The sustainable role of agricultural residues in future bioeconomy strategies and its dependency upon carbon returns to arable soils

Christhel Andrade Diaz

Université Fédérale
Toulouse Midi-Pyrénées

THÈSE

En vue de l'obtention du
DOCTORAT DE L'UNIVERSITÉ DE TOULOUSE

Délivré par l'Institut National des Sciences Appliquées de Toulouse

Présentée et soutenue par

Christhel ANDRADE DIAZ

Le 23 juin 2023

Le rôle des résidus agricoles dans des stratégies de bioéconomie durables et comment le retour de carbone aux sols conditionne la performance environnementale de ses stratégies

Ecole doctorale : **MEGEP - Mécanique, Energétique, Génie civil, Procédés**

Spécialité : **Génie des Procédés et de l'Environnement**

Unité de recherche :
TBI - Toulouse Biotechnology Institute, Bio & Chemical Engineering

Thèse dirigée par
Lorie HAMELIN et Ezequiel ZAMORA

Jury

Mme Birka WICKE, Rapporteure
M. Jorgen Eivind OLESEN, Rapporteur
Mme Sonja KEEL, Examinatrice
M. Jean-François SOUSSANA, Examinateur
M. Florent LEVAVASSEUR, Examinateur
Mme Lorie HAMELIN, Directrice de thèse
M. Ezequiel ZAMORA, Co-directeur de thèse
M. Etienne PAUL, Président

Université Fédérale
Toulouse Midi-Pyrénées

THESIS

Submitted in fulfillment of the requirements for the

DOCTORATE DEGREE OF THE UNIVERSITY OF TOULOUSE

Delivered by the Institute of Applied Sciences of Toulouse

Presented and defended by
Christhel ANDRADE DIAZ

The 23rd of June, 2023

The sustainable role of agricultural residues in future bioeconomy strategies and its dependency upon carbon returns to arable soils

---

Doctorate school: **MEGEP – Civil, Chemical, Power and Mechanical Engineering**
Major: **Chemical Engineering and Environment**

Research unit:
TBI – Toulouse Biotechnology Institute, Bio & Chemical Engineering

Supervisors:
Lorie HAMELIN and Ezequiel ZAMORA

Thesis Committee
Mrs. Brika Wicke, Rapporteur
Mr. Jorgen Eivind Olesen, Rapporteur
Mrs. Sonja Keel, Reviewer
Mr. Jean-François Soussana, Reviewer
Mr. Florent Levavasseur, Reviewer
Mrs. Etienne Paul, Reviewer
Mrs. Lorie Hamelin, Supervisor
Mrs. Ezequiel Zamora, Co-supervisor

ABSTRACT

Crop residues are a key feedstock to supply renewable carbon due to their relative abundance, flexibility to supply several bioeconomy pathways, and no land or food competition. Nevertheless, when left on the field, crop residues maintain the soil carbon balance, creating a tradeoff between supplying the bioeconomy and maintaining the soil carbon stocks. In France, it is recommended to maintain between 41 and 96% of the technically harvestable residue on soils to prevent soil organic carbon (SOC) losses, which precludes the supply of biomass to the bioeconomy. However, these restrictions have not considered the end-use of the residues or foreseen that bioeconomy processes generate, along with the main product, a residual biomass known as coproduct, which is rich in recalcitrant carbon that can be returned to soils.

This thesis aims to understand the interactions between the return of recalcitrant bioeconomy coproducts to soil and long-term SOC dynamics in a C-neutral harvest context. The term “C-neutral harvest” is defined as a situation where the harvesting of crop residues for a given bioeconomy management does not decrease the long-term SOC stocks, compared to a reference situation (BAU) where crop residues are not harvested. The thesis, thus, determines the amount of crop residues that could be harvested to supply the bioeconomy, in a spatially explicit manner and function of the bioeconomy pathway, while preserving or enhancing SOC stocks.

The interrelation between soil organic carbon dynamics and the recalcitrance of bioeconomy coproducts was investigated to provide a set of tools that integrate bioeconomy-derived coproducts within soil C models. The conversion rates of crop residues to bioeconomy coproducts, as well as the inherent recalcitrance of these coproducts, were exhaustively reviewed for five bioeconomy technologies (coproducts in brackets): i) pyrolysis (biochar), ii) gasification (char), iii) hydrothermal liquefaction (hydrochar), iv) anaerobic digestion (digestate), and v) lignocellulosic alcohol production (solid cake and liquid molasses). A harmonized database of over 600 data records was compiled to report average C conversion (C_C) and recalcitrance (C_R) coefficients for the coproducts under study.

A novel framework based on four interconnected modules that integrate the C_C and C_R coefficients of the five coproducts in the AMG and RothC soil models was developed. The models were applied to spatially explicitly assess the C-neutral harvest potential of crop residue to supply the bioeconomy in France (AMG) and Ecuador (RothC). In the case of RothC, the priming effect exerted by the input of the bioeconomy coproducts on crop-dedicated soils was also considered.

While returning the bioeconomy coproducts could allow exporting all the technically harvestable crop residues without imposing pressures on SOC stock (compared to a BAU situation), it

could impact other environmental variables disregarded by the soil C models (e.g., climate change, eutrophication, toxicity, among others). To shed light on the trade-off between carbon sequestration and environmental mitigation, a full life cycle assessment (LCA) was performed. Maritime biofuel production derived from residual crop biomass was studied for two processing pathways (biogas to liquefied gas, and bio-oil produced by pyrolysis) and was compared to a no-use scenario (BAU), including counterfactual biomass use. The integration of the SOC modeling results with the LCA conclusions allows the identification of the most suitable scenario for the valorization of crop residues.

Keywords: soil modeling, SOC, bioeconomy, recalcitrance, crop residues, coproducts

RÉSUMÉ

Les résidus de cultures sont une matière première essentielle pour fournir du carbone renouvelable en raison de leur abondance relative, de leur flexibilité pour approvisionner plusieurs voies bioéconomiques et de l'absence de concurrence foncière ou alimentaire. Néanmoins, lorsqu'ils sont laissés sur le terrain, les résidus de culture contribuent à maintenir le bilan carbone du sol, ce qui crée un compromis entre l'approvisionnement de la bioéconomie et le maintien des stocks de carbone du sol. En France, il est recommandé de maintenir entre 41 et 96 % des résidus techniquement récoltables sur les sols pour éviter les pertes de carbone organique du sol (COS), ce qui contraint l'approvisionnement en biomasse de la bioéconomie. Cependant, ces restrictions n'ont pas pris en compte l'utilisation finale des résidus ni prévu que les processus de bioéconomie génèrent, avec le produit principal, une biomasse résiduelle appelée coproduit, riche en carbone récalcitrant pouvant être restitué aux sols.

Cette thèse vise à comprendre les interactions entre le retour des coproduits récalcitrants de la bioéconomie dans le sol et la dynamique du COS à long terme dans un contexte de récolte neutre en C. Le terme “récolte neutre en C” est défini comme une situation où la récolte des résidus de culture pour une gestion bioéconomique ne diminue pas les stocks de COS à long terme, par rapport à une situation de référence (BAU) où les résidus de culture ne sont pas récoltés. La thèse détermine ainsi la quantité de résidus de culture qui pourrait être récoltée pour alimenter la bioéconomie, de manière spatialement explicite et en fonction d du type de transformation bioéconomique, tout en préservant ou en augmentant les stocks de COS.

L'interrelation entre la dynamique du COS et la recalcitrance des coproduits de la bioéconomie a été étudiée pour fournir un ensemble d'outils qui intègrent les coproduits dérivés de la bioéconomie dans les modèles du carbone du sol. Les taux de conversion des résidus de culture en coproduits de la bioéconomie, ainsi que la recalcitrance inhérente à ces coproduits, ont été revus de manière exhaustive pour cinq technologies de la bioéconomie (coproduits entre parenthèses) : i) pyrolyse (biochar), ii) gazéification (char), iii) hydrothermique liquéfaction (hydrochar), iv) digestion anaérobie (digestat) et v) production d'alcool lignocellulosique (fraction solide et mélasse liquide). Une base de données harmonisée de plus de 600 enregistrements de données a été compilée pour rapporter les coefficients moyens de (i) conversion du C (C_C) de la biomasse d’origine en coproduit et (ii) de recalcitrance (C_R) pour les coproduits étudié.

Un nouveau cadre basé sur quatre modules interconnectés qui intègrent les coefficients C_C et C_R des cinq coproduits étudiés dans les modèles de dynamique du carbone du sol AMG et RothC a été développé. Les modèles ont été appliqués pour évaluer de manière spatialement explicite le potentiel de récolte neutre en C des résidus de culture pour approvisionner la bioéconomie en France (AMG) et en Équateur (RothC). Dans le cas de RothC, le “priming effect” exercé par l'apport des coproduits de la bioéconomie sur les sols dédiés aux cultures a également été considéré.

Alors que le retour de certains coproduits de la bioéconomie pourrait permettre d'exporter tous les résidus de culture techniquement exploitables sans imposer de pressions sur le stock de COS (par rapport à une situation BAU), il pourrait avoir un impact sur d'autres variables environnementales ignorées par les modèles C du sol (par exemple, le changement climatique, l'eutrophisation, la toxicité, entre autres). Pour faire la lumière sur le compromis entre la séquestration du carbone et l'atténuation environnementale, une analyse de cycle de vie (ACV) a été réalisée. La production de biocarburants maritimes dérivés de la biomasse résiduelle des cultures a été étudiée pour deux voies de transformation (biogaz en gaz liquéfié, et bio-huile produite par pyrolyse) et a été comparée à un scénario sans utilisation (BAU). L'intégration des résultats de la modélisation SOC avec les conclusions de l'ACV permet d’identifier le scénario le plus adéquat pour la valorisation des résidus de culture.

Mots clés : modélisation des sols, COS, bioéconomie, récalcitrance, résidus de culture, coproduits

ACKNOWLEDGEMENTS

I wish to sincerely thank everyone who has contributed professionally and personally to making possible this Ph.D. along this three-year journey.

I would like to thank my supervisor and co-supervisor for their guidance along this hard endeavor. My most sincere gratitude goes to Dr. Lorie Hamelin, who welcomed me in Toulouse and has been a pillar for my professional formation. Thanks for believing in me and always encouraging me to go further in my academic life. These three years you have shown me your support and enthusiasm to pursue my goals and always strive for more. I appreciate the opportunities and doors you have opened to me by making me part of this project. Thanks for all the discussions, your contagious passion for science, dedication, confidence, and kind words, those have been key to completing this challenge. Moreover, I am deeply grateful for all the opportunities you have given me to forge my research skills by making me part of conferences, and project exchanges, and inviting me to all the work sessions, I have been part of during these years. Thanks a lot! My appreciation goes also to Dr. Ezequiel Zamora, thanks for inviting me to be part of this adventure, for all the discussions and side projects we have seen together, and for showing me the wonders of soil science and agronomy.

This research was only possible to become a reality, thanks to all the scientific advice I've received from experts, who have shown me the true open science by taking their time to answer my questions. In particular, I would like to express my gratitude to my coauthors, who have been a key part of this project. I want to express my thankfulness to Hugues Clivot for initiating me on soil modeling, thanks a lot for all the meetings and exchanges, and for being always available to help with my questions. Ariane Albers, a big shout-out goes for you too; thanks for all the discussions on shaping the papers and for helping me to improve my writing skills. Also, I cannot leave out Enrico Balugani, thanks for your enthusiasm and involvement in the project, and all the networking. I would like to take this opportunity to also extend my gratitude to people who played a key role in my PhD formation. Dr. Sergei Sokol, thanks for your patience while teaching me the R coding skills, without this I couldn't have succeeded on this challenge. Thanks to Shivesh Karan, my go-to source of GIS knowledge, thanks for introducing me to ArcGIS. Also, thanks to Dr. Henry Pachecho, for your support on the GIS data manipulation, and to Dr. Carlos Robles for his precious assistance on Python coding. During these three years, I have received the valuable advice and guidance of so many people, that I couldn't finish writing this thesis if I name each one, my most sincere thank you to all of you.

I take the opportunity to thank all my friends and colleagues of the EAD-7 and EAD-10 of TBI, and all the Cambioscopers, for their friendship, support, and joyful moments. You have made life beautiful in Toulouse. I take the opportunity to thank Patrick Brassard for sharing your experimental

data with me, even when it is yet unpublished, it plays a key part in my study. Thanks to Zhou, Pla, Gleeza, Ugo, Nia, and Seung Hye, for all the friendly exchanges, trips, and meals. You have kept me warm through the cold. Also, thanks to all the friends and nice people I have met in Toulouse that have helped me "survive", and thanks to my friends who have supported me with their nice words and encouragements, you are the reason why I have always kept my joy and energy. Thanks, my dear friends.

My biggest gratitude will always be to my family. My mom, dad, sister, and brother, as well as my furry family of dogs and cats (especially Ahomy and Lola, my faithful companions in the late nights), thank you for your unconditional love, patience, guidance, and support in all the challenges I take. Having you by my side is what keeps me strong to continue. Love you to the infinite.

This research was possible due to the financial support of the Embassy of France in Ecuador, through the project "Fonds de solidarité pour Projets Innovants" FSPI1 and the Universidad Técnica de Manabí (UTM), through the financial support for teachers pursuing graduate degrees. Thanks as well to the authorities and my colleagues in the UTM for their support since the very beginning of this road. I pass my appreciation as well to the Ministry of Agriculture of Ecuador, and especially Wilmer Jiménez, for providing valuable unpublished data that was used for paper 3 and the data paper of this thesis, and to the Sub-Secretary of Climate Change of Ecuador for the raw data on which the data paper was built.

Thanks again everyone, without all your support this would not have been possible!

LIST OF PUBLICATIONS AND COMMUNICATIONS

List of publications

1. **C. Andrade Diaz**, H. Clivot, A. Albers, E. Zamora-Ledezma, L. Hamelin. The crop residue conundrum: Maintaining long-term soil organic carbon stocks while reinforcing the bioeconomy, compatible endeavors? Applied Energy, 2023, https://doi.org/10.1016/j.apenergy.2022.120192.
2. **C. Andrade Diaz**, A. Albers, E. Zamora-Ledezma, L. Hamelin. The interplay between bioeconomy and long-term soil organic carbon stock maintenance: A systematic review. (*Under review in RSER*; pre-print available: https://doi.org/10.21203/rs.3.rs-1447842/v2).
3. **C. Andrade Diaz**, E. Balugani, E. Zamora-Ledezma, L. Hamelin. Modeling the long-term carbon storage potential from recalcitrant matter inputs in arable croplands (*Manuscript in preparation*).
4. **C. Andrade Diaz**, E. Zamora-Ledezma, L. Hamelin. Dataset for spatially-explicit pedoclimatic clustering of Ecuadorian croplands and biomass potential estimation. Data in Brief, 2023 (*Manuscript in preparation*)
5. **C. Andrade Diaz**, E. Zamora-Ledezma, L. Hamelin. The compromise between soil carbon storage and environmental mitigation from recovering crop residues for bioenergy: A life-cycle assessment for maritime fuels. (*Manuscript in preparation*).

Oral presentations and conference chairing

1. Considering the interactions between crop residues, bioeconomy conversion pathways, and the return of carbon to soils. *3rd Doctoral Colloquium Bioenergy DOC 2020*. **Oral presentation**, Leipzig, Germany.
2. Evaluación Metodológica para la modelación e interpretación de procesos de bioeconomía sobre el carbono orgánico en suelo: Caso de estudio Francia. *I Simposio Internacional de Ingeniería Agrícola – IV Convención Científica Internacional de la UTM 2020*. **Oral presentation**, Portoviejo, Ecuador.
3. Can long-term soil organic carbon stocks be maintained when considering the recalcitrant returns from bioeconomy processes? A national case study for France. *29th European Biomass Conference & Exhibition. 2021*. **Oral presentation**, online.

4. Recycling back carbon to the soil through biochar to maintain the long-term soil carbon stocks. *5th CIGR International Conference 2021 – Integrating agriculture and society through engineering*. **Oral presentation**, Québec, Canada.
5. Availability of Agricultural Biomass to supply bioeconomy technologies in Ecuador. *III Simposio Internacional de Ingeniería Agrícola – VI Convención Científica Internacional UTM 2022*. **Oral presentation**, Portoviejo, Ecuador.
6. Strengthening the bioeconomy in tropical countries while preserving soil organic carbon stocks by recycling recalcitrant coproducts: A case study for Ecuador. *EGU General Assembly 2023*. **Poster**, Vienna, Austria.
7. Technical, regulatory and economic issues and advantages: the challenges of setting up sustainable biochar sectors. **Round table** at the *First National Biochar Meetings*. Rennes, 2023.
8. **Co-convener** at the *VI Convención Científica Internacional UTM 2022 – V Congreso de Ingeniería Aplicada*. Portoviejo, 2022.
9. **Co-convener** at the *EGU General Assembly 2023* – Session SSS5.2 - Dynamics and functions of SOM pools under new and traditional soil amendments, with a special focus on pyrolytic carbon. Vienna, 2023.

SUPPLEMENTARY MATERIAL AND DATA

Modeling studies and LCAs rely on extensive data reported in the literature and thus require maximum transparency in the data collected and processed, as well as in the calculations performed. The supporting data of each paper in this thesis is listed in Table 0 and is available online at *Callisto – Dataverse - TBI - Toulouse Biotechnology Institute - T21018*. Additionally, each chapter ends by providing details about the Supplementary Information appended to the paper.

Table 0 : Supplementary files

Paper	Name and description of files	Doi link
1	**SI1.** Word file containing a detailed description of the methodology followed to perform the literature review in Chapter 2. This includes a further description of each bioeconomy pathway studied in this PhD work and the key soil models used by previous authors to model bioeconomy coproducts as soil amendments.	Available within this PhD manuscript in Appendix A1a
	SI2. Excel file presenting an exhaustive overview of the characteristics of 12 key soil models.	https://doi.org/10.21203/rs.3.rs-1447842/v1
	D1. Database to determine the Carbon recalcitrance (C_R) and carbon conversion (C_C) rate to bioeconomy coproducts. 2022. The database contains 8 excel files: 5 files presenting the full data reviewed to determine the C_R parameter for each bioeconomy pathway and 3 files are dedicated to Cc. 1 excel file presents the data used to determine the Cc parameter of the thermochemical pathways (Pyrolysis, Gasification, and hydrothermal liquefaction). 1 Excel file details the biomethane potential (BMP) reported for cereal derived biomass as well as the mass balance performed to determine the C balance. 1 Excel file presents the C_C for bioethanol coproducts. 1 metadata file in CSV format explains all the terminology used in this database	DOI: 10.48531/JBRU.CALMIP/WYWKIQ
2	**SI1.** Supplementary information of Paper 2 (Chapter 3). Contains details on the crop rotations and the adaptation of the bioeconomy coproducts in AMG.	Published at https://doi.org/10.1016/j.apenergy.2022.120199 and presented as Appendixes A2a and A2b.
	SI2. Excel file with summary results for paper 2. Present the percentage of area affected by ranges, the net and average SOC change and the sensitivity analysis.	
	D2. Dataset to assess the soil organic carbon evolution of French croplands in a bioeconomy perspective using the soil model AMG. 2022.	DOI: 10.48531/JBRU.CALMIP/AUEEEJ

Paper	Name and description of files	Doi link
	Contains 109 files corresponding to the processed results of the Paper 2. 3 R scripts detailing the data manipulation and results analysis. 9 CSV containing input data reporting cropping systems in France as PCUs and simulation units created in Launay et al., 2021 and formatted to be used in AMG (crops, irrigation, meteo4.5, organic fertilizer, SOC, tillage, surface), +1 metadata CSV. 8 CSV reporting main results for the combination of mean C_C and C_R for each scenario studied, 1 CSV for projected biomass annual yield in France from 2020 until 2120 based on the results obtained from STICS in the 4p1000 Report. 81 CSV files exploring the SA of the study.	
3	**SI1.** Word explaining further details considered in the study, such as pedoclimatic union description and details on the soil model adaptation.	
3, 5	**D3.** Spatially-explicit pedoclimatic clustering of Ecuadorian croplands and biomass potential estimation. (Database in preparation). This input data is accompanied by the parameters used for the baseline of cropping systems created for Ecuador. This whole dataset is presented as a separate data paper, companion of paper 3. Briefly, the data contained comprises: Excel with CR, CC, PE parameters reviewed, and summary average values used for the paper. CSV with yield of each crop per province. Input data CSV: TS, Constant, Initial. CSV results for each pathway. Meteorological data for EC. Shapefiles. **D4.** Outputs for the main scenarios and sensitivity analysis	https://doi.org/10.48531/JBRU.CALMIP/VLKG8V Presented with this thesis as Appendix A3a https://doi.org/10.48531/JBRU.CALMIP/54SOW9
4	**SI1**. Word file detailing the assumptions considered for preparing the mass and energy balances accounted in the LCA. **D5** Data Folder.: LCI files for 2pathways, and LCA results for all the pathways.	Presented in here as Appendix A4a https://doi.org/10.48531/JBRU.CALMIP/1JXQK3

TABLE OF CONTENTS

The list of figures, tables and appendixes are provided in each chapter

CHAPTER 1 : GENERAL INTRODUCTION & CONTEXT

1. CHAPTER 1: General introduction and context

1.1 Crop residues, bioeconomy, and soil organic carbon interplay

Bioenergy must represent at least 21% of the total global energy consumption by 2030 to meet the Paris target of maintaining the average temperature increase well below 2 °C above the pre-industrial era, according to IRENA [1]. In this context, and beyond the sole energy sector, various bioeconomy strategies are promoted by national and international bodies to supply the carbon-based products demanded by society from biological resources instead of fossil carbon (C) [2].

Crop residues are a key feedstock to supply renewable carbon due to their relative abundance, flexibility to supply several bioeconomy pathways, and no land or food competition [3]. A theoretical potential of 3800 PJ y^{-1} has been estimated for Europe [4], of which 987 – 1369 PJ y^{-1} have been reported for France alone [5]. Nevertheless, this potential is limited due to technical and environmental constraints. Crop residues represent an abundant source of carbon to maintain the soil carbon balance [6,7], therefore the removal rates are often limited to ca. 15 – 60% of the theoretical potential depending on the crop type [8–12]. In France, it is recommended to maintain between 41 and 96% of the technically harvestable residue on soils to prevent soil organic carbon (SOC) losses [13], which precludes the supply of biomass to the bioeconomy. However, these restrictions have not considered the end-use of the residues or foreseen that bioeconomy processes generate, along with the main product, a residual biomass known as coproduct, which is rich in recalcitrant carbon that can be returned to soils [14].

1.2 Contextualization

This section briefly explains some of the key general concepts used throughout this thesis. These concepts are further detailed in the subsequent chapters of the thesis.

1.2.1 Soil organic carbon

Topsoil (0 – 30 cm profile) contains approximately 700 Pg of organic carbon (SOC) at a global scale, representing the third largest pool in the C cycle [15,16]. SOC is the result of the decomposition and stabilization of soil organic matter (SOM), such as plant and animal residues. In agricultural systems, the C inputs from crop residues and organic fertilizers create a dynamic equilibrium with the C losses due to SOM decomposition [17] and keep the SOC stocks at relatively stable levels.

SOC plays a crucial role in maintaining and improving the soil structure, fertility, water holding capacity, and nutrient cycling [17]. Furthermore, SOC acts as a carbon sink, with a projected annual storage potential of 1.2 billion tons of C in agricultural soils (IPCC, 2014), helping to mitigate climate

change by storing carbon dioxide from the atmosphere. Managing and preserving SOC is essential for sustainable agriculture, ecosystem resilience, and global carbon balance [17,18].

1.2.2 Soil models

The changes in SOC stocks are only noticeable in the long term, with a minimum of five to ten years to be able to measure the changes. Soil models are thus useful to identify the effects of different practices on SOC evolution and define proper policies and strategies.

Soil models represent agroecological systems integrating the interaction of biotic elements with soil, weather, and management practices to simulate soil carbon, nitrogen, water, and biomass accumulation [19,20]. Diverse modeling approaches and continued advances in knowledge regarding the soil-atmosphere interactions have led to the development of more than 250 different soil models, and more models are being investigated and developed [21]. An ideal model must be based on a mechanistic understanding of the SOM dynamics to extrapolate the measured short-term local processes to long-term effects valid at different scales [22] (Fig 1).

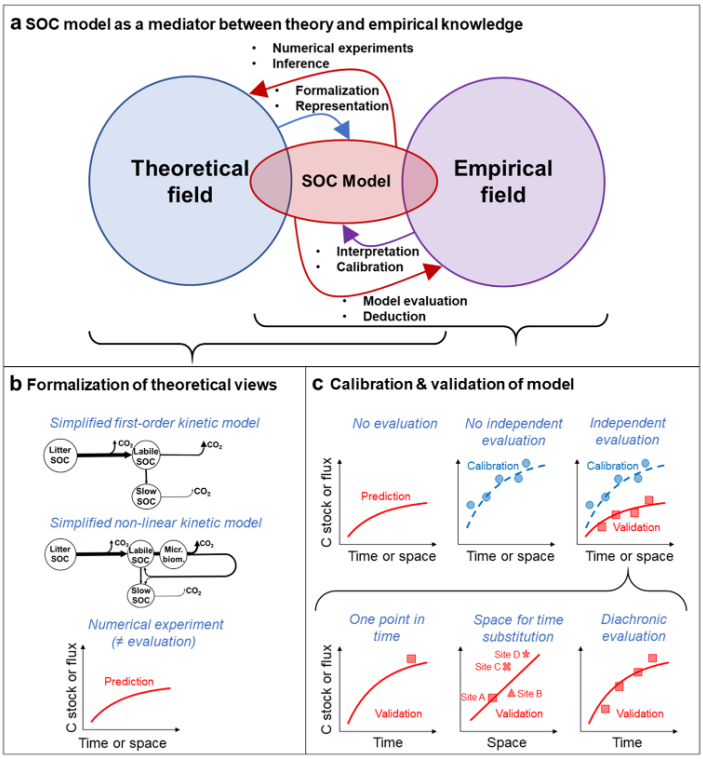

Fig 1.1 Representation of soil models integrating theoretical knowledge regarding soil mechanisms and empirical observations validating the theory. As shown in boxes b and c, the soil models contrast the theory with in-field evidence to provide calibrated values able to represent the local reality. *Source: Reused with permission from Le Nöe et al. [23].*

However there remain unresolved challenges regarding understanding the intrinsic soil dynamics, parameterization, and input data availability, thus no single ideal model exists. Moreover, depending on the purpose of the model the type of process and level of details incorporated in the model may vary. Models must be evaluated across all possible conditions, however, due to time and budget constraints this is virtually impossible to achieve, and thus it is preferred to increase the accuracy of a model for particular situations [19] and select the model adapted to the requirements. More details regarding general information and assumptions in soil models are presented in Chapter 2.

1.2.3 Bioeconomy coproducts

Bioeconomy set the scene to transition to reach the goal of climate neutrality by 2050 [24]. Currently, 9% of the total EU economy is represented by bioeconomy and 63% of the total biomass supply relies on agriculture, and a tenfold growth for bioenergy is projected by 2050 [25,26].

In its latest bioeconomy strategy [27], the European Commission defined bioeconomy as covering “all sectors and systems that rely on biological resources […], their functions and principles. It includes and interlinks land and marine ecosystems and the services they provide; all primary production sectors that use and produce biological resources, i.e., agriculture, forestry, fisheries and aquaculture; and all economic and industrial sectors that use biological resources and processes to produce food, feed, bio-based products, energy and services. […] health biotechnology and biological medicines are not included in the bioeconomy definition”.

The biomass used as feedstock for the bioeconomy processes can be derived from agriculture residues, wastes, and coproducts from biomass processing. Coproducts are defined as wastes resulting from a process or chemical reaction. They are not the principal product or service but can be often valorized through additional processing [28]. Bioeconomy coproducts are often rich in degradation-resistant carbon and may contain remaining of unconverted nutrients or toxic components in the raw biomass. However, the physicochemical characteristics of bioeconomy coproducts and potential reuse for secondary services vary according to the process conditions and characteristics of the original biomass.

1.2.4 Recalcitrance and Priming effect

All organic matter (OM) input to soils is subjected to a mineralization-stabilization process that conducts to SOC formation. Three possible mechanisms have been proposed to explain SOM stabilization, which are physical protection from microbial processes, limiting exposure to lytic enzymes by mineral associations, and OM recalcitrance by the preservation of the less biodegradable

inputs and the formation of stable humic molecules [29]. While physical protection and mineral aggregation are well-recognized mechanisms, the transformation of OM into degradation-resistant molecules remains a challenge [22].

The resistance to degradation exhibited by various bioeconomy coproducts is often referred to as recalcitrance [30,31]. The application of recalcitrant matter to soils can trigger a series of changes in the physicochemical composition of the soil and alter the behavior of soil microbiota. Recalcitrant coproducts have been reported to be mineralized at slower rates than their fresh OM counterpart. The change in mineralization rates leads to the so-called priming effects [32,33]. In fact, both faster and slower mineralization rates have been observed when the recalcitrant matter has been applied to soils [34], which hardens the endeavor of understanding the implications of recalcitrant coproducts as soil amendments.

Recalcitrance and priming effect are the key characteristics researched in the coproducts studied in this thesis and are further explored in chapters 2 to 4.

1.2.5 Sustainable maritime fuels (SMF)

The maritime industry accounts for 2 – 3% of global CO_2, 4 – 9% of SOx, and 10 – 15% of NOx emissions. These emissions are mainly related to the use of heavy fuel oil (HFO), which represents 77% (231 Mt) of the global marine fuel mix [35]. In response, various regulations are being put into action to limit maritime emissions [36–39]. The International Maritime Organization (IMO) targets to reduce the average carbon intensity of the sector by 70% and the total greenhouse gases (GHG) emissions by at least 50%, by 2050 (compared to 2008 levels) [40]. In this context, since 2020, the sulfur content in maritime fuels has been limited to 0.50% which limits the use of conventional maritime fuels [40,41].

Approximately 80% of international trading is done by merchant shipping, with a forecasted annual growth of 2.2% by 2027 [42]. Bulk carriers represent 43% of the global fleet with an estimated annual growth of 3.6% [43] and are thus a key vessel for transitioning to less carbon-intense maritime fuels.

The most common current marine fuels used in bulk carriers are HFO and marine diesel fuel oil (MFO), which are derived from the heavy distillates of refineries, contain long carbon chains, little aromatic components, and are thus deemed as of low quality and costs [35]. The use of marine distillate oils (MDO) and liquefied natural gas (LNG) are among the alternatives put in action to comply with the sulfur limitations, as well as desulphuring HFO and installing scrubber systems in the vessels to continue operating with HFOs.

Sustainable maritime fuels (SMF) produced from renewable sources, are another alternative towards GHG emissions reduction in the sector [44]. The technologies studied in this thesis deliver main products that can be refined to source the SMF demand. In particular, pyrolysis bio-oil can undergo a catalytic or hydro-cracking process [45] to deliver a fuel that can be used as replacement of HFO. Moreover, as shipping engines are already adapted to operate using the low quality HFO, cracking processes are not necessary during the upgrading of pyrolysis bio-oil, and a simple hydrotreatment to remove excessive O_2 is sufficient [40]. Biogas can also undergo bio-methanation to remove the CO_2 fraction and act as a replacement of LNG, which has aroused as one key alternative to comply with the sulfur regulation in the maritime industry [46].

In this sense a C-neutral harvest of crop residues for SMF production is an interesting alternative to supply the bioenergy sector. However, C-neutral harvest does not prevent unintended, environmental consequences arising from the conversion process and the use of the converted biomass. Therefore, understanding the eventual tradeoffs between the SOC maintenance and full environmental performance of the bioeconomy conversion process is required for defining the most environmentally-performant option to supply the crop residues streams. More details on maritime fuels are in Chapter 5 and Appendix A4a.

1.3 Thesis outline

Although supplying the most accessible source of renewable carbon, the bioeconomy implies many challenges in particular those posed by tapping into the potential of a large diversity of renewable biological resources (biodiversity, land use changes, ecosystem services) [47], which may disturb the nutrient cycle in the biosphere. Soils play a crucial role in food security, ecosystem services, and climate change mitigation [48] and their preservation is thus a primary goal limiting the supply of biomass to the bioeconomy.

SOC evolution in agricultural lands is acutely influenced by the pedoclimatic characteristics of the geographical area under study, as well as the anthropogenic influences related to farming management. The latter involves the amount and characteristics of the C inputs in the soil. However, current limitations on C harvesting to supply the bioeconomy, in terms of ensuring SOC stocks, disregard the final use of the crop residues and consequent potential return of recalcitrant C to maintain the SOC balance.

Therefore, this thesis aims to understand the interactions between the return of recalcitrant bioeconomy coproducts to soil and long-term SOC dynamics in a C-neutral harvest context. The term “C-neutral harvest” is defined as a situation where the harvesting of crop residues for a given bioeconomy conversion pathway does not decrease the long-term SOC stocks, compared to a

reference situation where crop residues are not harvested. In this study, five bioeconomy conversion pathways are studied, namely pyrolysis, gasification, hydrothermal liquefaction, anaerobic digestion, and second-generation bioethanol production.

Here we hypothesize that the return of the resulting coproducts from using crop residues in the bioeconomy provides recalcitrant carbon to soils, which in turn allows to harvest more crop residues while maintaining or even increasing SOC stocks, compared to a situation where crop residues remain on soils.

Accordingly, the main research question driving this study has been formulated as

"What is the C-neutral harvesting rate of crop residues in temperate and tropical environments, when considering the return of bioeconomy coproducts?"[1]

Based on the research gaps identified, the main research question, was divided into the following sub-questions (RQ):

1. **RQ1**. What are the key factors determining the interrelation between the supply of crop residues to the bioeconomy and the maintenance of SOC stocks in croplands?
2. **RQ2**. How much additional biomass from crop residues is available if a C-neutral harvest is practiced and recalcitrant bioeconomy coproducts are returned to soils, compared to business-as-usual approaches defining a harvest threshold?
3. **RQ3.** What are the trade-offs between a C-neutral harvest and the overall environmental performance of the bioeconomy conversion technology if the impacts related to the use of the principal product obtained in the bioeconomy pathway are fully addressed?

In order to answer these questions, the thesis builds on four research tasks (RT)

[1] This question has four implications: implies (i) that a particular bioeconomy conversion pathway is considered (five are considered in this thesis), (ii) that the bioeconomy e coproduct is returned to soils, (iii) that there is a temporal scope considered (several are studied), and (iv) that there is a geographical scope (two are considered herein, as detailed in the research objectives).

1. **RT1.** Investigate and quantify the carbon flows from crop residues in the five bioeconomy technologies under study, as well as the recalcitrance of the coproducts delivered in each pathway, and the ability of soil models to incorporate these characteristics.
2. **RT2.** Adapt a soil model to evaluate the medium- to long-term SOC dynamics of harvesting crop residues for the bioeconomy while returning the bioeconomy coproducts to soils.
3. **RT3**. Perform spatially-explicit assessments of C-neutral harvest potential of crop residue to supply the bioeconomy at the national level in temperate and tropical contexts, represented by France and Ecuador, respectively.
4. **RT3.1** Build the un-existing baseline of Ecuadorian cropping systems necessary to RO3, including a quantification of the theoretical potential of crop residues to supply the bioeconomy.
5. **RT4.** Perform a lifecycle assessment considering the full use of the main product and the return to soils of the coproducts.

To attain the research objectives and answer the research question, this thesis was conducted in four consecutive stages depicted in Fig 1.1.

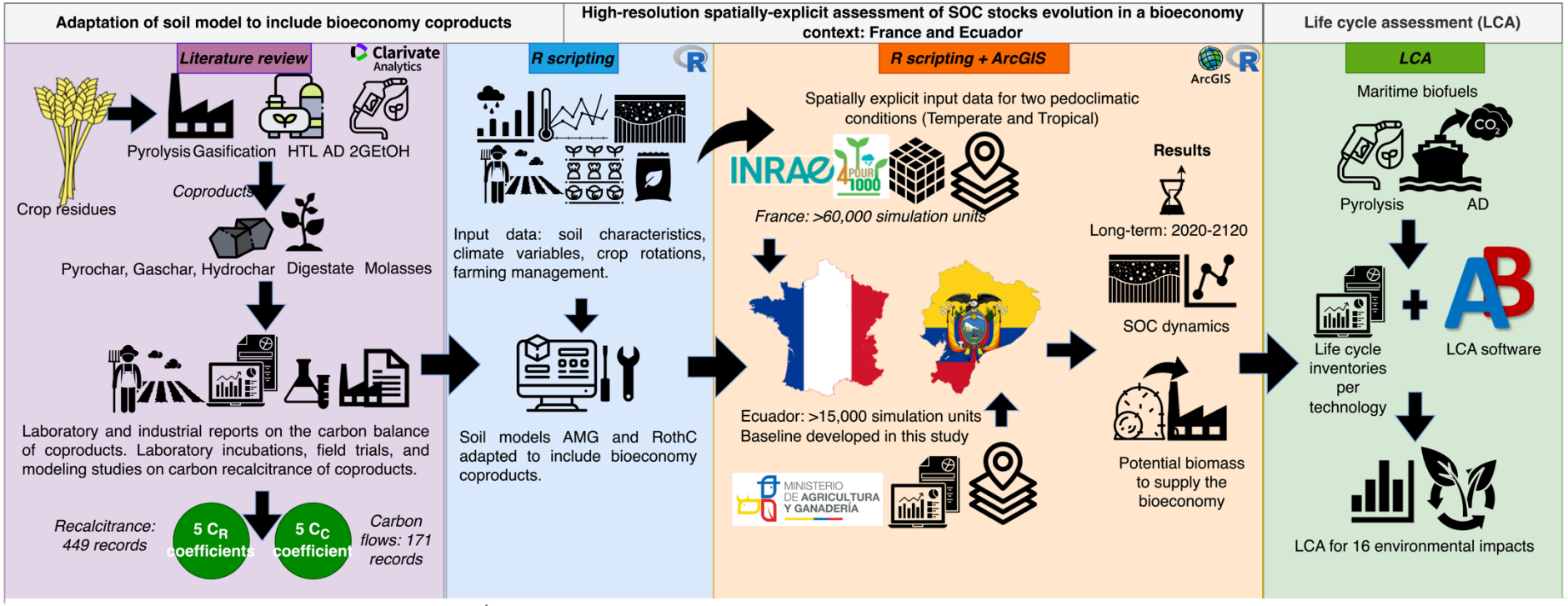

HTL: hydrothermal liquefaction; AD: anaerobic digestion; 2GEtOH: Éthanol Lignocellulosic ethanol. Icons retrieved from www.thenounproject.com

Fig.1.2 Research stages involved in this thesis

This thesis integrates an umbrella of disciplines that include agroecology, soil science, crop residues valorization for the bioeconomy and LCA. The scope (Fig. 1.2) of the study is mainly on the crop residues potential to supply the bioeconomy and how it interplays with the SOC dynamics in croplands.

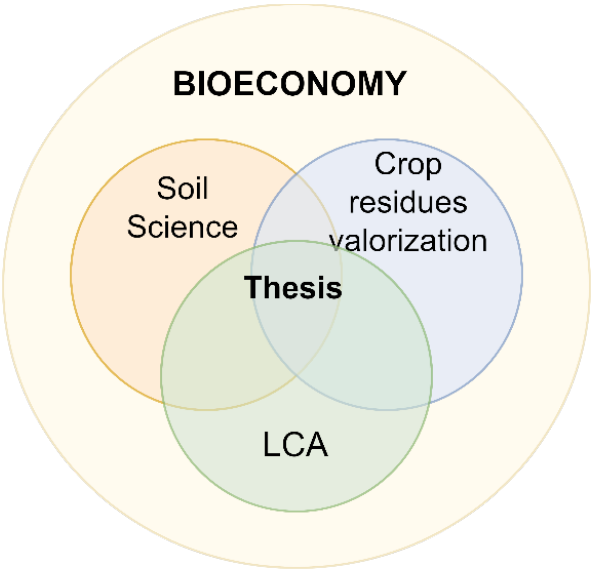

Fig 1.3. Scope of this PhD thesis

This thesis is composed of six chapters, illustrated in Fig 1.3. The research questions are addressed in chapters 2 to 5. Table 1.1. provides an overview of the research questions that are addressed in each chapter and the geographical and temporal scope considered. The final chapter summarizes the overall findings, answers the research questions, presents the conclusions and limitations of the thesis and highlights future perspectives within the research field.

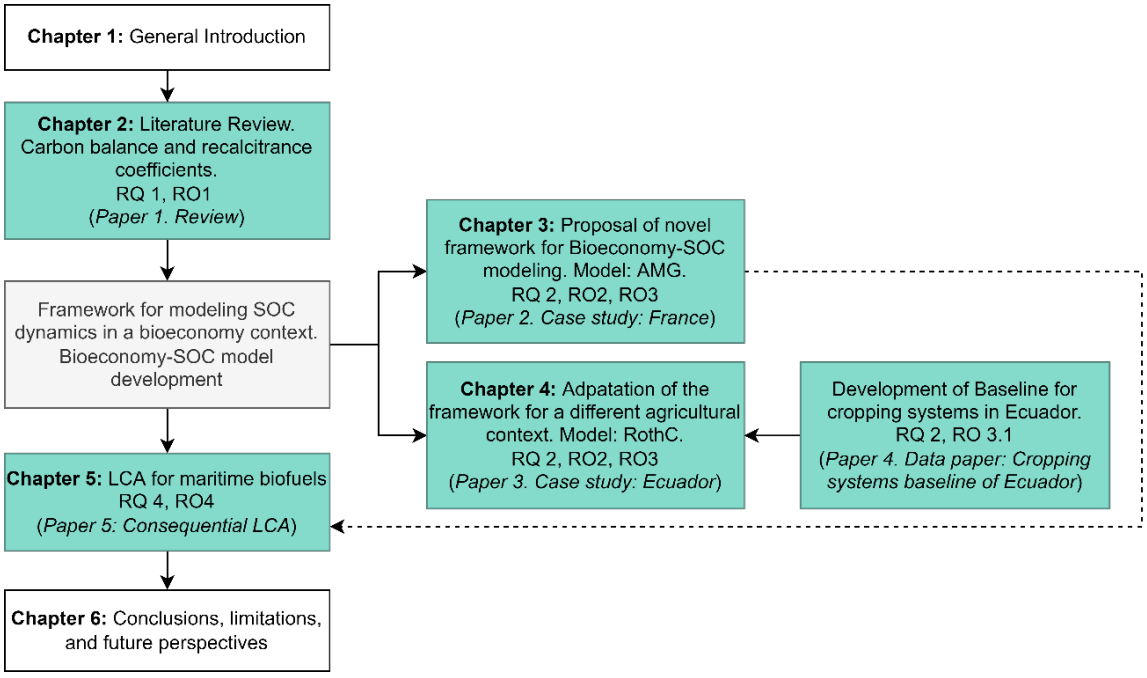

Fig 1.4. Simplified structure of the thesis with chapters and paper. Green boxes represent scientific papers.

Table 1.1. Overview of the thesis chapters and the research questions addressed

Chapter	Topic	Research question			Objectives	Geographical scope	Temporal scope
		1	2	3			
2	The interplay between bioeconomy and long-term soil organic carbon stock maintenance: A systematic review	X			RO1	-	-
3	The crop residue conundrum: Maintaining long-term soil organic carbon stocks while reinforcing the bioeconomy, compatible endeavors?		X		RO2, RO3	Temperate climate: France	100 years: 2020-2120
4	Modelling the long-term carbon storage potential from recalcitrant matter inputs in arable croplands		X		RO2, RO3, RO3.1	Tropical climate: Ecuador	20 years: 2020-2040 50 years: 2020-270
5	The compromise between soil carbon storage and environmental mitigation from recovering crop residues for bioenergy: A life-cycle assessment for maritime fuels			x	RO4	France	-

Chapter 2 establishes the theoretical fundaments of the interrelation between soil organic carbon dynamics and the recalcitrance of bioeconomy coproducts to integrate bioeconomy-derived coproducts within soil C models. The conversion rates of crop residues to bioeconomy coproducts, as well as the inherent recalcitrance of these coproducts, were exhaustively reviewed for five bioeconomy technologies (coproducts in brackets): i) pyrolysis (biochar), ii) gasification (char), iii) HTL (hydrochar), iv) AD (digestate), and v) 2GEtOH (solid cake and liquid molasses). A harmonized database of over 600 data records [37] was compiled to report average C conversion (C_C) and recalcitrance (C_R) coefficients for the coproducts under study. In parallel, twelve soil models (CENTURY, Daycent, DNDC, EPIC, Daisy, APSIM, STICS, CANDY, ORCHIDEE, RothC, AMG, and C-TOOL) were critically analyzed to unravel their ability to integrate bioeconomy coproducts through the incorporation of the derived C_C and C_R coefficients. This study provides a set of tools to develop more systematic methodologies to include bioeconomy coproducts within soil C models.

The cause-effect link between harvesting crop residues to supply the bioeconomy and long-term SOC evolution was investigated chapters 3 and 4. **Chapter 3** provides a novel framework based

on four interconnected modules that integrate the C_C and C_R coefficients of the five coproducts reviewed in chapter 1 within the AMG soil model. This chapter presents a high-resolution spatially explicit assessment, including more than 60,000 simulation units for the five bioeconomy deployments against a business-as-usual (BAU) reference scenario from 2020 to 2120, for the whole croplands of France. The BAU scenario considered the current farming management practices, derived from the 4p1000 study for France [38], and assumed that the crop residues were not harvested for the bioeconomy. The bioeconomy scenarios were as per the BAU but considered that all (100%) of the technically harvestable crop residues are harvested to supply the bioeconomy, followed by a partial return of C to soils as bioeconomy coproducts. The climatic variables were considered as projected by the Representative Concentration Pathway (RCP) 4.5 [39], downscaled by the model CNRM-CRFACS-CM5/CNRM-ALADIN63 [40]. This study proved that the amount of crop residue that could be harvested in a specific location depends on the spatially explicit characteristics of soil, climate, and farming management practices, as well as the use for which the residues are being collected. The results suggest an additional crop residue potential of 71-225 PJ (pathway-dependent) for the bioeconomy scenarios, without SOC decreases, compared to a typically suggested removal limit of 31.5% in France [8].

Although the AMG model has been well validated for temperate climates [41–43], it is yet to be validated for other climatic regions. To bridge this gap, **Chapter 4** adapts the bioeconomy-SOC modeling framework to be applied to tropical climates. A bioeconomy module was developed within the RothC model, and it was spatially explicitly assessed for the Ecuadorian croplands. The simulation units were created based on the SOC sequestration potential study developed by the Ministry of Agriculture of Ecuador [44,45] and the potential C inputs were determined as the average of the last nineteen years (2002-2020) of the production data reported in the Continuous Agricultural Production and Surface Survey [46]. The RothC model [47] adaptation was based on the RothC-biochar by Pulcher et al., 2022 [48] and included improved C_C and C_R values for the Ecuadorian crops. Furthermore, the model considered the effect exerted on SOC mineralization by the coproducts, also known as the priming effect. The future climate variables followed the RCP4.5 trajectory, based on an ensemble model (CSIRO-Mk3-6-0, GISS-E2-R, IPSL-CM5A-MR, MIROC-ESM) downscaled by the Climate Change Secretary of Ecuador [49]. Over 105,000 simulation units were included in this study.

While returning the bioeconomy coproducts could allow exporting all the technically harvestable crop residues without imposing pressures on SOC stock (compared to a BAU situation), it could impact other environmental variables disregarded by the soil C models (e.g., climate change, eutrophication, toxicity, among others). To shed light on the compromise between carbon sequestration and environmental mitigation, a full life cycle assessment was performed in **Chapter 5**.

The production of maritime biofuels derived from crop residual biomass was studied for five pathways, including the counterfactual use of the biomass. The vision of this section is to integrate the SOC modeling results with the LCA conclusions to derive the most adequate scenario for harnessing crop residues.

This thesis ends with an overall conclusion of the main findings of chapters 2 to 5, answers the research questions, highlights the limitations of the study, and provides future perspectives in **Chapter 6**.

Key novelties of this PhD work

- A harmonized database compiling 620 records reporting the conversion of the carbon in crop residues (i.e., cereals, maize, oilseed crops) into five bioeconomy coproducts, as well as their recalcitrance and mean residence time when applied in soils has been produced. A complementary database harmonizing 110 data records regarding the conversion of tropical crop residues (e.g., banana, cocoa, coffee, among others) into bioeconomy coproducts was also produced.
- Two soil carbon models, AMG and RothC, were adapted to include five bioeconomy coproducts as exogenous organic matter (EOM) inputs to soil, namely pyrochar (or biochar), gaschar, hydrochar, digestate, and molasses from second-generation bioethanol. The data preparation, model running, and output analysis were automatized using R.
- A novel framework for the spatially-explicit assessment of the long-term SOC dynamics of harvesting crop residues, supplying renewable carbon to the bioeconomy through five major bioeconomy pathways, and returning part of that carbon as recalcitrant coproducts was developed.
- The framework was applied with high resolution to the whole French croplands (>60,000 simulation units representing 84% of the country's arable land) to determine the available crop residues potential to supply the French bioeconomy while maintaining or increasing the SOC stocks, in comparison to a situation where crop residues would have been left on the fields.
- The framework was adapted for tropical lands and applied to determine the SOC storage potential of Ecuadorian croplands as a representative case of a tropical context, applied with high spatial granularity (>15,000 simulation units representing 52% of the country's arable lands).
- While the French baseline was already established before this Ph.D. study, the baseline for current cropping systems in Ecuador was not. National statistics on crop production and yields, as well as spatially-explicit soil and meteorological data were supplied by the Ecuadorian Ministries of Agriculture and Environment, respectively. From conciliating this with a variety

of additional data, a baseline quantifying the theoretical potential of harvestable crop residues to supply the bioeconomy in the country was created in this thesis. The projected evapotranspiration under the Representative Concentration Pathway (RCP) 4.5 was also produced during this thesis. All the data, maps, and scripts produced for this baseline is openly accessible and can be reused in further studies beyond SOC modeling.

- A full LCA was performed for the production of hydrotreated pyrolysis bio-oil and cryogenic liquefied biogas to replace heavy fuel oil and liquefied natural gas as maritime biofuels, respectively. This thesis delivers detailed inventories for the biofuels as well as the fossil fuels displaced. The two cases were chosen as end-of-intervals of the 5 pathways addressed to represent the trade-off between SOC enhancement vs overall environmental impacts of the full supply chain.

References

1. IRENA. Global Renewables Outlook. Energy Transformation 2050. Abu Dhabi: International Renewable Energy Agency; 2020.
2. Bugge M, Hansen T, Klitkou A. What Is the Bioeconomy? A Review of the Literature. Sustainability. 2016 Jul 19;8(7):691.
3. Swain MR, Singh A, Sharma AK, Tuli DK. Chapter 11 - Bioethanol Production From Rice- and Wheat Straw: An Overview. In: Bioethanol Production from Food Crops Sustainable Sources, Interventions, and Challenges. Academic Press; 2019. p. 19.
4. Hamelin L. A spatial approach to bioeconomy_ Quantifying the residual biomass potential in the EU-27. Renewable and Sustainable Energy Reviews. 2019;16.
5. Karan SK, Hamelin L. Crop residues may be a key feedstock to bioeconomy but how reliable are current estimation methods? Resources, Conservation and Recycling. 2021 Jan;164:105211.
6. Blanco-Canqui H. Crop Residue Removal for Bioenergy Reduces Soil Carbon Pools: How Can We Offset Carbon Losses? Bioenerg Res. 2013;14.
7. Carvalho JLN, Hudiburg TW, Franco HCJ, DeLucia EH. Contribution of above- and belowground bioenergy crop residues to soil carbon. GCB Bioenergy. 2017 Aug;9(8):1333–43.
8. Scarlat N, Martinov M, Dallemand JF. Assessment of the availability of agricultural crop residues in the European Union: Potential and limitations for bioenergy use. Waste Management. 2010 Oct 1;30(10):1889–97.
9. Monforti F, Lugato E, Motola V, Bodis K, Scarlat N, Dallemand JF. Optimal energy use of agricultural crop residues preserving soil organic carbon stocks in Europe. Renewable and Sustainable Energy Reviews. 2015 Apr 1;44:519–29.
10. Fischer G, Prieler S, van Velthuizen H, Berndes G, Faaij A, Londo M, et al. Biofuel production potentials in Europe: Sustainable use of cultivated land and pastures, Part II: Land use scenarios. Biomass and Bioenergy. 2010 Feb;34(2):173–87.
11. Haase M, Rösch C, Ketzer D. GIS-based assessment of sustainable crop residue potentials in European regions. Biomass and Bioenergy. 2016 Mar;86:156–71.
12. Panoutsou C, Kyriakos M. Sustainable biomass availability in the EU, to 2050. [Internet]. Concawe; 2021 Aug. Available from: https://www.concawe.eu/wp-content/uploads/Sustainable- Biomass-Availability-in-the-EU-Part-I-and-II-final-version.pdf
13. France Agrimer. L´Observatoire National des Ressources en Biomasse. Évaluation des ressources agricoles et agroalimentaires disponibles en France – édition 2020. Agrimer; 2020.
14. Hansen JH, Hamelin L, Taghizadeh-Toosi A, Olesen JE, Wenzel H. Agricultural residues bioenergy potential that sustain soil carbon depends on energy conversion pathways. 2020;12.
15. Paustian K, Collier S, Baldock J, Burgess R, Creque J, DeLonge M, et al. Quantifying carbon for agricultural soil management: from the current status toward a global soil information system. Carbon Management. 2019 Nov 2;10(6):567–87.
16. Batjes N h. Total carbon and nitrogen in the soils of the world. European Journal of Soil Science. 1996;47(2):151–63.
17. Wiesmeier M, Urbanski L, Hobley E, Lang B, von Lützow M, Marin-Spiotta E, et al. Soil organic carbon storage as a key function of soils - A review of drivers and indicators at various scales. Geoderma. 2019 Jan;333:149–62.
18. Meyer RS. Potential impacts of climate change on soil organic carbon and productivity in pastures of south eastern Australia. Agricultural Systems. 2018;13.
19. Bellocchi G, Rivington M, Matthews K, Acutis M. Deliberative processes for comprehensive evaluation of agroecological models. A review. Agron Sustain Dev. 2015 Apr;35(2):589–605.

20. Brilli L, Bechini L, Bindi M, Carozzi M, Cavalli D, Conant R, et al. Review and analysis of strengths and weaknesses of agro-ecosystem models for simulating C and N fluxes. Science of The Total Environment. 2017 Nov;598:445–70.
21. Manzoni S, Porporato A. Soil carbon and nitrogen mineralization: Theory and models across scales. Soil Biology and Biochemistry. 2009 Jul 1;41(7):1355–79.
22. Campbell EE. Current developments in soil organic matter modeling and the expansion of model applications: a review. Environ Res Lett. 2015;37.
23. Le Noë J, Manzoni S, Abramoff R, Bölscher T, Bruni E, Cardinael R, et al. Soil organic carbon models need independent time-series validation for reliable prediction. Commun Earth Environ. 2023 May 8;4(1):1–8.
24. Schoenmakere M, Hoogeveen Y, Gillabel J, Manshoven S. The circular economy and the bioeconomy: Partners in sustainability. [Internet]. LU: European Environment Agency.; 2018 [cited 2021 Apr 15]. Available from: https://data.europa.eu/doi/10.2800/02937
25. Gurría P, Ronzon T, Tamosiunas S, López R, García Condado S, Guillén J, et al. Biomass flows in the European Union: the Sankey biomass diagram – towards a cross set integration of biomass. [Internet]. LU: European Commission. Joint Research Centre.; 2017 [cited 2022 Feb 7]. Report No.: EUR 28565 EN. Available from: https://data.europa.eu/doi/10.2760/352412
26. M'barek R, Philippidis G, Ronzon T, European Commission, Joint Research Centre. Alternate global transition pathways to 2050: prospects for the bioeconomy. [Internet]. 2019 [cited 2021 Apr 15]. Available from: https://op.europa.eu/publication/manifestation_identifier/PUB_KJNA29862ENN
27. European Commission, Directorate-General for Research and Innovation. A sustainable bioeconomy for Europe : strengthening the connection between economy, society and the environment : updated bioeconomy strategy [Internet]. European Commission, Directorate-General for Research and Innovation; 2018. Available from: https://data.europa.eu/doi/10.2777/478385
28. Gomez San Juan M, Bogdanski A, Dubois O. Towards sustainable bioeconomy - Lessons learned from case studies. Rome: FAO; 2019 p. 132.
29. Cotrufo MF, Ranalli MG, Haddix ML, Six J, Lugato E. Soil carbon storage informed by particulate and mineral-associated organic matter. Nat Geosci. 2019 Dec;12(12):989–94.
30. Lehmann J, Hansel CM, Kaiser C, Kleber M, Maher K, Manzoni S, et al. Persistence of soil organic carbon caused by functional complexity. Nat Geosci. 2020 Aug;13(8):529–34.
31. Zimmerman AR. Abiotic and Microbial Oxidation of Laboratory-Produced Black Carbon (Biochar). Environ Sci Technol. 2010 Feb 15;44(4):1295–301.
32. Wang J, Xiong Z, Kuzyakov Y. Biochar stability in soil: meta-analysis of decomposition and priming effects. GCB Bioenergy. 2016 May;8(3):512–23.
33. Bernard L, Basile-Doelsch I, Derrien D, Fanin N, Fontaine S, Guenet B, et al. Advancing the mechanistic understanding of the priming effect on soil organic matter mineralisation. Functional Ecology. 2022;36(6):1355–77.
34. Chagas JKM, Figueiredo CC de, Ramos MLG. Biochar increases soil carbon pools: Evidence from a global meta-analysis. Journal of Environmental Management. 2022 Mar 1;305:114403.
35. Hsieh C wen C, Felby C. Biofuels for the marine shipping sector> An overview and analysis of sector infrastructure, fuel technologies and regulations. IEA Bioenergy; 2017. (Task 39).
36. Index of MEPC Resolutions and Guidelines related to MARPOL Annex VI [Internet]. [cited 2023 May 10]. Available from: https://www.imo.org/en/OurWork/Environment/Pages/Index-of-MEPC-Resolutions-and-Guidelines-related-to-MARPOL-Annex-VI.aspx

37. MARPOL. RESOLUTION MEPC.203(62): AMENDMENTS TO THE ANNEX OF THE PROTOCOL OF 1997 TO AMEND THE INTERNATIONAL CONVENTION FOR THE PREVENTION OF POLLUTION FROM SHIPS, 1973, AS MODIFIED BY THE PROTOCOL OF 1978 RELATING THERETO (Inclusion of regulations on energy efficiency for ships in MARPOL Annex VI). MEPC 62/24/Add.1 2011.
38. MARPOL. RESOLUTION MEPC.304(72) INITIAL IMO STRATEGY ON REDUCTION OF GHG EMISSIONS FROM SHIPS. MEPC 72/17/Add.1 2018.
39. MARPOL. MEPC RESOLUTION.366(79) INVITATION TO MEMBER STATES TO ENCOURAGE VOLUNTARY COOPERATION BETWEEN THE PORT AND SHIPPING SECTORS TO CONTRIBUTE TO REDUCING GHG EMISSIONS FROM SHIPS. MEPC 79/15/Add.1 2022.
40. Simonsen TI, Weiss ND, van Dyk S, van Thuijl E, Thomsen ST, Thomsen EST. Progress towards biofuels for marine shipping. IEA Bioenergy; 2021. (Task 39).
41. IMO. IMO's work to cut GHG emissions from ships [Internet]. 2023 [cited 2023 May 10]. Available from: https://www.imo.org/en/MediaCentre/HotTopics/Pages/Cutting-GHG-emissions.aspx
42. United Nations. Review of Maritime transport 2022: Navigating stormy waters. Geneva: United Nations; 2022. 174 p. (Review of maritime transport / United Nations Conference on Trade and Development, Geneva).
43. UNCTAD. A trade hope: the role of the black sea grain initiative in bringing Ukrainian grain to the world. UNCTAD; 2022.
44. SSI. Defining sustainability criteria for marine fuels: Fifteen issues, principles and criteria for zero and low carbon fuels for shipping [Internet]. The sustainable Shipping Initiative and Copenhagen Business School Maritime; 2021. Available from: https://www.sustainableshipping.org/wp-content/uploads/2021/09/Defining-sustainability-criteria-for-marine-fuels.pdf
45. Jahirul M, Rasul M, Chowdhury A, Ashwath N. Biofuels Production through Biomass Pyrolysis —A Technological Review. Energies. 2012 Nov 23;5(12):4952–5001.
46. Ardolino F, Cardamone GF, Parrillo F, Arena U. Biogas-to-biomethane upgrading: A comparative review and assessment in a life cycle perspective. Renewable and Sustainable Energy Reviews. 2021 Apr;139:110588.
47. Sevigné-Itoiz E, Mwabonje O, Panoutsou C, Woods J. Life cycle assessment (LCA): informing the development of a sustainable circular bioeconomy? Phil Trans R Soc A. 2021 Sep 20;379(2206):20200352.
48. Paustian K, Larson E, Kent J, Marx E, Swan A. Soil C Sequestration as a Biological Negative Emission Strategy. Front Clim. 2019 Oct 16;1:8.
49. Andrade C, Albers A, Zamora-Ledezma E, Hamelin L. Database to determine the Carbon recalcitrance and carbon conversion rate to bioeconomy coproducts [Internet]. Dataverse. TBI - Toulouse Biotechnology Institute - T21018; 2022. Available from: https://dataverse.callisto.calmip.univ-toulouse.fr/dataset.xhtml?persistentId=doi:10.48531/JBRU.CALMIP/WYWKIQ
50. Launay C, Constantin J, Chlebowski F, Houot S, Graux A, Klumpp K, et al. Estimating the carbon storage potential and greenhouse gas emissions of French arable cropland using high-resolution modeling. Glob Change Biol. 2021 Apr;27(8):1645–61.
51. Chen D, Rojas M, Samset BH, Cobb K, Diongue-Niang A, Edwards P, et al. Framing, Context, and Methods. In: Climate Change 2021: The Physical Science Basis Contribution of Working Group I to the Sixth Assessment Report of the Intergovernmental Panel on Climate Change. in Press. IPCC; 2021.
52. DRIAS, Météo-France, CERFACS, IPSL. CNRM-CERFACS-CM5/CNRM-ALADIN63-RCP4.5 [Internet]. DRIAS les futurs du climat. 2013 [cited 2020 Sep 1]. Available from: http://www.drias-climat.fr/commande

53. Clivot H, Mouny JC, Duparque A, Dinh JL, Denoroy P, Houot S, et al. Modeling soil organic carbon evolution in long-term arable experiments with AMG model. Environmental Modelling & Software. 2019 Aug 1;118:99–113.
54. Saffih-Hdadi K, Mary B. Modeling consequences of straw residues export on soil organic carbon. Soil Biology and Biochemistry. 2008 Mar;40(3):594–607.
55. Farina R, Sándor R, Abdalla M, Álvaro-Fuentes J, Bechini L, Bolinder MA, et al. Ensemble modelling, uncertainty and robust predictions of organic carbon in long-term bare-fallow soils. 2020;25.
56. Jiménez W, Sánchez D, Ruiz V, Manzano D, Armas D, Jiménez L, et al. Ecuador: SOil Organic Carbon Sequestration Potential National Map. National Report. Version 1.0. Global Soil Partnership. Ministry of Agriculture and Livestock of Ecuador.; 2021. Report No.: 1.0.
57. Peralta G, Di Paolo L, Luotto I, Omuto C, Mainka M, Viatkin K, et al. Global soil organic carbon sequestration potential map (GSOCseq v1.1) – Technical manual [Internet]. Rome: FAO; 2022. Available from: https://doi.org/10.4060/cb2642en
58. INEC. Encuesta de Superficie y Producción Agropecuaria Continua [Internet]. Ecuador: INEC, SENPLADES; 2021. Available from: https://anda.inec.gob.ec/anda/index.php/catalog/912#page=accesspolicy&tab=study-desc
59. Coleman K, Jenkinson DS. RothC-26.3 - A Model for the turnover of carbon in soil. In: Powlson DS, Smith P, Smith JU, editors. Evaluation of Soil Organic Matter Models [Internet]. Berlin, Heidelberg: Springer Berlin Heidelberg; 1996 [cited 2021 Apr 15]. p. 237–46. Available from: http://link.springer.com/10.1007/978-3-642-61094-3_17
60. Pulcher R, Balugani E, Ventura M, Greggio N, Marazza D. Inclusion of biochar in a C dynamics model based on observations from an 8-year field experiment. SOIL. 2022 Mar 17;8(1):199–211.
61. Armenta Porras GE, Villa Cedeño JL, Jácome P. Proyecciones Climáticas de Precipitación y Temperatura para Ecuadorm bajo distintos escenarios de cambio climático. Ecuador: Subsecretaría de Cambio Climático del Ecuador; 2016.

2. CHAPTER 2: LITERATURE REVIEW

The interplay between bioeconomy and long-term soil organic carbon stock maintenance: A systematic review

2. CHAPTER 2: LITERATURE REVIEW

2.1 Context

This chapter targets the following research questions and objectives:

1. **RQ 1:** What are the key factors determining the interrelation between the supply of crop residues to the bioeconomy and the maintenance of SOC stocks in croplands?
2. **RT 1:** Investigate and quantify the carbon flows from crop residues in the five bioeconomy technologies under study, as well as the recalcitrance of the coproducts delivered in each pathway, and the ability of soil models to incorporate these characteristics.

The conversion rates of crop residues to bioeconomy coproducts, as well as the inherent recalcitrance of these coproducts, were exhaustively reviewed for five bioeconomy technologies (coproducts in brackets): i) pyrolysis (biochar hereon pyrochar), ii) gasification (char hereon gaschar), iii) hydrothermal liquefaction (hydrochar), iv) anaerobic digestion (digestate), and v) lignocellulosic alcohol production (solid cake and liquid molasses). A harmonized database of over 600 data records and 20 types of crop residues was compiled to report average C conversion (C_C) and recalcitrance ($\overline{C_R}$) coefficients for the coproducts under study.

Key findings

- Pyrochar and gaschar are the most recalcitrant coproducts, with a $\overline{C_R}$ of 95%, and mean residence times (MRT) in soil over 100 years.
- Hydrochar has a lower content of aromatic functional groups than pyrochar and gaschar, and is thus less recalcitrant, with a $\overline{C_R}$ of 89%, and MRT on the decadal range.
- Digestate and bioethanol molasses are less recalcitrant than chars with $\overline{C_R}$ of 70% and 47%, respectively, and MRTs of approximately 1 year each.
- The $\overline{C_C}$ coefficient of gaschar and bioethanol molasses is 20%, 30 -36 % for hydrochar and digestate, and 45 – 50% for pyrochar.
- $\overline{C_C}$ and $\overline{C_R}$ can be adapted to soil models to simulate the SOC dynamics from bioeconomy coproducts soil application.

The content of this chapter is under review in Renewable and Sustainable Energy Reviews and has been made public as a preprint in Research Square at https://doi.org/10.21203/rs.3.rs-

List of figures

List of tables

The interplay between bioeconomy and long-term soil organic carbon stock maintenance: A systematic review

Christhel Andrade Díaz[a,b†], Ariane Albers[a], Ezequiel Zamora-Ledezma[c], Lorie Hamelin[a]

[a] Toulouse Biotechnology Institute (TBI), INSA, INRAE UMR792, and CNRS UMR5504, Federal University of Toulouse, 135 Avenue de Rangueil, F-31077, Toulouse, France

[b] Department of Chemical, Biotechnological and Food Processes, Faculty of Mathematical, Physics and Chemistry Sciences. Universidad Técnica de Manabí (UTM), 130150, Portoviejo, Ecuador.

[c] Faculty of Agriculture Engineering. Universidad Técnica de Manabí (UTM), 13132, Lodana, Ecuador.

Abstract

Crop residues' potential for the bioeconomy is often limited well below its full extent to prevent eventual soil organic carbon (SOC) depletion. However, when processed in the bioeconomy, biomass carbon can often be partially recovered in a stabilized degradation-resistant coproduct. This study reviews and interlinks the fundaments between these coproducts' process-dependent characteristics and behavior in soils and the use of soil models to predict the effect of replacing fresh crop residues with bioeconomy coproducts. Stemming from a revision of over 600 datasets, we synthesized and proposed average conversion coefficients from biomass C to coproduct ($\overline{C_C}$) and their inherent recalcitrance in soils ($\overline{C_R}$) for pyrolysis ($\overline{C_C}$: 48%, $\overline{C_R}$: 95%) and gasification ($\overline{C_C}$: 20%, $\overline{C_R}$: 95%) biochar, hydrochar ($\overline{C_C}$: 31%, $\overline{C_R}$: 83%), digestate ($\overline{C_C}$: 36%, $\overline{C_R}$: 68%) and lignocellulosic bioethanol solid ($\overline{C_C}$: 44%, $\overline{C_R}$: 42%) and liquid ($\overline{C_C}$: 21%, $\overline{C_R}$: 46%) coproducts. Different modeling approaches to incorporating stabilized organic matter into soils were investigated, as well as the input data requirements of a variety of soil models. This review study thus represents a steppingstone towards i) setting the fundaments for adapting soil models to the dynamics between crop residue harvest and return of C under multiple forms and ii) exploring future scenarios involving coproduct return as a strategy to increase the supply of renewable C for the bioeconomy while ensuring the maintenance of SOC stocks.

†Corresponding author. E-mail address: andraded@insa-toulouse.fr

Highlights

- The conversion of crop residues and eventual return to soils as coproducts is studied.
- Five bioeconomy coproducts are targeted: pyrochar, gaschar, hydrochar, digestate, and bioethanol effluent.
- Carbon conversion coefficients from crop residues to bioeconomy coproducts are compiled.
- Recalcitrance coefficients of coproducts are compiled.
- Soil models allowing to include bioeconomy coproducts return to soils are reviewed.

Keywords: biochar, coproducts, crop residues, digestate, hydrochar, lignocellulosic bioethanol, recalcitrance, soil models, SOC

Word count: Word count**:** 10,000 words

Graphical Abstract

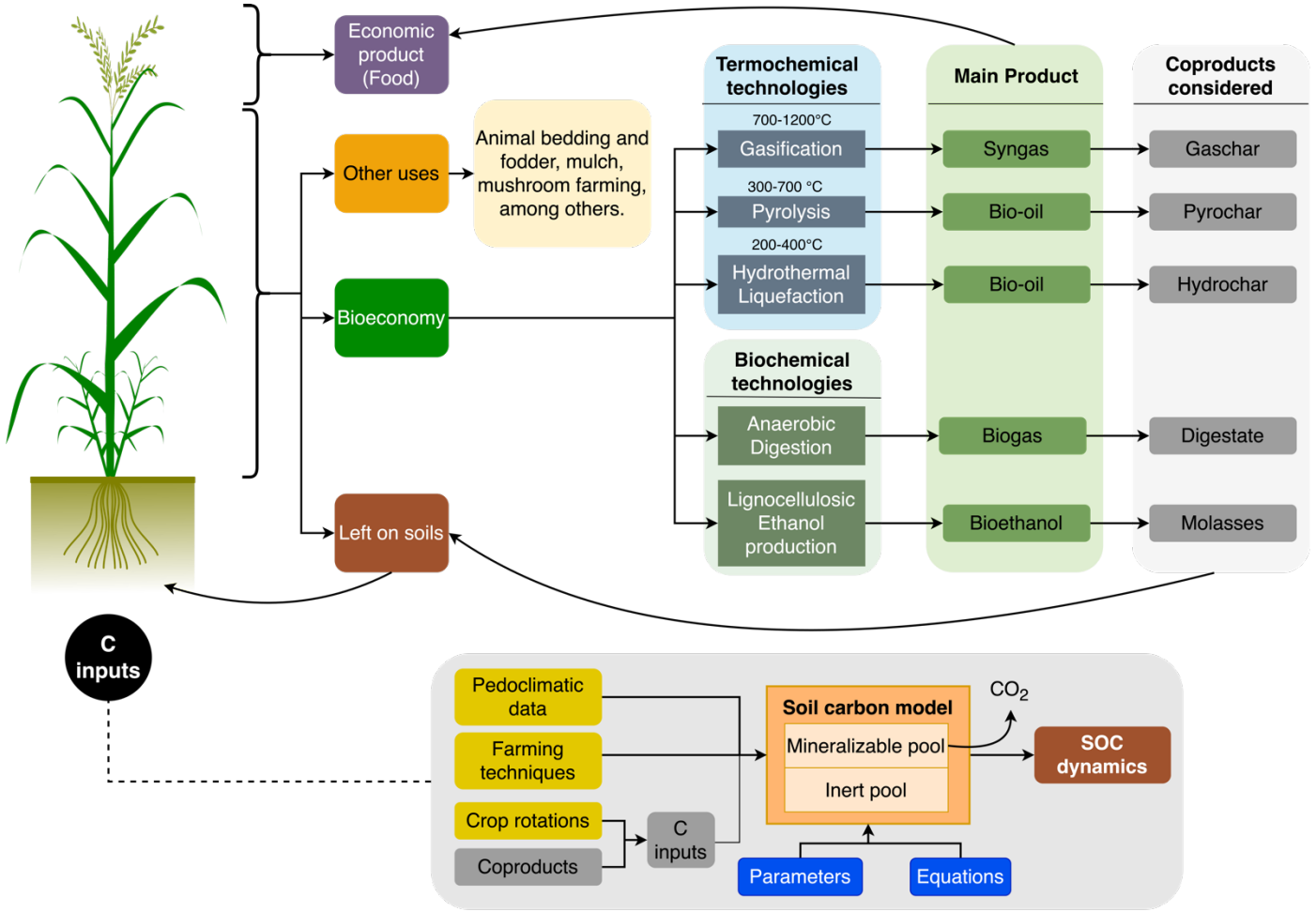

Fig 0. Graphical abstract of chapter 2

List of abbreviations

2GEtOH	Second-generation lignocellulosic bioethanol
AD	Anaerobic digestion
APSIM	Agricultural production systems simulator soil model
BC	Biochar
BC_{+100}	Stability of biochar over 100 years
$BC_{t1/2}$	Biochar half-life
BIOM	Metabolic pool
BmC	Carbon in biomass
BMP	Biomethane potential
BpC	Carbon in coproduct
BpY	Coproduct yield
C_A:	Active pool
CANDY	Carbon and nitrogen dynamics soil model
C_{BG}	C in biogas
C_C	Carbon conversion
C_{DG}	C inputs from digestate
C_{down}	Carbon transported from topsoil to subsoil
CDS	Condensed distillers solubles
CEC	Cation exchange capacity
C_{FOM}	C in the FOM pool
C_L	Carbon labile
C_m	Carbon mineralized
C_R	Carbon recalcitrance
C_{remain}	Carbon remaining
C_{remain}	Carbon remaining in soil at a given time
C_{rep}	C_{FOM} that enters the SOM pool in the CANDY soil model
$C_{retained}$	Carbon retained in soil after application
C_{runoff}	Carbon loss by runoff effects
CS	Stable pool
Db	Bulk density
DDGS	Distillers' dried grains with solubles
DEOM	Decomposable exogenous organic matter
DM	Dry matter
DNDC	Denitrification Decomposition soil model
DOC	Dissolved organic carbon
DPM	Decomposable plant material
EOM	Exogenous organic matter
EPIC	Environmental Policy Integrated Climate soil model
FBC	Fresh biochar
FOM	Fresh organic matter
f_r	C fraction prone to leaching and erosion
GHG	Greenhouse gas
Gt	Gigatons
HEOM	Humified exogenous organic matter
HTC	Hydrothermal carbonization
HTG	Hydrothermal gasification
HTL	Hydrothermal liquefaction
HUM	Humified matter
IPCC	Intergovernmental Pannel on Climate Change
IROC	Indicator of residual organic carbon
k	Decay rate
kL	Decay rate of the labile fraction
kR	Decay rate of the recalcitrant fraction
k_r	Erosion rate
k_{RBC}	Decay rate of RBC
LpH:	lower oxisol soil pH
Mg	Mega grams
MJ	Mega Joules
MPa	Mega Pascals
MRT	Mean residence time
MSW:	Municipal solid wastes
Nm^3	Normal cubic meter
PCM:	Pelletized cattle manure
PE	Priming effects
Pg	Petagrams
RBC	Recalcitrant biochar
REOM	Resistant exogenous organic matter
RMSE	Root mean square error
RothC	Rothamsted carbon model
RPM	Resistant plant material
SHF	Separate hydrolysis and fermentation
SOC	Soil organic carbon
SOM	Soil organic matter
SS:	Sewage sludge
SSF	Simultaneous saccharification and fermentation
STICS	Simulateur multidiscplinaire pour les cultures standard soil model
UpH:	upper oxisol soil pH
WDG	Wet distillers' grain
WOS	Web of science
YBC	Biochar yield
η	Substrate use efficiency coefficient in CANDY

1. Introduction

Facing an urgent need to reduce fossil carbon, as called for in the Paris Agreement [1] and as demonstrated by the IPCC [2], various national [3] and supranational [4,5] bodies promote bioeconomy as a strategy toward reaching climate neutrality by 2050 [6]. The vision is to use innovative technologies for processing and upgrading biological resources, to produce the carbon (C)-based products and services demanded by society without fossil carbon [7].

A key resource that has been identified for the bioeconomy is **crop residues** (e.g., cereal and oilseed straw, sugarbeet tops, maize stover), due to their relative abundance in high agricultural density regions [8,9], their versatility for several bioeconomy uses, no competition with food security [10], and the relative ease of their long-term storage.

However, their removal could affect ecosystem services (e.g., greenhouse gas mitigation, climate regulation, biodiversity, water infiltration, etc.) [11] and trigger loss in soil functions, which could indirectly impact food security by affecting biomass production (e.g., food, fibers, wood provision) and carbon sequestration; the latter being a key ecosystem service regulating the terrestrial carbon and nutrient cycle [12].

Soil organic carbon (SOC) is the third-largest pool in the global C cycle, with approximately 700 Pg at the top 30 cm, 1500 Pg at the top 1-m depth, and 2400 Pg at the top 2-m soil [15,16]. The SOC stocks represent about twice the C stocks in the atmosphere (860 Pg) and three times the C stocks in vegetation (450-650 Pg) [17,18]. Climate and soil conditions, as well as anthropogenic disturbances such as land use management and change, affect SOC stock dynamics [19]. About 116 Pg C for the top 2-m of soil was lost through cultivation since the onset of agriculture [20], which corresponds to a SOC stock loss of between 20% and 40% compared to uncultivated soils [21].

Since incorporating crop residues into soils (i.e., residues left on soils) contributes to maintaining or enhancing SOC stocks [26], various studies have proposed limiting crop residue removal between 15% and 60% of the residual biomass generated, depending on the biomass type, to ensure the maintenance of SOC stocks [27–31]. These removal rates have been proposed without considering any returns of C to the soil after the biomass is used in the bioeconomy, i.e., by recycling back the C from crop residues *via* eventual coproducts (e.g., biochar). Bioeconomy coproducts are rich in stabilized C, also referred to as recalcitrant C, and when returned to soils, maintain long-term SOC stock levels [32,33]. Their return to soil could thus allow greater amounts of biomass to be exported to the bioeconomy compared to a strategy limiting crop residue removal. The vision of this alternative

coproduct return strategy relies on the hypothesis that the amount of biomass available to supply renewable C to the bioeconomy is instead dependent on how biomass is converted and used [34–36].

Previous studies have reviewed the generalities of diverse bioeconomy pathways and described the production and composition of the resulting coproducts [37–44] and their effects on soil quality [38,45–50]. However, few studies have systematically reviewed the recalcitrant composition of bioeconomy coproducts (e.g., biochar, digestate, molasses) and how it affects SOC turnover (i.e., fraction mineralized and turnover rate). For instance, biochar stability in soils has been previously reviewed by some authors [33,51–56], including diverse process conditions, feedstocks, and other study limitations (e.g., Wang et al.[51] included only studies with stable isotopic techniques). Still, gaps in knowledge remain regarding biochar recalcitrance, specifically for crop residue feedstock, while similar studies do not exist for other coproducts. To our knowledge, there is currently no study that encompasses a systematic review of the recalcitrance of several bioeconomy coproducts (i.e., pyrolysis and gasification biochar, hydrochar, anaerobic digestate, and lignocellulosic ethanol coproducts) and their effect on SOC stock.

This study aims at providing, under a single study, the insights needed to i) further understand the interrelation between the potential use of crop residues for the bioeconomy and SOC stock preservation in a context where bioeconomy coproducts are returned to soils and ii) synthesize and propose pathway-dependent C balances and recalcitrance parameters that allow modeling the cycling of C from the feedstock throughout its bioeconomy conversion and final return to soils. The purpose is to provide a first study synthesizing the theoretical fundaments required for bioeconomy-adapted soil modeling frameworks.

This study thus reviews, in section 1, the key bioeconomy pathways associated with the conversion of crop residues and the C recalcitrance of associated coproducts, highlighting the implications for SOC simulation models. Section 2 describes the scope and methodology of the review and explains the variables influencing the SOC dynamics induced by bioeconomy coproduct application to soils. Section 3 presents an overview of the bioeconomy pathways considered and the variety of applicable operating conditions. It also presents and critically discusses the results of a literature compilation of over 600 records for (i) the carbon partitioning between the intended products and generated coproducts and (ii) the recalcitrance of the C in the coproducts that can be returned to soils. Finally, Section 4 presents an overview of the models, methods, and data used to simulate long-term changes in SOC stocks, including adaptations made to integrate bioeconomy coproducts as soil amendments.

2. Scope and methodology

2.1 Bioeconomy technologies considered and terminology

All the coproducts considered within this review result from processes aiming to convert the easily biodegradable C in the biomass into bioeconomy products and services. It addresses the technical aspects, operating conditions, and coproducts C balance and inherent recalcitrance of five bioeconomy technologies, considered the most common and promising processes for using crop residues (e.g., straw) to produce renewable gas and liquid hydrocarbons, considering the possibility of C return to soils through coproducts.

A conceptual review was conducted on the latest literature (**until July 2021**) reporting the technical conditions and process yields of these technologies, herein referred to as conversion pathways, followed by a systematic review of the available data reporting the stability of the coproducts in soils. Overall, 137 scientific papers, industry data, and grey literature were reviewed, producing 620 data records from which average coproduct C balance and recalcitrance values were derived (further detailed in sections 2.2 and 2.3). In some cases, the same dataset can be used for both. Data records also include unpublished data received as a courtesy from the authors. The data collected included only crop residue feedstock to the extent data were available, and in the case of data scarcity, the most representative proxies (wood and grass) were considered. In cases where a particular dataset was presented in more than one publication (due to consecutive publications with extended experiments), the most recent and complete study was prioritized. The searching procedure, including keywords, time range, and selection criteria, is further detailed in SI1.

The bioeconomy conversion pathways considered, with respective intended products and coproducts in brackets were pyrolysis (bio-oil, pyrochar), gasification (syngas, gaschar), hydrothermal liquefaction (HTL) (bio-oil, hydrochar), anaerobic digestion (AD) (biogas, digestate) and second-generation lignocellulosic bioethanol (2GEtOH) (bioethanol, liquid molasses, solid lignocellulosic cake). Molasses coproduct here refers to the residual liquid fraction obtained during bioethanol production, consisting mainly of hydrolyzed C5 and unconverted C6 sugars. Note that the solid pyrolysis coproduct is typically referred to as biochar. However, the term “biochar” has been increasingly expanded to encompass a wide variety of biomass-derived chars produced by either pyrolysis or gasification [33], and to some extent, HTL [39]. Therefore, the terms pyrochar, gaschar, and hydrochar are used herein to specifically refer to char from pyrolysis, gasification, and HTL, respectively. Section 3.1 briefly describes the process conditions of each technology.

We considered only coproducts that can return C to soils, and thus other coproducts stemming from the same reviewed pathways were excluded. For instance, pyrolysis generates a non-compressible gas coproduct that can be used for energy, and the bio-oil can be fractionated into heavy (oil) and light (vinegar) phases, the latter having biofungic properties [57]. Similarly, gasification generates tar, a mixture of organic compounds condensable at room temperature that can affect the gas quality and equipment efficiency [58], and ashes with very low C content that are typically disposed of in landfills [59].

2.2 Carbon flows from crop residue-to-bioeconomy coproduct (C_C)

A mass balance approach was used to account for the C flows from different crop residues throughout the production and conversion pathways to the final coproducts. Data were retrieved from a comprehensive literature review of reported yields and C content per coproduct and technology (see SI1). In total, 171 data records were collected from 73 studies. This includes 44 records for pyrochar, 25 for gaschar, 31 for hydrochar, 68 for digestate, and 3 for 2GEtOH coproducts (Table 1). The C fraction remaining in the coproduct, hereafter carbon conversion (C_C), was determined using **¡Error! No se encuentra el origen de la referencia.** for pyrochar, gaschar, hydrochar, digestate, and 2GEtOH coproducts (molasses and cake).

$$C_C = \frac{CpY * CpC}{BmC} \quad \text{(Eq.1)}$$

where *CpY* is the coproduct yield (kg coproduct kg^{-1} biomass), *CpC* is the C content in the coproduct (kg C kg^{-1} coproduct), and *BmC* is the initial C content in the biomass (kg C kg^{-1} biomass). C_C was determined for each study included in the database, and an average C_C ($\overline{C_C}$) was determined per coproduct type.

The $\overline{C_C}$ for digestate was determined using biomethane potential (BMP) values reported for different feedstock and specific digestion conditions (e.g., temperature) [60], which is further detailed in the supporting database [61]. The $\overline{C_C}$ of each coproduct is discussed in Section 3.2.

2.3 Coproduct recalcitrance (C_R) and mean residence time (MRT) in soils

The C remaining in the coproducts tends to be more resistant to microbial degradation when applied to soils as exogenous organic matter (EOM) than the original raw feedstock (e.g., straw). Here, the C fraction that is degraded over a short period and released as CO_2 (mineralization) was labeled as labile (C_L), while the more stable fraction that remains stored in the soil over the long-term during humus formation (humification) is called recalcitrant (C_R).

Understanding the C_R of coproducts and its effects on soils is a research field under development and relevant to climate [62], environmental, and agricultural sciences [63,64], and also to policymaking and economic development [65,66]. A major knowledge gap arises from the broad range of study conditions, in turn, associated with a large variety of feedstock and methods used to measure and model C_R, resulting in a wide range of estimated stability values [67]. Methods include the analysis of carbon structure, carbon oxidation resistance, thermal degradation, proximate analysis, laboratory incubations, field trial assays, and mathematical modeling [67,68].

Naisse et al.[69] found that the C stability of biochar and hydrochar cannot be reliably characterized by chemical reactivity, while incubation and field trials are considered to usually provide the most realistic results [68]. Although most methods are less reliable than incubations and field trials, they are frequently used as proxies to estimate the C degradation of (co)products due to their simplicity and time of execution [70].

Common drawbacks of laboratory incubations are difficulties in mimicking actual conditions in controlled environments, while for field trials the difficulty lies in proper monitoring of the C behavior in natural environments. Laboratory incubations are typically short-term assays (<1 year) that measure the CO_2 fluxes of the material being studied, alone or in a mixture with soil, under controlled conditions (i.e., an artificial environment). It helps to understand the effect of different parameters (e.g., soil texture, temperature, time, among others) on the degradation process but fails to replicate the interactions that occur in real environments [67,71]. Field trials are typically conducted for longer periods than laboratory incubations (>2-3 years) to measure the degradation of coproducts applied to fields. However, one difficulty is separating CO_2 fluxes from sources other than the coproduct, such as carbon losses from soil erosion, runoff water, and other environmental factors. Additionally, the results tend to be explicit for the study area only, requiring long-term evaluation periods. The lengthiest field trial inventoried for biochar lasted only 8.5 years [72], yet the expected stability is estimated to be over hundreds of years.

Some authors [54,68,73] consider incubation to be inadequate for determining the long-term C stability, especially for chars, and suggest that multi-carbon compartment modeling would allow predicting the long-term recalcitrance (amount of C remaining after a given time), as shown in (Eq.2a), Eq.2b, and (Eq.3) [55,56,73]:

$$C_m(t) = C_L\left(1 - e^{-k_L t}\right) + C_R\left(1 - e^{-k_R t}\right) \qquad \textit{(Eq.2a)}$$

$$C_{remain}(t) = C_L * e^{(-k_L t)} + C_R * e^{(-k_R t)} \qquad \textit{(Eq.2b)}$$

$$MRT = {}^{1}/_{k} \qquad \textit{(Eq.3)}$$

where C_m is the C mineralized at time *t*, C_{remain} is the C remaining at time *t*, C_L and C_R represent the labile and recalcitrant C fractions (%), respectively, k_L and k_R represent the mineralization rates of labile and recalcitrant fractions (d^{-1} or y^{-1}), and MRT (d or y) is the mean residence time of the (labile or recalcitrant fraction of) organic matter, defined as the inverse of the decay (or mineralization) rate *k* (either k_L or k_R) [55]. The MRT reflects the expected average time a C atom spends in a given soil pool [74], per fraction (i.e., from the recalcitrant or labile fraction).

There is a general agreement that incubation studies provide the most accurate value for C_L [73], which is essential for understanding the behavior of the C_R fraction and is thus the most popular method.

From the literature reviewed on coproduct recalcitrance, only studies based on incubation, field trials, and modeling were selected. For a given pathway, no differentiation by duration or type of soil used in the field and laboratory assays were made in the data compilation. The dataset includes 87 studies with 449 data records. This comprises 144 records for pyrochar, 36 for gaschar, 104 for hydrochar, 114 for digestate, and 51 for 2GEtOH coproducts. The amount of input C not mineralized after the assay was recorded as the C_R fraction of the coproduct. The mean C_R ($\overline{C_R}$) of each coproduct was determined after removing outliers and was defined as the average recalcitrance. The MRT values considered in the inventory are those explicitly reported in the original studies or calculated by other authors than the original, when relevant. If not provided, MRT values were not calculated to avoid introducing potential errors due to the high variability of the results related to the type of modeling applied (e.g., first-order, second-order, or n-order decay rate). The coproduct recalcitrance is discussed in section 3.2.

The complete dataset considered for C_C and C_R data is available in [61] and summarized in Table S1 and Table S2.

2.4 Review of SOC models

SOC models are mathematical representations for integrating, examining, and testing the understanding of complex soil dynamics in an endeavor to predict changes in response to environmental and anthropogenic factors across temporal and spatial scales [75,76]. Effects from biotic and abiotic factors such as soil, climate, and management practices are integrated into SOC models to simulate the dynamics of soil carbon, nitrogen, and water, as well as plant production [76,77].

The complexity of these biogeochemical processes varies considerably among models, for instance, regarding the number of inputs and driving variables needed (e.g., soil parameters,

meteorological data, farming practices), as well as the number of parameters required (e.g., soil pool fraction, mineralization rate in a given pool, C flows between the soil pools) to model the studied outputs (e.g., only C dynamics, C-N dynamics, plant growth, etc.). The selection of a model is thus a challenging endeavor, particularly given the high number of existing models in the literature (>250) developed over the last eight decades [79].

Some model evaluation and comparison attempts were performed under the same conditions and model calibrations [78], demonstrating the large variability in the predictions from different models. Models' generalities [75,79], limitations [77], accuracy [18,78], and sensitivity [80] have been previously assessed, yet, a clear ranking or validation of the models for specific sets of conditions (e.g., biome characteristics, crop type, farming practices, among others) has not been possible. Multi-model comparison studies suggested the use of an ensemble of models rather than a single one to obtain more reliable predictions (i.e., 13 models according to Sándor et al.[81] or 2-4 models with site-specific calibration according to Farina et al.[76]).

This review identifies the requirements and capabilities for modeling SOC dynamics from the interaction of crop residues with the bioeconomy. The characteristics of 12 models, as well as data inputs, outputs, and applicability to assess the SOC changes in croplands were reviewed (detailed in SI2): CENTURY [82], Daycent [83], DNDC (DeNitrification DeComposition) [84], EPIC (Environmental Policy Integrated Climate) [85], Daisy [86], APSIM (Agricultural production systems simulator) [87], STICS (Simulateur mulTIdiscplinaire pour les Cultures Standard) [88], CANDY (Carbon and Nitrogen Dynamics) [89], ORCHIDEE [90], RothC (Rothamsted carbon model) [91], AMG [92], and CTOOL [93]. These models were selected because i) they represent the most common modeling structures developed (e.g., multiple soil pools, each pool governed by a specific decay rate based on n-order equations), ii) are widely cited in the literature, and iii) have been used in simulations across different pedoclimatic systems [75,79,94].

Among the revised models, some propose adapted versions that consider bioeconomy coproducts as soil EOMs. These were examined with greater attention in Section 4, in an endeavor to uncover the considerations that allow predicting the coproducts' C behavior in soils, in order to perform similar, yet more systematic, adaptations in future research regarding SOC dynamics and the bioeconomy.

3. Bioeconomy

Although the technologies covered in this study are relatively well explored in earlier studies in terms of their technical and even economic and environmental performance, especially concerning

the main product they generate, less attention has been given to the process-dependent characteristics of their coproducts. Section 3.1 thus briefly describes each technology being studied and their possible variants in terms of operating conditions. Section 3.2 details the results of the literature review in terms of (i) average yield of coproducts & C partitioning between the coproducts intended as soil amendments and the other products, and (ii) coproduct recalcitrance.

3.1 Bioeconomy conversion pathways description

3.1.1 Pyrolysis

Pyrolysis is a thermal process where biomass is decomposed in an oxygen-free environment, in a range of temperatures from 300 to 700°C, to produce bio-oil, gas, and biochar hereon referred to as pyrochar (Fig.1) [38,95]. The biocrude oil is commonly further processed to separate the gas and vinegar fractions to obtain a more refined biocrude [57]. The oxygen-free environment is often ensured with the use of nitrogen (N_2) as a carrier gas. The bio-oil can be directly burned or subjected to further refinement to obtain an upgraded bio-oil suitable for transportation.

Pyrolysis processes can be classified as slow or fast depending on the heating rate. Slow pyrolysis is characterized by slow heating of the feedstock (<10°C s^{-1}) for minutes to days at temperatures above 400°C [35,95,96]. Fast pyrolysis employs higher heating rates for shorter times (>10°C s^{-1}, <2 s) at temperatures around 500°C (450-1000°C) [37,97]. Fast pyrolysis is optimal for bio-oil production, while slow pyrolysis delivers approximately equal ratios of products and favors biochar production [38,98]. The process conditions and product characteristics are further detailed in SI2.

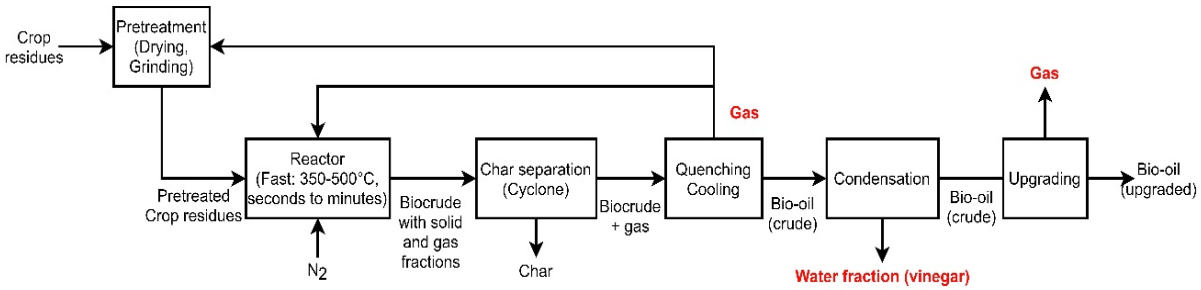

Fig.1. Generic process flow diagram of the pyrolysis process, here with crop residues as an input feedstock. Upgrading may or may not occur depending on the required quality of the final oil use (e.g., required if used as biofuel for transportation). Coproducts in red are outside the scope of this study.

3.1.2 Gasification

Gasification is a thermochemical conversion technology in which biomass is converted to a gaseous mixture of H_2, CO, CH_4, and CO_2, often referred to as syngas [99,100]. Gasification is performed at high temperatures (700-1200 °C) in the presence of a limited amount of oxidizing agent (i.e., air,

steam, oxygen, carbon dioxide, or a combination of these), in insufficient amounts to reach combustion [101,102]. The syngas is further treated to remove solid and aqueous fractions (gaschar and tar), particulates (dust and ashes), and other impurities (sulfur and ammonia), in order to produce clean syngas (Fig.2).

Full-scale gasification facilities commonly operate at atmospheric or higher pressures up to 33 bars and temperatures ranging between 800-1100°C [103,104], albeit agricultural residues are typically treated at 750-850°C [42]. The moisture content of the biomass must be maintained below 35% [105] with recommended levels of around 10-20% to avoid tar formation and failures in the system [103,106]. More details on the gasification products are in SI2.

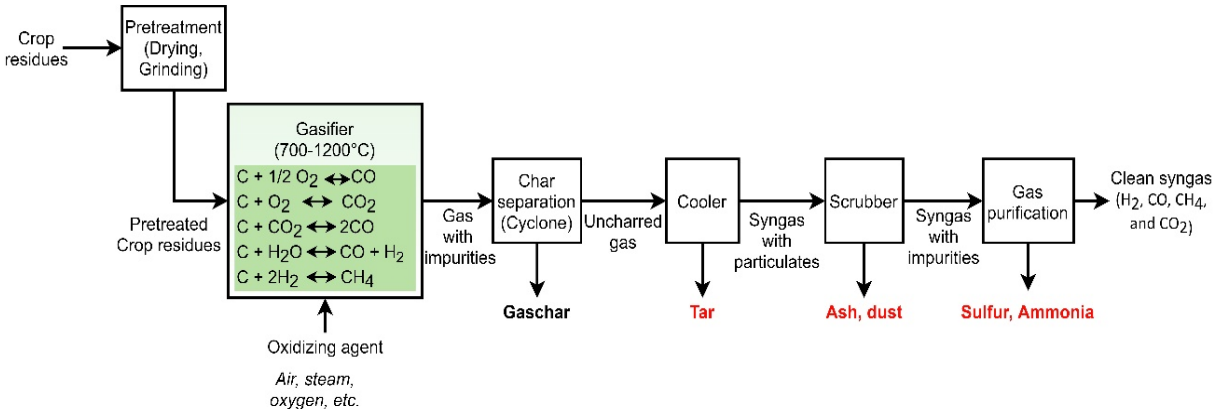

Fig.2. Generic process flow diagram of the gasification process, here with crop residues as an input feedstock. Coproducts in red are outside the scope of this study.

3.1.3 Hydrothermal Liquefaction

Both gasification and pyrolysis require the use of dry biomass (<10% moisture, [107]), which may involve additional upstream processes to prepare the feedstock. Hydrothermal Liquefaction (HTL) is a thermochemical process carried out in a liquid-phase medium and is acknowledged as a promising technology for biofuel production, in particular with wet feedstocks [41,108,109].

HTL allows the use of feedstock with only 5-20% dry matter (DM) [110] and is carried out at low temperatures of around 250-375°C, pressures of 4-25 MPa, and retention times of around 20-30 minutes [43,111]. Due to the moisture content of the feedstock and the liquid media in the reactor, the biocrude has high water content and must undergo an extra step to separate the biocrude oil from the aqueous phase [120] (Fig.3). The HTL bio-oil has lower oxygen and water contents, but higher viscosity than pyrolysis oil [111], and the HTL biochar is commonly referred to as hydrochar. SI2 further explains the various process configurations of HTL and its variants. Details on the expected yields are presented in section 3.2.

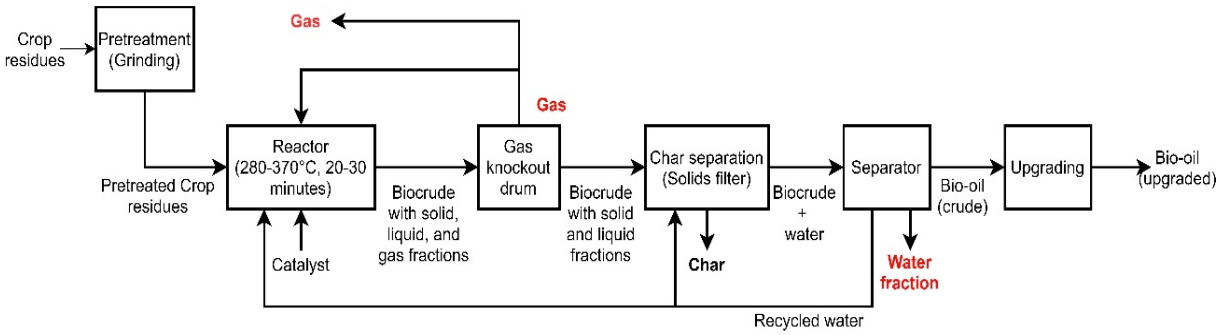

Fig.3. Generic process flow diagram of the hydrothermal liquefaction process, here with crop residues as an input feedstock. Coproducts in red are outside the scope of this study.

3.1.4 Anaerobic digestion

Anaerobic digestion (AD) is a biological process where, in the absence of oxygen, microorganisms decompose organic matter into i) biogas, which can be used to generate renewable energy, and ii) a coproduct known as digestate, typically used as fertilizer [112]. Through AD, carbohydrates, proteins, lipids, and other organic compounds are transformed into biogas, which is composed of methane (CH_4, 50-70%), carbon dioxide (CO_2, 30-50%), and traces of other gases (H_2S, NH_3, 1-5%), essentially depending on the input feedstock [113]. AD is among the most cost-effective and environmentally performant technologies for renewable energy due to its simplicity, low costs, and adaptability to diverse types of waste and biomass [114]. Therefore, the number of AD facilities is rising worldwide, with a subsequent increase in digestate production [113,115].

The process consists of a series of complex microbiological reactions that take place in four consecutive stages, namely hydrolysis, acidogenesis, acetogenesis, and methanogenesis (Fig.4). The reactions, influenced by the feedstock selection and operating parameters, govern the overall yield and characteristics of the biogas and digestate [116]. Additional details on AD are in SI2.

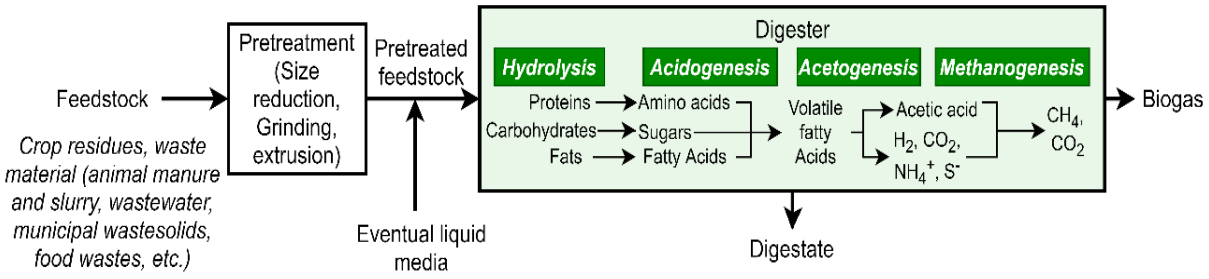

Fig.4. Generic process flow diagram of the anaerobic digestion process, here with the input feedstock including crop residues, waste material, wastewater, animal manure and slurry, and eventual mixture with a liquid media. Digestate contains all the undigested biomass and eventually added liquid media remaining after gas production.

3.1.5 Second-generation ethanol production

Bioethanol is a high-octane number biofuel produced by yeast fermentation of sugars, typically used in terrestrial transportation as a mixture with gasoline [117]. Bioethanol produced from lignocellulosic biomass is known as second-generation biofuel (2GEtOH). For bioethanol production, lignocellulosic biomass must follow a series of steps (Fig.5), involving i) a physical, chemical, or thermal pretreatment to release hemicellulose and cellulose from the matrix, ii) hydrolysis of polymers to simple sugars aided by acids, alkalis, or enzymes, and iii) fermentation of sugars by microorganisms followed by iv) a distillation process to purify the bioethanol [117–119]. During the process, approximately 95% of soluble sugars are transformed into ethanol and CO_2, while 1% become yeast cellular mass, and 4% are remaining coproducts [44].

The hydrolysis and fermentation stages can occur in a separate hydrolysis and fermentation (SHF) system or a simultaneous saccharification and fermentation (SSF) process. The non-fermentable components are removed as a stream called stillage, which can be separated into a solid (cake) and a liquid (molasses) fraction (Fig.5). Insights on the 2GEtOH process and products are in SI2.

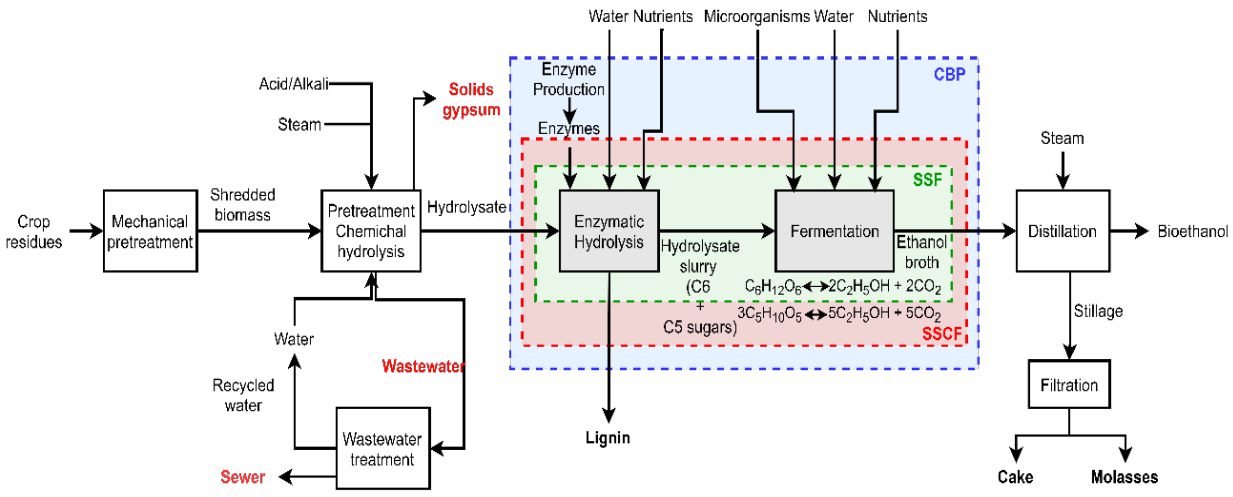

Fig.5. Generic process flow diagram of the lignocellulosic bioethanol production process, here illustrated for the case of enzymatic hydrolysis. Stillage can be used as obtained or separated in the solid and liquid fractions. SSF: Simultaneous saccharification and fermentation. SSCF: Simultaneous saccharification and co-fermentation. CBP: consolidated bioprocessing. WDG: Wet distillers' grains. Coproducts in red are out of the scope of this study.

3.2 Carbon conversion (C_C) and recalcitrance (C_R) results

Since the interest of this review is to analyze the potential of crop residues for the bioeconomy, process conditions favoring the production of the main economic product for each technology (i.e., bio-oil, syngas, biogas, and bioethanol), were selected, to the extent data were available. These are summarized in Table 1, where the coproducts of interest to be used as soil amendments are identified.

On this basis, average yields (CpY) of the defined coproducts, as well as their average C content (CpC), could be compiled and computed (Fig.6), on top of the parameters of interest within this study ($\overline{C_C}$ and $\overline{C_R}$; Fig.*6* and Fig.*7*, respectively).

Table 1. Process conditions, coproducts, and feedstocks included in the average results of Figs. 6-7, per technology.[†]

Process	Process Conditions selected	Coproduct of interest	Feedstocks included[a]	$\overline{MRT}$[g] years
Pyrolysis[b]	T: 350-700°C (<300°C, 300-500°C, >500°C), FS: DM>90%, RT: seconds to 2h	Pyrochar	Crop residues (wheat straw, maize stover, maize silage, rice straw, rice husks, rapeseed straw, rye straw, barley roots, soybean stover, sunflower straw, sugarcane bagasse), temporary grassland (switchgrass, ryegrass), peanut shell, poultry litter, digestate, green waste	632
Gasification[c]	T: 600-1200°C dry gasification, 300-550°C hydrothermal gasification, FS: DM>90%	Gaschar	Crop residues (wheat straw, maize stover, maize silage, rice straw), switchgrass, forestry residues (Vermont wood, pine wood), citrus peel, peanut shell, walnut shells	141
HTL[d]	T : 180-400°C, FS : DM<20%, RT : 30 minutes, Ot: K_2CO_3 catalyst	Hydrochar	Crop residues (wheat straw, maize stalks, maize silage, rice straw, barley straw), forestry residues (wood chips, poplar wood), straw digestate, draff, miscanthus, sugar beet pulp, vinasse, yeast	11
AD[e]	T: Mesophilic conditions (30-50°C). FS: Mixture of manure/slurry with crop residues, RT: 1-3 months.	Digestate	Wheat straw, rice straw, maize straw. Cattle manure, cattle slurry, pig slurry, poultry manure, food waste, paper, green waste, household waste, maize silage.	0.4
2GEtOH production[f]	Ot: Mechanical pretreatment; chemical and enzymatic hydrolysis, fermentation with S. cerevisiae, purification by distillation	Molasses Cake	Wheat straw, maize stover, wheat starch, non-fermentables from wheat bioethanol, DDGS, yeast concentrate, rapeseed meal, vinasse from sugarcane bagasse, vinasse from sugar beet	1

[†] T: temperature; FS: Feedstock; RT: Retention time; Ot: Other conditions; MRT: Mean residence time

[a] Feedstocks in italic are included only in the recalcitrance review to determine C_R

[b] For the C_R review, the minimum, and maximum pyrolysis temperatures were 250 and 800°C, respectively, and the assays were grouped by temperatures in low (< 300°C), medium (300-500°C), and elevated temperatures (>500°C).

[c] The use of wet biomass in gasification processes (hydrothermal gasification) is increasing as an energy strategy, thus these process conditions were included in this study.

[d] Due to the increasing use of catalysts in HTL processes to modify the products' yields and quality, processes with and without catalysts were included.

[e] Only the crop residues C is accounted for in the $\overline{Cc}$.

[f] For the lignocellulosic bioethanol production, the coproducts were grouped as a solid fraction (cake), a liquid fraction (molasses), and rapeseed meal, for the C_R coefficient. Due to the scarcity of data incubation and field trials for non-lignocellulosic bioethanol were included as proxies.

[g] The $\overline{MRT}$ values reported herein are averages from the whole dataset produced for the gasification, HTL, and AD technologies. For pyrolysis and 2GEtOH production, the MRT values shown correspond only to the 300-500°C group and molasses, respectively. The MRT shown for the AD technology stems from different conditions and incubation assays with a broad variety of timeframes (including studies carried out for less than a month), the recalcitrance derived herein is thus to be seen as an indicative figure only.

3.2.1 Carbon conversion results

The observed results are here compared, when possible, with available meta-studies. These were not included among the records considered herein [61], although some of the studies they contain are also considered in this study.

Results indicate, for pyrolysis, average pyrochar yields of 35% (DM) (n= 44), composed of 58% C, which reveals that 48% of the original C is in the pyrochar ($\overline{Cc}$) (Fig.6). This fits values reported in previous reviews (e.g., [33,37,38]), but is slightly above values that can be calculated with recent empirical equations [33], as further detailed in the SI1.

On average, the gaschar yield is 20% DM (Fig.6, n=25), with reported values ranging from 7% to 28%, this is further detailed in the repository data [61]. The gaschar yield is highly influenced by the oxidizing agent used for the gasification process, being double for oxygen (15.5%) compared with the use of steam (7.9%) [110]. Accordingly, the C content in gaschar varies in a wide range (20-90%, average 51%) depending on the process conditions (see [61]). The C content in gaschar compiled in this study fits the one reported in the review of You et al.[120] (20 - 60%), despite the higher-end interval herein. However, You et al.[120] showed that the total carbon content in gaschar can attain fractions well over 60% (weight). On the other hand, the 51% average shown here is slightly above the typical average of 38% reported by [50], likely because of the higher lignin content considered herein for the initial feedstocks.

In highly efficient processes, the fraction of C in wood-agricultural biomass that ends in the tar is less than 1% [148], while 20% ends in the gaschar ($\overline{Cc}$) (Fig.6). During gasification, the oxygen in the reactor oxidizes the C to CO_2, while it remains in the biochar in the pyrolysis reactor. This explains why the gaschar is among the coproducts with the lowest $\overline{Cc}$ value (Fig.6).

HTL can process a broad variety of feedstock with diverse compositions, thus the yield of the products varies in a wide range depending on the biomass (see [61]). Moreover, the use of catalysts may modify the yields and composition of the streams involved. Results indicate, on average, that HTL yields 25% hydrochar (by DM) (n=31) with a C content of 56%, which leads to a $\overline{Cc}$ coefficient of 31% (Fig.6). This is within reported HTL biocrude yields, ranging from 12 to 77% (by DM; for different process configurations) [110,122], with an average C content slightly below the one reported at 73% by Elliot et al.[123].

The amount of biomass converted to biogas depends on the initial feedstock. The studies considered herein reported BMPs varying between 60 and 468 Nm^3 CH_4 $tonne^{-1}$ dry biomass for agricultural residues, with an average BMP of 215 Nm^3 CH_4 $tonne^{-1}$ dry biomass (see [61]). According to these results, digestate represents, on average, 60% (DM) (n=66) of the products and coproducts generated during AD. The average C content of digestate is 49% (n=66) of the DM (Fig.6), which is in the range of 15- 55% reported by Wang and Lee [125]. Digestate $\overline{Cc}$ was estimated based on the volatile solids (VS) reduction reported by different authors (n=16) for straw and other crop residues during the digestion process. Accordingly, approximately 64% of biomass C is digested into biogas, representing a digestate $\overline{C_C}$ of 36% (Fig.6).

Bioethanol production results in 3 main streams in roughly equal proportions, by DM i) bioethanol, ii) non-fermentable constituents, and iii) carbon dioxide [126]. According to [127], the biomass conversion rates to bioethanol vary between 22% and 32%, i.e., 22-32% of the initial feedstock (DM) is converted to bioethanol. The results of Fig.6 indicate an average bioethanol yield of 0.225 kg kg^{-1} biomass DM (n=3), while the CO_2 emissions and coproducts represent a yield of 24% and 53% (split into 32% solid fraction and 21% liquid fraction), respectively, by DM. Given the low conversion rates achieved in the alcoholic fermentation of lignocellulosic biomass, the largest proportion of carbon from the initial feedstock is found in the residues, where it remains unconverted ($\overline{Cc}$ of 44% for the solid cake and 21% for the liquid molasses; Fig.6). These results are in accordance with industrial data (that could not be considered herein due to incomplete datasets), which report a solid fraction (lignin) yield of 32%-39% and 22%-35% molasses, on a dry basis [127].

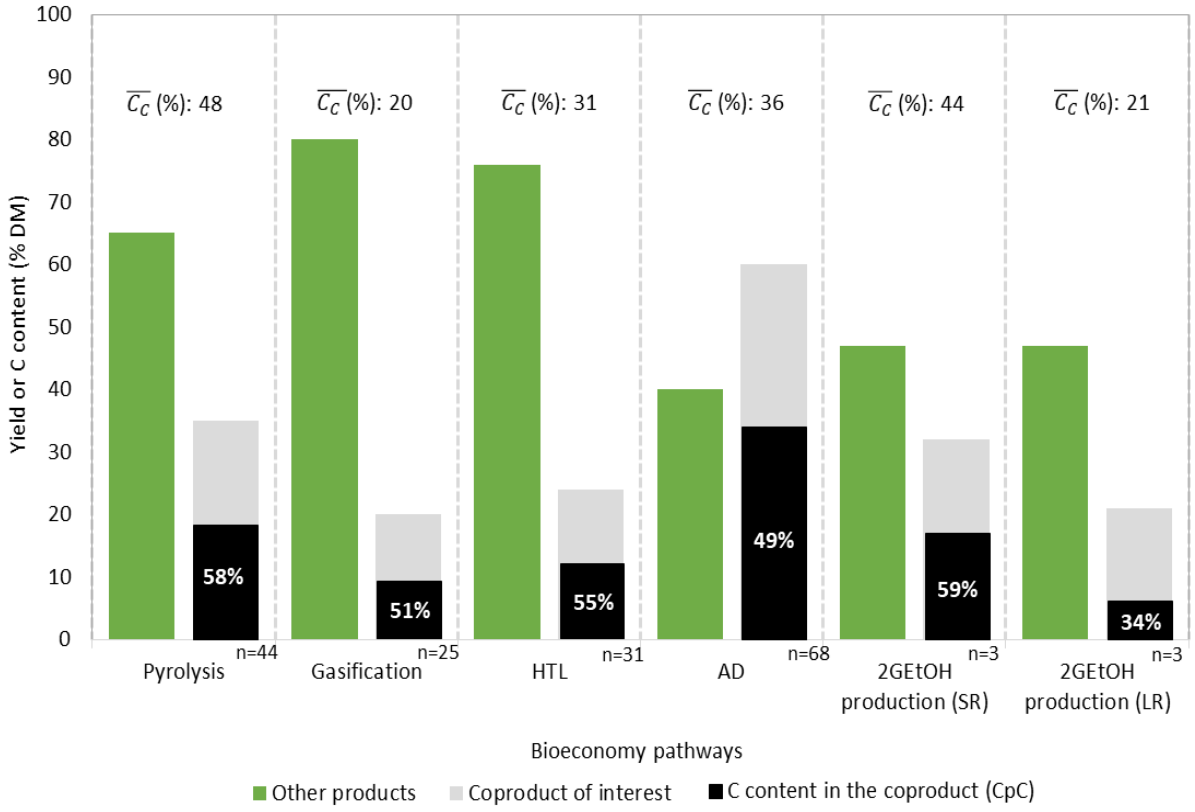

Fig.6. Yields (% of crop residues DM) of coproducts of interest (gray) and all other products (green; including the main product of interest), carbon (C) content of the coproducts of interest (% of the coproduct DM; black), and related percentage of initial C from crop residues transferred into coproducts ($\overline{Cc}$). SR: Solid residue (cake) from the 2GEtOH production; LR: Liquid residue (molasses) from the 2GEtOH production.

3.2.2 Recalcitrance of coproducts results

The degradation-resistant fraction of raw crop residues, commonly attributed to lignin, represents a high share of the C remaining in the bioeconomy coproducts. During thermochemical processes, the chemical structure of the recalcitrant C is changed producing different aromatic groups; whereas in the biochemical processes, only the labile C is removed from the biomass and the recalcitrant fraction remains as in the raw material. Therefore, the degree of recalcitrance of coproducts (C_R) varies between technologies (Fig.7, Table S2). This is reflected in Fig.7 where the C_R data compiled for each coproduct of interest are summarized, grouped by temperature ranges (pyrolysis), input feedstock (gasification, HTL, and AD), and type of coproduct used in the experimental assay (2GEtOH production). Through this section, the results of Fig.7 are analyzed jointly with a separate discussion of the literature review performed for each specific coproduct recalcitrance.

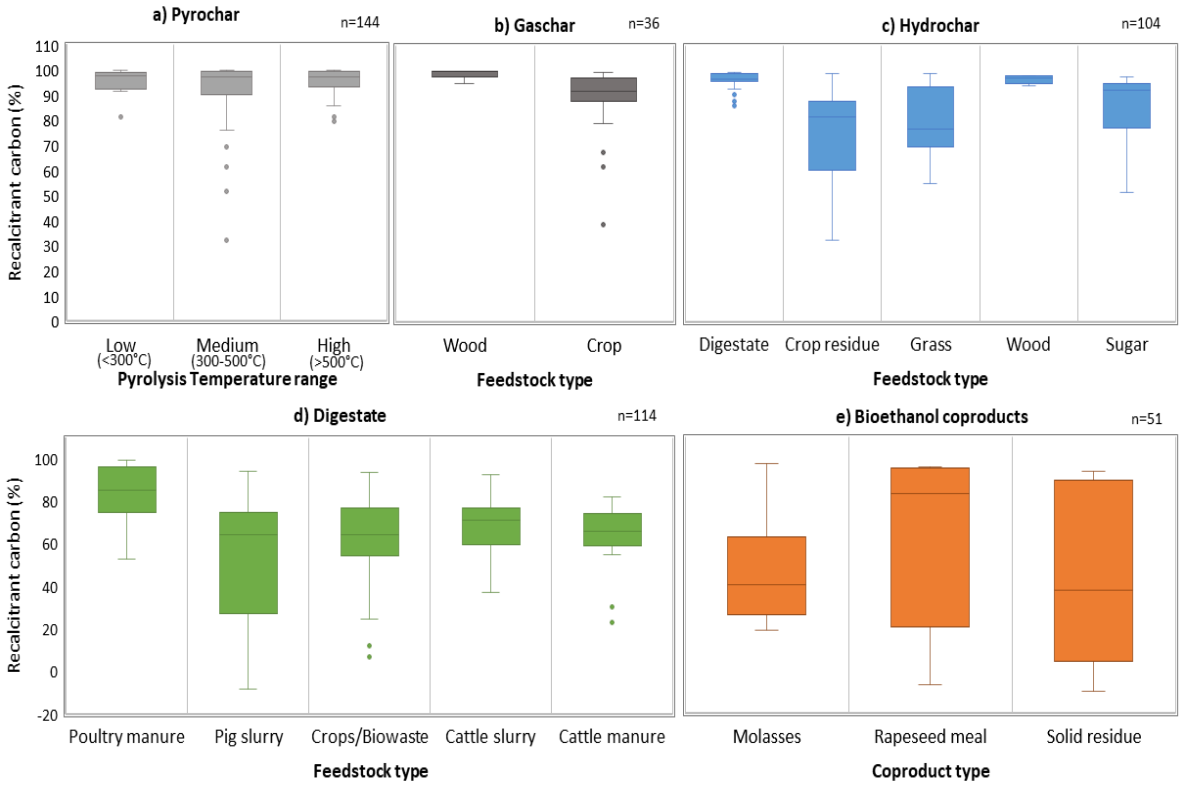

Fig.7. Boxplot of compiled carbon recalcitrance (C_R) data for the targeted bioeconomy technologies coproducts, grouped by temperature ranges (pyrolysis), input feedstock (gasification, HTL, and AD), and type of coproduct used in the experimental assay (2GEtOH production). n represents the number of records considered to build the boxplot. The C_R values computed herein represent the amount of C reported to be remaining in the coproduct after the incubation/field trial/modeling assay timeframe. Datapoints displayed correspond to outliers per technology.

3.2.2.1 Pyrochar and gaschar

From here onwards, the term biochar is used as an umbrella term to refer to the char product of both pyrolysis and gasification (jointly or indistinctively), else the terms pyrochar (pyrolysis char) and gaschar (gasification char) are used.

- ***Biochar (pyrochar and gaschar)***

The biochar recalcitrance is attributed to the presence of aromatic groups, which tend to increase with higher temperatures (see SI1) [51,128]. Furthermore, the biomass ash content influences the recalcitrance degree, because it acts as a barrier that impedes heat diffusion [52]. A high ash content thus hinders biomass dehydration and favors the formation of dissolved organic carbon (DOC), which is considered the main form of labile C in biochar [52].

Various studies have demonstrated that biochar (BC) is highly recalcitrant to both biotic and abiotic degradation, with approximately 80-97% of the organic carbon remaining unmineralized for hundreds to thousands of years [51,52,55,129]. This is attributed to the presence of C_L and C_R fractions [45,56,130], each one determined by the characteristics of the raw biomass and the conversion process conditions.

Wang et al.[51] found, based on 24 studies (n=128), that C_L represents approximately 3% of the biochar composition (MRT=108 days), while the C_R fraction represents the remaining 97% (MRT=556 years). The meta-analysis of Bai et al.[131] (56 studies) also found that biochar addition to soils increases SOC stocks, by 39%, on average. On the other hand, Zimmerman and Gao [56] determined, using a two-pool model, long-term losses of 2-59% for various biochars. The simulations of Zimmerman [131] uncovered average C losses of 10.3% after 100 years and 28.4% after 1000 years for microbial incubations, and 11.1% after 100 years and 28.8% after 1000 years for abiotic incubation of various biochars.

The recalcitrance of biochar can also be expressed by simple identifiers based on the elemental ratios between C, H, and O, which are plotted on the so-called Van-Krevelen diagram [38,45]. The ratio between hydrogen and carbon (H/C_{org}) is correlated with the presence of aromatic compounds and double bounding and is used to estimate the 100-year stability of biochar (BC_{+100}). A H/C_{org} of 0.5-0.7 is associated with a BC_{+100} of 50%, while an H/C_{org} of 0.4 denotes a BC_{+100} of 70% [68,71]. The O/C ratio indicates that a higher content of aromatic structures occurs when the oxygen content in the biochar is low and is used for expressing recalcitrance as half-life ($BC_{t1/2}$). Three ranges are typically used, with an estimated $BC_{t1/2}$ of 100 years for O/C >0.6, 100-1000 years for O/C between 0.2 and 0.6, and 1000 years for O/C <0.2 [38,54].

The interactions of biochar with soil properties influence the mineralization rate of biochar. It has been observed that biochar tends to mineralize faster in sandy soils than in clayey or mineral-enriched soils [52,132]. However, if poorly managed, plant roots can oxidize biochar, promoting higher mineralization and reducing the mitigation potential of biochar [134,135]. For instance, Zhang et al.[136] reported that application rates of biochar in the range of 10 to 40 t BC ha^{-1} can increase soil CO_2 and CH_4 emissions but reduce N_2O emissions by 15%, 16%, and 38%, respectively, as compared to a no-biochar situation, while application rates above 80 t BC ha^{-1} trigger net sequestration of 36% CO_2, 30% CH_4, and 65% N_2O.

- ***Pyrochar***

A total of 34 studies (n=144 datasets; details in [61]) were identified for crop residue-based pyrochar, collected from laboratory incubations, carbon modeling, and field trials. The studies were separated by process temperature as low (<300°C), medium (300-500°C), and high (>500°C) temperatures, with the main interest in the medium temperature group (Fig.7) since higher bio-oil (main product) yields are typically reported for this temperature range. After removing outliers, the data was reduced to 131 observations, with an average $\overline{C_R}$ (across all temperature ranges) of 96%. At medium temperatures, pyrochar showed a mean $\overline{C_R}$ of 95% (n=74), which is associated with an average $\overline{MRT}$ of 632 years and a mean incubation time of 279 days.

Compared to raw biomass, pyrochar mineralizes at a significantly slower rate. For instance, Knoblauch et al.[137], found that about 77% to 100% of rice husks were mineralized in soils, whereas only 4.4%-8.5% of pyrochar derived from rice husks was mineralized, for a similar timeframe. Similarly, Bruun et al.[95] observed that 53% of C was mineralized from wheat straw added to soils, while only 2.9% and 5.5% were mineralized for the slow and fast pyrolyzed residue, respectively.

Considering only studies conducted for more than one year (n=30), recalcitrance remains almost unchanged (~93%), while the $\overline{MRT}$ decreases to 604 years, for the medium temperatures group. For high (n=49) and low (n=10) temperatures, $\overline{C_R}$ is shown to be 97% The $\overline{C_R}$ value of low-temperature pyrochar may be biased by the small number of studies identified, thus this value remains highly uncertain.

Nevertheless, these results are consistent with the meta-analysis of Han et al.[52], who found that manure- and crop-based pyrochar are composed of a C_L fraction of 4.35%, while wood-based pyrochar is more recalcitrant with a C_L fraction of 1.32%. Despite the C_R fraction being considered to remain unchanged over the long term, various modeling studies have determined that in fact, a very slow mineralization process occurs in this fraction. Using Eq 2b, approximately 75% of the $\overline{C_R}$in pyrochar is reported to remain unmineralized after 100 years. The 100-year $\overline{C_R}$ predictions reported in this study are in accordance with Woolf et al.[33] and IPCC guidelines [138], suggesting respectively that 63-82% and 80% of the pyrochar is not mineralized after 100 years, thus remaining in soils.

- ***Gaschar***

In contrast to pyrochar, there is still scarce information about the C recalcitrance of gaschar, and incubation trials are needed to clarify the gaschar behavior in terms of long-term SOC dynamics [134,139]. Given the scarcity of information on gaschar recalcitrance, woody feedstocks were included besides crop residues to expand the number of records in the inventory, to derive the figures

presented in Fig.7. In total, ten publications were identified with 36 observations. The mean C recalcitrance ($\overline{C_R}$) was found to be 95% (n=33) for a mean incubation time of 523 days and a mean $\overline{MRT}$ of 141 years. Data were grouped by type of feedstock into crop residues- and wood-derived-gaschar, which represented a $\overline{C_R}$ (%) of 94% (n=20) and 100% (n=10), respectively (Fig.7).

Data were also grouped by gasification temperature in three groups (Table S2): low (500-600°C), medium (700-800°C), and high (>1200°C). The C recalcitrance ($\overline{C_R}$) was 95% for the medium and high-temperature groups. The low-temperature group showed recalcitrance near 100%. However, the latter value resulted from only one study where the incubation was carried out for 143 days.

Higher temperatures tend to produce a char with fewer surface functional groups, which is ascribed to increased resistance to microbial degradation; this explains the higher C stability in gaschar, as compared to pyrochar [52,128,140]. The results are aligned with the IPCC guidelines [138], suggesting that 89% (± 13%) of C remains in the soil after 100 years. Nevertheless, the MRT values of the dataset are considerably low compared to the centennial to millennial-scale values reported in e.g. [55,56].

3.2.2.2 Hydrochar

Compared to pyrochar, the literature on hydrochar recalcitrance is sparse, mainly because hydrochar is considered less attractive than pyrochar, at least when stemming from the HTL process. This is essentially attributed to the lower surface, porosity, and aromatic C groups in hydrochar than pyrochar [122]. From 104 datasets (16 studies), the average stability of hydrochar in soils obtained from different feedstocks was 89% (Fig.7, n=97, after outlier removal). For hydrochar from crop residues in isolation, the reported recalcitrance averages 83% with a mean $\overline{MRT}$ of 11 years (n=29).

The lower $\overline{C_R}$ and $\overline{MRT}$ of hydrochar compared to gaschar and pyrochar is attributed to the milder conditions and the water content allowed in the process. Under these conditions, hydrochar with a high number of aliphatic groups and O and H content is formed due to a lower evaporation rate, which leads to the formation of DOC in soils and more C lability [52].

3.2.2.3 Digestate

Digestate recalcitrance is attributed to the lignocellulosic matter content in the raw biomass, with the more labile components being converted to biogas during digestion [141].

A total of 17 studies (n=114) on digestate recalcitrance from different feedstocks were identified in this study. The average digestate C recalcitrance across all feedstocks combined was found to be 70% (n=104). Under the consideration of returning digestate to the soil as a strategy to harvest

more crop residues for AD, digestates were grouped by input feedstock, namely, cattle manure, cattle slurry, pig slurry, poultry manure, and crop residues/biowaste mixtures, the key feedstock of interest here. The average C recalcitrance for the crops/biowaste group was found to be 68% (n=31), which is similar to the value of 65% reported by Levavasseur et al.[142]

When possible, the mineralization of the raw biomass was compared to the digestates. Some studies have found digestate to be even twice as resistant to degradation as the undigested feedstock [143,144]. For instance, the application of undigested silage maize (100% C) produced a CO_2 loss of 104% (i.e., loss of C in the EOM and the native soil), while the application of digested silage maize (36% of the initial C) resulted in a 13% mineralization only [145]. On the other hand, Thomsen et al.[144] estimated, based on incubation assays, a recalcitrance of 12% for digested feedstock versus 14% for non-digested feedstock, concluding that anaerobic digestion has little influence on long-term C retention in soils. On average (n=20), this review found that digestate is 31% more stable than the raw biomass (details in the database compiled in Andrade et al.[61]); specifically, the stability of digestate from crop residues/biowaste mixtures is 35% higher than that of undigested biomass. Note that the original stable C in biomass is not altered during AD, thus the only difference between the raw and digested biomass is the labile C content. Therefore, the higher rate of CO_2 emissions in the raw biomass is ascribed to the labile fraction.

These results showed that while the C returned in digestate is only 36% (C_C) of that in undigested biomass, the removal of the labile C fraction lessens soil C mineralization when digestate is applied, allowing SOC stocks to be maintained longer than if crop residues were plowed back in soils. The $\overline{MRT}$ observed for digestate is only 1.2 years (0.4 years for crop residues digestate, Table 1), which can be biased by the short duration of the incubation assays and the lack of field trials included in the database [61].

3.2.2.4 Molasses

The potential use of coproducts from 2GEtOH as soil amendments has been poorly studied. Most studies address the behavior of the solid fraction only or molasses produced in first-generation bioethanol production (i.e., based on energy crops), while there are hardly any incubation studies to understand the recalcitrance of 2GEtOH molasses. Therefore, first-generation bioethanol coproducts were used as proxies of the 2GEtOH coproducts.

The compilation thus includes coproducts such as “non-fermentable solids”, “molasses”, “yeast concentrate”, “distiller’s grains”, “bagasse pith” and “biodiesel meal” obtained from the bioethanol production of different feedstocks (maize, sugarcane, sugar beet, wheat, rapeseed, potato;

details in Table S2 and Andrade et al.[61]). The average C recalcitrance for the ensemble of coproducts was 48% (Fig.7) with an MRT of 1.3 years (n=51). Separation of the residues into molasses, cake, and rapeseed meal resulted in recalcitrance values of 46%, 42%, and 68%, respectively.

There is evidence that the recalcitrance of bioethanol coproducts may be lower than that of the untreated biomass, probably because the chemical and enzymatic treatments alter the wall structure and disrupt the chemical bonds in lignin, allowing better access to soil microorganisms than in the raw biomass [64,146,147]. Soil application of molasses has been associated with increases in aliphatic carbon, salinity, and electrical conductivity of soils, as well as with higher CO_2 and N_2O emissions than untreated biomass [147,148]. The high mineralization rate of bioethanol coproducts is, however, associated with increased microbial activity, which in turn is associated with increased fertility and plant growth [118]. On the opposite, Cayuela et al.[146] observed stronger recalcitrance of the soil organic matter (SOM) for non-fermentable wheat residue from bioethanol production, compared to the recalcitrance observed with raw wheat residues. Further research is required to understand the actual recalcitrance of bioethanol coproducts and their effect on long-term soil quality.

3.2.2.5 Perspectives on recalcitrance

The application of bioeconomy coproducts (e.g., biochar, molasses, etc.) to soils needs to be further researched, as the presence of heavy metals and toxic substances may affect soil quality and soil C and N dynamics can be altered by the different feedstocks and processes. Nevertheless, some mechanisms have been proposed by [69,134,139,149,150] to understand how the application of specific bioeconomy coproducts can, now and in the future, affect soil C mineralization (commonly referred to as the negative priming effect when decreasing the mineralization rate). The key points to consider are:

a) The soil microbiome may evolve to adapt to use pyrochar or gaschar as a source of C instead of native SOM. Thus, the recalcitrant C would become the preferred C source, affecting long-term mineralization.
b) Biochar microporous structure adsorbs SOM particles, which reduces microbial accessibility to SOM, thus decreasing the microbial degradation of SOM. Higher process temperatures increase the microporosity of biochar, which explains the higher negative priming effect for biochar produced under gasification compared to pyrolysis or HTC.
c) Some functional groups in biochar or bioethanol molasses may be toxic to microorganisms, thus inhibiting their growth and enzymatic activity. The continued soil respiration even when coproducts are added may however be evidence to oppose this theory.

4. SOC modeling and bioeconomy

4.1 SOC modeling: general considerations

Soil models represent terrestrial systems linking soil, atmosphere, and plants, in different degrees depending on the model. Diverse modeling approaches are reported in the literature according to the mechanistic understanding of the SOM dynamics extrapolated to the system. Ideally, a soil model must be capable of extrapolating local short-term-measured processes to long-term effects valid at different scales [75]. However, challenges regarding understanding the intrinsic soil dynamics, parameterization, and input data availability remain unresolved thus no single ideal model exists, and the most adequate model must be selected for specific objectives [77].

RothC, AMG, and C-TOOL are SOC models with simple to moderate complexity to model C-dynamics only, while the other models reviewed here (CENTURY, Daycent, DNDC, EPIC, Daisy, APSIM, STICS, CANDY, ORCHIDEE) are agro-ecosystem models simulating plant-soil-atmosphere interactions [94] based on several sub-models, including a SOC model, and can thus predict C-N dynamics, soil-water, nutrients and energy balance, plant growth, and gaseous emissions. A detailed description of the models is provided in SI1 and SI2.

The decomposition and mineralization of SOM can be described via zero-order, first-order, or enzyme kinetics, and microbial growth rate functions [18]. However, most SOC models are based on conceptual compartments, commonly of two to five pools, each described by first-order-kinetics with a specific *k* constant, determining MRT () [75,151]. Despite the number of pools, and the values of *k* and MRT being distinctive for each model, they often include at least one pool to describe the decay process of C_L and another pool for C_R governing SOC stability. Therefore, incoming organic matter is partitioned among pools according to its decomposability.

Inputs required to run the different models (SI2) include soil characteristics (texture, bulk density, initial SOC stocks), climatic variables (air temperature, precipitations, and evapotranspiration), and management practices (crop rotations, fertilization, tillage, grazing, harvesting, among others). Models run at different timesteps (hourly, daily, monthly, or annual), therefore the input data provided must correspond to the time scale.

The models require estimates of the decomposability of the plant material and the number of C inputs from crop residues or EOMs. The C inputs from biomass are estimated from measured yields using allometric functions [18]. The stabilization process of the input material (plant and EOMs) is described using specific decomposition constants derived from chemically defined (e.g., chemical digestion, spectroscopy, among others) or kinetically defined fractions fitting the *k* and pool sizes to

CO_2 emissions observed from incubations [151]. The representation of the stabilization process within the model enables the long-term simulation of the molecules' persistence in soil (recalcitrance) [78].

Among the most popular models, CENTURY, DNDC, and RothC are the most accepted and dominate the SOM modeling literature [75], with CENTURY and RothC being used to set the basis for developing other models.

4.2 SOC modeling with bioeconomy coproduct

Here, the focus is on the models capable of representing bioeconomy coproducts C_R. Eight soil models that have been adapted to consider bioeconomy coproduct inputs were identified: Foereid et al.[152], RothC [35,36,151,153,154], Century [155], EPIC [156], APSIM [157], CANDY [158,159], AMG [142], and C-TOOL [34].

RothC has been the most adapted model for bioeconomy coproducts, while biochar is the most studied coproduct, followed by digestate. Model adaptation methods were determined by the complexity of the model and data availability, summarized in Table 2.

All the analyzed studies, but that of Dil and Oelberman [155], considered that the coproducts are composed of C_L and C_R fractions, which are then allocated in the different SOC pools according to specific partition coefficients and mineralize following a first-order *k*. Foereid et al.[152] and Dil and Oelberman [155] followed rather simplistic approaches to model the SOC dynamics from **biochar** application by not considering different SOC pools in the former and not deploying realistic turnover rates in the latter.

Foereid et al.[152] developed a biochar-soil model in Microsoft Excel using laboratory incubation data to define *k,* and field trial data to calibrate the model and describe leaching effects. Soil moisture and temperature effects were determined using the Daycent model. Biochar was considered to mineralize according to Eq.2b, with the labile *k* based on Whitman [160], while the recalcitrant *k* fit a turnover rate of 2,000 years in the stable fraction. The model also accounts for the C fraction prone to leaching and erosion (f_r), with an erosion rate (k_r) defined by adapting Eq.2b. Dil and Oelberman [155] included biochar in CENTURY as an organic matter input, representing the recalcitrance by 95% lignin content. This approach allocated biochar C in the slow pool following a turnover rate of 10-50 years, which is significantly lower than the reported biochar MRTs (Table S2).

AMG was parametrized for different **EOMs, including anaerobic digestates**, by Levavasseur et al.[142], based on the indicator of residual organic carbon (IROC) defined by Lashermes et al.[161]. The proportion of EOM input into SOC is represented by the humification coefficient (*h*), which corresponds to the IROC from the biochemical fractions of 24 EOMs (>600 datasets). The IROC of each

EOM was determined based on the C content of the soluble lignin and cellulose under the Van Soest [162] method and the proportion of C mineralized after a 3-day incubation [161].

RothC has been modified by Woolf and Lehmann [23], Mondini et al.[132], Lefebvre et al.[153], Pulcher et al.[153], and included within the BioEsoil tool [154] to model the SOC dynamics from **biochar, digestate, and bioethanol solid-residue** inputs:

- Woolf and Lehmann [35] modified the original decay rates of the decomposable plant material (DPM) and resistant plant material (RPM) pools to add the positive and negative priming effects of **biochar** addition to the soils. Simulations were performed for maize stalks as an input for pyrolysis. A 50% residue removal rate from croplands was assumed along with a biochar return to the soil, with a simulation frame of 100 years. The authors found a 30-60% increase in SOC stocks for biochar input instead of stalks.
- Mondini et al.[151] built additional SOC pools for eight types of EOM materials, including **anaerobic digestates** and **bioethanol residues**. New EOM decomposable (EOM-DEOM) and resistant (EOM-REOM) pools were added parallel to the standard model, while the humified EOM was directly incorporated into the standard humified matter (HUM) pool. The partitioning factors fDEOM, fREOM, fHEOM, and the mineralization rate constants kDEOM and kREOM were defined through short-time incubation experiments (224 curves). The model was used later [163] to predict the long-term SOC stocks in Italy, at a national scale, for future EOM scenarios.
- Lefebvre et al.[36] adapted **a biochar submodule** composed of fresh (FBC) and recalcitrant biochar (RBC) pools. The submodule considers the C_L fraction as fresh plant material, while the remaining C_R is allocated in the adapted RBC pool to be mineralized according to a k_{RBC} decay rate representing an 11.9% C lost in 100 years. A fraction of C is subtracted from RBC to represent the leaching (f_r) of biochar in natural ecosystems and a positive priming effect was included according to the Woolf and Lehmann [35] methodology.
- Pulcher et al.[153] collected data from an eight-year field trial to calibrate and validate a biochar module, represented by additional pools for the C_L (BClab) and C_R (BCrec) biochar fractions. The biochar mineralization rate of the labile (k_{LAB}) and recalcitrant (k_{REC}) fractions were defined using a double exponential decay model, previously estimated by Ventura et al.[150] and corrected by dividing by yearly average rate modifying factors (*a, b, c*) obtained from measurements performed in 2013, 2015, and 2020. Biochar was assumed to enter the BIO and HUM pools of RothC, with a fraction being mineralized, accounting for the sum of CO_2 emitted from the DPM, RPM, BIO, HUM, BClab, and BCrec pools. A 16% negative priming effect was included in the C balance of each pool.

- RothC was also included in the BioEsoil tool [154] to evaluate the effects of bioenergy technologies (i.e., incineration, AD, gasification, ethanol fermentation, and plant oil production) on SOC by considering the nutrient losses during the process and the potential recoveries from returning the coproducts to the soil following a yearly time step. However, only **digestate, gaschar, and incineration ashes** are regarded as inputs to soils in BioEsoil.

CANDY was used by Prays et al.[158] and Witing et al.[159] to predict the SOC dynamics from **digestate** applications. The fraction of C in the fresh organic matter (FOM) pool (C_{FOM}) that enters the SOM pool is labeled as C_{rep} flux and the substrate uses an efficiency parameter (η), which defines the potential to build new SOC. Prays et al.[158] performed incubation assays on six different maize-based digestates and performed inverse modeling to adjust η and k parameters to fit the observed mineralization rates. The adjusted parameters were then used by Witing et al.[159], where they determined the C_{rep} factor for different materials (i.e., crop residues, excrement, and digestate). The C inputs from digestate (C_{DG}) were calculated as the difference between the C_{FOM} and the C in biogas (C_{BG}), based on the reported biogas yields of different EOMs.

C-TOOL was adapted by Hansen et al.[34] to model **digestate**, based on the incubation results of Thomsen et al.[144]. For some substrates (e.g., manure), C-TOOL already artificially allocates, through a factor called f_{HUM}, a fraction of the EOM carbon input to the HUM pool (the rest being considered as labile and going to the FOM pool). By running iterations, Hansen et al.[34] determined that a f_{HUM} of 36.7% and 26.0% for, respectively, manure digestate and straw digestate was necessary to fit the results of Thomsen et al.[144]. The adapted model was used to predict the 300-years SOC evolution of applying straw-based digestate in soils in Denmark versus harvesting straw without any carbon return to soils.

EPIC was adapted and validated by Lychuk et al.[156] to determine maize yield, soil cation exchange capacity (CEC), pH, bulk density (Db), and SOC dynamics in soils amended with **biochar**. The biochar surface area and charge density were related to biochar additions to model the CEC and pH predictions. The soil-biochar mixture CEC (CEC_{mix}) was determined, and the extra CEC (CEC_{added}) compared to non-amended soil was used to determine the new pH (pH_{new}) using the equation by Magdoff and Barlett [164]. The SOC dynamics were modeled by allocating different fractions of biochar among the SOC pools. The bulk density is affected by SOC changes and thus was calculated by modifying the Adams [165] equation to consider the bulk density of the mineral soil (Db_m), SOM (Db_{SOM}), and biochar (Db_{BC}).

APSIM was adapted by Archontoulis et al.[157] by adding a biochar module that included ten parameters to define the **biochar** characteristics and 15 parameters concerning the soil-biochar

interactions. The coupled biochar module accounted for changes in soil OC, N mineralization and immobilization, CEC, NH_4 adsorption and desorption, water balance, and bulk density, as a response to biochar application. Unlike other adaptations, the APSIM biochar module considers a double-exponential decay rate, labile and recalcitrant fractions, allocation coefficients in the SOC pools, the amount of biochar lost during the application, and the efficiency of retaining biochar in the soil. The C fraction retained in the soil is allocated from the FOM to the metabolic (BIOM) and HUM pools. Positive and negative priming effects were determined according to the values reported by Woolf and Lehmann [35]. The authors assessed a range of values for the different parameters and compared the predictions to field observations, obtaining a mean relative absolute error between -0.4% and 13.1%.

Table 2. Overview of existing approaches to include the effects of bioeconomy coproducts within soil models

Model	Coproduct	Feedstock	Method[a]	Variables and parameters	Variable specifically defined within the study	Ref.
Foereid et al. Equations in Microsoft Excel	Biochar (pyrolysis, 500°C)	Pine and oak residues, maize stalks	$BCt(t) = BC0 \times [f_r * e^{-k_r t} + (1 - fr)]$ $BC(t) = BC0 \times [fC_L * e^{-k_L t} + (1 - fC_L) * e^{-k_R t}]$	fC_L =0.122, k_L= 0.0038 d^{-1}, fC_R = 1-C_L, MRT_R= 2000, k_R= 1.369 E^{-6} d^{-1} f_r=0.9, k_r=0.03 d^{-1} C_{m100y}= 11.68%, $C_{runoff100y}$= 76.09%, $C_{down100years}$=0.13%, C_{m2000y}= 20.65%, $C_{runoff2000y}$=74.83%, $C_{down2000years}$= 0.52%	BC(t): Mass of Biochar at time t, BC0: Biochar added	[152]
RothC 26.3	Biochar (Slow pyrolysis, 500°C)	Maize stalks	$BC(t) = BC0 \times [fC_L * e^{-k_L t} + (1 - fC_L) * e^{-k_R t}]$ $k'_{DPM} = k_{DPM}(1 + PE[BC])$ $k'_{RPM} = k_{RPM}(1 + PE[BC])$	C content= 37% (35-39%), C_L= 7.5% (5-10%), C_R = 1-C_L, ln(2)MRT_L= 3 (1-5), ln(2)MRT_R= 1000 (500-50000), +PE= 6.9%, (0-13.8%), -PE= 3.6% (1.1-6.1%). f_{BIO} and f_{HUM} as standard RothC (see SI2)	+PE: C mineralized as CO_2, -PE: C transferred to HUM k'_{DPM}, k'_{RPM}: modified decay rate in DPM and RPM pool	[35]
	8 EOMs, digestates and bioethanol residues		Additional pools: EOM-DEOM, EOM-REOM, EOM-HEOM. Average RMSE = 4.5%	f_{DEOM}= 0.09 (0-0.63) f_{REOM}= 0.70 (0.21-0.98) f_{HEOM}= 0.41 (0.06-0.78) k_{DEOM}= 89 y^{-1} (11-330) k_{REOM}= 0.4 y^{-1} (0.15-2.51) k_{HEOM}= 0.02 y^{-1}	EOM: Exogenous organic matter RMSE: Root mean square error	[151]
	Biochar (pyrolysis, 550°C)	Sugarcane bagasse and trash	Biochar submodule: FBC + RBC RBC= $C_R - C_{leached}$	C_L= 3%, C_R= 97%, k_{RBC}= 0.00119 y^{-1}, $C_{lost100years}$= 11.9%, $C_{leached}$= 5.83%, $C_{remain100years}$= 83%, +PE= 21% and 91%	FBC: Fresh biochar, RBC: Recalcitrant biochar pool k_{RBC}: decay rate in RBC	[36]

Model	Coproduct	Feedstock	Method[a]	Variables and parameters	Variable specifically defined within the study	Ref.
	Biochar (Gasification, 1200°C)	Maize silage	Additional pools: BClab and BCrec $k_{REC} = \frac{k_1}{a,b,c}$; $k_{LAB} = \frac{k_2}{a,b,c}$ $C\ output = C_{pool}\left(1 - e^{-a,b,c\ PE k_{pool}\frac{1}{12}}\right)$ k_1 and k_2 constants are as in Ventura et al. [161]. a, b,c are yearly average rate modifying factors corresponding to 2013, 2015, and 2020.	C_{2013}= 81%, C_{2015}= 63.3%, C_{2020}= 60.1%, k_1= 0.08 y^{-1}, k_2= 2.55 y^{-1}, C_L= 4%, C_R= 96%, k_{LAB}= 3.6 y^{-1}, k_{REC}= 0.14 y^{-1}, -PE= log (0.16)	BClab: Labile BC pool, BCrec: Recalcitrant BC pool, Cpool: Other RothC pools, k_{LAB}: BClab decay rate corrected, k_{REC}: BCrec decay rate corrected, k_1: BClab decay rate in 2015, k_2: BCrec decay rate in 2015, k_{pool}: decay rate of other RothC pools,	[153]
	Digestate, gaschar, ashes		FOM is distributed over the DPM and RPM, based on h according to $DPM/RPM = 2.0 - 2.174 * h$	Digestate produced: 50%, h: 0.75. Gaschar produced: 50%, h: 1. Incineration ashes produced : 5%, h: 1	Digestate, gaschar, and ashes produced: Residue produced in percentage (%) relative to feedstock mass. h : humification coefficient	[154]
Century	Biochar (pyrolysis, 450°C)	Wood residues	$\overline{CR}$ represented as 95% lignin content allocated in the slow pool ($\overline{MRT}$= 10-50 years). The N input from biochar was considered a mineral fertilizer	Biochar composition : 61.7% C, 0.24% N, 95% lignin, C:N ratio = 257		[155]
AMGv2	Manure, digestate, compost, SS, peat, MSW, PCM		AMG structure [22] $QC = QC_S + QC_A$ $\frac{dQC_A}{dt} = \sum_i m_i h_i - kQC_A$	h= IROC for the different EOMs in Lashermes et al. [171]. Digestate h= 0.65.	QC: Total SOC, C_A: Active pool, C_S: Stable pool, m_i: C input, h: humification rate, k: mineralization rate of the C_A	[142]
CANDY	Digestate		Inverse modeling to fit the parameters to experimental observations	k= 0.279-0.575 d^{-1} η= 0.802 to 0.890.		[158]

Model	Coproduct	Feedstock	Method[a]	Variables and parameters	Variable specifically defined within the study	Ref.
	Digestate		$C_{DG} = C_{FOM} - C_{BG}$	C inputs year 2000= 2905 kg C ha^{-1} (1524 kg Crep ha^{-1}). C inputs year 2011= 2965 kg C ha^{-1} (1567 kg Crep ha^{-1}). Crep = 53%. η as determined in Prays et al., 2017.	C inputs year 2000: Carbon input in the year 2000 C inputs year 2011: Carbon input in the year 2000	[159]
CTOOLv2	Digestate	Manure, straw	Inverse modeling: Iterative calculation of f_{HUM} to fit the experimental C remaining data of Thomsen et al. [155]	Digested biomass-$C_{remain20y}$ – Raw biomass-$C_{remain20y}$ = 14%, Manure digestate: h=36.7%, Straw digestate: h=26.0%	Digested biomass-$C_{remain20y}$ – Raw biomass-$C_{remain20y}$: Percentage of C remaining in digestate after 20 years	[34]
EPIC	Biochar		$CECmix = \frac{CECsoil + \left(\frac{BCrate}{Msoil}\right) \times CECbiochar}{1 + \left(\frac{BCrate}{Msoil}\right)}$ $CECadded = \frac{(CECmix - CECsoil)10}{OM_{bc\&soil}}$ $pHnew = \frac{UpH - LpH}{1 + e^{-a(X_{new} - T)}} + LpH$ $X_{new} = \left(T - \frac{1}{A}\left(ln\left(\frac{UpH - LpH}{pH - LpH}\right) - 1\right)\right) + CECadded$ $Db = \frac{100}{\frac{SOM}{Db_{SOM}} + \frac{100 - SOM - BC}{Dm} + \frac{BC}{Db_{BC}}}$	Biochar characteristics: Db_{BC}= 0.64 Mg m^{-3}, 72.9% C, 0.76% N, 4.6% ash, C:N= 120, H:C= 0.018, and O:C= 0.26 Biochar in SOC pools: fActive= 2%, fSlow= 60%, fPassive= 38% pH: Modified Magdoff and Barlett (1985) equation pH=soil pH, UpH= 7.30055, LpH= 3.495, A= 1.08, T= 6.6 Db: Modified Adams (1973) equation Db_{SOM}= 0.244 Mg m^{-3} Average error= 30% (yield) and 8% (SOC)	BCrate is the rate of biochar addition, Msoil is the mass of a slice of soil in 1 ha, CECbiochar is the CEC of biochar, UpH: upper oxisol pH, LpH: lower oxisol pH. $OM_{bc\&soil}$: organic matter content within the soil and biochar mixture	[156]

Model	Coproduct	Feedstock	Method[a]	Variables and parameters	Variable specifically defined within the study	Ref.
APSIM	Biochar		PE is considered for each pool and k is modified according to Woolf and Lehmann [49]: $BC(t) = BC0 \times [fC_L * e^{-k_L t} + (1 - fC_L) * e^{-k_R t}]$ $k'_{DPM} = k_{DPM}(1 + PE[BC])$ $k'_{RPM} = k_{RPM}(1 + PE[BC])$	C content= 17-88%, C_L= 3-30%, MRT_L=0.3-25, MRT_R= 50-50000, $C_{retained}$= 40%, f_{BIO}= 0.05, f_{HUM}= 0.95 $+PE_{FOM}$= 0.1 (0-0.138) m^2 kg^{-1} C, $-PE_{FOM}$= 0.05 (-0.30-0-0.15) m^2 kg^{-1} C, $+PE_{BIO}$= 0.1 (0-0.15) m^2 kg^{-1} C, $-PE_{BIO}$= 0.05 (-0.15-0) m^2 kg^{-1} C, $+PE_{HUM}$= 0.1 (0-0.15) m^2 kg^{-1} C MRAE = -0.4% to 13.1%	+PE: C mineralized as CO_2, -PE: C transferred to HUM. MRAE: mean relative absolute error	[157]

[a]Values in parenthesis represent the whole range of values, L: Labile, R: Recalcitrant, k: decay rate, f: partition factor, C_m: C mineralized, C_{runoff}: C lost by runoff, C_{down}: C transported from topsoil to subsoil, $C_{retained}$: C retained in soils, $C_{leached}$: C lost by leaching, C_{remain}: C remaining at a given time, MRT: Mean residence time (years), PE: Priming Effect, [BC]: concentration of biochar in the soil, Db: bulk density, CEC: Cation exchange capacity, C_L: Labile carbon, C_R: Recalcitrant carbon, k_L : decay rate in labile pool, k_R : decay rate in recalcitrant pool, MRT_L: Mean Residence time in labile pool, MRT_R: Mean Residence time in recalcitrant pool, f_r: fraction of C available for runoff, k_r: runoff rate, +PE: positive priming effect, -PE: negative priming effect, $OM_{bc\&soil}$: organic matter content within the soil and biochar mixture, Db_{SOM}: Bulk density of SOM, Db_{BC}: Bulk density of biochar, UpH= upper oxisol pH, LpH= lower oxisol pH, f_{BIO}: fraction of C transferred to BIO, f_{HUM}: fraction of C transferred to HUM, f_{DEOM}: fraction of C transferred to DEOM , f_{REOM}: fraction of C transferred to REOM, f_{HEOM}: fraction of C transferred to HEOM, h: humification coefficient, η: substrate use efficiency, EOM: Exogenous organic matter, SOC: Soil organic carbon, SOM: Soil organic Matter, FPM: Fresh Plant Material, FOM: Fresh Organic Matter, DPM: Decomposable plant material, RPM: resistant plant material, BIO: Microbial Biomass, HUM: Humified organic matter, LAOC: Labile Added Organic Carbon, DEOM: decomposable exogenous organic matter, REOM: resistant exogenous organic matter, HEOM: humified exogenous organic matter, IROC: indicator of residual organic carbon, FBC: Fresh biochar, RBC: Resistant biochar, SS: Sewage sludge, MSW: municipal solid wastes, PCM: pelletized cattle manure, RMSE: root mean square error, MRAE: mean relative absolute error.

The most relevant strengths and weaknesses of the models in Table 2 were categorized in Fig.8 to determine the current SOC models with the major potential to simulate the interplay between crop residue removal and their partial return to soils as bioeconomy coproducts. Models with limited input data, easy procedures, and friendly interfaces are commonly preferred by decision-makers [149]. Therefore, the considered "desirable characteristics" are simple and modifiable structures, based on simple processes, widely validated across diverse land and climate types, and requiring easily accessible national scale data inputs. The ability to determine other dynamics beyond C evolution was also considered desirable. However, it must be highlighted that defining a characteristic as a strength or weakness depends on the user´s purpose for using the model.

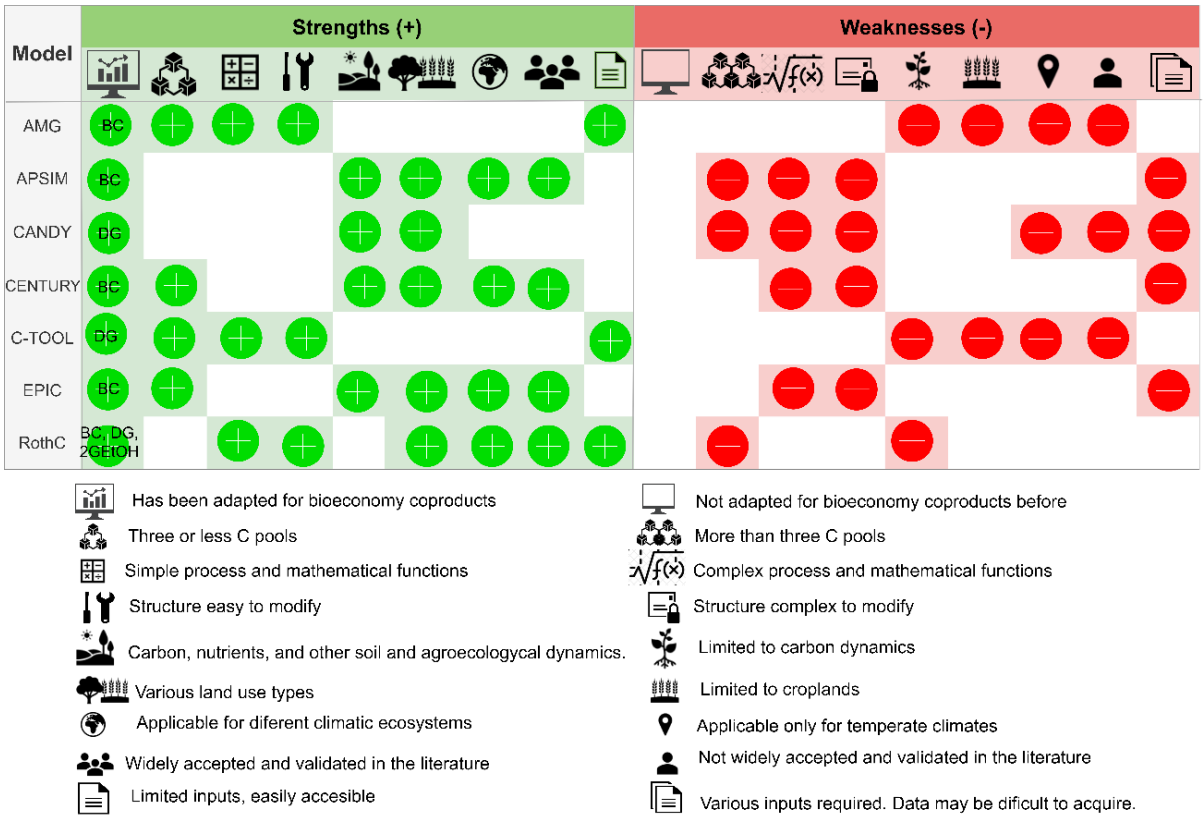

Fig.8. Comparison of promising SOC models to include bioeconomy coproducts return to soils. BC: Biochar, DG: Digestate, 2GEtOH: Second generation-lignocellulosic bioethanol.

5. Conclusions

The main conclusions resulting from this study can be summarized as follows:

- This study compiled data from over 600 literature records to provide the foundations required to uncover the synergies between bioeconomy conversion pathways and long-term SOC stock maintenance with a focus on crop residues. This allowed computing average C conversion ($\overline{Cc}$) and C recalcitrance ($\overline{C_R}$) coefficients for pyrochar, gaschar, hydrochar, digestate, and

lignocellulosic bioethanol molasses. The $\overline{C_R}$ was further refined by process conditions and feedstock types. These coefficients can be further adapted within soil models to assess the bioeconomy coproduct implications in SOC stock evolution.

- Pyrochar and gaschar presented the highest $\overline{C_R}$ coefficients (95%), followed by hydrochar (89%), digestate (70%), and lignocellulosic bioethanol coproducts (47%). However, while a relatively high amount of experimental data was available for pyrochar (n=144), hydrochar (n=104), and digestate (n=114), there were relatively scarce data for gaschar (n=36) and lignocellulosic bioethanol coproducts (n=51). Moreover, values associated specifically with crop residues tend to present larger variation ranges than other lignocellulosic feedstock for gaschar (ranging between 39–99%) and hydrochar (ranging between 33–97%). For pyrolysis, a medium operating temperature (300 –500 °C), i.e., the condition considered when bio-oil is the intended product, similarly leads to wider $\overline{C_R}$ variability (33–100%) than low (<300°C, 82–100%) or high (>500°C, 80–100%) operating temperatures.
- Of the C in the initial biomass feedstock, only 20% end up in the gaschar or lignocellulosic bioethanol molasses (liquid fraction), while it is 30 – 36% for hydrochar and digestate and 45%-50% for the lignocellulosic bioethanol solid fraction and pyrochar.
- MRT represents the average lifetime of the coproducts in soils. Pyrochar has the highest average MRT (3014 years), while the lowest MRT was reported for digestates (1.23 years). However, MRT values are influenced by the modeling equations selected, the incubation duration, and the frequency of respirometry measurements and the results in this study are biased by the small number of studies reporting expected MRTs (216) compared with the total data records (449).
- One major critique of incubation trials and field experiments is the duration of the experiments, which tends to be shorter than the expected half-life of the coproducts, especially for pyrochar and gaschar. The lengthiest reported field trial experiment was conducted for only 8.5 years for pyrochar, while the shortest assays had durations of over one week for digestate. Modeling has allowed determining the long-term behavior of coproducts in soils; however, it requires a set of consecutive measurements to determine the C kinetics and results are highly influenced by the order of the equation (zero, first, second, n), which is related to the defined C fractions in the coproducts.
- Incubation and field trial experiments are typically focused on the C mineralization process, sometimes including N emissions and fertilization effects, but tend to disregard other environmental aspects such as toxicity, biodiversity, or soil physical quality (e.g., CEC, salinity, erosion, etc.).

- Adapting a SOC simulation model to consider the interplay between bioeconomy and SOC is challenging, with one hurdle being the limited knowledge of the behavior of stabilized matter in real (and future) environments. To date, some models, including RothC, Century, AMG, CANDY, EPIC, APSIM, C-TOOL, and empirical simplistic models, have been adapted to some extent to include bioeconomy coproducts (e.g., biochar, digestate, bioethanol non-fermentable residues) with acceptable precision. These were thoroughly reviewed, including the methods used to incorporate coproduct recalcitrance within the models, when applicable. RothC was highlighted as the most adaptable model due to its simplicity and limited data requirements. Nevertheless, adapting more complex models may provide a more comprehensive understanding of the diverse effects of stabilized matter in soil dynamics beyond carbon. The $\overline{C_R}$ and $\overline{C_C}$ values compiled herein for a wide variety of bioeconomy coproducts, nevertheless, represent a major steppingstone for feeding this upcoming generation of adapted SOC models and therefore allow for better anticipating the interplay between crop residues and bioeconomy.

Data availability

The data that support the findings of this study are openly available in "TBI - Toulouse Biotechnology Institute - T21018" at https://doi.org/10.48531/JBRU.CALMIP/WYWKIQ [18]

Acknowledgments

This work was carried out within the framework of the research project Cambioscop (https://cambioscop.cnrs.fr), partly financed by the French National Research Agency, Programme Investissement d'Avenir (ANR-17-MGPA-0006), and Region Occitanie (18015981). C. Andrade was additionally funded by the French Embassy in Ecuador under the Project "Fonds de Solidarité pour Projets Innovants" (FSPI) and the French Ministry for Europe and Foreign Affairs.

Author contributions

Christhel Andrade Díaz: Conceptualization, Methodology, Data curation, Formal analysis, visualization, Investigation, Writing - original draft, Writing - review & editing. **Ariane Albers**: Writing - review & editing. **Ezequiel Zamora-Ledezma:** Writing - review & editing, Funding acquisition, and Supervision. **Lorie Hamelin:** Conceptualization, Methodology, Writing - review & editing, Funding acquisition, Project administration, Resources, and Supervision.

Competing interests

The authors declare no competing interests.

Supporting documents and data

This **Chapter 2** remains a synthesis mentioning the key characteristics of the bioeconomy conversion pathways studied, the final average coefficients representing the bioeconomy coproducts, and the soil models considered for including recalcitrant bioeconomy coproducts. The full data reporting the carbon content, yields, recalcitrance, and mean residence time of five bioeconomy coproducts was compiled in a harmonized database transparently documented in separated Appendix files and online repositories. Also, process conditions of each technology, and the structure of all the models reviewed are detailed in the appendixes:

- **Appendix A1a:** Supplementary information of the article
- **Appendix A1b:** Table summarizing the structures and parameters of twelve soil models.
- **Background data:** The database produced along with this paper is openly available in the following repository: https://doi.org/10.48531/JBRU.CALMIP/WYWKIQ

Towards Chapter 3

Besides proposing a set of coefficients defined as the carbon conversion (C_C) and carbon recalcitrance (C_R), to describe the amount of carbon converted from crop residues to bioeconomy coproducts and to represent the recalcitrant nature of the coproducts, respectively for pyrolysis biochar (pyrochar), gasification char (gaschar), HTL hydrochar, and AD digestate, **Chapter 2** also investigated several soil models and the feasibility of including the studied coproducts in them. Soil carbon models as RothC, AMG, or C-Tool present simple structures more easily adaptable to include novel inputs as source of C. Therefore, the C_C and C_R coefficients can be adapted to the soil carbon models to represent the amount of carbon input to croplands as recalcitrant coproducts, and the fraction of carbon that will be allocated in each soil pool. Also, the database produced within this study reports mineralization rates and mean residence time of each carbon fraction of the coproducts. Yet, the parameters of each coproduct have not been yet included in the models. Moreover, SOC dynamics depend on pedoclimatic conditions and farming management, and are thus spatial explicit. Accordingly, **Chapter 3**, proposes the adaptation of the soil model AMG to include the five coproducts reviewed in **Chapter 2** and presents a novel framework for the spatial explicit application of the new bioeconomy adapted AMG.

References for Chapter 2

[1] UNFCCC. Paris Agreement to the United Nations Framework Convention on Climate Change. 2015.

[2] IPCC. Global Warming of 1.5°C. An IPCC Special Report on the impacts of global warming of 1.5°C above pre-industrial levels and related global greenhouse gas emission pathways, in the context of strengthening the global response to the threat of climate change, sustainable development, and efforts to eradicate poverty [Masson-Delmotte, V., P. Zhai, H.-O. Pörtner, D. Roberts, J. Skea, P.R. Shukla, A. Pirani, W. Moufouma-Okia, C. Péan, R. Pidcock, S. Connors, J.B.R. Matthews, Y. Chen, X. Zhou, M.I. Gomis, E. Lonnoy, T. Maycock, M. Tignor, and T. Waterfield (eds.)]. IPCC; 2018.

[3] IACGB. Global Bioeconomy Policy Report (IV): A decade of bioeconomy policy development around the world. Berlin: International Advisory Council on Global Bioeconomy; 2020.

[4] European Commission, Directorate-General for Research and Innovation. A sustainable bioeconomy for Europe : strengthening the connection between economy, society and the environment : updated bioeconomy strategy. European Commission, Directorate-General for Research and Innovation; 2018.

[5] Gomez San Juan M, Bogdanski A, Dubois O. Towards sustainable bioeconomy - Lessons learned from case studies. Rome: FAO; 2019.

[6] Schoenmakere M, Hoogeveen Y, Gillabel J, Manshoven S. The circular economy and the bioeconomy: Partners in sustainability. LU: European Environment Agency.; 2018.

[7] Bugge M, Hansen T, Klitkou A. What Is the Bioeconomy? A Review of the Literature. Sustainability 2016;8:691. https://doi.org/10.3390/su8070691.

[8] Karan SK, Hamelin L. Crop residues may be a key feedstock to bioeconomy but how reliable are current estimation methods? Resources, Conservation and Recycling 2021;164:105211. https://doi.org/10.1016/j.resconrec.2020.105211.

[9] Hamelin L. A spatial approach to bioeconomy_ Quantifying the residual biomass potential in the EU-27. Renewable and Sustainable Energy Reviews 2019:16.

[10] Sarkar S, Skalicky M, Hossain A, Brestic M, Saha S, Garai S, et al. Management of Crop Residues for Improving Input Use Efficiency and Agricultural Sustainability. Sustainability 2020;12:9808. https://doi.org/10.3390/su12239808.

[11] Sevigné-Itoiz E, Mwabonje O, Panoutsou C, Woods J. Life cycle assessment (LCA): informing the development of a sustainable circular bioeconomy? Phil Trans R Soc A 2021;379:20200352. https://doi.org/10.1098/rsta.2020.0352.

[12] Paustian K, Larson E, Kent J, Marx E, Swan A. Soil C Sequestration as a Biological Negative Emission Strategy. Front Clim 2019;1:8. https://doi.org/10.3389/fclim.2019.00008.

[13] Yaashikaa PR, Senthil Kumar P, Varjani S. Valorization of agro-industrial wastes for biorefinery process and circular bioeconomy: A critical review. Bioresource Technology 2022;343:126126. https://doi.org/10.1016/j.biortech.2021.126126.

[14] Strapasson A, Woods J, Chum H, Kalas N, Shah N, Rosillo-Calle F. On the global limits of bioenergy and land use for climate change mitigation. GCB Bioenergy 2017;9:1721–35. https://doi.org/10.1111/gcbb.12456.

[15] Paustian K, Collier S, Baldock J, Burgess R, Creque J, DeLonge M, et al. Quantifying carbon for agricultural soil management: from the current status toward a global soil information system. Carbon Management 2019;10:567–87. https://doi.org/10.1080/17583004.2019.1633231.

[16] Batjes N h. Total carbon and nitrogen in the soils of the world. European Journal of Soil Science 1996;47:151–63. https://doi.org/10.1111/j.1365-2389.1996.tb01386.x.

[17] Friedlingstein P, Jones MW, O'Sullivan M, Andrew RM, Hauck J, Peters GP, et al. Global Carbon Budget 2019. Earth Syst Sci Data 2019;11:1783–838. https://doi.org/10.5194/essd-11-1783-2019.

[18] Smith P, Soussana J-F, Angers D, Schipper L, Chenu C, Rasse DP, et al. How to measure, report and verify soil carbon change to realize the potential of soil carbon sequestration for atmospheric greenhouse gas removal. Global Change Biology 2020;26:219–41. https://doi.org/10.1111/gcb.14815.

[19] Köck K, Leifeld J, Fuhrer J. A model-based inventory of sinks and sources of CO2 in agricultural soils in Switzerland: development of a concept 2013:189.

[20] Correction for Sanderman et al., Soil carbon debt of 12,000 years of human land use. Proceedings of the National Academy of Sciences 2018;115:E1700–E1700. https://doi.org/10.1073/pnas.1800925115.

[21] Davidson EA, Ackerman IL. Changes in soil carbon inventories following cultivation of previously untilled soils. Biogeochemistry 1993;20:161–93. https://doi.org/10.1007/BF00000786.

[22] FAO. Land use in agriculture by the numbers. Sustainable Food and Agriculture 2020. https://www.fao.org/sustainability/news/detail/en/c/1274219/.

[23] Minasny B, Malone BP, McBratney AB, Angers DA, Arrouays D, Chambers A, et al. Soil carbon 4 per mille. Geoderma 2017;292:59–86. https://doi.org/10.1016/j.geoderma.2017.01.002.

[24] Lessmann M, Ros GH, Young MD, de Vries W. Global variation in soil carbon sequestration potential through improved cropland management. Global Change Biology 2022;28:1162–77. https://doi.org/10.1111/gcb.15954.

[25] Zomer RJ, Bossio DA, Sommer R, Verchot LV. Global Sequestration Potential of Increased Organic Carbon in Cropland Soils. Sci Rep 2017;7:15554. https://doi.org/10.1038/s41598-017-15794-8.

[26] Blanco-Canqui H, Lal R. Crop Residue Removal Impacts on Soil Productivity and Environmental Quality. Critical Reviews in Plant Sciences 2009;28:139–63. https://doi.org/10.1080/07352680902776507.

[27] Fischer G, Prieler S, van Velthuizen H, Berndes G, Faaij A, Londo M, et al. Biofuel production potentials in Europe: Sustainable use of cultivated land and pastures, Part II: Land use scenarios. Biomass and Bioenergy 2010;34:173–87. https://doi.org/10.1016/j.biombioe.2009.07.009.

[28] Haase M, Rösch C, Ketzer D. GIS-based assessment of sustainable crop residue potentials in European regions. Biomass and Bioenergy 2016;86:156–71. https://doi.org/10.1016/j.biombioe.2016.01.020.

[29] Monforti F, Lugato E, Motola V, Bodis K, Scarlat N, Dallemand JF. Optimal energy use of agricultural crop residues preserving soil organic carbon stocks in Europe. Renewable and Sustainable Energy Reviews 2015;44:519–29. https://doi.org/10.1016/j.rser.2014.12.033.

[30] Panoutsou C, Kyriakos M. Sustainable biomass availability in the EU, to 2050. Concawe; 2021.

[31] Scarlat N, Fahl F, Lugato E, Monforti-Ferrario F, Dallemand JF. Integrated and spatially explicit assessment of sustainable crop residues potential in Europe. Biomass and Bioenergy 2019;122:257–69. https://doi.org/10.1016/j.biombioe.2019.01.021.

[32] Blanco-Canqui H. Crop Residue Removal for Bioenergy Reduces Soil Carbon Pools: How Can We Offset Carbon Losses? Bioenerg Res 2013:14.

[33] Woolf D, Lehmann J, Ogle S, Kishimoto-Mo AW, McConkey B, Baldock J. Greenhouse Gas Inventory Model for Biochar Additions to Soil. Environ Sci Technol 2021:acs.est.1c02425. https://doi.org/10.1021/acs.est.1c02425.

[34] Hansen JH, Hamelin L, Taghizadeh-Toosi A, Olesen JE, Wenzel H. Agricultural residues bioenergy potential that sustain soil carbon depends on energy conversion pathways 2020:12.

[35] Woolf D, Lehmann J. Modelling the long-term response to positive and negative priming of soil organic carbon by black carbon. Biogeochemistry 2012:13.

[36] Lefebvre D, Williams A, Meersmans J, Kirk GJD, Sohi S, Goglio P, et al. Modelling the potential for soil carbon sequestration using biochar from sugarcane residues in Brazil. Sci Rep 2020;10:19479. https://doi.org/10.1038/s41598-020-76470-y.

[37] Qambrani NA, Rahman MdM, Won S, Shim S, Ra C. Biochar properties and eco-friendly applications for climate change mitigation, waste management, and wastewater treatment: A review. Renewable and Sustainable Energy Reviews 2017;79:255–73. https://doi.org/10.1016/j.rser.2017.05.057.

[38] Ippolito JA, Cui L, Kammann C, Wrage-Mönnig N, Estavillo JM, Fuertes-Mendizabal T, et al. Feedstock choice, pyrolysis temperature and type influence biochar characteristics: a comprehensive meta-data analysis review. Biochar 2020;2:421–38. https://doi.org/10.1007/s42773-020-00067-x.

[39] Ponnusamy VK, Nagappan S, Bhosale RR, Lay C-H, Duc Nguyen D, Pugazhendhi A, et al. Review on sustainable production of biochar through hydrothermal liquefaction: Physico-chemical properties and applications. Bioresource Technology 2020;310:123414. https://doi.org/10.1016/j.biortech.2020.123414.

[40] Kumar R, Strezov V, Weldekidan H, He J, Singh S, Kan T, et al. Lignocellulose biomass pyrolysis for bio-oil production: A review of biomass pre-treatment methods for production of drop-in fuels. Renewable and Sustainable Energy Reviews 2020;123:109763. https://doi.org/10.1016/j.rser.2020.109763.

[41] Gollakota ARK, Kishore N, Gu S. A review on hydrothermal liquefaction of biomass. Renewable and Sustainable Energy Reviews 2018;81:1378–92. https://doi.org/10.1016/j.rser.2017.05.178.

[42] Molino A, Larocca V, Chianese S, Musmarra D. Biofuels Production by Biomass Gasification: A Review. Energies 2018;11:811. https://doi.org/10.3390/en11040811.

[43] Mathanker A, Das S, Pudasainee D, Khan M, Kumar A, Gupta R. A Review of Hydrothermal Liquefaction of Biomass for Biofuels Production with a Special Focus on the Effect of Process Parameters, Co-Solvents, and Extraction Solvents. Energies 2021;14:4916. https://doi.org/10.3390/en14164916.

[44] Zabed H, Sahu JN, Suely A, Boyce AN, Faruq G. Bioethanol production from renewable sources: Current perspectives and technological progress. Renewable and Sustainable Energy Reviews 2017;71:475–501. https://doi.org/10.1016/j.rser.2016.12.076.

[45] Joseph S, Cowie AL, Van Zwieten L, Bolan N, Budai A, Buss W, et al. How biochar works, and when it doesn't: A review of mechanisms controlling soil and plant responses to biochar. GCB Bioenergy 2021:gcbb.12885. https://doi.org/10.1111/gcbb.12885.

[46] Teglia C, Tremier A, Martel J-L. Characterization of Solid Digestates: Part 1, Review of Existing Indicators to Assess Solid Digestates Agricultural Use. Waste Biomass Valor 2011;2:43–58. https://doi.org/10.1007/s12649-010-9051-5.

[47] Alkharabsheh HM, Seleiman MF, Battaglia ML, Shami A, Jalal RS, Alhammad BA, et al. Biochar and Its Broad Impacts in Soil Quality and Fertility, Nutrient Leaching and Crop Productivity: A Review. Agronomy 2021;11:993. https://doi.org/10.3390/agronomy11050993.

[48] Ameloot N, Graber ER, Verheijen FGA, De Neve S. Interactions between biochar stability and soil organisms: review and research needs: Biochar stability and soil organisms. Eur J Soil Sci 2013;64:379–90. https://doi.org/10.1111/ejss.12064.

[49] Möller K. Effects of anaerobic digestion on soil carbon and nitrogen turnover, N emissions, and soil biological activity. A review. Agron Sustain Dev 2015;35:1021–41. https://doi.org/10.1007/s13593-015-0284-3.

[50] Nkoa R. Agricultural benefits and environmental risks of soil fertilization with anaerobic digestates: a review. Agron Sustain Dev 2014;34:473–92. https://doi.org/10.1007/s13593-013-0196-z.

[51] Wang J, Xiong Z, Kuzyakov Y. Biochar stability in soil: meta-analysis of decomposition and priming effects. GCB Bioenergy 2016;8:512–23. https://doi.org/10.1111/gcbb.12266.

[52] Han L, Sun K, Yang Y, Xia X, Li F, Yang Z, et al. Biochar's stability and effect on the content, composition and turnover of soil organic carbon. Geoderma 2020;364:114184. https://doi.org/10.1016/j.geoderma.2020.114184.

[53] Singh N, Abiven S, Torn MS, Schmidt MWI. Fire-derived organic carbon turnover in soils on a centennial scale. Biogeochemistry: Soils; 2011. https://doi.org/10.5194/bgd-8-12179-2011.

[54] Spokas KA. Review of the stability of biochar in soils: predictability of O:C molar ratios. Carbon Management 2010:15.

[55] Lehmann J, Abiven S, Kleber M, Pan G, Singh BP, Sohi SP, et al. Persistence of biochar in soil. Biochar for Environmental Management. 2nd Edition, 2015, p. 48.

[56] Zimmerman A, Gao B. The Stability of Biochar in the Environment. In: Ladygina N, Rineau F, editors. Biochar and Soil Biota, CRC Press; 2013, p. 1–40. https://doi.org/10.1201/b14585-2.

[57] Brassard P, Godbout S, Hamelin L. Framework for consequential life cycle assessment of pyrolysis biorefineries: A case study for the conversion of primary forestry residues. Renewable and Sustainable Energy Reviews 2021;138:110549. https://doi.org/10.1016/j.rser.2020.110549.

[58] Rakesh N, Dasappa S. A critical assessment of tar generated during biomass gasification - Formation, evaluation, issues and mitigation strategies. Renewable and Sustainable Energy Reviews 2018;91:1045–64. https://doi.org/10.1016/j.rser.2018.04.017.

[59] Di Gianfilippo M, Costa G, Pantini S, Allegrini E, Lombardi F, Astrup TF. LCA of management strategies for RDF incineration and gasification bottom ash based on experimental leaching data. Waste Management 2016;47:285–98. https://doi.org/10.1016/j.wasman.2015.05.032.

[60] Zhang Y, Kusch-Brandt S, Salter AM, Heaven S. Estimating the Methane Potential of Energy Crops: An Overview on Types of Data Sources and Their Limitations. Processes 2021;9:1565. https://doi.org/10.3390/pr9091565.

[61] Andrade C, Albers A, Zamora-Ledezma E, Hamelin L. Database to determine the Carbon recalcitrance and carbon conversion rate to bioeconomy coproducts 2022. https://doi.org/10.48531/JBRU.CALMIP/WYWKIQ.

[62] Lehmann J, Cowie A, Masiello CA, Kammann C, Woolf D, Amonette JE, et al. Biochar in climate change mitigation. Nat Geosci 2021;14:883–92. https://doi.org/10.1038/s41561-021-00852-8.

[63] Melo LCA, Lehmann J, Carneiro JS da S, Camps-Arbestain M. Biochar-based fertilizer effects on crop productivity: a meta-analysis. Plant Soil 2022;472:45–58. https://doi.org/10.1007/s11104-021-05276-2.

[64] Cayuela ML, Oenema O, Kuikman PJ, Bakker RR, Van Groenigen JW. Bioenergy by-products as soil amendments? Implications for carbon sequestration and greenhouse gas emissions: C and N dynamics from bioenergy by-products in soil. GCB Bioenergy 2010:no-no. https://doi.org/10.1111/j.1757-1707.2010.01055.x.

[65] Panoutsou C, Germer S, Karka P, Papadokostantakis S, Kroyan Y, Wojcieszyk M, et al. Advanced biofuels to decarbonise European transport by 2030: Markets, challenges, and policies that impact their successful market uptake. Energy Strategy Reviews 2021;34:100633. https://doi.org/10.1016/j.esr.2021.100633.

[66] IPCC. Climate Change and Land: an IPCC special report on climate change, desertification, land degradation, sustainable land management, food security, and greenhouse gas fluxes in terrestrial ecosystems. IPCC; 2019.

[67] Söderqvist H. Carbon Stability of Biochar -Methods for assessment and indication. KTH Royal Institute of Technology; 2019.

[68] Leng L, Huang H, Li H, Li J, Zhou W. Biochar stability assessment methods: A review. Science of The Total Environment 2019;647:210–22. https://doi.org/10.1016/j.scitotenv.2018.07.402.

[69] Naisse C, Girardin C, Lefevre R. Effect of physical weathering on the carbon sequestration potential of biochars and hydrochars in soil. GCB Bioenergy 2014:9.

[70] Jindo K, Sonoki T. Comparative Assessment of Biochar Stability Using Multiple Indicators. Agronomy 2019;9:254. https://doi.org/10.3390/agronomy9050254.

[71] Budai A, Zimmerman AR, Cowie AL, Webber JBW, Singh BP, Glaser B, et al. Biochar Carbon Stability Test Method: An assessment of methods to determine biochar carbon stability 2014:30.

[72] Kuzyakov Y, Bogomolova I, Glaser B. Biochar stability in soil: Decomposition during eight years and transformation as assessed by compound-specific 14C analysis. Soil Biology and Biochemistry 2014;70:229–36. https://doi.org/10.1016/j.soilbio.2013.12.021.

[73] Leng L, Xu X, Wei L, Fan L, Huang H, Li J, et al. Biochar stability assessment by incubation and modelling: Methods, drawbacks and recommendations. Science of The Total Environment 2019;664:11–23. https://doi.org/10.1016/j.scitotenv.2019.01.298.

[74] Watson RT, Noble IR, Bolin B, Ravindranath NH, Verardo DJ, Dokken DJ. Chapter 4: Additional Human-Induced Activities. Land Use, Land-Use Change and Forestry - Special Report, UK: IPCC; 2000.

[75] Campbell EE. Current developments in soil organic matter modeling and the expansion of model applications: a review. Environ Res Lett 2015:37.

[76] Farina R, Sándor R, Abdalla M, Álvaro-Fuentes J, Bechini L, Bolinder MA, et al. Ensemble modelling, uncertainty and robust predictions of organic carbon in long-term bare-fallow soils 2020:25. https://doi.org/10.1111/gcb.15441.

[77] Bellocchi G, Rivington M, Matthews K, Acutis M. Deliberative processes for comprehensive evaluation of agroecological models. A review. Agron Sustain Dev 2015;35:589–605. https://doi.org/10.1007/s13593-014-0271-0.

[78] Brilli L, Bechini L, Bindi M, Carozzi M, Cavalli D, Conant R, et al. Review and analysis of strengths and weaknesses of agro-ecosystem models for simulating C and N fluxes. Science of The Total Environment 2017;598:445–70. https://doi.org/10.1016/j.scitotenv.2017.03.208.

[79] Manzoni S, Porporato A. Soil carbon and nitrogen mineralization: Theory and models across scales. Soil Biology and Biochemistry 2009;41:1355–79. https://doi.org/10.1016/j.soilbio.2009.02.031.

[80] Cavalli D, Bellocchi G, Corti M, Marino Gallina P, Bechini L. Sensitivity analysis of C and N modules in biogeochemical crop and grassland models following manure addition to soil. Eur J Soil Sci 2019:ejss.12793. https://doi.org/10.1111/ejss.12793.

[81] Sándor R, Ehrhardt F, Grace P, Recous S, Smith P, Snow V, et al. Ensemble modelling of carbon fluxes in grasslands and croplands. Field Crops Research 2020;252:107791. https://doi.org/10.1016/j.fcr.2020.107791.

[82] Parton WJ, Schimel DS, Cole CV, Ojima DS. Analysis of Factors Controlling Soil Organic Matter Levels in Great Plains Grasslands. Soil Science Society of America Journal 1987;51:1173–9. https://doi.org/10.2136/sssaj1987.03615995005100050015x.

[83] Parton WJ, Ojima DS, Cole CV, Schimel DS. A general model for soil organic matter dynamics: sensitivity to litter chemistry, texture and management. Quantitative Modeling of Soil Forming Processes 1994;39:147–67.

[84] Li C, Frolking S, Frolking TA. A model of nitrous oxide evolution from soil driven by rainfall events: 1. Model structure and sensitivity. Journal of Geophysical Research: Atmospheres 1992;97:9759–76. https://doi.org/10.1029/92JD00509.

[85] Williams JR, Jones CA, Dyke PT. A modeling approach to determining the relationship between erosion and soil productivity [EPIC, Erosion-Productivity Impact Calculator, mathematical models]. Trans ASAE, 1984.

[86] Hansen S, Jensen HE, Nielsen NE, Svendsen H. DAISY: Soil Plant Atmosphere System Model. Copenhagen: The National Agency for Environmental Protection; 1990.

[87] Keating BA, Carberry PS, Hammer GL, Probert ME, Robertson MJ, Holzworth D, et al. An overview of APSIM, a model designed for farming systems simulation. European Journal of Agronomy 2003;18:267–88. https://doi.org/10.1016/S1161-0301(02)00108-9.

[88] Brisson N, Mary B, Ripoche D, Jeuffroy M-H, Ruget F, Nicoullaud BB, et al. STICS: a generic model for the simulation of crops and their water and nitrogen balances. I. Theory and parameterization applied to wheat and corn. Agronomie 1998;18:311.

[89] Franko U, Oelschlägel B, Schenk S. Simulation of temperature-, water- and nitrogen dynamics using the model CANDY. Ecological Modelling 1995;81:213–22. https://doi.org/10.1016/0304-3800(94)00172-E.

[90] Krinner G, Viovy N, de Noblet-Ducoudré N, Ogée J, Polcher J, Friedlingstein P, et al. A dynamic global vegetation model for studies of the coupled atmosphere-biosphere system: DVGM FOR COUPLED CLIMATE STUDIES. Global Biogeochem Cycles 2005;19. https://doi.org/10.1029/2003GB002199.

[91] Coleman K, Jenkinson DS. RothC-26.3 - A Model for the turnover of carbon in soil. In: Powlson DS, Smith P, Smith JU, editors. Evaluation of Soil Organic Matter Models, Berlin, Heidelberg: Springer Berlin Heidelberg; 1996, p. 237–46. https://doi.org/10.1007/978-3-642-61094-3_17.

[92] Andriulo A, Mary B, Guerif J. Modelling soil carbon dynamics with various cropping sequences on the rolling pampas. Agronomie 1999;19:365–77. https://doi.org/10.1051/agro:19990504.

[93] Petersen BM, Olesen JE, Heidmann T. A flexible tool for simulation of soil carbon turnover. Ecological Modelling 2002;151:1–14. https://doi.org/10.1016/S0304-3800(02)00034-0.

[94] Goglio P, Smith WN, Grant BB, Desjardins RL, McConkey BG, Campbell CA, et al. Accounting for soil carbon changes in agricultural life cycle assessment (LCA): a review. Journal of Cleaner Production 2015;104:23–39. https://doi.org/10.1016/j.jclepro.2015.05.040.

[95] Bruun EW. Effects of slow and fast pyrolysis biochar on soil C and N turnover dynamics. Soil Biology 2012:7.

[96] Mohan D, Pittman CU, Steele PH. Pyrolysis of wood/biomass for bio-oil: A critical review. Energy and Fuels 2006;20:848–89. https://doi.org/10.1021/ef0502397.

[97] Lammens T. Advanced Biofuels from Fast Pyrolysis Bio-Oil. BTG Bioliquids B.V. 2021.

[98] Tomczyk A. Biochar physicochemical properties: pyrolysis temperature and feedstock kind effects. Rev Environ Sci Biotechnol 2020:25.

[99] Heidenreich S, Foscolo PU. New concepts in biomass gasification. Progress in Energy and Combustion Science 2015;46:72–95. https://doi.org/10.1016/j.pecs.2014.06.002.

[100] Roos CJ. Clean heat and power using biomass gasification for industrial and agricultural projects. Northwest CHP Application Center; 2010.

[101] Farzad S, Mandegari MA, Görgens JF. A critical review on biomass gasification, co-gasification, and their environmental assessments. Biofuel Res J 2016;3:483–95. https://doi.org/10.18331/BRJ2016.3.4.3.

[102] Hanchate N, Ramani S, Mathpati CS, Dalvi VH. Biomass gasification using dual fluidized bed gasification systems: A review. Journal of Cleaner Production 2021;280:123148. https://doi.org/10.1016/j.jclepro.2020.123148.

[103] Ahmad M, Ok YS, Kim B-Y, Ahn J-H, Lee YH, Zhang M, et al. Impact of soybean stover- and pine needle-derived biochars on Pb and As mobility, microbial community, and carbon stability in a contaminated agricultural soil. Journal of Environmental Management 2016;166:131–9. https://doi.org/10.1016/j.jenvman.2015.10.006.

[104] Molino A, Chianese S, Musmarra D. Biomass gasification technology: The state of the art overview. Journal of Energy Chemistry 2016;25:10–25. https://doi.org/10.1016/j.jechem.2015.11.005.

[105] Lodato C, Hamelin L, Tonini D, Astrup TF. Towards sustainable methane supply from local bioresources: Anaerobic digestion, gasification, and gas upgrading. Applied Energy 2022;323:119568. https://doi.org/10.1016/j.apenergy.2022.119568.

[106] Widjaya ER, Chen G, Bowtell L, Hills C. Gasification of non-woody biomass: A literature review. Renewable and Sustainable Energy Reviews 2018;89:184–93. https://doi.org/10.1016/j.rser.2018.03.023.

[107] Jahirul M, Rasul M, Chowdhury A, Ashwath N. Biofuels Production through Biomass Pyrolysis —A Technological Review. Energies 2012;5:4952–5001. https://doi.org/10.3390/en5124952.

[108] Zhu Z, Toor SS, Rosendahl L, Yu D, Chen G. Influence of alkali catalyst on product yield and properties via hydrothermal liquefaction of barley straw. Energy 2015;80:284–92. https://doi.org/10.1016/j.energy.2014.11.071.

[109] Seehar TH, Toor SS, Sharma K, Nielsen AH, Pedersen TH, Rosendahl LA. Influence of process conditions on hydrothermal liquefaction of eucalyptus biomass for biocrude production and investigation of the inorganics distribution. Sustainable Energy Fuels 2021;5:1477–87. https://doi.org/10.1039/D0SE01634A.

[110] Watson J, Wang T, Si B, Chen W-T, Aierzhati A, Zhang Y. Valorization of hydrothermal liquefaction aqueous phase: pathways towards commercial viability. Progress in Energy and Combustion Science 2020;77:100819. https://doi.org/10.1016/j.pecs.2019.100819.

[111] Knorr D, Lukas J, Schoen P. Production of Advanced Biofuels via Liquefaction - Hydrothermal Liquefaction Reactor Design: April 5, 2013. 2013. https://doi.org/10.2172/1111191.

[112] Schievano A, Adani F, Tambone F, D'Imporzano G, Scaglia B, Genevini PL. What is the digestate? 2009.

[113] Xu F, Li Y. Biomass Digestion. Encyclopedia of Sustainable Technologies, Elsevier; 2017, p. 197–204. https://doi.org/10.1016/B978-0-12-409548-9.10108-3.

[114] Fagerström A, Al Seadi T, Rasi S, Briseid T, Murphy JD, IEA Bioenergy Task 37, et al. The role of anaerobic digestion and biogas in the circular economy. 2018.

[115] Rigby H, Smith RS. New markets for digestate from anaerobic digestion. WRAP 2011.

[116] Sarker S, Lamb JJ, Hjelme DR, Lien KM. A Review of the Role of Critical Parameters in the Design and Operation of Biogas Production Plants. Applied Sciences 2019;9:1915. https://doi.org/10.3390/app9091915.

[117] Bušić A, Marđetko N, University of Zagreb, Faculty of Food Technology and Biotechnology, Pierottijeva 6, 10000 Zagreb, Croatia, Kundas S, Belarussian National Technical University, Power Plant Construction and Engineering Services Faculty, Nezavisimosti Ave. 150, 220013 Minsk, Belarus, Morzak G, et al. Bioethanol Production from Renewable Raw Materials and its Separation and Purification: a Review. Food Technol Biotechnol 2018;56. https://doi.org/10.17113/ftb.56.03.18.5546.

[118] Alotaibi KD, Schoenau JJ. Enzymatic activity and microbial biomass in soil amended with biofuel production byproducts. Applied Soil Ecology 2011;48:227–35. https://doi.org/10.1016/j.apsoil.2011.03.002.

[119] Arora R, Sharma NK, Kumar S, Sani RK. Chapter 9 - Lignocellulosic Ethanol: Feedstocks and Bioprocessing. Bioethanol Production from Food Crops. Sustainable Sources, Interventions, and Challenges, Academic Press; 2019, p. 21.

[120] You S, Ok YS, Chen SS, Tsang DCW, Kwon EE, Lee J, et al. A critical review on sustainable biochar system through gasification: Energy and environmental applications. Bioresource Technology 2017;246:242–53. https://doi.org/10.1016/j.biortech.2017.06.177.

[121] Valin S, Ravel S, Pons de Vincent P, Thiery S, Miller H, Defoort F, et al. Fluidised Bed Gasification of Diverse Biomass Feedstocks and Blends—An Overall Performance Study. Energies 2020;13:3706. https://doi.org/10.3390/en13143706.

[122] Cao L, Zhang C, Chen H, Tsang DCW, Luo G, Zhang S, et al. Hydrothermal liquefaction of agricultural and forestry wastes: state-of-the-art review and future prospects. Bioresource Technology 2017;245:1184–93. https://doi.org/10.1016/j.biortech.2017.08.196.

[123] Elliott DC, Sealock LJ, Phelps MR, Neuenschwander GG, Hart TR. Development of a catalytic system for gasification of wet biomass. 1993. https://doi.org/10.2172/10120451.

[124] Birman J, Burdloff J, De Peufeilhoux H, Erbs G, Feniou M, Lucille P-L. Geographical analysis of biomethane potential and costs in Europe in 2050. ENGIE; 2021.

[125] Wang W, Lee D-J. Valorization of anaerobic digestion digestate: A prospect review. Bioresource Technology 2021;323:124626. https://doi.org/10.1016/j.biortech.2020.124626.

[126] Rosentrater KA, Lehman RM. Predicting Stability of Distiller's Wet Grains (DWG) with Color Analysis. Food Bioprocess Technol 2010:9.

[127] European Commission. Building up the future, technology status and reliability of the value chains: sub group on advanced biofuels : sustainable transport forum. LU: European Commission. Directorate General for Mobility and Transport.; 2018.

[128] He Y, Zhou X, Jiang L, Li M, Du Z, Zhou G, et al. Effects of biochar application on soil greenhouse gas fluxes: a meta-analysis. GCB Bioenergy 2017;9:743–55. https://doi.org/10.1111/gcbb.12376.

[129] Zimmerman AR, Gao B, Ahn M-Y. Positive and negative carbon mineralization priming effects among a variety of biochar-amended soils. Soil Biology and Biochemistry 2011;43:1169–79. https://doi.org/10.1016/j.soilbio.2011.02.005.

[130] Herath HMSK, Camps-Arbestain M, Hedley MJ, Kirschbaum MUF, Wang T, van Hale R. Experimental evidence for sequestering C with biochar by avoidance of CO_2 emissions from original feedstock and protection of native soil organic matter. GCB Bioenergy 2015;7:512–26. https://doi.org/10.1111/gcbb.12183.

[131] Zimmerman AR. Abiotic and Microbial Oxidation of Laboratory-Produced Black Carbon (Biochar). Environ Sci Technol 2010;44:1295–301. https://doi.org/10.1021/es903140c.

[132] Singh M, Sarkar B, Sarkar S, Churchman J, Bolan N, Mandal S, et al. Stabilization of Soil Organic Carbon as Influenced by Clay Mineralogy. Advances in Agronomy 2018;148:52. https://doi.org/10.1016/bs.agron.2017.11.001.

[133] Bai X, Huang Y, Ren W, Coyne M, Jacinthe P, Tao B, et al. Responses of soil carbon sequestration to climate-smart agriculture practices: A meta-analysis. Glob Change Biol 2019;25:2591–606. https://doi.org/10.1111/gcb.14658.

[134] Ventura M, Alberti G, Viger M, Jenkins JR, Girardin C, Baronti S, et al. Biochar mineralization and priming effect on SOM decomposition in two European short rotation coppices. GCB Bioenergy 2015;7:1150–60. https://doi.org/10.1111/gcbb.12219.

[135] Wu M. Soil organic carbon content affects the stability of biochar in paddy soil 2016:8.

[136] Zhang Q, Xiao J, Xue J, Zhang L. Quantifying the Effects of Biochar Application on Greenhouse Gas Emissions from Agricultural Soils: A Global Meta-Analysis. Sustainability 2020;12:3436. https://doi.org/10.3390/su12083436.

[137] Knoblauch C, Maarifat A-A, Pfeiffer E-M, Haefele SM. Degradability of black carbon and its impact on trace gas fluxes and carbon turnover in paddy soils. Soil Biology and Biochemistry 2011;43:1768–78. https://doi.org/10.1016/j.soilbio.2010.07.012.

[138] IPCC. 2019 Refinement to the 2006 IPCC Guidelines for National Greenhouse Gas Inventories - Appendix4: Method for Estimating the Change in Mineral Soil Organic Carbon Stocks from Biochar Amendments: Basis for Future Methodological Development. IPCC; 2019.

[139] Hansen V, Müller-Stöver D, Imparato V, Krogh PH, Jensen LS, Dolmer A, et al. The effects of straw or straw-derived gasification biochar applications on soil quality and crop productivity: A farm case study. Journal of Environmental Management 2017;186:88–95. https://doi.org/10.1016/j.jenvman.2016.10.041.

[140] Hansen V, Müller-Stöver D, Munkholm LJ, Peltre C, Hauggaard-Nielsen H, Jensen LS. The effect of straw and wood gasification biochar on carbon sequestration, selected soil fertility indicators and functional groups in soil: An incubation study. Geoderma 2016;269:99–107. https://doi.org/10.1016/j.geoderma.2016.01.033.

[141] Askri A, Laville P, Trémier A, Houot S. Influence of Origin and Post-treatment on Greenhouse Gas Emissions After Anaerobic Digestate Application to Soil. Waste Biomass Valor 2016;7:293–306. https://doi.org/10.1007/s12649-015-9452-6.

[142] Levavasseur F, Mary B, Christensen BT, Duparque A, Ferchaud F, Kätterer T, et al. The simple AMG model accurately simulates organic carbon storage in soils after repeated application of exogenous organic matter. Nutrient Cycling in Agroecosystems 2020:15.

[143] Chen R, Blagodatskaya E, Senbayram M, Blagodatsky S, Myachina O, Dittert K, et al. Decomposition of biogas residues in soil and their effects on microbial growth kinetics and enzyme activities. Biomass and Bioenergy 2012;45:221–9. https://doi.org/10.1016/j.biombioe.2012.06.014.

[144] Thomsen IK, Olesen JE, Møller HB, Sørensen P, Christensen BT. Carbon dynamics and retention in soil after anaerobic digestion of dairy cattle feed and faeces. Soil Biology and Biochemistry 2013;58:82–7. https://doi.org/10.1016/j.soilbio.2012.11.006.

[145] Béghin-Tanneau R, Guérin F, Guiresse M, Kleiber D, Scheiner JD. Carbon sequestration in soil amended with anaerobic digested matter. Soil and Tillage Research 2019;192:87–94. https://doi.org/10.1016/j.still.2019.04.024.

[146] Cayuela ML, Kuikman P, Bakker R, van Groenigen JW. Tracking C and N dynamics and stabilization in soil amended with wheat residue and its corresponding bioethanol by-product: a ^{13} C/ ^{15} N study. GCB Bioenergy 2014;6:499–508. https://doi.org/10.1111/gcbb.12102.

[147] Bera T, Vardanyan L, Inglett KS, Reddy KR, O'Connor GA, Erickson JE, et al. Influence of select bioenergy by-products on soil carbon and microbial activity: A laboratory study. Science of The Total Environment 2019;653:1354–63. https://doi.org/10.1016/j.scitotenv.2018.10.237.

[148] Parnaudeau V, Condom N, Oliver R, Cazevieille P, Recous S. Vinasse organic matter quality and mineralization potential, as influenced by raw material, fermentation and concentration processes. Bioresource Technology 2008:10.

[149] Hansen V, Müller-Stöver D, Ahrenfeldt J, Holm JK, Henriksen UB, Hauggaard-Nielsen H. Gasification biochar as a valuable by-product for carbon sequestration and soil amendment. Biomass and Bioenergy 2015;72:300–8. https://doi.org/10.1016/j.biombioe.2014.10.013.

[150] Ventura M, Alberti G, Panzacchi P, Vedove GD, Miglietta F, Tonon G. Biochar mineralization and priming effect in a poplar short rotation coppice from a 3-year field experiment. Biol Fertil Soils 2019;55:67–78. https://doi.org/10.1007/s00374-018-1329-y.

[151] Mondini C, Cayuela ML, Sinicco T, Fornasier F, Galvez A, Sánchez-Monedero MA. Modification of the RothC model to simulate soil C mineralization of exogenous organic matter. Biogeochemistry: Soils; 2017. https://doi.org/10.5194/bg-2016-551.

[152] Foereid B, Lehmann J, Major J. Modeling black carbon degradation and movement in soil. Plant Soil 2011;345:223–36. https://doi.org/10.1007/s11104-011-0773-3.

[153] Pulcher R, Balugani E, Ventura M, Greggio N, Marazza D. Inclusion of biochar in a C dynamics model based on observations from an 8-year field experiment. SOIL 2022;8:199–211. https://doi.org/10.5194/soil-8-199-2022.

[154] Bonten LTC, Elferink EV, Zwart K. Tool to assess effects of bio-energy on nutrient losses and soil organic matter 2014:22.

[155] Dil M, Oelbermann M. Evaluating the long-term effects of pre-conditioned biochar on soil organic carbon in two southern Ontario soils using the century model. Chapter 13. In: Oelbermann M, editor. Sustainable agroecosystems in climate change mitigation, The Netherlands: Wageningen Academic Publishers; 2014, p. 249–68. https://doi.org/10.3920/978-90-8686-788-2_13.

[156] Lychuk TE, Izaurralde RC, Hill RL, McGill WB, Williams JR. Biochar as a global change adaptation: predicting biochar impacts on crop productivity and soil quality for a tropical soil with the Environmental Policy Integrated Climate (EPIC) model. Mitig Adapt Strateg Glob Change 2015;20:1437–58. https://doi.org/10.1007/s11027-014-9554-7.

[157] Archontoulis SV, Huber I, Miguez FE, Thorburn PJ, Rogovska N, Laird DA. A model for mechanistic and system assessments of biochar effects on soils and crops and trade-offs. GCB Bioenergy 2016;8:1028–45. https://doi.org/10.1111/gcbb.12314.

[158] Prays N, Dominik P, Sänger A, Franko U. Biogas residue parameterization for soil organic matter modeling. PLoS ONE 2018;13:e0204121. https://doi.org/10.1371/journal.pone.0204121.

[159] Witing F, Prays N, O'Keeffe S, Gründling R, Gebel M, Kurzer H-J, et al. Biogas production and changes in soil carbon input - A regional analysis. Geoderma 2018;320:105–14. https://doi.org/10.1016/j.geoderma.2018.01.030.

[160] Whitman T. Biochar as carbon sequestration mechanism: decomposition, modelling, and policy. M.Sc. Cornell University, 2010.

[161] Lashermes G, Nicolardot B, Parnaudeau V, Thuriès L, Chaussod R, Guillotin ML, et al. Indicator of potential residual carbon in soils after exogenous organic matter application. European Journal of Soil Science 2009;60:297–310. https://doi.org/10.1111/j.1365-2389.2008.01110.x.

[162] Van Soest PJ, Wine RH. Use of Detergents in the Analysis of Fibrous Feeds. IV. Determination of Plant Cell-Wall Constituents. Journal of Association of Official Analytical Chemists 1967;50:50–5. https://doi.org/10.1093/jaoac/50.1.50.

[163] Mondini C, Cayuela ML, Sinicco T, Fornasier F, Galvez A, Sánchez-Monedero MA. Soil C Storage Potential of Exogenous Organic Matter at Regional Level (Italy) Under Climate Change Simulated by RothC Model Modified for Amended Soils. Front Environ Sci 2018;6:144. https://doi.org/10.3389/fenvs.2018.00144.

[164] Magdoff FR, Bartlett RJ. Soil pH Buffering Revisited. Soil Science Society of America Journal 1985;49:145–8. https://doi.org/10.2136/sssaj1985.03615995004900010029x.

[165] Adams WA. The Effect of Organic Matter on the Bulk and True Densities of Some Uncultivated Podzolic Soils. Journal of Soil Science 1973;24:10–7. https://doi.org/10.1111/j.1365-2389.1973.tb00737.x.

[166] Clivot H, Mouny J-C, Duparque A, Dinh J-L, Denoroy P, Houot S, et al. Modeling soil organic carbon evolution in long-term arable experiments with AMG model. Environmental Modelling & Software 2019;118:99–113. https://doi.org/10.1016/j.envsoft.2019.04.004.

3. CHAPTER 3: SOC modeling for the bioeconomy in temperate contexts – French case study

The crop residue conundrum

3. CHAPTER 3: SOC modeling for the bioeconomy in temperate contexts – French case study

3.1 Context

This chapter targets the following research questions and objectives:

1. **RQ2**. How much additional biomass is available if bioeconomy coproducts are returned to soils, compared to an approach not considering the bioeconomy/recalcitrance effect?
2. **RO2.** Adapt a soil model to evaluate the long-term SOC dynamics of harvesting crop residues for the bioeconomy while returning the bioeconomy coproducts to soils.
3. **RO3**. Perform spatially explicit assessments of C-neutral harvest potential of crop residue to supply the bioeconomy at national level in temperate and tropical contexts, represented by France and Ecuador, respectively.

Key findings

- The soil model AMG has been adapted to include pyrochar, gaschar, hydrochar, digestate, and bioethanol molasses.
- A SOC – bioeconomy modelling framework, applicable to different spatial resolutions and geographical areas has been developed in this chapter.
- A surplus potential of 71 -125 PJ could be available in France if a C-neutral harvest entailing the return of bioeconomy coproducts is applied to maintain the SOC stocks at the same level as in a reference scenario where crop residues are not harvested.

The content of this chapter was published in Applied Energy in 2023 and is reproduced with permission of the journal. The numbering of the sections, figures, tables, and appendixes are kept as in the published version.

***Citation**: Christhel Andrade Díaz, Hugues Clivot, Ariane Albers, Ezequiel Zamora-Ledezma, Lorie Hamelin, The crop residue conundrum: Maintaining long-term soil organic carbon stocks while reinforcing the bioeconomy, compatible endeavors?, Applied Energy, Volume 329, 2023, 120192, ISSN 0306-2619, https://doi.org/10.1016/j.apenergy.2022.120192.*

List of figures

List of tables

Applied Energy 329 (2023) 120192

Contents lists available at ScienceDirect

Applied Energy

journal homepage: www.elsevier.com/locate/apenergy

The crop residue conundrum: Maintaining long-term soil organic carbon stocks while reinforcing the bioeconomy, compatible endeavors?

Christhel Andrade Díaz [a,b,*], Hugues Clivot [c], Ariane Albers [a], Ezequiel Zamora-Ledezma [d], Lorie Hamelin [a]

[a] Toulouse Biotechnology Institute (TBI), INSA, INRAE UMR792, and CNRS UMR5504, Federal University of Toulouse, 135 Avenue de Rangueil, F-31077, Toulouse, France
[b] Department of Chemical, Biotechnological and Food Processes, Faculty of Mathematical, Physics and Chemistry Sciences. Universidad Técnica de Manabí (UTM), 130150 Portoviejo, Ecuador
[c] Université de Reims Champagne-Ardenne, INRAE, FARE, UMR A 614, Reims, France
[d] Faculty of Agriculture Engineering. Universidad Técnica de Manabí (UTM), 13132 Lodana, Ecuador

HIGHLIGHTS

- The interaction between soil organic carbon, crop residues, and bioeconomy conversion was investigated.
- The AMG soil carbon model was adapted to include five bioeconomy coproducts.
- Crop residues' potential for the bioeconomy is spatially explicit and depends on the conversion pathway.
- Returning biochar to soils can maintain and even double SOC stocks if all the available crop residues are harvested.
- Additional 71 – 225 PJ biomass are available for the bioeconomy with coproducts returning to soils.

GRAPHICAL ABSTRACT

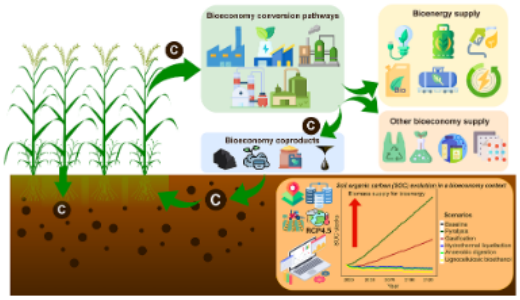

ARTICLE INFO

Keywords:
SOC modeling
Recalcitrance
Biochar
Hydrochar
Bioethanol molasses
Digestate

ABSTRACT

Crop residues are a key bulk feedstock for supplying renewable carbon for bioenergy production and the broader bioeconomy without compromising food security. However, it is frequently advised to harvest no more than half of this potential to ensure the preservation of soil organic carbon (SOC) stocks. In this study, we challenge this recommendation and demonstrate that the crop residue potential allowing to maintain long-term SOC stocks is spatially differentiated and strongly dependent upon the bioeconomy conversion pathway for which it is intended. We assessed the interaction between the residues' usage for the bioeconomy and the maintenance of SOC stocks over 100 years by considering the coproduct return to soils from five bioeconomy pathways: pyrolysis, gasification, hydrothermal liquefaction, anaerobic digestion, and lignocellulosic ethanol production. To compare the long-term SOC changes from these scenarios against a reference where crop residues are unharvested, we developed a novel framework, applicable to any site or region, by coupling a SOC model that includes recalcitrant organic matter deriving from a bioeconomy calculation module. The adapted SOC model considers the recalcitrance to degradation of each coproduct, while the bioeconomy module determines the share of carbon

* Corresponding author.
E-mail address: andraded@insa-toulouse.fr (C. Andrade Díaz).

https://doi.org/10.1016/j.apenergy.2022.120192
Received 22 July 2022; Received in revised form 23 September 2022; Accepted 16 October 2022
Available online 14 November 2022

The crop residue conundrum: maintaining long-term soil organic carbon stocks while reinforcing the bioeconomy, compatible endeavors?

Christhel Andrade Díaz,*[a,b] Hugues Clivot, [c] Ariane Albers, [a] Ezequiel Zamora-Ledezma [d] and Lorie Hamelin [a]

[a] Toulouse Biotechnology Institute (TBI), INSA, INRAE UMR792, and CNRS UMR5504, Federal University of Toulouse, 135 Avenue de Rangueil, F-31077, Toulouse, France.

[b] Department of Chemical, Biotechnological and Food Processes, Faculty of Mathematical, Physics and Chemistry Sciences. Universidad Técnica de Manabí (UTM), 130150 Portoviejo, Ecuador.

[c] Université de Reims Champagne-Ardenne, INRAE, FARE, UMR A 614, Reims, France.

[d] Faculty of Agriculture Engineering. Universidad Técnica de Manabí (UTM), 13132 Lodana, Ecuador.

* Corresponding author: andraded@insa-toulouse.fr. ORCID: 0000-0002-2448-6186

Highlights

- The interaction between soil organic carbon, crop residues, and bioeconomy conversion was investigated.
- The AMG soil carbon model was adapted to include five bioeconomy coproducts.
- Crop residues' potential for the bioeconomy is spatially explicit and depends on the conversion pathway.
- The return of biochar to soils can maintain and even double SOC stocks if all the available crop residues are harvested compared to non-harvesting.
- Additional 71 – 225 PJ biomass are available for the bioeconomy with coproducts returning to soils.

Abstract

Crop residues are a key bulk feedstock for supplying renewable carbon for bioenergy production and the broader bioeconomy without compromising food security. However, it is frequently advised to harvest no more than half of this potential to ensure the preservation of soil organic carbon (SOC) stocks. In this study, we challenge this recommendation and demonstrate that the crop residue potential allowing to maintain long-term SOC stocks is spatially differentiated and strongly dependent upon the bioeconomy conversion pathway for which it is intended. We assessed the interaction between the residues' usage for the bioeconomy and the maintenance of SOC stocks over 100 years by considering the coproduct return to soils from five bioeconomy pathways: pyrolysis, gasification, hydrothermal liquefaction, anaerobic digestion, and lignocellulosic ethanol production. To compare the long-term SOC changes from these scenarios against a reference where crop residues are unharvested, we developed a novel framework, applicable to any site or region, by coupling a SOC model that includes recalcitrant organic matter deriving from a bioeconomy calculation module. The adapted SOC model considers the recalcitrance to degradation of each coproduct, while the bioeconomy module determines the share of carbon from the crop residues ending in the coproducts. The framework was tested and applied with a high spatial resolution (> 60,000 simulation units) to the context of French croplands over the period of 2020–2120, with state-of-the-art sensitivity analyses. The case study results revealed, among others, that an additional crop residue potential equivalent to 71–225 PJ (pathway-dependent) could be available for the French bioeconomy without SOC decreases, compared to applying a stringent removal limit of 31.5%.

Keywords

SOC modeling, recalcitrance, biochar, hydrochar, bioethanol molasses, digestate

Graphical abstract

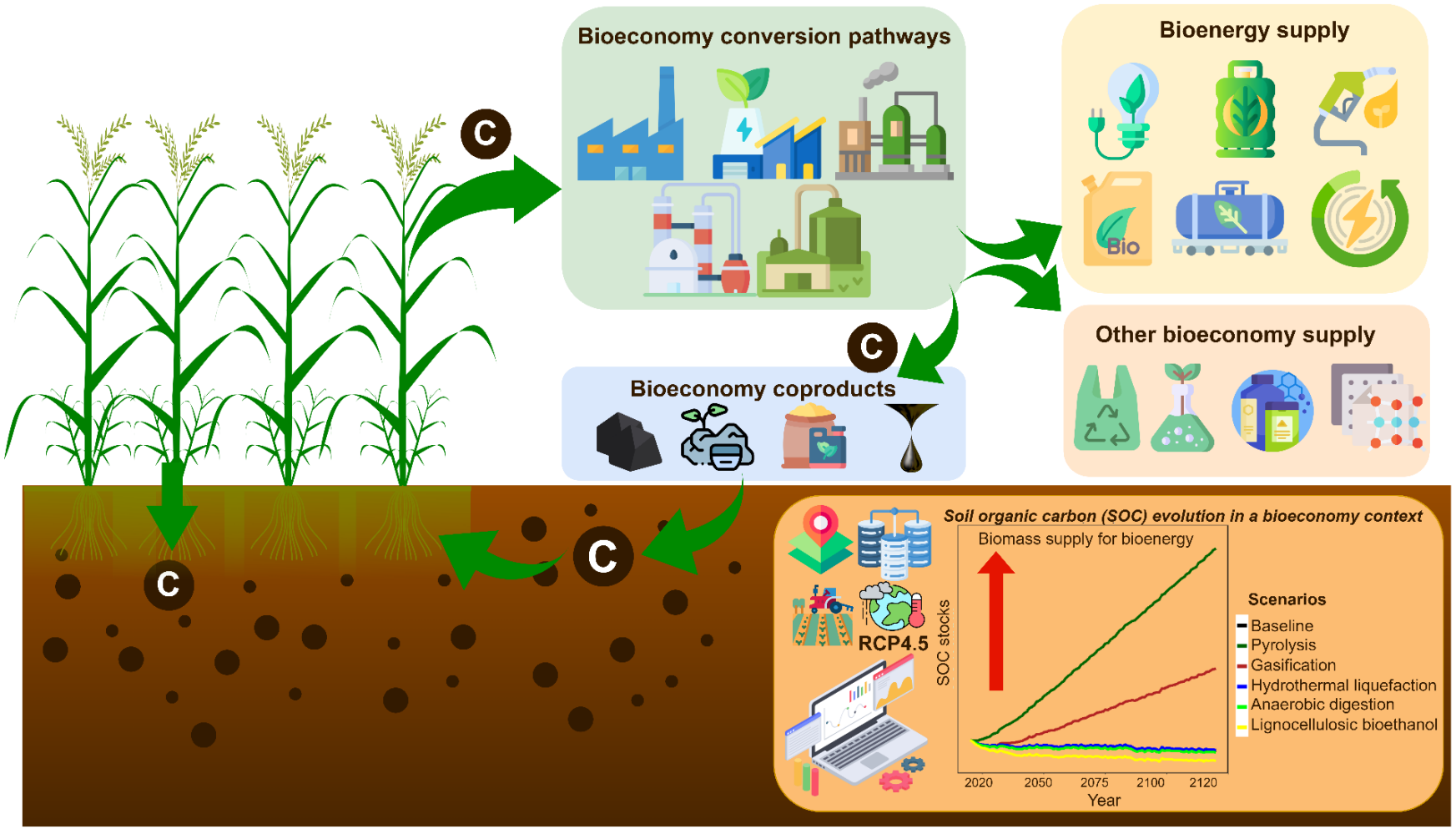

Fig 0. Graphical Abstract of Chapter 3.

List of abbreviations

2GEtOH	Second-generation bioethanol
AD	Anaerobic digestion
APCU	Agricultural pedoclimatic units
APSIM	Agricultural production systems simulator
BAU	Business as usual
CA	Active SOC pool
CANDY	Carbon and nitrogen dynamics model
Cc	Carbon conversion
CERFACS	European Center for Advanced Research and Training in Scientific Computing
C_L	Carbon labile
CNRM	National Meteorological Research Centre
C_R	Carbon recalcitrance
C_S	Stable SOC pool
DM	Dry matter
EOM	Exogenous organic matter
EPIC	Environmental Policy Integrated Climate Model
FOM	Fresh organic matter
h	Retention coefficient
h_a	Retention coefficient for the active SOC pool
HI	Harvest Index
h_s	Retention coefficient for the stable SOC pool
HTL	Hydrothermal liquefaction
k	Mineralization rate constant
MRT	Mean residence time
OM	Organic matter
PCU	Pedoclimatic units
RCP	Representative concentration pathway
RE	Extra-root carbon
RothC	Rothamsted carbon model
RP	Proportion of carbon in the harvested product
RR	Root carbon
RS	Proportion of carbon in the above-ground residues
SA	Sensitivity analysis
SI	Supplementary Information
SOC	Soil organic carbon
STICS	Multidisciplinary simulator for standard crops
SU	Simulation units

1. Introduction

In alignment with the Paris Agreement [1], the European Union [2], the United Kingdom [3], China [4], and other countries [5] have set the goal of achieving carbon neutrality by the mid-century. According to the International Renewable Energy Agency, a global bioenergy share of at least 21% of the total energy consumption by 2030 is required, to meet the Paris target of limiting global average temperature increases well below 2°C above pre-industrial levels. [6,7] This implies a myriad of solutions to avoid the use of fossil carbon (C), such as increased electrification, use of bioenergy for energy services that cannot be immediately electrified, use of biomass and direct air carbon capture to supply carbon feedstock for energy and non-energy services, as well as ensuring the cycling of the carbon already in circulation within the technosphere. [8] Additionally, it involves increasing carbon sinks, among others in agricultural soils, including grasslands.

Crop residues are leftovers from harvest operations and are a key feedstock supplying renewable carbon. In fact, crop residues are widely available in large quantities, at low costs, and with short harvest cycles, besides not directly competing with food security. [9,10] In Europe alone, a theoretical potential of 3800 PJ y^{-1} was estimated [11] which is equivalent to the gross annual electricity generation of France and Germany combined. [12]

Crop residues include a variety of streams, such as dry stalks and leaves of (i) cereals, (ii) oilseed crops, and (iii) stems and leaves from tubers. [13] Current uses of crop residues include animal fodder and bedding, mushroom production, or mulch to preserve soil moisture, among others. [11,14]

When left unharvested on the field (i.e., ploughed back into the soils), crop residues can contribute to soil organic carbon (SOC) and play a crucial role in the long-term quality, nutrient balance, and agronomic functions of soils. Increasing removal rates reduces the soil organic matter inputs. This creates a tradeoff between the use of crop residue for the bioeconomy (here defined as the supply of both energy and non-energy services without fossil carbon) and SOC stock maintenance. [15,16] To address this trade-off, various studies have suggested limiting the removal to rates between 15% and 60% of the theoretical harvest potential (depending on the crop type). [14,17–20] These restrictions significantly reduce the supply of renewable carbon from crop residues to the bioeconomy and bioenergy production systems.

Bioeconomy processes convert the degradable portion of biomass into a main product (e.g., bio-oil, biogas, biomaterials), while the more degradation-resistant portion remains a coproduct (e.g., biochar, digestate, molasses). This coproduct can be applied to soils as exogenous organic matter (EOM) to maintain or enhance their SOC stocks. [21] EOM is a heterogeneous material and can be composed of recalcitrant and labile fractions. The labile fractions tend to be mineralized (i.e., as CO_2 emissions) within 1 – 2 years following their application to the soil, while the recalcitrant fractions exhibit longer mean residence times (MRT [22]) in soils, typically ranging on the decadal scale, promoting SOC storage. [22,23] SOC stock evolution depends on the coproduct applied as well as the site-specific conditions and cropping systems (i.e., a combination of soil properties, climate, crop rotations, and other management practices). [24,25] Spatially explicit considerations are thus needed in order to address the conundrum between long-term SOC storage and the supply of a renewable C feedstock to the bioeconomy.

Soil C models can simulate long-term SOC dynamics, taking into consideration different cropping systems, soil properties, and climates. [26] The decomposition of organic matter involves complex processes influenced by the characteristics of the biomass, eventual stabilization treatment, degree of recalcitrance, pedoclimatic conditions, and interactions with the soil microbiota, among others. An accurate prediction of the coproducts' carbon persistence in soils is therefore challenging. [27,28] Some soil models have been adapted to simulate the return of bioeconomy coproducts into soils. This includes, for instance, RothC [29–31], Century [32], APSIM [33], and EPIC [34] for biochar; CTOOL [35], AMG [36], CANDY [37], and RothC [28] for digestate. RothC has also been adapted to consider bioethanol coproducts, such as the non-fermentable residue [28], and was used to develop BioEsoil, a tool to evaluate the effect of residues from bioenergy processes (i.e., gasification and incineration) on soil organic matter. [38] However, these studies are coproduct-specific and often limited to very specific parcels.

For instance, the interaction between harvesting crop residues to supply the bioeconomy and its effect on long-term SOC stocks has been explored in Hansen et al. [35], where the authors found that for Danish soils, the amount of crop residues that can be harvested for pathways that do not involve C returns is one-fourth of what can be harvested on average if the digestate is returned to soils. Hansen et al. [35] assessed only one bioeconomy conversion pathway (i.e., anaerobic digestion) and used a rather coarse spatial representation of Danish croplands limited to two types of crop rotations and three types of soils. Similarly, Woolf and Lehmann [30] predicted that removing 50% of crop residues for bioenergy in three specific locations of Colombia, Kenya, and

the USA could lead to SOC stock increases of 30–60% in 100 years when the corresponding biochar is applied to soils. To date, only a few studies have used a soil model that includes different EOM inputs coupled with large-scale spatial information. One notable example is the study of Mondini et al. [39], where eight types of EOMs (including a variety of bioethanol, biodiesel, and anaerobic digestion coproducts) were simulated for Italy. However, the study of Mondini et al. [39] did not focus on the removal-return relationship of crop residues per se, but on the input of 1 t C ha^{-1} of various EOMs to increase SOC. Moreover, their study excludes any char coproduct from thermochemical conversion pathways (these being a high focus in the perspective of carbon sequestration [40]), and the relevance of their recalcitrance data is questionable, being based on a single incubation experiment with a duration of only 7-37 days.

To our knowledge, no study has addressed the effect on SOC stocks from crop residue removal and C return to the soil from various bioeconomy conversion pathways involving the return of recalcitrant carbon, to determine the crop residues' potential made available for the bioeconomy. In this work, we challenge the idea that the biomass potential from crop residues must be limited by a given removal rate to maintain organic carbon in arable soils. Instead, we propose that such potential is deeply intertwined with the use of residual biomass within the bioeconomy and return of the coproduct to the soil. This is based on the rationale that coproducts returned to soil are more recalcitrant to degradation than the original raw biomass.

This study aims at: (i) further understanding the cause-effect link between the “C-neutral harvest” of crop residues (defined below) and the usage of these residues for bioenergy and the broader bioeconomy; and (ii) addressing how this cause-effect link differs among the major existing bioeconomy pathways where a C return to the soil is possible. Therefore, this study proposes a methodology to evaluate the maximum amount of crop residue to harvest for supplying the bioeconomy while assuring the maintenance or enhancement of SOC stocks in croplands. Doing so, it provides a novel framework based on a soil C model including specific composition and recalcitrance characteristics for various bioeconomy coproducts, to spatially explicitly assess the interplay between preserving SOC stocks and supplying renewable carbon for the bioeconomy and bioenergy provision.

We modeled the SOC evolution of all arable topsoils (0–30 cm depth) in France, with and without crop residue harvest for different bioeconomy pathways, as an illustrative case study. The study is limited to determining the spatially explicit crop residues' potential to deliver C for bioeconomy systems and its impact on SOC stock evolution. Therefore, the implications related to

the produced energy and non-energy services (e.g., considering energy and product substitutions, induced gaseous and non-gaseous emissions, etc.), were out of the scope of this work. The term "C-neutral harvest" is herein employed to designate situations where the long-term (here defined as 100 years) SOC stocks of a given bioeconomy management do not decrease, compared to a reference situation where crop residues are directly incorporated into soils. It encompasses a similar vision to what previous studies have referred to as "sustainable harvest" [14] but explicitly differentiates between what it covers (quantification of SOC stocks only) and what it disregards (e.g., other aspects of long-term sustainability such as biodiversity or soil fertility).

2. Methods

The modeling framework assesses the long-term SOC stock effects of using crop residues for different bioeconomy technologies, considering different management practices on arable topsoils. It quantifies the amount of harvestable crop residues that can be removed from fields for bioeconomy, while an alternative coproduct is returned to meet the condition of maintaining or even increasing the SOC stock levels, as compared to a reference situation where residues are left on the field. The bioeconomy scenarios considered here include bio-oil production by pyrolysis and hydrothermal liquefaction (HTL), biogas production by gasification and anaerobic digestion (AD), and second-generation bioethanol (2GEtOH) production by alcoholic fermentation of lignocellulosic biomass. The five technologies studied represent bioenergy pathways, but their output products can also be used as biomaterials or feedstock for the chemical industry, thereby covering the broader bioeconomy. This is why the term bioeconomy is used through the study rather than the more limiting bioenergy scope.

The framework is based on high-resolution data on climate, soil, and agricultural practices and a SOC model that simulates the SOC stock changes in cropping systems receiving coproduct inputs with specific recalcitrance properties. It is here applied to specific spatial units of metropolitan France, with a temporal scope of 100 years, over the years 2020-2120. While the framework is applied to a specific case study, it may be replicated for any region.

The state of C in arable soils, agricultural practices, soil, and climate at the beginning of the timeframe is here referred to as the initial conditions. Two developments over the timeframe are considered: (i) a business as usual (BAU) scenario reflecting current practices where part of the harvestable crop residues (ca. 46%; details in SI1.2) are already being exported for livestock (as bedding and fodder) and the rest is left on fields, and (ii) bioeconomy scenarios, which are similar

to the BAU, except that the share of crop residues left on fields is instead harvested, used in five different bioenergy technologies, and partly returned to fields as a coproduct. The BAU is a measure-stick against which the five bioeconomy scenarios are contrasted.

The physicochemical properties of soil and the future meteorological variables (further detailed in sections 2.2 and 2.3) are the same for the BAU and bioeconomy scenarios. Similarly, the same rotations, farming management practices (section 2.2), and crop yields (SI1.2) are repeated cycle after cycle. The impact on crop yields from replacing the raw biomass with stabilized EOM was excluded to emphasize the effect of crop residue removal alone. [41] The effects on soil water resulting from replacing crop residues with bioeconomy coproducts, as well as the change in nutrient input to soils, were also not considered. The technical harvestable rate and amount of crop residues already used for livestock are crop-dependent (Table SI1.1) and are assumed to remain constant during the modeling timeframe.

The structure of the framework consists of four main modules (Fig. 1), further detailed in the subsequent subsections: description of the simulation units (Module 1); definition of the bioeconomy scenarios, carbon conversion from residues to coproducts, and recalcitrance of coproducts (Module 2); modeling SOC stock changes and collecting related input data (Module 3); and sensitivity analysis (Module 4). The process was automated using R [42], and the scripts for the model calculations, as well as the input and processed data, are all documented in an open repository in Andrade et al. [43].

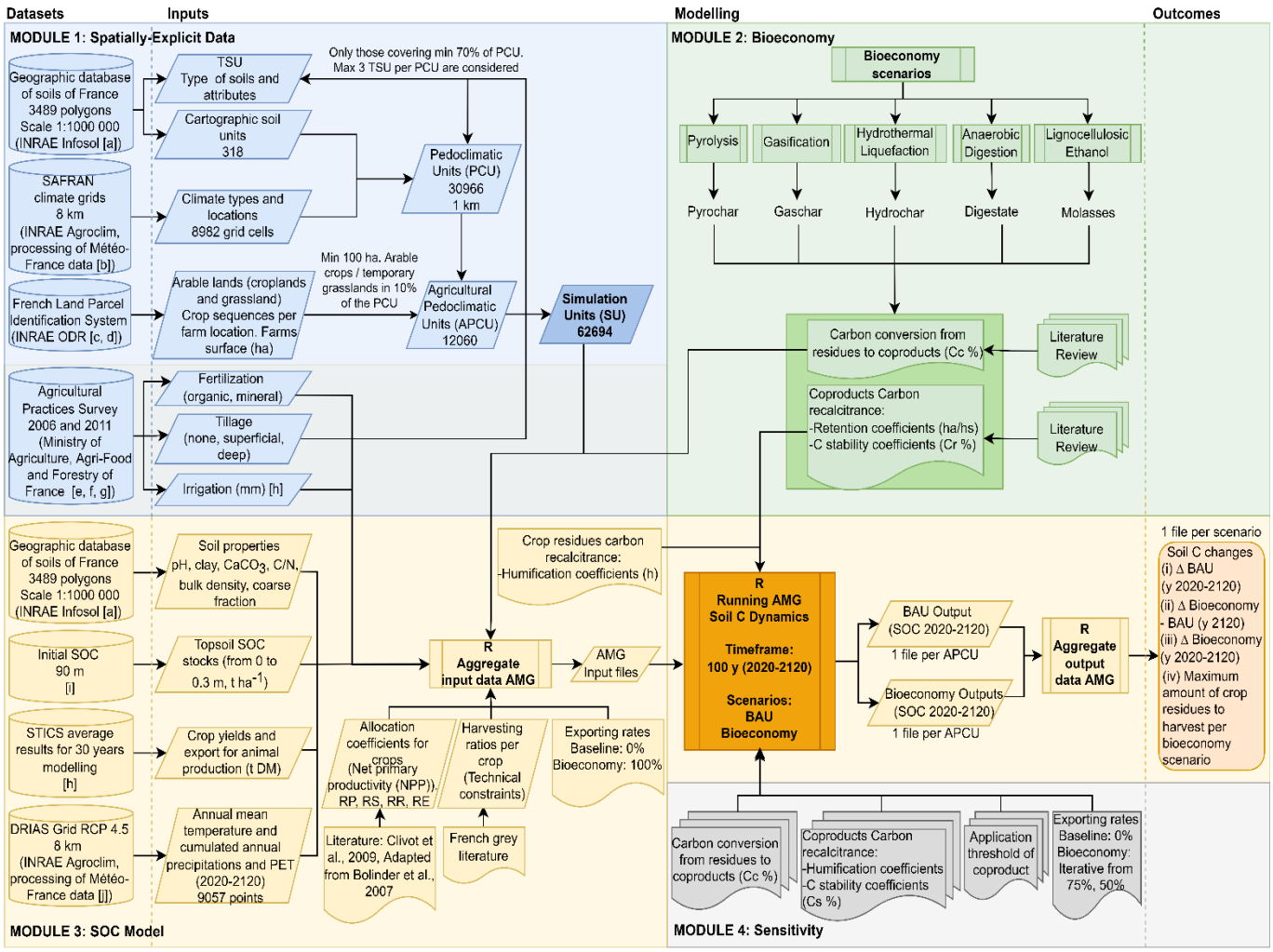

Fig. 1 Spatially explicit modeling framework, as applied to metropolitan France, to quantify the long-term soil organic carbon difference between crop residues left on land and their harvest for five distinct bioeconomy pathways, with the return of the coproduct. [a] [194], [b] Based on Durand et al.[195] after adaptation of Launay et al.[19], [c] [196], [d] [197], [e] [198], [f] [199], [g] [200], [h] [19], [i] [201], [j] CNRM-CERFACS-CM5--CNRM/ALADIN 63. Model GCM / RCM – correction ADAMONT. Institution : Météo-France/French National Center for Meteorological Research, [202]. PET: Potential Evapotranspiration, RP: Relative Carbon allocation coefficient for the agricultural product, RR: Relative Carbon allocation coefficient for roots, RS: Relative Carbon allocation coefficient for straw or any post-harvest residue, RE: Relative Carbon allocation coefficient for extra root material, BAU: Business-as-Usual, SOC: Soil organic carbon, STICS: Soil-crop model used in Launay et al.[19], DRIAS: Spatially explicit database for France projections of climate scenarios, SAFRAN: Spatially explicit database for France climate. *Figure legend*: Cylinders: database, parallelogram: data input, rectangle: process, rectangle with inner bars: process embedded within another process, curved bottom rectangle: manually input data sets, rounded rectangle: output.

2.1 Module 1: Spatially explicit data

The aim of Module 1 is to define representative simulation units (SU) for the case under study, reflecting the variety of soils, climates, crop rotations, and farming practices in a spatially explicit manner. Here, Module 1 is entirely built upon the study of Launay et al. [46], launched within the frame of the French efforts within the international 4p1000 initiative [54], acknowledged as the most comprehensive and updated spatially explicit representation of cropping systems in France.

Launay et al. [46] defined a set of fundamental concepts briefly described as follows : pedoclimatic units (PCU) are defined as a unique combination of soil properties (coarse fraction, clay content, pH, etc.) and meteorological variables (temperature, precipitation, and potential evapotranspiration) (French climate and soil types are identified in SI1.1). When found on arable lands, these are referred to as agricultural PCUs (APCU). French APCUs combine soil-mapping units (1:1000,000; [44]) and the French SAFRAN climate grids (8x8 km; [45,55]) with identified crop rotations per PCU retrieved from the French Land Parcel Identification System. [48,56] A total of 12,060 APCUs with more than 100 ha of agricultural area, at least 10% having arable crops and/or temporary grasslands, were identified. This selection represents 84% of the French cropland.

The crop rotations selected by Launay et al. [46] include 12 different crops, temporary grasslands, and cover crops (further detailed in SI1.2). Winter wheat is the most representative crop, providing 65% of the available residual biomass (dry matter). These rotations cover 4.79 Mha and were deemed a fair representation of the 18.35 Mha of French arable crops and temporary grasslands in 2006-2012. Farming practices —involving organic fertilization, cover crops, irrigation, tillage, and current use of crop residues— were determined from a survey conducted by the French Ministry of Agriculture, Agri-Food, and Forestry over the period 2006-2011 [51,57].

The combination of APCUs, crop rotations, and farming practices yielded 62,694 simulation units (SI1.1). Further details on the crop rotation and yields are presented in SI1.2.

2.2 Module 2: Bioeconomy scenarios

All the bioeconomy scenarios involve two key parameters that are crucial to answering the research questions of this study, and both depend upon the feedstock and process conditions. These parameters are (i) the amount of C from the harvested crop residues (of a given SU; Fig. 1) that will end up in the coproducts (of a given bioeconomy pathway) returned to fields, and (ii) the coproduct C recalcitrance to degradation. The former is hereafter referred to as carbon conversion (C_C) and the latter as carbon recalcitrance (C_R). Recalcitrance represents the most stable

biochemical fraction of organic products. Here, C_R is the fraction of the coproduct that cannot be readily mineralized and that decomposes slower than the more labile fraction of the organic coproduct. [22] Labile carbon (C_L) is defined as 1-C_R and is assumed to be entirely processed by soil microorganisms within one year.

Thermochemical processes, such as gasification, pyrolysis, and HTL, exposing biomass to elevated temperatures for long periods of time, produce biochar with more aromatic compounds than for processes operated at low temperatures and short times. Coproducts with higher content of aromatics are related to higher degrees of recalcitrance. [59–61] Various studies have determined that the recalcitrant fraction of biochar exhibits MRTs from decades to millennia. [22,62] HTL, which is carried out at lower temperatures than pyrolysis and gasification, using relatively wet feedstock, produces a less recalcitrant char than pyrolysis. Gasification, which employs higher temperatures than HTL and pyrolysis, yields char with a higher degree of recalcitrance than pyrolysis char. [63]

In this work, only the return of the char produced in each thermochemical technology is considered, and other coproducts generated (e.g., tar, ashes) are excluded. To avoid confusion between the coproducts assessed in each scenario, we refer to pyrolysis, gasification, and HTL char as pyrochar, gaschar, and hydrochar, respectively.

Biochemical processes, such as AD and 2GEtOH, are carried out using microorganisms and lower temperatures than thermochemical technologies. The outputs of AD are biogas and digestate, while alcoholic fermentation produces bioethanol and a residue that is often separated into a lignin-rich solid and a liquid fraction known as molasses. The solid coproduct is typically combusted for heat and power, involving no carbon fraction to be returned to soils. Therefore, for the biochemical pathways, we consider only digestate (from AD) and molasses (from 2GEtOH production) as EOMs. The carbon stability and soil MRT of molasses and digestate are considered lower than for chars (Table 1).

The C_R and C_C presented in Table 1 stem from a comprehensive compilation and data reconciliation of over 600 records from laboratory assays, field trials, and modeling experiments involving a wide variety of feedstock, including crop residues, as detailed in Andrade et al. [63,64]. To the extent possible, the C_C and C_R values used herein were derived from studies involving straw-like feedstock. Table 1 summarizes the C_C and C_R values considered, along with the identification of the coproduct returned to fields and the other products generated during the conversion process for each scenario. The bioeconomy conversion pathways are further described in SI1.3.

Table 1. Overview of the bioeconomy scenarios considered in the study, and implications in terms of the carbon conversion and carbon recalcitrance parameters.

Scenario	Process Conditions	Coproduct returned to soils	Other products generated[a]	Carbon conversion (C_C)[b] %	Carbon recalcitrance (C_R)[b] %	MRT[c] Years	Key process reference[h]
BAU	Crops residues left on soil	None	None	n/a	n/a	n/a	[46]
Pyrolysis[d]	350 – 700 °C, from seconds to 2h, typically fed with a biomass DM>90%	Pyrochar[e]	**Bio-oil**, non-condensable gases	44 [34 – 54]	95 [90 – 99]	> 100	[22,65,66]
Gasification	600 – 1200°C dry gasification. 300-550°C hydrothermal gasification, typically fed with a DM>90%	Gaschar	**Syngas**, tar, ashes	20 [14 – 25]	95 [90 – 99]	> 100	[67–69]
Hydrothermal Liquefaction[f]	180 – 400°C, use of K_2CO_3 catalyst to enhance bio-oil production; typically fed with a DM<20%	Hydrochar	**Bio-oil**, non-condensable gases	31 [12 – 45]	83 [80 – 96]	< 26	[70,71]
Anaerobic[g] Digestion	Mesophilic conditions (30 – 50°C). 1-3 months. Typically, wet digestion, with DM in the digester<35%	Digestate	**Biogas**	33 [30 – 40]	68 [58 – 77]	< 26	[72–74]
Lignocellulosic bioethanol	Pretreatment, acid, and enzymatic hydrolysis, fermentation with *S. cerevisiae, purification by* distillation. The effluent is separated into a solid fraction and liquid molasses	Molasses	**Bioethanol**, solid fraction	24 [18 – 30]	45 [28 – 60]	< 26	[10,75,76]

DM: dry matter, n/a: not applicable, MRT: Mean residence time, C_C: carbon conversion, C_R: carbon recalcitrance. [a] The main product considered driving the investment in this bioeconomy scenario, under the specified conditions, is indicated in bold; [b] C_C: C fraction of initial crop residue transferred to the co-product returned to fields, C_R: C fraction of the coproduct allocated to the stable biochemical fraction. The values presented herein are averages from

Andrade et al. [63], based on a compilation of 188, 61, 135, 182, and 54 records, for pyrochar, gaschar, hydrochar, digestate, and molasses, respectively. Ranges in brackets represent quartiles 1 and 3. The labile fraction (C_L) is obtained as 1 - C_R; [c] The MRT is used within soil models and allows defining the fraction of C_R to allocate to the different soil organic carbon pools. Coproducts with C_R fractions exhibiting MRT of 7 – 26 years are considered to be slowly mineralized [77] in the soil model used in this study, while any coproduct with an MRT longer than 100 years are considered as virtually inert (see section 2.3). For this reason, MRTs are here expressed as <26 y or >100 y; [d] Pyrolysis can be classified as fast (300 – 500°C, seconds of retention time) or slow (500-700°C, minutes to hours). Slow conditions tend to favor the production of biochar, whereas a fast process is optimal for bio-oil production. From an economic standpoint, the pyrolysis scenario in this study aims to maximize the bio-oil yields, thus the process conditions of the studies included are those of a fast process when possible [65]. [e] Also commonly referred to as "biochar". [f] The use of catalysts, especially K_2CO_3 accelerates the water-gas shift reaction in low-temperature hydrothermal liquefaction processes, which yields higher rates of bio-oil (targeted product) than hydrochar. The use of catalysts tends to be more common [78], therefore, the C_C and C_R values stem from such process conditions. [g] Some simulation units involve the use of manure as an organic fertilizer. To keep the focus on the impacts from crop residues, we did not consider this manure to be digested. C_C accounts only for the carbon in crop residues transferred to the digestate. [h] Only key references are mentioned; the full compilation of reviewed studies is presented in Andrade et al. [63].

2.3 Module 3: Soil organic carbon model

Module 3 describes the SOC model used and the adaptations considered in this study, as well as how the bioeconomy scenarios have been compared to the BAU scenario.

2.3.1 AMG model: Overview

For both the BAU and bioeconomy scenarios, the evolution of topsoil SOC stocks (0-30 cm) was simulated with the AMGv2 SOC model, detailed in Clivot et al. [77]. AMG is a French SOC model, first described in Andriulo et al. [79], which simulates the carbon dynamics of agricultural topsoils at an annual timestep. The model successfully predicted the changes in SOC stocks of various cropping systems under different pedoclimatic conditions in France and Europe [77,80,81] and has notably been calibrated for 26 EOM types. [36] AMG splits the organic matter (OM) into three different pools (shown as boxes in Fig. 2). The fresh OM inputs from above- (crop residues) and below- (crop roots and root exudates) ground plant compartments, as well as inputs from EOM (e.g., manure, bioeconomy coproducts), represent the fresh organic matter (FOM) pool, which is assumed to be annually decomposed (Fig. 2a). The C in the FOM pool is labeled as C_{FOM}. The proportion of C_{FOM} incorporated into the active SOC pool (C_A) is determined by a retention coefficient (*h*). The fraction of C_{FOM} that does not enter C_A (1-*h*) is mineralized as CO_2. The C_A pool

is affected by a mineralization process following first-order kinetics with a *k* mineralization rate. The stable SOC pool (C_S) is set at 65% of the initial SOC by default and is considered inert during the simulation for sites with an arable land history. [77]

2.3.2 Model input data

AMG minimum input data comprises crop rotations, climate, soil physicochemical properties, initial SOC stocks, and farming practices (including the maximal soil tillage depth, irrigation water amounts, EOM inputs, and crop residue management). Crop rotation information includes annual yield, moisture content of the harvested product, harvest indexes (HI), and C allocation coefficients determining the proportion of C in the harvested product (RP), above-ground residues (RS), root C (RR), and extra-root C (RE) (Fig. 1; module 3). It also includes the fraction of residues that can be technically harvested per crop type.

Instead of calculating the absorbed C by the plant, an indirect method based on HI and allocation coefficients was used, as set out in the method proposed for calculating C inputs for AMGv2 [77], adapted from Bolinder et al. [82]. The technically harvestable fraction for each crop was also taken as defined in AMGv2 (further details in Table SI1.1) and varied from 55% to 91%. Meteorological data comprise the mean annual air temperature and the annual water balance, the latter being determined as the difference between the water inputs (accumulated precipitation and irrigation) and potential evapotranspiration. In this study, the spatially explicit meteorological data were retrieved for the years 2020 to 2100, from SICLIMA (last updated May 2013 [83]), for the RCP4.5 climate trajectory (Representative Concentration Pathway [84]), downscaled by the model CNRM-CERFACS-CM5/CNRM-ALADIN63. These projections were not available beyond 2100. Therefore, for the period from 2101 to 2120, average values from the last decade (i.e., from 2091 to 2100) were used.

Soil-related data include initial SOC stocks, pH, bulk density, coarse fraction, clay content, C:N ratio, and $CaCO_3$ content. Initial SOC stocks were retrieved from Mulder et al.[52] and used as processed by Launay et al. [46] to correspond to the APCU resolution, while the other soil parameters were retrieved from Jamagne et al. [44]. AMG also requires information regarding farming practices, as detailed in Module 1.

Default *h* values (FOM-dependent) given in AMG for crop residues and non-coproduct EOMs (e.g., animal manure) [36,77] were used, while for the bioeconomy, the *h* values of coproducts were determined individually. The actual mineralization rate (k) of the active SOC pool, which

depends on environmental response functions, is calculated for each year and each situation as defined in Clivot et al. [77].

2.3.3 AMG adapted for bioeconomy processes

We adapted the calculation method for C inputs and the model to include the C_C and C_R values of pyrochar, gaschar, hydrochar, digestate, and lignocellulosic bioethanol molasses. The adapted version of AMG allows determining the SOC evolution of the different bioeconomy scenarios by deriving retention coefficients from C_R values. The C input from the coproducts is determined using the initial C in the crop residues and the C_C coefficient.

We grouped the C_R values per coproduct as highly recalcitrant (pyrochar and gaschar) and less recalcitrant (hydrochar, digestate, and molasses), to define the C retention time in the soil associated with each coproduct. The recalcitrance and the MRT values in Table 1 were used to set the h coefficient per coproduct and allocate the C to the soil pools (C_A or C_S), respectively. Two retention coefficients were defined to differentiate between the fraction integrating the active pool (h_a) and the stable pool (h_s).

For the highly recalcitrant coproducts, with MRTs longer than the modeling timeframe, the C_R fraction (95%; Table 1) was considered virtually inert and was directly allocated into the stable pool as h_s (Fig 2b), while the labile fraction was assumed to be entirely lost as CO_2 and no h_a was considered. For the less recalcitrant coproducts hydrochar, digestate, and bioethanol molasses, we assumed that the labile fraction C_L (1-C_R; 17%, 32%, and 36%, respectively) was mineralized in the first year and the remaining recalcitrant fraction corresponded to h_a (here equivalent to C_R) and was fully allocated to the active pool (Fig. 2a). The derived h_a coefficient for the digestate (0.68) is close to the value of 0.65 proposed by Levavasseur et al. [36]. No reference allowing for a similar comparison was found for the other coproducts studied. The adaptation of AMG for the bioeconomy is further detailed in SI1.4.

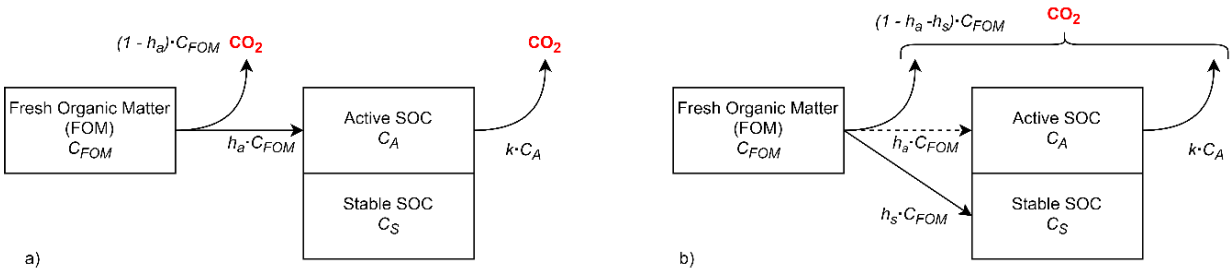

Fig. 2 AMG configuration implemented in this study (adapted from Clivot et al., [22]): a) AMG (for all streams but pyro- and gaschar), and b) adaptation of AMG (for pyro- and gaschar). SOC: Soil organic carbon, FOM: fresh organic matter, C_{FOM}: carbon in the fresh organic matter, $h_a.C_{FOM}$: fraction of C_{FOM} allocated to the active pool C_A, $h_s.C_{FOM}$: fraction of C_{FOM} allocated into the stable pool C_S, h_a: retention coefficient integrating a fraction of FOM into the active pool, h_s: retention coefficient integrating a fraction of FOM into the stable pool, k: mineralization rate constant, dotted line: FOM fraction allocated to the active SOC pool (see section 2.5).

2.3.4 AMG output analysis

The difference in changes of SOC stocks between a given bioeconomy scenario and the BAU was determined based on equation (1):

$$\Delta SOC_{\ bio-BAU}(\%) = \frac{SOC_{fbio} - SOC_{fBAU}}{SOC_{fBAU}} * 100 \qquad (1)$$

where $\Delta SOC_{bio\text{-}BAU}$ (%) is the percent change in SOC by shifting from BAU to bioeconomy, SOC_{fbio} corresponds to the SOC stocks at the end of the simulation, f, (here f = year 100) for the bioeconomy scenario, and SOC_{fBAU} is the SOC stocks at the end of the simulation for the BAU scenario. Positive values of $\Delta SOC_{bio\text{-}BAU}$ represent an increase in SOC stocks for the bioeconomy scenarios as compared to the BAU scenarios, while negative values reflect SOC losses from shifting to the bioeconomy.

For a given scenario (BAU or bioeconomy), the change in SOC stocks over 100 years was calculated as the final SOC stock minus the initial SOC, as shown in equation (2):

$$\Delta SOC_{0-100_i}(\%) = \frac{SOC_{100i} - SOC_0}{SOC_0} * 100 \qquad (2)$$

where $\Delta SOC_{0\text{-}100_i}$ (%) is the percent change of SOC stocks from the initial conditions (year 2020) until the end of the simulation (year 2120); SOC_0 corresponds to the initial SOC stocks and SOC_{100i} to the final SOC stocks (after 100 years), per scenario *i*.

The difference between the scenarios BAU and bioeconomy was calculated at a national scale as the total net SOC change (Mt C) for all the APCUs areas (equation (3)):

$$Total\ national\ \Delta SOCnet = \sum_i^j (SOC_{bio} - SOC_{BAU})_j * PondCoef_{SU_j xAPCU_i} * S_{APCU_i} \quad (3)$$

Total national ΔSOC net (in Mt C) is the sum of the difference between the SOC stocks under the bioeconomy and the BAU scenarios at the year 2120 per SU, times the ponderation coefficient ($PondCoef_{SUxAPCU}$) of the SU surface in the APCU surface, times the surface of the APCU (S_{APCU}). The total APCU surface is 14.89 Mha (SI1.1) but after the selection criteria in Module 1, only 3.5 Mha were included in the SUs. $PondCoef_{SUxAPCU}$ corresponds to the weight of a SU area in each APCU required to scale the SOC change per SU to the APCU scale (j=identity of the SU within a given APCU, i =identity of the APCU).

2.4 Module 4: Sensitivity Analysis

The characteristics and amount of carbon input have a great influence on SOC stock changes. [85] We performed a sensitivity analysis (SA) on the key parameters governing the amount of C returned to the soil, namely, C_C and C_R. As shown in Table 1, both C_C and C_R can vary within ranges conditioned by the process performance (itself depending on the specific process conditions) and the type of assay used for their determination (affecting C_R only). These ranges were retrieved from the review of Andrade et al.[63]. Here, the first and third quartiles of Andrade et al.[63] were used to set “low” and “high” levels for C_C and C_R for all coproducts (Table SI1.2). Combinations of low, mean, and high $C_C$and C_R were tested for a total of eight new sets of C_C and C_R combinations per scenario.

Since the long-term recalcitrance behavior of biochar is poorly understood due to the lack of long-term experimental evidence compared to reported half-lifetimes ranging from decadal- to millennial scales [86,87], an additional SA was performed on the procedure used to partition C_R within AMG SOC pools. It was performed for the pyrolysis scenario as a representative case of a highly recalcitrant EOM. In the initial method (section 2.3.3), the recalcitrant fraction was considered completely inert during the simulation and was fully allocated to the C_S pool. Yet, various studies suggest that the recalcitrant fraction may not be completely inert but rather follow a very slow decay rate. [59,66] Therefore, an alternative partition of the recalcitrant fraction between C_A and C_S was considered. To this end, it was considered that 75% of the C fraction remains after 100 years, meaning that 25% of the initial C is mineralized during the timeframe.

[63,86] Of this 25%, a fraction corresponds to a very labile fraction readily mineralized in the first year (4%) while the remaining corresponds to the mineralizable recalcitrant fraction, which is allocated to the C_A pool to be slowly mineralized. More details are provided in SI1.5. The values for pyrochar covered those found in the literature and suggested by the IPCC [88], which proposes that around 80% of C in biochar remains after 100 years for pyrolysis temperatures of 450-600°C. Table SI1.2 summarizes all the combinations investigated in the SA.

Excessive application of biochar may be toxic to soil microbiota, which may reduce plant growth and increase CH_4 and CO_2 emissions. [66,89] To avoid this negative effect, a last SA was performed to explore the effects of exporting all the available harvestable crop residues followed by the return of a lower amount of coproduct than generated. Accordingly, an extra scenario was modeled, limiting the soil application rate of pyro- and gaschar to not exceed a total of 50 Mg C ha^{-1} regularly applied over 100 years, as suggested by Woolf et al.[58] to allow char storage in the soil and ensure positive or neutral effects on plant yields. The analysis of alternative storage options for the portion of char not returned to the soil is out of the scope of this work.

Finally, for occurrences where $\Delta SOC_{bio\text{-}BAU}$ (equation (1)) was negative, the percentage of retrieved residues from fields was decreased in steps of 25% from its initial 100% value until 0%. These iterations were performed only for scenarios showing negative $\Delta SOC_{bio\text{-}BAU}$ to identify possible compromises between bioeconomy exports and SOC maintenance.

3. Results

3.1 Business as usual and bioeconomy scenarios over 100 years

The BAU scenario predicted a potential decrease of the topsoil SOC stocks by a mean of 2% (Table 2) in the APCUs over 100 years, which represents a C loss of 18 Mt C on the French national scale. This small number masks considerable spatial variation. For example, approximately 63% of the simulated areas show SOC stocks predicted to decline over 100 years, with a maximum decrease of 27% in some APCUs. APCUs displaying SOC stock increase may raise their levels by up to 85%, mainly in the Central and Western regions (Fig 3).

Crop residues are unavailable for the bioeconomy in 10% of the areas because they are already exported for other services. Therefore, these areas did not present any change in the bioeconomy scenarios compared with the BAU scenario. At the national level, the SOC change over 100 years associated

with each bioeconomy scenario varies greatly; it ranges from -34.9 (for molasses) to +774.2 Mt C (for pyrochar) (Table 2), a 22-fold difference reflecting the importance of the coproducts' C_C and C_R parameters.

The highest additional SOC storage, as compared to the BAU, was observed for pyrochar application (+106%), while the highest SOC loss was associated with molasses return (-4.4%) (Table 2). Note that SOC change is highly variable across the country (Fig. 4), reflecting the large variety of underlying pedoclimatic conditions and cropping practices. This applies to both the BAU (Fig. 3) and the bioeconomy scenarios (Fig. 4).

The simulations for the pyrolysis and gasification scenarios show enhanced SOC levels in all APCUs (100% of the areas) after 100 years, with the highest potential for SOC sequestration in the Southwestern and Central regions (Fig. 4. a,c). On the national level, the SOC stock improvement potential of pyrochar was two times that of gaschar, with a mean increase of 106% and 43%, respectively, after 100 years.

The return of hydrochar is shown to ensure SOC sequestration in 88% of the area (Table S2.4), with a maximum increase of 4%. On a national scale, this scenario represents an average SOC change of 1.1%, with a maximum increase of 4% (Table 2, Fig. 4). Digestate application was shown to slightly increase SOC stocks (to a maximum of 0.8%) in 50% of the simulated areas (Table 2), with an overall insignificant mean SOC loss of 0.1%, expected on a national scale over the timeframe, compared to the BAU scenario. For molasses, the expected SOC stocks after 100 years are lower than in the BAU scenario by a mean of 4.4% on a national scale, representing a potential SOC loss of 35 Mt C (Table 2).

For the scenarios depicting SOC losses (i.e., HTL, AD, and 2GEtOH), exporting rates were re-adjusted (75% and 50%). Decreases in the export rates did not influence the overall percentage of areas affected (Table S2.1), thus no lower exporting values were tested.

3.2 Key results for overall carbon returns

The Southwest of France tends to exhibit the largest SOC changes (both positive and negative) among the different scenarios, while the SOC changes in the Northwest tend to be lower (Fig 4). Digestate may contribute to building up SOC stocks in the North-Central area of France, with predicted losses in the Southwestern and Northern regions. For the HTL scenario, SOC losses are predicted to occur, but in the Northern region.

Compared to the current practice of leaving the crop residues on the field to preserve SOC stocks, the conversion of crop residues into bio-oil and syngas for the French energy system followed by the return of

pyrochar and gaschar to the soil represents a total surplus C input of 774 Mt C and 316 Mt C in the long term, respectively (Table 2). For the pyrolysis scenarios, approximately 57% of the areas revealed a SOC stock increase of over 100% (Table S2.1), attaining a maximum increase of 409% (Fig. 4). In 85% of the modeled areas, the consecutive application of gaschar could increase SOC stocks by approximately 80%, as compared to the BAU (maximum +178%) (Table S2.1; Table S2.4).

Despite SOC stocks being shown to be reduced in approximately 3% of the areas (up to 1.8%) for the HTL scenario, a total additional C storage of 8.9 Mt C can be expected at the national level in the long term. Similarly, although the AD scenario yielded SOC losses in 40% of the areas (up to -3.5%), the SOC change observed in this scenario is insignificant. Notably, the vast majority of those areas (37%) may attain SOC losses of only 1.3%, comparable to the SOC improvements (50% of the area) shown to reach only 0.7% (Table S2.4). The bioethanol scenario would only yield SOC losses on 100% of the French croplands.

At the national level, the crop residue potential (dry matter), after considering the harvest constraints of Table S1.1, is 18.7 Mt (Table 3) for 2021 (the theoretical potential, i.e., without these machinery-related constraints, is 30.4 Mt). Of this, 100% (18.7 Mt) can be harvested for pyrolysis and/or gasification processes without any SOC decrease, compared to the BAU scenario, based on the results of this study. If we exclude the areas with expected SOC losses, only 98% (18.3 Mt) and 53% (9.96 Mt) can be used for HTL and AD, respectively.

Table 2. National 100-year soil organic carbon changes from the business as usual to the bioeconomy ($\Delta SOC_{bio-BAU}$) scenarios, in total Mt C and %, at an exporting rate of 100%, at year 2120. Values in % are provided as national averages of all APCUs[a].

Bioeconomy scenarios	Total national $\Delta SOC_{bio-BAU}$[c]	Min.[d]	Max.[d]	Average national $\Delta SOC_{bio-BAU}$[e]	σ[f]	Min.[d]	Max.[d]
	(Mt C)			(%)			
BAU[b]	-17.8	-0.1	0.1	-2.2	14.8	-27.0	84.9
Pyrolysis	774.0	2.5E-5	0.5	106.0	69.3	0.1	409.0
Gasification	316.0	8.6E-6	0.2	43.3	29.3	0.1	177.0
HTL	8.9	-4.4E-3	9.3E-3	1.1	0.8	-1.8	4.1
AD	-0.8	-8.6E-3	1.5E-3	-0.1	0.4	-3.5	0.7
Lignocellulosic bioethanol	-34.9	-3.3E-2	-2.5E-6	-4.4	2.9	-14.2	-1.2E-4

SOC: Soil organic carbon, BAU: Business as usual, APCU: Agricultural pedoclimatic units. [a] To ensure tractability, results are presented with a maximum of three significant digits. [b] BAU scenario corresponds to ΔSOC_{0-100}: change from BAU at year 100 vs BAU at year 0; [c] Sum of all the modeled APCUs; [d] Minimum and maximum $\Delta SOC_{bio-BAU}$ reported over all APCU; [e] Average SOC change for all the modeled APCUs: change from bioeconomy scenario at year 2120 vs BAU at year 2120¸ [f] Standard deviation.

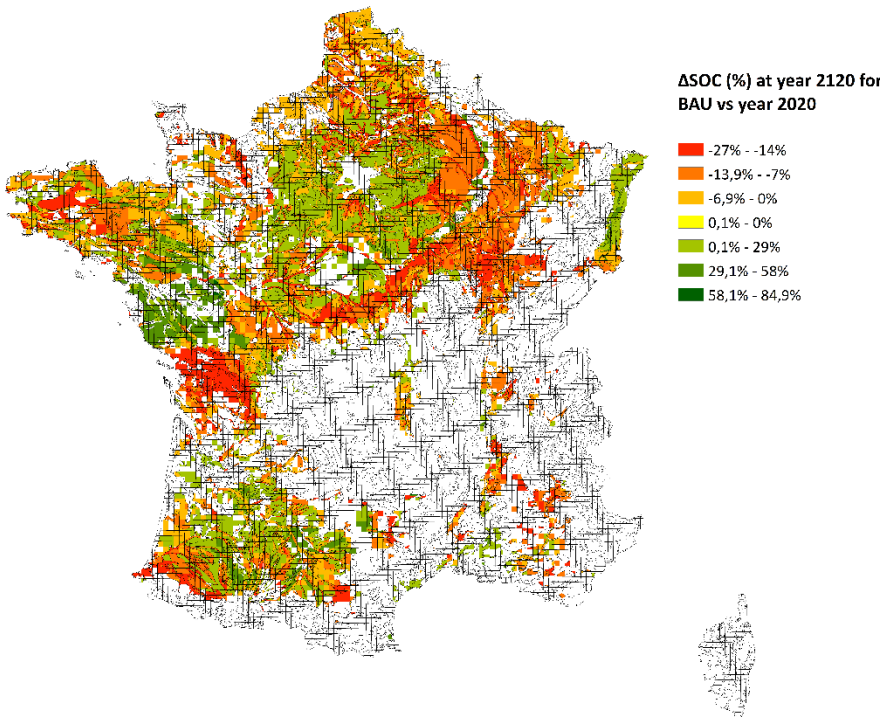

Fig 3. Predicted long-term soil organic carbon (SOC) stocks for the business as usual (BAU) scenario in 2120.

Table 3. National harvestable crop residues potential per scenario for the year 2021, calculated with a fixed limit and the methodology developed herein. Only areas shown to maintain or increase soil organic carbon stocks are considered[a].

Crops included in this study [b]	National crop residue potential [c]	Current potential using a fixed ratio of 31.50% [d]		C-neutral harvest potentials (this study) [f]							
				Pyrolysis scenario[g]		Gasification scenario[g]		HTL scenario[h]		AD scenario[h]	
	(Mt DM)	(Mt DM)	PJ [e]	(Mt DM)	PJ [e]	(Mt DM)	PJ [e]	(Mt DM)	PJ [e]	(Mt DM)	PJ [e]
Winter wheat	11.5	3.6	63.3	11.5	201.0	11.5	201.0	11.4	199.0	9.4	164.0
Grain maize	5.3	1.7	29.5	5.3	93.6	5.3	93.6	5.3	93.3	0.2	3.2
Protein peas	7.8E-04	2.5E-04	4.3E-03	7.8E-04	1.4E-02	7.8E-04	1.37E-02	6.7E-04	1.18E-02	3.3E-14	5.8E-13
Rapeseed	0.9	0.3	5.2	0.9	16.5	0.9	16.5	0.9	16.5	0.4	7.0
Sunflower	0.4	0.1	2.1	0.4	6.7	0.4	6.7	0.4	6.7	8.5E-04	1.5E-02
Sugar beet	0.6	0.2	3.3	0.6	10.3	0.6	10.3	0.4	6.3	3.5E-03	0.1
Total	18.7	5.9	103.0	18.7	328.0	18.7	328.0	18.4	322.0	10.0	174.0

HTL: Hydrothermal Liquefaction, AD: Anaerobic Digestion, DM: dry matter.[a] To ensure tractability, results are presented with a maximum of three significant digits; [b] Crops considered in French croplands that generate residues; [c] Based on (i) yields obtained from the STICS simulation tool, for the year 2021 [46], (ii) on the consideration that only 56% crop residues are not already used, and (iii) technical harvesting fractions defined in AMGv2 (Table S1.1); [d] This fixed ratio is the mean of the values suggested by France Agrimer [90], who recommend that 41-96% of the technically harvestable straw must be left on soils; [e] Considering a generic low heating value: 17.5 GJ t^{-1}; [f] C-neutral harvest represents a share of: 100% of national crop residues potential (DM) for pyrolysis and gasification, 98% for HTL, and 53% for AD (see results of Fig. 4). The lignocellulosic bioethanol scenario is not considered because this does not provide any additional potential compared to the BAU scenario. [g] 100% of areas providing crop residues to be harvested; [h] These values do not consider the residues from the specific areas where SOC stock is shown to decrease, it thus only covers: 88% of the modeled areas for HTL and 50% for AD.

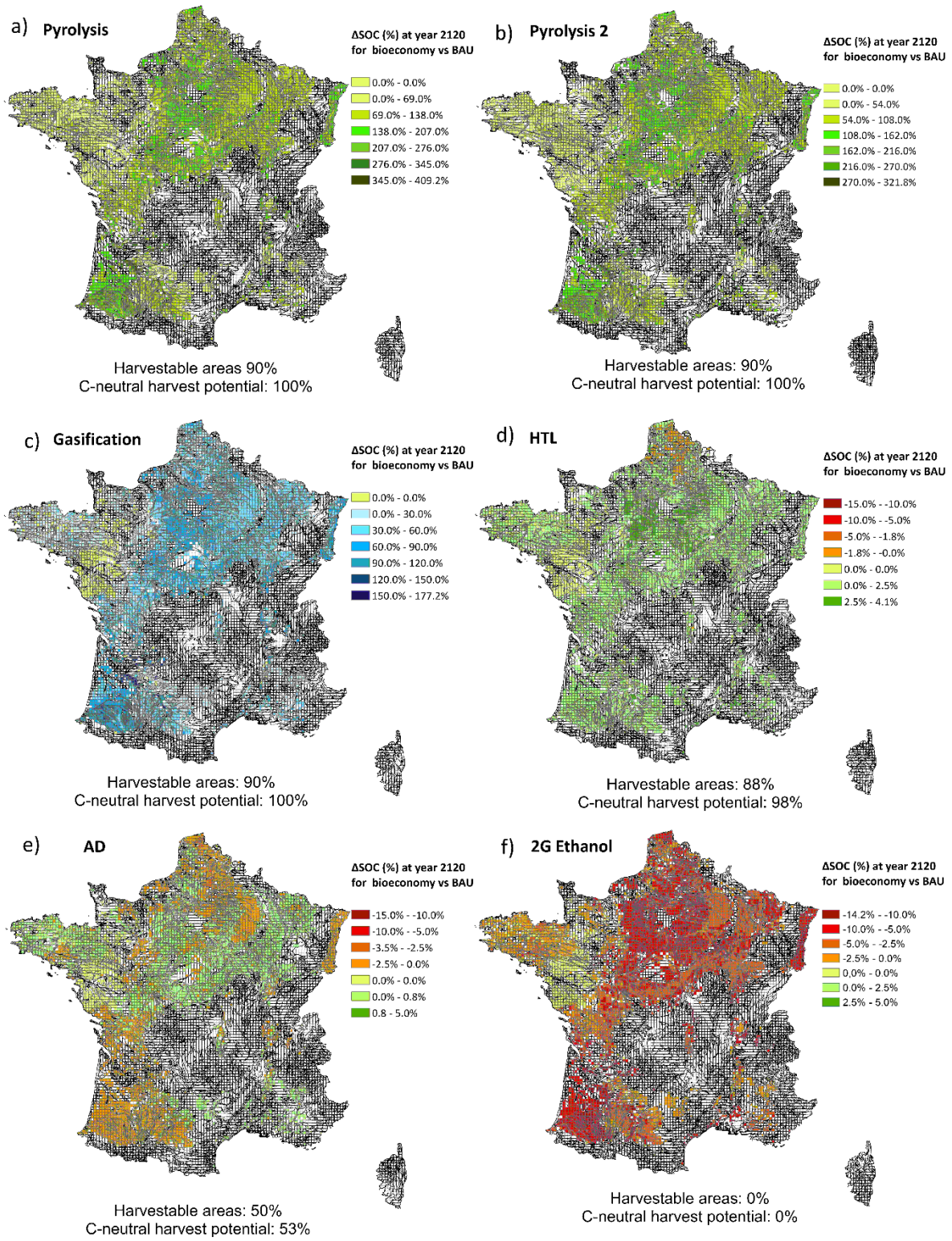

Fig 4. Spatially explicit soil organic carbon stocks relative to the business-as-usual scenario (year 2120) if the available harvestable crop residues are used for bioeconomy ($\Delta SOC_{bio\text{-}BAU}$%) a) Pyrolysis (with C_S pool of AMG only; default), b) pyrolysis (with C_A and C_S pool of AMG; sensitivity), c) gasification, d) hydrothermal liquefaction, e) anaerobic digestion, f) lignocellulosic bioethanol. White grids were not included in the simulations. BAU: Business as usual, C_S: Carbon stable pool of AMG, CA: Carbon active pool of AMG. Harvestable areas discard areas generating crop residues already being exported for livestock (as bedding or fodder; areas with 0-0%, these

represent 10% of all areas) as well as those where soil organic carbon decreases are observed. C-neutral harvest potential is the share of crop residues that can be "neutrally" harvested out of the total amount generated (excluding amount already exported for livestock). For example, 90% of the areas can be harvested for pyrolysis, which corresponds to 100% of the residues generated (and not already used for livestock).

3.3 Sensitivity Analysis

The SA allowed the evaluation of the uncertainty of the potential national SOC changes in 2120 due to the variability of the C_C and C_R coefficients relative to the mean coefficient value (Fig. 5). All variations discussed within this section are relative to the results obtained with the mean C_C and C_R.

For the pyrolysis scenario, the different combinations of C_C and C_R coefficients affected the additional SOC stocks, ranging between -29% and +30%, equivalent to 549 Mt C and 1009 Mt C (Table S2.3), at a national level. A one-at-a-time test showed that the SOC results were more sensitive to C_C, ranging between -25% and +25%, while Cr ranged between -6% and +5%. The additional SOC stocks for all the SA tested in the gasification scenario varied between -40% and +36%, equivalent to 187-431 Mt C. C_R variability contributed to SOC changes between –6% and +5%, while C_C alone affected the results from -36% to +30%. From these results, it is observed that C_C has the greatest influence on the pyrolysis and gasification scenarios, one reason being the greater range of values compared to C_R (Fig.S4, Fig.S6).

For the low recalcitrance scenarios, the variation of the coefficients caused the results to vary from C losses to potential additional C storage. The HTL scenario result is affected by -4.8% to +7.6%. High C_C values for any given C_R, result in C sequestration in areas that are shown to lose SOC stocks with the mean coefficients. The opposite was observed for low C_C values, which resulted in SOC losses for all the APCUs (Fig. S7). Due to the diverse possible conditions of the HTL technology, the C_C coefficients in this scenario were tested for a broader range (0.12-0.45; Table 1) than other technologies, which produced a higher effect for C_C than for C_R.

The national SOC change ranges from -16 Mt C to +24 Mt C for the different coefficients in the AD scenario, representing changes of -2 to +3%. The combination of high C_C and C_R resulted in SOC losses in only 0.2% of the simulated areas, compared to 40% for the mean values of the parameters (Table S2.1).

Similarly, lower C_C and C_R values resulted in SOC stocks decreasing in all areas (Fig S8). For the molasses scenario, the combination of maximum and minimum values of C_C and C_R represented a SOC stock variation of -61% to +48% (Table S2.3), with losses observed in all APCUs.

The C_R partitioning between the C_A and the C_S pools of AMG (Pyrolysis 2) resulted in cumulated additional SOC stocks of 617 Mt C compared to the BAU scenario by 2120 (Table S2.2). This represents a difference of -21% compared to a 100% C allocation of the recalcitrant pyrochar to the C_S pool only, with variability in the SOC stock results ranging from -39% to -10% for all the SA coefficient combinations (Table S2.3). Albeit the net additional C stored differed for the two C_R allocation methods, the trend observed was the same, with expected SOC increases in all APCUs. For the Pyrolysis 2 scenario, 36% of the areas predicted SOC to increase above 100% (Fig. S5).

If all the harvestable crop residues are exported for pyrolysis or gasification, but only 50 t C ha^{-1} are regularly recycled to the soils throughout the 100 years to avoid the toxic effects of excessive char application, no SOC decreases are observed as a result, on all APCU (Table S2.2).

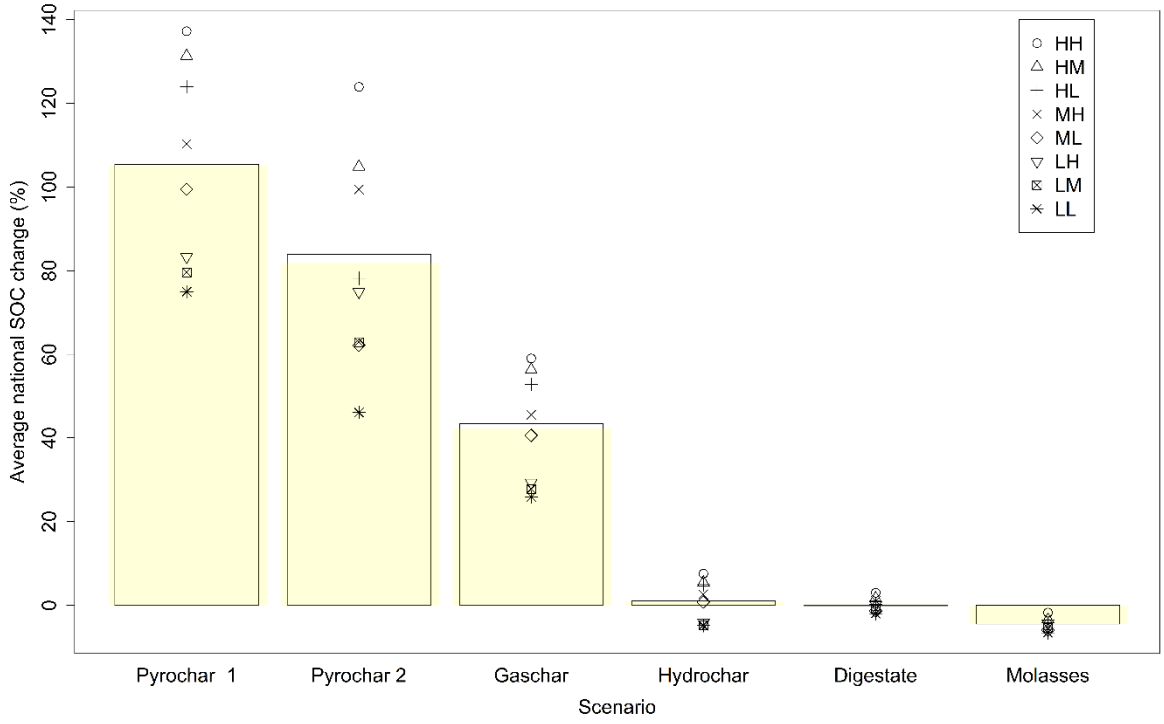

Fig 5. Sensitivity analysis describing a combination of low (L), mean (M), and high (H) carbon conversion (C_C) and carbon recalcitrance (C_R) values for each bioeconomy scenario, with an extra scenario for pyrolysis (Pyrochar2) considering an alternative method to partition the recalcitrant fractions into soil organic carbon pools in AMG. The bars show the mean value (M C_C + M C_R) while yellow shades represent the average of all nine points (SOC at year 2120; in comparison to the business as usual) for the different C_C and C_R combinations in a given scenario. SOC : Soil organic carbon.

4. Discussion

4.1 Implications for decision making

The bioeconomy-AMG soil model developed in this study supplies the first open-source framework to assess the interaction between five promising bioeconomy pathways (pyrolysis, gasification, HTL, AD, and 2GEtOH production) and SOC evolution, in order to understand where and whether crop residues should be harvested as feedstock for future energy and bioeconomy systems. One key implication of this framework is that it reveals a smart, region-specific biomass potential ensuring a C-neutral harvest higher than otherwise thought. This enhanced potential can then be converted into e.g., more bioenergy to supply electricity, heat, and transportation industries, without incurring extra pressures on land use changes or competition with the food industry.

In fact, in France, it is suggested to limit the harvest of cereal straw to leaving a share of 41%-96% of the technically harvestable residues on the soil to preserve its agronomic functions. [90] Similarly, ADEME [91] determined that despite 46-69% of the projected energy demand in France must be supplied by renewable sources by 2050, only 21% of crop residues (by weight) generated could be mobilized for the specific needs of biogas production, due to agronomical soil functions and issues related to competitive use. Our results suggest that this threshold may be too stringent in a C-neutral harvesting context, even for anaerobic digestion, where a 75% harvest (and return) rate implies SOC losses below 1% in 37.5% of the areas (maximum loss of 2.6%, in 2.5% of the areas).

The results of this study demonstrated that the harvest potential is 100% (of the technically harvestable feedstock not already used) unless the residues are to be used for bioethanol (then 0% removal). If to be conservative, we consider export rates of 0% in the areas where SOC losses are projected with anaerobic digestion and HTL, a reduction of the corresponding crop residue potential of 80% and 3% would be observed, respectively (based on 30.4 Mt dry matter harvestable in 2021). Comparing this with a generic 31.5% harvesting limit (middle of the above range suggested to be left on the soil for France), it involves that between 4.1 (anaerobic digestion) and 12.8 (for pyrolysis and gasification) Mt dry matter of additional crop residues are obtained by applying our framework. This corresponds to an added supply of 71 – 225PJ y^{-1} (considering a low heating value of 17.5 GJ t^{-1} DM), the equivalent of the gross electricity generation in Greece and Austria, respectively [12].

Another implication of the framework developed within this study is its usefulness within the context of C farming initiatives [92], where farmers could be paid to sequester carbon in

their soils. In fact, the framework reveals areas with enhanced ability to support, without negative consequences on the SOC stocks, a given conversion pathway, as well as sensitive areas where crop residue harvesting requires a more careful look at the actual conversion pathway to be used. Thus, the model can be used to provide advice for resource management for bioeconomy development in specific locations.

4.2 Long-term spatially explicit coproduct potential for soil organic carbon stocks

The BAU scenario predicted a slight average SOC decrease (2% for 100 years) in the simulated areas, which is consistent with the potential prolongation of average decreases in SOC stocks observed over the past decades in temperate croplands in France, Belgium, and Germany. [77,93–95] The simulated decrease is, however, lower than that of 14% obtained by Riggers et al.[96] in German croplands with a multi-model ensemble for the same climate projection (RCP 4.5) and unchanged (current) C inputs for the 2014–2099 period. The BAU scenario predicted SOC losses in around 63% of all simulated areas (Fig. 3). This conforms to the trends observed in Launay et al.[46], where SOC decreases in 55% of the simulated areas (using the STICS model) were observed after 30 years. The regional differences observed can be explained by the influence of the initial SOC stocks, climate, soil, and cropping system characteristics. For instance, simulation units where crop rotations include temporary grasslands and/or cover crops showed a greater SOC build up potential than rotations including only arable crops; this was also observed by Launay et al. [46] for the BAU scenario.

Current French cropping systems must increase the C inputs by 42% on average to reach the 4‰ target, while recent studies predict a required increase of 283% for Germany. [96,97] However, decreasing SOC stock trends under a BAU scenario have been identified in this work and others. [46,97] In this context, the management of crop residues, allowing SOC stocks to increase as in the biochar scenarios (pyrochar, gaschar, and hydrochar) and partially in the digestate scenario, could represent alternatives toward the 4‰ goals.

Results differed considerably among the recalcitrance groups (high and low) because the adapted AMG allocates the recalcitrant C as inert for the highly recalcitrant coproducts, whereas it is allocated to the decomposable active pool for the less recalcitrant coproducts. The steady-state reached in the active pool is never attained in the stable one, allowing the highly recalcitrant products to continue building up SOC stocks over the long term.

Due to the novelty of this work, there are currently few literary sources available for result comparison. However, some studies are available for SOC modeling using pyrochar and digestate amendments. For instance, Lefebvre et al. [29] reported a 127% SOC increase in 20

years in Brazilian sugarcane fields by replacing sugarcane residues with pyrochar. Likewise, Woolf and Lehmann [30] found that the export of 50% of maize residues for pyrochar production, with the subsequent addition of pyrochar to soils, can increase SOC stocks by 30% –60% over 100 years. Bodilis et al. [99] observed a slight decrease in SOC stocks in French croplands after digestate application as compared to undigested biomass using AMG. To the contrary, Mondini et al. [39] reported a 2-fold SOC increase after digestate application on Italian lands, compared to undigested crop residues using a modified version of RothC.

While pyrochar, gaschar, and even hydrochar are clearly outlined as attractive scenarios for SOC improvement, the digestate scenario projects insignificant SOC stock changes compared to the BAU scenario. Evidence suggests that anaerobic digestion of plant residue has little effect on SOC stocks in the long term compared to fresh plant-derived C. [100,101] The difference between the raw and digested residual biomass lies in the labile C fraction. The removal of the labile fraction reduces CO_2 emissions from the digestate, compared to the raw feedstock. Besides C, bioavailable nutrients are concentrated in digestate, often in a form that is more assimilable for plants, which makes it an attractive fertilizer. [102] Using digestate as fertilizer can offset the C emissions incurred by mineral fertilizer production and application, though it can also involve higher N losses under specific conditions due to its greater propensity to volatilization following digestion. [103] Areas depicting SOC decreases should therefore be analyzed in detail to determine whether other benefits (energy and nutrient recovery) are worth the risk of losing soil C.

The SOC stocks decreased in all APCUs with the 2GEtOH scenario, which reflects the changed lignin condensation of the biomass exerted by the chemical and enzymatic treatments, allowing the soil microorganisms to decompose the coproducts at a faster rate. [21,23,104] It is associated with increased microbial activity, which may improve fertility and plant growth. [105] Nevertheless, soil application of molasses has been associated with negative impacts on soil characteristics (e.g., increased salinity and electrical conductivity) and increased greenhouse gas emissions compared to untreated biomass. [21,23] Our results suggest not exchanging the crop residue provision to soils with bioethanol coproducts if the objective is to prevent SOC losses.

4.3 Strengths and limitations

The scarcity and high variability of data regarding the coproduct's C recalcitrance and the challenge of representing long-term effects on real environments based on short-term laboratory studies require caution in the analysis of the results. The main conclusions do not

regard the absolute values predicted but the trends related to the sensitivity of the model to the parameters used. We tested a wide range of plausible values for key parameters. The conclusions drawn for each technology can provide insightful decision support concerning the crop residues' potential for bioeconomy.

Our results partially show the bioeconomy cause-effect link between the usage of the crop residues and their export potential, with different long-term SOC stock predictions among scenarios. Using coproducts as EOM inputs to the soil is expected to modify the soil's physical, chemical, and biological characteristics in diverse ways. Soil changes can be altered by i) net primary production due to changes in the amount and quality of input carbon and nutrients, ii) addition of extra organic compounds to the soils, and iii) soil microbiota adaptation to use the C in the coproducts (this C being structurally different to the one in plant residues). [41,106] An excessive application of bioeconomy coproducts may alter soil physicochemical properties and induce other environmental impacts (e.g., climate change). Moreover, the C in the raw biomass is readily available, while in the stabilized matter the C may be unavailable for microorganisms, which could affect soil functioning and fertility. The SA demonstrated that 100% of the crop residues can be exported to increase the bioeconomy provision while restraining the possible negative effects of biochar, by limiting the application, without affecting the SOC stocks.

Some limitations can be identified in the adapted model and the case studied here. Changes in soil fertility induced by the addition of coproducts were not considered, as well as the potential changes in soil structure and quality due to limitations of the model. [66,107] Besides, nitrogen dynamics (i.e., nitrate leaching and NH_3 emissions) and atmospheric emissions were not evaluated. It was beyond the scope of this work to analyze the overall environmental effects of the different bioeconomy strategies (i.e., accounting for the substituted energy and products by the main bioeconomy products), here focusing on SOC changes only. Similarly, how to prioritize the distribution of each crop residue to each bioeconomy technology was not addressed. These considerations, however, need to be assessed in future studies (e.g., life cycle assessment) to have a holistic understanding of the environmental impacts of exporting crop residues for each technology.

Moreover, the exchange of crop residues with bioeconomy coproducts can influence the soil water retention capacity and crop yield. The physical structure (e.g., high microporosity, large surface area, and particle size) of chars (pyrochar, gaschar, and hydrochar) encourages the retention of water in their pores, which improves the water-holding capacity of soils [65,108,109]. Furthermore, the addition of chars improves the soil aggregate stability, which prevents nutrients from leaching [66,110]. The increased moisture, stability, and nutrient

retention, in turn improve the yield of crops [41,111]. Similarly, the high moisture and nutrient content in digestate and bioethanol molasses allow improving the soil's moisture and fertility [103,105]. A change in crop yields will in turn change the available crop residues and SOC dynamics. Besides the soil implications, the increased crop residue supply for bioeconomy or bioenergy production will demand extra resources such as water, chemicals (e.g., catalysts, O_2 and N_2 carriers, among others), and even bigger facilities to process the extra residues. However, these water-energy nexus implications were not considered herein due to the lack of quantified evidence to integrate it.

Another limitation of the study regards the validation of the bioeconomy-adapted AMG. Despite AMG having been well validated in previous studies [77,80,81,112], especially for temperate regions, currently, there is no available experimental data regarding the long-term SOC evolution of croplands after the application of the studied coproducts that can be used to validate the bioeconomy adapted AMG.

Results may vary for different future climate trajectories; our case study considered the RCP4.5 trajectory only. This study considers unchanged cropping systems and crop yields throughout the 100 years. The impact of this hypothesis could be challenged in future works by e.g., using ADEME [91] projections of cropping systems in France, namely one complying with the Factor 4 initiative, and another prolonging the current trends. Factor 4, a national strategy that aims to divide GHG emissions by a factor of 4 by 2050, envisions better agricultural practices and fewer livestock while the current trends would lead to higher yields for grass, cereal-, and oleaginous crops. These changes in the cropping systems may affect the SOC dynamics and the ability to export crop residues.

We assumed that all cover crops are maintained on soils and all temporary grasslands are exported, while currently approximately 50% of cover crops and 11% of temporary grasslands are being collected on a national scale for anaerobic digestion. [91] This surplus provision of digested feedstock may improve the results obtained for the AD scenario. Moreover, we only considered the changes in recalcitrance for the crop residues digested and not for the co-substrates used. Around 50% of the simulation units involve the presence of manure besides other organic amendments, which could be co-digested, resulting in C inputs decline but C recalcitrance improvements. Nevertheless, this effect is expected to be of minor importance considering previous works (e.g., Thomsen et al.[101]).

Finally, note that the SOC losses observed for hydrochar, digestate, and molasses could be compensated if coupled with other strategies, such as i) redistribution of coproducts from areas showing increased SOC stocks, ii) introduction of specific cover crops, iii) changes in farming

management, and iv) mix of bioeconomy coproduct return. This was, however, beyond the scope of the study.

5. Conclusions

This study demonstrated that the harvesting potential of crop residues is affected by the process for which the biomass is destined and is spatially explicit in order to preserve long-term SOC stocks.

The partial return of crop residues C to soils, as stabilized coproducts, was shown to maintain and even increase SOC stocks in comparison to levels attained by simply leaving the residues on soils, allowing for the supply of more feedstock to the bioeconomy. The study thus confirmed that current practices applying a fixed removal threshold deprive the bioeconomy of an important amount of biomass, whose carbon would otherwise be lost as CO_2 emissions rather than contribute to enhancing SOC levels.

Pyrochar and gaschar have been shown to raise SOC stocks in all the French croplands when used as soil C inputs in place of crop residues. Except for croplands in the Northern region, the HTL scenario predicted an increase in SOC stocks in 88% of the areas. For digestate, minor SOC gains resulted in only 50% of the areas. The return of C via molasses resulted in clear losses of SOC stocks throughout all croplands.

By modifying the AMG soil carbon model to consider the recalcitrance of returned bioeconomy coproducts, this study provides a spatially explicit operational tool that can supply science-based support for future decisions on the usage of crop residues for bioeconomy and/or renewable energy systems, for a variety of locations and data granularity.

Nevertheless, further research is required regarding recalcitrance, particularly for bioethanol coproducts and gasification char, for which studies are scarce and the understanding of the C stability and MRT effects on SOC evolution remains an issue.

Data availability

The data that support the findings of this study are openly available in [43] at https://doi.org/10.48531/JBRU.CALMIP/WYWKIQ.

Author Contributions

Conceptualization and methodology, C.A., A.A., and L.H.; software and formal analysis, C.A. and H.C.; data curation, investigation, and visualization, C.A.; writing – original draft, C.A.; writing – review &

editing C.A., L.H., A.A., H.C., and E.Z.L; funding acquisition, C.A., L.H., and E.Z.L.; supervision L.H. and E.Z.L.; project administration L.H.

Conflicts of interest

There are no conflicts to declare.

Acknowledgments

This work was carried out within the framework of the research project Cambioscop (https://cambioscop.cnrs.fr), partly financed by the French National Research Agency, Programme Investissement d'Avenir (ANR-17-MGPA-0006), and Region Occitanie (18015981). C. Andrade was additionally funded by the French Embassy in Ecuador under the Project "Fonds de Solidarité pour Projets Innovants" (FSPI).

Authors are grateful to Camille Launay for providing the initial data and helping with our questions, Serguei Sokol for helping with data manipulation in R, and Julie Constantin and Olivier Therond for initiating the collaboration and data share from the INRAE 4p1000 project. The authors thank Pr. Steven Abbott and Dr. Mark Landon for proofreading the manuscript.

Credits

The graphical abstract has been designed using free icons resources from Flaticon.com (authors: Freepik, Surang, Monkik, Ultimaterm, Kosonicon, Vectorsmarket15, Backwoods, PongsakornRed, Aficons studio, Bqlqn, Smashicons).

Disclosure

This manuscript has been submitted as a preprint to Research Square, [113] https://doi.org/10.21203/rs.3.rs-1447950/v2 and is currently available as a journal article in Applied Energy [114]

Supporting documents and data

This **Chapter 3** presents a novel framework adapting the soil model AMG to include five bioeconomy coproducts, namely pyrochar, gaschar, hydrochar, digestate; and molasses derived from the production of second-generation bioethanol. The framework is applied to a case study for French croplands, and thus all the data inputs used in this chapter, as well as the outputs results from the model for each scenario (BAU and bioeconomy) and sensitivity analysis are summarized in the accompanying appendixes:

- **Appendix A2a:** Supplementary information of the article.
- **Appendix A2b:** Summary of the results
- **Background data:** The complete database produced along with this paper reporting the input and output data of the model, as well as the scripts used is openly available in the following repository: https://doi.org/10.48531/JBRU.CALMIP/AUEEEJ

Towards Chapter 4

This **Chapter 3** proposes a framework for the spatially-explicit assessment of crop residues potential to supply the bioeconomy in a C-neutral harvest context at a national scale. The AMG soil model was adapted to include five coproducts and was then applied in the specific case study of French croplands. Although the application of the model requires specific input data for the geographic area under study, the framework developed in this chapter can be applied to other contexts besides France and at different spatial resolution. SOC dynamics in croplands are deeply defined by the specific pedoclimatic context and agricultural practices. Therefore, the conclusions derived in this chapter are not universal and specific local assessments must be performed for each particular context. Due to their prodigious combination of soil and climate characteristics, tropical lands are expected to contribute to approximately 70% of the global carbon sequestration until 2050. However, these same characteristics confluence to produce highly fertile soils which are overly exploited by the agroindustry in tropical regions. In **Chapter 4**, we apply the framework developed in chapter 3, for Ecuadorian croplands as a representative case of a tropical biome. The framework is adapted for the local conditions and second soil model, widely tested in tropical countries, is adapted for the bioeconomy.

References Chapter 3

[1] UNFCCC. Paris Agreement to the United Nations Framework Convention on Climate Change. 2015.

[2] European Comission. Regulation (EU) 2021/1119 of the European Parliament and of the Council of 30 June 2021 establishing the framework for achieving climate neutrality and amending Regulations (EC) No 401/2009 and (EU) 2018/1999 ('European Climate Law'). PE/27/2021/REV/1. vol. 32021R1119. 2021.

[3] Department for Business, Energy & Industrial Strategy. Net Zero Strategy: Build Back Greener. UK: HM Government UK; 2021.

[4] Energy Transitions Commission. China 2050: A fully developed rich zero-carbon economy. China: Energy Transitions Commission; 2019.

[5] Energy & Climate Intelligence Unit. Net zero emissions race. 2022 Scorecard. Net Zero Scorecard 2022. https://eciu.net/netzerotracker (accessed February 27, 2022).

[6] IRENA. REmap 2030. A Renewable Energy Roadmap. Summary of findings. Abu Dhabi: International Renewable Energy Agency; 2014.

[7] IRENA. Global Renewables Outlook. Energy Transformation 2050. Abu Dhabi: International Renewable Energy Agency; 2020.

[8] Shapiro-Bengtsen S, Hamelin L, Møllenbach Bregnbæk L, Zou L, Münster M. Should Residual Biomass be used for Fuels, Power and Heat, or Materials? Assessing Costs and Environmental Impacts for China in 2035. Energy Environ Sci 2022. https://doi.org/10.1039/D1EE03816H.

[9] Sadh PK, Duhan S, Duhan JS. Agro-industrial wastes and their utilization using solid state fermentation: a review. Bioresour Bioprocess 2018;5:1. https://doi.org/10.1186/s40643-017-0187-z.

[10] Swain MR, Singh A, Sharma AK, Tuli DK. Chapter 11 - Bioethanol Production From Rice- and Wheat Straw: An Overview. Bioethanol Production from Food Crops. Sustainable Sources, Interventions, and Challenges, Academic Press; 2019, p. 19.

[11] Hamelin L, Borzęcka M, Kozak M, Pudełko R. A spatial approach to bioeconomy: Quantifying the residual biomass potential in the EU-27. Renewable and Sustainable Energy Reviews 2019;100:127–42. https://doi.org/10.1016/j.rser.2018.10.017.

[12] BP. Statistical Review of World Energy 2021. 70th Edition. BP; 2021.

[13] Karan SK, Hamelin L. Crop residues may be a key feedstock to bioeconomy but how reliable are current estimation methods? Resources, Conservation and Recycling 2021;164:105211. https://doi.org/10.1016/j.resconrec.2020.105211.

[14] Scarlat N, Fahl F, Lugato E, Monforti-Ferrario F, Dallemand JF. Integrated and spatially explicit assessment of sustainable crop residues potential in Europe. Biomass and Bioenergy 2019;122:257–69. https://doi.org/10.1016/j.biombioe.2019.01.021.

[15] Blanco-Canqui H. Crop Residue Removal for Bioenergy Reduces Soil Carbon Pools: How Can We Offset Carbon Losses? Bioenerg Res 2013:14.

[16] Morais TG, Teixeira RFM, Domingos T. Detailed global modelling of soil organic carbon in cropland, grassland and forest soils. PLOS ONE 2019:27.

[17] Fischer G, Prieler S, van Velthuizen H, Berndes G, Faaij A, Londo M, et al. Biofuel production potentials in Europe: Sustainable use of cultivated land and pastures, Part II: Land use scenarios. Biomass and Bioenergy 2010;34:173–87. https://doi.org/10.1016/j.biombioe.2009.07.009.

[18] Haase M, Rösch C, Ketzer D. GIS-based assessment of sustainable crop residue potentials in European regions. Biomass and Bioenergy 2016;86:156–71. https://doi.org/10.1016/j.biombioe.2016.01.020.

[19] Monforti F, Lugato E, Motola V, Bodis K, Scarlat N, Dallemand JF. Optimal energy use of agricultural crop residues preserving soil organic carbon stocks in Europe. Renewable and Sustainable Energy Reviews 2015;44:519–29. https://doi.org/10.1016/j.rser.2014.12.033.

[20] Panoutsou C, Maniatis K. Sustainable biomass availability in the EU, to 2050. Concawe; 2021.

[21] Cayuela ML, Oenema O, Kuikman PJ, Bakker RR, Van Groenigen JW. Bioenergy by-products as soil amendments? Implications for carbon sequestration and greenhouse gas emissions: C and N dynamics from bioenergy by-products in soil. GCB Bioenergy 2010:no-no. https://doi.org/10.1111/j.1757-1707.2010.01055.x.

[22] Lehmann J, Abiven S, Kleber M, Pan G, Singh BP, Sohi SP, et al. Persistence of biochar in soil. Biochar for Environmental Management. 2nd Edition, 2015, p. 48.

[23] Bera T, Vardanyan L, Inglett KS, Reddy KR, O'Connor GA, Erickson JE, et al. Influence of select bioenergy by-products on soil carbon and microbial activity: A laboratory study. Science of The Total Environment 2019;653:1354–63. https://doi.org/10.1016/j.scitotenv.2018.10.237.

[24] Wiesmeier M, Urbanski L, Hobley E, Lang B, von Lützow M, Marin-Spiotta E, et al. Soil organic carbon storage as a key function of soils - A review of drivers and indicators at various scales. Geoderma 2019;333:149–62. https://doi.org/10.1016/j.geoderma.2018.07.026.

[25] Muth DJ, Bryden KM, Nelson RG. Sustainable agricultural residue removal for bioenergy: A spatially comprehensive US national assessment. Applied Energy 2013;102:403–17. https://doi.org/10.1016/j.apenergy.2012.07.028.

[26] Smith P, Soussana J-F, Angers D, Schipper L, Chenu C, Rasse DP, et al. How to measure, report and verify soil carbon change to realize the potential of soil carbon sequestration for atmospheric greenhouse gas removal. Global Change Biology 2020;26:219–41. https://doi.org/10.1111/gcb.14815.

[27] Lehmann J, Hansel CM, Kaiser C, Kleber M, Maher K, Manzoni S, et al. Persistence of soil organic carbon caused by functional complexity. Nat Geosci 2020;13:529–34. https://doi.org/10.1038/s41561-020-0612-3.

[28] Mondini C, Cayuela ML, Sinicco T, Fornasier F, Galvez A, Sánchez-Monedero MA. Modification of the RothC model to simulate soil C mineralization of exogenous organic matter. Biogeochemistry: Soils; 2017. https://doi.org/10.5194/bg-2016-551.

[29] Lefebvre D, Williams A, Meersmans J, Kirk GJD, Sohi S, Goglio P, et al. Modelling the potential for soil carbon sequestration using biochar from sugarcane residues in Brazil. Sci Rep 2020;10:19479. https://doi.org/10.1038/s41598-020-76470-y.

[30] Woolf D, Lehmann J. Modelling the long-term response to positive and negative priming of soil organic carbon by black carbon. Biogeochemistry 2012:13.

[31] Pulcher R, Balugani E, Ventura M, Greggio N, Marazza D. Inclusion of biochar in a C dynamics model based on observations from an 8-year field experiment. SOIL 2022;8:199–211. https://doi.org/10.5194/soil-8-199-2022.

[32] Dil M, Oelbermann M. Evaluating the long-term effects of pre-conditioned biochar on soil organic carbon in two southern Ontario soils using the century model. Chapter 13. In: Oelbermann M, editor. Sustainable agroecosystems in climate change mitigation, The Netherlands: Wageningen Academic Publishers; 2014, p. 249–68. https://doi.org/10.3920/978-90-8686-788-2_13.

[33] Archontoulis SV, Huber I, Miguez FE, Thorburn PJ, Rogovska N, Laird DA. A model for mechanistic and system assessments of biochar effects on soils and crops and trade-offs. GCB Bioenergy 2016;8:1028–45. https://doi.org/10.1111/gcbb.12314.

[34] Lychuk TE, Izaurralde RC, Hill RL, McGill WB, Williams JR. Biochar as a global change adaptation: predicting biochar impacts on crop productivity and soil quality for a tropical soil with the Environmental Policy Integrated Climate (EPIC) model. Mitig Adapt Strateg Glob Change 2015;20:1437–58. https://doi.org/10.1007/s11027-014-9554-7.

[35] Hansen JH, Hamelin L, Taghizadeh-Toosi A, Olesen JE, Wenzel H. Agricultural residues bioenergy potential that sustain soil carbon depends on energy conversion pathways 2020:12.

[36] Levavasseur F, Mary B, Christensen BT, Duparque A, Ferchaud F, Kätterer T, et al. The simple AMG model accurately simulates organic carbon storage in soils after repeated application of exogenous organic matter. Nutrient Cycling in Agroecosystems 2020:15.

[37] Witing F, Prays N, O'Keeffe S, Gründling R, Gebel M, Kurzer H-J, et al. Biogas production and changes in soil carbon input - A regional analysis. Geoderma 2018;320:105–14. https://doi.org/10.1016/j.geoderma.2018.01.030.

[38] Bonten LTC, Elferink EV, Zwart K. Tool to assess effects of bio-energy on nutrient losses and soil organic matter 2014:22.

[39] Mondini C, Cayuela ML, Sinicco T, Fornasier F, Galvez A, Sánchez-Monedero MA. Soil C Storage Potential of Exogenous Organic Matter at Regional Level (Italy) Under Climate Change Simulated by RothC Model Modified for Amended Soils. Front Environ Sci 2018;6:144. https://doi.org/10.3389/fenvs.2018.00144.

[40] Smith P, Nkem J, Calvin K, Campbell D, Cherubini F, Grassi G, et al. Interlinkages Between Desertification, Land Degradation, Food Security and Greenhouse Gas Fluxes: Synergies, Trade-offs and Integrated Response Options. Climate Change and Land: an IPCC special report on climate change, desertification, land degradation, sustainable land management, food security, and greenhouse gas fluxes in terrestrial ecosystems. P.R. Shukla, J. Skea, E. Calvo Buendia, V. Masson-Delmotte, H.-O. Portner, D. C. Roberts, P. Zhai, R. Slade, S. Connors, R. van Diemen, M. Ferrat, E. Haughey, S. Luz, S. Neogi, M. Pathak, J. Petzold, J. Portugal Pereira, P. Vyas, E. Huntley, K. Kissick, M. Belkacemi, J. Malley, (eds.), IPCC; 2019.

[41] Oldfield EE, Bradford MA, Wood SA. Global meta-analysis of the relationship between soil organic matter and crop yields. SOIL 2019;5:15–32. https://doi.org/10.5194/soil-5-15-2019.

[42] R Core Team. R: A language and environment for statistical computing 2021.

[43] Andrade C, Clivot H, Albers A, Zamora-Ledezma E, Hamelin L. Dataset to assess the soil organic carbon evolution of French croplands in a bioeconomy perspective using the soil model AMG 2022. https://doi.org/10.48531/JBRU.CALMIP/AUEEEJ.

[44] Jamagne M, Hardy R, King D. La base de données géographique des sols de France. Étude et Gestion des Sols 1995:16.

[45] Durand Y, Brun E, Guyomarc'H G, Lesaffre B. A meteorological estimation of relevant parameters for snow models 1993:7.

[46] Launay C, Constantin J, Chlebowski F, Houot S, Graux A, Klumpp K, et al. Estimating the carbon storage potential and greenhouse gas emissions of French arable cropland using high-resolution modeling. Glob Change Biol 2021;27:1645–61. https://doi.org/10.1111/gcb.15512.

[47] Ministère de l'Agriculture et de l'Alimentation. Géoportail. Registre Parcellaire Graphique (RPG) n.d. https://www.geoportail.gouv.fr/donnees/registre-parcellaire-graphique-rpg-2010 (accessed March 12, 2021).

[48] Leenhardt D, Therond O, Mignolet C. Quelle représentation des systèmes de culture pour la gestion de l'eau sur un grand territoire ? gronomie, Environnement & Sociétés,Association Française d'Agronomie (Afa), 2012;2:77–89.

[49] Agreste. Enquete pratiques culturales 2006 n.d. https://agreste.agriculture.gouv.fr/agreste-web/disaron/Dos8/detail/ (accessed October 20, 2020).

[50] Agreste. Recensement agricole 2010 2010. https://agreste.agriculture.gouv.fr/agreste-web; http://agreste.agriculture.gouv.fr/recensement-agricole-2010//methodon/S-RA%202010/methodon/ (accessed October 20, 2020).

[51] Graux A-I, Resmond R, Casellas E, Delaby L, Faverdin P, Le Bas C, et al. High-resolution assessment of French grassland dry matter and nitrogen yields. European Journal of Agronomy 2020;112:125952. https://doi.org/10.1016/j.eja.2019.125952.

[52] Mulder VL, Lacoste M, Richer-de-Forges AC, Martin MP, Arrouays D. National versus global modelling the 3D distribution of soil organic carbon in mainland France. Geoderma 2016;263:16–34. https://doi.org/10.1016/j.geoderma.2015.08.035.

[53] DRIAS les futurs du climat n.d. http://www.drias-climat.fr/.

[54] 4p1000. L'Initiative Internationale "4 Pour 1000" Les Sols Pour La Sécurité Alimentaire et Le Climat n.d. https://www.4p1000.org (accessed January 10, 2021).

[55] Bertuzzi P, Clastre P. Information sur les mailles SAFRAN 2021. https://doi.org/10.57745/1PDFNL.

[56] Levavasseur F, Martin P, Scheurer O. RPG Explorer, notice d'utilisation 2015:114.

[57] Lafargue I. Enquête pratiques culturales grandes cultures et prairies 2011. Application d'intrants sur maïs grain: quelles évolutions en 2011?. France: Ministry of Agriculture, Agri-Food and Forestry; 2013.

[58] Woolf D, Amonette JE, Street-Perrott FA, Lehmann J, Joseph S. Sustainable biochar to mitigate global climate change. Nat Commun 2010;1:56. https://doi.org/10.1038/ncomms1053.

[59] Han L, Sun K, Yang Y, Xia X, Li F, Yang Z, et al. Biochar's stability and effect on the content, composition and turnover of soil organic carbon. Geoderma 2020;364:114184. https://doi.org/10.1016/j.geoderma.2020.114184.

[60] He S, Boom J, van der Gaast R, Seshan K. Hydro-pyrolysis of lignocellulosic biomass over alumina supported Platinum, Mo2C and WC catalysts. Frontiers of Chemical Science and Engineering 2018;12:155–61. https://doi.org/10.1007/s11705-017-1655-x.

[61] Wang J, Xiong Z, Kuzyakov Y. Biochar stability in soil: meta-analysis of decomposition and priming effects. GCB Bioenergy 2016;8:512–23. https://doi.org/10.1111/gcbb.12266.

[62] Zimmerman A, Gao B. The Stability of Biochar in the Environment. In: Ladygina N, Rineau F, editors. Biochar and Soil Biota, CRC Press; 2013, p. 1–40. https://doi.org/10.1201/b14585-2.

[63] Andrade C, Albers A, Zamora-Ledezma E, Hamelin L. A review on the interplay between bioeconomy and soil organic carbon stocks maintenance. PREPRINT (Version 2) Available at Research Square 2022. https://doi.org/10.21203/rs.3.rs-1447842/v1.

[64] Andrade C, Albers A, Zamora-Ledezma E, Hamelin L. Database to determine the Carbon recalcitrance and carbon conversion rate to bioeconomy coproducts 2022. https://doi.org/10.48531/JBRU.CALMIP/WYWKIQ.

[65] Ippolito JA, Cui L, Kammann C, Wrage-Mönnig N, Estavillo JM, Fuertes-Mendizabal T, et al. Feedstock choice, pyrolysis temperature and type influence biochar characteristics: a comprehensive meta-data analysis review. Biochar 2020;2:421–38. https://doi.org/10.1007/s42773-020-00067-x.

[66] Joseph S, Cowie AL, Van Zwieten L, Bolan N, Budai A, Buss W, et al. How biochar works, and when it doesn't: A review of mechanisms controlling soil and plant responses to biochar. GCB Bioenergy 2021:gcbb.12885. https://doi.org/10.1111/gcbb.12885.

[67] Molino A, Larocca V, Chianese S, Musmarra D. Biofuels Production by Biomass Gasification: A Review. Energies 2018;11:811. https://doi.org/10.3390/en11040811.

[68] Ventura M, Alberti G, Panzacchi P, Vedove GD, Miglietta F, Tonon G. Biochar mineralization and priming effect in a poplar short rotation coppice from a 3-year field experiment. Biol Fertil Soils 2019;55:67–78. https://doi.org/10.1007/s00374-018-1329-y.

[69] Watson J, Zhang Y, Si B, Chen W-T, de Souza R. Gasification of biowaste: A critical review and outlooks. Renewable and Sustainable Energy Reviews 2018;83:1–17. https://doi.org/10.1016/j.rser.2017.10.003.

[70] Malghani S, Jüschke E, Baumert J, Thuille A, Antonietti M, Trumbore S, et al. Carbon sequestration potential of hydrothermal carbonization char (hydrochar) in two contrasting soils; results of a 1-year field study. Biology and Fertility of Soils 2015;51:123–34. https://doi.org/10.1007/s00374-014-0980-1.

[71] Watson J, Wang T, Si B, Chen W-T, Aierzhati A, Zhang Y. Valorization of hydrothermal liquefaction aqueous phase: pathways towards commercial viability. Progress in Energy and Combustion Science 2020;77:100819. https://doi.org/10.1016/j.pecs.2019.100819.

[72] Hamelin L, Naroznova I, Wenzel H. Environmental consequences of different carbon alternatives for increased manure-based biogas. Applied Energy 2014;114:774–82. https://doi.org/10.1016/j.apenergy.2013.09.033.

[73] Sarker S, Lamb JJ, Hjelme DR, Lien KM. A Review of the Role of Critical Parameters in the Design and Operation of Biogas Production Plants. Applied Sciences 2019;9:1915. https://doi.org/10.3390/app9091915.

[74] Zhang Y, Kusch-Brandt S, Salter AM, Heaven S. Estimating the Methane Potential of Energy Crops: An Overview on Types of Data Sources and Their Limitations. Processes 2021;9:1565. https://doi.org/10.3390/pr9091565.

[75] Tonini D, Hamelin L, Astrup TF. Environmental implications of the use of agro-industrial residues for biorefineries: application of a deterministic model for indirect land-use changes. GCB Bioenergy 2016;8:690–706. https://doi.org/10.1111/gcbb.12290.

[76] Wietschel L, Messmann L, Thorenz A, Tuma A. Environmental benefits of large-scale second-generation bioethanol production in the EU: An integrated supply chain network optimization and life cycle assessment approach. Journal of Industrial Ecology 2021;25:677–92. https://doi.org/10.1111/jiec.13083.

[77] Clivot H, Mouny J-C, Duparque A, Dinh J-L, Denoroy P, Houot S, et al. Modeling soil organic carbon evolution in long-term arable experiments with AMG model. Environmental Modelling & Software 2019;118:99–113. https://doi.org/10.1016/j.envsoft.2019.04.004.

[78] Mathanker A, Das S, Pudasainee D, Khan M, Kumar A, Gupta R. A Review of Hydrothermal Liquefaction of Biomass for Biofuels Production with a Special Focus on the Effect of Process Parameters, Co-Solvents, and Extraction Solvents. Energies 2021;14:4916. https://doi.org/10.3390/en14164916.

[79] Andriulo A, Mary B, Guerif J. Modelling soil carbon dynamics with various cropping sequences on the rolling pampas. Agronomie 1999;19:365–77. https://doi.org/10.1051/agro:19990504.

[80] Farina R, Sándor R, Abdalla M, Álvaro-Fuentes J, Bechini L, Bolinder MA, et al. Ensemble modelling, uncertainty and robust predictions of organic carbon in long-term bare-fallow soils 2020:25. https://doi.org/10.1111/gcb.15441.

[81] Saffih-Hdadi K, Mary B. Modeling consequences of straw residues export on soil organic carbon. Soil Biology and Biochemistry 2008;40:594–607. https://doi.org/10.1016/j.soilbio.2007.08.022.

[82] Bolinder MA, Janzen HH, Gregorich EG, Angers DA, VandenBygaart AJ. An approach for estimating net primary productivity and annual carbon inputs to soil for common agricultural crops in Canada. Agriculture, Ecosystems & Environment 2007;118:29–42. https://doi.org/10.1016/j.agee.2006.05.013.

[83] DRIAS, Météo-France, CERFACS, IPSL. CNRM-CERFACS-CM5/CNRM-ALADIN63-RCP4.5. DRIAS les futurs du climat 2013. http://www.drias-climat.fr/commande (accessed September 1, 2020).

[84] Chen D, Rojas M, Samset BH, Cobb K, Diongue-Niang A, Edwards P, et al. Framing, Context, and Methods. Climate Change 2021: The Physical Science Basis. Contribution of Working Group I to the Sixth Assessment Report of the Intergovernmental Panel on Climate Change. in Press, IPCC; 2021.

[85] Keel SG, Leifeld J, Mayer J, Taghizadeh-Toosi A, Olesen JE. Large uncertainty in soil carbon modelling related to method of calculation of plant carbon input in agricultural systems: Uncertainty in soil carbon modelling. Eur J Soil Sci 2017;68:953–63. https://doi.org/10.1111/ejss.12454.

[86] Woolf D, Lehmann J, Ogle S, Kishimoto-Mo AW, McConkey B, Baldock J. Greenhouse Gas Inventory Model for Biochar Additions to Soil. Environ Sci Technol 2021:acs.est.1c02425. https://doi.org/10.1021/acs.est.1c02425.

[87] Zimmerman AR. Abiotic and Microbial Oxidation of Laboratory-Produced Black Carbon (Biochar). Environ Sci Technol 2010;44:1295–301. https://doi.org/10.1021/es903140c.

[88] IPCC. 2019 Refinement to the 2006 IPCC Guidelines for National Greenhouse Gas Inventories - Appendix4: Method for Estimating the Change in Mineral Soil Organic Carbon Stocks from Biochar Amendments: Basis for Future Methodological Development. IPCC; 2019.

[89] Zhang Q, Xiao J, Xue J, Zhang L. Quantifying the Effects of Biochar Application on Greenhouse Gas Emissions from Agricultural Soils: A Global Meta-Analysis. Sustainability 2020;12:3436. https://doi.org/10.3390/su12083436.

[90] France Agrimer. L´Observatoire National des Ressources en Biomasse. Évaluation des ressources agricoles et agroalimentaires disponibles en France – édition 2020. Agrimer; 2020.

[91] ADEME, GrDF, GRTgaz. Un mix de gaz 100% renouvelable en 2050. Étude de faisabilité technico-économique. ADEME, GRDF, GRTgaz; 2018.

[92] European Commission, Directorate-General for Climate Action, Radley G, Keenleyside C, Frelih-Larsen A, McDonald H, et al. Setting up and implementing result-based carbon farming mechanisms in the EU : technical guidance handbook. Publications Office of the European Union; 2021. https://doi.org/10.2834/056153.

[93] Goidts E, van Wesemael B. Regional assessment of soil organic carbon changes under agriculture in Southern Belgium (1955–2005). Geoderma 2007;141:341–54. https://doi.org/10.1016/j.geoderma.2007.06.013.

[94] Meersmans J, Van Wesemael B, Goidts E, Van Molle M, De Baets S, De Ridder F. Spatial analysis of soil organic carbon evolution in Belgian croplands and grasslands, 1960-2006: Spatial Analysis of soil organic carbon evolution. Global Change Biology 2011;17:466–79. https://doi.org/10.1111/j.1365-2486.2010.02183.x.

[95] Steinmann T, Welp G, Holbeck B, Amelung W. Long-term development of organic carbon contents in arable soil of North Rhine–Westphalia, Germany, 1979–2015. European Journal of Soil Science 2016;67:616–23. https://doi.org/10.1111/ejss.12376.

[96] Riggers C, Poeplau C, Don A, Frühauf C, Dechow R. How much carbon input is required to preserve or increase projected soil organic carbon stocks in German croplands under climate change? Plant Soil 2021;460:417–33. https://doi.org/10.1007/s11104-020-04806-8.

[97] Martin MP, Dimassi B, Román Dobarco M, Guenet B, Arrouays D, Angers DA, et al. Feasibility of the 4 per 1000 aspirational target for soil carbon: A case study for France. Glob Change Biol 2021;27:2458–77. https://doi.org/10.1111/gcb.15547.

[98] Bai X, Huang Y, Ren W, Coyne M, Jacinthe P, Tao B, et al. Responses of soil carbon sequestration to climate-smart agriculture practices: A meta-analysis. Glob Change Biol 2019;25:2591–606. https://doi.org/10.1111/gcb.14658.

[99] Bodilis A-M, Trochard R, Lechat G, Airiau A, Lambert L, Hruschka S. Impact de l'introduction d'unités de méthanisation à la ferme sur le bilan humique des sols. Analyse sur 10 exploitations agricoles de la région Pays de la Loire. Fourrages 2015.

[100] Möller K. Effects of anaerobic digestion on soil carbon and nitrogen turnover, N emissions, and soil biological activity. A review. Agron Sustain Dev 2015;35:1021–41. https://doi.org/10.1007/s13593-015-0284-3.

[101] Thomsen IK, Olesen JE, Møller HB, Sørensen P, Christensen BT. Carbon dynamics and retention in soil after anaerobic digestion of dairy cattle feed and faeces. Soil Biology and Biochemistry 2013;58:82–7. https://doi.org/10.1016/j.soilbio.2012.11.006.

[102] Wentzel S, Schmidt R, Piepho H-P, Semmler-Busch U, Joergensen RG. Response of soil fertility indices to long-term application of biogas and raw slurry under organic farming. Applied Soil Ecology 2015;96:99–107. https://doi.org/10.1016/j.apsoil.2015.06.015.

[103] Reibel A. Valorisation agricole des digestats : Quels impacts sur les cultures, le sol et l'environnement ? Revue de littérature. GERE, ADEME; 2018.

[104] Cayuela ML, Kuikman P, Bakker R, van Groenigen JW. Tracking C and N dynamics and stabilization in soil amended with wheat residue and its corresponding bioethanol by-product: a ^{13} C/ ^{15} N study. GCB Bioenergy 2014;6:499–508. https://doi.org/10.1111/gcbb.12102.

[105] Alotaibi KD, Schoenau JJ. Enzymatic activity and microbial biomass in soil amended with biofuel production byproducts. Applied Soil Ecology 2011;48:227–35. https://doi.org/10.1016/j.apsoil.2011.03.002.

[106] Hansen V, Müller-Stöver D, Imparato V, Krogh PH, Jensen LS, Dolmer A, et al. The effects of straw or straw-derived gasification biochar applications on soil quality and crop productivity: A farm case study. Journal of Environmental Management 2017;186:88–95. https://doi.org/10.1016/j.jenvman.2016.10.041.

[107] Drosg B, Fuchs W, Seadi TA, Madsen M, Linke B. Nutrient Recovery by Biogas Digestate Processing. IEA Bioenergy; 2015.

[108] Ndede EO, Kurebito S, Idowu O, Tokunari T, Jindo K. The Potential of Biochar to Enhance the Water Retention Properties of Sandy Agricultural Soils. Agronomy 2022;12:311. https://doi.org/10.3390/agronomy12020311.

[109] Gondim RS, Muniz CR, Lima CEP, Santos CLAD. EXPLAINING THE WATER-HOLDING CAPACITY OF BIOCHAR BY SCANNING ELECTRON MICROSCOPE IMAGES. Rev Caatinga 2018;31:972–9. https://doi.org/10.1590/1983-21252018v31n420rc.

[110] de Jager M, Röhrdanz M, Giani L. The influence of hydrochar from biogas digestate on soil improvement and plant growth aspects. Biochar 2020;2:177–94. https://doi.org/10.1007/s42773-020-00054-2.

[111] Glaser B, Wiedner K, Seelig S, Schmidt H-P, Gerber H. Biochar organic fertilizers from natural resources as substitute for mineral fertilizers. Agron Sustain Dev 2015;35:667–78. https://doi.org/10.1007/s13593-014-0251-4.

[112] Martin M, Dimassi B, Picaud C, Millet F, Bardy M, Boulonne L, et al. Methodes de Comptabilisation du stockage de carbone organique des sols sous l´effet des pratiques culturales CSOPRA. ADEME; 2018.

[113] Andrade C, Clivot H, Albers A, Zamora-Ledezma E, Hamelin L. The crop residue conundrum: maintaining long-term soil organic carbon stocks while reinforcing the bioeconomy, compatible endeavors? Research Square: PREPRINT 2022. https://doi.org/doi.org/10.21203/rs.3.rs-1447950/v2.

[114]. Andrade Díaz C, Clivot H, Albers A, Zamora-Ledezma E, Hamelin L. The crop residue conundrum: Maintaining long-term soil organic carbon stocks while reinforcing the bioeconomy, compatible endeavors? Applied Energy. 2023 Jan 1;329:120192.

4. CHAPTER 4: SOC modeling for the bioeconomy in tropical contexts:

Long-term SOC dynamics in Tropical lands

4. CHAPTER 4: SOC modeling for the bioeconomy in tropical contexts – Ecuadorian case study

4.1 Context

This chapter answers the specific research questions:

1. **RQ2**. How much additional biomass is available if bioeconomy coproducts are returned to soils, compared to an approach not considering the bioeconomy/recalcitrance effect?
2. **RO2.** Adapt a soil model to evaluate the long-term SOC dynamics of harvesting crop residues for the bioeconomy while returning the bioeconomy coproducts to soils.
3. **RO3**. Perform spatially explicit assessments of C-neutral harvest potential of crop residue to supply the bioeconomy at the national level in temperate and tropical contexts, represented by France and Ecuador, respectively.
4. **RO3.1** Build the baseline of Ecuadorian cropping systems with potential to supply the bioeconomy development in the country.

While the AMG soil model used in **Chapter 3** has been widely validated for temperate climates, it cannot be directly used in tropical lands due to a lack of validation for this particular pedoclimatic conditions. Therefore, this study adapted the framework to include bioeconomy coproducts within the RothC soil model, which has been tested in a wider array of climates as reviewed in **Chapter 2.** Besides the soil model itself, another marked difference with the study of Andrade et al. 2023 is the inclusion of crops commonly found in tropical regions, which have a higher lignin content than the typical cereal-like crops included in **Chapter 3.** The model was tested with a high spatial resolution for Ecuadorian croplands as a representative case. To this end, three main stages were performed within this work. First, we performed a spatial-explicit assessment of the crop residue potential in Ecuador, which has produced the first baseline representing current cropping systems for the country and assessing the potential for the bioeconomy and soil C inputs. This stage is presented as a data paper included in **Appendix A3a**. In the second stage, we adapted the soil model RothC to include four bioeconomy coproducts: pyrochar, gaschar, hydrochar, and digestate, as defined in **Chapter 3**. Based on the conclusions observed using AMG for the bioethanol scenario, this scenario was not considered in this chapter. Finally, the croplands baseline developed for Ecuador was applied in the newly adapted RothC-Bioeconomy to perform the spatial explicit SOC modeling in Ecuadorian croplands, for the four bioeconomy coproducts. The stages two and three are presented in this chapter.

Key findings

- The database defining CC coefficients in Chapter 1 was extended with new 110 data records to account for tropical crop residues.
- The baseline cropping systems and potential crop residues of Ecuador has been defined. A detailed spatial explicit database reporting biomass yields and derived above- and belowground C inputs to soil has been produced.
- A total potential of 113 PJ crop residues is available in the assessed cropland portion (52% of Ecuadorian croplands).
- The cumulated monthly evapotranspiration for Ecuador, for the period 2020 – 2070, under the RCP 4.5 projection, at a 4km spatial resolution was produced in this chapter.
- The RothC soil model was adapted to include pyrochar, gaschar, hydrochar, and digestate, resulting in the RothC-Bioeconomy model.

The content of this chapter is being prepared for submission to peer review and the databases developed are transparently documented in the open repositories declared along the chapter.

List of figures

List of tables

Modelling the long-term carbon storage potential from recalcitrant matter inputs in tropical arable croplands

Christhel Andrade Diaz[a,b*], Enrico Balugani[c], Ezequiel Zamora-Ledezma[d], Lorie Hamelin[a]

[a] Toulouse Biotechnology Institute (TBI), INSA, INRAE UMR792, and CNRS UMR5504, Federal University of Toulouse, 135 Avenue de Rangueil, F-31077, Toulouse, France

[b] Department of Chemical, Biotechnological and Food Processes, Faculty of Mathematical, Physics and Chemistry Sciences. Universidad Técnica de Manabí (UTM), 130150, Portoviejo, Ecuador.

[c] Department of Physics and Astronomy, Università di Bologna, Bologna, Italy

[d] Ecosystems Functioning and Climate Change Research Group FAGROCLIM, Faculty of Agriculture Engineering. Universidad Técnica de Manabí (UTM), 13132, Lodana, Ecuador.

* andraded@insa-toulouse.fr, christhel.andrade@utm.edu.ec,

Abstract

The urgency to achieve climate neutrality and limit global warming requires a transition to low fossil carbon use. Crop residues, an abundant source of renewable carbon, remain underutilized, among others due to soil conservation practices. Soil organic carbon (SOC) plays a crucial role in tropical croplands by supporting soil health, nutrient availability, and biogeochemical cycles. The incorporation of exogenous organic matter (EOM) amendments has the potential to enhance carbon storage and fertility. This study conducted in Ecuador, a biodiversity hotspot, aims to identify SOC stock vulnerabilities, estimate SOC storage potential and changes in CO_2 fluxes in tropical cropping systems resulting from changes in crop residue harvest for use within the bioeconomy, when a subsequent recalcitrant EOM application is involved. A spatially-explicit modeling framework representing the agricultural area into 15,782 agricultural pedoclimatic units was employed to assess the potential for SOC storage and to quantify resulting CO_2 emission changes in tropical cropping systems. Four scenarios were analyzed, all implying the conversion of crop residues into bioeconomy products as well as recalcitrant EOMs. The RothC soil model, adapted to incorporate additional carbon pools for labile (C_L) and recalcitrant (C_R) fractions, as well as the priming effect, was utilized alongside high-resolution data to evaluate SOC storage potential for each scenario. Baseline SOC stocks ranged from 7.43 to 235 t C ha^{-1}, with an average of 61.76 t C ha^{-1}. At the national level, the business-as-usual (BAU) scenario, i.e., crop residues removal, projected a potential 4% increase in SOC stocks by 2040 and a 7% increase by 2070. However, SOC stocks decreased in 79% of the study area. The simulations

demonstrated the potential to supply 113 PJ biomass for the bioeconomy without incurring SOC losses in the pyrolysis and gasification scenarios. Harvesting residual biomass with co-product return led to a 19-39% reduction in CO_2 emissions over 50 years, depending on the scenario. Sensitivity analyses revealed the priming effect as a particularly sensitive parameter for the results.

Keywords

Soil organic carbon, exogenous organic matter, RothC, crop residues, carbon sink, bioeconomy, priming effect, biochar, digestate, gaschar, hydrochar

Highlights

- The soil model RothC was adapted to simulate the long-term SOC dynamics of recalcitrant exogenous organic matter inputs.
- The adapted RothC was used to estimate the SOC storage potential of croplands amended with recalcitrant EOMs in tropical lands.
- The changes in CO_2 emissions were studied for various scenarios involving the harvest of crop residues and return of recalcitrant EOMs.
- The baseline of current cropping systems of Ecuador was developed with high spatial resolution.

Graphical abstract

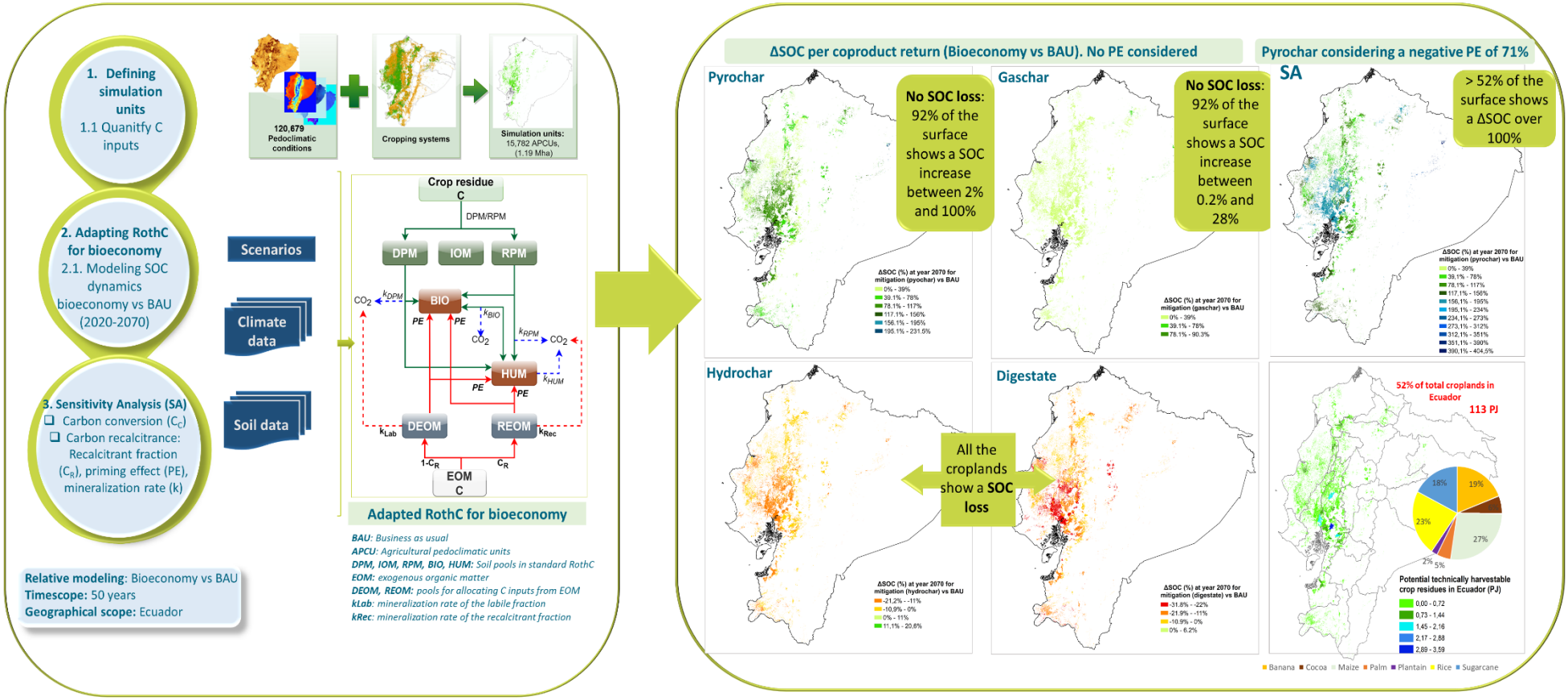

Fig 0 Graphical abstract summarizing Chapter 4

List of abbreviations

Acronym	Description
AD	Anaerobic Digestion
AMG	Model simulating soil C at annual time steps
APCU	Agricultural Pedoclimatic Units
APSIM	Agricultural Production Systems Simulator
BAU	Business as Usual
BIO	Microbial biomass
C	Carbon
CANDY	Carbon and Nitrogen Dynamics model
C_C	Carbon Conversion
Century	Century Model
C_L	Carbon Labile fraction
CO_2	Carbon dioxide
CO_{2_BAU}	CO_2-C Emissions in the BAU Scenario
CO_{2_bio}	CO_2-C Emissions in the Mitigation Scenario
C_R	Carbon Recalcitrance fraction
CTOOL	Cropping System TOOL
DEOM	Decomposable Exogenous Organic Matter
DM	Dry Matter
DPM	Decomposable Plant Material
EOM	Exogenous Organic Matter
EPIC	Environmental Policy Integrated Climate model
ESPAC	National Continuous Agricultural Production and Surface Survey of Ecuador
HTL	Hydrothermal Liquefaction
HUM	Humified organic matter
IEA	International Energy Agency
IOM	Inert Organic Matter
IPCC	Intergovernmental Panel on Climate Change
ISRIC	International Soil Reference and Information Centre
k	Decay Rate
k_L	Mineralization Rate of the Labile Fraction
k_{Lab}	Mineralization rate of the labile fraction
k_R	Mineralization Rate of the Recalcitrant Fraction
k_{Rec}	Mineralization rate of the recalcitrant fraction
MAG	Ministry of Agriculture of Ecuador

MRT	Mean Residence Time
Mt C	Megatonnes of Carbon
PCU	Primary Crop Unit
PE	Priming Effect
Pg	Petagram (1 billion metric tons)
Pyrochar	Pyrolysis biochar
RCP	Representative Concentration Pathway
REOM	Recalcitrant Exogenous Organic Matter
RothC	Rothamsted Carbon Model
RPM	Resistant Plant Material
RPR	Residue to Product Ratio
RtS	Root to Shoot Ratio
SA	Sensitivity Analysis
S_{APCU}	Surface area of Agricultural Production and Consumption Unit
SI	Supplementary Information
SOC	Soil Organic Carbon
$SOC_{\_BAU}$	SOC stocks in the BAU scenario
$SOC_{\_bio}$	SOC stocks in the mitigation scenario
SOC_0	Initial SOC stocks
SOCS	Soil Organic Carbon Sequestration
$SOC_{t,i,x}$	Final SOC stocks at time t, APCU i, and scenario x
SOC_{tBAU}	SOC stock at time t for the BAU scenario
SOC_{tbio}	SOC stock at time t for the mitigation scenario
SPEI	Standardized Precipitation Evapotranspiration Index
t	Time
w	Pondering Coefficient
ΔCO_2	Difference in CO_2 emissions between mitigation and BAU scenarios
ΔCO_2 (t C ha^{-1} y^{-1})	Amount of CO_2-C emitted or avoided by each mitigation scenario at the end of the simulation
$\Delta SOC_{0\text{-}t,i,x}$ (%)	Percent change of SOC stocks from initial conditions to the end of the simulation
$\Delta SOC_{bio\text{-}BAU}$ (%)	Weighted average SOC change observed per scenario at a national scale
$\Delta SO_{Cbio\text{-}BAUi}$ (%)	SOC stocks change percentage observed by implementing a mitigation scenario, relative to the BAU, in the APCU i
ΔSOC_{net}	Net change in SOC stocks at the national level

1. Introduction

The ambitious goal of climate neutrality by 2050 [1,2] set to commit to the Paris Agreement [3] target to limit global warming well below 2°C calls for actions ensuring a transition toward low fossil carbon (C) use [4]. Biomass, particularly crop residues, constitutes one of the largest streams supplying renewable C, with an estimated production of 5 billion metric tons in 2013 [5]. However, this potential is not fully exploited as crop residues are usually left on the agricultural fields to conserve the soil organic carbon (SOC) budget [6,7]. Typically, a precautionary principle is applied, suggesting a crop-dependent threshold ranging from 15% to 60% [8] to avoid SOC losses related to the harvest of crop residues.

Soil organic carbon is especially important for soil health and functioning in tropical croplands due to their high soil biodiversity and fertility, as well as year-round intensive agricultural practices that promote soil degradation and carbon losses [9]. Tropical soils can store large amounts of carbon, and the incorporation of organic matter through the use of cover crops and the application of organic amendments can help maintain soil health and fertility [10,11].

In addition, soil organic carbon plays a crucial role in supporting biogeochemical cycles and plant nutrition in tropical croplands [12,13]. Soil organic matter can enhance the mineralization and availability of nutrients such as nitrogen, phosphorus, and sulfur, which are often limiting factors in tropical soils [14,15]. Moreover, soil organic matter can also improve soil structure, water-holding capacity, and infiltration, leading to increased soil productivity and crop yields in tropical croplands [9,16].

Given the high potential for soil carbon sequestration especially in tropical croplands, there is a need for effective strategies to increase soil organic carbon stocks and mitigate carbon losses. This can be achieved through the implementation of sustainable agricultural practices, which aims to minimize soil disturbance and maintain soil cover with the use of cover crops and mulching [14]. Furthermore, the use of organic amendments such as compost and manure can also promote soil carbon sequestration and improve soil health in tropical croplands [13,17]. Overall, the maintenance and enhancement of soil organic carbon are crucial for the sustainable management of tropical croplands and the provision of ecosystem services such as carbon sequestration, nutrient cycling, and food security.

In this context, agricultural soils can behave either as a source or sink of C in response to stress induced by farming management practices [10]. Various studies have addressed diverse agricultural

practices to induce SOC sequestration, including the insertion of cover crops [11] and grasslands [18,19] in crop rotations and the recycling of organic resources [20] as exogenous organic matter (EOM) to soils. EOM can be defined as any byproduct material of biological origin derived from industries, livestock breeding, or municipal wastes, that can be applied as a soil amendment to promote C storage, enhance soil fertility, and reduce soil degradation [21,22].

The potential of various EOMs (e.g., manure, compost, sewage sludge) to improve agriculture and offset environmental impacts has been studied by various authors [21–24], with results depending on the specific pedoclimatic characteristics associated with the soil and the composition of the EOM, itself determined by the original feedstock and production conditions. Nevertheless, the application of EOMs to soils is highlighted as an attractive strategy for building up SOC stocks while recycling material otherwise considered waste. Moreover, previous studies have revealed that the actual harvesting potential of crop residues to supply bioeconomy services could increase if the coproduct of the process returns to the soil as an EOM [8,25,26].

Due to the high costs associated with SOC measurements, soil models able to simulate the soil response to EOM application are a valuable tool for developing soil C sequestration policies [27]. Previous studies have investigated the inclusion of EOMS with varying degrees of recalcitrance, such as biochar and digestate, in soil models, including RothC [26,28–30], Century [31], APSIM [32], EPIC [33], CTOOL [25], AMG [34], and CANDY [35]. Notably, Andrade Diaz et al. [8] have included five different EOMs simultaneously in AMG and applied the model to French croplands. However, SOC modeling including recalcitrant EOMs has been predominantly studied for temperate regions and research is needed to expand their application to other biomes.

In fact, according to IPCC [36] tropics can potentially sequestrate 1.1 – 1.6 Pg C yr^{-1}, which represents approximately 70% of the global potential carbon sequestration from 1995 to 2050. On the other hand, the favorable pedoclimatic conditions, wide crop biodiversity, and high soil fertility allow for year-round intensive agricultural practices that promote soil degradation and carbon losses in tropical croplands [12]. Tropical croplands are thus key for supplying renewable carbon to the bioeconomy if C sequestration strategies can be implemented.

This study aims to estimate at a high-spatial-resolution the i) SOC storage potential of tropical cropping systems under various scenarios entailing the harvest of crop residues followed by the application of recalcitrant EOM, and iii) the CO_2 emissions mitigation potential of these scenarios. We modeled the SOC dynamics of Ecuadorian croplands (0 – 30 cm), with and without harvesting crop residues to supply various bioeconomy pathways, allowing for the return of recalcitrant EOMs. Albeit Ecuador is a well-known biodiversity hotspot, vulnerabilities regarding the maintenance of SOC stocks

have already been identified [37,38] and were thus selected as an illustrative case of tropical lands. When it comes to CO_2 mitigation, the scope of the work is only related to the changes in crop residues management from the soil perspective. A complete assessment should also consider the full biomass conversion processes and activities, as well as substitution effects, which is outside the scope of this work.

2. Methods

2.1 Modelling framework

We used a spatially-explicit approach to assess the SOC storage potential in tropical lands, under four mitigation scenarios involving the conversion of crop residues into stabilized EOMs as compared to a business-as-usual (BAU) reference scenario where crop residues remain on soils. The study was based on the framework developed by Andrade et al. [8] and applied with a high-spatial resolution for the Ecuadorian croplands as a representative case. A near-term (2020-2040) and long-term (2020-2070) timeframe were considered for all the scenarios. The BAU scenario reflects the current cropping systems of Ecuador and assumes that crop residues (100%) are left on soils as a source of C. As opposed, each mitigation scenario considers that all the technically harvestable crop residues are exported to supply the bioeconomy and then partially returned as a stabilized EOM rich in recalcitrant carbon. The BAU is then a benchmark for contrasting the mitigation scenarios. The EOMs considered here are biochar produced under gasification and fast pyrolysis, hydrochar from hydrothermal liquefaction (HTL), and digestate from anaerobic digestion (AD). To avoid confusion between the mitigation scenarios, biochar is referred as pyrochar and gaschar for the pyrolysis and gasification processes, respectively.

The framework entails four consecutive stages (Fig 1) detailed in the subsequent sections: i) first, we clustered the country according to its pedoclimatic characteristics and define the area of study, ii) then, we described the baseline cropping systems and quantify the spatially explicit potential of crop residues in Ecuador, iii) thereafter, the RothC [39] soil model was adapted and applied with high resolution to determine the SOC storage potential of each mitigation scenario (compared to the BAU), and iv) we finally performed a sensitivity analysis to evaluate the influence of the key parameters driving the soil model.

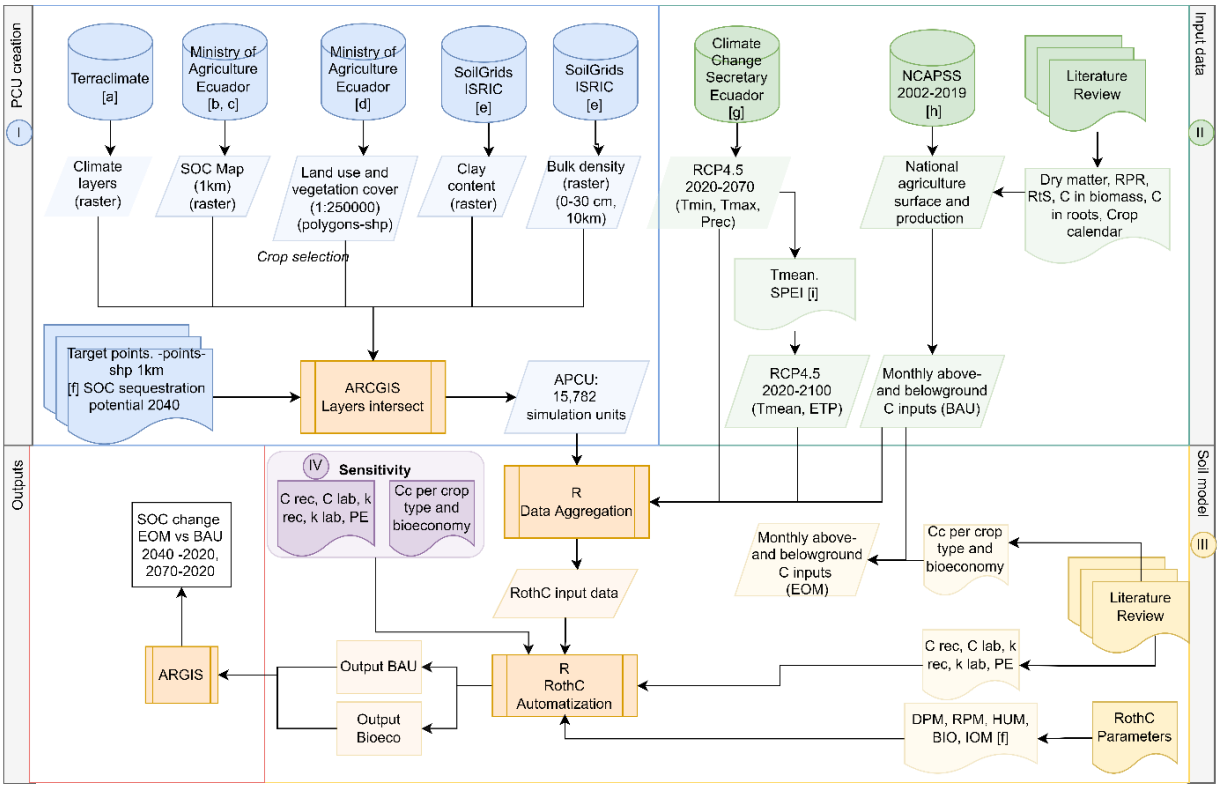

Fig. 3 Modelling framework applied for Ecuador, to quantify the spatially-explicit long-term SOC storage potential under four mitigation scenarios, entailing the return of exogenous organic matter. ISRIC: International Soil Reference and Information Centre, NCAPSS: National Continuous Agricultural Production and Surface Survey of Ecuador, known as ESPAC, RPR: residue to product ratio, RtS: root to shoot ratio, RCP: Representative concentration pathway, SOC: soil organic carbon, EOM: exogenous organic matter, BAU : business as usual, DPM, RPM, HUM, BIO, HUM : soil pools in RothC. [a] [40], [b] [41], [c] [37], [d] [42], [e] [43], [f] [38], [g] [44], [h] [45], [i] [46]

2.2 Spatially explicit cropping systems

The wide pedoclimatic diversity of Ecuadorian croplands was represented by the so-called agricultural pedoclimatic units (APCU, [8]), which are unique combinations of soil characteristics, meteorological variables, and crop rotations in agricultural lands. The creation of the APCUs is thoroughly detailed in the supplementary information (SI)1, while the original and processed data are transparently documented in “a companion data paper [47]”, inhere we succinctly explore the essential concepts to build the APCUs. The APCUs were built upon the contribution of the Ministry of Agriculture of Ecuador (MAG) for the global Soil Organic Carbon Sequestration (SOC) map [37,38], by intersecting the national SOC stock map at 0-30 cm [41], the climate layers extracted from Terraclimate [40] and the national land use map for the period 2009 – 2015 [42]. The average data reported for the period 2016 – 2019 on the National Continuous Agricultural Production and Surface Survey (ESPAC; [48]) was used to select the study area based on crop yields and surface. The selected representative

crops include 10 different annual, semi perennial and perennial species (i.e., banana, barley, cocoa, coffee, maize, rice, plantain, oil palm, sugarcane, and wheat) (Table S1), representing 95% of the national production and over 90% of the national croplands surface [47]. The APCUs included in this study where only those dedicated to the selected crops, with at least 10 ha of surface, and for which the Ecuadorian SOC sequestration map presented successfully modelled SOC stocks for 2040 under a BAU development [38]. This selection yielded 15,782 APCUs covering 1.19 Mha, which represents 52% of the total Ecuadorian croplands (further detailed in SI1) in 2009-2015.

The potential residual biomass contributing to the soil C inputs in the BAU scenario was determined based on the average yield extracted from the data reported on the historical ESPAC for the period 2002-2019. The above- and belowground C inputs per APCU were calculated by multiplying the main product yield (t ha^{-1}) per crop by the residue-to-product (RPR; [49]) and root-to-shoot (RtS, [50]) ratios and the corresponding C content (see Andrade et al. [47]), respectively. The C inputs in the mitigation scenarios were determined as in the BAU, with the premise that all the technically harvestable fraction (Table S1) was mobilized to supply the bioeconomy and partially returned to the soils as a recalcitrant EOM. The detailed procedure to determine the potential crop residues and C inputs in the Ecuadorian cropping systems is detailed in SI1 and in the associated data paper.

2.3 Mitigation scenarios

The mitigation scenarios consider the application of four different EOMs to offset SOC stock losses and climate change. The EOM-SOC dynamics are directly affected by the quantity of C in the EOM and its recalcitrance to degradation when input in soils. The recalcitrance represents the fraction of carbon in the EOM that is more resistant to mineralization [51] and is represented by the carbon recalcitrance (C_R) coefficient. The more easily degradable fraction of carbon is referred to as labile (C_L), and is expressed as $1 - C_R$. The amount of carbon input through each EOM is affected by the carbon conversion (C_C) coefficient [52]. Both C_C and C_R are specific for each EOM and are governed by the process conditions and the feedstock material composition.

The EOMs included in this study are pyrochar produced under fast pyrolysis conditions, gaschar obtained as a coproduct of gasification, hydrochar produced from hydrothermal liquefaction (HTL), and digestate resulting from anaerobic digestion (AD). The process conditions assumed to produce each of the EOMs are described in SI1. While thermochemical processes (i.e., pyrolysis, gasification, and HTL) are conducted under extreme pressure and temperature conditions that favour the appearance of aromatic carbon related to high C_R values [53], biochemical processes, such as AD, do not change the original structure of the C contained in the raw biomass [54]. The C_R and C_C values used were retrieved from the study by Andrade et al. [52]; the former taken directly as presented in the

original study, whereas the latter included the expansion of the database to include the tropical crop residues assessed in this study (Table 1).

Due to their recalcitrant nature, EOMs used as soil amendments can change the normal rate of SOC mineralization. This effect is commonly referred to as priming effect (PE) and is considered to be positive (+PE) if the mineralization rates observed in the BAU are accelerated by the input of the EOM, and negative (-PE) if the rate is slower [55]. Due to the tremendous role played by the mineralization rate on SOC dynamics [30], the PE was considered a key parameter to assess the EOM-SOC dynamics in this study (Table 1).

Table 1. Mitigation scenarios and inner characteristics of the carbon structure of the EOMs included in this study. [a]

EOM	Production conditions	C_C		C_R [b]	C_L	PE[c]	k_L [b] (y^{-1})	k_R [b] (y^{-1})
		Cereal straw [b]	Fibres and leaves [c]					
Pyrochar	350°C – 700°C, seconds to 2 hours, DM > 90%	0.44	0.51	0.95	0.05	0.286	118.00	0.003
Gaschar	600°C – 1200°C, DM > 90%	0.20	0.31	0.95	0.05	0.449	69.67	0.007
Hydrochar [d]	180°C – 400°C, catalyst, DM < 20%	0.31	0.31	0.89	0.11	0.803	27.64	0.099
Digestate	Mesophilic: 30°C – 50°C, 1-3 months, DM < 35%	0.36	0.69	0.68	0.32	0.803	199.96	0.815

C_C: Carbon conversion C_R: Carbon recalcitrant fraction, C_L: carbon labile fraction (1-C_R), PE: Priming effect, k_L: mineralization rate of the labile fraction, k_R: mineralization rate of the recalcitrant fraction. [a] Parameters considered for the main simulations of this study, considered as the default average parameters. PE is 1 for the main simulations and the PE reported in here is only considered for the sensitivity analysis (section 2.5). [b] Value used as in Andrade Díaz et al. (2023). [c] Average value from 110 data records reported in Andrade et al. [56] to include lignin rich crop residues. PE values of pyrochar and gaschar were defined according to the global meta-analysis by [57]. PE for pyrochar was used as the percent change of the organic carbon content in the soil observed by the application of biochar produced at medium temperature (350 – 600°C) and the value observed for high temperatures (> 600 °C) was used as proxy for gaschar. The determination of PE as presented in here is further detailed in section 2.4.4 and SI1. PE for digestate was calculated from a meta-analysis (unpublished) including 79 data records contrasting the SOC changes observed after the application of digestate with a control situation where no digestate is applied. [d] No data regarding the hydrochar represented in this study was found, therefore C_C and C_R defined in Andrade Díaz et al. (2023) for cereal residues were used as a proxy. Since HTL processes tolerate wet feedstocks as in AD processes, and the recalcitrance lifetime of hydrochar was found to be on the decadal scale as opposed to the hundreds found for other biochar (pyrochar and gaschar) [53,58], the PE defined for digestate was used as a proxy for hydrochar.

2.4 SOC modeling

2.4.1 Soil model RothC Overview

The Rothamsted Carbon model (RothC) 26.3 [39] is a widely used multicompartment model for predicting soil carbon turnover. It was initially developed to simulate the SOC dynamics in croplands and later expanded to forests and grasslands. RothC has been tested and well-validated under different soils and climates worldwide, including tropical regions [59–62].

The model operates in a monthly timestep and is structured to allocate the carbon inputs in five different soil compartments (Fig. 2a). The decomposable plant material (DPM), resistant plant material (RPM), microbial biomass (BIO), and Humified organic matter (HUM) compartments are considered active and mineralize the C inputs according to specific decay rates (*k*) in each pool, following first-order kinetics. The inert organic matter (IOM) pool is a small compartment resistant to decomposition. The *k* values for the active pools are constants in decreasing order: k_{DPM}= 10 y^{-1}, k_{RPM}= 0.30 y^{-1}, k_{BIO}= 0.66 y^{-1}, k_{HUM}= 0.02 y^{-1}, with a mean residence time (MRT) of 1 k^{-1}.

The carbon inputs are split between DPM and RPM according to the DPM: RPM ratio of the material. The default DPM: RPM ratio for croplands and grasslands is 1.44 (i.e., the material contains 59% DPM and 41% RPM). A portion of the carbon in each compartment is mineralized as CO2 and the remaining fraction is allotted in the BIO (46%) and HUM (54%) pools. The soil clay content determines the proportion of emitted CO_2.

2.4.2 Adapted RothC for the mitigation scenarios

We adapted RothC to include two extra pools to allocate the labile (C_L) and recalcitrant (C_R) carbon fractions of the EOMs under study (Fig2b). The model, hereon RothC-Bioeconomy, is built upon the study of Pulcher et al. [30] for including biochar in RothC. The C_L and C_R coefficients (Table 1) distribute the EOM's C between the decomposable exogenous organic matter (DEOM) and the recalcitrant exogenous organic matter (REOM) pools, respectively. RothC-Bioeconomy assumes that the EOM is partly mineralized into CO_2 and the remaining C is transferred to the BIO and HUM pools. The carbon mineralization in the DEOM and REOM pools is defined by their respective mineralization rates (k_L and k_R) and is affected by the priming effect of the EOM. The size (C_L and C_R) and mineralization rates (k_L and k_R) allotted to the DEOM and REOM pools are EOM-dependent and were used as reported in the study of Andrade et al. [52], as further detailed in SI1.

The pyrochar PE was retrieved from the global meta-analysis by Chagas et al. [57], where the mean effect on SOC stocks determined for the application of biochar produced at pyrolysis temperatures ranging from 350°C to 600°C was used to represent the pyrochar PE in this study. Due

to lack of information regarding the PE of gaschar, the SOC change determined by Chagas et al. [57] for pyrolysis temperatures above 600°C was used as a proxy for gaschar PE. A meta-study (*unpublished)* was performed to contrast the SOC stocks attained under digestate application against a control situation with no digestate inputs and it was used to derive the PE of digestate. The data used to determine the digestate PE is openly reported in Andrade et al. [56]. If no PE is considered by the input of the EOM, then PE is set as 1. If the EOM input involves a PE on the mineralization rates, then the PE value is summed or subtracted from 1, for a positive and negative PE, respectively. The details on implementing the RothC-Bioeconomy parameters (i.e., C_C, C_R, k_L, k_R, and PE) are further explored in SI1.

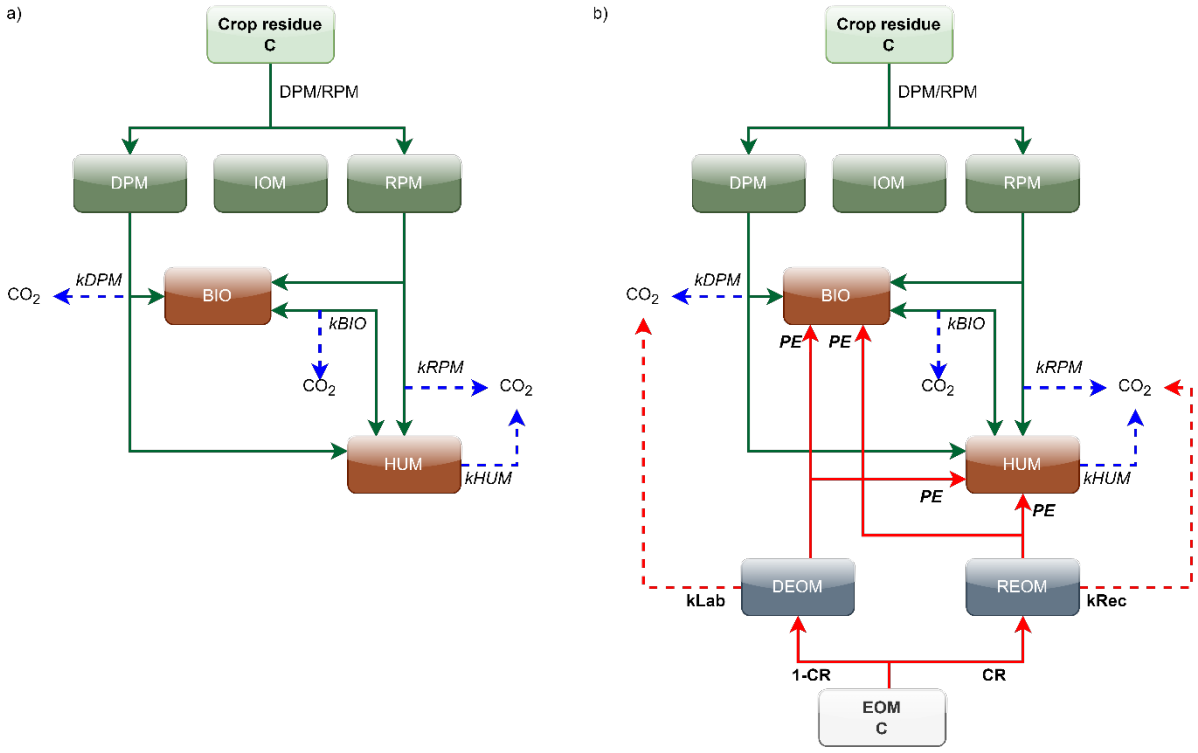

Fig 2. RothC model a) original configuration, and b) RothC-Bioeconomy adapted in this study. DPM: Degradable Plant Material. RPM: Resistant Plant Material. BIO: Microbial Biomass. HUM: Humified Organic Matter. IOM; Inert organic matter. k: mineralization rate. PE: Priming effect. EOM: Exogenous organic matter. DEOM: decomposable exogenous organic matter. REOM: recalcitrant exogenous organic matter. EOM: exogenous organic matter. k_{Lab}: mineralization rate of the labile fraction. k_{Rec}: mineralization rate of the recalcitrant fraction. Green solid line represents the allocation of the crop residue carbon in the soil pools. Red solid line depicts the allocation of EOM carbon in the soil pools. Dotted lines represent mineralization of the carbon inputs as CO_2.

2.4.3 Input data for RothC-Bioeconomy

RothC requires minimal and relatively easily obtainable climate, soil, and management data. The climate data comprises monthly rainfall (mm), monthly evapotranspiration (mm), and average monthly air temperature (°C). The temperature and precipitation data for the period 2020 – 2070, were obtained from the Sub-secretary of Climate Change of Ecuador [44], for the RCP4.5 climate trajectory (Representative Concentration Pathway; [63], downscaled by the ensemble model IPSL-CM5A-MR/MIROC-ESM/GISS-E2-R/CSIRO-Mk3-6-0. The evapotranspiration was calculated using the Thornthwaite method [61,64] within the Standardized Precipitation Evapotranspiration Index (SPEI package SPEI v1.7, updated 2019) package [46,65]. The preparation of the spatially-explicit meteorological data is detailed in [47]. Soil data includes clay content (%) at simulation depth, initial (0 - 30 cm) SOC stocks (t C ha^{-1}), and initial SOC allocation among the different pools. Data regarding SOC stocks and allocation across the soil pools, as well as the clay content (%), were retrieved from the contribution of MAG to the Global SOC sequestration potential map [37,38] at a 1km resolution. The bulk density was retrieved from Soilgrids [43].

The management data comprise information on whether the soil is covered or bare, an estimate of the decomposability of the plant material (DPM:RPM ratio), and the monthly input of carbon (t C ha^{-1}) from the crop residues, farmyard manure, and other EOMs. The DPM:RPM ratio used was 1.44 as suggested by default in RothC for cropping systems [39]. The monthly above- and belowground C inputs were calculated based on the average (years 2022 to 2019) production data reported in the ESPAC [45] for the sow/harvest schedule of the crops included in this study (Fig S1), as further detailed in SI1.

2.4.4 SOC storage potential calculation

The SOC storage potential of any mitigation scenario, compared to the BAU, is determined as the SOC change observed at the end of the simulations in each scenario (mitigation *vs* BAU). The SOC stocks change is calculated in each APCU using Eq (1) [8] and scaled at national level as the weighted average according to the APCU surface (Eq (2)).

$$\Delta SOC_{\ bio-BAU_i}(\%) = \left(\frac{SOC_{tbio} - SOC_{tBAU}}{SOC_{tBAU}}\right)_i * 100 \qquad (4)$$

$$\Delta \widetilde{SOC}_{\ bio-BAU}(\%) = \Delta SOC_{\ bio-BAU_i} * w_i \qquad (5)$$

where $\Delta SOC_{bio\text{-}BAUi}$ (%) is the SOC stocks change percentage observed by implementing a mitigation scenario, relative to the BAU, in the APCU i. SOC_{tbio} is the SOC stock at time t for the mitigation scenario and SOC_{tBAU} is the SOC stock at time t for the BAU scenario. Here, t corresponds to

December at the years 2040 and 2070 for the near-term and long-term simulations, respectively. Scenarios representing a potential SOC storage, as compared to the BAU, return positive $\Delta SOC_{bio\text{-}BAU}$ values, while scenarios with a SOC losing potential return a negative $\Delta SOC_{bio\text{-}BAU}$. $\widetilde{\Delta SOC}_{bio-BAU}(\%)$ is the weighted average SOC change observed per scenario at a national scale, considering a pondering coefficient w, which represents the contribution of the surface of APCU i to the total surface simulated. The net SOC storage potential of the mitigation scenarios, defined as the total Mt C gained or loss (mitigation vs BAU) at a national level (only APCUs studied) is calculated using Eq (3):

$$Total\ national\ \Delta SOCnet = \sum_i (SOC_{bio} - SOC_{BAU})_i * S_{APCU\,i} \qquad (6)$$

Total national ΔSOC net (in Mt C) is the sum of the difference between the SOC stocks in the mitigation and the BAU scenarios at the end year (2040 or 2070) per APCU, times the APCU surface (S_{APCU}). The total croplands surface of Ecuador is 2.19 Mha but after the selection criteria described in section 2.2, only 1.19 Mha were included in the study (see SI).

The SOC stocks change in time, for a given scenario (mitigation or BAU) is calculated as the SOC observed at the final year minus the initial SOC stocks (Eq (4)).

$$\Delta SOC_{0-t_{i,x}}(\%) = \frac{SOC_{t,i,x} - SOC_0}{SOC_0} * 100 \qquad (4)$$

where $\Delta SOC_{0\text{-}t,i,x}$ (%) is the percent change of SOC stocks from the initial conditions (year 2020) until the end of the simulation (near-term: 2040, long-term: 2070); SOC_0 corresponds to the initial SOC stocks and $SOC_{t,I,x}$ to the final SOC stocks at time t, APCU i, and scenario x.

RothC calculates the SOC storage has a direct effect on the CO_2 flux from soil, which are accounted as the difference of the CO_2 outflows [38] in the mitigation scenario *vs* the BAU (Eq 5).

$$\Delta CO_2 = CO_{2\_bio} - CO_{2\_BAU} \qquad (5)$$

where ΔCO_2 (t C ha^{-1} y^{-1}) is the amount of CO_2-C emitted or avoided by each mitigation scenario at the end of the simulation, for CO_{2_bio} representing the emissions in the mitigation scenario and CO_{2_BAU} the emissions in the BAU.

2.5 Sensitivity analysis

The carbon inputs, EOM's recalcitrance, and priming effect parameters included in the adapted RothC-Bioeconomy can vary in function of the process performance [52]. Moreover, knowledge gaps are still open regarding the PE of the studied EOMs thus entailing important differences on PE values across the available literature [57,66].

The effects of carbon inputs and of recalcitrance values have been addressed in a previous publication [8]. Therefore, we here focus on addressing the effect of PE for the pyrochar scenario as a representative of high negative PE (i.e., 71.4% slower mineralization rates, [57]). To this end, we ran a simulation for which all the parameters were as default (Table 1) but instead of using a PE of 1, the PE was set to be the one presented in Table 1.

3. Results

3.1 SOC evolution in the BAU scenario

The SOC stocks in Ecuadorian croplands (i.e., only the PCUs included in this study), at the baseline (2020), range from 7.43 to 235 t C ha^{-1} (average 61.76 t C ha^{-1}), which represents 70.2 Mt C for the 1.19 Mha inhere studied (SI). At the national level, the BAU results show a potential increase of the national SOC stock by a mean of 4% and 7% in the short- (2040) and long-term (2070), respectively (Table 2). Despite this expected average increase, SOC stocks are, by 2040, shown to decrease in 79% of the simulated areas (up to 65% loss), representing a loss of 0.984 MtC (Fig S3). However, this loss stabilizes to 0.77 MtC (up to -90%) by 2070, due to a slight recovery between 2040-2070. The SOC lost in Ecuadorian croplands induces total cumulated emission of 304.51 Mt CO_2-C at the end of the simulations. The spatial explicitness of the study revealed the influence of the cropping systems diversity on the SOC dynamics. The highest SOC sequestration is observed in the areas with presence of sugarcane, followed by areas dedicated to banana, while the highest SOC loss is observed in the areas dedicated to cereal crops (i.e., rice and maize) (Fig S2).

3.2 Exogenous organic matter linked to SOC dynamics

The potential SOC storage (Table 2), as well as the area affected (Fig 3 and 4), differed greatly among the mitigation scenarios, with national SOC changes ranging from -7 (AD) to 17.70 (Pyrolysis) Mt C in 2040 and from -10.5 to 44.7 Mt C in 2070. Pyrochar shows the highest SOC storage, with a potential increase by a mean of 64% (max 231%) compared to the BAU, while the greatest SOC loss is observed in the AD scenario with a mean change of -15.3% (min -31.8%).

Pyrochar shows increased SOC stocks in all (100%) the simulated areas for the two timeframes studied. However, a 3-fold increase of SOC sequestering potential is observed between 2040 and 2070, with SOC changes ranging from 0.5 to 69% in 2040 and from 2 to 231% in 2070.

Albeit gaschar predicted additional SOC stocks of 1.24 Mt C ($\Delta SOC_{EOMvsBAU}$ of 1.5%) at a national scale, approximately 8.58% of the simulated area could decrease SOC stocks (up to -12.3%) in the near term (2040). The SOC loss observed, could be compensated by sustained gaschar inputs, attaining additional 12.03 Mt C ($\Delta SOC_{EOMvsBAU}$ of 15%) by 2070, with no SOC losses observed in any

PCU. This difference reveals a 10-fold increase on SOC storage in 30 years of gaschar inputs. Moreover, while 60% of the simulated area predicted a maximum SOC increase of 2% by 2040, approximately 54% of the areas show a maximum increase of 16.5% by 2070.

The SOC storage response to the exchange of crop residues by EOMs produced under mild process conditions (i.e., hydrochar and digestate) is highly spatially heterogeneous (Figs 3 and 4) and is greatly influenced by the time extension of the simulations. For instance, at the near-term simulations (2040), the HTL scenario shows SOC stocks changes ranging from -14.8% to 13.1% (mean of -4.6%), which results in a SOC loss of 3.52 Mt C at a national scale. For the same period, the AD scenario shows a cumulated loss of 7.08 Mt C compared to BAU, with SOC variations across the PCUs ranging from -29.1% to 3% (mean of -10%). If the simulations are extended until 2070, the long-term SOC stocks are predicted to loss 6.43 and 10.5 Mt C under the HTL and AD scenarios, respectively. These losses represent a mean SOC change of -9.1% and -15.3% for each scenario. We must note that the SOC loss observed for both scenarios and both timeframes represent 99.9% of the simulated area, this due to positive SOC storage observed in only 1 single PCU covering 19.4 ha.

3.3 CO_2 emissions and key spatial observations

All the EOM scenarios represent a significative mitigation potential for CO_2 emissions, compared to the BAU scenario at the near- and long-term timeframes (Table 2). The pyrolysis and gasification scenarios represent a 40% decrease of CO_2-C emissions, with net reductions of 125 and 126 Mt C, respectively at the year 2070. Despite the negative effect on SOC stocks shown by the AD and HTL scenarios, the CO_2 emissions are reduced by 32% and 20%, which represents national CO_2-C emissions reduction of 99.2 and 61.65 Mt C in each scenario.

The highest SOC storage potential achieved by the conversion of crop residues into recalcitrant EOM is observed in the Northeast and Central West regions, for the pyrolysis and gasification scenarios. In particular, the provinces of Imbabura, Orellana, Guayas, Manabí, El Oro, and Loja show the greatest SOC stocks increase across the simulated area. On the opposite, these areas showed the most marked SOC stock losses for the HTL and AD scenarios (Fig 3, 4).

3.4 Sensitivity analysis

Various combinations of carbon input (C_C), recalcitrant fraction (C_R), mineralization rates (k_R and k_L), and PE were tested according to Table S4. Across the different parametric configurations, the greatest effect was related to the priming effect. A one-at-a-time test for the pyrolysis scenario, allowed comparing the SOC stock evolution under the average expected PE of pyrochar (-0.714) against the default scenario of this study where the PE was set to zero (Fig 5). This allowed to separate the PE

from the other set of parameters that could have been tested. The SOC stocks were doubled in the pyrochar scenario. This test revealed that if we consider the PE, pyrochar SOC storage potential is increased, representing 2.54-fold the potential SOC storage observed with no PE by the year 2040, with an expected decrease to 1.8-fold if the timeframe is extended to 2070.

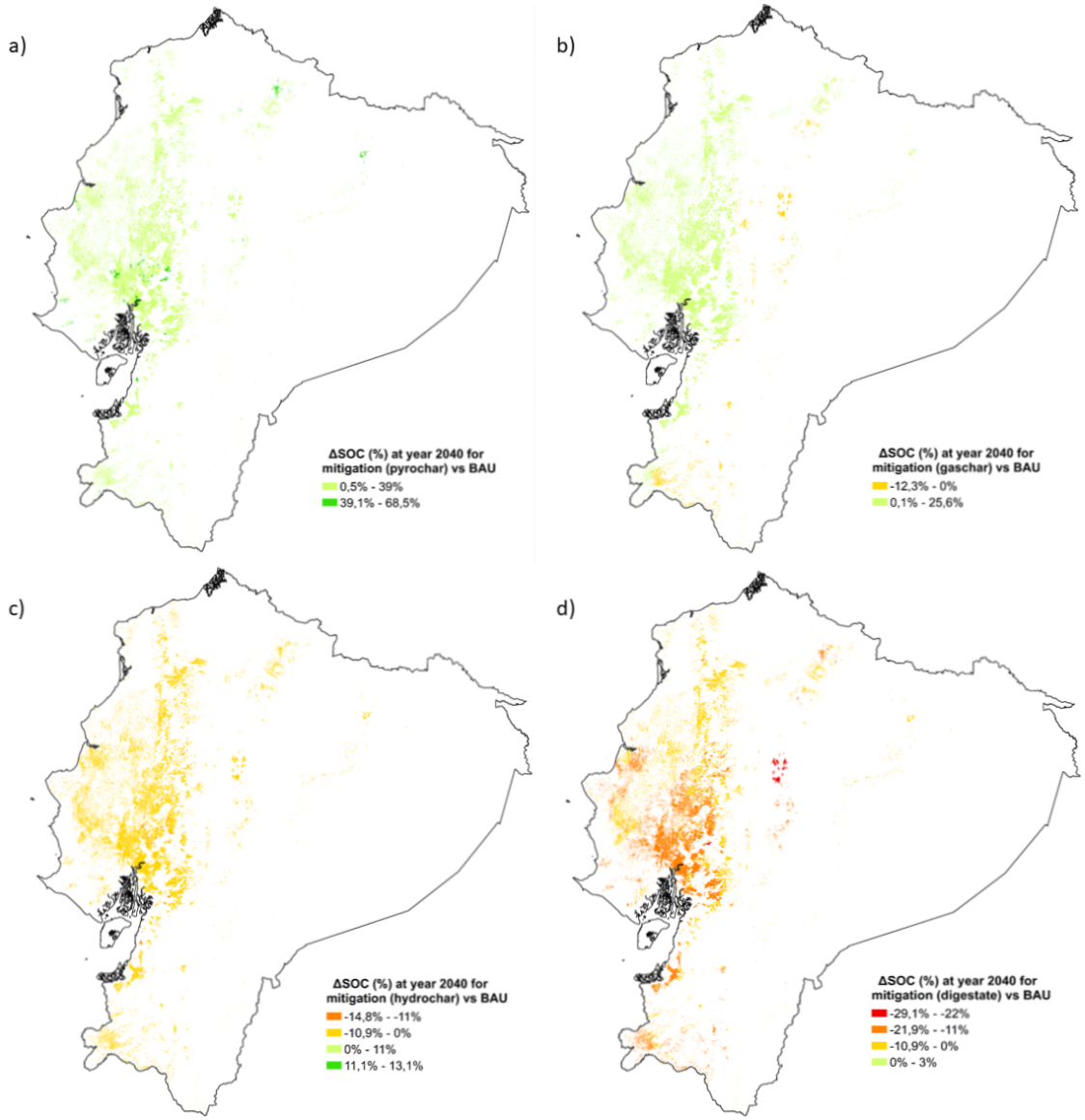

Fig 3. SOC change between EOM scenarios and BAU at year 2040 a) pyrochar, b) gaschar, c) hydrochar d) digestate. Fixed ranges are used for comparison purposes, net values are presented in [68]. Minimum and maximum values presented. White areas were not included in the simulations.

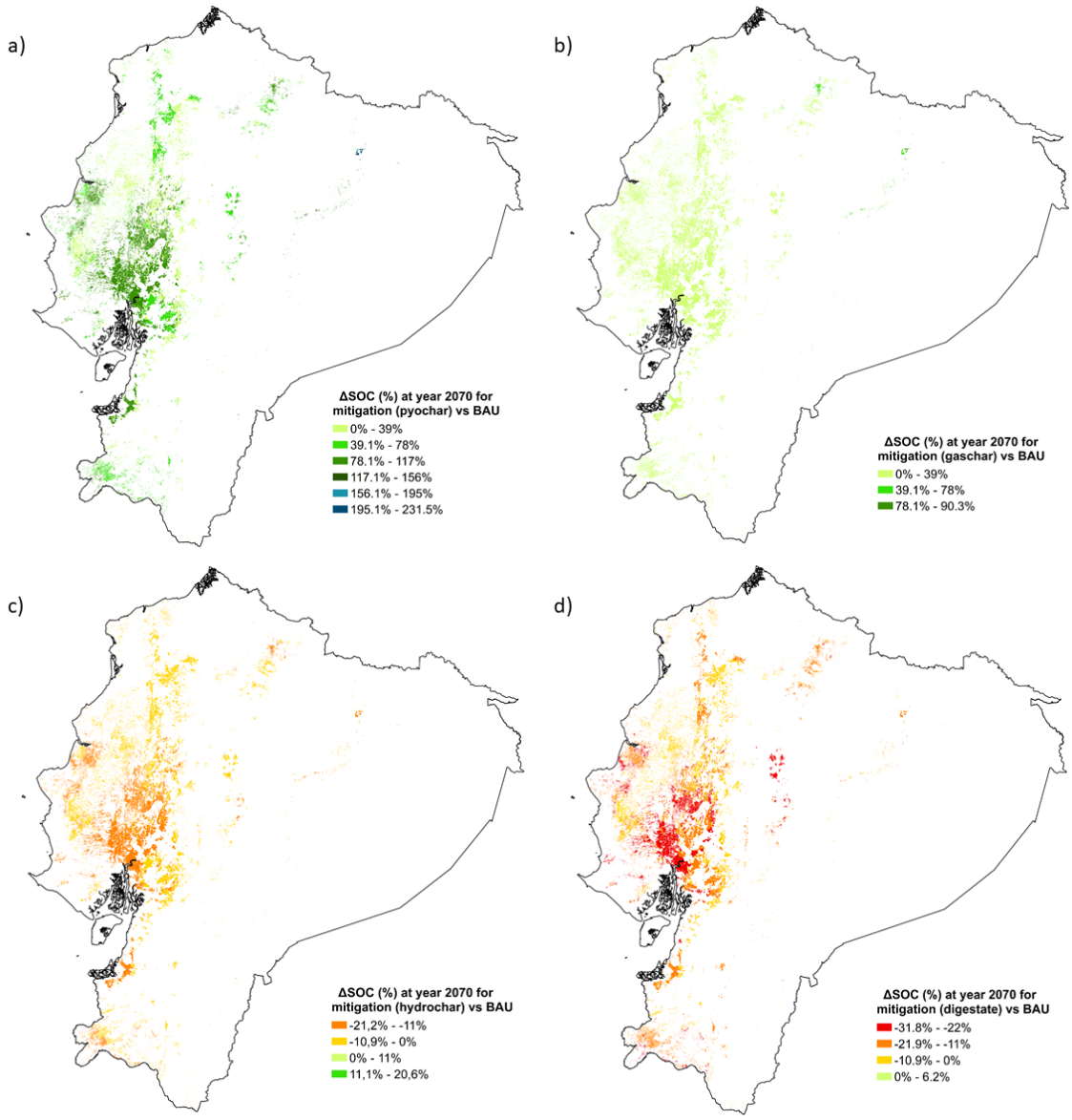

Fig 4. SOC change between EOM scenarios and BAU at year 2070 a) pyrochar, b) gaschar, c) hydrochar d) digestate. Fixed ranges are used for comparison purposes, net values are presented in [68]. Minimum and maximum values presented. White areas were not included in the simulations

Table2. Soil organic carbon storage potential and CO_2 emissions avoided of the mitigation scenarios, relative to the BAU, for the near-term (2040) and long-term (2070) simulations, at a national level. Results shown as total MtC and weighted average percentage for all the APCUs. [a]

Scenario	2040								2070							
	Total national SOC change [c]				Average national SOC change [d]				Total national SOC change [c]				Average national SOC change [d]			
	Total	Min [e]	Max [e]	CO_2 [f]	Mean	Min [e]	Max [e]	CO_2 [f]	Total	Min [e]	Max [e]	CO_2 [f]	Mean	Min [e]	Max [e]	CO_2 [f]
	Mt C				%				Mt C				%			
BAU [b]	-1.0	-0.2	1.1	125.8	3.7	-65.4	738.9	-	-0.8	-0.3	1.7	304.5	6.7	-89.6	1167.6	-
Pyrolysis	14.7	2.8E-6	0.4	-47.0	21.1	0.5	68.5	-34.3	44.7	1.3E-5	1.3	-125.3	64.3	2.2	231.5	-39.4
Gasification	1.2	-1.4E-2	0.1	-47.0	1.5	-12.3	25.6	-34.3	12.0	1.6E-6	0.5	-126.2	15.3	0.2	90.3	-39.6
HTL	-3.5	1.2E-4	-0.1	-38.7	-4.6	-14.8	13.1	-28.4	-6.4	1.7E-4	-0.2	-99.2	-9.1	-21.2	20.6	-31.2
AD	-7.1	-0.2	2.8E-5	-21.85	-10.0	-29.1	3.0	-16.0	-10.5	-0.3	5E-05	-61.7	-15.3	-31.8	6.2	-19.2
Pyrolysis_PE [g]	36.4	6.55E-05	1.1	-	54.1	14.8	154.6	-	79.8	9.5E-5	2.5	-	120.9	27.5	404.5	-

SOC: Soil organic carbon, BAU: Business as usual, HTL: Hydrothermal liquefaction, AD: anaerobic digestion, APCU: Agricultural pedoclimatic units. [a] Results are presented with a maximum of three significant digits to ensure tractability. [b] BAU scenario represents the change between SOC at the year of study (2040 or 2070) vs initial SOC at 2020 under the BAU conditions. [c] Sum of all APCUs. [d] Average SOC change for an APCU at national scale, considering the APCU surface to obtain the weighted average. [e] Minimum and maximum result observed across all the APCUs modeled. [f] Avoided C-CO_2 emissions. The C used in the main product delivered by the mitigation scenario has been deducted from the avoided C-CO_2 emissions to prevent overestimation of the mitigation potential of each scenario. [g] One at a time sensitivity analysis performed for the pyrolysis scenario, considering same parameters as pyrolysis with the difference of using a negative PE of 0.714. CO2 emissions avoided were not accounted for this scenario.

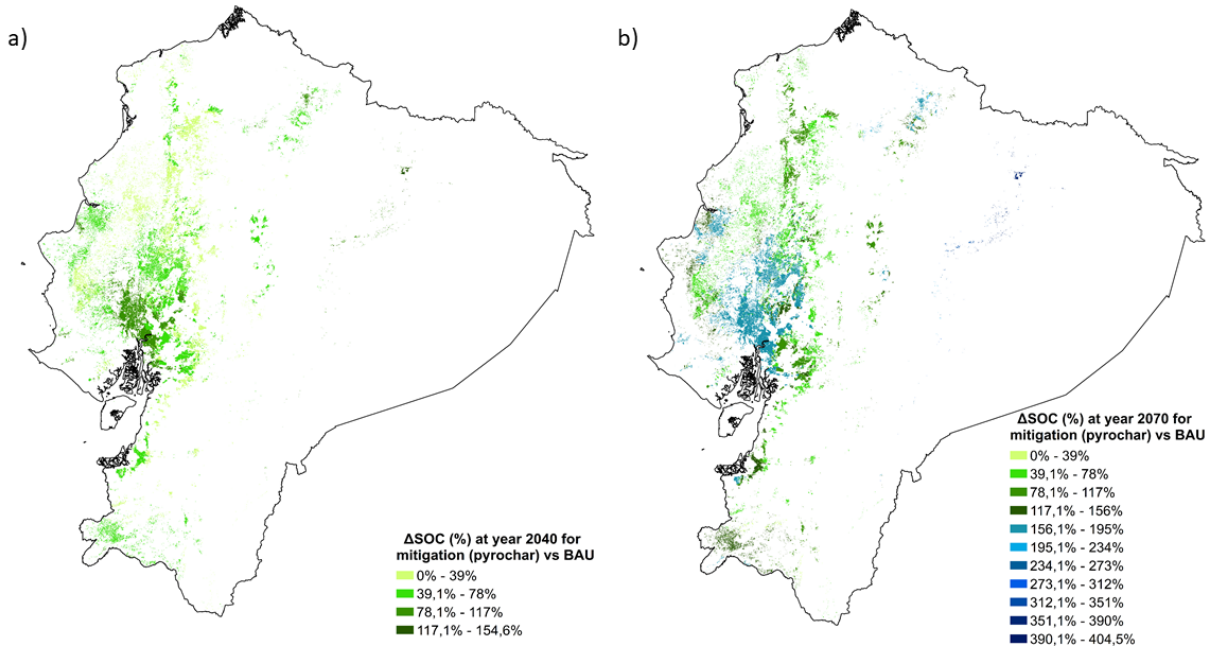

Fig 5. One at a time sensitivity analysis for the pyrochar scenario, considering a negative priming effect of 0.714 for the year a) 2040 and b) 2070. White areas were not included in the simulations.

4. Discussion

4.1 Carbon storage potential in Ecuador

Agricultural practices in Ecuador are highly intensive in frequency and rely primarily on monoculture systems. This intensity is mainly related to the favorable pedoclimatic conditions found in tropical regions, where one harvest season can last as fast as two months and a new season starts immediately (SI). These, however, pose great pressure to soils and the current cropping systems are projected to lose SOC stocks by 0.77 Mt C in the near term. Our observations follow the same trends as the potential SOC sequestration map contribution to the global database [38], which reports projected SOC losses of 0.6 MtC for the same period (2040). The insight regarding SOC storage in the BAU scenario, for 20 and 50 years, is explored in SI1 and the results are contrasted to those of FAO [37]. The temperature and high humidity have a direct relationship with OM mineralization because hot and humid environments can stimulate microbial enzymatic activity [69]. However, the relative nature of our results, comparing the bioeconomy vs the BAU scenario, neutralizes all the functions accounted equally in both developments, and results are related to the main structural differences across the scenarios. As expected, pyrochar has a weighted average SOC storage potential of 21% in the 2040 scenario, (Fig4a) which increases by 3-fold in the 2070 projections (Fig5a). This potential is attributed both to the recalcitrant nature and carbon content of pyrochar, which represents 50% of the C in the raw biomass for the typical lignin-rich residues found in Ecuador (Table 1). Besides SOC

storage, pyrochar can contribute to soils health by increasing the water holding capacity, aggregates stability and nutrient retention in the micropores which diminishes the leakage of nutrients [70–73]. Although gaschar is also composed of 95% recalcitrant carbon, the process efficiency yields less amounts in the gaschar and therefore in the soil C flow balance. Accordingly, the reduced C inputs have a greater negative effect in the near term, which is neutralized in the long-term. The SOC losses observed in the near-term gaschar application which are offset in the long-term assessment, highlights the importance of the temporal scope of SOC modeling. Overall, pyrochar and gaschar can be completely harvested with expected increase of SOC stocks by 2070, thus supplying extra 113 PJ for the bioeconomy.

Both hydrochar and digestate are less recalcitrant than the pyrochar and gaschar. The recalcitrant fractions are 0.89 and 0.68, each corresponding to a MRT of ca. 11 years and 1.2 years, for the hydrochar and digestate respectively. The lower recalcitrant and carbon inputs considered in these scenarios affect the overall soil C balance negatively. Andrade Diaz et al. 2023, showed that hydrochar could potentially prevent SOC losses in 87% of French croplands (10% considered not included) if all the technically harvestable crop residues are collected, while digestate would have the same effect on 50% of the surface. The expected positive effect on the French case is mainly related to lower temperatures, which are recognized to avoid microbial stimulation.

4.2 Implications of the priming effect

The approximate 2-fold increased on SOC storage potential observed with the PE is attributed to the lower rates of mineralization exerted by the interaction of biochar with the biochemical functions of soils. Wang et al [51]., demonstrated that biochar application improves the soils moisture retention and decrease the N bioavailability on soils. The combination of these effects resulted in improved structures on the microbial communities and induced carbon utilisation regulation for the microorganisms. The PE still poses a conundrum on soil sciences with results observed ranging from positive to negative effects. However, the average biochar PE observed [57] is on the negative side, attributed to the better carbon utilisation induced by the presence of biochar. The input of recalcitrant matter to soils, leads to a better distribution and usage of carbon reserves, and thus the lower mineralization rates observed, which are often assorted with microbial respiration, do not necessarily denote less microbial activity. Whereas PE has been relatively well studied for pyrochar, the PE exerted by the other coproducts remains a knowledge gap. For instance, digestate, which is often rich in N, poses an opposed effect to that observed with biochar, by providing extra N. However, research in this area is still necessary to understand the extent of the PE and the inclusion of microbial pools on SOC models is promoted [74] as the new step for more realistic ready to go conversion pathways.

4.3 *Strengths and limitations of the study*

Despite Ecuador's economy being highly sustained by the agriculture sector [75], there is sparse information that systematically documents the spatially explicit farming management practices in the country (e.g., crop rotations, amount and frequency of irrigation, depth of tillage, among others). Moreover, neither the projected future evapotranspiration rates nor the spatially-explicit biomass disponible in the country have been previously documented. In this study, we present the baseline crop residue potential in Ecuador for ten crops deemed as key for the bioeconomy (see section 2), which expands and updates the Bioenergy Atlas of Ecuador [76] with high spatial resolution. Also, we deliver the spatially explicit evapotranspiration (mm) in a monthly timestep until the year 2070 according to the RCP4.5 (see companion data paper).

Besides the construction and conveyance of the baseline data used (see companion data paper) for the specific case of Ecuador, this study draws key insights for each mitigation scenario investigated, to support science-based decisions regarding the potential of crop residues in tropical croplands. For instance, the policies endeavoured by the Ecuadorian government to attain the goals of circular economy [77], which rely on the research and development of bioenergy [78] and biomaterials can be supported by the RothC-Bioeconomy tool presented in here.

However, it is worth noting, that data remains scarce and highly variable for both the baseline preparation and the soil model adaptation. Therefore, the conclusions to retain rely on the general trends observed and the sensitivity of the model rather than the absolute values foreseen.

Limitations encountered on the baseline preparation regard the lack of information on crop rotations and residues management. Despite information on crop rotations has been reported at parcel levels in Ecuador [79], this is not compatible to be scaled at the national level and fine granularity considered in the study. Consequently, the assumption of no crop rotations along the year may influence the overall C inputs. Moreover, the C inputs and exports are directly dependent on the RPR, RtS, and crop residue composition, which is highly variable across the literature [7,49,80,81]. [49] denoted a high variability on the potential biomass production depending on the equation used to estimate the RPR. This calls for attention on the overall net value of crop residues potential reported in here (see companion data paper). Another limitation is the knowledge on the current use of the crop residues, which can be delivered to animals or used for the bioeconomy. In fact, the BAU scenario considers that all the residues remain on fields while grey literature reports that farmers burn crop residues open-to comply with the intense harvesting cycles in Ecuador. This consideration may create unbalances on the amount of C inputs in real life *vs* the simulated scenarios because the ashes

remaining from open burning are nearly C depleted [82] while the studied scenarios consider that all (BAU) or a part (mitigation) of the C remains on soils.

Another source of uncertainty is related to the size and recalcitrance of the EOMs, based on C_C and C_R, respectively. Sparse literature reports the C balance for the EOMs studied (i.e., biochar, digestate, hydrochar, gaschar) using tropical crops (e.g., coffee, cocoa, banana, among others) as feedstocks or their C recalcitrance, for processes fed with the tropical crops considered. While the C_C and C_R parameters used for cereal-based crop residues stem from an exhaustive review comprising over 600 data records [52], scarce data provides useful information to derive the same parameters for tropical crop residues. The PE, which plays a key role on the SOC evolution in the mitigation scenarios is still hardly understood by soil scientists, and the values observed are in extreme ranges. For instance, Zimmerman et al., 2019, reported that the application of biochar prepared from sugarcane increased the SOC mineralization in 91%, while the global metanalysis of Moura found an average decrease by 71.4%. More research regarding the microbial response to the recalcitrant EOMs is needed, which could provide science-based data to stablish the microbial degradation processes in the soil model [83].

5. Conclusions

The high temperatures, extreme moisture variation (high rain and high evapotranspiration), and intensive agricultural practices promote the loss of SOC stocks in tropical croplands. Our results show that soil application of recalcitrant EOMs as a replacement of harvested crop residues could aid to maintain the carbon balance and even promote higher SOC sequestration than if crop residues remained on soils, while providing renewable carbon for the bioeconomy.

The simulated APCUs, representing 52% of croplands in Ecuador, can deliver extra 113 PJ biomass from crop residues to supply the bioeconomy goals in the country, with no SOC losses expected, for the pyrolysis and gasification scenarios, compared to the BAU. In fact, SOC is expected to double in 8% of the cropland surface in the pyrolysis scenario in 50 years. The recalcitrance of digestate and hydrochar EOMs produced in the AD and HTL scenarios, respectively, does not compensate for the lesser C inputs returned, triggering SOC losses in all the studied APCUs.

Moreover, harvesting residual biomass with return of the co-products brings GHG mitigation in comparison to leaving the residues on land, translating into 19-39% reduction of CO_2 emissions over 50 years, depending on the bioeconomy pathway (C supplied to the bioeconomy already accounted as extra source of emissions).

Data availability

The data that support the findings of this study are openly available in "TBI - Toulouse Biotechnology Institute - T21018" at https://doi.org/10.48531/JBRU.CALMIP/VLKG8V [56] (input data) and https://doi.org/10.48531/JBRU.CALMIP/54SOW9 [68] (output data).

Acknowledgements

This work was carried out within the framework of the research project Cambioscop (https://cambioscop.cnrs.fr), partly financed by the French National Research Agency, Programme Investissement d'Avenir (ANR-17-MGPA-0006), and Region Occitanie (18015981). C. Andrade was additionally funded by the French Embassy in Ecuador under the Project "Fonds de Solidarité pour Projets Innovants" (FSPI) and the French Ministry for Europe and Foreign Affairs and by a partial Scholarship from the Universidad Técnica de Manabí, Ecuador (UTM).

The authors would like to thank Wilmer Jimenez and the Ministry of Agriculture of Ecuador for providing the backup data used to produce the Ecuadorian National Report for the Global Soil Organic Carbon Sequestration Potential Map, the Subsecretary of Climate Change of Ecuador for providing the climate projections for Ecuador, and Carlos Robles for helping with the climate data extraction.

Author contributions

Christhel Andrade Díaz: Conceptualization, Methodology, Data curation, Formal analysis, visualization, Investigation, Writing - original draft, Writing - review & editing. **Enrico Balugani**: Formal analysis, methodology. **Ezequiel Zamora-Ledezma:** Conceptualization, methodology, Writing - review & editing, Funding acquisition, and Supervision. **Lorie Hamelin:** Conceptualization, Methodology, Writing - review & editing, Funding acquisition, Project administration, Resources, and Supervision.

Supporting documents and data

Chapter 4 implements the framework developed in **Chapter 3** to a different climate context, using Ecuador as a case study to apply the newly adapted SOC – Bioeconomy model RothC-Bioeconomy. This chapter produced the cropping system baseline for Ecuador, detailing the crop residues potential of the country, a soil model suitable for bioeconomy contexts, and a spatial explicit prediction of SOC dynamics in Ecuador until 2040 and 2070. The large amount of data used and produced during this chapter, as well as the detailed manipulation procedure are transparently documented in the appendixes and databases associated:

- **Appendix A3a:** Data paper presenting the cropping systems baseline of Ecuador.
- **Appendix A3b:** Supplementary information of the paper, detailing the adaptation of the soil model.
- **Background data:** The database containing the input data prepared in this chapter is openly available in the following repository: DOI: 10.48531/JBRU.CALMIP/WYWKIQ. The database presenting the final output obtained with the SOC model are allocated in the repository: https://doi.org/10.48531/JBRU.CALMIP/54SOW9.

Towards Chapter 5

Albeit agriculture is a pillar of the Ecuadorian economy, the sector is mainly sustained by artisanal agriculture, thus data involving cropping systems are not well systematized in the country. The lack of policies to incentive better farming practices has been translated into uninformed farmers that deploy intensive agriculture systems. No systematic information exists reporting the management activities regarding crop rotations or residue disposal or valorization. Moreover, although the mapping registry of croplands is of high spatial resolution, the statistical survey reporting national production is of gross spatial granularity at a province scale, which diminishes the valuable details found in the land use map. Here, we developed the first baseline for current cropping systems in the country, containing pedological, climatic, and farming management practices, with high spatial resolution. This baseline includes the ten key crops representing the national production. This chapter also produced a second SOC-Bioeconomy model, able to simulate the SOC dynamics under a bioeconomy context in tropical croplands. Due to the great difference between temperate (France) and tropical (Ecuador) biomes, the results observed in **Chapter 4** differ from those in **Chapter 3**. However, in both contexts, biochar

(pyrochar and gaschar) highlights as a promising alternative for maintaining or building SOC stocks while supplying renewable carbon to the bioeconomy.

Nonetheless, the scope of the studies developed in Chapters 3 and 4, remained on SOC dynamics and only the carbon balances of the studied processes were studied. Accordingly, chapter 3 and 4, did not consider any other environmental implication beyond SOC stocks, nor the net mass and energy balances involved in the process. Policy makers require thorough studies to take informed-based decisions, therefore Chapter 5 deals with the full environmental implications involved in the bioeconomy conversion pathways. In that sense, the next chapter aims to unravel the tradeoffs between supplying renewable C to the bioeconomy while maintaining the SOC reserves and the full environmental implications of this decision.

References for Chapter 4

1. IEA. Net Zero by 2050 – A roadmap for the Global Energy Sector [Internet]. IEA; 2021 [cited 2023 May 3]. Available from: https://www.iea.org/reports/net-zero-by-2050
2. Energy & Climate Intelligence Unit. Net zero emissions race. 2022 Scorecard [Internet]. Net Zero Scorecard. 2022 [cited 2022 Feb 27]. Available from: https://eciu.net/netzerotracker
3. UNFCCC. Paris Agreement to the United Nations Framework Convention on Climate Change. Dec 12, 2015.
4. Araújo OQF, de Medeiros JL. How is the transition away from fossil fuels doing, and how will the low-carbon future unfold? Clean Techn Environ Policy. 2021 Jul 1;23(5):1385–8.
5. Cherubin MR, Oliveira DM da S, Feigl BJ, Pimentel LG, Lisboa IP, Gmach MR, et al. Crop residue harvest for bioenergy production and its implications on soil functioning and plant growth: A review. Sci agric (Piracicaba, Braz). 2018 May;75(3):255–72.
6. Blanco-Canqui H. Crop Residue Removal for Bioenergy Reduces Soil Carbon Pools: How Can We Offset Carbon Losses? Bioenerg Res. 2013;14.
7. Scarlat N, Fahl F, Lugato E, Monforti-Ferrario F, Dallemand JF. Integrated and spatially explicit assessment of sustainable crop residues potential in Europe. Biomass and Bioenergy. 2019 Mar 1;122:257–69.
8. Andrade Díaz C, Clivot H, Albers A, Zamora-Ledezma E, Hamelin L. The crop residue conundrum: Maintaining long-term soil organic carbon stocks while reinforcing the bioeconomy, compatible endeavors? Applied Energy. 2023 Jan 1;329:120192.
9. Lal R. Soil carbon sequestration to mitigate climate change. Geoderma. 2004 Nov 1;123(1):1–22.
10. Lal R. World crop residues production and implications of its use as a biofuel. Environment International. 2005 May 1;31(4):575–84.
11. Poeplau C, Don A. Carbon sequestration in agricultural soils via cultivation of cover crops – A meta-analysis. Agriculture, Ecosystems & Environment. 2015 Feb 1;200:33–41.
12. Francaviglia R, Almagro M, Vicente-Vicente JL. Conservation Agriculture and Soil Organic Carbon: Principles, Processes, Practices and Policy Options. Soil Systems. 2023 Mar;7(1):17.
13. Rolando JL, Turin C, Ramírez DA, Mares V, Monerris J, Quiroz R. Key ecosystem services and ecological intensification of agriculture in the tropical high-Andean Puna as affected by land-use and climate changes. Agriculture, Ecosystems & Environment. 2017 Jan 2;236:221–33.
14. Henry M, Tittonell P, Manlay RJ, Bernoux M, Albrecht A, Vanlauwe B. Biodiversity, carbon stocks and sequestration potential in aboveground biomass in smallholder farming systems of western Kenya. Agriculture, Ecosystems & Environment. 2009 Jan 1;129(1):238–52.
15. Sainju UM, Singh BP, Whitehead WF. Long-term effects of tillage, cover crops, and nitrogen fertilization on organic carbon and nitrogen concentrations in sandy loam soils in Georgia, USA. Soil and Tillage Research. 2002 Jan 1;63(3):167–79.
16. Bolliger A, Magid J, Amado JCT, Skóra Neto F, Ribeiro M de F dos S, Calegari A, et al. Taking Stock of the Brazilian "Zero-Till Revolution": A Review of Landmark Research and Farmers' Practice. In: Advances in Agronomy [Internet]. Academic Press; 2006 [cited 2023 May 9]. p. 47–110. Available from: https://www.sciencedirect.com/science/article/pii/S0065211306910025
17. Lessmann M, Ros GH, Young MD, de Vries W. Global variation in soil carbon sequestration potential through improved cropland management. Global Change Biology. 2022;28(3):1162–77.

18. Johnston AE, Poulton PR, Coleman K, Macdonald AJ, White RP. Changes in soil organic matter over 70 years in continuous arable and ley–arable rotations on a sandy loam soil in England. European Journal of Soil Science. 2017;68(3):305–16.
19. Lemaire G, Gastal F, Franzluebbers A, Chabbi A. Grassland–Cropping Rotations: An Avenue for Agricultural Diversification to Reconcile High Production with Environmental Quality. Environmental Management. 2015 Nov 1;56(5):1065–77.
20. Launay C, Constantin J, Chlebowski F, Houot S, Graux A, Klumpp K, et al. Estimating the carbon storage potential and greenhouse gas emissions of French arable cropland using high-resolution modeling. Glob Change Biol. 2021 Apr;27(8):1645–61.
21. Moinard V, Levavasseur F, Houot S. Current and potential recycling of exogenous organic matter as fertilizers and amendments in a French peri-urban territory. Resources, Conservation and Recycling. 2021 Jun 1;169:105523.
22. Mondini C, Cayuela ML, Sinicco T, Fornasier F, Galvez A, Sánchez-Monedero MA. Soil C Storage Potential of Exogenous Organic Matter at Regional Level (Italy) Under Climate Change Simulated by RothC Model Modified for Amended Soils. Front Environ Sci. 2018 Nov 29;6:144.
23. Le Noë J, Billen G, Garnier J. How the structure of agro-food systems shapes nitrogen, phosphorus, and carbon fluxes: The generalized representation of agro-food system applied at the regional scale in France. Science of The Total Environment. 2017 May 15;586:42–55.
24. Nowak B, Nesme T, David C, Pellerin S. To what extent does organic farming rely on nutrient inflows from conventional farming? Environ Res Lett. 2013 Dec;8(4):044045.
25. Hansen JH, Hamelin L, Taghizadeh-Toosi A, Olesen JE, Wenzel H. Agricultural residues bioenergy potential that sustain soil carbon depends on energy conversion pathways. 2020;12.
26. Woolf D, Lehmann J. Modelling the long-term response to positive and negative priming of soil organic carbon by black carbon. Biogeochemistry. 2012;13.
27. Karhu K, Gärdenäs AI, Heikkinen J, Vanhala P, Tuomi M, Liski J. Impacts of organic amendments on carbon stocks of an agricultural soil — Comparison of model-simulations to measurements. Geoderma. 2012 Nov 1;189–190:606–16.
28. Lefebvre D, Williams A, Meersmans J, Kirk GJD, Sohi S, Goglio P, et al. Modelling the potential for soil carbon sequestration using biochar from sugarcane residues in Brazil. Sci Rep. 2020 Dec;10(1):19479.
29. Mondini C, Cayuela ML, Sinicco T, Fornasier F, Galvez A, Sánchez-Monedero MA. Modification of the RothC model to simulate soil C mineralization of exogenous organic matter [Internet]. Biogeochemistry: Soils; 2017 Jan [cited 2020 Jul 3]. Available from: https://www.biogeosciences-discuss.net/bg-2016-551/bg-2016-551.pdf
30. Pulcher R, Balugani E, Ventura M, Greggio N, Marazza D. Inclusion of biochar in a C dynamics model based on observations from an 8-year field experiment. SOIL. 2022 Mar 17;8(1):199–211.
31. Dil M, Oelbermann M. Chapter 13. Evaluating the long-term effects of pre-conditioned biochar on soil organic carbon in two southern Ontario soils using the century model. In: Oelbermann M, editor. Sustainable agroecosystems in climate change mitigation [Internet]. The Netherlands: Wageningen Academic Publishers; 2014 [cited 2022 Mar 2]. p. 249–68. Available from: https://www.wageningenacademic.com/doi/10.3920/978-90-8686-788-2_13
32. Archontoulis SV, Huber I, Miguez FE, Thorburn PJ, Rogovska N, Laird DA. A model for mechanistic and system assessments of biochar effects on soils and crops and trade-offs. GCB Bioenergy. 2016 Nov;8(6):1028–45.
33. Lychuk TE, Izaurralde RC, Hill RL, McGill WB, Williams JR. Biochar as a global change adaptation: predicting biochar impacts on crop productivity and soil quality for a tropical soil with the Environmental Policy Integrated Climate (EPIC) model. Mitig Adapt Strateg Glob Change. 2015 Dec;20(8):1437–58.

34. Levavasseur F, Mary B, Christensen BT, Duparque A, Ferchaud F, Kätterer T, et al. The simple AMG model accurately simulates organic carbon storage in soils after repeated application of exogenous organic matter. Nutrient Cycling in Agroecosystems. 2020;15.
35. Witing F, Prays N, O'Keeffe S, Gründling R, Gebel M, Kurzer HJ, et al. Biogas production and changes in soil carbon input - A regional analysis. Geoderma. 2018 Jun;320:105–14.
36. AR4 Climate Change 2007: Synthesis Report — IPCC [Internet]. [cited 2023 May 17]. Available from: https://www.ipcc.ch/report/ar4/syr/
37. FAO. Global Soil Organic Carbon Sequestration Potential Map – GSOCseq v.1.1 : Technical report [Internet]. Rome, Italy: FAO; 2022 [cited 2023 Jan 13]. 179 p. Available from: https://www.fao.org/documents/card/en/c/cb9002en
38. Jiménez W, Sánchez D, Ruiz V, Manzano D, Armas D, Jiménez L, et al. Ecuador: SOil Organic Carbon Sequestration Potential National Map. National Report. Version 1.0. Global Soil Partnership. Ministry of Agriculture and Livestock of Ecuador.; 2021. Report No.: 1.0.
39. Coleman K, Jenkinson DS. RothC-26.3 - A Model for the turnover of carbon in soil. In: Powlson DS, Smith P, Smith JU, editors. Evaluation of Soil Organic Matter Models [Internet]. Berlin, Heidelberg: Springer Berlin Heidelberg; 1996 [cited 2021 Apr 15]. p. 237–46. Available from: http://link.springer.com/10.1007/978-3-642-61094-3_17
40. Abatzoglou JT, Dobrowski SZ, Parks SA, Hegewisch KC. TerraClimate, a high-resolution global dataset of monthly climate and climatic water balance from 1958–2015. Sci Data. 2018 Jan 9;5(1):170191.
41. MAG, MAATE, FAO, GSP. Mapeo digital de Carbono orgánico en los suelos del Ecuador. [Internet]. Quito, Ecuador; 2021. Report No.: Segunda Edición. Available from: sipa.agricultura.gob.ec
42. MAG, IEE, SENPLADES. Mapa de cobertura y uso de la tierra del Ecuador continental, 2009- 2015, escala 1: 25.000. Versión editada por el Ministerio de Agricultura y Ganadería 2020. Ecuador; 2015.
43. Hengl T, Jesus JM de, Heuvelink GBM, Gonzalez MR, Kilibarda M, Blagotić A, et al. SoilGrids250m: Global gridded soil information based on machine learning. PLOS ONE. 2017 Feb 16;12(2):e0169748.
44. Armenta Porras GE, Villa Cedeño JL, Jácome P. Proyecciones Climáticas de Precipitación y Tmperatura para Ecuador, bajo distintos escenarios de cambio climático. Ecuador: Subsecretaría de Cambio Climático del Ecuador; 2016.
45. MAG. Sistema de Información Pública Agropecuaria [Internet]. Sistemaa de Información Pública Agropecuaria: Estadísticas. 2023. Available from: http://sipa.agricultura.gob.ec/index.php/sipa-estadisticas/estadisticas-productivas
46. Beguería S, Vicente-Serrano SM, Reig F, Latorre B. Standardized precipitation evapotranspiration index (SPEI) revisited: parameter fitting, evapotranspiration models, tools, datasets and drought monitoring. International Journal of Climatology. 2014;34(10):3001–23.
47. Andrade Díaz C, Zamora-Ledezma E, Hamelin L. Dataset for defining the spatially explicit baseline of cropping systems in Ecuadorian croplands and estimating the crop residues potential. 2023.
48. INEC. Encuesta de Superficie y Producción Agropecuaria Continua [Internet]. Ecuador: INEC, SENPLADES; 2021. Available from: https://anda.inec.gob.ec/anda/index.php/catalog/912#page=accesspolicy&tab=study-desc
49. Karan SK, Hamelin L. Crop residues may be a key feedstock to bioeconomy but how reliable are current estimation methods? Resources, Conservation and Recycling. 2021 Jan;164:105211.
50. Rogers HH, Prior SA, Runion GB, Mitchell RJ. Root to shoot ratio of crops as influenced by CO2. Plant Soil. 1995 Jul 1;187(2):229–48.
51. Wang J, Xiong Z, Kuzyakov Y. Biochar stability in soil: meta-analysis of decomposition and priming effects. GCB Bioenergy. 2016 May;8(3):512–23.

52. Andrade C, Albers A, Zamora-Ledezma E, Hamelin L. A review on the interplay between bioeconomy and soil organic carbon stocks maintenance. PREPRINT (version 2) available at Research Square [Internet]. 2022 Mar 16 [cited 2022 Mar 16]; Available from: https://www.researchsquare.com
53. Han L, Sun K, Yang Y, Xia X, Li F, Yang Z, et al. Biochar's stability and effect on the content, composition and turnover of soil organic carbon. Geoderma. 2020 Apr;364:114184.
54. Möller K. Effects of anaerobic digestion on soil carbon and nitrogen turnover, N emissions, and soil biological activity. A review. Agron Sustain Dev. 2015 Jul;35(3):1021–41.
55. Bernard L, Basile-Doelsch I, Derrien D, Fanin N, Fontaine S, Guenet B, et al. Advancing the mechanistic understanding of the priming effect on soil organic matter mineralisation. Functional Ecology. 2022;36(6):1355–77.
56. Andrade Díaz C, Zamora-Ledezma E, Hamelin L. Database: Dataset for defining the spatially explicit baseline of cropping systems in Ecuadorian croplands and estimating the crop residues potential. Dataverse - TBI - Toulouse Biotechnology Institute - T21018. 2023 May;
57. Chagas JKM, Figueiredo CC de, Ramos MLG. Biochar increases soil carbon pools: Evidence from a global meta-analysis. Journal of Environmental Management. 2022 Mar 1;305:114403.
58. Lehmann J, Cowie A, Masiello CA, Kammann C, Woolf D, Amonette JE, et al. Biochar in climate change mitigation. Nat Geosci. 2021 Dec;14(12):883–92.
59. Fantin V, Buscaroli A, Buttol P, Novelli E, Soldati C, Zannoni D, et al. The RothC Model to Complement Life Cycle Analyses: A Case Study of an Italian Olive Grove. Sustainability. 2022 Jan 5;14(1):569.
60. Gottschalk P, Smith JU, Wattenbach M, Bellarby J, Stehfest E, Arnell N, et al. How will organic carbon stocks in mineral soils evolve under future climate? Global projections using RothC for a range of climate change scenarios. 2012;21.
61. Morais TG, Teixeira RFM, Domingos T. Detailed global modelling of soil organic carbon in cropland, grassland and forest soils. PLOS ONE. 2019;27.
62. Nemo, Klumpp K, Coleman K, Dondini M, Goulding K, Hastings A, et al. Soil Organic Carbon (SOC) Equilibrium and Model Initialisation Methods: an Application to the Rothamsted Carbon (RothC) Model. Environ Model Assess. 2017 Jun 1;22(3):215–29.
63. Chen D, Rojas M, Samset BH, Cobb K, Diongue-Niang A, Edwards P, et al. Framing, Context, and Methods. In: Climate Change 2021: The Physical Science Basis Contribution of Working Group I to the Sixth Assessment Report of the Intergovernmental Panel on Climate Change. in Press. IPCC; 2021.
64. Thornthwaite CW. An Approach toward a Rational Classification of Climate. Geographical Review. 1948;38(1):55–94.
65. Vicente-Serrano SM, Beguería S, López-Moreno JI. A Multi-scalar drought index sensitive to global warming: The Standardized Precipitation Evapotranspiration Index – SPEI. Journal of Climate. 2010;23:1696–718.
66. Zimmerman AR, Ouyang L. Priming of pyrogenic C (biochar) mineralization by dissolved organic matter and vice versa. Soil Biology and Biochemistry. 2019 Mar 1;130:105–12.
67. Andrade C, Albers A, Zamora-Ledezma E, Hamelin L. Database to determine the Carbon recalcitrance and carbon conversion rate to bioeconomy coproducts [Internet]. Dataverse. TBI - Toulouse Biotechnology Institute - T21018; 2022. Available from: https://dataverse.callisto.calmip.univ-toulouse.fr/dataset.xhtml?persistentId=doi:10.48531/JBRU.CALMIP/WYWKIQ
68. Andrade Díaz C. Dataset for Modelling the long-term carbon storage potential from recalcitrant matter inputs in tropical arable croplands. TBI - Dataverse; 2023.
69. Bai X, Huang Y, Ren W, Coyne M, Jacinthe P, Tao B, et al. Responses of soil carbon sequestration to climate-smart agriculture practices: A meta-analysis. Glob Change Biol. 2019 Aug;25(8):2591–606.

70. Ippolito JA, Cui L, Kammann C, Wrage-Mönnig N, Estavillo JM, Fuertes-Mendizabal T, et al. Feedstock choice, pyrolysis temperature and type influence biochar characteristics: a comprehensive meta-data analysis review. Biochar. 2020 Dec;2(4):421–38.
71. Zhang Q, Xiao J, Xue J, Zhang L. Quantifying the Effects of Biochar Application on Greenhouse Gas Emissions from Agricultural Soils: A Global Meta-Analysis. Sustainability. 2020 Apr 23;12(8):3436.
72. Ndede EO, Kurebito S, Idowu O, Tokunari T, Jindo K. The Potential of Biochar to Enhance the Water Retention Properties of Sandy Agricultural Soils. Agronomy. 2022 Jan 25;12(2):311.
73. Glaser B, Wiedner K, Seelig S, Schmidt HP, Gerber H. Biochar organic fertilizers from natural resources as substitute for mineral fertilizers. Agron Sustain Dev. 2015 Apr;35(2):667–78.
74. Woolf D, Lehmann J. Microbial models with minimal mineral protection can explain long-term soil organic carbon persistence. Sci Rep. 2019 Dec;9(1):6522.
75. Orejuela-Escobar LM, Landázuri AC, Goodell B. Second generation biorefining in Ecuador: Circular bioeconomy, zero waste technology, environment and sustainable development: The nexus. Journal of Bioresources and Bioproducts. 2021 May 1;6(2):83–107.
76. MEER, MCPEC, INP. Atlas Bioenergético del Ecuador. Ecuador: Ministry of Electricity and Renewable Energy; 2014.
77. Ministerio de Produccion; comercio exterior, invversiones y pesca. Libro Blanco de Economia circular de Ecuador. Ecuador; 2021.
78. Posso F, Siguencia J, Narváez R. Residual biomass-based hydrogen production: Potential and possible uses in Ecuador. International Journal of Hydrogen Energy. 2020 May 11;45(26):13717–25.
79. Nguema A, Norton GW, Alwang J, Taylor DB, Barrera V, Bertelsen M. FARM-LEVEL ECONOMIC IMPACTS OF CONSERVATION AGRICULTURE IN ECUADOR. Experimental Agriculture. 2013 Jan;49(1):134–47.
80. Bentsen NS, Felby C, Thorsen BJ. Agricultural residue production and potentials for energy and materials services. Progress in Energy and Combustion Science. 2014 Feb 1;40:59–73.
81. Fischer G, Prieler S, van Velthuizen H, Berndes G, Faaij A, Londo M, et al. Biofuel production potentials in Europe: Sustainable use of cultivated land and pastures, Part II: Land use scenarios. Biomass and Bioenergy. 2010 Feb;34(2):173–87.
82. Andrade CA, Zambrano-Intriago LA, Oliveira NS, Vieira JS, Quiroz-Fernández LS, Rodríguez-Díaz JM. Adsorption Behavior and Mechanism of Oxytetracycline on Rice Husk Ash: Kinetics, Equilibrium, and Thermodynamics of the Process. Water Air Soil Pollut. 2020 Mar 2;231(3):103.
83. Lehmann J, Hansel CM, Kaiser C, Kleber M, Maher K, Manzoni S, et al. Persistence of soil organic carbon caused by functional complexity. Nat Geosci. 2020 Aug;13(8):529–34.

5. CHAPTER 5: LCA for Maritime biofuels:

To harvest or not? Tradeoffs between SOC maintenance and overall environmental performance of harvesting crop residues for the bioeconomy

5. CHAPTER 5: LCA for maritime fuels – Tradeoffs between SOC maintenance and overall environmental performance

5.1 Context

The tools developed in Chapters 3 and 4 reveal that for some conversion pathways (e.g., pyrolysis) all the technically available crop residues can be supplied to the bioeconomy under a C-neutral harvest strategy (*see Chapter 3*). However, if we consider the environmental impacts generated over the full supply chain, including the use of the main product and what it replaces, the most interesting conversion pathway may differ from the ones ensuring a C-neutral harvest.

Here, we performed a full LCA for the pyrolysis and anaerobic digestion processes studied in the previous chapters, as end-of-intervals of all the pathways addressed to represent the tradeoff between sequestration of additional SOC (in comparison to BAU) and the overall impacts of the supply chain. We considered the case of upgrading the bio-oil and biogas produced in each conversion pathway, to supply the service of sustainable maritime fuels (SMF), to displace the use of conventional fossil maritime fuels. This was selected given the rising interest in SMF and because both products can be used to this end.

The life cycle inventories (LCI) build upon previously published studies for the base technologies (fast pyrolysis and anaerobic digestion). To these, it was however necessary to include the upgrading procedures and combustion in marine vessels.

The case of pyrolysis considered a catalytic hydrotreatment to remove oxygen from the bio-crude and produce stabilized bio-oil suitable as a drop-in biofuel to substitute heavy fuel oil. The pyrolysis-biocrude LCI was developed from the study by Brassard et al. [40] and adapted to cereal-like feedstock using unpublished laboratory results kindly provided by Brassard et al. [54]. The upgrading process was modeled based on the catalytic hydrodeoxygenation process by Jones [55].

The anaerobic digestion scenario considered an upgrading process comprising cryogenic liquefaction, to produce bio-liquefied natural gas (bio-LNG) suitable to replace fossil LNG. The LCI for the anaerobic digestion process was retrieved from the anaerobic digestion module developed by Javourez [40] and the cryogenic-liquefaction upgrading was incorporated into the module. The LCA was performed using Activity Browser, with the Ecoinvent 3.9.1 consequential database, and the environmental impacts included in the EFv3.1 model.

The LCA presented inhere follows the transparency requirements of the ISO standards 14040 and 14044 [36,37] but is not ISO-compliant as it does not contain a state-of-the-art uncertainty analysis. It, nevertheless, allows answering the research questions and objectives 3 and 4, respectively:

- **RQ3.** What are the trade-offs between a C-neutral harvest and the overall environmental performance of the bioeconomy conversion technology if the use of the principal product obtained in the bioeconomy pathway is considered in a holistic manner?
- **RO4.** Perform a lifecycle assessment considering the full use of the main product and the return to soils of the coproducts.

The content of this chapter is being prepared for submission to peer review and the databases developed are transparently documented in the open repositories declared along the chapter.

.

List of figures

List of tables

To harvest or not? Tradeoffs between SOC maintenance and overall environmental performance of harvesting crop residues for the bioeconomy

Christhel Andrade Diaz[a,b*], Ezequiel Zamora-Ledezma[c], Lorie Hamelin[a]

[a] Toulouse Biotechnology Institute (TBI), INSA, INRAE UMR792, and CNRS UMR5504, Federal University of Toulouse, 135 Avenue de Rangueil, F-31077, Toulouse, France

[b] Department of Chemical, Biotechnological and Food Processes, Faculty of Mathematical, Physics and Chemistry Sciences. Universidad Técnica de Manabí (UTM), 130150, Portoviejo, Ecuador.

[c] Ecosystems Functioning and Climate Change Research Group FAGROCLIM, Faculty of Agriculture Engineering. Universidad Técnica de Manabí (UTM), 13132, Lodana, Ecuador.

* andraded@insa-toulouse.fr, christhel.andrade@utm.edu.ec,

Abstract

The transition to zero-net emissions raises trade-offs between the services competing for sustainable carbon sources. Here, we performed a consequential LCA to understand the full environmental performance of managing 1 tonne of wet crop residue to produce sustainable marine fuels, while preserving or enhancing the SOC stocks in French croplands. Three management scenarios were considered: i) decay of crop residues on soils (reference), ii) conversion of crop residues to hydrotreated pyrolysis oil (HPO) to replace heavy fuel oil in maritime transportation, with biochar return to soil, and iii) conversion of crop residues to cryogenic liquefied biomethane (bio-LNG) to replace liquefied natural gas in cargo ships, with digestate return to soil. Besides the replacement of fossil fuels, a system boundaries expansion was applied to account for the valorization of the coproducts obtained along the whole supply chain of each system. Results per tonne of crop residues show, for all impacts assessed, a better environmental performance of using crop residues for maritime biofuels in comparison to their direct ploughing to soils, for all environmental impacts assessed. Notably, major GHG savings are observed, representing avoided emissions of 563 and 946 $kgCO_{2e}tww^{-1}$ of crop residues for the HPO and bio-LNG, respectively. The impact was scaled to the national potential that can be harvested for each pathway without losing SOC stocks (C-neutral harvest), implying a greater potential for the HPO pathway. While bio-LNG was the most performant pathway per tonne of residues (except for marine eutrophication and particulate matter), the scaled results show greater savings with the HPO pathway, except for freshwater eutrophication and water scarcity. The results show that converting crop residues to biofuels while returning the recalcitrant

coproduct of the conversion pathway to soils allows, in the HPO case, net environmental benefits for all the assessed environmental impacts as well as for SOC stocks. While bio-LNG shows net savings in most impacts, it shows a net impact for marine eutrophication because of the nitrogen losses associated with the digestate management. Overall, the results do not show, for the assessed pathways and impacts, a trade-off between SOC maintenance and net environmental impacts, if a C-neutral harvest is ensured with the co-product return to soil. This reflects the importance of fossil fuels substitution beyond the sole climate impact.

Keywords

LCA, maritime biofuels, cryogenic liquified biomethane, climate change

1. Introduction

Bioeconomy, in particular bioenergy, plays a key role in achieving the 2050-climate-neutrality goal pledged by national [1–3] and supranational [4–6] entities. However, the transition to low fossil carbon economies raises trade-offs between the involved sectors striving for renewable carbon. One current issue is that posed by the soil carbon lock-up and crop residue harvesting [7–9] competition. Soil organic carbon (SOC) is crucial for soil health because it regulates the biogeochemical cycles involved in soil fertility [10], crop productivity [11], and climate change mitigation through carbon sequestration [12]. However, the SOC dynamics and evolution are regulated by the equilibria between C inputs from plants and exogenous organic matter (EOM) (e.g., animal manure, organic fertilizers) [13,14] and the outputs related to heterotrophic respiration [15]. Therefore, recommendations suggest limiting the harvesting of crop residues to generic values depending on the crop type [7,16–18] to avoid SOC disturbances. These constraints hinder the sourcing of green carbon to feed bioeconomy conversion pathways.

Previous studies [19,20] have investigated the concurrence between SOC enhancement and crop residues removal, with clear positive synergies observed when the final use of crop residues is accounted for and the carbon is partly returned in a transformed stabilized state (e.g., biochar, digestate, hydrochar) [21,22]. Moreover, the SOC response to changes in C inputs in agricultural lands is spatially explicit, in other words, it depends on the specific site pedology, climate, and farming management practices [14,23,24].

Our previous study [20] determined the spatial-explicit amount of crop residues that can be harvested in French croplands to be used in five specific bioeconomy conversion pathways while preserving SOC stocks. There, we demonstrated that the often-suggested removal limit (31.5% of

harvestable biomass in France [25]) can be well surpassed without losing SOC if the bioeconomy coproduct is returned to the soil (i.e., pyrolysis and gasification biochar, hydrochar, and digestate) allowing a surplus 71-225 PJ for the bioeconomy. The study was later replicated in a tropical context, for the specific case of Ecuador (Chapter 3), revealing similar conclusions with an estimated C-neutral harvest potential of 113 PJ from crop residues. However, the scope of these studies was constrained to the soil carbon balance and disregarded other aspects associated with crop residue harvesting. In fact, no previous study has simultaneously evaluated the potential of crop residues to supply the bioeconomy while restraining SOC stock diminishment and assessing the whole environmental implications along the supply chain of the conversion pathway.

This study thus aims at shedding light on the SOC stocks, crop residues, and bioeconomy supply tradeoffs with a special focus on the overall environmental impact of harvesting crop residues for biofuel production, beyond sole SOC stock preservation. To this end, we performed a life cycle assessment (LCA) for biofuel production through pyrolysis and anaerobic digestion, both retained as end-of-intervals conversion pathways in the study of Andrade Diaz et al. [20][3].

The LCA is applied to the specific case of sustainable maritime fuels (SMF) for cargo ships [26]. Therefore, we compare the conventional management of harvestable crop residues (no harvest) to the use of crop residues to produce upgraded fuels as substitutes for marine conventional fuels. The comparison to other upgrading technologies or valorization alternatives (e.g., CHP, grid injection, etc.) is out of the scope of this study.

The case of maritime fuels was selected as a key sector for biofuel implementation because sea transport represents ca. 80% of international trade, consuming 330 Mt of maritime fuels per year, of which 77% is heavy fuel oil (HFO) [27]. This consumption accounts for 2-3% of global CO_2, 4-9% SOx, and 10-15% of NOx emissions [28], with a forecasted increase of over 30% from 2015 until 2050, only in the European Union (EU) [29]. In order to address the sea-transport-derived emissions, some regulations have been imposed by the International Maritime Organization (IMO) [30] and the sector has been recently included for the first time in the greenhouse gas emission (GHG) reductions commitment of the EU [31]. The IMO aims to reduce by 50% the total GHG maritime transport emissions by 2050 (compared to 2008) while the EU targets an 80% reduction in the same period (compared to 2020 levels), with special attention to vessels over 5000 gross tonnage (e.g., cargo ships)

[3] Also, in Chapter 4 of this thesis.

[29,32,33]. Accordingly, since 2020 maritime fuels must comply with the low sulfur fuel regulation [34,35], which sets the maximum sulfur content of maritime biofuels at 0.5%.

Cargo vessels are predominantly fueled with HFO, which is a low-quality end-of-the-barrel residue from petrol refinement. However, the use of liquefied natural gas (LNG) and marine distillate oil (MDO) for sea transportation has increased to comply with sulfur regulations [28]. In this context, the transition to SMFs is of foremost importance. Therefore, inhere we studied the production of stabilized pyrolysis oil, suitable to substitute HFO and the displacement fossil liquefied natural gas (LNG) by liquefied biomethane, also known as bio-LNG, produced by anaerobic digestion.

2. Methods

2.1 Life cycle assessment implementation

A consequential modeling approach was implemented according to the ISO 14040844 LCA standards [36,37] to track the environmental impacts of SMF. Accordingly, a system boundaries expansion approach was followed to assess displacement multifunctionality and the consequences of using crop residues for SMF production. The main goal of the LCA was to unravel the tradeoffs between the C-neutral harvest of crop residues to supply the bioeconomy and the overall environmental impacts related to the use for which the crop residues are streamed. The consequential methodology [38] considers the counterfactual use of the resources (i.e., the otherwise use of crop residues) and the avoided or induced effects of supplying the resources to the conversion pathways (e.g., coproducts valorization, heat requirements meet through other sources). The functional unit (FU) was defined as ***"the management of one wet tonne of harvestable crop residues per year"***. The FU is common for all the scenarios as the same crop residue composition is considered across the cases to allow comparing the environmental implications of the different management options. The harvestable portion considers the technical constraints described in Andrade Diaz et al. [20].

The geographical scope of the study was set to France, which defined the type of crop residues, energy mix, and legal implications of the scenarios. However, most of the inputs required in the conversion processes were considered to be internationally traded. Therefore, data were selected prioritizing the French scope, and when international markets were required, the "Global", "Rest of the World" or "Europe" scope were selected. The temporal scope was set to reflect future optimal performance, in particular, the heat requirements were considered to be electrically supplied as defined in the long-term scenarios proposed by Su-ungkavatin [39].

To the extent possible, only marginal suppliers (described in SI1) reacting to a change in demand were considered. Foreground life cycle inventories (LCI), i.e., specific to this study, were built

on previous similar works by Brassard et al. [40], Su-ungkavatin [39], and Javourez [41] and were expanded based on published literature and stoichiometry balances as further detailed in the supplementary information (SI) 1. Background LCI data were retrieved from the Ecoinvent 3.9.1 consequential database [42]. The LCI data for each scenario, detailing all the input and output flows involved in each operation is detailed in SI2 and SI3 [43]. The environmental impacts of these flows were calculated using the Environmental Footprint (EF) v3.1 Life Cycle Impact Assessment (LCIA) methodology [44] with the open-access software Brightway 2.0 through the Activity Browser interface [45]. Five environmental impacts are addressed (key substances contributing to the impact in brackets): Climate change with a 100-year horizon (CC; CO_2, CH_4, N_2O), respiratory inorganics reflecting particulate matter emissions (PM; soot, NOx, SO_2), eutrophication from exceeding phosphorus (freshwater) and nitrogen (marine) emissions in water reservoirs, and water scarcity (WS). These impacts were selected at the light of key global environmental stakes such as climate change and planetary boundaries where the safe operating space is exceeded, and in the light of issues specific to the maritime sector, such as the exhaust emissions from ships [33]. For the climate change impact in particular, the biogenic CO_2 emissions were considered following a so-called 0/0 approach [46] (uptake and releases having a characterization factor of 0 kg CO_2e per kg CO_2, while induced sequestration flows have a characterization factor of -1 kg CO_2e per kg CO_2 sequestered). This approach considers that biogenic CO_2 emissions are part of a short cycle where exchanges between the different reservoirs over short periods (from a few months to several decades) are stable. Conversely, fossil CO_2 emissions are associated with long cycles requiring millions of years to reach equilibrium.

2.2 Case scenario description

The LCA scenarios reflect the conversion of crop residues to SMFs for cargo vessels. Cargo vessels are predominantly fueled by HFO and propelled using two—stroke engines [47]. However, the IMO [33] reports a 7% decrease in HFO consumption triggered by a 6% and 0.9% increase in marine diesel oil and liquefied natural gas (LNG) over the period 2012 – 2018. To comply with the market trends, the SMFs scenarios consider i) the substitution of HFO by drop-in pyrolysis bio-oil, and ii) the use of liquefied biomethane (bio-LNG) from anaerobic digestion as an alternative for fossil-LNG. In accordance with the aim of this study, the reference scenario comprises a situation where crop residues are managed by plowing them back into arable fields to avoid diminishing SOC stocks [24]. The pyrolysis and anaerobic digestion conversion pathways were selected because i) they can produce oil and gas fuels ready to replace the current market fuels, and ii) they represent the extremes of the pathways addressed in our previous studies (Chapters 3 and 4) evaluating the C-neutral potential of crop residues to supply the bioeconomy.

Both scenarios assess the harvesting of crop residues to source the conversion pathways to produce the selected SMF and return a C-rich coproduct suitable to be spread on soils as a source of Carbon. The observations for 1 wet tonne of crop residue, are then scaled to the national potential C-neutral harvest determined by Andrade et al. [20], to contrast the overall environmental implications of supplying crop residues to the bioeconomy while maintaining the SOC stocks in French croplands.

The crop residues composition, reference scenario y combustion emissions of the fossil fuels are detailed in the SI1.

2.2.1 Pyrolysis scenario: Hydrotreated pyrolysis oil (HPO)

As the main goal of the case study is to supply SMF for cargo shipping, a fast pyrolysis process was selected to favor the bio-crude yields [48]. Along with the bio-crude secondary coproducts in solid (biochar) and gaseous (syngas) states are produced. Pyrolysis biocrude has high water ($\sim$15-30%) and oxygen (20 – 50%) contents, high acidity (pH 2.5 – 3), low heating values (15 -18 MJ kg^{-1}) [49], and may contain traces of ashes, solids, alkali, among others [48] which detriment its potential as a drop-in fuel [27]. Therefore, the biocrude must undergo an upgrading process in order to remove oxygen and increase the H:C ratio to fit fuel standards. Upgrading alternatives for pyrolysis bio-oil include solvent addition, fractionation, catalytic and no-catalytic hydrodeoxygenation (HDO), hot condensation, and catalytic hydrocracking, among others [48,50]. Among these, catalytic HDO coupled with hydrocracking distillation can produce a high-quality bio-oil with suitable quality to completely replace fossil oils [51,52]. However, since ship propulsion systems already operate low-quality fuels, such as HFO, the highly refined pyrolysis oil is more attractive for the aviation than maritime sector. Therefore, here we consider an upgrading process performed by a two-column HDO to produce stable bio-oil, instead of a refined biofuel. The hydrotreated pyrolysis oil (HPO) is then of suitable quality to completely replace HFO in slow-speed engines [32]. The process flow diagram for the HPO, including all the unit operations, counterfactual utilization, and displaced products is shown in Figure 1 and the details are further explored in SI1.

Briefly, the scenario considers four stages, namely i) biomass supply and pretreatment, ii) fast pyrolysis, iii) HDO upgrading, and iv) HPO combustion onboard. The system boundaries expansion, further explained in section 2.3, includes what is affected by harvesting the crop residues for HPO and the use of the coproducts.

The biomass supply stage accounts for the crop residues harvesting and transportation while the pretreatment considers the storage, size reduction, and moisture conditioning. The harvested crop residues are considered to be baled and stored until their use, with a 4.8% mass loss during storing [53]. The pretreatment includes size reduction to 1 – 3 mm by means of grinding (1% mass loss as

dust), which favors the heat transfer during pyrolysis [40] and drying to achieve a maximum of 10% water content as required by the reactor. The fast pyrolysis process was modeled according to the study by Brassard et al. [40] and the biocrude, aqueous phase (hereon vinegar), biochar and syngas yields reflected the results obtained at a semi-pilot scale auger reactor for the pyrolysis of wheat straw [54] as a proxy of the crop residues in France (the crop residue composition is detailed in SI1). The pyrolysis products are considered to be separated by a condensation system operating with a glycol-water mixture (50:50). The pyrolysis bio-crude is upgraded to reduce the oxygen content to be suitable for substituting HFO to fuel cargo vessels. The coproducts are recovered and used within the system boundaries (Fig.1).

The upgrading process consists of a catalytic HDO in multiple fixed bed reactors to attain a bio-oil with less than 2% content oxygen. The HDO upgrading was modelled according to the PNL report by Jones [55], and assumptions from Elliot [56] and Vienescu [49] were also considered. The process comprises three stages: i) stabilization, ii) first hydrotreatment, and ii) second hydrotreatment. The three stages require H_2 and catalysts supply. The stabilization and first HDO stage employ a Ruthenium catalyst, while the second HDO is performed using a Molybdenum based catalyst. The overall H_2 consumption of the upgrading stage is of 5.8% H_2 per biocrude feed. The H_2 is assumed to be produced by alkaline water electrolysis according to the model by Javourez [41]. The H_2 plant assumes the partial recovery of excess heat but due to lack of current technology the O_2 is considered to be vented (this is not represented in Fig 1). The pyrolysis, HDO, and H_2 plant details are compiled in SI1.

The upgraded bio-oil is assumed to be combusted onboard the cargo ship, with emissions assumed according to the Fourth IMO GHG study for MDO.

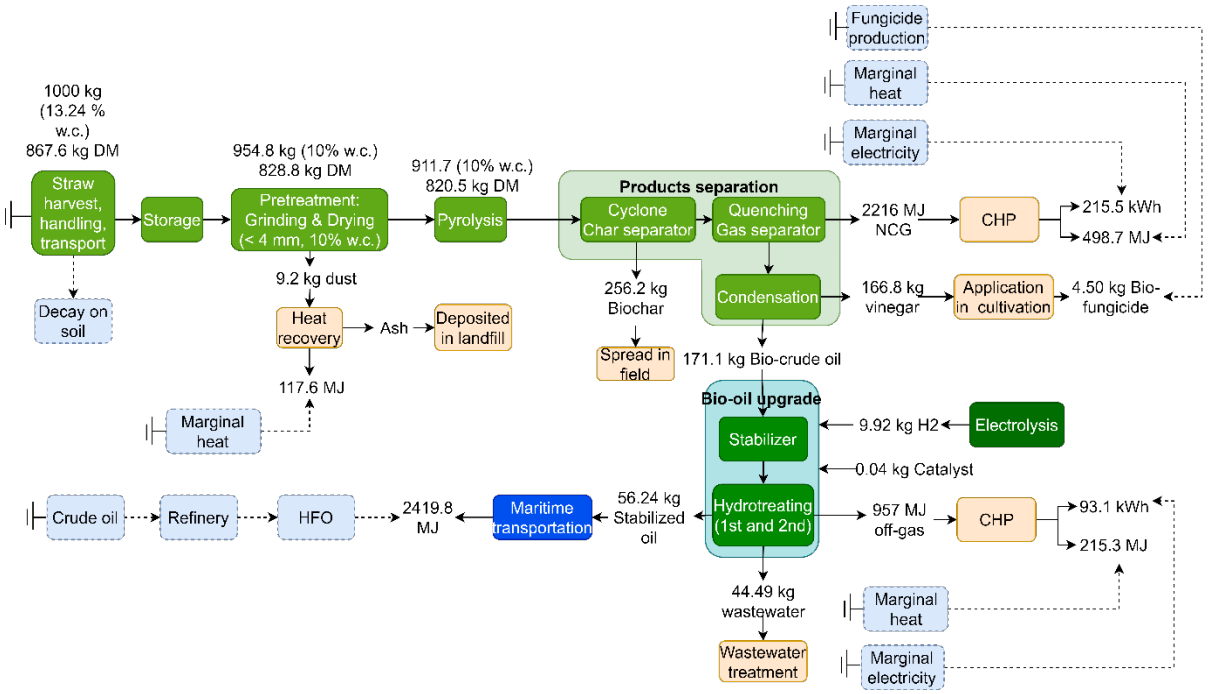

Fig 1. Process flow diagram for the hydrotreated pyrolysis oil (HPO) scenario. The process comprises a first fast-pyrolysis stage, followed by an upgrading process to remove oxygen excess from the bio-crude. The upgrading process is performed by a two column hydrotreatment, preceded by a stabilization process [55]. Doted arrows and boxes represent avoided/displaced products and services as a consequence of implementing the process. The final product stabilized oil displaces HFO to fuel cargo vessels for deep-sea shipping. The non-condensable-gases (NCG) produced during the pyrolysis and hydrotreatment processes is considered to be used for heat and power cogeneration (CHP), avoiding marginal heat and electricity for the energy mix of France as further detailed in SI1. The electrolysis also produces heat (partly recovered, thus avoiding marginal heat) and oxygen (here not recovered).

2.2.2 Anaerobic Digestion (AD) scenario: Cryogenic liquefied biomethane (bio-LNG)

Biogas produced during AD can be directly burned or upgraded to be used as transportation biofuel or injected in the electricity grid. LNG has been one alternative to replace HFO in order to comply with the low sulphur regulations, thus cargo vessels are already transitioning to use this type of fuel [57]. Biogas can be upgraded to biomethane by CO_2 removal, and then compressed to be used as bio-LNG to substitute the fossil-based LNG. Among the myriad of technologies to upgrade biogas to biomethane, cryogenic upgrading is an attractive alternative because it allows to recover CO_2 and compress the CH_4 to be used directly as LNG [58,59]. For this scenario, we considered the cryogenic upgrading of biomethane, by successive steps of compression and freezing (Cryopure technology) to be used in cargo vessels running on steam turbines [28]. This procedure, allows obtaining, besides bio-LNG, pure CO_2, which can be used for other technologies.

The anaerobic digestion (AD) scenario was built on the module developed by Javourez [41] and expanded to include the biogas upgrading as liquefied natural gas (bio-LNG). The AD process considers an infinitely stirred mesophilic bioreactor and includes the following stages: i) pre-treatment, ii) methanation, iii) digestate storage, iv) digestate spreading, and v) biogas valorization. The pretreatment includes the collection of straw as bales, comminution, and extrusion, with an average 3% mass loss [60]. The diffuse feedstock is transported to the collection platform (40 km assumed) and then to the AD facility (40 km assumed), accounting for 80 km of transportation (assumed based on the gasification module of [41]). The pretreated residues are assumed to be ensiled before entering the AD process, with a 1.95% mass loss. The biomethane yield was estimated to be 75% of the theoretical biomethane potential (TBMP), based on Tonini et al. [61] while the TBMP was calculated based on the Symon and Busswell [62], equation using the biochemical composition of the input feedstock.

The heat and electricity requirements were assumed to be represented by 8% auto consumption. The biogas valorization as bio-LNG considers the cryogenic separation of CH_4 based on the sublimation condensation of CO_2 at different temperatures [59]. The bio-LNG is considered to have a CO_2 content below 50 ppm to avoid freezing problems in the process [58]. The cryogenic bio-LNG was assumed to substitute liquefied natural gas (LNG) for marine transportation.

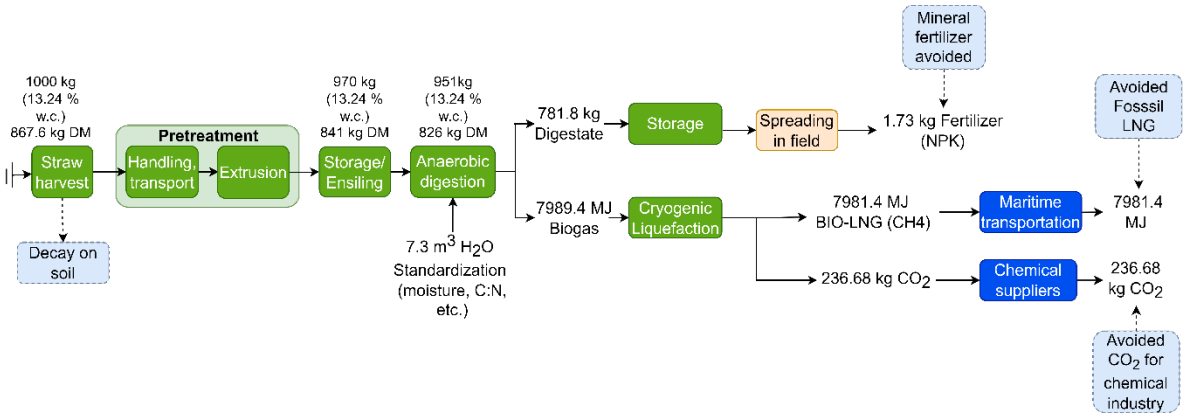

Fig 2. Process flow diagram for the bio-LNG scenario. The process comprises a first stage of anaerobic digestion in a mono-digestion system, at mesophilic conditions and including the addition of water to attain the required humidity for the process (>65 %). The biogas is upgraded by cryogenic liquefaction to obtain liquefied biomethane referred to as bio-LNG, which has similar characteristics to fossil liquefied natural gas (LNG). Here, doted lines and boxes represent the avoided/displaced services and products as a consequence of implementing the case scenario. The bio-LNG is considered to displace fossil-LNG as maritime fuel for cargo vessels.

The life cycle inventories (LCI) per technology are based on previously published works and adapted to include the upgrading to produce drop-in fuels suitable for maritime transport in carrier ships. Pyrolysis LCA (biocrude) was based on Brassard et al. [40,54], whereas the bio-LNG scenario is

built on the AD module developed by Javourez [41] and expanded to include the cryogenic upgrading according to the Cryopure process [58,63,64]. The bio-LNG was modeled to be fuel a bulk carrier to substitute fossil LNG. The detailed life cycle inventories are presented in the supplementary information SI and repository [43].

2.3 System boundaries

The system boundaries of the scenarios follow a well-to-wake approach [65], including all the processes from the raw materials acquisition to the fuel production and use onboard, accounting for the utilities, waste management, and emissions associated with each life stage of the process. The systems are illustrated in Figures 1 and 2 and the LCIs are detailed in SI 1, 2, and 3. This study aims to compare the tradeoffs between a C-neutral [20] harvest of crop residues to supply the bioeconomy with the overall environmental implications of the system. Capital goods are included to the extent possible, with a few exceptions because of a lack of data (i.e., ship vessel construction, engine production). Yet, these appear in both what is induced (maritime transportation with biofuel) and avoided (maritime transportation with conventional fuels), and it is considered reasonable to neglect eventual differences in the engines (in terms of the environmental impacts related to their production).

The use of crop residues to produce SMFs avoids counterfactual management. This counterfactual is considered as the reference business-as-usual (BAU) scenario, where the residues decay on soil (i.e., ploughing considered here). Moreover, various coproducts are released along the supply chains in each scenario and are considered to displace marginal services. In the HPO scenario dust, biochar, syngas, and an aqueous stream (vinegar) are produced during the fast pyrolysis stage with an extra syngas release in the upgrading stage (Fig 1). In the bio-LNG scenario, the coproducts of the whole conversion chain are digestate and CO_2 (Fig 3). We consider that dust and syngas can be recovered for energy production to displace marginal heat and electricity from the future energy mix of France [39]. Similarly, digestate, vinegar, and biochar are recovered to be spread on fields as soil amendments. Digestate and vinegar are considered to displace mineral fertilizers and inorganic pesticides, respectively, while biochar is used for carbon sequestration (i.e., fertilizing properties of biochar not accounted for). The purified CO_2 stream from the bio-LNG production is accounted to supply the chemical industry, displacing commercial CO_2. It should be noted that the final use of CO_2 is not accounted for, and only the avoided production of CO_2 from fossil sources is considered.

3. Results

The study examines the environmental impacts of three scenarios and presents the findings for five impact categories. Figure 3 illustrates the key contributors to each impact category for the three scenarios. The bars in the figure represent the positive (above zero) or negative (below zero, avoided processes) environmental impacts, while the triangle indicates the overall net environmental performance of each scenario. The environmental impacts for the other categories assessed within the EFv3.1 methodology are shown in Appendixes SI2 and SI3 for the HPO and bio-LNG scenarios, respectively. The environmental impacts are expressed and analyzed for 1 tonne of wet crop residues ($1t_{ww}$).

3.1 Analysis per environmental impact

3.1.1 Climate change

The results for climate change are accounted for on a 0/0 methodology, as explained in section 2.1. Figure 3 shows that both biofuel pathways allow environmental reductions on climate change compared to the BAU. Harvesting and using crop residues for bioeconomy purposes avoids approximately 1519 $kgCO_{2eq}.t_{ww}^{-1}$ that would otherwise be emitted if the residues were simply ploughed into the soils.

The full supply chain for the HPO achieves a net reduction of 562.5 kg $CO_{2eq}.t_{ww}^{-1}$ compared to the BAU. The 20 $t.day^{-1}$ input modeled in the HPO system can therefore reduce 2700 $MgCO_2$ per year. The major contributor to emissions reduction is the potential C sequestration through biochar spreading, for which 75% of the C is assumed to remain in the soil as SOC after 100 years [66,67]. The biochar recalcitrance can thus induce the sequestration of 463.6 $kgCO_2.t_{ww}^{-1}$. Moreover, replacing HFO with HPO, results in a net reduction of ca. 234.33 kg $CO_2.t_{ww}^{-1}$, emissions, accounting for the emissions induced by the HPO (3.7 $kgCO_2.t_{ww}^{-1}$) and avoided by HFO (-238.0 kg $CO_{2eq}.t_{ww}^{-1}$) production and combustion. The positive emissions are mainly related to the supply and pretreatment stage, attaining 133.3 $kgCO_{2eq}.t_{ww}^{-1}$. The pyrolysis and HDO stages represent emissions of 53.2 $kgCO_2$, of which 52% corresponds to the pyrolysis process, 8% to the condensation of the pyrolysis products, and 40% to the HDO upgrading of the biocrude. The counterfactual use of coproducts other than biochar (i.e., dust generated during grinding, vinegar and syngas from pyrolysis, and syngas from pyrolysis) represent a total emission of 36.1 $kgCO_{2eq}.t_{ww}^{-1}$. These emissions are offset by the avoided heat, electricity, and pesticide application, which represents 87.2 $kgCO_{2eq}$.tww. Therefore, considering the consequences of valorizing the HPO coproducts represents an emissions reduction of 52 $kCO_{2eq}.t_{ww}^{-1}$.

The bio-LNG pathway represents total emission reductions of 945.5 $kgCO_2.t_{ww}^{-1}$, of which 84% are attributed to the substitution of fossil LNG (avoided 856.33 $kgCO2_e.t_{ww}^{-1}$ production and use) by bio-LNG (emitted 62.7 $kgCO_{2eq}.t_{ww}^{-1}$) combustion to fuel the cargo vessel. While the pretreatment and AD stages release 36.63 $kgCO_{2eq}.t_{ww}^{-1}$, the cryogenic liquefaction avoids the emission of 238.7 kg $CO_{2eq}.t_{ww}^{-1}$. Both the AD and upgrading stages account for the emissions related to methane slips during the process and pipeline injection. Albeit digestate avoids 71.3 $kgCO_{2eq}.t_{ww}^{-1}$ by replacing mineral fertilizers, its management (i.e., storage and spreading) releases 121.6 $kgCO_{2eq}.t_{ww}^{-1}$ with a total net contribution to emissions of 50.2 $kgCO_{2eq}.t_{ww}^{-1}$.

3.1.2 Freshwater eutrophication (EUF)

The SMFs scenarios avoid 8.66 $x10^{-3}$ $kgPO_{4eq}.t_{ww}^{-1}$ emissions. This represents a 198% reduction in freshwater eutrophication for the HPO system, compared to the BAU. Overall, the whole HPO supply chain emits 0.03 $kgPO_{4eq}.t_{ww}^{-1}$ to freshwaters, which is counterbalanced by the reduction of 0.043 $kgPO_{4eq}.t_{ww}^{-1}$ emissions. While the HPO production and upgrading process, comprised of the pyrolysis, condensation, and HDO, represents 61% of the EUF emissions, its use to replace HFO contributes to 7% of the EUF reduction. The major contributor to decreasing EUF (76%) corresponds to the biopesticide avoided. Moreover, despite the recovery of coproducts (except vinegar) and their application (e.g., syngas and dust combustion, biochar spreading, etc.) representing emissions of 0.007 $kgPO4_{eq}.t_{ww}^{-1}$ to freshwater, these emissions are almost neutralized (-0.007 $kgPO_{4eq}.t_{ww}^{-1}$) by the avoided heat and electricity they provide.

The bio-LNG represents higher EUF reductions than HPO, with total emission reductions of 0.09 $kgPO_{4eq}.t_{ww}^{-1}$. The whole supply chain induces the emission of 0.012 0.007 $kgPO_{4eq}.t_{ww}^{-1}$, of which the digestate management (storage and spread) is the main contributor (74%), followed by the pretreatment operations (20%). Due to the CO_2 recovery associated, the cryogenic liquefaction has a net negative EUF impact, with a reduction of 0.06 kg $PO_{4eq}.t_{ww}^{-1}$. Moreover, bio-LNG displaces fossil LNG, which reduces emissions by 0.025 $kgPO_{4eq}.t_{ww}^{-1}$. Albeit digestate represents the greatest EUF impact, it induces avoiding a mineral fertilizer, which is composed of ca. 9% phosphates (P_2O_5) and thus represents 16% fewer PO_{4eq} emissions.

3.1.3 Marine water eutrophication (EUM)

The whole HPO supply chain reduces this impact by 147% compared to the BAU. The HPO combustion is the major contributor to EUM, representing 84% of the total emissions. However, the main contributor to the EUM reduction is the avoided HFO, accounting for 93% of the avoided emissions. Therefore, the net balance for the onboard fuel combustion is negative, achieving emissions of -0.60 $kgN_{eq}.t_{ww}^{-1}$ (HPO and HFO combustion accounted). The coproducts utilization accounted by the

system boundaries expansion (i.e., combustion of dust and syngas, biochar soil application, vinegar application) represents 0.06 $kgN_{eq}.t_{ww}^{-1}$, which are offset by the avoided services of marginal heat and electricity, as well as chemical pesticide replacement, which reduce emissions by 0.136 $kgN_{eq}.t_{ww}^{-1}$.

The bio-LNG scenario EUM reduction is 41% of the HPO and 60% of the EUM. While the storage and bio-LNG use did not contribute to the freshwater eutrophication represented by P emissions, the NH_3, N_2O and NOx emissions observed in these operations are contributors to the marine eutrophication represented by N. The main contributor to this impact is digestate management (storage and spread), which releases 1.31 $kgN_{eq}.t_{ww}^{-1}$, accounting for 55% of the positive emissions. However, the effect of digestate is partially offset by a reduction of 0.63 $kgN_{eq}.t_{ww}^{-1}$ resulting from avoiding mineral fertilizers. The major contribution to the EUM impact reduction (61%) compared to the BAU in the bio-LNG scenario is attributed to the fossil LNG replacement by bio-LNG.

3.1.4 Respiratory Inorganics, representing particulate matter (PM) emissions

This impact represents the impact on human health (disease incidence) by NOx, SO_2, and particulates (<10µm and <2.5µm) as the main pollutants. This is the only category analyzed where a SMF has worse environmental performance than the BAU. Here the bio-LNG has a positive impact on $4.9E^{-5}$ disease incidence whereas $1.6E^{-6}$ disease is avoided by ploughing the crop residues in soils (BAU). In fact, almost the whole supply chain of bio-LNG represents positive PM emissions with reductions observed only by avoiding the fossil LNG ($-1.2E^{-5}$ disease incidence) and mineral fertilizer ($-7.6E^{-6}$ disease incidence). The major emissions are related to the digestate management (storage and spread) accounting for 73% of the disease incidence of PM. This is explained by the high N content in digestate, which is emitted during storage and is later mineralized, relatively fast, when applied on fields.

On the opposite, the HPO scenario represents major PM disease incidence reductions compared to the BAU ($-9.27x10^{-5}$ disease incidence). HFO is a residue like fuel, for which high SOx, NOx, and PM emissions have been attributed compared to other maritime fuels. Therefore, this impact is of major importance when analyzing the replacement of HFO by SMFs. Accordingly, the avoided combustion of HFO by implementing HPO is responsible for 97% of the $1.58E^{-4}$ disease incidence reduction. Likely, the HPO combustion contributes to 77% of the scenario disease incidence. The other operations represent minor flows in this impact category compared to the onboard combustion of the fuels.

3.1.5 Water scarcity

The bio-LNG shows the best performance to avoid water scarcity, which corresponds to 3.4-fold the reductions observed in the BAU. The reductions are attributed to the upgrading stage and the

avoided use of fossil LNG and mineral fertilizer. These three operations, contribute almost equally to the offset of water scarcity, representing 39%, 32%, and 29% of the total reduction, respectively. The whole supply chain represents total induced water scarcity of 6.20 $m^3w_{eq}.t_{ww}^{-1}$, of which 46% is attributed to the water addition process during the AD stage.

The HPO scenario represents approximately 50% of the reductions observed for the bio-LNG. The unit processes along the supply chain represent a positive (thus impactful) WS impact, with total consumption of 28.6 $m^3w_{eq}.t_{ww}^{-1}$. However, the avoided products (HFO, fungicide, heat, and electricity) represent a 2.6-fold reduction of emissions, yielding a net impact of -46.9 $m^3w_{eq}.t_{ww}^{-1}$. Of these, the avoided fungicide represents 60% of the WS reduction, followed by heat production (31%).

3.2 Overall environmental impacts and SOC implications

The results show that the SMFs have a better environmental performance for all the five impact categories as compared to the BAU scenario. The major contributors to the impacts reduction are the avoided fossil fuel combustion and the coproducts and services replaced/avoided by the system expansion. Beyond the environmental impacts assessed, this study aims to analyze the overall trade-offs between the whole environmental impacts along the supply chain and the SOC stocks maintenance achieved by returning the recalcitrant coproduct released before the upgrading process. Table 1 shows the environmental impacts scaled to the total biomass available for a C-neutral harvest of crop residues, considering the national potential of France as reported by Andrade Diaz et al., [20].

For the crop residues potential of 18.7 Mt DM.$year^{-1}$ (13.24% water content), the BAU scenario would emit 32.17 $MgCO_{2eq}$, which are related to an average loss of 178 kt C per year as SOC (considering an annualization over 100 years). The results show, that the SMFs scenarios are both favorable in terms of SOC sequestration and climate change mitigation. For the HPO scenario, based on the SOC results, 100% of the crop residues potential can be harvested to supply the pyrolysis process with no SOC expected to decrease. Therefore, the return of biochar in the HPO scenario builds up average annual SOC stocks by 7740 kt C (considering an annualization over 100 years). while avoiding 11.91 $MgCO_2$eq due to the substitution of HFO by HPO. All the impacts included in the study are as well scaled to the national crop residues potential (C-neutral harvest potential), which represents a 21-fold of the results shown in Fig 3 for the BAU and HPO scenarios.

For biogas with digestate return, the C-neutral harvest of crop residues was shown to be possible in approximately 50% of French croplands, with a national potential of 10 Mt DM.$year^{-1}$. Accordingly, the bio-LNG has 1.7-fold the climate change mitigation potential of the HPO. Scaling the results at national level for a C-neutral harvest results in a higher mitigation potential for the HPO, which corresponds to 1.1-fold that of bio-LNG.

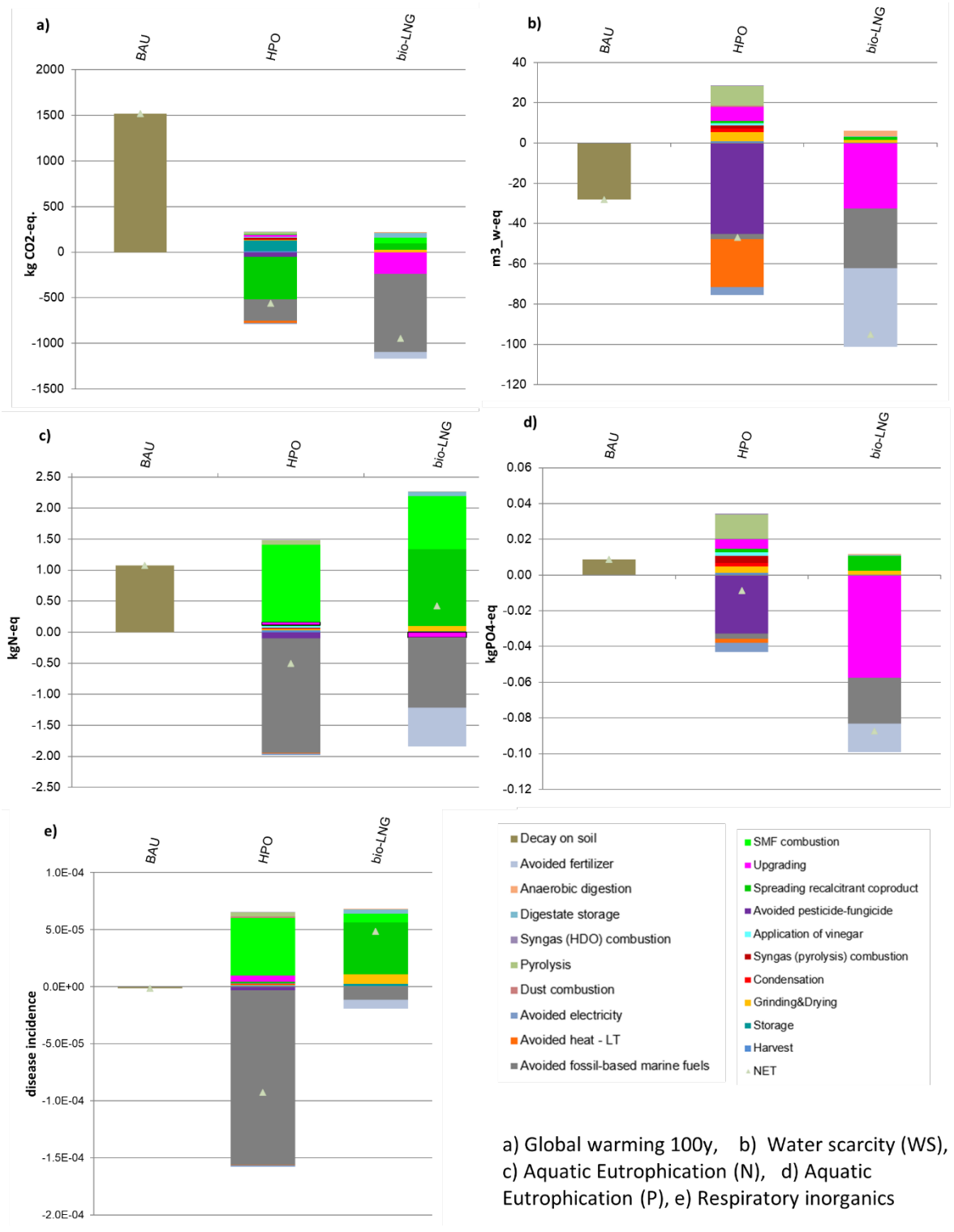

Fig 3. Environmental impacts contribution per process for each scenario. Net process contribution represented as a triangle. SMF: Sustainable maritime fuels; HDO: hydrodeoxygenation; BAU: business as usual, HPO: hydrotreated pyrolysis oil; bio-LNG: liquefied biomethane.

Table 1. Tradeoffs between SOC and the whole environmental performance of the bioeconomy supply chain for producing HPO and bio-LNG to fuel the maritime industry. Results per tonne of crop residues and scaled to the C-neutral harvest potential involved for each technology, as defined in Andrade et al. [20].

		Results per tonne of crop residues			Results scaled to the national C-neutral harvest potential involved by the technology		
Parameter	**Units**	**BAU**	**Pyrolysis**	**Anaerobic Digestion**	**BAU**	**Pyrolysis [e]**	**Anaerobic Digestion [e, f]**
Crop residue potential per technology [a]	Mt DM	1.00	1.00	1.00	21.18	21.18	11.32
C sequestered in soil, per year [b]	kt C	-	-	-	-178.0 [c]	7740.00	7.60
Climate change GWP100 [d]	$MgCO_{2\text{-eq}}$	0.02	-562.50	-945.47	32.17	-11911.51	-10706.52
Eutrophication Freshwater (P)	$kgPO_{4\text{-eq}}$	0.01	-0.01	-0.09	0.19	-0.18	-0.99
Eutrophication Marine (N)	$kgN_{\text{-eq}}$	1.08	-0.50	0.43	22.82	-10.68	4.82
Particulate matter[g] formation	disease incidence	$-1.63x10^{-6}$	$-9.27x10^{-5}$	$4.88x10^{-5}$	$-3.45x10^{-5}$	$-1.96x10^{-3}$	$5.5\ x10^{-4}$
Water scarcity	$m^3\_w_{\text{-eq}}$	-28.14	-46.90	-95.07	-595.87	-933.19	-1076.58

[a] At the national scale of France considering 3.48 Mha of croplands, as determined using the soil-plant model STICS by Launay et al., [68] and used in Andrade-Díaz et al., [20] in AMG. A water content (w.c.) of 13.24% is considered according to [69] [b] Relative SOC sequestration within the technologies, compared to the BAU, for a 100-years' timeframe [20] comprising the period 2020 – 2120. Here, the results of Andrade Diaz [20] were divided to 100 to obtain the sequestration rate per year. [c] SOC change in baseline corresponds to the difference between year 2120 and year 2020. [d] The offset potential considers that the whole supply chain CO_2 emissions related to crop residues are neutralized due to their biogenic nature according to the 0/0 methodology [46]. In other words, the CO_2 emitted along the process has a biological source being sourced from the crop residues and once emitted plants will uptake to lock the biogenic carbon cycle (ref). [e] The biomass potential and SOC sequestration accounts only for the "base" processes, namely pyrolysis and anaerobic digestion, and thus not consider the SOC effects of the upgrading technology. The environmental impacts consider the whole supply chain for the scenarios studied (HPO and bio-LNG). [f] Only Areas with no expected SOC decrease are considered. [g] in units of disease incidence per kg of PM2.5 emitted.

4. Discussion

4.1 Potential of biofuels for the maritime sector regarding climate impact goals

Albeit biofuels are currently increasing their share on the road and aviation energy mix their use on the maritime sector is still limited due to a myriad of technical and policy drawbacks, e.g., engine incompatibility to combust the novel fuels in current vessels. Historically, cargo ships have been fueled by low-quality HFO, which are bottom-of-the-barrel leftover from the refining of petrol [47] entailing low costs. Accordingly, the current fleet has been designed with slow-speed propulsion systems with limited suitability to different fuels [28]. Since emissions regulations had not been put in action before the last decade [29] , the maritime industry actors have continued to favor the low-cost low-quality HFO and new vessels and engines capable to carry and burn new alternative fuels are still under research and development [32]. However, the latest GHG emission reduction target set by the IMO [30] along with the 0.5% sulfur limit and the latest inclusion of the maritime industry within the emissions target of European call for immediate action to transition to renewable fuels.

The IEA [32] has estimated that lignocellulosic fuels have the potential to supply all the maritime fuel demand (455-805 Mt oil equivalent potential *vs* 330 Mt oil equivalent demand) while reducing the industry emissions, otherwise expected to increase by 30% in 2050 [30] Yet, there are also multiples competing demands on lignocellulosic resources, as discussed in e.g. [70]. All the environmental impacts addressed showed a better environmental performance for the SMFs scenarios than the BAU. In summary, the CC, EUM, and WS impacts were better performing for the bio-LNG, while the EUF and PM presented the most pronounced emissions reduction in the HPO scenario.

Approximately 137% and 162% GHG emission reduction can be attained if crop residues are harvested and transformed to HPO and bio-LNG, and used to substitute HFO and LNG, respectively. These tremendous emissions savings are mainly related to the avoided mineralization of crop residues on fields, which would else be released as CO_2, and by the replacement of the fossil counterpart fuel as well as the marginal heat, electricity and fertilizer/pesticides currently used. In this study, we considered an optimistic energetic performant future, where all the energy services (heat and electricity) are electrified. If more conventional sources of heat would else be used (and replaced), the emission reduction would be even larger, as more heat is produced than used.

In fact, compared to the fossil alternatives the SMF represent over 90% less $CO_{2\text{-eq}}$ emissions. The HPO combustion represents a 98% reduction of GHG emissions as compared to the HFO. Likely, the combustion of bio-LNG represents 92% less CO_{2eq} emissions than the fossil alternative. Our results are in accordance with previous studies, where it has been reported that approximately 50 to 90 % of

the life cycle impacts are related to the avoided fossil alternative [71], highlining the ability of bio-LNG to reduce 90% of the fossil LNG GHG emissions [72].

Besides GHG emissions, the maritime industry is responsible for NOx, SOx, and PM emissions [33], which represents a main environmental risk. Therefore, the marine water eutrophication (N) and particulate matter (NOx, SOx, and PM) impacts are of key importance in the maritime transport's context. Replacing HFO with HPO, reduces the PM impact by 67% and the marine eutrophication by 33%. Likely, transitioning to bio-LNG shows 36% less PM impact and 24% less marine eutrophication.

4.2 Trade-offs with SOC sequestration

Both the HPO and bio-LNG allow recovering a C-rich coproduct, deemed as recalcitrant [66,73], that can be applied on soils as C amendment, namely biochar and digestate, respectively. Nonetheless, the different nature of both products was considered within the modeled LCA, producing contrasting results for each. Biochar, which is composed by 95% recalcitrant carbon (i.e., degradation resistant carbon) is expected to heavily remain in soils, i.e. 75% of its C after 100 years [66]. This represented 82% of the GHG emission reduction for the HPO scenario. However, it does not affect any of the other four impact categories.

On the other hand, digestate has been reported to have a behavior similar to crop residues [74,75] with the difference that the labile fraction responsible of the major share of CO_2 emissions in the BAU has been removed and converted to biogas. The recalcitrant carbon fraction of digestate has a short mean residence time (ca. 1.2 years) associated [66]. Moreover, the nitrogen content in the digestate is concentrated during the AD process (as other fractions are lost to the gas phase), while the ratio inorganic : organic N is enhanced as a result of the process, granting fertilizing properties [76]. Results show that digestate is the major contributor in four of the five impacts investigated for the bio-LNG scenario. For instance, the digestate mineralization during storage and on field is responsible of 55% of the positive CO_{2eq} emissions (not through CO_2, but CH_4 and N_2O losses), 58% of the eutrophication of marine water, 75% eutrophication of freshwater, and 73% of particulate matter formation in the bio-LNG scenario. These emissions are directly related to either the high N and P content of digestate.

However, although digestate contribute to the major share of emissions in the bio-LNG scenario, these are offset by the reduced and avoided overall emissions along the whole supply chain. Aligned with the aim of this study, we have compared the trade-off of the C-neutral harvest of the crop residues to produce the SMFs and the full environmental impacts associated.

Scaling the environmental impacts of one wet tonne of crop residues to the national C-neutral harvest potential of each technology in France (Table 1), shows that HPO is the most environmentally performant scenario both in terms of emissions and SOC sequestration. Interestingly, the bio-LNG potential to offset water scarcity and freshwater eutrophication is 5.5-and 1.15-fold that of HPO, even when harvesting only half the same amount of crop residues. Overall, Table 1 does not show any trade-offs between the addressed environmental impacts and SOC stocks maintenance for the investigated SMFs scenarios. The C-neutral harvest of crop residues thus pose major environmental savings if the recalcitrant coproducts are returned to soils, allowing to not simply maintain SOC stocks, but to improve them.

The LCA results reveal, that the precautionary practice of leaving the crop residues on soils results in higher GHG emissions than valorizing the residues for biofuel production. This also applies for all other environmental impacts addressed. Harvesting crop residues to produce biofuels, here HPO and bio-LNG for maritime use, while ensuring the return of the C-rich coproducts to soils is a win-win option because it allows to sequester C in soils, provide the energy service to displace fossil fuels, and consequently reduce the overall GHG emissions along with other environmental impacts of the system.

Despite the bio-LNG scenario is environmentally performant to reduce C-related emissions, digestate is held responsible of major N losses, including N_2O, NH_3, and nitrate losses to water. This is critically detrimental for the overall scenario performance because N_2O represent almost 300 times the global warming potential of CO_2. It is also detrimental to other impacts, most importantly the marine eutrophication (Table 1), being one of the two impacts where a net positive impact is observed. Therefore, measures to reduce the soil-denitrification induced by digestate application need to be addressed. As the N_2O result from the nitrification and oxidation of ammonium, already existing techniques such as nitrification inhibitors can be used [77]. Other techniques regarding microbial enrichment [78] and farming management activities (e.g., tillage, irrigation) [79] can be implemented in order to offset the N-flux contribution from digestate. Techniques such as digestate acidification at the spreading stage can also limit nitrogen losses (here NH_3) and hence reduce the marine eutrophication impact. Moreover, biochar has well recognized N-offset properties [80] and could be applied in tandem with digestate to create synergies from the nutrient-fertilizer effect of digestate and reduced C and N mineralization from biochar.

4.3 Key aspects to consider

Though comparing the renewable fuels *vs* the fossil ones, HPO shows a better environmental performance than fossil HFO, bio-LNG exhibits less overall emission along the whole supply chain, per wet tonne of crop residue. This is in part explained because the system modeled in this study considers

that the cryogenic upgrading allows separating a CO_2 stream, which can then be recovered to avoid the production of fossil derived CO_2 for the chemical industry. In fact, avoiding this fossil-derived CO2 has a significant impact (~0.9 $kgCO_{2e}$ per kg fossil CO_2 avoided). However, it remains unclear to which extent a 100% recovery can be considered representative of future biogas plants as the recovery efficiency could be lower. Moreover, the biogas injection to the cryogenic liquefaction process may entail some gas slips [64] that were considered negligible herein (yet, losses were considered at the moment to inject the non-upgraded biogas to the biogas pipelines transporting the gas to the upgrading site).

In fact, fossil LNG has been promoted to reduce GHG emissions in the maritime sector compared to other fossil fuels. However, this characteristic is counterpoised by the risk of slipping CH_4 while processing the natural gas, which has a global warming potential 30 times that of CO_2. It has been determined that a 3.5% natural gas slip on ship operation, may result in 3 to 9% higher emissions than HFO. Therefore, it is crucial to evaluate the possible fugitive losses during the LNG production process [81]. The fossil LNG used from Ecoinvent 3.9.1, assumes an 8.6% natural gas consumption to run the liquefaction process, a 0.05% gas leakage, and that all the CO_2 separated is emitted. These assumptions are fundamentally different than those consider in the bio-LNG scenario, where we have considered an optimized future in terms of energy performance, and the full recovery of the separated CO_2. However, as we considered a bio-LNG driven future where the biogas is transported through a dedicated pipeline to the upgrading facilities located next to the harbor port, we penalized the upgrading process by assuming a total 1.70% leakage due to the pipeline injection and upgrading operation. In order to have transparent comparisons, it is necessary to consider the same leakage assumptions for the fossil and biofuel scenarios, which could be considered in further sensitivity analyses.

The cryogenic upgrading of biomethane is still limited due to technology development issues, high costs, and high energy consumption to comply with the cryogenic process requirements [82]. However, according to the Danish Energy Agency [64], this technology may develop in future years due to the lower energy costs envisioned at commercial scale, high purity of the biomethane, expected leakages below 1%, and possibility to recover coproducts such as CO_2 and N.

Regarding the HPO process, pyrolysis oil is not considered a drop-in fuel due to the lack of compliance with fuels standards (e.g., high water content, high O_2 content, acidity). However, when upgraded, the stabilized oil, here HPO, is an attractive biofuel for the sea transport able to replace HFO with notorious reduced emissions in multiple impact categories. Nonetheless, fast pyrolysis remains at a pioneer stage and the potential development of this technology at commercial scale is still uncertain [64]. Moreover,

one critique that detracts the hydrodeoxygenation performance is the high requirement of H_2, which can represent 15% [49,52] of the produced biofuel and is mainly supplied by steam reforming of fossil fuels [55]. Here, we modeled the production of the H_2 by means of alkaline electrolysis [41]. One consequential benefit of using electrolysis-derived H_2 is the ability to recover O_2, which can reach up to 95% of efficiency. However, to remain conservative, we considered no O_2 recovery in this study. Recovering and substituting conventional O_2 could increase the environmental performance of the HPO scenario and could be analyzed in further sensitivity analyses.

5. Conclusion

The analysis of the LCA results observed here coupled to the SOC stocks simulations allows inferring that harvesting the crop residues to supply the bioeconomy, followed by the return of the recalcitrant coproducts to soils, allows to not only maintain, but to improve the soils C budget, while at the same time triggering emission reduction for the climate change, marine and freshwater eutrophication, particulate matter, and water scarcity environmental impact by replacing fossil fuels and marginal energy (i.e., electricity and heat).

For the particular case of HPO and bio-LNG studied in here, these biofuels have the potential to offset over 90% of the GHG emissions produced by the combustion of the traditional fossil HFO and LNG. HPO is of key interest to reduce the particulate matter impact of HFO by 67%, associated with NOx, SOx, and PM emissions, which is a key issue in the sea transport mitigation goals. Similarly, bio-LNG has the highest potential to reduce freshwater eutrophication, climate change, and water scarcity if the whole system is considered. The results show that managing crop residues by just plowing them back to soils, does not only hamper the biomass supply to the bioeconomy but also results in higher environmental impacts as well as lower SOC stocks.

However, the validity of our study relies on the transparency and representativeness of the data used in the models. Current LCI data related to maritime biofuels are still sparse, and existing studies are often not directly comparable, which complicates a further in-depth assessment of a full well-to-wake LCA for the sea transport industry. From the perspective of decision-making, the results shown here must be considered under the umbrella of a further sensitivity and uncertainty analysis to shed light on the sensitive and uncertain parameters the model involved.

Data availability

This manuscript is supported by a supplementary information document and the LCI foreground database is openly available in "TBI - Toulouse Biotechnology Institute - T21018" at https://doi.org/10.48531/JBRU.CALMIP/1JXQK3 [43]

Supporting documents and data

The supplementary information accompanying this paper is presented in Appendix A4a.

References for Chapter 5

1. Energy & Climate Intelligence Unit. Net zero emissions race. 2022 Scorecard [Internet]. Net Zero Scorecard. 2022 [cited 2022 Feb 27]. Available from: https://eciu.net/netzerotracker
2. Department for Business, Energy & Industrial Strategy. Net Zero Strategy: Build Back Greener. UK: HM Government UK; 2021 Oct. (Climate Change Act).
3. Energy Transitions Commission. China 2050: A fully developed rich zero-carbon economy [Internet]. China: Energy Transitions Commission; 2019. Available from: https://www.energy-transitions.org/publications/china-2050-a-fully-developed-rich-zero-carbon-economy
4. European Comission. Regulation (EU) 2021/1119 of the European Parliament and of the Council of 30 June 2021 establishing the framework for achieving climate neutrality and amending Regulations (EC) No 401/2009 and (EU) 2018/1999 ('European Climate Law'). PE/27/2021/REV/1 [Internet]. 2021. Available from: http://data.europa.eu/eli/reg/2021/1119/oj
5. IEA. Net Zero by 2050 – A roadmap for the Global Energy Sector [Internet]. IEA; 2021 [cited 2023 May 3]. Available from: https://www.iea.org/reports/net-zero-by-2050
6. IPCC. Global Warming of 1.5°C. An IPCC Special Report on the impacts of global warming of 1.5°C above pre-industrial levels and related global greenhouse gas emission pathways, in the context of strengthening the global response to the threat of climate change, sustainable development, and efforts to eradicate poverty [Masson-Delmotte, V., P. Zhai, H.-O. Pörtner, D. Roberts, J. Skea, P.R. Shukla, A. Pirani, W. Moufouma-Okia, C. Péan, R. Pidcock, S. Connors, J.B.R. Matthews, Y. Chen, X. Zhou, M.I. Gomis, E. Lonnoy, T. Maycock, M. Tignor, and T. Waterfield (eds.)]. IPCC; 2018.
7. Blanco-Canqui H. Crop Residue Removal for Bioenergy Reduces Soil Carbon Pools: How Can We Offset Carbon Losses? Bioenerg Res. 2013;14.
8. Katherine Rodriguez Caceres, Francy Blanco Patino, Julian Araque Duarte, Viatcheslav Kafarov. Assessment of the energy potential of agricultural residues in non-interconnected zones of colombia: case study of choco and putumayo. Chemical Engineering Transactions. 2016 Jun;50:349–54.
9. Carvalho JLN, Hudiburg TW, Franco HCJ, DeLucia EH. Contribution of above- and belowground bioenergy crop residues to soil carbon. GCB Bioenergy. 2017 Aug;9(8):1333–43.
10. Lal R. Soil carbon sequestration to mitigate climate change. Geoderma. 2004 Nov 1;123(1):1–22.
11. Meyer RS. Potential impacts of climate change on soil organic carbon and productivity in pastures of south eastern Australia. Agricultural Systems. 2018;13.
12. Paustian K, Larson E, Kent J, Marx E, Swan A. Soil C Sequestration as a Biological Negative Emission Strategy. Front Clim. 2019 Oct 16;1:8.

13. Autret B, Mary B, Chenu C, Balabane M, Girardin C, Bertrand M, et al. Alternative arable cropping systems: A key to increase soil organic carbon storage? Results from a 16 year field experiment. Agriculture, Ecosystems & Environment. 2016 Sep;232:150–64.
14. Mondini C, Cayuela ML, Sinicco T, Fornasier F, Galvez A, Sánchez-Monedero MA. Soil C Storage Potential of Exogenous Organic Matter at Regional Level (Italy) Under Climate Change Simulated by RothC Model Modified for Amended Soils. Front Environ Sci. 2018 Nov 29;6:144.
15. Fujisaki K, Chevallier T, Chapuis-Lardy L, Albrecht A, Razafimbelo T, Masse D, et al. Soil carbon stock changes in tropical croplands are mainly driven by carbon inputs: A synthesis. Agriculture, Ecosystems & Environment. 2018 May 1;259:147–58.
16. Scarlat N, Fahl F, Lugato E, Monforti-Ferrario F, Dallemand JF. Integrated and spatially explicit assessment of sustainable crop residues potential in Europe. Biomass and Bioenergy. 2019 Mar 1;122:257–69.
17. Fischer G, Prieler S, van Velthuizen H, Berndes G, Faaij A, Londo M, et al. Biofuel production potentials in Europe: Sustainable use of cultivated land and pastures, Part II: Land use scenarios. Biomass and Bioenergy. 2010 Feb;34(2):173–87.
18. Monforti F, Lugato E, Motola V, Bodis K, Scarlat N, Dallemand JF. Optimal energy use of agricultural crop residues preserving soil organic carbon stocks in Europe. Renewable and Sustainable Energy Reviews. 2015 Apr 1;44:519–29.
19. Hansen JH, Hamelin L, Taghizadeh-Toosi A, Olesen JE, Wenzel H. Agricultural residues bioenergy potential that sustain soil carbon depends on energy conversion pathways. 2020;12.
20. Andrade Díaz C, Clivot H, Albers A, Zamora-Ledezma E, Hamelin L. The crop residue conundrum: Maintaining long-term soil organic carbon stocks while reinforcing the bioeconomy, compatible endeavors? Applied Energy. 2023 Jan 1;329:120192.
21. Woolf D, Lehmann J. Modelling the long-term response to positive and negative priming of soil organic carbon by black carbon. Biogeochemistry. 2012;13.
22. Lefebvre D, Williams A, Meersmans J, Kirk GJD, Sohi S, Goglio P, et al. Modelling the potential for soil carbon sequestration using biochar from sugarcane residues in Brazil. Sci Rep. 2020 Dec;10(1):19479.
23. Zhang Q, Xiao J, Xue J, Zhang L. Quantifying the Effects of Biochar Application on Greenhouse Gas Emissions from Agricultural Soils: A Global Meta-Analysis. Sustainability. 2020 Apr 23;12(8):3436.
24. Stella T, Mouratiadou I, Gaiser T, Berg-Mohnicke M, Wallor E, Ewert F, et al. Estimating the contribution of crop residues to soil organic carbon conservation. Environmental Research Letters. 2019 Sep 6;14(9):094008.
25. France Agrimer. L´Observatoire National des Ressources en Biomasse. Évaluation des ressources agricoles et agroalimentaires disponibles en France – édition 2020. Agrimer; 2020.
26. SSI. Defining sustainability criteria for marine fuels: Fifteen issues, principles and criteria for zero and low carbon fuels for shipping [Internet]. The sustainable Shipping Initiative and Copenhagen Business School Maritime; 2021. Available from: https://www.sustainableshipping.org/wp-content/uploads/2021/09/Defining-sustainability-criteria-for-marine-fuels.pdf
27. Hsieh C wen C, Felby C. Biofuels for the marine shipping sector> An overview and analysis of sector infrastructure, fuel technologies and regulations. IEA Bioenergy; 2017. (Task 39).
28. United Nations. Review of Maritime transport 2022: Navigating stormy waters. Geneva: United Nations; 2022. 174 p. (Review of maritime transport / United Nations Conference on Trade and Development, Geneva).
29. European Union Parliament. Fit for 55 package. 2021.

30. Index of MEPC Resolutions and Guidelines related to MARPOL Annex VI [Internet]. [cited 2023 May 10]. Available from: https://www.imo.org/en/OurWork/Environment/Pages/Index-of-MEPC-Resolutions-and-Guidelines-related-to-MARPOL-Annex-VI.aspx
31. European Union Parliament. REGULATION OF THE EUROPEAN PARLIAMENT AND OF THE COUNCIL amending Regulation (EU) 2015/757 in order to provide for the inclusion of maritime transport activities in the EU Emissions Trading System and for the monitoring, reporting and verification of emissions of additional greenhouse gases and emissions from additional ship types. PE-CONS 10/23 Apr 20, 2023.
32. Simonsen TI, Weiss ND, van Dyk S, van Thuijl E, Thomsen ST, Thomsen EST. Progress towards biofuels for marine shipping. IEA Bioenergy; 2021. (Task 39).
33. IMO. Fourth IMO GHG Study 2020 [Internet]. IMO; 2020. Available from: https://wwwcdn.imo.org/localresources/en/OurWork/Environment/Documents/Fourth%20IMO%20GHG%20Study%202020%20-%20Full%20report%20and%20annexes.pdf
34. MARPOL. RESOLUTION MEPC.304(72) INITIAL IMO STRATEGY ON REDUCTION OF GHG EMISSIONS FROM SHIPS. MEPC 72/17/Add.1 2018.
35. MARPOL. MEPC RESOLUTION.366(79) INVITATION TO MEMBER STATES TO ENCOURAGE VOLUNTARY COOPERATION BETWEEN THE PORT AND SHIPPING SECTORS TO CONTRIBUTE TO REDUCING GHG EMISSIONS FROM SHIPS. MEPC 79/15/Add.1 2022.
36. ISO. ISO 14040:2006 [Internet]. ISO. 2014 [cited 2023 May 10]. Available from: https://www.iso.org/fr/standard/37456.html
37. ISO. ISO 14044:2006 [Internet]. ISO. 2014 [cited 2023 May 10]. Available from: https://www.iso.org/fr/standard/38498.html
38. Brandão M, Martin M, Cowie A, Hamelin L, Zamagni A. Consequential Life Cycle Assessment: What, How, and Why? In: Abraham MA, editor. Encyclopedia of Sustainable Technologies [Internet]. Oxford: Elsevier; 2017 [cited 2023 May 10]. p. 277–84. Available from: https://www.sciencedirect.com/science/article/pii/B9780124095489100685
39. Su-ungkavatin P. Assessing the environmental performance of future sustainable aviation systems: methodological development and evaluation by life cycle assessment. [France]: INSA Toulouse; 2022.
40. Brassard P, Godbout S, Hamelin L. Framework for consequential life cycle assessment of pyrolysis biorefineries: A case study for the conversion of primary forestry residues. Renewable and Sustainable Energy Reviews. 2021 Mar;138:110549.
41. Javourez U. Transforming residual biomass into food and feed – Towards an LCA optimization platform. [France]: INSA Toulouse; 2023.
42. Ecoinvent. Ecoinvent 3.9.1 database. 2022.
43. Andrade Díaz C. Database: LCIs for : To harvest or not? Tradeoffs between SOC maintenance and overall environmental performance of harvesting crop residues for the bioeconomy. Datavers.Callisto; 2023.
44. European Comission. COMMISSION RECOMMENDATION of 16.12.2021 on the use of the Environmental Footprint methods to measure and communicate the life cycle environmental performance of products and organisations [Internet]. 2021. Available from: https://environment.ec.europa.eu/system/files/2021-12/Commission%20Recommendation%20on%20the%20use%20of%20the%20Environmental%20Footprint%20methods_0.pdf
45. Steubing B, de Koning D, Haas A, Mutel CL. The Activity Browser — An open source LCA software building on top of the brightway framework. Software Impacts. 2020 Feb 1;3:100012.

46. Cucurachi S, Steubing B, Siebler F, Navarre N, Caldeira C, Sala S. Prospective LCA methodology for Novel and Emerging Technologies for BIO-based products - The PLANET BIO project [Internet]. JRC Publications Repository. 2022 [cited 2023 May 15]. Available from: https://publications.jrc.ec.europa.eu/repository/handle/JRC129632
47. Comer B, Olmer N, Mao X, Roy B, Rutherford D. Prevalence of heavy fuel oil and black carbon in Arctic shipping, 2015 to 2025. International Council on Clean Transportation; 2017.
48. Oasmaa A, Lehto J, Solantausta Y, Kallio S. Historical Review on VTT Fast Pyrolysis Bio-oil Production and Upgrading. Energy Fuels. 2021 Apr 1;35(7):5683–95.
49. Vienescu DN, Wang J, Le Gresley A, Nixon JD. A life cycle assessment of options for producing synthetic fuel via pyrolysis. Bioresource Technology. 2018 Feb 1;249:626–34.
50. Sorunmu Y, Billen P, Spatari S. A review of thermochemical upgrading of pyrolysis bio-oil: Techno-economic analysis, life cycle assessment, and technology readiness. GCB Bioenergy. 2020;12(1):4–18.
51. Peters JF, Iribarren D, Dufour J. Biomass Pyrolysis for Biochar or Energy Applications? A Life Cycle Assessment. Environ Sci Technol. 2015 Apr 21;49(8):5195–202.
52. Iribarren D, Peters JF, Dufour J. Life cycle assessment of transportation fuels from biomass pyrolysis. Fuel. 2012 Jul 1;97:812–21.
53. Emery I, Dunn JB, Han J, Wang M. Biomass Storage Options Influence Net Energy and Emissions of Cellulosic Ethanol. Bioenerg Res. 2015 Jun 1;8(2):590–604.
54. Brassard P. Mass balance and LCA inventory of bio-oil production by fast pyrolysis of wheat straw. Unpublished study, received as a courtesy from the authors. 2022;
55. Jones S, Meyer P, Snowden-Swan L, Padmaperuma A, Laboratory PNN. Process Design and Economics for the Conversion of Lignocellulosic Biomass to Hydrocarbon Fuels: Fast Pyrolysis and Hydrotreating Bio-oil Pathway. 2013;97.
56. Elliott DC. Transportation fuels from biomass via fast pyrolysis and hydroprocessing. WIREs Energy and Environment. 2013;2(5):525–33.
57. Aronietis R, Sys C, van Hassel E, Vanelslander T. Forecasting port-level demand for LNG as a ship fuel: the case of the port of Antwerp. Journal of Shipping and Trade. 2016 Jul 20;1(1):2.
58. Pellegrini LA, De Guido G, Langé S. Biogas to liquefied biomethane via cryogenic upgrading technologies. Renewable Energy. 2018 Aug 1;124:75–83.
59. Florio C, Fiorentino G, Corcelli F, Ulgiati S, Dumontet S, Güsewell J, et al. A Life Cycle Assessment of Biomethane Production from Waste Feedstock Through Different Upgrading Technologies. Energies. 2019 Jan;12(4):718.
60. Hamelin L, Naroznova I, Wenzel H. Environmental consequences of different carbon alternatives for increased manure-based biogas. Applied Energy. 2014 Feb;114:774–82.
61. Tonini D, Hamelin L, Astrup TF. Environmental implications of the use of agro-industrial residues for biorefineries: application of a deterministic model for indirect land-use changes. GCB Bioenergy. 2016;8(4):690–706.
62. Symons GE, Buswell AM. The Methane fermentation of carbohydrates. Journal of the American Chemical Society. 1933;
63. Yousef AM, El-Maghlany WM, Eldrainy YA, Attia A. Upgrading biogas to biomethane and liquid CO2: A novel cryogenic process. Fuel. 2019 Sep 1;251:611–28.
64. Danish Energy Agency, Energinet. Technology Data. Renewable fuels. [Internet]. 2017. Available from: http://www.ens.dk/teknologikatalog
65. Carvalho F, O'Mally J, Osipova L, Pavlenko N. Keu issues in LCA methodology for marine fuels. ICCT; 2023 Apr.

66. Andrade C, Albers A, Zamora-Ledezma E, Hamelin L. A review on the interplay between bioeconomy and soil organic carbon stocks maintenance. PREPRINT (version 2) available at Research Square [Internet]. 2022 Mar 16 [cited 2022 Mar 16]; Available from: https://www.researchsquare.com
67. Lehmann J, Cowie A, Masiello CA, Kammann C, Woolf D, Amonette JE, et al. Biochar in climate change mitigation. Nat Geosci. 2021 Dec;14(12):883–92.
68. Launay C, Constantin J, Chlebowski F, Houot S, Graux A, Klumpp K, et al. Estimating the carbon storage potential and greenhouse gas emissions of French arable cropland using high-resolution modeling. Glob Change Biol. 2021 Apr;27(8):1645–61.
69. Karan S. Cambioscop RO1: Dataset on characterization, quantity and current use of French residual biomasses. 2022 Nov 28 [cited 2023 May 10];1. Available from: https://data.mendeley.com/datasets/b9sx3h3584
70. Su-ungkavatin P, Tiruta-Barna L, Hamelin L. Biofuels, electrofuels, electric or hydrogen?: A review of current and emerging sustainable aviation systems. Progress in Energy and Combustion Science. 2023 May 1;96:101073.
71. Al-Enazi A, Okonkwo EC, Bicer Y, Al-Ansari T. A review of cleaner alternative fuels for maritime transportation. Energy Reports. 2021 Nov 1;7:1962–85.
72. Hacatoglu K, McLellan PJ, Layzell DB. Production of Bio-Synthetic Natural Gas in Canada. Environ Sci Technol. 2010 Mar 15;44(6):2183–8.
73. Gómez N, Rosas JG, Singh S, Ross AB, Sánchez ME, Cara J. Development of a gained stability index for describing biochar stability: Relation of high recalcitrance index (R50) with accelerated ageing tests. Journal of Analytical and Applied Pyrolysis. 2016 Jul;120:37–44.
74. Möller K. Effects of anaerobic digestion on soil carbon and nitrogen turnover, N emissions, and soil biological activity. A review. Agron Sustain Dev. 2015 Jul;35(3):1021–41.
75. Thomsen IK, Olesen JE, Møller HB, Sørensen P, Christensen BT. Carbon dynamics and retention in soil after anaerobic digestion of dairy cattle feed and faeces. Soil Biology and Biochemistry. 2013 Mar;58:82–7.
76. Alburquerque JA, de la Fuente C, Campoy M, Carrasco L, Nájera I, Baixauli C, et al. Agricultural use of digestate for horticultural crop production and improvement of soil properties. European Journal of Agronomy. 2012 Nov;43:119–28.
77. De Notaris C, Abalos D, Mikkelsen MH, Olesen JE. Potential for the adoption of measures to reduce N2O emissions from crop residues in Denmark. Science of The Total Environment. 2022 Aug 20;835:155510.
78. Jonassen KR, Hagen LH, Vick SHW, Arntzen MØ, Eijsink VGH, Frostegård Å, et al. Nitrous oxide respiring bacteria in biogas digestates for reduced agricultural emissions. ISME J. 2022 Feb;16(2):580–90.
79. Hassan MU, Aamer M, Mahmood A, Awan MI, Barbanti L, Seleiman MF, et al. Management Strategies to Mitigate N2O Emissions in Agriculture. Life (Basel). 2022 Mar 17;12(3):439.
80. Wu D, Ren C, Ren D, Tian Y, Li Y, Wu C, et al. New insights into carbon mineralization in tropical paddy soil under land use conversion: Coupled roles of soil microbial community, metabolism, and dissolved organic matter chemodiversity. Geoderma. 2023 Apr 1;432:116393.
81. Baresic D, Smith T, Raucci C, Rehmatulla N, Narula K, Rojon I. LNG as a marine fuel in the EU: Market, bunkering infrastructure investments and risks in the context of GHG reductions. London: UMAS - Transport and Environment; 2018.
82. Naquash A, Qyyum MA, Chaniago YD, Riaz A, Yehia F, Lim H, et al. Separation and purification of syngas-derived hydrogen: A comparative evaluation of membrane- and cryogenic-assisted approaches. Chemosphere. 2023 Feb 1;313:137420.

6. CHAPTER 6: Conclusions, limitations, and future perspectives

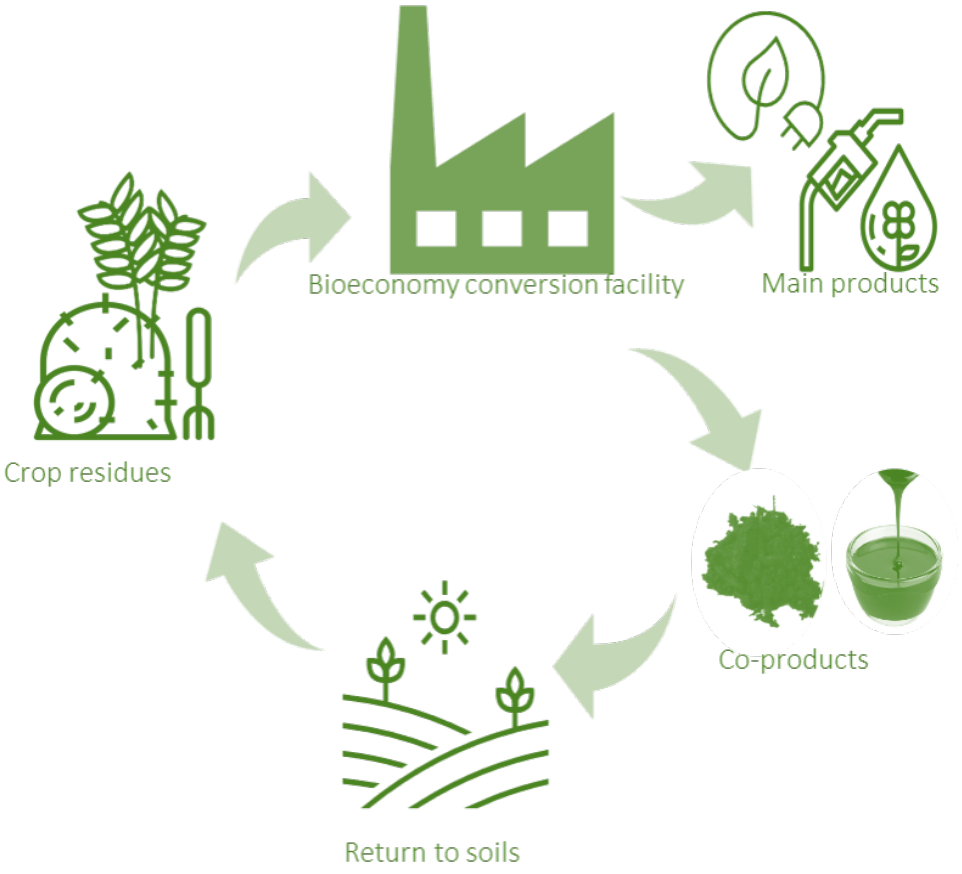

6. CHAPTER 6 : Conclusions, limitations, and future perspective

6.1 Summary and key findings

The aim of this thesis was to understand the interactions between the return of recalcitrant bioeconomy coproducts to soil and the long-term SOC dynamics in a C-neutral harvest context. To do so, the research questions and objectives shown in **Chapter 1** have been answered and fulfilled.

First, the notion of "C-neutral harvest" has been introduced and defined as a situation where the long-term SOC stocks do not decrease when crop residues are managed to supply a bioeconomy conversion pathway, compared to a reference situation where the residues are left on soils. This thesis has identified and parametrized the factors interrelating the use of crop residues for the bioeconomy and the SOC dynamics in croplands when a return of the bioeconomy coproducts to soils is considered. Here, a novel framework was developed to integrate the parametrized factors within soil models, providing useful tools for decision-making regarding the management of crop residues. The study was performed spatially explicitly with high resolution, providing insights for the specific contexts of national French and Ecuadorian croplands. Moreover, a full life cycle assessment of the whole bioeconomy supply chain contrasted the SOC-driven observations with the full environmental performance of the C-neutral harvest of crop residues. This work is thus the first, to the author's knowledge, to propose a SOC assessment methodology for multiple bioeconomy coproducts, applicable to various climate contexts, focused on supplying renewable C to the bioeconomy.

The **RO1** was achieved in **Chapter 2** through an exhaustive literature review harmonizing 620 data records that trail the carbon balance and recalcitrance of pyrochar, gaschar, hydrochar, digestate, and the solid (cake) and liquid (molasses) fraction remaining after the second-generation alcohol production. The carbon balances were systematically sequenced to express a coefficient defined as "carbon conversion C_C", which tailors the fraction of carbon remaining in the coproducts at the end of the bioeconomy conversion pathway. Based on laboratory incubations, field trials, and modeling assays, the fraction of recalcitrant carbon in the coproducts was expressed as the "recalcitrant carbon C_R" coefficient. The C_R coefficient was categorized into various subgroups related to the variability of the coproducts, driven by the process conditions and assessment methodology. **Chapter 2** also presents a depth revision of twelve soil models with the aim of understanding their ability to integrate bioeconomy coproducts. Eight models [1–10] were identified as already adapted for including other inputs than plants and manure, and thus the procedures were thoroughly documented to derive a tailored procedure for including the coproducts studied in this thesis. Fig 6.1 summarizes the products

delivered on Chapter 2 to reach RO1. The completion of **RO1** led to answering **RQ1,** namely "What are the key factors determining the interrelation between the supply of crop residues to the bioeconomy and the maintenance of SOC stocks in croplands?" Albeit soil models present different configurations based on the interactions considered (e.g., plant-atmosphere, SOC only, C-N, etc.) [11–13], the SOC focused models can be simplified by two key functions: i) the size of the C input and ii) the time that the carbon will remain in the soil pool. The latter function is in turn related to defining the soil pool where the carbon fraction will be allocated, which is also simplified by representing the carbon as labile and recalcitrant. Therefore, the C_C and C_R coefficients are useful parameters to interrelate the effect of harvesting crop residues, converting them to recalcitrant coproducts while supplying renewable carbon to the bioeconomy, and retuning to the soils as C amendments. The C_C allows thus measuring the C input returning, and the C_R defines the amount of recalcitrant carbon allocated in the most stable soil pool.

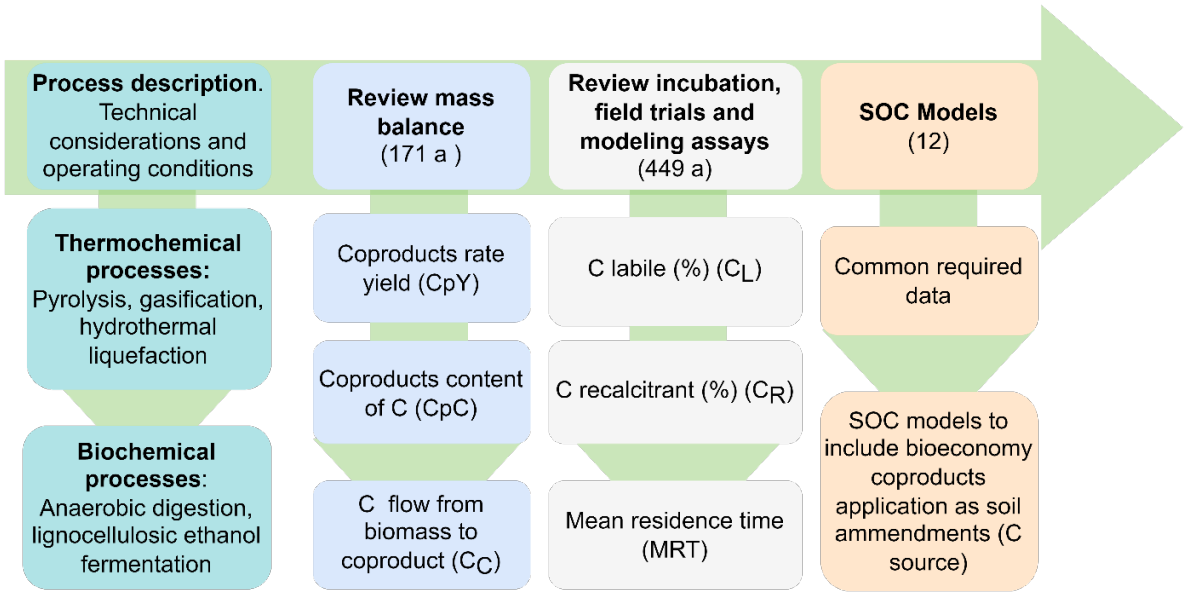

Fig 6.1. Approach followed in the review presented in Chapter 2 and main deliverables.

While Chapter 2, framed by the RO1 and RQ1 set the theoretical basis of this thesis, the main research question is primarily answered by achieving **RO2** and **RO3**, both interlinked to **RQ2 (**How much additional biomass from crop residues is available if a C-neutral harvest is practiced and recalcitrant bioeconomy coproducts are returned to soils, compared to business-as-usual approaches defining a harvest threshold?). The SOC-bioeconomy framework integrating the harvest of crop residues to supply the bioeconomy with the return of recalcitrant coproducts was developed in **Chapter 3** and applied to French croplands. **Chapter 3** thus adapted the C_C and C_R parameters within the SOC model AMG [14,15] by allocating the recalcitrant carbon in the coproducts to the inert soil pool in the case of pyrochar and gaschar (i.e., coproducts with mean residence lives longer than the

simulation timeframe) (**RO2**). The newly adapted AMG was then used to model the bioeconomy-induced SOC dynamics in French croplands at a national scale with high spatial resolution (**RO3**). The study comprised over 60,000 simulation units in a horizon of 100 years (2020-2120) and entails plausible variations in the C_C and C_R coefficients to assess the sensitivity of the model, resulting in 79 scenarios modeled for the five coproducts. Chapter 3 provides a tailored answer for the main research question for each coproduct, in the temperate context. The study revealed a 100% C-neutral harvest rate (of the technically harvestable fraction) for both the pyro- and gaschar scenarios with SOC stocks expected to increase by 106% and 43% for each scenario respectively. For the hydrochar and digestate, the harvest rates were of 98% and 53%, respectively, while for the bioethanol-molasses it is not possible to achieve a C-neutral harvest (0%). Note that the actual amount of crop residues is spatially explicit and is influenced by the pedoclimatic conditions (i.e., soil characteristics and meteorological variables) and farming management (e.g., crop rotations, application of organic fertilizer, irrigation) and this value can be retrieved from the maps provided within the study and from the detailed files deposed in the accompanying database. The identified harvest rates are higher than the one proposed by Agrimer (31.5%) [16] for France, entailing an additional supply of 71 – 225 PJ (digestate and pyrochar represented in these extremes), which answers the **RQ2**.

The framework developed in **Chapter 3** was adapted to a tropical context, for the representative case of Ecuador, to answer the second part of the main research question. AMG has been well tested and validated with good results for temperate lands [12,15] but has yet to be validated and calibrated for tropical contexts. Therefore, a second SOC model well tested in tropical regions, namely RothC, was adapted in the second part of the thesis. **Chapter 4** thus adapts the RothC model for pyrochar, gaschar, hydrochar, and digestate and then applies it to model near- and long-term SOC dynamics in Ecuadorian croplands. Based on the results of Chapter 3, the bioethanol molasses was deemed as not performant for C-neutral harvest scenarios and was thus not included in the Ecuadorian case. Ecuador is a megadiverse country, characterized by the high fertility of agricultural soils and a high economic dependency on the agroindustry. However, cropping systems have not been yet systematized and farming management information is practically non-existent. Moreover, the productivity information is reported only at Province scale (i.e., Ecuador is comprised by 24 provinces), which hampers the high spatial resolution of the land-use map of the country (250m). To achieve **RO3** for Ecuador, the previously inexistent baseline for the cropping systems of the country was developed, including the quantification of the potential crop residues production, potential above- and belowground carbon flows, and projected climate variables under the RCP4.5. This baseline (**RO3.1**) is thus one key deliverable of this thesis, involving an intense level of data manipulation and maps production and was therefore valorized as a side data paper (Appendix A3a). The Ecuadorian

cropping systems revealed a 100% C-neutral harvest rate for the pyrochar and gaschar scenarios in the long-term frame (2020-2070). This result is aligned with the ones observed for the French case, although the net level of C sequestration was observed to be markedly lower in the tropical case. The less recalcitrant products hydrochar and digestate demonstrated non-C-neutral harvest potential in the tropical context. A potential surplus 113 PJ was quantified for Ecuador by means of a C-neutral harvest, with expected SOC increases (answer to **RQ2**). Figure 6.2 integrates the tools produced within this thesis, which can serve to support decision making related to crop residues mobilization and SOC implications.

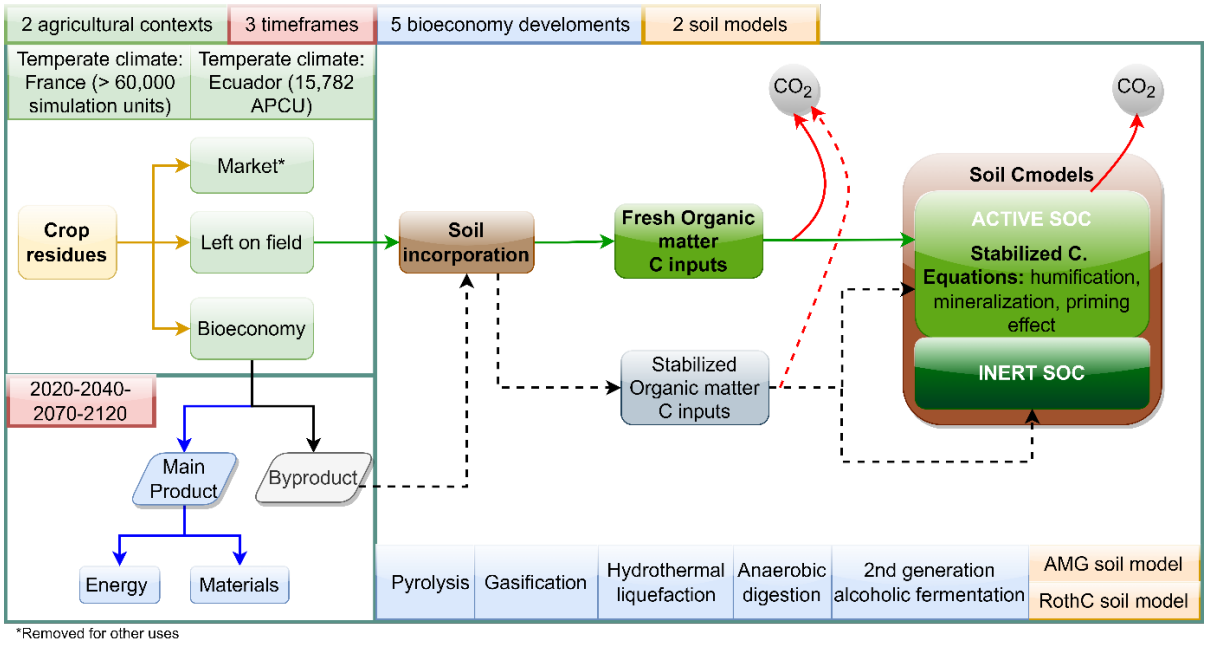

Fig 6.2. Summary and integration of chapters 3 and 4. Five bioeconomy conversion pathways were studied and adapted into two soil models (AMG and RothC), for two agricultural contexts (temperate and tropical), and three timeframes (20, 50, and 100 years), modeled with high spatial resolution. The models represent tools able to support policy and decision makers regarding crop residues management, and the results provide ready to use maps to locate areas where a bioeconomy development may be of greater or lesser interest in terms of SOC sequestration. Solid lines represent the flow of carbon from crop residues. Dotted lines represent the carbon flows from bioeconomy coproducts.

Chapters 3 and 4 are the core of this thesis and several observations can be extracted to understand the results. Despite the net results differ, there is a clear trend favoring the return of pyrochar and gaschar as a SOC enhancement strategy. The difference observed in the net values attained and moreover on the opposed results for the hydrochar and digestate scenarios are related to the intrinsic characteristics of the coproducts (C_C and C_R) and the pedoclimatic variability across the systems. Thermochemical bioeconomy processes exhaust the readily degradable carbon in crop residues into a main economic product while the degradation resistant carbon is converted in aromatic

functional groups. The higher aromaticity of a coproduct results in lesser mineralization when used as a soil amendment. Therefore, thermochemically produced coproducts, such as pyrochar, gaschar, and to some extent hydrochar are highly recalcitrant coproducts.

Under mild process conditions, the readily degradable carbon is converted into the main product, while the lignin fractions remain unchanged, exhibiting the same characteristics as in the unconverted biomass. For the case of anaerobic digestion, digestate contains the same lignin as in the untreated parental feedstock, and the difference between undigested and digested matter lies within the labile fraction, which is removed during the biogas production. The hydrolysis process performed during the bioethanol production breaks the lignin walls in crop residues, and thus molasses is rich in a form of non-so-recalcitrant carbon, that is readily available for microorganisms. While soil application of molasses could be used to improve microbial activity of soils targeting fertility goals, it is not attractive as a carbon sequestration strategy. Tropical climates are exposed to extreme meteorological conditions, such as high temperature, intense raining seasons and excessive evapotranspiration (attributed to the high temperatures). All these conditions converge to promote SOC mineralization [17] which is observed in lower SOC stocks in the studied scenarios, compared to the temperate context, where the colder climate allows for better SOC retention [18]. The differences observed between the two case studies are also related to the models' configuration. RothC requires less input information and thus the SOC dynamics are entirely influenced by the climate and clay content. On the other hand, AMG computes for more parameters, including farming practices as irrigation or tillage, and considers more soil parameters (e.g., $CaCO_3$, pH). Moreover, the inclusion of the recalcitrant products in AMG was achieved by allocating the pyrochar and gaschar in the inert pool, while in RothC they were allocated in the humified pool. However, one key point of improvement applied in RothC was the consideration of the priming effect. In fact, the sensitivity analysis showed change of directions in the results (from positive to negative and vice versa) when the priming effects were accounted. However, the priming effect of coproducts like biochar and digestate remains an open question in soil science, which makes a difficult endeavor to set a definite value to this parameter. Moreover, while the recalcitrance of biochar has been more or less validated across different soil systems, the priming effect is highly variable across regions and conversion pathways [19].

The results observed in chapters 3 and 4 indicate that crop residues can be completely harvested for pyrolysis processes with marked expected SOC improvements if the biochar is returned to soils. However, these chapters did not account for other environmental impacts that could arise by the management of crop residues as a bioeconomy feedstock, nor the energy balance of the pathways. This leads to **RQ3 (**What are the trade-offs between a C-neutral harvest and the overall environmental performance of the bioeconomy conversion technology if the impacts related to the use of the

principal product obtained in the bioeconomy pathway are fully addressed?). The LCA presented in chapter 5 shows that harvesting the crop residues for supplying the bioeconomy with maritime biofuels does not only improve SOC stocks but contributes to environmental mitigation for the five environmental impacts considered. The avoided fossil fuels, as well as the substitution associated to the various coproducts produced along the conversion processes led to net environmental benefits for almost all impact categories (i.e., the benefits associated to these substitutions are greater than the impacts associated with the conversion processes). Solely the particulate matter and freshwater eutrophication represented increased impacts for the bio-LNG. Moreover, for the case of anaerobic digestion, the selection of a cryogenic upgrading with CO2 recovery results in already negative emissions in the production stage. However, the assumptions considered in the LCIs developed in chapter 5 envision a better energy performant future (electrified) and should be contrasted with other possible alternatives.

6.2 Limitations of the study

Several limitations were encountered during this study. Here the most prominent limitations are highlighted as a voice of alert for the use and interpretation of the results.

- Although biochar recalcitrance has been a hotspot on soil science for already over a decade, the interaction with the soil microbiome and induced priming effects from soil application are still unknown. This knowledge gap is open mainly because of the difficulty and high costs [21] associated to perform long-term observations, moreover biochar has an expected mean residence life over the hundreds of years, which makes their understanding a difficult endeavor. Studies indicate that biochar can improve the soil physicochemical characteristics which can promote fertility and productivity. Moreover, microorganisms have demonstrated to be able to adapt to new sources of C, thus it is possible that the application of the coproducts may exert changes in the short-term, but these will attain the equilibrium in the long-term. However, this pose another question, if the microorganisms can adapt in the long-term, will it mean a reduction on the GHG offset potential of recalcitrant materials as biochar? These questions are still open and research is ongoing to elucidate an answer.
- One key issue to consider when dealing with soil models, is the ability of transforming the real-life observations into mathematical equations and extrapolating lab-scale results to open fields. Therefore, selecting a soil model depends on the aim for which it is going to be used and the validity to the physical area that is expected to represent.
- The C_C and C_R parameters derived within this thesis are highly influenced by the conversion pathway conditions. A high variability on operational conditions is thus translated to a high

variability on the potential carbon balance of the process and composition of the coproducts, which determines the inner recalcitrance. This limitation was considered through the sensitivity analyses performed for the two case studies.

- While this study is driven by the SOC stocks dynamics, the application of the bioeconomy coproducts may alter the normal function of soils, which could result in changes on fertility and productivity. Zhang et al, has observed in his metadata analysis, that the amount of biochar application plays a key role on the soil response. Excessive values of coproducts may result toxic or create a barrier impeding soil respiration, while too low values may not induce any positive effect and only contribute to GHG emissions. This was slightly considered by modeling one scenario where the biochar application was limited to 50tC ha-1 in 100 years, which did not affect the previous conclusions.
- Besides the questions regarding the parameters characterizing the coproducts, limitations were also encountered regarding the data inputs. For instance, the French case study reused the 4p1000 data base (ref.) which was modelled with STICS, and for which all the cereals were considered as wheat. This assumption was maintained in our study. Also, when we modeled digestate, we considered the crop residues to be subjected to a mono-digestion process. A co-digestion process including manure or slurry may result in different SOC dynamics. SOC evolution is tightly dependent to climate variables, in this study we considered the RCP4.5 projections, however, other climate trajectories may cause a variation in the results, mainly for the anaerobic digestion scenario where the SOC balance was close to the BAU.
- Ecuador representation is limited due to lack of data on crop rotations, irrigation, and farming management. Moreover, here we considered that crop residues are left on soils and contribute to input C but in fact, the most common practice in the country is open-field burning. This induces CO_2 emissions and the material remaining on soils are mainly C-depleted ashes (90% Silica). In fact, the relative results from the bioeconomy compared to BAU would be greater than shown in here if the combustion scenario would have been considered as BAU.
- Detailed foreground data to build the LCIs for the maritime biofuel scenarios is hardly available. Moreover, it has been identified that LCA studies on maritime fuels lack harmony among them, which hardens the comparison between studies. Most of the studies; however, relay on similar data, which is in cases the result of one single laboratory experiment but considered as a referent by the number of studies citing it.

6.3 Future perspectives and further research

The limitations encountered during this research and described in section 6.2, are open knowledge gaps that call for further investigation to better comprehend the bioeconomy-SOC interactions.

Currently, investigations are trying to understand the coproducts effect on the soil microbiota and finding ways to translate the laboratory observations to mathematical models [22]. Several ongoing modelling and experimental projects try to converge to a unanimous response regarding the biochar behavior in soils and their link effect to other environmental impacts. These efforts are needed to better represent the potential effects that recalcitrant matter could exert on soil health [23,24]

The commitment of nations and institutions towards the net-zero goals have resulted in series of regulations and incentives programs that incentive GHG emissions reduction and C sequestration. The interest of the industrials on addressing soil challenges is expected to increase along with alternatives to maintain C in soils. In this context, tools like the models and databases developed in this thesis result valuable to explore SOC sequestration alternatives.

Here we studied each conversion pathway as a separated scenario. A more realistic representation must assess the simultaneous implementation of various pathways to evaluate the competitions and synergies among them and derive the best management alternative.

Inclusion of parallel C sequestration practices in these scenarios were SOC is expected to decrease may result in an interesting alternative to valorize the crop residues without imposing pressures to SOC stocks. For instance, the inclusion of cover crops or temporary grasslands in crop rotations has demonstrated to be an efficient alternative for SOC improvements. Coupling the introduction of cover crops, with the application of coproducts like digestate or molasses, may help to offset the negative results.

The maritime sector is transitioning a transformation era. It has been included for the first time within the European Union GHG targets/ Moreover, the IMO is imposing more regulations to decrease the emissions from sea transport. These regulations can only be met by replacing fossil fuels with renewable fuels (e.g., biofuels, but also electricity). These transitions have resulted in a clear need of robust databases modeling maritime biofuels for LCA studies. In fact, the IMO has called for a harmonized methodology to perform well-to-wake LCAs for sea transport. This poses a great opportunity to develop studies like the one conducted in this thesis, coupling SOC modeling with LCA methodologies to shed light to the tradeoffs between environmental impacts.

References for Chapter 6

1. Foereid B, Lehmann J, Major J. Modeling black carbon degradation and movement in soil. Plant Soil. 2011 Aug 1;345(1):223–36.
2. Mondini C, Cayuela ML, Sinicco T, Fornasier F, Galvez A, Sánchez-Monedero MA. Modification of the RothC model to simulate soil C mineralization of exogenous organic matter [Internet]. Biogeochemistry: Soils; 2017 Jan [cited 2020 Jul 3]. Available from: https://www.biogeosciences-discuss.net/bg-2016-551/bg-2016-551.pdf
3. Lefebvre D, Williams A, Meersmans J, Kirk GJD, Sohi S, Goglio P, et al. Modelling the potential for soil carbon sequestration using biochar from sugarcane residues in Brazil. Sci Rep. 2020 Dec;10(1):19479.
4. Archontoulis SV, Huber I, Miguez FE, Thorburn PJ, Rogovska N, Laird DA. A model for mechanistic and system assessments of biochar effects on soils and crops and trade-offs. GCB Bioenergy. 2016 Nov;8(6):1028–45.
5. Dil M, Oelbermann M. Chapter 13. Evaluating the long-term effects of pre-conditioned biochar on soil organic carbon in two southern Ontario soils using the century model. In: Oelbermann M, editor. Sustainable agroecosystems in climate change mitigation [Internet]. The Netherlands: Wageningen Academic Publishers; 2014 [cited 2022 Mar 2]. p. 249–68. Available from: https://www.wageningenacademic.com/doi/10.3920/978-90-8686-788-2_13
6. Levavasseur F, Mary B, Christensen BT, Duparque A, Ferchaud F, Kätterer T, et al. The simple AMG model accurately simulates organic carbon storage in soils after repeated application of exogenous organic matter. Nutrient Cycling in Agroecosystems. 2020;15.
7. Pulcher R, Balugani E, Ventura M, Greggio N, Marazza D. Inclusion of biochar in a C dynamics model based on observations from an 8-year field experiment. SOIL. 2022 Mar 17;8(1):199–211.
8. Prays N, Dominik P, Sänger A, Franko U. Biogas residue parameterization for soil organic matter modeling. Sihi D, editor. PLoS ONE. 2018 Oct 12;13(10):e0204121.
9. Lychuk TE, Izaurralde RC, Hill RL, McGill WB, Williams JR. Biochar as a global change adaptation: predicting biochar impacts on crop productivity and soil quality for a tropical soil with the Environmental Policy Integrated Climate (EPIC) model. Mitig Adapt Strateg Glob Change. 2015 Dec;20(8):1437–58.
10. Hansen JH, Hamelin L, Taghizadeh-Toosi A, Olesen JE, Wenzel H. Agricultural residues bioenergy potential that sustain soil carbon depends on energy conversion pathways. 2020;12.
11. Campbell EE. Current developments in soil organic matter modeling and the expansion of model applications: a review. Environ Res Lett. 2015;37.
12. Le Noë J, Manzoni S, Abramoff R, Bölscher T, Bruni E, Cardinael R, et al. Soil organic carbon models need independent time-series validation for reliable prediction. Commun Earth Environ. 2023 May 8;4(1):1–8.
13. Farina R, Sándor R, Abdalla M, Álvaro-Fuentes J, Bechini L, Bolinder MA, et al. Ensemble modelling, uncertainty and robust predictions of organic carbon in long-term bare-fallow soils. 2020;25.
14. Andriulo A, Mary B, Guerif J. Modelling soil carbon dynamics with various cropping sequences on the rolling pampas. Agronomie. 1999;19(5):365–77.
15. Clivot H, Mouny JC, Duparque A, Dinh JL, Denoroy P, Houot S, et al. Modeling soil organic carbon evolution in long-term arable experiments with AMG model. Environmental Modelling & Software. 2019 Aug 1;118:99–113.
16. France Agrimer. L´Observatoire National des Ressources en Biomasse. Évaluation des ressources agricoles et agroalimentaires disponibles en France – édition 2020. Agrimer; 2020.
17. Wu D, Ren C, Ren D, Tian Y, Li Y, Wu C, et al. New insights into carbon mineralization in tropical paddy soil under land use conversion: Coupled roles of soil microbial community, metabolism, and dissolved organic matter chemodiversity. Geoderma. 2023 Apr 1;432:116393.

18. Amelung W, Bossio D, de Vries W, Kögel-Knabner I, Lehmann J, Amundson R, et al. Towards a global-scale soil climate mitigation strategy. Nat Commun. 2020 Oct 27;11(1):5427.
19. Chagas JKM, Figueiredo CC de, Ramos MLG. Biochar increases soil carbon pools: Evidence from a global meta-analysis. Journal of Environmental Management. 2022 Mar 1;305:114403.
20. Brandão M, Martin M, Cowie A, Hamelin L, Zamagni A. Consequential Life Cycle Assessment: What, How, and Why? In: Abraham MA, editor. Encyclopedia of Sustainable Technologies [Internet]. Oxford: Elsevier; 2017 [cited 2023 May 10]. p. 277–84. Available from: https://www.sciencedirect.com/science/article/pii/B9780124095489100685
21. Vanino S, Pirelli T, Di Bene C, Bøe F, Castanheira N, Chenu C, et al. Barriers and opportunities of soil knowledge to address soil challenges: Stakeholders' perspectives across Europe. Journal of Environmental Management. 2023 Jan 1;325:116581.
22. Woolf D, Lehmann J. Microbial models with minimal mineral protection can explain long-term soil organic carbon persistence. Sci Rep. 2019 Dec;9(1):6522.
23. Amonette JE, Blanco-Canqui H, Hassebrook C, Laird DA, Lal R, Lehmann J, et al. Integrated biochar research: A roadmap. Journal of Soil and Water Conservation. 2021;76(1):24A-29A.
24. Lehmann J, Kleber M. The contentious nature of soil organic matter. Nature. 2015 Dec;528(7580):60–8.

END

The sustainable role of agricultural residues in future bioeconomy strategies and its dependency upon carbon returns to arable soils

PhD Thesis presented by Christhel Andrade Díaz

Appendixes

This document compiles all the appendixes related to the PhD thesis manuscript entitled **"The sustainable role of agricultural residues in future bioeconomy strategies and its dependency upon carbon returns to arable soils**". Each appendix presents its own table of contents as well as the lists of tables, figures, and references.

- **Appendix A1a:** Supplementary information of chapter 2, section 1.
- **Appendix A1b:** Supplementary information of chapter 2, section 2
- **Appendix A2a:** Supplementary information of chapter 3, section 1
- **Appendix A2b:** Supplementary information of chapter 3, section 2
- **Appendix A3a:** Data paper associated to chapter 4
- **Appendix A3b:** Supplementary information of chapter 4, section 1
- **Appendix A4a:** Supplementary information of chapter LCA details

Appendix A1a

Supplementary Information of Chapter 2 – Section 1

The content of this appendix is part of the supplementary information accompanying the paper 1 of this thesis and is currently under review in Renewable and Sustainable Energy Reviews. The numbering of the sections, figures and tables are as presented in the original document.

The background data of this appendix is available in the following repository: https://doi.org/10.48531/JBRU.CALMIP/WYWKIQ

The interplay between bioeconomy and long-term soil organic carbon stock maintenance: A systematic review

Supplementary Information 1

Christhel Andrade[a,b*], Ariane Albers[a], Ezequiel Zamora-Ledezma[c], Lorie Hamelin[a]

[a] Toulouse Biotechnology Institute (TBI), INSA, INRAE UMR792, and CNRS UMR5504, Federal University of Toulouse, 135 Avenue de Rangueil, F-31077, Toulouse, France

[b] Department of Chemical, Biotechnological and Food Processes, Faculty of Mathematical, Physics and Chemistry Sciences. Universidad Técnica de Manabí (UTM), 130150, Portoviejo, Ecuador.

[c] Faculty of Agriculture Engineering. Universidad Técnica de Manabí (UTM), 13132, Lodana, Ecuador.

* Corresponding author: andraded@insa-toulouse.fr

Contents

List of Tables

1 Review Methodology

The review was conducted in two consecutive stages to collect the data records regarding the C flows and recalcitrance per technology, used in this study, which are available in Andrade et al. [1]. First, the literature was reviewed to collect information on recalcitrance of coproducts when applied in soils, limited to laboratory incubations, field trials, and modelling studies. Data was retrieved from an exhaustive systematic revision on Web of Science (WOS). The search criteria included “All databases”, all years of publication until September 2020 (1950-2020), (key) search terms “recalcitrance”, “carbon mineralization”, “carbon stability”, “soil incubation”, “stability in soil”, followed by the words “biochar”, “hydrochar”, “molasses”, “digestate” in a separate search for each coproduct. Given the scarcity on studies regarding bioethanol coproducts recalcitrance, we performed an extra search using the word “vinasse” instead of “molasses” along with the mentioned key search terms. All the papers were revised and only those presenting C mineralization data which allowed to determine the C lost only from the coproduct during the incubation were kept. The C recalcitrance search included only crop residue feedstock to the extent of data availability, and in the case of data scarcity, the most representative proxies (wood and grass) were considered. All studies per technology were considered, without differentiation by duration or type of soil used in field and laboratory assays. If results from the same experiment were in more than one publication, only the data for the studies with the longest duration were selected.

In a second stage, to determine the carbon flows per technology, data was retrieved from a non-exhaustive literature revision of reported yields and C content per coproduct and technology. Papers retrieved for the recalcitrance database, which presented the products yields and C content, or allowed to perform carbon mass balances, were as well included in this step. To expand the database, an extra data search was performed using WOS, searching in “All databases”, including all years of publication (from 1950 until July 2021), using the search terms “mass balance”, “carbon balance”, “carbon pathway” followed by the words “biochar”, “hydrochar”, “molasses”, “digestate” in a separate search for each coproduct. The search term “biomethane potential” was used specifically for digestate. Unpublished data was also obtained as courtesy from some authors. The C balance included crop residue feedstock to the extent of data availability, and in the case of data scarcity, the most representative proxies (wood and grass) were considered. If data was present in more than one publication (due to consecutive publications with extended experiments), we chose the most actual and complete study.

A conceptual review was carried out to describe each bioeconomy pathway, including process generalities and working conditions. Likely, SOC models were reviewed by checking the official website of each model, the user manual, and highlighted literature (e.g., first apparition of the model, adaptations of the model, usage across different climates).

2 Bioeconomy conversion pathways description

2.1 Pyrolysis

Pyrolysis employs high temperatures in absence of oxygen to convert biomass into bio-oil syngas and a solid residue herein called pyrochar. Bio-oil, which releases lower amounts of SOx and NOx than fossil fuels, can be combusted in turbines for power and heat generation or upgraded to be used as transportation fuel [2]. Biochar can be used for pollutants sorption, as a precursor for the production of activated carbon, as a soil amendment to improve soil quality and fertility [3–5], or buried in soils as a way to induce additional negative emissions [6–8].

The yields of the products depend on the feedstock characteristics and the process conditions, such as residence time, temperature, pressure, etc. [2,9,10]. A recent review on biochar [11] found correlations between the residence time and product yields as well as between the process temperature and the characteristics of the products in pyrolysis processes.

Fast pyrolysis is optimal for bio-oil production, with yields of around 75% bio-oil as further detailed in section **3.2** of the main text, while slow pyrolysis delivers approximately equal ratios of products and favors biochar production with typical yields of 35% biochar [9,11].

The biochar yield observed in this study is slightly higher than the yield derived from using the empirical equation proposed by Woolf et al. [12] (Eq 4) to estimate what the authors referred to as the dry ash-free biochar yield (Y_{BC}). Applied for a low temperature (T) (350-450°C) pyrolysis of wheat straw with a lignin content (L) of 12.3% [12], a pyrochar yield of 25-29% (by DM) is predicted.

$$Y_{BC} = 0.1261 + 0.5391e^{-0.004T} + 0.002733L \quad \text{(Eq 4)}$$

This difference can be explained because the value reported by Woolf et al.[12] was defined only for wheat straw, while in this study, the feedstock was considered as a mixture of various cereal straws.

Pyrolysis temperature plays a key role in the chemical and structural properties of biochar. During pyrolysis, an array of reactions such as dehydration, cleavage, and

decarboxylation take place, which are favored at higher temperatures [2,11]. Elevated temperatures promote the volatilization of other elements, mainly H and O, hence increasing the C content in the biochar and producing biochar with fewer O- functional groups. Moreover, longer exposures to heat allow the production of a higher number of aromatic compounds, resulting in more recalcitrant biochar [13,14]. Large proportions of aliphatic compounds in biochar are related to more lability and solubility in soils [15].

Biochar produced at high temperatures is considered more recalcitrant (i.e., has more aromatic groups) [11] compared to low temperatures, while long residence times yield more biochar than fast processes [16]. Due to the beneficial properties of biochar on soil [17], biochar production may be the main driver in some pyrolysis systems. In those cases, the process will aim to produce the highest amount of high-quality biochar, therefore, a compromise between pyrolysis type (fast vs slow) and temperature (high vs low) is required.

2.2 Gasification

Gasification is a complex process that encompasses a series of steps such as volatilization of the biomass, cracking and reforming of the volatiles, and gasification of the chars formed [85]; the reactions involved in these processes are the water-gas shift, Boudouard, steam reforming, and methanation reactions [19–21]. Besides syngas, other light hydrocarbons (HCs), as well as a mixture of residual materials, composed of char, ashes, and tar, are produced, as shown in (Eq 5)(Eq *5*) [22].

$$Biomass + H_2O \xrightarrow{gasification} CO + H_2 + H_2O + CO_2 + CH_4 + HCs + tars + char \quad \text{(Eq 5)}$$

Syngas can be directly used for heat and power generation, upgraded to produce transportation fuels, or used for chemical feedstock production [18]. Like pyrolysis biochar, gasification char can be valorized for different uses, including as an amendment to enhance soil health [23].

Typical conversion efficiencies of biomass DM to syngas range between 50 and 70%, with the amount of tar formed and the heating value of syngas being dependent on the oxidizing agent. The use of air as an oxidizing agent introduces considerable amounts of nitrogen to the process, which dilutes the CO and H_2 concentrations, and yields syngas with heating values of 4-10 MJ Nm^{-3}. Pure oxygen can produce syngas with heating values up to 28 MJ Nm^{-3} and the highest CO concentration, nevertheless its use is limited due to elevated costs. Steam is an attractive agent as it yields high H_2 concentrations and heating values in the range of 10-18 MJ Nm^{-3}. [19,20]

The main challenges of gasification are tar formation and moisture control of the biomass. Various authors have comprehensively reviewed the implications of the feedstock and operating conditions for biomass gasification, as well as the chemical reactions involved, the reactor design, pretreatments, tar removal processes, and novel gasification technologies using catalysts or supercritical fluids [18–21,24–27]. Still, there is scarce information regarding the char C recalcitrance and its behavior when used as a soil amendment, as further detailed in section **3.2.2** of the main text.

2.3 Hydrothermal Liquefaction

Compared to other thermochemical processes, HTL is considered a more energy-effective technology as it allows the use of a wide variety of feedstocks, from lignocellulosic to algal biomass [28], without previous drying steps, and as it produces a biocrude with lower oxygen and water content, yields less tar, and requires lower amounts of chemical additives and heat consumption [29–32].

During HTL, biomass undergoes, as in the case of gasification, multiple reactions, including hydrolysis, dehydration, polymerization, Maillard reaction, decarboxylation, and repolymerization reactions [29,32], to convert the carbohydrates in the feedstock into biocrude, biochar, and gases**Fig.**.

Catalysts can influence the HTL processes to improve the bio-oil yield and properties, decrease the hydrochar yield [28], reduce operation times, hinder secondary reactions, such as repolymerization and cracking of long-chain hydrocarbons, and reduce the pressure and temperature dependency of the process [33]. This effect is influenced by the type of catalyst, process conditions, and biomass used [30]. Basic catalysts are preferred in HTL operations over acid catalysts, to avoid system corrosion. For instance, K_2CO_3 accelerates the water-gas shift reaction in HTL processes conducted at low temperatures. Zhu et al. [34] found that C conversion from the feedstock to hydrochar decreased from 41% to 9% when K_2CO_3 was applied.

It should be noted that there is a similar process called hydrothermal carbonization (HTC), where instead of bio-oil, the intended product is hydrochar. This yields approximately 50-70% hydrochar (of the initial DM; [35,36]), while the hydrochar yield is approximately 25% with HTL, as further detailed in section 3.2. Similarly, an alternative process referred to as hydrothermal gasification (HTG) has been developed to focus on the gas as the main product. The HTC processes are normally carried out at lower temperatures than HTL, commonly from 180 to 250 °C at 2–10 MPa [37] and for longer time (hours) than HTL. HTG, on the other hand, operates at temperatures above 400°C [38], in the range of 650-700 °C or 400 – 550°C if catalysts

are used [39], which favors the formation of syngas (80 – 95 % C converts to gas), with minor hydrochar production in comparison to HTL [40].

2.4 Anaerobic Digestion

The co-digestion of a mixture of two or more substrates, typically organic wastes and animal manure, is commonly used to ensure consequent biogas production. According to the type of substrates being used, the process may be carried out in wet (typically <20% DM) or dry (typically well above 20% DM) systems [41], though the former is the most commonly implemented [42].

Most anaerobic digestion systems (wet and dry) operate at temperatures around 30-40°C or 50-60°C [43]. Although some organisms can produce biogas at higher or lower temperatures, lower methane rates have been observed at psychrophilic temperatures (~10°C), and accumulation of fatty acids is associated with temperatures above 60°C [44]. The optimal retention times are reported to be between 10 and 25 days [46].

During AD, the more readily degradable components are converted to biogas while the non- or less-readily degradable materials remain in the digestate [47,48]. Digestate is mainly composed of lignin, cellulose, and hemicellulose [49]. During AD, cellulose and hemicellulose degrade at about 50% and 80%, respectively, while the lignin remains unconverted. Digestate commonly contains 9-13% DM, of which between 28 and 47% correspond to the total carbon content [45,48], as further detailed in section **3.2**. Besides carbon, digestate is rich in nitrogen, potassium, phosphorus, and other minerals, which makes it attractive as a fertilizer or soil conditioner [52].

2.5 Second-generation lignocellulosic bioethanol

The energy content of cellulosic bioethanol ranges between 16.7-21.2 MJ L^{-1} depending on the feedstock, which represents around 66% of the energy content in gasoline [53]. In contrast with gasoline, bioethanol contains 35% oxygen, denoting a 15% higher combustion efficiency [54]. Wheat, rice, corn, and sugarcane residues are the most common feedstocks for lignocellulosic bioethanol, also called second-generation biofuel (2GEtOH).

Bioethanol production involves a series of steps to hydrolyze the complex polymers in the biomass, into soluble sugars, which are fermented with the aid of microorganisms. The hydrolysis process can be performed using chemicals, enzymes, or a mixture of both, and can take place in separate rectors for the hydrolysis and fermentation processes (SHF) or in one single reactor where all the steps are carried on (SSF) [55,56].

The acid hydrolysis can be carried out using dilute (4%) or concentrated (70 – 77%) acids (e.g., H_2SO_4, HCl, H_3PO_4, HNO_3) for short times at high temperatures (180°C), or long times (minutes – hours) at low temperatures (120°C), while the alkaline hydrolysis (e.g., NaOH, KOH, NH_4OH) can be performed at room temperature lasting from seconds to days [54]. The enzymatic hydrolysis usually occurs under mild conditions: low pressure, long retention times in the range of 48-72h, pH around 5, and temperatures below 50°C [54–56]. The fermentation process can be carried out by different microorganisms, including yeast, bacteria, and fungi, of which the yeast *Saccharomyces cerevisiae* is the most frequently used.

While the SHF system allows optimal temperatures for each process (50°C for hydrolysis, and 28-32°C for fermentation), the SSF configuration involves one reactor operated at temperatures around 38°C where the hydrolyzed sugars are fermented immediately. Higher bioethanol yields and lower process duration and costs have been observed for SSF processes, compared to SHF, and are the most common systems at pilot scale [55].

After removing the cellulose and hemicellulose from the biomass for bioethanol production, the more complex sugars, such as lignin, remain in the coproducts at a 3-fold higher concentration than the original substrate [57]. Before distillation, the non-fermentable components are removed as a stream called stillage, rich in waxes, yeast cells, soluble nutrients, and lignin content [58,59]. Stillage can be utilized as animal fodder, fertilizer, or to produce energy (i.e., electricity and biogas) [60]. Stillage typically undergoes filtration, from which liquid and solid fractions are generated, each suitable for different uses. The resulting liquid fraction is known as molasses, of which approximately 15% is recycled as process water [61] and the remaining fraction can be used as feedstock for biogas production in anaerobic digestion facilities [62] or condensed by evaporation. The solid fraction, composed of small unfermentable biomass particles, is hereon referred to as cake. Contrarily to first-generation processes, the 2GEtOH cake has a poor quality to be used as animal feed and is thus typically burned to produce energy [62].

Bioethanol coproducts have a higher C concentration than the original crop residues [57], with the largest fraction of C ending in the solid residue. Moreover, the lignin and N concentration of bioethanol coproducts can triple that of the raw feedstock, which makes them attractive as soil amendments [57].

3 Carbon conversion

Table S1. Summary of Carbon conversion data (C_C)

Conversion Pathway	Coproduct	Total papers reviewed	Total data collected	Coproduct of interest yield (%)	Other products yield[a] (%)	SD	C content in the coproduct (%)	SD	C_C (%)	SD	n[b]	Ref.[c] (n)	Ref.
Gasification	Gaschar	5	25	20	80	7	51	22	20	7	25	5	[22,63,64]; Borooah et al., 2021 (unpublished). Courtesy of R. Borooah, during EUBCE 2021. Sungkavatin et al., 2021 (unpublished). Courtesy of P. Sungkavatin, INSA Toulouse, France. Unpublished data from on-going work, supplied in 2021
Pyrolysis	Pyrochar	21	44	35	65	7	58	13	48	10	44	21	[65–84] ; Brassard et al. 2021 on wheat straw (unpublished). Courtesy of P. Brassard, IRDA, Canada. Unpublished data from on-going work, supplied in 2021
HTL	Hydrochar	10	31	24	76	16	55	8	31	22	31	10	[29,34,85–93]
AD	Digestate	34	68	69	31	14	25	10	36	14	16	9	[94–127]
2GEtOH[d]	Liquid fraction	3	3	21	47	11	34	5	21	15	3	3	[124,128,129]
	Solid fraction			33	47	18	59	26	44	21			

HTL: Hydrothermal Liquefaction; AD: Anaerobic Digestion; 2GEtOH: Second Generation Bioethanol; SD: Standard deviation. [a] Includes the main product and other produced coproducts; [b] number of data records; [c] Number of references after outliers' removal; [d] The other products consist of bioethanol and CO_2 only

4 Carbon recalcitrance

Table S2. Summary of data collected on C recalcitrance

Conversion Pathway	Coproduct	Subclasification	Total papers reviewed	Total data collected	Average Results							Data records		Ref.
					% C recalcitrant	% C labile	SD	Incubation days	SD	MRT years	SD	n [a]	Ref. [b] (n)	
Gasification	Gaschar	All	10	36	95	5	5	523	893	141	219	33	10	[23,130–135,135–138]
		500-600°C			100	0	0	140	0	n/a	n/a	9	1	
		700-800°C			95	5	3	349	429	n/a	n/a	6	3	
		>1200°C			95	5	4	876	1269	n/a	n/a	15	6	
Pyrolysis	Pyrochar	All temperatures and feedstocks	34	144	96	4	5	264	367	3014	23352	131	32	[18,67–74,77,79,80,82,84,139–158]
		<300°C			97	3	3	705	474	106	84	10	4	
		300-500°C			95	5	6	249	403	632	2068	74	26	
		>500°C			97	3	4	193	183	6616	36773	49	17	
HTL	Hydrochar	All feedstock	16	104	89	11	11	199	167	10	7	97	15	[135,139,150,159–171]
		Crop residues			83	17	18	201	148	11	6	29	8	
		Grass			77	23	13	352	190	4	4	12	5	
		Sugar			85	15	15	100	94	10	8	21	3	
		Wood			96	4	2	186	170	10	4	7	4	
AD	Digestate	All feedstocks	17	114	70	30	15	147	118	1.23	1.99	104	16	[49,140,144,172–185]
		Cattle manure			66	34	11	230	120	0.67	0.37	21	5	
		Cattle slurry			72	28	11	105	72	0.03	0.02	20	4	
		Crops/Biowaste			68	32	14	122	121	0.40	0.00	31	6	
		Pig slurry			53	47	33	168	130	1.89	2.35	21	7	
		Poultry manure			85	15	0	87	8	1.38	0.71	13	2	
2GEtOH	Cake and molasses	All coproducts	10	51	47	53	31	164	127	1.3	1.2	51	10	[57,140,144,186–192]
		Rapeseed meal			68	32	30	147	169	2.8	1.3	8	3	
		Solid Residue			42	58	33	161	128	1	1	28	6	
		Vinasse			46	54	22	192	81	1	0	15	4	

HTL: Hydrothermal Liquefaction; AD: Anaerobic Digestion; 2GEtOH: Second Generation Bioethanol; SD: Standard deviation. [a] number of data records; [b] Number of references after outliers' removal.

5 Soil carbon models previously adapted for bioeconomy coproducts

5.1 Century

CENTURY [193] is a biogeochemical plant-soil nutrient cycling model designed to simulate the carbon and nutrient dynamics for different types of ecosystems. It integrates the effects of soil characteristics, climatic conditions, and agricultural management, including crop rotation systems and tillage practices, to analyze the effects of management and global change on productivity and sustainability of agroecosystems. Century is able to simulate the long-term plant growth and soil carbon C, nitrogen N, phosphorus P, sulfur S, and water dynamics to centuries and millennia for grassland, agricultural crop, forest, and savanna systems. The model runs in a monthly timestep and is based on three soil organic matter pools, considered as active, slow, and passive, with different decomposition rates, above and belowground pools and a surface microbial pool. CENTURY has been run and tested across a variety of pedoclimatic conditions across the world [194–199]. CENTURY has been further modified into the daily timestep version Daycent [200,201], which has been used in different studies around the world more frequently than Century in the last times [202,203]. Daycent maintains the same structure, inputs, and simulation outputs as CENTURY but in a daily basis and includes other processes such as GHG emissions assessment.

5.2 CANDY

CANDY (Carbon and Nitrogen Dynamics) [204] is an integrated agroecosystem model to simulate soil C and N dynamics, temperature, and water balance in a daily timestep. The model runs on a user interface built over a complex structure composed of four modules dedicated to i) temperature, ii) hydrological processes considering water drainage, interception of water by crops, runoff, potential and actual evapotranspiration, iii) crop dynamics, and iv) organic matter turnover [205]. While some modules are mandatory, others can be turned off according to the user requirements and thus the modeling objective must be clearly defined at the beginning to prepare the corresponding input data. The organic matter turnover and steady state is calculated based on an option defined as biological active time (BAT), which corresponds to the time required under optimal conditions (laboratory) to produce the same C-turnover as in real conditions (field) [206]. The C and N dynamics are calculated simultaneously based on the properties of the organic inputs (eg., manure, slurry, straw, compost) and the above and below ground plant material (i.e., residues, roots) not harvested. A simplified version of CANDY, the CANDY Carbon Balance (CCB), was derived to calculate the SOM dynamics on an annual time-step at field scale [206]. CANDY and CCB have been validated across different European locations [206–209].

5.3 RothC

Unlike agroecosystem models, which include a global balance of different subsystems, macromolecules, and nutrients, the Rothamsted Carbon model (RothC) 26.3 [210] is a soil process model focused on carbon dynamics. RothC is the most commonly used model to simulate SOC dynamics due to its simplicity and ability to be modified to include different considerations specific to the studied system. It simulates the SOC dynamics in a monthly timestep, in cropland, forests and grasslands, and has been tested under different soils and climates around the globe [211–213]. The standard structure of RothC- 26.3 splits the carbon inputs into five different compartments with a specific decay rate (k) for each compartment following first-order kinetics. Four compartments are considered as active pools, these are the decomposable plant material (DPM, k_{DPM}= 10 y^{-1}), resistant plant material (RPM, k_{RPM}= 0.30 y^{-1}), microbial biomass (BIO, 0.66 y^{-1}) and the Humified organic matter (HUM, k_{HUM}= 0.02 y^{-1}). The fifth pool, the inert organic matter (IOM), is a small compartment resistant to decomposition. The model is based on relatively few soil parameters and requires limited and easily accessible input data, it has been parametrized for C inputs from plant sources and farmyard manure. The uncertainty in SOC stocks predicted by RothC has been estimated to be ±6.8–8.5 % when site specific data on climate, soil, and net primary productivity (NPP) are available (Falloon and Smith 2003).

5.4 C-TOOL

C-TOOL [214] is a soil C model to simulate the medium- to long-term SOC dynamics of agricultural soils on a monthly basis. The latest version C-TOOL v2.3 is described in details in [215]. The model is represented by three C pools in topsoil (0 – 0.25 m) and subsoil (0.25 – 1 m), namely, Fresh Organic Matter (FOM; carbon half-life <1 y), Humified Organic Matter (HUM; carbon half-life 50 years), and carbon in Resistant Organic Matter (ROM; carbon half-life of 600-800 years). Carbon is modelled to move across the pools and soil layers. The C in one pool is mineralized and emitted as CO2 following a first-order kinetics reaction, dependent on temperature and clay content, while the more resistant organic matter is transferred to the other pools. C-TOOL has been validated and used to predict SOC dynamics in different cropping systems over Europe (Denmark, UK, Sweden) [209,216,217]. The inputs required are limited to only average monthly air temperature, soil clay content, initial soil C:N ratio, C input to topsoil. Besides crop inputs, C-TOOL admits the input of manure as a C source. The model is not properly parametrized on soils with more than 6% organic carbon and should be applied with caution for soils exposed to prolonged dry seasons or water-logged soils [218].

5.5 AMG

AMG [219] is a SOC model that simulates soil carbon dynamics in agricultural soils following an annual timestep. The latest version of the model AMGv2 is detailed in [220]. The model has been validated and used to predict SOC dynamics for different cropping systems across different pedoclimatic conditions [209,220,221](Clivot 2019, Farina et al., 2020, Saffih-Hdadi and Mary 2008), in diverse locations, including France, Great Britain, Argentina [209,222–224] . AMGv2 splits the carbon from organic matter (OM) into three different compartments. The OM from crop residues, roots and EOM is allocated into the fresh organic matter (FOM) pool, where it could be decomposed or humified and is divided into an active pool (CA) and a stable (Cs) pool. The proportion of C that is incorporated into the CA pool is fixed by the humification coefficient (h) and is affected by the mineralization process following a first order kinetic with a k mineralization constant. The remaining fraction of C (1-h) is mineralized as CO_2. The stable Cs pool is considered completely recalcitrant to mineralization. The mean residence time (MRT) of the active CA pool ranges from 7 to 26 years, while the stable Cs pool, which is set as 65% of total SOC by default, is considered inert during all the simulated period [220].

The relative root mean square error of AMGv2 was calculated in Clivot et al. [220] to be 5.3%, which is comparable with the values for Century (6.8% [225]– 13.1% [226]), RothC (9.9% [225]), C-TOOL (6.1% [218]), and CCB (8.5%[206]).

5.6 EPIC

The Environmental Policy Integrated Climate (EPIC) [227] is an agroecosystem model developed to assess the effect of land management on soil quality. EPIC was originally developed to evaluate the effects of land management on soil erosion alone [227] and was later expanded to include other components of agriculture, such as soil and water quality, carbon cycling, nutrients cycling, plant growth and competition, pesticide fate, weather, greenhouse gas emissions, and economics [228,229]. The model operates on a daily timestep and is able to perform long-term simulations in the millennial timeframe (1-4000 years) [229]. The simulation area, is a unit area of homogeneous land-use, management, soil aspects, geomorphology, and weather, typically up to 100 ha [230]. An extension model, the Agricultural Policy Environmental eXtender (APEX), was incorporated to EPIC to facilitate the simultaneous simulation of multiple field-scenarios, encompassing various land managements.

EPIC is a complex model that requires a large number of input data regarding the management activities (e.g., crop rotations, fertilization, harvesting, irrigation, burning, among others) and plant information (e.g., leaf area index, harvest index, photosynthetically active radiation, root depth, etc.) [228]. However, it remains among the most used models and is continuously improved and validated across various pedoclimatic systems [230,231]. For instance, the EPIC-APEX algorithms have been

configured to be able to generate weather information at the run time, five different evapotranspiration equations can be selected, and specific parameters for over 80 crops (100 if grass and trees are included) are now embedded within the model [229,232]. Moreover, EPIC has been calibrated and validated in various agricultural systems [230], including the United States [233], Argentina [234], China [231], and several European locations [209,235].

5.7 APSIM

The Agricultural Production Systems Simulator (APSIM) [236] is an agroecosystem model that simulates the interactions between soil and plant growth in cropping systems [237,238]. APSIM is built within a suite of biophysical modules that integrate various plant (i.e., crops, pastures, and trees), animal, soil, climate (i.e., solar radiation, maximum and minimum temperatures, rainfall), and management interactions [239]. The model operates on a daily timestep to simulate crop rotations soil C, N, P, and water dynamics, as well as soil pH and erosion [237]. The organic matter module includes tillage, leaching, and decomposition parameters of various crops to allocate the plant organic matter across three soil pools, namely, fresh organic matter (FOM), biological organic matter (BIOM), and humified organic matter (HUM) [240].

APSIM has been extensively used and validated in various agricultural contexts, especially in Africa [241–243] and Australia [244–247], and more recently in Asia [237,248]. The model is continuously improved with new submodules added to develop new modeling capacities [249–251] in an international initiative.

References SI 1.1

[1] Andrade C, Albers A, Zamora-Ledezma E, Hamelin L. Database to determine the Carbon recalcitrance and carbon conversion rate to bioeconomy coproducts 2022. https://doi.org/10.48531/JBRU.CALMIP/WYWKIQ.

[2] Kumar R, Strezov V, Weldekidan H, He J, Singh S, Kan T, et al. Lignocellulose biomass pyrolysis for bio-oil production: A review of biomass pre-treatment methods for production of drop-in fuels. Renewable and Sustainable Energy Reviews 2020;123:109763. https://doi.org/10.1016/j.rser.2020.109763.

[3] Laird DA, Novak JM, Collins HP, Ippolito JA, Karlen DL, Lentz RD, et al. Multi-year and multi-location soil quality and crop biomass yield responses to hardwood fast pyrolysis biochar. Geoderma 2017;289:46–53. https://doi.org/10.1016/j.geoderma.2016.11.025.

[4] Greco G, Di Stasi C, Rego F, González B, Manyà JJ. Effects of slow-pyrolysis conditions on the products yields and properties and on exergy efficiency: A comprehensive assessment for wheat straw. Applied Energy 2020;279:115842. https://doi.org/10.1016/j.apenergy.2020.115842.

[5] Dai Y, Zhang N, Xing C, Cui Q, Sun Q. The adsorption, regeneration and engineering applications of biochar for removal organic pollutants: A review. Chemosphere 2019;223:12–27. https://doi.org/10.1016/j.chemosphere.2019.01.161.

[6] Smith P. Soil carbon sequestration and biochar as negative emission technologies. Glob Change Biol 2016;22:1315–24. https://doi.org/10.1111/gcb.13178.

[7] Schmidt H-P, Anca-Couce A, Hagemann N, Werner C, Gerten D, Lucht W, et al. Pyrogenic carbon capture and storage. GCB Bioenergy 2019;11:573–91. https://doi.org/10.1111/gcbb.12553.

[8] Werner C, Schmidt H-P, Gerten D, Lucht W, Kammann C. Biogeochemical potential of biomass pyrolysis systems for limiting global warming to 1.5 °C. Environ Res Lett 2018;13:044036. https://doi.org/10.1088/1748-9326/aabb0e.

[9] Tomczyk A. Biochar physicochemical properties: pyrolysis temperature and feedstock kind effects. Rev Environ Sci Biotechnol 2020:25.

[10] Gabhane JW, Bhange VP, Patil PD, Bankar ST, Kumar S. Recent trends in biochar production methods and its application as a soil health conditioner: a review. SN Appl Sci 2020;2:1307. https://doi.org/10.1007/s42452-020-3121-5.

[11] Ippolito JA, Cui L, Kammann C, Wrage-Mönnig N, Estavillo JM, Fuertes-Mendizabal T, et al. Feedstock choice, pyrolysis temperature and type influence biochar characteristics: a comprehensive meta-data analysis review. Biochar 2020;2:421–38. https://doi.org/10.1007/s42773-020-00067-x.

[12] Woolf D, Lehmann J, Ogle S, Kishimoto-Mo AW, McConkey B, Baldock J. Greenhouse Gas Inventory Model for Biochar Additions to Soil. Environ Sci Technol 2021:acs.est.1c02425. https://doi.org/10.1021/acs.est.1c02425.

[13] He Y, Zhou X, Jiang L, Li M, Du Z, Zhou G, et al. Effects of biochar application on soil greenhouse gas fluxes: a meta-analysis. GCB Bioenergy 2017;9:743–55. https://doi.org/10.1111/gcbb.12376.

[14] Wang J, Xiong Z, Kuzyakov Y. Biochar stability in soil: meta-analysis of decomposition and priming effects. GCB Bioenergy 2016;8:512–23. https://doi.org/10.1111/gcbb.12266.

[15] Han L, Sun K, Yang Y, Xia X, Li F, Yang Z, et al. Biochar's stability and effect on the content, composition and turnover of soil organic carbon. Geoderma 2020;364:114184. https://doi.org/10.1016/j.geoderma.2020.114184.

[16] Qambrani NA, Rahman MdM, Won S, Shim S, Ra C. Biochar properties and eco-friendly applications for climate change mitigation, waste management, and wastewater treatment: A review. Renewable and Sustainable Energy Reviews 2017;79:255–73. https://doi.org/10.1016/j.rser.2017.05.057.

[17] Joseph S, Cowie AL, Van Zwieten L, Bolan N, Budai A, Buss W, et al. How biochar works, and when it doesn't: A review of mechanisms controlling soil and plant responses to biochar. GCB Bioenergy 2021:gcbb.12885. https://doi.org/10.1111/gcbb.12885.

[18] Ahmad M, Ok YS, Kim B-Y, Ahn J-H, Lee YH, Zhang M, et al. Impact of soybean stover- and pine needle-derived biochars on Pb and As mobility, microbial community, and carbon stability in a contaminated agricultural soil. Journal of Environmental Management 2016;166:131–9. https://doi.org/10.1016/j.jenvman.2015.10.006.

[19] Molino A, Larocca V, Chianese S, Musmarra D. Biofuels Production by Biomass Gasification: A Review. Energies 2018;11:811. https://doi.org/10.3390/en11040811.

[20] Watson J, Zhang Y, Si B, Chen W-T, de Souza R. Gasification of biowaste: A critical review and outlooks. Renewable and Sustainable Energy Reviews 2018;83:1–17. https://doi.org/10.1016/j.rser.2017.10.003.

[21] Widjaya ER, Chen G, Bowtell L, Hills C. Gasification of non-woody biomass: A literature review. Renewable and Sustainable Energy Reviews 2018;89:184–93. https://doi.org/10.1016/j.rser.2018.03.023.

[22] Carpenter DL, Bain RL, Davis RE, Dutta A, Feik CJ, Gaston KR, et al. Pilot-Scale Gasification of Corn Stover, Switchgrass, Wheat Straw, and Wood: 1. Parametric Study and Comparison with Literature. Ind Eng Chem Res 2010;49:1859–71. https://doi.org/10.1021/ie900595m.

[23] Hansen V, Müller-Stöver D, Imparato V, Krogh PH, Jensen LS, Dolmer A, et al. The effects of straw or straw-derived gasification biochar applications on soil quality and crop productivity: A farm case study. Journal of Environmental Management 2017;186:88–95. https://doi.org/10.1016/j.jenvman.2016.10.041.

[24] Farzad S, Mandegari MA, Görgens JF. A critical review on biomass gasification, co-gasification, and their environmental assessments. Biofuel Res J 2016;3:483–95. https://doi.org/10.18331/BRJ2016.3.4.3.

[25] Hanchate N, Ramani S, Mathpati CS, Dalvi VH. Biomass gasification using dual fluidized bed gasification systems: A review. Journal of Cleaner Production 2021;280:123148. https://doi.org/10.1016/j.jclepro.2020.123148.

[26] Heidenreich S, Foscolo PU. New concepts in biomass gasification. Progress in Energy and Combustion Science 2015;46:72–95. https://doi.org/10.1016/j.pecs.2014.06.002.

[27] Molino A, Chianese S, Musmarra D. Biomass gasification technology: The state of the art overview. Journal of Energy Chemistry 2016;25:10–25. https://doi.org/10.1016/j.jechem.2015.11.005.

[28] Grande L, Pedroarena I, Korili SA, Gil A. Hydrothermal Liquefaction of Biomass as One of the Most Promising Alternatives for the Synthesis of Advanced Liquid Biofuels: A Review. Materials 2021;14:5286. https://doi.org/10.3390/ma14185286.

[29] Seehar TH, Toor SS, Sharma K, Nielsen AH, Pedersen TH, Rosendahl LA. Influence of process conditions on hydrothermal liquefaction of eucalyptus biomass for biocrude production and investigation of the inorganics distribution. Sustainable Energy Fuels 2021;5:1477–87. https://doi.org/10.1039/D0SE01634A.

[30] Toor SS, Rosendahl L, Rudolf A. Hydrothermal liquefaction of biomass: A review of subcritical water technologies. Energy 2011;36:2328–42. https://doi.org/10.1016/j.energy.2011.03.013.

[31] Cao L, Zhang C, Chen H, Tsang DCW, Luo G, Zhang S, et al. Hydrothermal liquefaction of agricultural and forestry wastes: state-of-the-art review and future prospects. Bioresource Technology 2017;245:1184–93. https://doi.org/10.1016/j.biortech.2017.08.196.

[32] Castello D, Pedersen T, Rosendahl L. Continuous Hydrothermal Liquefaction of Biomass: A Critical Review. Energies 2018;11:3165. https://doi.org/10.3390/en11113165.

[33] Mathanker A, Das S, Pudasainee D, Khan M, Kumar A, Gupta R. A Review of Hydrothermal Liquefaction of Biomass for Biofuels Production with a Special Focus on the Effect of Process Parameters, Co-Solvents, and Extraction Solvents. Energies 2021;14:4916. https://doi.org/10.3390/en14164916.

[34] Zhu Z, Toor SS, Rosendahl L, Yu D, Chen G. Influence of alkali catalyst on product yield and properties via hydrothermal liquefaction of barley straw. Energy 2015;80:284–92. https://doi.org/10.1016/j.energy.2014.11.071.

[35] Wei J, Guo Q, Song X, Ding L, Mosqueda A, Liu Y, et al. Effect of hydrothermal carbonization temperature on reactivity and synergy of co-gasification of biomass hydrochar and coal. Applied Thermal Engineering 2021;183:116232. https://doi.org/10.1016/j.applthermaleng.2020.116232.

[36] Nakason K, Panyapinyopol B, Kanokkantapong V, Viriya-empikul N, Kraithong W, Pavasant P. Characteristics of hydrochar and hydrothermal liquid products from hydrothermal carbonization of corncob. Biomass Conv Bioref 2018;8:199–210. https://doi.org/10.1007/s13399-017-0279-1.

[37] Yang C, Wang S, Yang J, Xu D, Li Y, Li J, et al. Hydrothermal liquefaction and gasification of biomass and model compounds: a review. Green Chem 2020;22:8210–32. https://doi.org/10.1039/D0GC02802A.

[38] Watson J, Wang T, Si B, Chen W-T, Aierzhati A, Zhang Y. Valorization of hydrothermal liquefaction aqueous phase: pathways towards commercial viability. Progress in Energy and Combustion Science 2020;77:100819. https://doi.org/10.1016/j.pecs.2019.100819.

[39] GRTgaz, Enea Consulting. Potentiel de la Gazéification Hydrothermale en France. Une technologie innovante pour le traitement des déchets et des résidus de biomasses liquides et leur conversion en gaz renouvelable. France: 2019.

[40] Ghavami N, Özdenkçi K, Salierno G, Björklund-Sänkiaho M, De Blasio C. Analysis of operational issues in hydrothermal liquefaction and supercritical water gasification processes: a review. Biomass Conv Bioref 2021. https://doi.org/10.1007/s13399-021-02176-4.

[41] Akinbomi JG, Patinvoh RJ, Taherzadeh MJ. Current challenges of high-solid anaerobic digestion and possible measures for its effective applications: a review. Biotechnology for Biofuels and Bioproducts 2022;15:52. https://doi.org/10.1186/s13068-022-02151-9.

[42] Fortune Business Insights. Europe Biogas Plant Market Size, Analysis & Forecast [2028]. Fortune Business Insights 2022. https://www.fortunebusinessinsights.com/europe-biogas-plant-market-106351 (accessed October 3, 2022).

[43] Schnürer A, Jarvis Å. Microbiology of the biogas process 2016:168.

[44] Scherer PA, Vollmer G-R, Fakhouri T, Martensen S. Development of a methanogenic process to degrade exhaustively the organic fraction of municipal “grey waste” under thermophilic and hyperthermophilic conditions. Water Science and Technology 2000;41:83–91. https://doi.org/10.2166/wst.2000.0059.

[45] Atelge MR, Atabani AE, Banu JR, Krisa D, Kaya M, Eskicioglu C, et al. A critical review of pretreatment technologies to enhance anaerobic digestion and energy recovery. Fuel 2020;270:117494. https://doi.org/10.1016/j.fuel.2020.117494.

[46] Sarker S, Lamb JJ, Hjelme DR, Lien KM. A Review of the Role of Critical Parameters in the Design and Operation of Biogas Production Plants. Applied Sciences 2019;9:1915. https://doi.org/10.3390/app9091915.

[47] Schievano A, Adani F, Tambone F, D’Imporzano G, Scaglia B, Genevini PL. What is the digestate? 2009.

[48] Askri A, Laville P, Trémier A, Houot S. Influence of Origin and Post-treatment on Greenhouse Gas Emissions After Anaerobic Digestate Application to Soil. Waste Biomass Valor 2016;7:293–306. https://doi.org/10.1007/s12649-015-9452-6.

[49] Marcato C-E, Mohtar R, Revel J-C, Pouech P, Hafidi M, Guiresse M. Impact of anaerobic digestion on organic matter quality in pig slurry. International Biodeterioration & Biodegradation 2009;63:260–6. https://doi.org/10.1016/j.ibiod.2008.10.001.

[50] Möller K. Effects of anaerobic digestion on soil carbon and nitrogen turnover, N emissions, and soil biological activity. A review. Agron Sustain Dev 2015;35:1021–41. https://doi.org/10.1007/s13593-015-0284-3.

[51] Teglia C, Tremier A, Martel J-L. Characterization of Solid Digestates: Part 1, Review of Existing Indicators to Assess Solid Digestates Agricultural Use. Waste Biomass Valor 2011;2:43–58. https://doi.org/10.1007/s12649-010-9051-5.

[52] Rigby H, Smith RS. New markets for digestate from anaerobic digestion. WRAP 2011.

[53] Wyman CE. Ethanol fuel 2004.

[54] Zabed H, Sahu JN, Suely A, Boyce AN, Faruq G. Bioethanol production from renewable sources: Current perspectives and technological progress. Renewable and Sustainable Energy Reviews 2017;71:475–501. https://doi.org/10.1016/j.rser.2016.12.076.

[55] Bušić A, Marđetko N, University of Zagreb, Faculty of Food Technology and Biotechnology, Pierottijeva 6, 10000 Zagreb, Croatia, Kundas S, Belarussian National Technical University, Power Plant Construction and Engineering Services Faculty, Nezavisimosti Ave. 150, 220013 Minsk, Belarus, Morzak G, et al. Bioethanol Production from Renewable Raw Materials and its Separation and Purification: a Review. Food Technol Biotechnol 2018;56. https://doi.org/10.17113/ftb.56.03.18.5546.

[56] Swain MR, Singh A, Sharma AK, Tuli DK. Chapter 11 - Bioethanol Production From Rice- and Wheat Straw: An Overview. Bioethanol Production from Food Crops. Sustainable Sources, Interventions, and Challenges, Academic Press; 2019, p. 19.

[57] Johnson JMF, Reicosky D, Sharratt B, Lindstrom M, Voorhees W, Carpenter-Boggs L. Characterization of Soil Amended with the By-Product of Corn Stover Fermentation. SOIL SCI SOC AM J 2004;68:9.

[58] Alotaibi KD, Schoenau JJ. Enzymatic activity and microbial biomass in soil amended with biofuel production byproducts. Applied Soil Ecology 2011;48:227–35. https://doi.org/10.1016/j.apsoil.2011.03.002.

[59] Rosentrater KA, Lehman RM. Predicting Stability of Distiller's Wet Grains (DWG) with Color Analysis. Food Bioprocess Technol 2010:9.

[60] Wietschel L, Messmann L, Thorenz A, Tuma A. Environmental benefits of large-scale second-generation bioethanol production in the EU: An integrated supply chain network optimization and life cycle assessment approach. Journal of Industrial Ecology 2021;25:677–92. https://doi.org/10.1111/jiec.13083.

[61] Kim Y, Mosier NS, Hendrickson R, Ezeji T, Blaschek H, Dien B, et al. Composition of corn dry-grind ethanol by-products: DDGS, wet cake, and thin stillage. Bioresource Technology 2008:12.

[62] Danish Energy Agency, Energinet. Technology Data. Renewable fuels. 2017.

[63] Nanda S, Reddy SN, Vo D-VN, Sahoo BN, Kozinski JA. Catalytic gasification of wheat straw in hot compressed (subcritical and supercritical) water for hydrogen production. Energy Sci Eng 2018;6:448–59. https://doi.org/10.1002/ese3.219.

[64] Pei H, Jin B, Huang Y. Quantitative analysis of mass and energy flow in rice straw gasification based on mass and carbon balance. Renewable Energy 2020;161:846–57. https://doi.org/10.1016/j.renene.2020.08.014.

[65] Alburquerque JA, Salazar P, Barrón V, Torrent J, del Campillo M del C, Gallardo A, et al. Enhanced wheat yield by biochar addition under different mineral fertilization levels. Agron Sustain Dev 2013;33:475–84. https://doi.org/10.1007/s13593-012-0128-3.

[66] Brassard P, Godbout S, Hamelin L. Framework for consequential life cycle assessment of pyrolysis biorefineries: A case study for the conversion of primary forestry residues. Renewable and Sustainable Energy Reviews 2021;138:110549. https://doi.org/10.1016/j.rser.2020.110549.

[67] Bruun EW. Effects of slow and fast pyrolysis biochar on soil C and N turnover dynamics. Soil Biology 2012:7.

[68] Bruun EW, Hauggaard-Nielsen H, Ibrahim N, Egsgaard H, Ambus P, Jensen PA, et al. Influence of fast pyrolysis temperature on biochar labile fraction and short-term carbon loss in a loamy soil. Biomass and Bioenergy 2011;35:1182–9. https://doi.org/10.1016/j.biombioe.2010.12.008.

[69] Bruun S, Clauson-Kaas S, Bobuľská L, Thomsen IK. Carbon dioxide emissions from biochar in soil: role of clay, microorganisms and carbonates: CO_2 emissions from biochar in soil. Eur J Soil Sci 2014;65:52–9. https://doi.org/10.1111/ejss.12073.

[70] Bruun S, Jensen ES, Jensen LS. Microbial mineralization and assimilation of black carbon: Dependency on degree of thermal alteration. Organic Geochemistry 2008:7.

[71] Conz RF, Abbruzzini TF, Andrade CA de, MIlori D, Cerri CEP. Effect of Pyrolysis Temperature and Feedstock Type on Agricultural Properties and Stability of Biochars. Agricultural Sciences 2017:20.

[72] Hamer U, Marschner B, Brodowski S, Amelung W. Interactive priming of black carbon and glucose mineralisation. Organic Geochemistry 2004;35:823–30. https://doi.org/10.1016/j.orggeochem.2004.03.003.

[73] Herath HMSK, Camps-Arbestain M, Hedley M, Van Hale R, Kaal J. Fate of biochar in chemically- and physically-defined soil organic carbon pools. Organic Geochemistry 2014;73:35–46. https://doi.org/10.1016/j.orggeochem.2014.05.001.

[74] Hilscher A, Knicker H. Degradation of grass-derived pyrogenic organic material, transport of the residues within a soil column and distribution in soil organic matter fractions during a 28month microcosm experiment. Organic Geochemistry 2011;42:42–54. https://doi.org/10.1016/j.orggeochem.2010.10.005.

[75] Karaosmanoğlu F, Işığıgür-Ergüdenler A, Sever A. Biochar from the Straw-Stalk of Rapeseed Plant. Energy Fuels 2000;14:336–9. https://doi.org/10.1021/ef9901138.

[76] Kerré B, Hernandez-Soriano MC, Smolders E. Partitioning of carbon sources among functional pools to investigate short-term priming effects of biochar in soil: A 13C study. Science of The Total Environment 2016;547:30–8. https://doi.org/10.1016/j.scitotenv.2015.12.107.

[77] Knoblauch C, Maarifat A-A, Pfeiffer E-M, Haefele SM. Degradability of black carbon and its impact on trace gas fluxes and carbon turnover in paddy soils. Soil Biology and Biochemistry 2011;43:1768–78. https://doi.org/10.1016/j.soilbio.2010.07.012.

[78] Kuzyakov Y, Subbotina I, Chen H, Bogomolova I, Xu X. Black carbon decomposition and incorporation into soil microbial biomass estimated by 14C labeling. Soil Biology and Biochemistry 2009;41:210–9. https://doi.org/10.1016/j.soilbio.2008.10.016.

[79] Maestrini B. Ryegrass-derived pyrogenic organic matter changes organic carbon and nitrogen mineralization in a temperate forest soil. Soil Biology 2014:11.

[80] Saffari N. Biochar type and pyrolysis temperature effects on soil quality indicators and structural stability. Journal of Environmental Management 2020:12.

[81] Windeatt JH, Ross AB, Williams PT, Forster PM, Nahil MA, Singh S. Characteristics of biochars from crop residues: Potential for carbon sequestration and soil amendment. Journal of Environmental Management 2014;146:189–97. https://doi.org/10.1016/j.jenvman.2014.08.003.

[82] Yin Y. Effects of Rice Straw and Its Biochar Addition on Soil Labile Carbon and Soil Organic Carbon 2014:8.

[83] Yue Y, Lin Q, Irfan M, Chen Q, Zhao X, Li G. Slow Pyrolysis as a Promising Approach for Producing Biochar from Sunflower Straw. BioResources 2018;13:7455–69.

[84] Zhu X, Mao L, Chen B. Driving forces linking microbial community structure and functions to enhanced carbon stability in biochar-amended soil. Environment International 2019:11.

[85] Huang H, Yuan X, Zhu H, Li H, Liu Y, Wang X, et al. Comparative studies of thermochemical liquefaction characteristics of microalgae, lignocellulosic biomass and sewage sludge. Energy 2013;56:52–60. https://doi.org/10.1016/j.energy.2013.04.065.

[86] Liu H-M, Li M-F, Sun R-C. Hydrothermal liquefaction of cornstalk: 7-Lump distribution and characterization of products. Bioresource Technology 2013;128:58–64. https://doi.org/10.1016/j.biortech.2012.09.125.

[87] Murakami K, Kasai K, Kato T, Sugawara K. Conversion of rice straw into valuable products by hydrothermal treatment and steam gasification. Fuel 2012;93:37–43. https://doi.org/10.1016/j.fuel.2011.09.050.

[88] Sharma K, Shah AA, Toor SS, Seehar TH, Pedersen TH, Rosendahl LA. Co-Hydrothermal Liquefaction of Lignocellulosic Biomass in Supercritical Water. Energies 2021;14:1708. https://doi.org/10.3390/en14061708.

[89] Wang C, Pan J, Li J, Yang Z. Comparative studies of products produced from four different biomass samples via deoxy-liquefaction. Bioresource Technology 2008;99:2778–86. https://doi.org/10.1016/j.biortech.2007.06.023.

[90] Wang Y, Wu L, Wang C, Yu J, Yang Z. Investigating the influence of extractives on the oil yield and alkane production obtained from three kinds of biomass via deoxy-liquefaction. Bioresource Technology 2011;102:7190–5. https://doi.org/10.1016/j.biortech.2011.04.060.

[91] Yin S, Zhang N, Tian C, Yi W, Yuan Q, Fu P, et al. Effect of Accumulative Recycling of Aqueous Phase on the Properties of Hydrothermal Degradation of Dry Biomass and Bio-Crude Oil Formation. Energies 2021;14:285. https://doi.org/10.3390/en14020285.

[92] Zhao B, Wang H, Hu Y, Gao J, Zhao G, Ray MB, et al. Hydrothermal Co-Liquefaction of Lignite and Lignocellulosic Biomass with the Addition of Formic Acid: Study on Product Distribution, Characteristics, and Synergistic Effects. Ind Eng Chem Res 2020;59:21663–75. https://doi.org/10.1021/acs.iecr.0c04619.

[93] Zhu Z, Toor SS, Rosendahl L, Chen G. Analysis of product distribution and characteristics in hydrothermal liquefaction of barley straw in subcritical and supercritical water. Environ Prog Sustainable Energy 2014;33:737–43. https://doi.org/10.1002/ep.11977.

[94] Badger DM, Bogue MJ, Stewart DJ. Biogas production from crops and organic wastes. 1. Results of batch digestions. New Zealand Journal of Science 1979;22:11–20.

[95] Bareha Y, Affes R, Moinard V, Buffet J, Girault R. A simple mass balance tool to predict carbon and nitrogen fluxes in anaerobic digestion systems. Waste Management 2021;135:47–59. https://doi.org/10.1016/j.wasman.2021.08.020.

[96] Bauer S. PNNL and LanzaTech team to make new jet fuel. PNNL News 2019:2018–20.

[97] Funke A, Mumme J, Koon M, Diakité M. Cascaded production of biogas and hydrochar from wheat straw: Energetic potential and recovery of carbon and plant nutrients. Biomass and Bioenergy 2013;58:229–37. https://doi.org/10.1016/j.biombioe.2013.08.018.

[98] Gao J, Li J, Wachemo AC, Yuan H, Zuo X, Li X. Mass conversion pathway during anaerobic digestion of wheat straw. RSC Adv 2020;10:27720–7. https://doi.org/10.1039/D0RA02441D.

[99] Gissén C, Prade T, Kreuger E, Nges IA, Rosenqvist H, Svensson S-E, et al. Comparing energy crops for biogas production – Yields, energy input and costs in cultivation using digestate and mineral fertilisation. Biomass and Bioenergy 2014;64:199–210. https://doi.org/10.1016/j.biombioe.2014.03.061.

[100] Hamelin L, Naroznova I, Wenzel H. Environmental consequences of different carbon alternatives for increased manure-based biogas. Applied Energy 2014;114:774–82. https://doi.org/10.1016/j.apenergy.2013.09.033.

[101] Hashemi B, Sarker S, Lamb JJ, Lien KM. Yield improvements in anaerobic digestion of lignocellulosic feedstocks. Journal of Cleaner Production 2021;288:125447. https://doi.org/10.1016/j.jclepro.2020.125447.

[102] Heeg K, Pohl M, Sontag M, Mumme J, Klocke M, Nettmann E. Microbial communities involved in biogas production from wheat straw as the sole substrate within a two-phase solid-state anaerobic digestion. Systematic and Applied Microbiology 2014;37:590–600. https://doi.org/10.1016/j.syapm.2014.10.002.

[103] Jerger DE, Chynoweth DP, Isaacson HR. Anaerobic digestion of sorghum biomass. Biomass 1987;14:99–113. https://doi.org/10.1016/0144-4565(87)90013-8.

[104] Jurado E, Gavala HN, Skiadas IV. Enhancement of methane yield from wheat straw, miscanthus and willow using aqueous ammonia soaking. Environmental Technology 2013;34:2069–75. https://doi.org/10.1080/09593330.2013.826701.

[105] Kakuk B, Kovács KL, Szuhaj M, Rákhely G, Bagi Z. Adaptation of continuous biogas reactors operating under wet fermentation conditions to dry conditions with corn stover as substrate. Anaerobe 2017;46:78–85. https://doi.org/10.1016/j.anaerobe.2017.05.015.

[106] Kreuger E, Nges I, Björnsson L. Ensiling of crops for biogas production: effects on methane yield and total solids determination. Biotechnol Biofuels 2011;4:44. https://doi.org/10.1186/1754-6834-4-44.

[107] Lehtomäki A, Viinikainen TA, Rintala JA. Screening boreal energy crops and crop residues for methane biofuel production. Biomass and Bioenergy 2008;32:541–50. https://doi.org/10.1016/j.biombioe.2007.11.013.

[108] Lehtomäki A, Huttunen S, Rintala JA. Laboratory investigations on co-digestion of energy crops and crop residues with cow manure for methane production: Effect of crop to manure ratio. Resources, Conservation and Recycling 2007;51:591–609. https://doi.org/10.1016/j.resconrec.2006.11.004.

[109] Lehtomäki A, Björnsson L. Two-Stage Anaerobic Digestion of Energy Crops: Methane Production, Nitrogen Mineralisation and Heavy Metal Mobilisation. Environmental Technology 2006;27:209–18. https://doi.org/10.1080/09593332708618635.

[110] Li H, Tan F, Ke L, Xia D, Wang Y, He N, et al. Mass balances and distributions of C, N, and P in the anaerobic digestion of different substrates and relationships between products and substrates. Chemical Engineering Journal 2016;287:329–36. https://doi.org/10.1016/j.cej.2015.11.003.

[111] Misri B. Case Study 11. Hay and crop residues in India and Nepal[7]. FAO 2016. https://www.fao.org/3/X7660E/x7660e0q.htm#fn7 (accessed March 12, 2022).

[112] Mussoline W. Enhanced Methane Production from Pilot-Scale Anaerobic Digester Loaded with Rice Straw. TOENVIEJ 2013;6:32–9. https://doi.org/10.2174/1874829520131205001.

[113] Mussoline W, Esposito G, Lens P, Garuti G, Giordano A. Electrical energy production and operational strategies from a farm-scale anaerobic batch reactor loaded with rice straw and piggery wastewater. Renewable Energy 2014;62:399–406. https://doi.org/10.1016/j.renene.2013.07.043.

[114] Nges IA, Wang B, Cui Z, Liu J. Digestate liquor recycle in minimal nutrients-supplemented anaerobic digestion of wheat straw. Biochemical Engineering Journal 2015;94:106–14. https://doi.org/10.1016/j.bej.2014.11.023.

[115] Parawira W, Murto M, Zvauya R, Mattiasson B. Anaerobic batch digestion of solid potato waste alone and in combination with sugar beet leaves. Renewable Energy 2004;29:1811–23. https://doi.org/10.1016/j.renene.2004.02.005.

[116] Patil PN, Gogate PR, Csoka L, Dregelyi-Kiss A, Horvath M. Intensification of biogas production using pretreatment based on hydrodynamic cavitation. Ultrasonics Sonochemistry 2016;30:79–86. https://doi.org/10.1016/j.ultsonch.2015.11.009.

[117] Petersson A, Thomsen MH, Hauggaard-Nielsen H, Thomsen AB. Potential bioetanol and biogas production using lignocellulosic biomass from winter rye, oilseed rape and faba bean. Biomass & Bioenergy 2007;31:812–9. https://doi.org/10.1016/j.biombioe.2007.06.001.

[118] Pohl M, Heeg K, Mumme J. Anaerobic digestion of wheat straw – Performance of continuous solid-state digestion. Bioresource Technology 2013;146:408–15. https://doi.org/10.1016/j.biortech.2013.07.101.

[119] Pohl M, Mumme J, Heeg K, Nettmann E. Thermo- and mesophilic anaerobic digestion of wheat straw by the upflow anaerobic solid-state (UASS) process. Bioresource Technology 2012;124:321–7. https://doi.org/10.1016/j.biortech.2012.08.063.

[120] Sharma SK, Mishra IM, Sharma MP, Saini JS. Effect of particle size on biogas generation from biomass residues. Biomass 1988;17:251–63. https://doi.org/10.1016/0144-4565(88)90107-2.

[121] Svensson LM, Christensson K, Björnsson L. Biogas production from crop residues on a farm-scale level in Sweden: scale, choice of substrate and utilisation rate most important parameters for financial feasibility. Bioprocess Biosyst Eng 2006;29:137–42. https://doi.org/10.1007/s00449-006-0064-1.

[122] Szerencsits M, Weinberger C, Kuderna M, Feichtinger F, Erhart E, Maier S. Biogas from Cover Crops and Field Residues: Effects on Soil, Water, Climate and Ecological Footprint 2015;9:4.

[123] Tonini D, Hamelin L, Alvarado-Morales M, Astrup TF. GHG emission factors for bioelectricity, biomethane, and bioethanol quantified for 24 biomass substrates with consequential life-cycle assessment. Bioresource Technology 2016;208:123–33. https://doi.org/10.1016/j.biortech.2016.02.052.

[124] Tonini D, Hamelin L, Astrup TF. Environmental implications of the use of agro-industrial residues for biorefineries: application of a deterministic model for indirect land-use changes. GCB Bioenergy 2016;8:690–706. https://doi.org/10.1111/gcbb.12290.

[125] Zauner E, Küntzel U. Methane production from ensiled plant material. Biomass 1986;10:207–23. https://doi.org/10.1016/0144-4565(86)90054-5.

[126] Zhang Y, Kusch-Brandt S, Salter AM, Heaven S. Estimating the Methane Potential of Energy Crops: An Overview on Types of Data Sources and Their Limitations. Processes 2021;9:1565. https://doi.org/10.3390/pr9091565.

[127] Zieliński M, Dębowski M, Kisielewska M, Nowicka A, Rokicka M, Szwarc K. Cavitation-based pretreatment strategies to enhance biogas production in a small-scale agricultural biogas plant. Energy for Sustainable Development 2019;49:21–6. https://doi.org/10.1016/j.esd.2018.12.007.

[128] Ching D. Upgrading of biomass: alternative ways for biomass treatment. Master. KTH, 2014.

[129] Johnson E. Integrated enzyme production lowers the cost of cellulosic ethanol. Biofuels, Bioprod Bioref 2016;10:164–74. https://doi.org/10.1002/bbb.1634.

[130] Abdulrazzaq H, Jol H, Husni A, Abu-Bakr R. Characterization and Stabilisation of Biochars Obtained from Empty Fruit Bunch, Wood, and Rice Husk. BioResources 2014;9:2888–98. https://doi.org/10.15376/biores.9.2.2888-2898.

[131] Fidel R, Laird D, Parkin T. Effect of Biochar on Soil Greenhouse Gas Emissions at the Laboratory and Field Scales. Soil Syst 2019;3:8. https://doi.org/10.3390/soilsystems3010008.

[132] Hansen V, Müller-Stöver D, Munkholm LJ, Peltre C, Hauggaard-Nielsen H, Jensen LS. The effect of straw and wood gasification biochar on carbon sequestration, selected soil fertility indicators and functional groups in soil: An incubation study. Geoderma 2016;269:99–107. https://doi.org/10.1016/j.geoderma.2016.01.033.

[133] Hansen V, Müller-Stöver D, Ahrenfeldt J, Holm JK, Henriksen UB, Hauggaard-Nielsen H. Gasification biochar as a valuable by-product for carbon sequestration and soil amendment. Biomass and Bioenergy 2015;72:300–8. https://doi.org/10.1016/j.biombioe.2014.10.013.

[134] Müller-Stöver D, Ahrenfeldt J, Holm JK, Shalatet SGS, Henriksen U, Hauggaard-Nielsen H. Soil application of ash produced by low-temperature fluidized bed gasification: effects on soil nutrient dynamics and crop response. Nutr Cycl Agroecosyst 2012;94:193–207. https://doi.org/10.1007/s10705-012-9533-x.

[135] Naisse C, Girardin C, Lefevre R. Effect of physical weathering on the carbon sequestration potential of biochars and hydrochars in soil. GCB Bioenergy 2014:9.

[136] Pereira EIP, Suddick EC, Six J. Carbon Abatement and Emissions Associated with the Gasification of Walnut Shells for Bioenergy and Biochar Production. PLOS ONE 2016:15.

[137] Ventura M, Alberti G, Panzacchi P, Vedove GD, Miglietta F, Tonon G. Biochar mineralization and priming effect in a poplar short rotation coppice from a 3-year field experiment. Biol Fertil Soils 2019;55:67–78. https://doi.org/10.1007/s00374-018-1329-y.

[138] Ventura M, Alberti G, Viger M, Jenkins JR, Girardin C, Baronti S, et al. Biochar mineralization and priming effect on SOM decomposition in two European short rotation coppices. GCB Bioenergy 2015;7:1150–60. https://doi.org/10.1111/gcbb.12219.

[139] Bamminger C, Marschner B, Jüschke E. An incubation study on the stability and biological effects of pyrogenic and hydrothermal biochar in two soils: Biological effects of different biochars in two soils. Eur J Soil Sci 2014;65:72–82. https://doi.org/10.1111/ejss.12074.

[140] Cayuela ML, Oenema O, Kuikman PJ, Bakker RR, Van Groenigen JW. Bioenergy by-products as soil amendments? Implications for carbon sequestration and greenhouse gas emissions: C and N dynamics from bioenergy by-products in soil. GCB Bioenergy 2010:no-no. https://doi.org/10.1111/j.1757-1707.2010.01055.x.

[141] Chen G. Decomposition temperature sensitivity of biochars with different stabilities affected by organic carbon fractions and soil microbes 2019:11.

[142] Cross A, Sohi SP. The priming potential of biochar products in relation to labile carbon contents and soil organic matter status. Soil Biology 2011:8.

[143] Farrell M. Microbial utilisation of biochar-derived carbon. Science of the Total Environment 2013:10.

[144] Galvez A, Sinicco T, Cayuela ML, Mingorance MD, Fornasier F, Mondini C. Short term effects of bioenergy by-products on soil C and N dynamics, nutrient availability and biochemical properties. Agriculture, Ecosystems & Environment 2012;160:3–14. https://doi.org/10.1016/j.agee.2011.06.015.

[145] Hernandez-Soriano MC, Kerré B, Kopittke PM, Horemans B, Smolders E. Biochar affects carbon composition and stability in soil: a combined spectroscopy-microscopy study. Sci Rep 2016;6:25127. https://doi.org/10.1038/srep25127.

[146] Kuzyakov Y, Bogomolova I, Glaser B. Biochar stability in soil: Decomposition during eight years and transformation as assessed by compound-specific 14C analysis. Soil Biology and Biochemistry 2014;70:229–36. https://doi.org/10.1016/j.soilbio.2013.12.021.

[147] Lehmann J, Abiven S, Kleber M, Pan G, Singh BP, Sohi SP, et al. Persistence of biochar in soil. Biochar for Environmental Management. 2nd Edition, 2015, p. 48.

[148] Lu W, Ding W, Zhang J, Li Y, Luo J, Bolan N, et al. Biochar suppressed the decomposition of organic carbon in a cultivated sandy loam soil: A negative priming effect. Soil Biology and Biochemistry 2014;76:12–21. https://doi.org/10.1016/j.soilbio.2014.04.029.

[149] Luo X. Effects of biochar on carbon mineralization of coastal wetland soils in the Yellow River Delta, China. Ecological Engineering 2016:8.

[150] Malghani S. Chars produced by slow pyrolysis and hydrothermal carbonization vary in carbon sequestration potential and greenhouse gases emissions. Soil Biology 2013:10.

[151] Nguyen BT, Lehmann J, Hockaday WC, Joseph S, Masiello CA. Temperature Sensitivity of Black Carbon Decomposition and Oxidation 2010:8.

[152] Nguyen BT, Lehmann J. Black carbon decomposition under varying water regimes. Organic Geochemistry 2009:8.

[153] Sarfaraz Q. Characterization and carbon mineralization of biochars produced from different animal manures and plant residues 2020:9.

[154] Shen Y, Zhu L, Cheng H, Yue S, Li S. Effects of Biochar Application on CO2 Emissions from a Cultivated Soil under Semiarid Climate Conditions in Northwest China. Sustainability 2017;9:1482. https://doi.org/10.3390/su9081482.

[155] Wu M. Soil organic carbon content affects the stability of biochar in paddy soil 2016:8.

[156] Zimmerman A, Gao B. The Stability of Biochar in the Environment. In: Ladygina N, Rineau F, editors. Biochar and Soil Biota, CRC Press; 2013, p. 1–40. https://doi.org/10.1201/b14585-2.

[157] Zimmerman AR. Abiotic and Microbial Oxidation of Laboratory-Produced Black Carbon (Biochar). Environ Sci Technol 2010;44:1295–301. https://doi.org/10.1021/es903140c.

[158] Zimmerman AR, Gao B, Ahn M-Y. Positive and negative carbon mineralization priming effects among a variety of biochar-amended soils. Soil Biology and Biochemistry 2011;43:1169–79. https://doi.org/10.1016/j.soilbio.2011.02.005.

[159] Bai M, Wilske B, Buegger F, Esperschütz J, Kammann CI, Eckhardt C, et al. Degradation kinetics of biochar from pyrolysis and hydrothermal carbonization in temperate soils. Plant Soil 2013;372:375–87. https://doi.org/10.1007/s11104-013-1745-6.

[160] Baronti S, Alberti G, Camin F, Criscuoli I, Genesio L, Mass R, et al. Hydrochar enhances growth of poplar for bioenergy while marginally contributing to direct soil carbon sequestration. GCB Bioenergy 2017;9:1618–26. https://doi.org/10.1111/gcbb.12450.

[161] Dicke C, Lanza G, Mumme J, Ellerbrock R, Kern J. Effect of Hydrothermally Carbonized Char Application on Trace Gas Emissions from Two Sandy Soil Horizons. J Environ Qual 2014;43:1790–8. https://doi.org/10.2134/jeq2013.12.0513.

[162] Eibisch N, Helfrich M, Don A, Mikutta R, Kruse A, Ellerbrock R, et al. Properties and Degradability of Hydrothermal Carbonization Products. J Environ Qual 2013;42:1565–73. https://doi.org/10.2134/jeq2013.02.0045.

[163] Gajić A, Ramke H-G, Hendricks A, Koch H-J. Microcosm study on the decomposability of hydrochars in a Cambisol. Biomass and Bioenergy 2012;47:250–9. https://doi.org/10.1016/j.biombioe.2012.09.036.

[164] Gronwald M, Vos C, Helfrich M, Don A. Stability of pyrochar and hydrochar in agricultural soil - a new field incubation method. Geoderma 2016;284:85–92. https://doi.org/10.1016/j.geoderma.2016.08.019.

[165] Malghani S, Jüschke E, Baumert J, Thuille A, Antonietti M, Trumbore S, et al. Carbon sequestration potential of hydrothermal carbonization char (hydrochar) in two contrasting soils; results of a 1-year field study. Biology and Fertility of Soils 2015;51:123–34. https://doi.org/10.1007/s00374-014-0980-1.

[166] Qayyum MF, Steffens D, Reisenauer HP, Schubert S. Kinetics of Carbon Mineralization of Biochars Compared with Wheat Straw in Three Soils. J Environ Qual 2012;41:1210–20. https://doi.org/10.2134/jeq2011.0058.

[167] Santana A, Bisinoti M, Melo C, Ferreira O, Moreira A. DISPONIBILIDADE DE NUTRIENTES E CARBONO ORGÂNICO EM SOLOS CONTENDO CARVÃO HIDROTÉRMICO LAVADO E NÃO LAVADO E COMPARAÇÃO COM SOLOS ANTROPOGÊNICOS. QN 2019. https://doi.org/10.21577/0100-4042.20170339.

[168] Schimmelpfennig S. Degradation of Miscanthus×giganteus biochar, hydrochar and feedstock under the influence of disturbance events. Applied Soil Ecology 2017:16.

[169] Schimmelpfennig S, Müller C, Grünhage L, Koch C, Kammann C. Biochar, hydrochar and uncarbonized feedstock application to permanent grassland—Effects on greenhouse gas emissions and plant growth. Agriculture, Ecosystems & Environment 2014;191:39–52. https://doi.org/10.1016/j.agee.2014.03.027.

[170] Schulze M, Mumme J, Funke A, Kern J. Effects of selected process conditions on the stability of hydrochar in low-carbon sandy soil. Geoderma 2016;267:137–45. https://doi.org/10.1016/j.geoderma.2015.12.018.

[171] Steinbeiss S, Gleixner G, Antonietti M. Effect of biochar amendment on soil carbon balance and soil microbial activity. Soil Biology and Biochemistry 2009;41:1301–10. https://doi.org/10.1016/j.soilbio.2009.03.016.

[172] Alburquerque JA, de la Fuente C, Bernal MP. Chemical properties of anaerobic digestates affecting C and N dynamics in amended soils. Agriculture, Ecosystems & Environment 2012;160:15–22. https://doi.org/10.1016/j.agee.2011.03.007.

[173] Askri A. Valorisation des digestats de methanisation en agriculture: Effets sur les cycles biogeochimiques du carbone et de l´azote. PhD. AgroParis Tech, 2015.

[174] Béghin-Tanneau R, Guérin F, Guiresse M, Kleiber D, Scheiner JD. Carbon sequestration in soil amended with anaerobic digested matter. Soil and Tillage Research 2019;192:87–94. https://doi.org/10.1016/j.still.2019.04.024.

[175] Bernal MP, Kirchmann H. Carbon and nitrogen mineralization and ammonia volatilization from fresh, aerobically and anaerobically treated pig manure during incubation with soil. Biol Fertil Soils 1992;13:135–41. https://doi.org/10.1007/BF00336268.

[176] Chen R, Blagodatskaya E, Senbayram M, Blagodatsky S, Myachina O, Dittert K, et al. Decomposition of biogas residues in soil and their effects on microbial growth kinetics and enzyme activities. Biomass and Bioenergy 2012;45:221–9. https://doi.org/10.1016/j.biombioe.2012.06.014.

[177] de la Fuente C, Alburquerque JA, Clemente R, Bernal MP. Soil C and N mineralisation and agricultural value of the products of an anaerobic digestion system. Biol Fertil Soils 2013;49:313–22. https://doi.org/10.1007/s00374-012-0719-9.

[178] Dietrich M, Fongen M, Foereid B. Greenhouse gas emissions from digestate in soil. International Journal of Recycling Organic Waste in Agriculture 2020;9:1–19. https://doi.org/10.30486/ijrowa.2020.1885341.1005.

[179] Johansen A, Carter MS, Jensen ES, Hauggard-Nielsen H, Ambus P. Effects of digestate from anaerobically digested cattle slurry and plant materials on soil microbial community and emission of CO2 and N2O. Applied Soil Ecology 2013;63:36–44. https://doi.org/10.1016/j.apsoil.2012.09.003.

[180] Mukherjee S, Weihermueller L, Tappe W, Vereecken H, Burauel P. Microbial respiration of biochar- and digestate-based mixtures. Biol Fertil Soils 2016;52:151–64. https://doi.org/10.1007/s00374-015-1060-x.

[181] Nielsen K, Roß C-L, Hoffmann M, Muskolus A, Ellmer F, Kautz T. The Chemical Composition of Biogas Digestates Determines Their Effect on Soil Microbial Activity. Agriculture 2020;10:244. https://doi.org/10.3390/agriculture10060244.

[182] Sánchez M, Gomez X, Barriocanal G, Cuetos MJ, Morán A. Assessment of the stability of livestock farm wastes treated by anaerobic digestion. International Biodeterioration & Biodegradation 2008;62:421–6. https://doi.org/10.1016/j.ibiod.2008.04.002.

[183] Schouten S, van Groenigen JW, Oenema O, Cayuela ML. 'Bioenergy from cattle manure? Implications of anaerobic digestion and subsequent pyrolysis for carbon and nitrogen dynamics in soil.' GCB Bioenergy 2012;4:751–60. https://doi.org/10.1111/j.1757-1707.2012.01163.x.

[184] Thomsen IK, Olesen JE, Møller HB, Sørensen P, Christensen BT. Carbon dynamics and retention in soil after anaerobic digestion of dairy cattle feed and faeces. Soil Biology and Biochemistry 2013;58:82–7. https://doi.org/10.1016/j.soilbio.2012.11.006.

[185] Viaene J. Co-ensiling, co-composting and anaerobic co-digestion of vegetable crop residues: Product stability and effect on soil carbon and nitrogen dynamics. Scientia Horticulturae 2017:12.

[186] Amin AE-EAZ. Bagasse Pith-Vinasse Biochar Effects on Carbon Emission and Nutrient Release in Calcareous Sandy Soil. J Soil Sci Plant Nutr 2020;20:220–31. https://doi.org/10.1007/s42729-019-00125-9.

[187] Cayuela ML, Kuikman P, Bakker R, van Groenigen JW. Tracking C and N dynamics and stabilization in soil amended with wheat residue and its corresponding bioethanol by-product: a ^{13}C/ ^{15}N study. GCB Bioenergy 2014;6:499–508. https://doi.org/10.1111/gcbb.12102.

[188] de A. Sousa JG, Cherubin MR, Cerri CEP, Cerri CC, Feigl BJ. Sugar cane straw left in the field during harvest: decomposition dynamics and composition changes. Soil Res 2017;55:758. https://doi.org/10.1071/SR16310.

[189] Mondini C, Cayuela ML, Sinicco T, Fornasier F, Galvez A, Sánchez-Monedero MA. Modification of the RothC model to simulate soil C mineralization of exogenous organic matter. Biogeochemistry: Soils; 2017. https://doi.org/10.5194/bg-2016-551.

[190] Muniyasamy S. Biodegradable green composites from bioethanol co-product and poly(butylene adipate-co-terephthalate). Industrial Crops and Products 2013:8.

[191] Parnaudeau V, Condom N, Oliver R, Cazevieille P, Recous S. Vinasse organic matter quality and mineralization potential, as influenced by raw material, fermentation and concentration processes. Bioresource Technology 2008:10.

[192] Yamaguchi CS, Ramos NP, Carvalho CS, Pires AMM, de Andrade CA. Sugarcane straw decomposition and carbon balance as a function of initial biomass and vinasse addition to soil surface 2017;76:10.

[193] Parton WJ, Schimel DS, Cole CV, Ojima DS. Analysis of Factors Controlling Soil Organic Matter Levels in Great Plains Grasslands. Soil Science Society of America Journal 1987;51:1173–9. https://doi.org/10.2136/sssaj1987.03615995005100050015x.

[194] Falloon P, Smith P. Simulating SOC changes in long-term experiments with RothC and CENTURY: model evaluation for a regional scale application. Soil Use and Management 2002;18:101–11. https://doi.org/10.1111/j.1475-2743.2002.tb00227.x.

[195] Palosuo T, Foereid B, Svensson M, Shurpali N, Lehtonen A, Herbst M, et al. A multi-model comparison of soil carbon assessment of a coniferous forest stand. Environmental Modelling & Software 2012;35:38–49. https://doi.org/10.1016/j.envsoft.2012.02.004.

[196] Silva-Olaya AM. Modelling SOC response to land use change and management practices in sugarcane cultivation in South-Central Brazil. Plant Soil 2017:16.

[197] Lugato E, Jones A. Modelling Soil Organic Carbon Changes Under Different Maize Cropping Scenarios for Cellulosic Ethanol in Europe. Bioenerg Res 2015;8:537–45. https://doi.org/10.1007/s12155-014-9529-2.

[198] Cerri CEP, Easter M, Paustian K, Killian K, Coleman K, Bernoux M, et al. Simulating SOC changes in 11 land use change chronosequences from the Brazilian Amazon with RothC and Century models. Agriculture, Ecosystems & Environment 2007;122:46–57. https://doi.org/10.1016/j.agee.2007.01.007.

[199] Monforti F, Lugato E, Motola V, Bodis K, Scarlat N, Dallemand JF. Optimal energy use of agricultural crop residues preserving soil organic carbon stocks in Europe. Renewable and Sustainable Energy Reviews 2015;44:519–29. https://doi.org/10.1016/j.rser.2014.12.033.

[200] Del Grosso SJ, Parton WJ, Mosier AR, Hartman MD, Brenner J, Ojima DS, et al. Simulated interaction of carbon dynamics and nitrogen trace gas fluxes using the DAYCENT model. Modeling Carbon and Nitrogen Dynamics for Soil Management 2001;303:332.

[201] Parton WJ, Ojima DS, Cole CV, Schimel DS. A general model for soil organic matter dynamics: sensitivity to litter chemistry, texture and management. Quantitative Modeling of Soil Forming Processes 1994;39:147–67.

[202] Necpálová M, Anex RP, Fienen MN, Del Grosso SJ, Castellano MJ, Sawyer JE, et al. Understanding the DayCent model: Calibration, sensitivity, and identifiability through inverse modeling. Environmental Modelling & Software 2015;66:110–30. https://doi.org/10.1016/j.envsoft.2014.12.011.

[203] Oliveira DMS, Paustian K. Predicting soil C changes over sugarcane expansion in Brazil using the DayCent model 2017:11.

[204] Franko U, Oelschlägel B, Schenk S. Simulation of temperature-, water- and nitrogen dynamics using the model CANDY. Ecological Modelling 1995;81:213–22. https://doi.org/10.1016/0304-3800(94)00172-E.

[205] Franko U. Simulating trends in soil organic carbon in long-term experiments using the CANDY model 1997:12.

[206] Franko U, Kolbe H, Thiel E, Ließ E. Multi-site validation of a soil organic matter model for arable fields based on generally available input data. Geoderma 2011;166:119–34. https://doi.org/10.1016/j.geoderma.2011.07.019.

[207] Puhlmann M, Kuka K, Franko U. Comparison of methods for the estimation of inert carbon suitable for initialisation of the CANDY model 2006:11.

[208] Ghaley BB. Simulation of Soil Organic Carbon Effects on Long-Term Winter Wheat (Triticum aestivum) Production Under Varying Fertilizer Inputs. Frontiers in Plant Science 2018;9:9.

[209] Farina R, Sándor R, Abdalla M, Álvaro-Fuentes J, Bechini L, Bolinder MA, et al. Ensemble modelling, uncertainty and robust predictions of organic carbon in long-term bare-fallow soils 2020:25. https://doi.org/10.1111/gcb.15441.

[210] Coleman K, Jenkinson DS. RothC-26.3 - A Model for the turnover of carbon in soil. In: Powlson DS, Smith P, Smith JU, editors. Evaluation of Soil Organic Matter Models, Berlin, Heidelberg: Springer Berlin Heidelberg; 1996, p. 237–46. https://doi.org/10.1007/978-3-642-61094-3_17.

[211] Morais TG, Teixeira RFM, Domingos T. Detailed global modelling of soil organic carbon in cropland, grassland and forest soils. PLOS ONE 2019:27.

[212] Klumpp K, Coleman K, Dondini M, Goulding K, Hastings A, Jones MB, et al. Soil Organic Carbon (SOC) Equilibrium and Model Initialisation Methods: an Application to the Rothamsted Carbon (RothC) Model n.d.:15.

[213] Gottschalk P, Smith JU, Wattenbach M, Bellarby J, Stehfest E, Arnell N, et al. How will organic carbon stocks in mineral soils evolve under future climate? Global projections using RothC for a range of climate change scenarios 2012:21.

[214] Petersen BM, Olesen JE, Heidmann T. A flexible tool for simulation of soil carbon turnover. Ecological Modelling 2002;151:1–14. https://doi.org/10.1016/S0304-3800(02)00034-0.

[215] Taghizadeh-Toosi A, Christensen BT, Hutchings NJ, Vejlin J, Kätterer T, Glendining M, et al. C-TOOL: A simple model for simulating whole-profile carbon storage in temperate agricultural soils. Ecological Modelling 2014;292:11–25. https://doi.org/10.1016/j.ecolmodel.2014.08.016.

[216] Hansen JH, Hamelin L, Taghizadeh-Toosi A, Olesen JE, Wenzel H. Agricultural residues bioenergy potential that sustain soil carbon depends on energy conversion pathways 2020:12.

[217] Keel SG, Leifeld J, Mayer J, Taghizadeh-Toosi A, Olesen JE. Large uncertainty in soil carbon modelling related to method of calculation of plant carbon input in agricultural systems: Uncertainty in soil carbon modelling. Eur J Soil Sci 2017;68:953–63. https://doi.org/10.1111/ejss.12454.

[218] Taghizadeh-Toosi A, Olesen JE. Modelling soil organic carbon in Danish agricultural soils suggests low potential for future carbon sequestration. Agricultural Systems 2016;145:83–9. https://doi.org/10.1016/j.agsy.2016.03.004.

[219] Andriulo A, Mary B, Guerif J. Modelling soil carbon dynamics with various cropping sequences on the rolling pampas. Agronomie 1999;19:365–77. https://doi.org/10.1051/agro:19990504.

[220] Clivot H, Mouny J-C, Duparque A, Dinh J-L, Denoroy P, Houot S, et al. Modeling soil organic carbon evolution in long-term arable experiments with AMG model. Environmental Modelling & Software 2019;118:99–113. https://doi.org/10.1016/j.envsoft.2019.04.004.

[221] Saffih-Hdadi K, Mary B. Modeling consequences of straw residues export on soil organic carbon. Soil Biology and Biochemistry 2008;40:594–607. https://doi.org/10.1016/j.soilbio.2007.08.022.

[222] Nowak B, Marliac G. Optimization of carbon stock models to local conditions using farmers' soil tests: A case study with AMGv2 for a cereal plain in central France n.d.:13.

[223] Autret B, Mary B, Chenu C, Balabane M, Girardin C, Bertrand M, et al. Alternative arable cropping systems: A key to increase soil organic carbon storage? Results from a 16 year field experiment. Agriculture, Ecosystems & Environment 2016;232:150–64. https://doi.org/10.1016/j.agee.2016.07.008.

[224] Milesi Delaye LA, Irizar AB, Andriulo AE, Mary B. Effect of Continuous Agriculture of Grassland Soils of the Argentine Rolling Pampa on Soil Organic Carbon and Nitrogen. Applied and Environmental Soil Science 2013;2013:1–17. https://doi.org/10.1155/2013/487865.

[225] Falloon P, Smith P. Simulating SOC changes in long-term experiments with RothC and CENTURY: model evaluation for a regional scale application. Soil Use and Management 2002;18:101–11. https://doi.org/10.1111/j.1475-2743.2002.tb00227.x.

[226] Dimassi B, Guenet B, Saby NPA, Munoz F, Bardy M, Millet F, et al. The impacts of CENTURY model initialization scenarios on soil organic carbon dynamics simulation in French long-term experiments. Geoderma 2018;311:25–36. https://doi.org/10.1016/j.geoderma.2017.09.038.

[227] Williams JR, Jones CA, Dyke PT. A modeling approach to determining the relationship between erosion and soil productivity [EPIC, Erosion-Productivity Impact Calculator, mathematical models]. Trans ASAE, 1984.

[228] Izaurralde RC, Mcgill WB, Williams JR. Development and application of the EPIC model for carbon cycle, greenhouse-gas mitigation, and biofuel studies. M Liebig, AJ Franzluebbers and R Follett; Academic Press, Waltham, MA, United States(US).; 2012.

[229] Gerik T, Williams JR, Dagitz S, Magre M, Meinardus A, Steglich E, et al. Environmental Policy Integrated Cimate Model - User's Manual version 0810 2015.

[230] Wang X, Kemanian AR, Williams JR. Special Features of the EPIC and APEX Modeling Package and Procedures for Parameterization, Calibration, Validation, and Applications. Methods of Introducing System Models into Agricultural Research, vol. 2, Wiley Online Library; 2011.

[231] Wang XC, Li J, Tahir MN, Hao MD. Validation of the EPIC model using a long-term experimental data on the semi-arid Loess Plateau of China. Mathematical and Computer Modelling 2011;54:976–86. https://doi.org/10.1016/j.mcm.2010.11.025.

[232] Wang X, R. Williams J, W. Gassman P, Baffaut C, C. Izaurralde R, Jeong J, et al. EPIC and APEX: Model Use, Calibration, and Validation. Transactions of the ASABE 2012;55:1447–62. https://doi.org/10.13031/2013.42253.

[233] Izaurralde R, Williams JR, McGill W, Rosenberg N, Jakas M. Simulating soil C dynamics with EPIC: Model description and testing against long-term data 2006. https://doi.org/10.1016/J.ECOLMODEL.2005.07.010.

[234] Bernardos JN, Viglizzo EF, Jouvet V, Lértora FA, Pordomingo AJ, Cid FD. The use of EPIC model to study the agroecological change during 93 years of farming transformation in the Argentine pampas. Agricultural Systems 2001;69:215–34. https://doi.org/10.1016/S0308-521X(01)00027-0.

[235] Balkovič J, van der Velde M, Schmid E, Skalský R, Khabarov N, Obersteiner M, et al. Pan-European crop modelling with EPIC: Implementation, up-scaling and regional crop yield validation. Agricultural Systems 2013;120:61–75. https://doi.org/10.1016/j.agsy.2013.05.008.

[236] Keating BA, Carberry PS, Hammer GL, Probert ME, Robertson MJ, Holzworth D, et al. An overview of APSIM, a model designed for farming systems simulation. European Journal of Agronomy 2003;18:267–88. https://doi.org/10.1016/S1161-0301(02)00108-9.

[237] Gaydon DS, Balwinder-Singh, Wang E, Poulton PL, Ahmad B, Ahmed F, et al. Evaluation of the APSIM model in cropping systems of Asia. Field Crops Research 2017;204:52–75. https://doi.org/10.1016/j.fcr.2016.12.015.

[238] Mohanty M, Probert ME, Reddy KS, Dalal RC, Mishra AK, Subba Rao A, et al. Simulating soybean–wheat cropping system: APSIM model parameterization and validation. Agriculture, Ecosystems & Environment 2012;152:68–78. https://doi.org/10.1016/j.agee.2012.02.013.

[239] APSIM. APSIM: The Leading Software Framework for Agricultural Systems Modelling and SimulationPSIM. APSIM n.d. https://www.apsim.info/.

[240] Thorburn PJ, Probert ME, Robertson FA. Modelling decomposition of sugar cane surface residues with APSIM–Residue. Field Crops Research 2001;70:223–32. https://doi.org/10.1016/S0378-4290(01)00141-1.

[241] Akponikpè PBI, Gérard B, Michels K, Bielders C. Use of the APSIM model in long term simulation to support decision making regarding nitrogen management for pearl millet in the Sahel. European Journal of Agronomy 2010;32:144–54. https://doi.org/10.1016/j.eja.2009.09.005.

[242] Delve RJ, Probert ME, Cobo JG, Ricaurte J, Rivera M, Barrios E, et al. Simulating phosphorus responses in annual crops using APSIM: model evaluation on contrasting soil types. Nutr Cycl Agroecosyst 2009;84:293–306. https://doi.org/10.1007/s10705-008-9243-6.

[243] Kisaka MO, Mucheru-Muna M, Ngetich FK, Mugwe JN, Mugendi DN, Mairura F, et al. Using APSIM-model as a decision-support-tool for long-term integrated--nitrogen-management and maize productivity under semir-arid condiutions in Kenya. Experimental Agriculture 2016;52:279–99. https://doi.org/10.1017/S0014479715000095.

[244] Thorburn PJ, Biggs JS, Collins K, Probert ME. Using the APSIM model to estimate nitrous oxide emissions from diverse Australian sugarcane production systems. Agriculture, Ecosystems & Environment 2010;136:343–50. https://doi.org/10.1016/j.agee.2009.12.014.

[245] O'Leary GJ, Liu DL, Ma Y, Li FY, McCaskill M, Conyers M, et al. Modelling soil organic carbon 1. Performance of APSIM crop and pasture modules against long-term experimental data. Geoderma 2016;264:227–37. https://doi.org/10.1016/j.geoderma.2015.11.004.

[246] Chauhan YS, Solomon KF, Rodriguez D. Characterization of north-eastern Australian environments using APSIM for increasing rainfed maize production. Field Crops Research 2013;144:245–55. https://doi.org/10.1016/j.fcr.2013.01.018.

[247] Asseng S, Keating BA, Fillery IRP, Gregory PJ, Bowden JW, Turner NC, et al. Performance of the APSIM-wheat model in Western Australia. Field Crops Research 1998;57:163–79. https://doi.org/10.1016/S0378-4290(97)00117-2.

[248] Balwinder-Singh, Gaydon DS, Humphreys E, Eberbach PL. The effects of mulch and irrigation management on wheat in Punjab, India—Evaluation of the APSIM model. Field Crops Research 2011;124:1–13. https://doi.org/10.1016/j.fcr.2011.04.016.

[249] Holzworth DP, Huth NI, deVoil PG, Zurcher EJ, Herrmann NI, McLean G, et al. APSIM – Evolution towards a new generation of agricultural systems simulation. Environmental Modelling & Software 2014;62:327–50. https://doi.org/10.1016/j.envsoft.2014.07.009.

[250] Cichota R, Vogeler I, Sharp J, Verburg K, Huth N, Holzworth D, et al. A protocol to build soil descriptions for APSIM simulations. MethodsX 2021;8:101566. https://doi.org/10.1016/j.mex.2021.101566.

[251] Archontoulis SV, Huber I, Miguez FE, Thorburn PJ, Rogovska N, Laird DA. A model for mechanistic and system assessments of biochar effects on soils and crops and trade-offs. GCB Bioenergy 2016;8:1028–45. https://doi.org/10.1111/gcbb.12314.

Appendix A1b

Supplementary Information of Chapter 2 – Section 2

This appendix summarizes the general characteristics and parameters of 12 soil models investigated in Paper 1. It is reproduced from the original version in excel.

The interplay between bioeconomy and long-term soil organic carbon stock maintenance: A systematic review

Supplementary Information 2

Christhel Andrade[a,b*], Ariane Albers[a], Ezequiel Zamora-Ledezma[c], Lorie Hamelin[a]

[a] Toulouse Biotechnology Institute (TBI), INSA, INRAE UMR792, and CNRS UMR5504, Federal University of Toulouse, 135 Avenue de Rangueil, F-31077, Toulouse, France

[b] Department of Chemical, Biotechnological and Food Processes, Faculty of Mathematical, Physics and Chemistry Sciences. Universidad Técnica de Manabí (UTM), 130150, Portoviejo, Ecuador.

[c] Faculty of Agriculture Engineering. Universidad Técnica de Manabí (UTM), 13132, Lodana, Ecuador.

* Corresponding author: andraded@insa-toulouse.fr

Model	Latest Version Model type	Pools (#)	Carbon pools (size %)	MRT (years)	Soil depth (cm)	Land use types	Climate	Timescale Timestep	Inputs			Outputs	Adapted to new C inputs		Accepted		Locations tested	Ref
									Climate	Soil	Farming		Yes	No	High	Low		
CENTURY [1]	Century 5.0 Agro-ecosystem	3	Active SOM pool (2%) Slow SOM pool (45-60%,) Passive SOM pool (45-50%,)	0.5-1 10-50 400-4000	0-15, 15-30, 30-45, 45-60, 60-90	Grasslands , Croplands, Forest, Lands, Savanna	Tropical, Temperate	Long-term Monthly	Average, min and max air temperature. Sum of monthly precipitations. Atmospheric nitrogen.	Soil texture (sand, clay, silt and water fractions). Initial SOC (g C m^{-2}). Initial C:N ratio. BD, pH, wilting point, field capacity, initial N, P, and S.	Crop sequences. Defined or calculated plant lignin, N, P, and S content. Cultivation options. Fertilization. Fires. Grazing. Harvesting schedules. Irrigation. OM addition	Long term C, N, P, and S dyamics for plant-soil systems. Plant growth, nutrient cycling, and soil SOM dynamics	X		X		EU, USA, Italy, Amazon, Global	[1], [2], [3], [4], [5], [6], [7]
DAYCENT [8]	DayCent4.5 Agro-ecosystem	3	Active SOM pool (2-5%) Slow SOM pool (45-60%) Passive SOM pool (45-50%)	0.5-1 10-50 400-2000	0-15, 15-30, 30-45, 45-60, 60-90	Grasslands, Croplands, Forest, Lands, Savanna	Tropical, Temperate	Long-term Daily	Min and max air temperature. Min and max precipitations	Soil texture (sand, clay, silt and water fractions). Initial SOC (gC m^{-2}). Initial C:N ratio. BD, pH, wilting point, field capacity, initial N, P, and S.	Crop sequences. Defined or calculated plant ligning, N, P and S content. Cultivation options. Fertilization. Fires. Grazing. Tillage. Harvesting schedules. Irrigation. OM addition. Planting schedule. Amount and schedule of nutrient amendments	Long term C, N, P, and S dyamics for plant-soil systems. Plant growth, nutrient cycling and soil organic matter (SOM) dynamics. Daily N gas flux, CH_4 uptake, CO_2 flux, actual evapotranspiration. Water flows		X	X		USA, EU, China, Global, Canada, Ireland, Australia, UK, Argentina, New Zealand	[8], [9], [10], [11], [12], [13], [14], [15], [16], [17], [18], [19], [20], [21]
RothC (Rothamsted Carbon model) [22]	RothC 26.3 C turnover	5	DPM (Crops: 59%, FYM : 49%, Wood: 20%). RPM (Crops: 41%, FYM: 49%, Wood:20%).	0.10 3.33	0-23	Grasslands, Croplands, Forest	Tropical, Temperate Dry Mid-term	Monthly or annual	Monthly rainfall (mm), monthly open pan evaporation (mm), and average monthly air temperature (°C)	Clay content (%), degree of soil cover (vegetatated or bare), initial SOC stocks (t C ha^{-1}). IOM (t C ha^{-1}). Depth of the soil layer (cm)	Monthly input of plant residue (t C ha^{-1}). Monthly input of FYM manure (tC ha^{-1}). Estimate of the decomposability of the input material	Turnover of soil total organic carbon, microbial biomass carbon, and delta 14C (from which the equivalent radiocarbon age	X		X		UK, India, Australia, France, Japan, Italy, Mexico, Colombia, China, Ireland,	[22], [23], [24], [25], [26], [27], [28], [29],

Model	Latest Version	Model type	Pools (#)	Carbon pools (size %)	MRT (years)	Soil depth (cm)	Land use types	Climate	Timescale	Timestep	Inputs			Outputs	Adapted to new C inputs		Accepted		Locations tested	Ref
											Climate	Soil	Farming		Yes	No	High	Low		
				BIO (46%). HUM (54%, FYM : 2%) IOM	1.52 50.00 50 000								(DPM/RPM ratio). Soil tillage depth (cm)	of the soil can be calculated in non-waterlogged topsoil. CO_2 emissions and C inputs in soil (inverse modeling).					Spain, Slovakia, Africa, Switzerland, Syria, Czech Republic, Hungary, Sweden, Global	[30], [31], [32], [33], [34], [35], [36]
AMG [37]	AMGv2	C turnover	3	FOM Active Carbon Organic Matter (CA) (60%) Stable Carbon Organic Matter (CS) (40%)	< 1 7-26 Inert	0-30	Croplands	Temperate	Long-term	Yearly	Mean annual air temperature (°C). Difference between the annual sum of precipitation and the annual sum of evapotranspiration values (mm)	Clay and carbonate contents (%), pH, C:N ratio, soil bulk density, SOC content (t C ha^{-1}), depth to compute SOC stocks	Crop rotation. Crop yields (t ha^{-1} y^{-1}) or C inputs directly measured. Tillage depth, irrigation, type, rate and year of EOM application. Harvesting and fate of the residue	Annual SOC turnover	X			X	France, Argentina, UK, Togo	[37], [38], [39], [40], [41], [42], [43], [44], [45], [46]
C-TOOL [47]	C-TOOL 2.3	C turnover	3	FOM HUM (51%) ROM (49%)	0.69 52.08 2159.83	Topsoil 0-25 Subsoil 25-100	Croplands	Temperate	Mid-term	Monthly	Average monthly air temperature (°C). Average monthly precipitations (mm). Optional atmospheric 14C content	Clay content (%). C:N ratio. Initial SOC (Mg C ha^{-1}). Bulk density	Yearly input of plant residues (Mg C ha^{-1}). Yearly input of FYM manure (Mg C ha^{-1})	Annual SOC turnover and CO_2	X			X	Denmark, UK, Sweden	[47], [48], [49], [50], [51], [52]
CANDY (Carbon and Nitrogen Dynamics)	CANDY3.Agro	-	4	FOM	2.5	0-200 (by	Cropland	Cold and	Short	Daily	Daily mean air temperature (°C)	Soil moisture (%). Clay and fine silt	Annual N deposition from	Soil C and N dynamics. SOC	X			X	Germany, USA, UK,	[53], [54],

Model	Latest Version Model tune	Pools (#)	Carbon pools (size %)	MRT (years)	Soil depth (cm)	Land use types	Climate	Timescale Timestep	Inputs			Outputs	Adapted to new C inputs		Accepted		Locations tested	Ref
									Climate	Soil	Farming		Yes	No	High	Low		
			AOM	7.14	layers of 10 cm)				. Daily precipitation (mm). Daily global radiation (MJ m^{-2}) or daily sunshine (h)	particles ≤ 6.3 µm (%). Depth of the soil layer (dm).	atmosphere (kg ha^{-1}). Crop rotation, date of sowing, date of emergence, date of harvest. Main product (dt ha^{-1}), crop nitrogen uptake (kg ha^{-1}). Increase of livestock units and decrease of livestock units (premanent grasslands). Organic inputs date, amount (kg ha^{-1}), type (manure, slurry, and compost), C content. Mineral fertilizer type, date and amount (kg ha^{-1}). Tillage type, date and depth (cm).	stocks, OM turnover, N uptake by crops, leaching and water quality. Water balance CANDY calculates a Biological Active Tme (BAT) to assess the OM turnover and steady state. Fertilizer application scheme.					Russia, Ukraine, Belarus	[55], [56], [57], [58], [59]
			S-SOM	20														
			LTS-SOM	Inert														
DAISY [60]	DAISY6.32	Agro-ecosystem	3 to 6	AOM fast (40%)	0.05	-	Croplands	Cold and temperate	Short-term Hourly	Average air temperature, Precipitation, Global radiation. Weather station location (longitude and latitude), elevation,	Soil texture (clay, sit and sand fractions). Humus content and C:N ratio. Maximum root depth. Location of the groundwater, wether the soil is drained. Data is required for all the	Date, rate and type of fertilizer. Irrigation: amount, type of application, and mineral fertilizer in the water. Tillage. Crop rotations. Harvesting time,	Water, heat, solute, and OM balances. Crop production. Water flow, drain, uptake by plants, infiltration and run-off.		X		X	Denmark, UK, Chile, Czech Republic,	[60], [61], [62], [63], [64], [65], [66], [67], [59]
			AOM slow (60%; To SMB fast: 50%, To SMB slow: 50%)	0.23														
			SMB fast (50%, To	0.27														

Model	Latest Version Model tune	Pools (#)	Carbon pools (size %)	MRT (years)	Soil depth (cm)	Land use types	Climate	Timescale Timestep	Inputs			Outputs	Adapted to new C inputs		Accepted		Locations tested	Ref
									Climate	Soil	Farming		Yes	No	High	Low		
			SOM fast:60%)						recorded at field or surface, screen height, average temperature, Wet and dry deposition of NH_4 and NO_3. Additional : Vapor pressure, relative humidity and wind speed.	horizons. Additional: BD, average yearly carbon input before the simulation, N yield from a non-fertilized crop, retention curve of a point (field capacity, wilting point), saturated hydraulic conductivity, unsaturated hydraulic conductivity. Detailed: Moisture content over time, drain flow, nitrate content in soil moisture, nitrate concentration in drain flow	stubble height, and fate of residuals. Crop yield, root depth of the crop. Additional: DM and N content of individual crop parts, crop height, canopy cover, LAI.	Simulation of C and N dynamics. Degradation, sorptionm uptake and transport of agrochemicals and pesticides.						
			SMB slow (50%, To SOM fast:60%)	14.81														
			SOM fast (60%)	19.57														
			SOM slow (To SOM slow: 10%)	1014.71														
			SOM inert	Inert														
ORCHIDEE (Organizing Carbon and Hydrology in Dynamic Ecosystems) [68]	2	Agro-cosystem	3	Active SOM pool (2%)	0.5-1	0-200 (11 layers)	Croplands, Grasslasnd, Forest lands, Bare	Tropical, Temperate, Boreal	Short-term, Mid-term, Long-term Half hourly, Daily Annual	Daily minimum and maximum near-surface air temperature (K). Wind speed (m s^{-1}). Daily Precipitation (mm d^{-1}). Surface air pressure (hPa). Solar and infrared incoming	Soil map. Moisture (%). Clay content (%). Floodplain map to route the runoff processes. Irrigation map	Initial vegetation distribution. LAI if biogeochemical processes are off. 14 plant functional types: tree or grass (tropical, temperate, and boreal), needleleaf or broadleaf, evergreen, summer-green or	CO_2, H_2O and C fluxes. Heat exchanged with the atmosphere. Half hourly photosynthesis and energy balance. Daily C dynamics, including allocation, respiration, foliar	X	X			Africa, Brazil, France, Scotland, UK, USA, Cina, Belgium, Germany	[68], [69], [70], [71], [72], [73], [74], [75]

Model	Latest Version Model tune	Pools (#)	Carbon pools (size %)	MRT (years)	Soil depth (cm)	Land use types	Climate	Timescale Timestep	Inputs			Outputs	Adapted to new C inputs		Accepted		Locations tested	Ref
									Climate	Soil	Farming		Yes	No	High	Low		
			Slow SOM pool (45-60%)	10-50					radiation (W m^{-2}). Specific humidity (kg kg^{-1}). CO_2 concentration		rain green crops. Amount of FOC ammended (g C kg^{-1} dry soil). Lignin:C ratio of FOC, C:N ratio of FOC	developmetn and SOM decomposition.						
			Passive SOM pool** (45-50%)	400-4000														
EPIC (Environmental Policy Integrated Climate) [76]	V.0810 - V.1102	Soil erosion	3[a]	Structural litter (lignin). Allocated in Slow pool (70%) Metabolic liter. Allocated in Biomass pool (55-60%) Microbial biomass (3 - 5%)	13.59-2950	Topsoil and subsoils (10 layers)	Cropland	Temperate Tropical	Longterm Daily	Monthly mean and standard deviation, and daily values of of max and min air temperatue (°C), precipitation (mm), solar radiation (MJ/m2 or Langley), relative humidity, and wind speed (m/s). Probability of wet day after dry day and viceversa, rain (days/month), and maximum half hour rainfall (mm).	Farm location. Soil albedo, initial water content, depth to water, CaCO3 content, thickness of the layer, bulk density, san and silt content, pH, initial organic N concentration, CEC, coarse fragment, Initial NO3, Initial labile P, P sorption ratio, etc.	Schedule for crop rotations, tillage, and management events (fertilizing, harvesting, sowing. EPIC provides an editable databse with the characteristics and growth of 56 crops (100 plants including trees and grasses). Type of machinery used for tillage operations. Fertilizer name, cost, and composition. Solubility, half-life, and carbon adsroption coeffcieitne of pesticides applied.	Soil physical properties variation. Changes in soil, water, nutrient uptake, pesticide fate, and crop yields. Water quality, N and C cycling, climate change impacts, erosion effects, and atmospheric CO_2 effects	X		X		USA, China, Canada, Argentina, Germany, Italy, Cambodia, South Africa	[76], [77], [78], [79], [80], [81], [82], [83], [84]
			Slow humus (30 - 70%)															
			Passive humus	Inert														
APSIM The Agric v7.1		Agro-ecosy	3[b]	FOM FOM1 (fast) FOM2 (slow)	5.55 - 1142.86	Topsoils and subsoil	Grasslands,	Global	Longt	Daily	Daily radiation, minimum and maximum	APSIM module contains generic soil profiles for different	Types of crop, pastures, and surface residues.	Soil water, C, N, and P dynamics, cycling of nitrate,	X		X		Australia, New	[85], [86], [87],

Model	Latest Version	Model type	Pools (#)	Carbon pools (size %)	MRT (years)	Soil depth (cm)	Land use types	Climate	Timescale	Timestep	Inputs			Outputs	Adapted to new C inputs		Accepted		Locations tested	Ref
											Climate	Soil	Farming		Yes	No	High	Low		
				FOM3 (medium) BIOM HUM IOM	Inert	s. No maximum deep, but for agricultural soils 0-200					temperature and precipitation	locations. Variables : texture, SOC content, rooting depth	Tillage, grazing, intercropping, irrigation, fertilization, LAI, height of crops.	ammonium and other solutes, nitrification and denitrification processes, N_2, N_2O emissions, crop P uptake and growth, citrate efflux,					Zealand, Africa, Asia,	[88], [89], [90], [91], [92], [93], [94]
STICS (Simulateur mulTIdisciplinaire pour les Cultures Standard) [95]	STICSv.10	Agro-ecosystem	6	Microbial Biomass Humified Stable pool (65%)	36-2062	0-30 cm	Croplands	Temperate	Longterm	Daily	Radiation, min and max temeratures, rainfall, reference evapotranspiration wind, and humidity.	Water content. Mineral and organic N content. Root density distribution. Bulk density. Initial SOC. pH, $CaCO_3$	Crops above-ground biomass, N content, LAI, number of crops, harvested organs. Crop temperature. Senescence (leaf timespan). Fertilization, crop rotation, grazing, sowing, tillage	Plant growth, water, C and N fluxes. It allows to consider biomass or grain productivity and quality, N storage, nitrate leaching, N_2, N_2O, NH_3, and CO_2 emissions.		X		X	France, Canada	[95], [96], [97], [97], [98], [99], [20]
DNDC (DeNitrification-DeComposition) [100]	v9.5	Agro-ecosystems	6	Very labile litter Labile litter Resistant litter Labile microbes Resistant microbes Labile humads Resistant humads Passive hum	-	0-50 (by layers of 10 cm)	Grasslands, Cropland	Global. Tested arround the world	Longterm	Day - Year	Daily precipitation and max and min temperatures	BD, texture, clay fraction, porosity, conductivity, pH, organic carbon content, field capacity, wilting point.. Soil thermal and hydraulic propierties. Location coordinates. GIS	Crop rotations and manure addition. LAI. Cropping practices: fertilization, irrigation, tillage, flooding, grazing, and weeding. Nutrients addition. Annual litter and root C input.	Soil physical parameters: temperature, moisture, pH, redox potential, erosion. Plant growth (crop yield). Soil C and N dynamics, dissolved organic carbon, N leaching, gasseous emissions (e.g., N_2O, NO, N_2,		X	X		USA, Costa Rica, Europe, Australia, UK, Canada, India, China, Japan, Thailand, New Zealand, Germany, Belgium, Canada, Ireland, France, Switzerland, Netherlands,	[100], [101], [102], [103], [104], [105], [106], [107],

Model	Latest Version	Model type	Pools (#)	Carbon pools (size %)	MRT (years)	Soil depth (cm)	Land use types	Climate	Timescale	Timestep	Inputs			Outputs	Adapted to new C inputs		Accepted		Locations tested	Ref
											Climate	Soil	Farming		Yes	No	High	Low		
														NH_3, CH_4 and CO_2)					UK, France, Morocco	[108], [20], [109], [90], [110]

[a] 3 pools plus 2 pools for litter matter decomposition; [b] 3 pools plus 3 pools for FOM decomposition. DPM: Decomposable plant material; RPM: Resistant plant material; BIO: Microbial Biomass; HUM: Humified organic matter; IOM: Inert Organic Matter; SOM: Soil Organic Matter; FYM: Farmyard manure; FOM: Fresh Organic Matter; EOM: Exogenous Organic Matter; SOC: Soil Organic Carbon; MRT: Mean Residence Time; ROM: Resistant Organic Matter; AOM: Active soil Organic Matter; S-SOM: Stabilized soil organic Matter; LTS-SOM: Long term stabilized soil organic matter; BAOM: Biological Active soil Organic Matter; BAT: Biological Active Time; FOC: Fresh Organic Carbon; SMB: Soil microbial biomass; SOM: Soil Orgnaic Matter; FOM: Fresh Organic Matter; FOMS: Soluble fraction of FOM; FOML: Labile fraction of FOM; FOMR: Resistant fraction of FOM; LAI: Leaf Area Index; BD: Bulk density; DOM: Dissolved Organic Matter; AOM: Active Organic Matter; ROM: Refractory Organic Matter; Min: Minimum; Max: Maximum; OM: Organic matter; USA: United States of America; EU: European Union; UK: United Kingdom

References SI 1.2

[1] Parton WJ, Schimel DS, Cole CV, Ojima DS. Analysis of Factors Controlling Soil Organic Matter Levels in Great Plains Grasslands. Soil Science Society of America Journal 1987;51:1173–9. https://doi.org/10.2136/sssaj1987.03615995005100050015x.

[2] Parton B, Ojima D, Del Grosso S, Keough C. CENTURY tutorial. Supplement to Century User's Manual 2001.

[3] Falloon P, Smith P. Simulating SOC changes in long-term experiments with RothC and CENTURY: model evaluation for a regional scale application. Soil Use and Management 2002;18:101–11. https://doi.org/10.1111/j.1475-2743.2002.tb00227.x.

[4] Cerri CEP, Paustian K, Bernoux M, Victoria RL, Melillo JM, Cerri CC. Modeling changes in soil organic matter in Amazon forest to pasture conversion with the Century model: MODELING SOM IN AMAZON FOREST-PASTURE CONVERSION. Global Change Biology 2004;10:815–32. https://doi.org/10.1111/j.1365-2486.2004.00759.x.

[5] Sobocká J, Balkovič J, Lapin M. A CENTURY 5 model using for estimation of soil organic matter behaviour at predicted climate change. Soil & Water Res 2008;2:25–34. https://doi.org/10.17221/2099-SWR.

[6] Cerri CEP, Easter M, Paustian K, Killian K, Coleman K, Bernoux M, et al. Simulating SOC changes in 11 land use change chronosequences from the Brazilian Amazon with RothC and Century models. Agriculture, Ecosystems & Environment 2007;122:46–57. https://doi.org/10.1016/j.agee.2007.01.007.

[7] Lugato E, Jones A. Modelling Soil Organic Carbon Changes Under Different Maize Cropping Scenarios for Cellulosic Ethanol in Europe. Bioenerg Res 2015;8:537–45. https://doi.org/10.1007/s12155-014-9529-2.

[8] Parton WJ, Ojima DS, Cole CV, Schimel DS. A general model for soil organic matter dynamics: sensitivity to litter chemistry, texture and management. Quantitative Modeling of Soil Forming Processes 1994;39:147–67.

[9] Parton WJ, Holland EA, Del Grosso SJ, Hartman MD, Martin RE, Mosier AR, et al. Generalized model for NO x and N2O emissions from soils. Journal of Geophysical Research: Atmospheres 2001;106:17403–19. https://doi.org/10.1029/2001JD900101.

[10] Del Grosso SJ, Parton WJ, Mosier AR, Hartman MD, Brenner J, Ojima DS, et al. Simulated interaction of carbon dynamics and nitrogen trace gas fluxes using the DAYCENT model. Modeling Carbon and Nitrogen Dynamics for Soil Management 2001;303:332.

[11] Stehfest E, Müller C. Simulation of N2O emissions from a urine-affected pasture in New Zealand with the ecosystem model DayCent. Journal of Geophysical Research: Atmospheres 2004;109. https://doi.org/10.1029/2003JD004261.

[12] Li Y, Chen D, Zhang Y, Edis R, Ding H. Comparison of three modeling approaches for simulating denitrification and nitrous oxide emissions from loam-textured arable soils. Global Biogeochemical Cycles 2005;19. https://doi.org/10.1029/2004GB002392.

[13] Li X, Meixner T, Sickman JO, Miller AE, Schimel JP, Melack JM. Decadal-scale Dynamics of Water, Carbon and Nitrogen in a California Chaparral Ecosystem: DAYCENT Modeling Results. Biogeochemistry 2006;77:217–45. https://doi.org/10.1007/s10533-005-1391-z.

[14] Del Grosso SJ, Parton WJ, Mosier AR, Walsh MK, Ojima DS, Thornton PE. DAYCENT National-Scale Simulations of Nitrous Oxide Emissions from Cropped Soils in the United States. Journal of Environmental Quality 2006;35:1451–60. https://doi.org/10.2134/jeq2005.0160.

[15] Stehfest E, Heistermann M, Priess JA, Ojima DS, Alcamo J. Simulation of global crop production with the ecosystem model DayCent. Ecological Modelling 2007;209:203–19. https://doi.org/10.1016/j.ecolmodel.2007.06.028.

[16] Del Grosso SJ, Halvorson AD, Parton WJ. Testing DAYCENT Model Simulations of Corn Yields and Nitrous Oxide Emissions in Irrigated Tillage Systems in Colorado. J Environ Qual 2008;37:1383–9. https://doi.org/10.2134/jeq2007.0292.

[17] Fitton N, Datta A, Hastings A, Kuhnert M, Topp CFE, Cloy JM, et al. The challenge of modelling nitrogen management at the field scale: simulation and sensitivity analysis of N $\less$sub$\greater$2$\less$/sub$\greater$ O fluxes across nine experimental sites using DailyDayCent. Environ Res Lett 2014;9:095003. https://doi.org/10.1088/1748-9326/9/9/095003.

[18] Necpálová M, Anex RP, Fienen MN, Del Grosso SJ, Castellano MJ, Sawyer JE, et al. Understanding the DayCent model: Calibration, sensitivity, and identifiability through inverse modeling. Environmental Modelling & Software 2015;66:110–30. https://doi.org/10.1016/j.envsoft.2014.12.011.

[19] Bista P, Machado S, Ghimire R, Del Grosso SJ, Reyes-Fox M. Simulating Soil Organic Carbon in a Wheat–Fallow System Using the Daycent Model. Agronomy Journal 2016;108:2554–65. https://doi.org/10.2134/agronj2016.04.0202.

[20] Sansoulet J, Pattey E, Kröbel R, Grant B, Smith W, Jégo G, et al. Comparing the performance of the STICS, DNDC, and DayCent models for predicting N uptake and biomass of spring wheat in Eastern Canada. Field Crops Research 2014;156:135–50. https://doi.org/10.1016/j.fcr.2013.11.010.

[21] Della Chiesa T, Piñeiro G, Del Grosso SJ, Parton WJ, Araujo PI, Yahdjian L. Higher than expected N2O emissions from soybean crops in the Pampas Region of Argentina: Estimates from DayCent simulations and field measurements. Science of The Total Environment 2022;835:155408. https://doi.org/10.1016/j.scitotenv.2022.155408.

[22] Jenkinson D s., Coleman K. Calculating the annual input of organic matter to soil from measurements of total organic carbon and radiocarbon. European Journal of Soil Science 1994;45:167–74. https://doi.org/10.1111/j.1365-2389.1994.tb00498.x.

[23] Coleman K, Jenkinson DS. RothC-26.3 - A Model for the turnover of carbon in soil. In: Powlson DS, Smith P, Smith JU, editors. Evaluation of Soil Organic Matter Models, Berlin, Heidelberg: Springer Berlin Heidelberg; 1996, p. 237–46. https://doi.org/10.1007/978-3-642-61094-3_17.

[24] Falloon PD, Smith P, Smith JU, Szabó J, Coleman K, Marshall S. Regional estimates of carbon sequestration potential: linking the Rothamsted Carbon Model to GIS databases 1998:6.

[25] Jenkinson DS, Coleman K. The turnover of organic carbon in subsoils. Part 2. Modelling carbon turnover. European Journal of Soil Science 2008:14.

[26] Barančíková G, Halás J, Gutteková M, Makovníková J, Nováková M, Skalský R, et al. Application of RothC model to predict soil organic carbon stock on agricultural soils of Slovakia. Soil & Water Res 2010;5:1–9. https://doi.org/10.17221/23/2009-SWR.

[27] González-Molina L, Etchevers-Barra JD, Paz-Pellat F, Díaz-Solis H, Fuentes-Ponce MH, Covaleda-Ocón S, et al. Performance of the RothC-26.3 model in short-term experiments in Mexican sites and systems. J Agric Sci 2011;149:415–25. https://doi.org/10.1017/S0021859611000232.

[28] Molina LG, Moreno Pérez E del C, Krishnamurty LR, Pérez AB, Miguel AM. Simulación de los cambios de carbono orgánico del suelo en sistema de cultivo con higuerilla por el modelo RothC. Pesq agropec bras 2012;47:1647–54. https://doi.org/10.1590/S0100-204X2012001100012.

[29] Peltre C, Christensen BT, Dragon S, Icard C, Kätterer T, Houot S. RothC simulation of carbon accumulation in soil after repeated application of widely different organic amendments. Soil Biology 2012:20.

[30] Jiang G, Shirato Y, Xu M, Yagasaki Y, Huang Q, Li Z, et al. Testing the modified Rothamsted Carbon Model for paddy soils against the results from long-term experiments in southern China. Soil Science and Plant Nutrition 2013;59:16–26. https://doi.org/10.1080/00380768.2012.733923.

[31] Farina R, Sándor R, Abdalla M, Álvaro-Fuentes J, Bechini L, Bolinder MA, et al. Ensemble modelling, uncertainty and robust predictions of organic carbon in long-term bare-fallow soils 2020:25. https://doi.org/10.1111/gcb.15441.

[32] Nemo, Klumpp K, Coleman K, Dondini M, Goulding K, Hastings A, et al. Soil Organic Carbon (SOC) Equilibrium and Model Initialisation Methods: an Application to the Rothamsted Carbon (RothC) Model. Environ Model Assess 2017;22:215–29. https://doi.org/10.1007/s10666-016-9536-0.

[33] Meyer RS. Potential impacts of climate change on soil organic carbon and productivity in pastures of south eastern Australia. Agricultural Systems 2018:13.

[34] Mishra G. Modeling soil organic carbon dynamics under shifting cultivation and forests using Rothc model. Ecological Modelling 2019:9.

[35] Morais TG, Teixeira RFM, Domingos T. Detailed global modelling of soil organic carbon in cropland, grassland and forest soils. PLOS ONE 2019:27.

[36] Shirato Y. Use of models to evaluate carbon sequestration in agricultural soils. Soil Science and Plant Nutrition 2020;66:21–7. https://doi.org/10.1080/00380768.2019.1702477.

[37] Andriulo A, Mary B, Guerif J. Modelling soil carbon dynamics with various cropping sequences on the rolling pampas. Agronomie 1999;19:365–77. https://doi.org/10.1051/agro:19990504.

[38] Saffih-Hdadi K, Mary B. Modeling consequences of straw residues export on soil organic carbon. Soil Biology and Biochemistry 2008;40:594–607. https://doi.org/10.1016/j.soilbio.2007.08.022.

[39] Kintché K, Guibert H, Sogbedji JM, Levêque J, Tittonell P. Carbon losses and primary productivity decline in savannah soils under cotton-cereal rotations in semiarid Togo. Plant Soil 2010;336:469–84. https://doi.org/10.1007/s11104-010-0500-5.

[40] Milesi Delaye LA, Irizar AB, Andriulo AE, Mary B. Effect of Continuous Agriculture of Grassland Soils of the Argentine Rolling Pampa on Soil Organic Carbon and Nitrogen. Applied and Environmental Soil Science 2013;2013:1–17. https://doi.org/10.1155/2013/487865.

[41] Autret B, Mary B, Chenu C, Balabane M, Girardin C, Bertrand M, et al. Alternative arable cropping systems: A key to increase soil organic carbon storage? Results from a 16 year field experiment. Agriculture, Ecosystems & Environment 2016;232:150–64. https://doi.org/10.1016/j.agee.2016.07.008.

[42] Clivot H, Mouny J-C, Duparque A, Dinh J-L, Denoroy P, Houot S, et al. Modeling soil organic carbon evolution in long-term arable experiments with AMG model. Environmental Modelling & Software 2019;118:99–113. https://doi.org/10.1016/j.envsoft.2019.04.004.

[43] Martinez JP, Crespo C, Rozas HS, Echeverría H, Studdert G, Martinez F, et al. Soil organic carbon in cropping sequences with predominance of soya bean in the argentinean humid Pampas n.d.:11.

[44] Mary B, Clivot H, Blaszczyk N, Labreuche J, Ferchaud F. Soil carbon storage and mineralization rates are affected by carbon inputs rather than physical disturbance: Evidence from a 47-year tillage experiment. Agriculture, Ecosystems & Environment 2020;299:106972. https://doi.org/10.1016/j.agee.2020.106972.

[45] Levavasseur F, Mary B, Christensen BT, Duparque A, Ferchaud F, Kätterer T, et al. The simple AMG model accurately simulates organic carbon storage in soils after repeated application of exogenous organic matter. Nutrient Cycling in Agroecosystems 2020:15.

[46] Nowak B, Marliac G. Optimization of carbon stock models to local conditions using farmers' soil tests: A case study with AMGv2 for a cereal plain in central France n.d.:13.

[47] Petersen BM, Olesen JE, Heidmann T. A flexible tool for simulation of soil carbon turnover. Ecological Modelling 2002;151:1–14. https://doi.org/10.1016/S0304-3800(02)00034-0.

[48] Taghizadeh-Toosi A, Christensen BT, Hutchings NJ, Vejlin J, Kätterer T, Glendining M, et al. C-TOOL: A simple model for simulating whole-profile carbon storage in temperate agricultural soils. Ecological Modelling 2014;292:11–25. https://doi.org/10.1016/j.ecolmodel.2014.08.016.

[49] Taghizadeh-Toosi A, Christensen BT, Glendining M, Olesen JE. Consolidating soil carbon turnover models by improved estimates of belowground carbon input. Scientific Reports 2016;6:32568. https://doi.org/10.1038/srep32568.

[50] Taghizadeh-Toosi A, Olesen JE. Modelling soil organic carbon in Danish agricultural soils suggests low potential for future carbon sequestration. Agricultural Systems 2016;145:83–9. https://doi.org/10.1016/j.agsy.2016.03.004.

[51] Keel SG, Leifeld J, Mayer J, Taghizadeh-Toosi A, Olesen JE. Large uncertainty in soil carbon modelling related to method of calculation of plant carbon input in agricultural systems: Uncertainty in soil carbon modelling. Eur J Soil Sci 2017;68:953–63. https://doi.org/10.1111/ejss.12454.

[52] Hansen JH, Hamelin L, Taghizadeh-Toosi A, Olesen JE, Wenzel H. Agricultural residues bioenergy potential that sustain soil carbon depends on energy conversion pathways 2020:12.

[53] Franko U, Oelschlägel B, Schenk S. Simulation of temperature-, water- and nitrogen dynamics using the model CANDY. Ecological Modelling 1995;81:213–22. https://doi.org/10.1016/0304-3800(94)00172-E.

[54] Franko U. Simulating trends in soil organic carbon in long-term experiments using the CANDY model 1997:12.

[55] Puhlmann M, Kuka K, Franko U. Comparison of methods for the estimation of inert carbon suitable for initialisation of the CANDY model 2006:11.

[56] Franko U, Kuka K, Romanenko IA, Romanenkov VA. Validation of the CANDY model with Russian long-term experiments 2007:13.

[57] Smith P, Smith JU, Franko U, Kuka K, Romanenkov VA, Shevtsova LK, et al. Changes in mineral soil organic carbon stocks in the croplands of European Russia and the Ukraine, 1990–2070; comparison of three models and implications for climate mitigation. Reg Environ Change 2007;7:105–19. https://doi.org/10.1007/s10113-007-0028-2.

[58] Franko U, Kolbe H, Thiel E, Ließ E. Multi-site validation of a soil organic matter model for arable fields based on generally available input data. Geoderma 2011;166:119–34. https://doi.org/10.1016/j.geoderma.2011.07.019.

[59] Ghaley BB. Simulation of Soil Organic Carbon Effects on Long-Term Winter Wheat (Triticum aestivum) Production Under Varying Fertilizer Inputs. Frontiers in Plant Science 2018;9:9.

[60] Hansen S, Jensen HE, Nielsen NE, Svendsen H. DAISY: Soil Plant Atmosphere System Model. Copenhagen: The National Agency for Environmental Protection; 1990.

[61] Jensen LS, Mueller T, Nielsen NE, Hansen S, Crocker GJ, Grace PR, et al. Simulating trends in soil organic carbon in long-term experiments using the soil-plant-atmosphere model DAISY. Geoderma 1997;81:5–28. https://doi.org/10.1016/S0016-7061(97)88181-5.

[62] Hansen S. Daisy, a flexible Soil-Plant-Atmosphere system Model 2002:47.

[63] Müller T, Magid J, Jensen LS, Nielsen NE. Decomposition of plant residues of different quality in soil—DAISY model calibration and simulation based on experimental data. Ecological Modelling 2003;166:3–18. https://doi.org/10.1016/S0304-3800(03)00114-5.

[64] Bruun S, Christensen BT, Hansen EM, Magid J, Jensen LS. Calibration and validation of the soil organic matter dynamics of the Daisy model with data from the Askov long-term experiments. Soil Biology and Biochemistry 2003;35:67–76. https://doi.org/10.1016/S0038-0717(02)00237-7.

[65] Müller T, Thorup-Kristensen K, Magid J, Jensen LS, Hansen S. Catch crops affect nitrogen dynamics in organic farming systems without livestock husbandry—Simulations with the DAISY model. Ecological Modelling 2006;191:538–44. https://doi.org/10.1016/j.ecolmodel.2005.05.026.

[66] Hansen S, P. Abrahamsen, C. T. Petersen, M. Styczen. Daisy: Model Use, Calibration, and Validation. Transactions of the ASABE 2012;55:1317–35. https://doi.org/10.13031/2013.42244.

[67] Salazar O, Nájera F, Tapia W, Casanova M. Evaluation of the DAISY model for predicting nitrogen leaching in coarse-textured soils cropped with maize in the Mediterranean zone of Chile. Agricultural Water Management 2017;182:77–86. https://doi.org/10.1016/j.agwat.2016.12.005.

[68] Krinner G, Viovy N, de Noblet-Ducoudré N, Ogée J, Polcher J, Friedlingstein P, et al. A dynamic global vegetation model for studies of the coupled atmosphere-biosphere system: DVGM FOR COUPLED CLIMATE STUDIES. Global Biogeochem Cycles 2005;19. https://doi.org/10.1029/2003GB002199.

[69] Morales P, Sykes MT, Prentice IC, Smith P, Smith B, Bugmann H, et al. Comparing and evaluating process-based ecosystem model predictions of carbon and water fluxes in major European forest biomes. Global Change Biol 2005;11:2211–33. https://doi.org/10.1111/j.1365-2486.2005.01036.x.

[70] Tan K, Ciais P, Piao S, Wu X, Tang Y, Vuichard N, et al. Application of the ORCHIDEE global vegetation model to evaluate biomass and soil carbon stocks of Qinghai-Tibetan grasslands. Global Biogeochemical Cycles 2010;24. https://doi.org/10.1029/2009GB003530.

[71] Verbeeck H, Peylin P, Bacour C, Bonal D, Steppe K, Ciais P. Seasonal patterns of CO 2 fluxes in Amazon forests: Fusion of eddy covariance data and the ORCHIDEE model. J Geophys Res 2011;116:G02018. https://doi.org/10.1029/2010JG001544.

[72] Traore AK, Ciais P, Vuichard N, Poulter B, Viovy N, Guimberteau M, et al. Evaluation of the ORCHIDEE ecosystem model over Africa against 25 years of satellite-based water and carbon measurements. Journal of Geophysical Research 2014:22.

[73] Guenet B, Moyano FE, Peylin P, Ciais P, Janssens IA. Towards a representation of priming on soil carbon decomposition in the global land biosphere model ORCHIDEE (version 1.9.5.2). Geosci Model Dev 2016;9:841–55. https://doi.org/10.5194/gmd-9-841-2016.

[74] Raoult N, Ottlé C, Peylin P, Bastrikov V, Maugis P. Evaluating and Optimizing Surface Soil Moisture Drydowns in the ORCHIDEE Land Surface Model at In Situ Locations. Journal of Hydrometeorology 2021;22:1025–43. https://doi.org/10.1175/JHM-D-20-0115.1.

[75] Mahmud K, Scott RL, Biederman JA, Litvak ME, Kolb T, Meyers TP, et al. Optimizing Carbon Cycle Parameters Drastically Improves Terrestrial Biosphere Model Underestimates of Dryland Mean Net CO2 Flux and its Inter-Annual Variability. Journal of Geophysical Research: Biogeosciences 2021;126:e2021JG006400. https://doi.org/10.1029/2021JG006400.

[76] Williams JR, Jones CA, Dyke PT. A modeling approach to determining the relationship between erosion and soil productivity [EPIC, Erosion-Productivity Impact Calculator, mathematical models]. Trans ASAE, 1984.

[77] Bernardos JN, Viglizzo EF, Jouvet V, Lértora FA, Pordomingo AJ, Cid FD. The use of EPIC model to study the agroecological change during 93 years of farming transformation in the Argentine pampas. Agricultural Systems 2001;69:215–34. https://doi.org/10.1016/S0308-521X(01)00027-0.

[78] Izaurralde R, Williams JR, McGill W, Rosenberg N, Jakas M. Simulating soil C dynamics with EPIC: Model description and testing against long-term data 2006. https://doi.org/10.1016/J.ECOLMODEL.2005.07.010.

[79] Farina R, Seddaiu G, Orsini R, Steglich E, Roggero PP, Francaviglia R. Soil carbon dynamics and crop productivity as influenced by climate change in a rainfed cereal system under contrasting tillage using EPIC. Soil and Tillage Research 2011;112:36–46. https://doi.org/10.1016/j.still.2010.11.002.

[80] Wang X, Kemanian AR, Williams JR. Special Features of the EPIC and APEX Modeling Package and Procedures for Parameterization, Calibration, Validation, and Applications. Methods of Introducing System Models into Agricultural Research, vol. 2, Wiley Online Library; 2011.

[81] Wang X, R. Williams J, W. Gassman P, Baffaut C, C. Izaurralde R, Jeong J, et al. EPIC and APEX: Model Use, Calibration, and Validation. Transactions of the ASABE 2012;55:1447–62. https://doi.org/10.13031/2013.42253.

[82] Izaurralde RC, Mcgill WB, Williams JR. Development and application of the EPIC model for carbon cycle, greenhouse-gas mitigation, and biofuel studies. M Liebig, AJ Franzluebbers and R Follett; Academic Press, Waltham, MA, United States(US).; 2012.

[83] Balkovič J, van der Velde M, Schmid E, Skalský R, Khabarov N, Obersteiner M, et al. Pan-European crop modelling with EPIC: Implementation, up-scaling and regional crop yield validation. Agricultural Systems 2013;120:61–75. https://doi.org/10.1016/j.agsy.2013.05.008.

[84] Gerik T, Williams JR, Dagitz S, Magre M, Meinardus A, Steglich E, et al. Environmental Policy Integrated Cimate Model - User's Manual version 0810 2015.

[85] Keating BA, Carberry PS, Hammer GL, Probert ME, Robertson MJ, Holzworth D, et al. An overview of APSIM, a model designed for farming systems simulation. European Journal of Agronomy 2003;18:267–88. https://doi.org/10.1016/S1161-0301(02)00108-9.

[86] Thorburn PJ, Biggs JS, Collins K, Probert ME. Using the APSIM model to estimate nitrous oxide emissions from diverse Australian sugarcane production systems. Agriculture, Ecosystems & Environment 2010;136:343–50. https://doi.org/10.1016/j.agee.2009.12.014.

[87] Akponikpè PBI, Gérard B, Michels K, Bielders C. Use of the APSIM model in long term simulation to support decision making regarding nitrogen management for pearl millet in the Sahel. European Journal of Agronomy 2010;32:144–54. https://doi.org/10.1016/j.eja.2009.09.005.

[88] Balwinder-Singh, Gaydon DS, Humphreys E, Eberbach PL. The effects of mulch and irrigation management on wheat in Punjab, India—Evaluation of the APSIM model. Field Crops Research 2011;124:1–13. https://doi.org/10.1016/j.fcr.2011.04.016.

[89] Holzworth DP, Huth NI, deVoil PG, Zurcher EJ, Herrmann NI, McLean G, et al. APSIM – Evolution towards a new generation of agricultural systems simulation. Environmental Modelling & Software 2014;62:327–50. https://doi.org/10.1016/j.envsoft.2014.07.009.

[90] Giltrap D, Vogeler I, Cichota R, Luo J, van der Weerden T, de Klein C. Comparison between APSIM and NZ-DNDC models when describing N-dynamics under urine patches. New Zealand Journal of Agricultural Research 2015;58:131–55. https://doi.org/10.1080/00288233.2014.987876.

[91] O'Leary GJ, Liu DL, Ma Y, Li FY, McCaskill M, Conyers M, et al. Modelling soil organic carbon 1. Performance of APSIM crop and pasture modules against long-term experimental data. Geoderma 2016;264:227–37. https://doi.org/10.1016/j.geoderma.2015.11.004.

[92] Kisaka MO, Mucheru-Muna M, Ngetich FK, Mugwe JN, Mugendi DN, Mairura F, et al. Using APSIM-model as a decision-support-tool for long-term integrated--nitrogen-management and maize productivity under semir-arid condiutions in Kenya. Experimental Agriculture 2016;52:279–99. https://doi.org/10.1017/S0014479715000095.

[93] Gaydon DS, Balwinder-Singh, Wang E, Poulton PL, Ahmad B, Ahmed F, et al. Evaluation of the APSIM model in cropping systems of Asia. Field Crops Research 2017;204:52–75. https://doi.org/10.1016/j.fcr.2016.12.015.

[94] Cichota R, Vogeler I, Sharp J, Verburg K, Huth N, Holzworth D, et al. A protocol to build soil descriptions for APSIM simulations. MethodsX 2021;8:101566. https://doi.org/10.1016/j.mex.2021.101566.

[95] Brisson N, Mary B, Ripoche D, Jeuffroy M-H, Ruget F, Nicoullaud BB, et al. STICS: a generic model for the simulation of crops and their water and nitrogen balances. I. Theory and parameterization applied to wheat and corn. Agronomie 1998;18:311.

[96] Launay C, Constantin J, Chlebowski F, Houot S, Graux A, Klumpp K, et al. Estimating the carbon storage potential and greenhouse gas emissions of French arable cropland using high-resolution modeling. Glob Change Biol 2021;27:1645–61. https://doi.org/10.1111/gcb.15512.

[97] Brisson N, Launay M, Mary B, Beaudoin N. Conceptual basis, formalisations and parameterization of the STICS crop model. Editions Quae; 2009.

[98] Coucheney E, Buis S, Launay M, Constantin J, Mary B, García de Cortázar-Atauri I, et al. Accuracy, robustness and behavior of the STICS soil-crop model for plant, water and nitrogen outputs. Environ Model Softw 2015;64:177–90. https://doi.org/10.1016/j.envsoft.2014.11.024.

[99] Bergez JE, Raynal H, Launay M, Beaudoin N, Casellas E, Caubel J, et al. Evolution of the STICS crop model to tackle new environmental issues: New formalisms and integration in the modelling and simulation platform RECORD. Environmental Modelling & Software 2014;62:370–84. https://doi.org/10.1016/j.envsoft.2014.07.010.

[100] Li C, Frolking S, Frolking TA. A model of nitrous oxide evolution from soil driven by rainfall events: 1. Model structure and sensitivity. Journal of Geophysical Research: Atmospheres 1992;97:9759–76. https://doi.org/10.1029/92JD00509.

[101] Li C, Frolking S, Harriss R. Modeling carbon biogeochemistry in agricultural soils. Global Biogeochemical Cycles 1994;8:237–54. https://doi.org/10.1029/94GB00767.

[102] Li C, Frolking S, Crocker GJ, Grace PR, Klír J, Körchens M, et al. Simulating trends in soil organic carbon in long-term experiments using the DNDC model. Geoderma 1997;81:45–60. https://doi.org/10.1016/S0016-7061(97)00080-3.

[103] Smith WN, Desjardins RL, Grant B, Li C, Lemke R, Rochette P, et al. Testing the DNDC model using N 2 O emissions at two experimental sites in Canada. Can J Soil Sci 2002;82:365–74. https://doi.org/10.4141/S01-048.

[104] Cai Z, Sawamoto T, Li C, Kang G, Boonjawat J, Mosier A, et al. Field validation of the DNDC model for greenhouse gas emissions in East Asian cropping systems. Global Biogeochemical Cycles 2003;17. https://doi.org/10.1029/2003GB002046.

[105] Babu YJ, Li C, Frolking S, Nayak DR, Adhya TK. Field Validation of DNDC Model for Methane and Nitrous Oxide Emissions from Rice-based Production Systems of India. Nutr Cycl Agroecosyst 2006;74:157–74. https://doi.org/10.1007/s10705-005-6111-5.

[106] Abdalla M, Kumar S, Jones M, Burke J, Williams M. Testing DNDC model for simulating soil respiration and assessing the effects of climate change on the CO2 gas flux from Irish agriculture. Global and Planetary Change 2011;78:106–15. https://doi.org/10.1016/j.gloplacha.2011.05.011.

[107] Leip A, Busto M, Corazza M, Bergamaschi P, Koeble R, Dechow R, et al. Estimation of N2O fluxes at the regional scale: data, models, challenges. Current Opinion in Environmental Sustainability 2011;3:328–38. https://doi.org/10.1016/j.cosust.2011.07.002.

[108] Li C, Salas W, Zhang R, Krauter C, Rotz A, Mitloehner F. Manure-DNDC: a biogeochemical process model for quantifying greenhouse gas and ammonia emissions from livestock manure systems. Nutr Cycl Agroecosyst 2012;93:163–200. https://doi.org/10.1007/s10705-012-9507-z.

[109] Smith W, Grant B, Qi Z, He W, VanderZaag A, Drury CF, et al. Development of the DNDC model to improve soil hydrology and incorporate mechanistic tile drainage: A comparative analysis with RZWQM2. Environmental Modelling & Software 2020;123:104577. https://doi.org/10.1016/j.envsoft.2019.104577.

[110] Chaki AK, Gaydon DS, Dalal RC, Bellotti WD, Gathala MK, Hossain A, et al. How we used APSIM to simulate conservation agriculture practices in the rice-wheat system of the Eastern Gangetic Plains. Field Crops Research 2022;275:108344. https://doi.org/10.1016/j.fcr.2021.108344.

Appendix A2a

Supplementary Information of Chapter 3 – Section 1

The content of this appendix was published as supplementary information of the paper in doi.org/10.1016/j.apenergy.2022.120192 in Applied Energy, and is reproduced with permissions from the journal. The numbering of the sections, figures and tables are as presented in the original document.

The background data of this appendix is available in the following repository: https://doi.org/10.48531/JBRU.CALMIP/AUEEEJ

The crop residue conundrum: maintaining long-term soil organic carbon stocks while reinforcing the bioeconomy, compatible endeavors?

Supplementary Information 1

Christhel Andrade-Díaz[1,2,*], Hugues Clivot[3], Ariane Albers[1], Ezequiel Zamora-Ledezma[4], and Lorie Hamelin[1]

[1] Toulouse Biotechnology Institute (TBI), INSA, INRAE UMR792, and CNRS UMR5504, Federal University of Toulouse, 135 Avenue de Rangueil, F-31077, Toulouse, France.

[2] Department of Chemical, Biotechnological and Food Processes, Faculty of Mathematical, Physics and Chemistry Sciences. Universidad Técnica de Manabí (UTM), 130150 Portoviejo, Ecuador.

[3] Université de Reims Champagne Ardenne, INRAE, FARE, UMR A 614, Reims, France.

[4] Faculty of Agriculture Engineering. Universidad Técnica de Manabí (UTM), 13132 Lodana, Ecuador.

*Corresponding author: andraded@insa-toulouse.fr . ORCID: 0000-0002-2448-6186

Contents

List of Figures

List of Tables

1. Pedoclimatic data

The climate of France can be grouped into 8 typologies [1] as shown in Fig S1, while the soil texture of the agricultural lands [2] can be defined as sandy, balanced, silty, or clayey according to Fig S2.

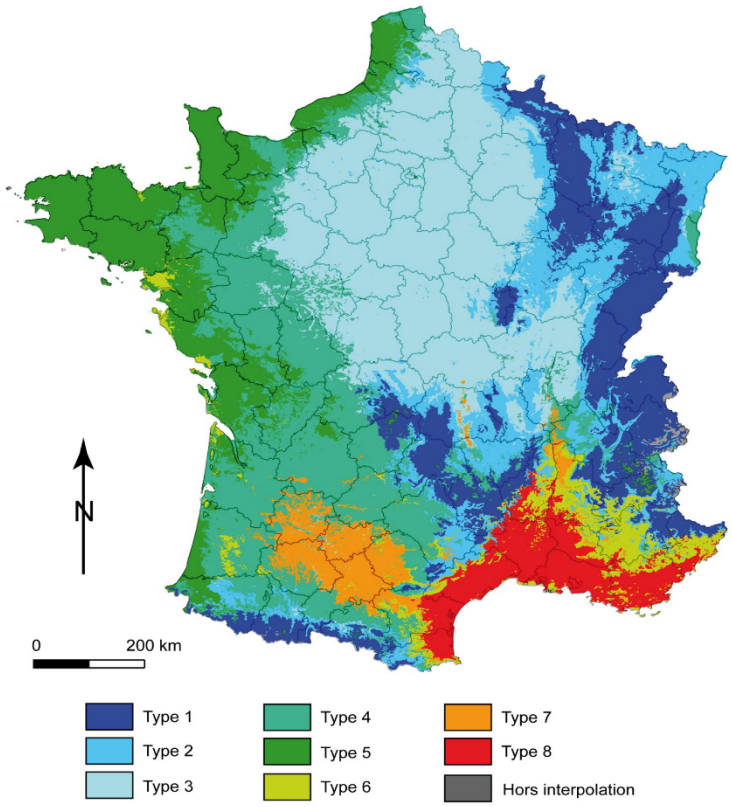

Fig S1. France climate typologies. Type 1: mountain climates, Type 2: the semi-continental climate and the climate of the mountain margins, Type 3: The degraded oceanic climate of the central and northern plains, Type 4: Altered oceanic climate, Type 5: The frank oceanic climate, Type 6: The altered Mediterranean climate, Type 7: The climate of the South-West Basin, Type 8: The frank Mediterranean climate, Hors interpolation: Out of interpolation. [1]

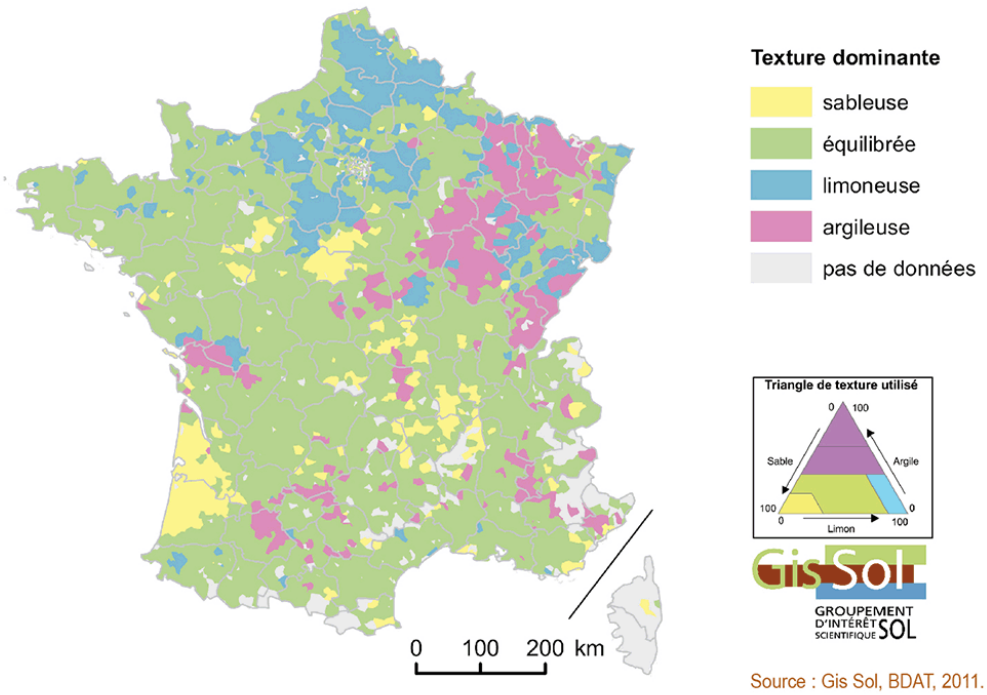

Fig S2. Dominant soil textures of the agricultural lands of France. Sableuse : sandy, équilibrée : balanced, limoneuse : silty, argileuse : clayey, pas de données : no data. Retrieved from. [2]

The APCUs in Launay et al. [3] were created using the SAFRAN grid, while the climate data input to the model in this work came from DRIAS RCP4.5, therefore some points of the grid were lost during the adaptation. Besides, we used Launay et al. [3] yields obtained from STICS modeling, where some simulation units were lost during the modeling, thus no yields were available for those units. Changing the climate grid and recycling the simulated yields are major differences from Launay et al. [3] and resulted in 11,784 APCU and 60,390 simulation units in this study vs 12,060 APCU and 62,694 simulation units in Launay et al. [3]. This also affected the total area included in the study, which decreased from 18.35 Mha to 14.89 Mha at the APCU level, and from 4.79 Mha to 3.48 Mha at the simulation unit level.

2. Crop rotations

The crop rotations were retrieved from Launay et al. [3]. Due to the high resolution of the data, a total of 1,472 crop rotations were included (or 1,588 if we considered the type of tillage as a differentiation in the rotation). The crops included in the rotations are grain and silage maize, winter wheat, winter and spring peas, rapeseed, sunflower, and sugar beet. The crop rotations also included temporary grasslands, alfalfa, and cover crops (mustard and ray-grass). Temporary grasslands, alfalfa, and cover crops were not considered to be exported for bioeconomy because they are already being fully used for other purposes such as animal

bedding and fodder (temporary grasslands and alfalfa) or are generally left on soils to maintain N levels (cover crops).

The original retrieved data included only 33 years of information, with rotation durations varying from 1 to 13 years. To account for the 100 years of modeling, we recycled the 33 years of original data. As a limitation of this work, the recycling of each 33 years meant that for some simulation units the rotations at year 33 were not completed, but the following year 34 presented the crop corresponding to the first crop in the sequence.

The product yield of each crop depends on the pedoclimatic characteristics and farming management; therefore, it varies among simulation units. We obtained the spatially explicit yields from the STICS results modeled in Launay et al. [3] and used the average value for the 30 years considered there. This means that for a given simulation unit, the grain yield in tonnes per ha of a given crop in the sequence will be the same throughout the 100 years of the modeling done in this work.

The total annual production of each crop (cover crops excluded) for the starting year 2020, as well as the technical harvestable fraction, are shown in Table S1.1. To determine the most representative crop in arable lands in France, the mean contribution of each crop to the whole mix of the considered crops was determined for the 100-year timeframe (Fig S3). The amount of crop residues currently exported is specific to each simulation unit and varies among the years according to the crop sequences. However, on average for 100 years on a national scale, 466,656 tonnes grain ha^{-1} y^{-1} (DM) are produced on the cropland surface included in this study, of which 46% of the residues are already being used for animals. The dataset containing the crop sequences, annual yields, and information about the current exporting of the crop sequences per simulation unit and the scripts to determine the total annual yield per crop, annual crop contribution to the mix, and annual percentage of crops exported are available in Andrade et al. [4] at https://doi.org/10.48531/JBRU.CALMIP/AUEEEJ. It must be noted that crops indicating current exports refer to a 100% exporting rate of the harvestable crop residue.

Table S1.1. Crop residues considered to be exported for bioeconomy and the technical harvestable fraction of the residues.

Crops included in this study	Crop residue considered for bioeconomy	Estimated crop residue potential at a national scale (Mtonnes y^{-1} DM)[a]	Technical harvestable fraction of residues	Estimated available harvestable crop residue potential at a national scale (Mtonnes y^{-1} DM)[a]
Winter wheat[b]	YES	35.43	0.60	11.48
Grain maize	YES	14.15	0.70	5.35
Silage maize	NO	0.26	0	0.00
Protein peas[c]	YES	2.41E-3	0.60	7.80E-4
Rapeseed	YES	3.18	0.55	0.94
Sunflower	YES	0.89	0.80	0.38
Sugarbeet	YES	1.20	0.91	0.59
Alfalfa	NO	0.05	0	0.00
Temporary grasslands (English ryegrass)	NO	1.13	0	0.00
Potential biomass available for the bioeconomy[c]		**30.39**		**18.74**

[a] Average yield for all the simulation units in the year 2021, determined with STICs. The yields vary with the year due to the crop rotations; [b] The crop rotations used here were the same as in Launay et al.[3]. They performed the SOC simulations using STICS and all the cereal-like crops (wheat, barley, oats, rice, etc.) were considered to be winter wheat. Since we recycled the crop rotations, we also consider the ensemble of cereal-like crops to be winter wheat; [c] winter peas and spring peas are considered protein peas in AMG, thus the total yield was calculated as a mixture of the two types of peas.

[c]Total crop residues considered for bioeconomy minus the fraction already exported for other services (46%).

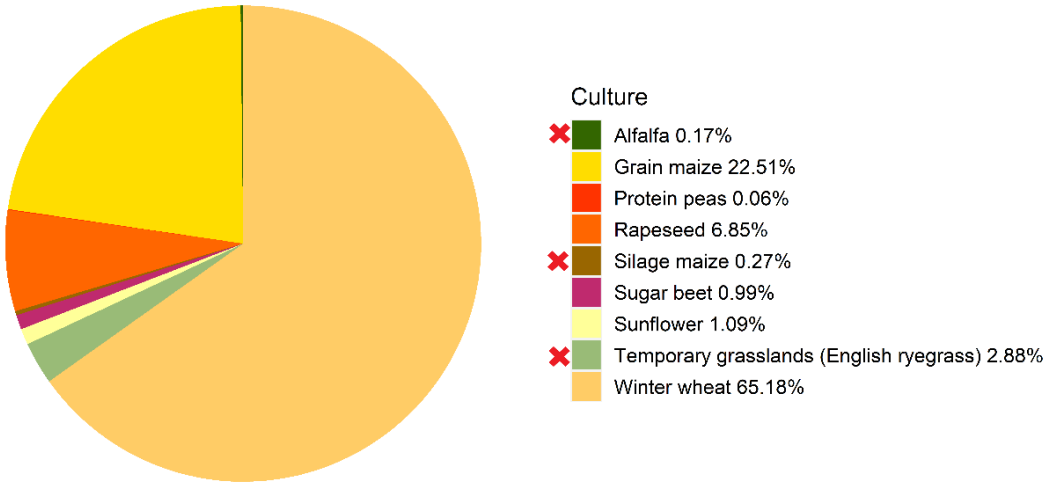

Fig S3. Contribution of each type of crop to the total residual biomass production (DM) in France (average for a 2020 – 2120 timeframe). Red cross (x) indicates crops not harvested in the bioeconomy scenarios.

3. Bioeconomy technologies

The conditions assumed for each considered technology are briefly explained in this section.

Pyrolysis: Pyrochar coproduct

Pyrolysis is a thermochemical process that converts biomass to bio-oil at high temperatures in the absence of oxidants, with the coproduction of gas and biochar, hereafter referred to as pyrochar. The process can be classified as fast or slow pyrolysis. Fast pyrolysis comprises mid-range temperatures and low times (300-500°C, seconds to a few minutes), which enhance the production of bio-oil (75-50% bio-oil, 12-20% pyrochar, and 20-40% gas). [5] Slow pyrolysis is carried out at high temperatures and longer retention times (500-700°C, minutes), favoring higher yields of pyrochar (30% bio-oil, 35% pyrochar). [6] From an economic viewpoint (i.e., higher yield of bio-oil), we consider the use of the crop residues in a fast pyrolysis process. This set of conditions produces highly recalcitrant pyrochar, with a 95% fraction of recalcitrant carbon and an average mean residence time in soil (MRT) of 632 years. [7]

Gasification: Gaschar coproduct

Gasification is a thermochemical process, which, as opposed to pyrolysis, is carried out in the presence of an oxidant agent. Gasification generates syngas and co-products, such as gaschar, tar, and ashes. Since gasification is carried out at higher temperatures than pyrolysis (700-1200°C), it has been noted that a lower amount of biochar is produced (10%) but of higher

stability than that produced under pyrolysis processes. [8] In this study, we considered a gasification process carried out at temperatures ranging from 800-1200°C, followed by the return of the resulting gaschar to the arable land. We did not consider the tar (undesirable co-product) or the ashes (high in silica and low in C) as EOM to the soil. Gaschar is defined as being slightly more recalcitrant than pyrochar. However, due to the sparsity of studies regarding gaschar compared to pyrochar, the recalcitrant fraction of the former has been defined as 95% as in pyrochar, with a MRT of 141 years. [7]

Hydrothermal Liquefaction: Hydrochar coproduct

Hydrothermal liquefaction (HTL) is a thermochemical process carried out at low temperatures of around 280-370°C with retention times of around 20-30 minutes. HTL use wet biomass (15-20% dry matter) in contrast to pyrolysis and gasification, which require a pre-treatment to dry the matter to >90%.[9] HTL produces bio-oil and a solid residue called "hydrochar". Note that there is a similar process called hydrothermal carbonization (HTC), in which the main product is hydrochar and not bio-oil. HTC processes involve higher temperatures (300-450°C) over a longer period comprising hours, making HTL hydrochar constitutively different from HTC hydrochar. Catalysts can enhance the efficiency of HTL processes, especially alkali catalysts such as K_2CO_3. [10] We consider an HTL process at temperature ranges of 300-400°C aided by catalysts with the hydrochar as an EOM to soil. Due to the HTL operational conditions, the produced hydrochar contains more aliphatic groups than pyro- and gaschar, which is related to lower degrees of recalcitrance. On average, hydrochar is composed of 83% recalcitrant carbon with an expected MRT of ca. 11 years. [7]

Anaerobic Digestion: Digestate coproduct

In the anaerobic digestion (AD) process, the organic constituents of the biomass are decomposed by microorganisms in the absence of oxygen. AD generates biogas, which is composed of methane, carbon dioxide, and traces of other gases, as well as a coproduct known as digestate. AD uses a wide variety of biomass-based feedstock, which could be wet (15-35% DM) or dry (10%). The most common AD processes co-digest more than one substrate, at mesophilic temperatures (30-40°C) with retention times varying according to the feedstock (typically 10-25 days). The AD scenario of this study consists of a mixture of crop residues and manure (cattle, pig, and poultry), whereby the C return to the soil is computed from crop residue only. The digestate produced during anaerobic digestion is composed of the non-digestible matter in the feedstock, with an average recalcitrance fraction of 68%. Thomsen et al. [11] determined that 14% of the recalcitrant carbon in digestate remains after 20 years.

Lignocellulosic ethanol: Molasses coproduct

Bioethanol is a biofuel produced from the fermentation of sugars in biomass and its conversion into alcohol by microorganisms. [12] In this work, we consider that crop residues are exposed to an acid pretreatment that frees cellulose and hemicellulose, followed by the hydrolysis to glucose and xylose, which are fermented to ethanol by the action of *Saccharomyces cerevisiae*, and finally purified by distillation. [13] The unconverted fractions are directed to a residual stream known as stillage, which is centrifuged to separate the liquid fraction (molasses) and the solid fraction. [14] The solid fraction is normally used as an animal feed supplement and for energy production in power plants, therefore, here we only consider the return of the bioethanol molasses to the soil. Molasses has significantly lower recalcitrance than the other coproducts included in this study. On average, the bioethanol molasses is composed of 45% recalcitrant carbon, with a MRT of ca. 1 year. [7] Note that only a few studies have determined the mineralization kinetics of bioethanol molasses, and thus the values may not be representative of the real MRT.

4. Carbon inputs from bioeconomy and AMGv2 adaption

Modifications were performed on AMGv2 to consider the input of the bioeconomy co-products as C sources in the soil.

4.1 Calculation of C inputs: Carbon conversion (C_C)

We define C conversion (C_C) as the percentage of initial C in the biomass that is present in the co-product. It is the mass of C in the solid co-product divided by the mass of C in the initial dry biomass (Eq S1).

$$\%C_C = \frac{CpY * CpC}{BmC} * 100 \quad \text{(Eq S1)}$$

where C_C is the carbon conversion (%), CpY is the coproduct yield (kg Cp kg^{-1} biomass), which corresponds to the amount of coproduct resulting from the treatment of 1 kg of feedstock during the bioeconomy process, CpC is the carbon content in the co-product (kg C kg^{-1} Bp), and BmC is the initial carbon content in the biomass (kg C kg^{-1} biomass).

Andrade et al. [7], reviewed the literature to determine the C pathway from crop residues to understand the amount of feedstock C that is present in each coproduct considered in this work. The study employed Eq S1 to determine the C_C coefficient used for each technology.

BmC was determined for each technology dataset ranging from 0.41-0.5 kg C kg^{-1} biomass DM in Andrade et al. [7].

C_C is a parameter fed to AMG that allows determining the C input based on the crop yields. C_C was used in Eq (S2) to determine the amount of C from a given co-product that would be applied in a given simulation unit per year.

$$TCpC = Wt(dm)_i * WtCc_i * Cc \quad \text{(Eq S2)}$$

where TCpC is the total coproduct C applied [t C ha^{-1} y^{-1}], $Wt(dm)_i$ is the crop residues mass available for crop i [t crop residues ha^{-1} y^{-1}], $WtCc_i$ is the Crop residue carbon content for crop residue i [t C t^{-1} crop]. The suffix i denotes the different crops that could be included in the rotation. AMG follows an annual timestep, therefore, it allows for input of only one main crop per year.

$Wt(dm)_I$ is determined for each crop in each simulation unit based on the HI and allocation coefficients [15] and the grain yield [t biomass DM ha^{-1} y^{-1}] input, while WtCCi was defined as 0.444 g C g^{-1} biomass DM. [16]

4.2 AMG adaptation: Carbon Recalcitrance (C_R) of bioeconomy coproducts

The soil carbon partitioning in AMG is described by Eq S3 and Eq S4. [16]

$$QC = QC_S + QC_A \quad \text{(Eq S3)}$$

$$\frac{dQC_A}{dt} = \sum_i m_i h_i - kQC_A \quad \text{(Eq S4)}$$

where QC is the total SOC stock (t ha^{-1}), QC_A and QC_S are the C stocks of the active and stable C pools (t ha^{-1}) respectively, m_i is the annual C input from organic residue i (t ha^{-1} yr^{-1}), h is its humification or retention coefficient and k is the mineralization rate constant of the active C pool (yr^{-1}).

The bioeconomy coproducts are assumed to be composed of two carbon fractions, one called labile, and another known as stable or recalcitrant. The labile fraction is easily mineralizable as CO_2, while the recalcitrant fraction is less prone to degradation and is mineralized at a slower rate than the former one. The size (%) of each fraction and the time of residence in the soil of the recalcitrant one vary for each coproduct as a function of the technology conditions.

For the less recalcitrant coproducts (digestate, hydrochar, molasses), the labile fraction has sizes of around 20 – 50%, while the recalcitrant fraction of this group tends to exhibit MRT values lower than 26 years, which are values considered to be close to the MRT of the active pool. Thus, for this group of products, the fraction remaining after one year (*h*) is considered to correspond to the recalcitrant fraction defined by the coefficient C_R. Therefore, C_R is defined as the active retention coefficient (h_a) and is completely allocated in the active pool C_A where it will be slowly mineralized.

The recalcitrant fraction of the highly recalcitrant co-products (pyrochar and gaschar) constitutes 95% of the coproduct total carbon and exhibits MRTs longer than the 100 years of simulation conducted here, thus they were treated by way of simplification as inert in our modeling approach. For this group, the adapted AMG version considers that the recalcitrant fraction determined by C_R is directly allocated in the C_S pool of the model as the stable retention coefficient (h_s). The labile fraction (5%) is considered to be readily mineralized at the annual time step.

5. Sensitivity Analyses (SA)

Based on the range of C_C and C_R values reported on [7], an average result was obtained for the distinct types of feedstocks considered for a given technology. Then, the first and third quartiles were selected as a low and a high value, respectively, to be tested in the SA. This approach permitted testing the range of values observed while not being influenced by the less likely-to-happen extreme values. This approach results in three levels for each parameter.

The “main scenarios” for each technology consisted of the combination of the average values of each parameter (C_{Cmean} – C_{Rmean}). The SA constituted new scenarios, which considered the different possible combinations between the two coefficients and the three levels. Combining a mean value with a low or high value would allow identifying the sensitivity of the model to the change in the parameter modified as low or high (i.e., C_{Cmean}- C_{Rhigh} allows to identify the effect of C_R). The combinations between low and high values allowed identifying the combined effect of changing both parameters (i.e., C_{Clow}- C_{Rlow}, C_{Clow}- C_{Rhigh}, etc.).

The manner of determining C_R plays a role in the modeled SOC evolution. We considered this source of uncertainty by calculating C_S under two different methods for the pyrolysis scenario.

In the **first method,** as explained in the main body, section 2.3.3, we considered that the recalcitrant fraction would be allocated directly in the C_S pool, and we assumed that nothing would be allocated in the active pool C_A.

Various modeling assays linked to laboratory incubations and field trials have determined that the recalcitrant fraction would not be inert but would follow a very low decay rate. Therefore, in the **second method**, we determined the amount of C mineralized during the first year based on incubation assays lasting less than 1 year. It was noted that 80% of the labile fraction (5% of total C) would be mineralized in the first couple of months and the other 20% would have a mean life of 10 years. [6] In that sense, 4% of the biochar would be directly mineralized in the first year, and the remaining 1% would be allocated to the C_A pool to be slowly mineralized.

The C lost in 100 years has been determined by various authors for different crop residues-based biochar [17–19] using Eq S5. [20]

$$M_t = M_1\left(1 - e^{-k_1 t}\right) + M_2\left(1 - e^{-k_2 t}\right) \qquad \text{(Eq S5)}$$

where Mt is the Carbon mineralized in mg C g^{-1} biochar at time t, M_1 is the labile mineralizable fraction, M_2 is the recalcitrant C fraction, and k_1 and k_2 are the first-order degradation rate constants for the labile and recalcitrant pools, respectively.

Mean values of 26% C lost in 100 years have been obtained in Andrade et al. [7] from the studies performing modeling in a 100-year timeframe. This value falls under the IPCC [21] guidelines, which suggest that 80% (±11%) of biochar (pyrolysis, 450-600°C) remains after 100 years. Although evidence suggests that biochar losses in a century could be significantly low [22], and the MRT obtained from the ensemble of works in Andrade et al. [7] at pyrolysis temperatures of 300 – 500°C is 632 years, we opt to be conservative. Therefore, we defined that 75% of pyrochar is inert during the 100 years of modeling and is allocated in the C_S pool as the h_s coefficient. After considering the losses in the first year ($1\text{-}h_s$), the labile fraction, and the inert fraction (100 years), the h_a coefficient was calculated to be 0.21 using Eq S6.

$$h_{a\_pyro} = 1 - (80\%)(C_L) - h_S \qquad \text{Eq S6}$$

where h_{a_pyro} is the active retention coefficient for the pyrochar scenario alternative method, C_L is the labile fraction of pyrochar (5%), and h_S is the stable pool corresponding to the inert fraction of pyrochar for 100 years (75%).

As was done for the first method, we examined three levels of h_a and h_S, based on the mean value and the first and third quartiles presented in [7]. The combination of "main scenarios" and "SA scenarios" yielded a total of 54 scenarios explored (Table SI2). Considering the limitations regarding the return of pyrochar and gaschar and decreasing the export rate in the scenarios exhibiting SOC losses, a total of 24 extra scenarios were generated. In total, including the BAU scenario, 79 scenarios were explored in this work.

Table S1.2. Different combinations of parameters considered for sensitivity. The recalcitrant carbon has been split between the retention coefficients for the active and stable soil pools.

Bioeconomy pathways	Recalcitrance (C_R)						(C_C)		
	h_a			h_S					
	Low	Mean	High	Low	Mean	High	Low	Mean	High
Pyrochar[a]	n/a	n/a	n/a	90	95	99	34	44	54
Pyrochar[b]	36	21	7	60	75	89	34	44	54
Gaschar	n/a	n/a	n/a	90	95	99	14	20	25
Hydrochar	80	83	96	n/a	n/a	n/a	12	31	45
Digestate	58	68	77	n/a	n/a	n/a	29	39	49
Lignocellulosic bioethanol molasses	28	45	60	n/a	n/a	n/a	18	24	30

C_R: Carbon recalcitrance, h_a : retention coefficient in the active pool, h_s : retention coefficient in the stable pool, C_C : Carbon conversion

[a] First method of introducing C_R for inert fractions in AMG

[b] Second method of introducing C_R for inert fractions in AMG

n/a under h denotes that the C_A pool was not considered in the model while under C_S denotes that the C_S pool was not considered in the model.

A total of 9 extra SA tests were performed to assess the effects of limiting the pyrochar and gaschar application rate and decreasing the exporting rate when SOC losses were observed (AD, HTL, and 2G Ethanol production scenarios).

1.1 SA Result Figures

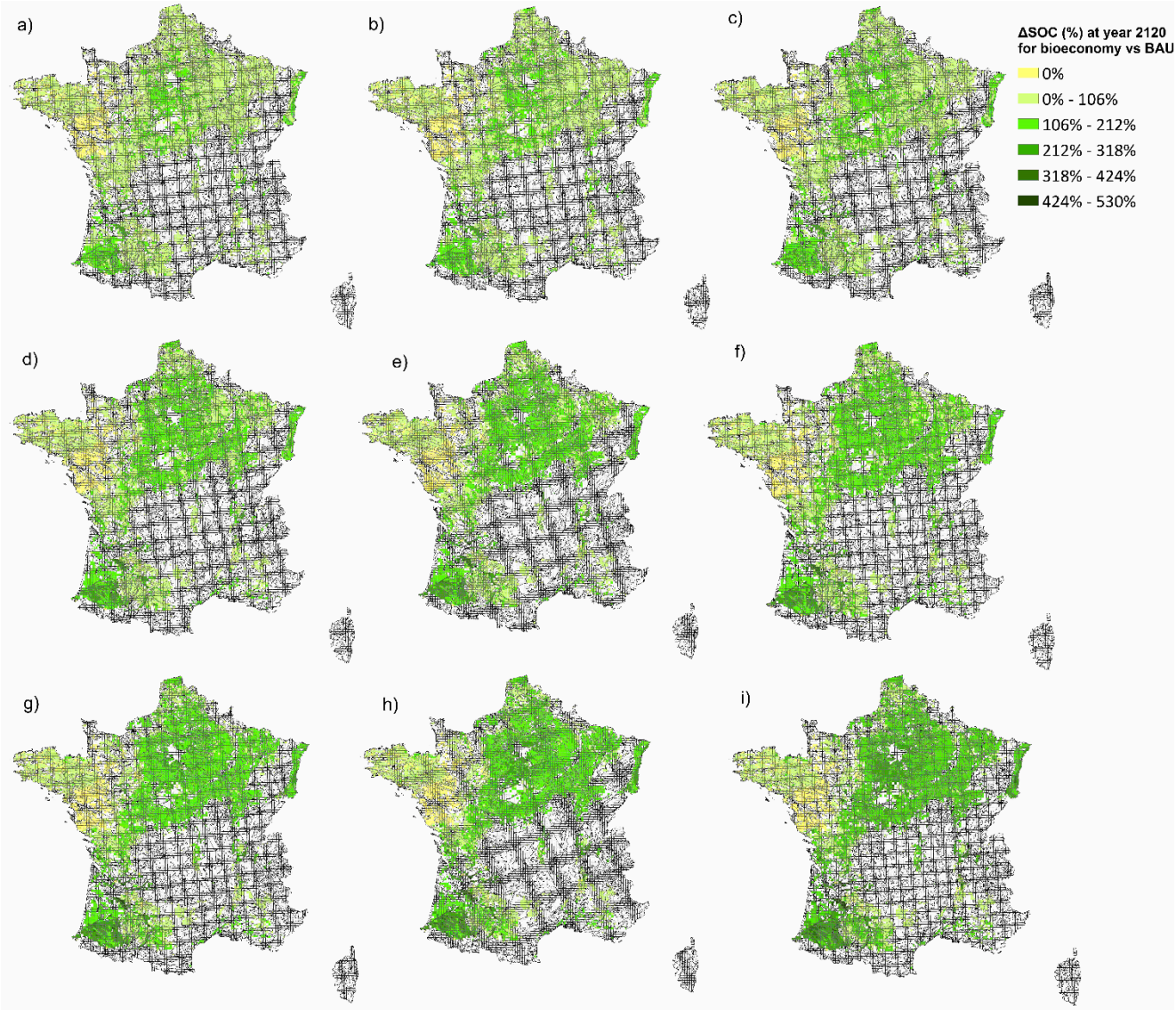

Fig S4. Sensitivity analyses (SA) for the pyrolysis scenario determined without the active pool: a) LL: Low C_C – Low C_R, b) LM: Low C_C – Mean C_R, c) LH: Low C_C - High C_R, d) ML: Mean C_C – Low C_R, e) MM: Mean C_C – Mean C_R (Main scenario), f) MH: Mean C_C – High C_R, g) HL: High C_C – Low C_R, g) HM: High Cc – Mean C_R, i) HH: High C_C – High C_R

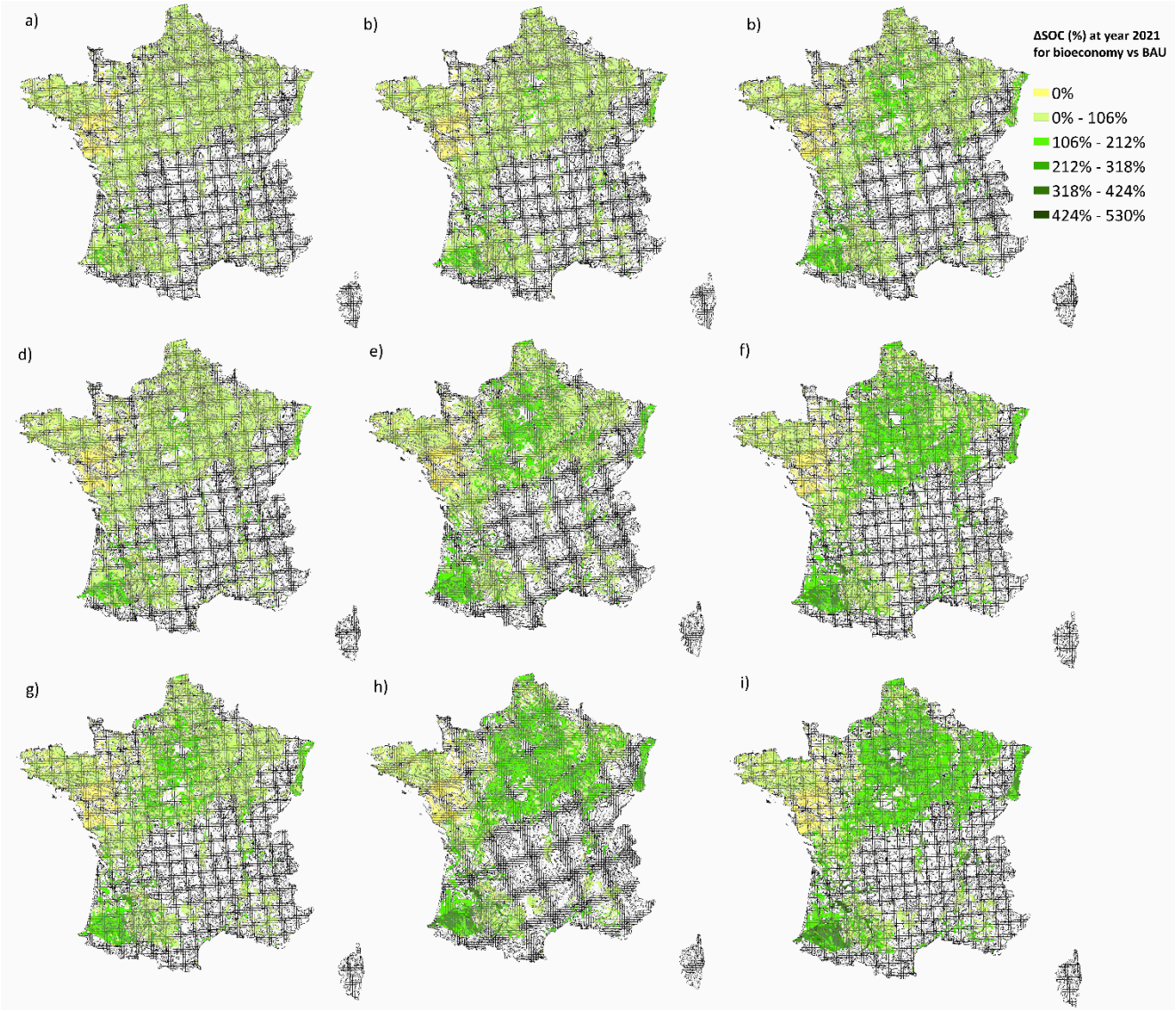

Fig S5. Sensitivity analyses (SA) for the pyrolysis scenario determined with the active and stable pools: a) LL: Low C_C – Low C_R, b) LM: Low C_C – Mean C_R, c) LH: Low C_C - High C_R, d) ML: Mean C_C – Low C_R, e) MM: Mean C_C – Mean C_R (Main scenario), f) MH: Mean C_C – High C_R, g) HL: High C_C – Low C_R, g) HM: High C_C – Mean C_R, i) HH: High C_C – High C_R

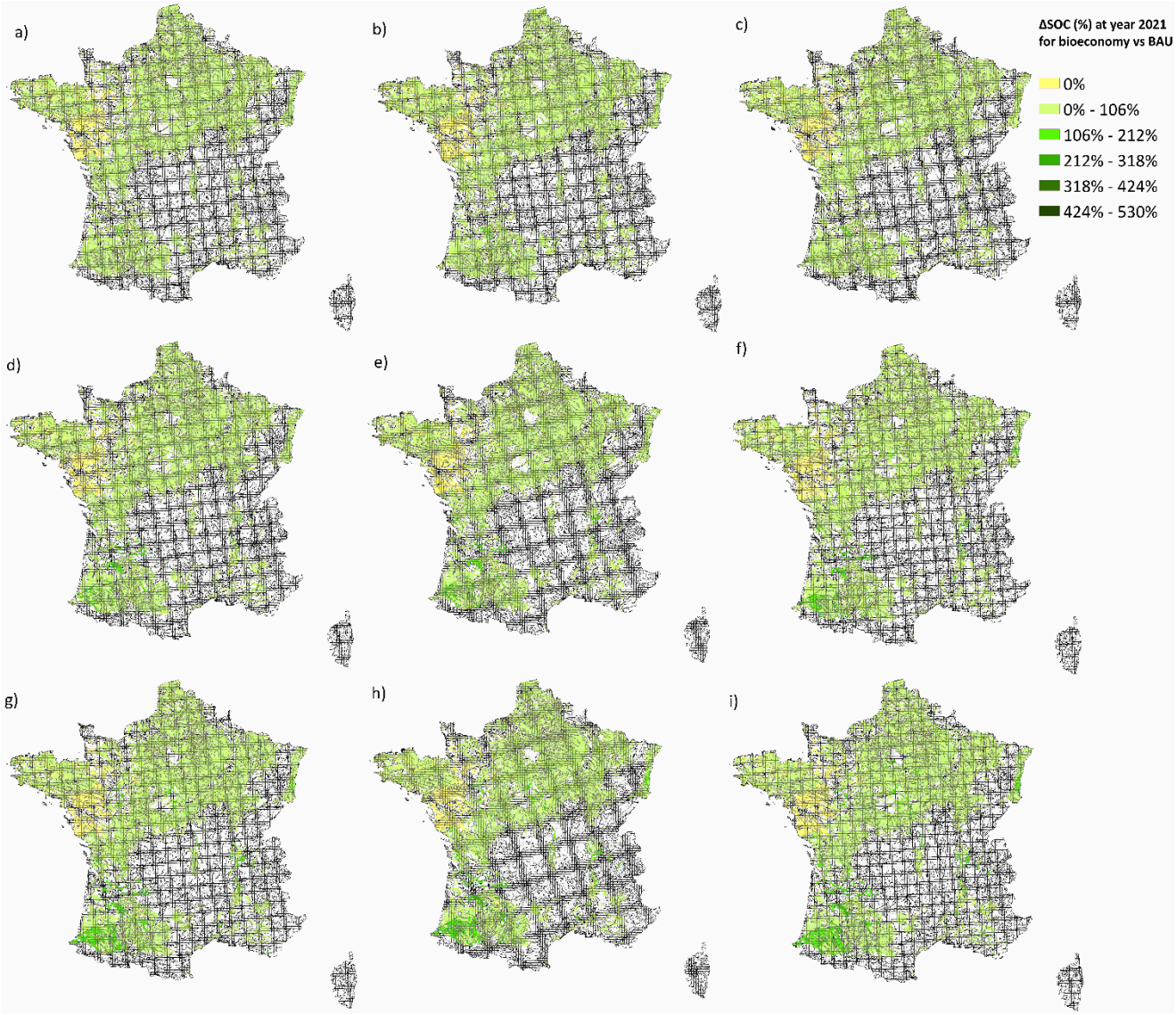

Fig S6. Sensitivity analyses (SA) for the gasification scenario: a) LL: Low C_C – Low C_R, b) LM: Low C_C – Mean C_R, c) LH: Low C_C - High C_R, d) ML: Mean C_C – Low C_R, e) MM: Mean C_C – Mean C_R (Main scenario), f) MH: Mean C_C – High C_R, g) HL: High C_C – Low C_R, g) HM: High C_C – Mean C_R, i) HH: High C_C – High C_R

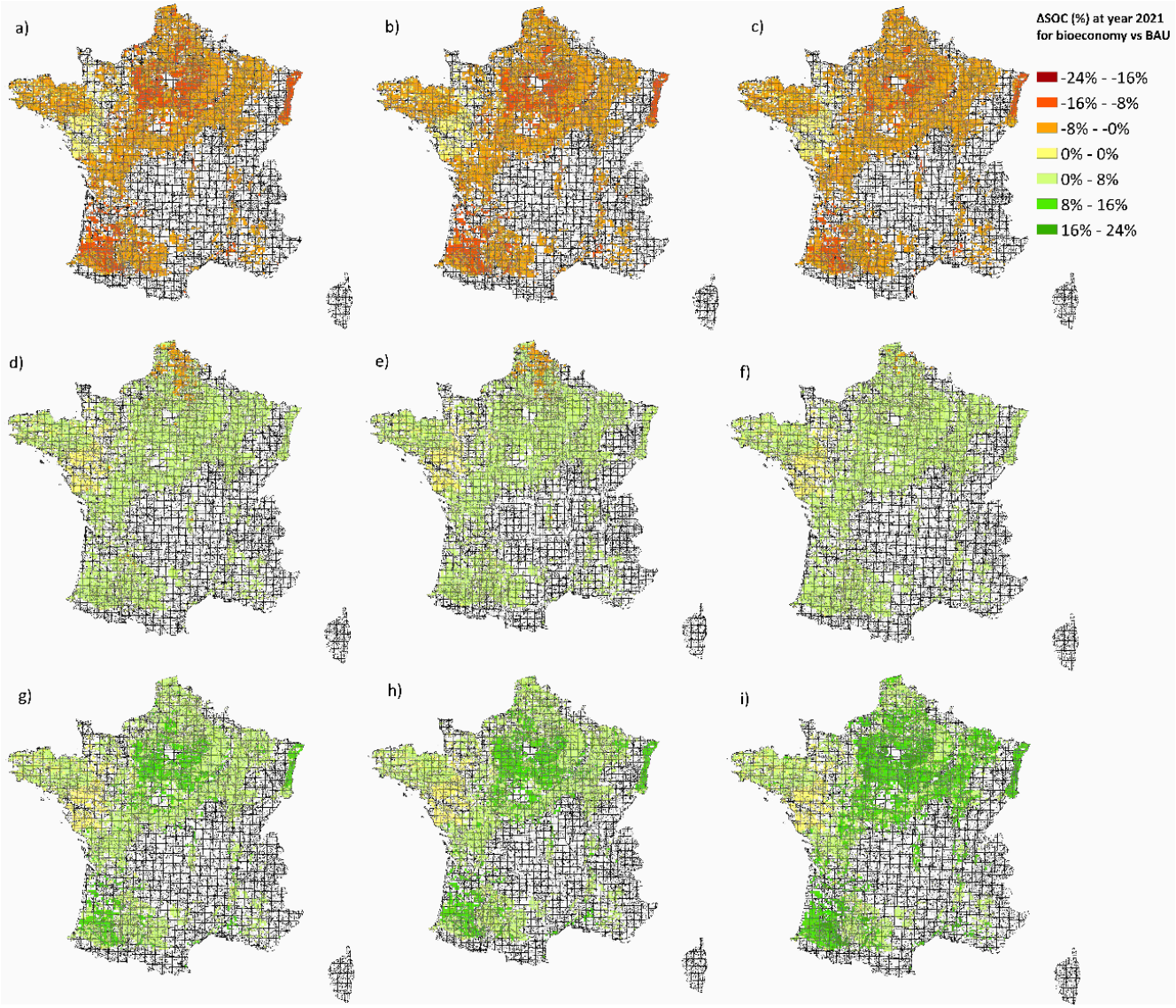

Fig S7. Sensitivity analyses (SA) for the hydrothermal liquefaction scenario: a) LL: Low C_C – Low C_R, b) LM: Low C_C – Mean C_R, c) LH: Low C_C - High C_R, d) ML: Mean C_C – Low C_R, e) MM: Mean C_C – Mean C_R (Main scenario), f) MH: Mean C_C – High C_R, g) HL: High C_C – Low C_R, g) HM: High C_C – Mean C_R, i) HH: High C_C – High C_R

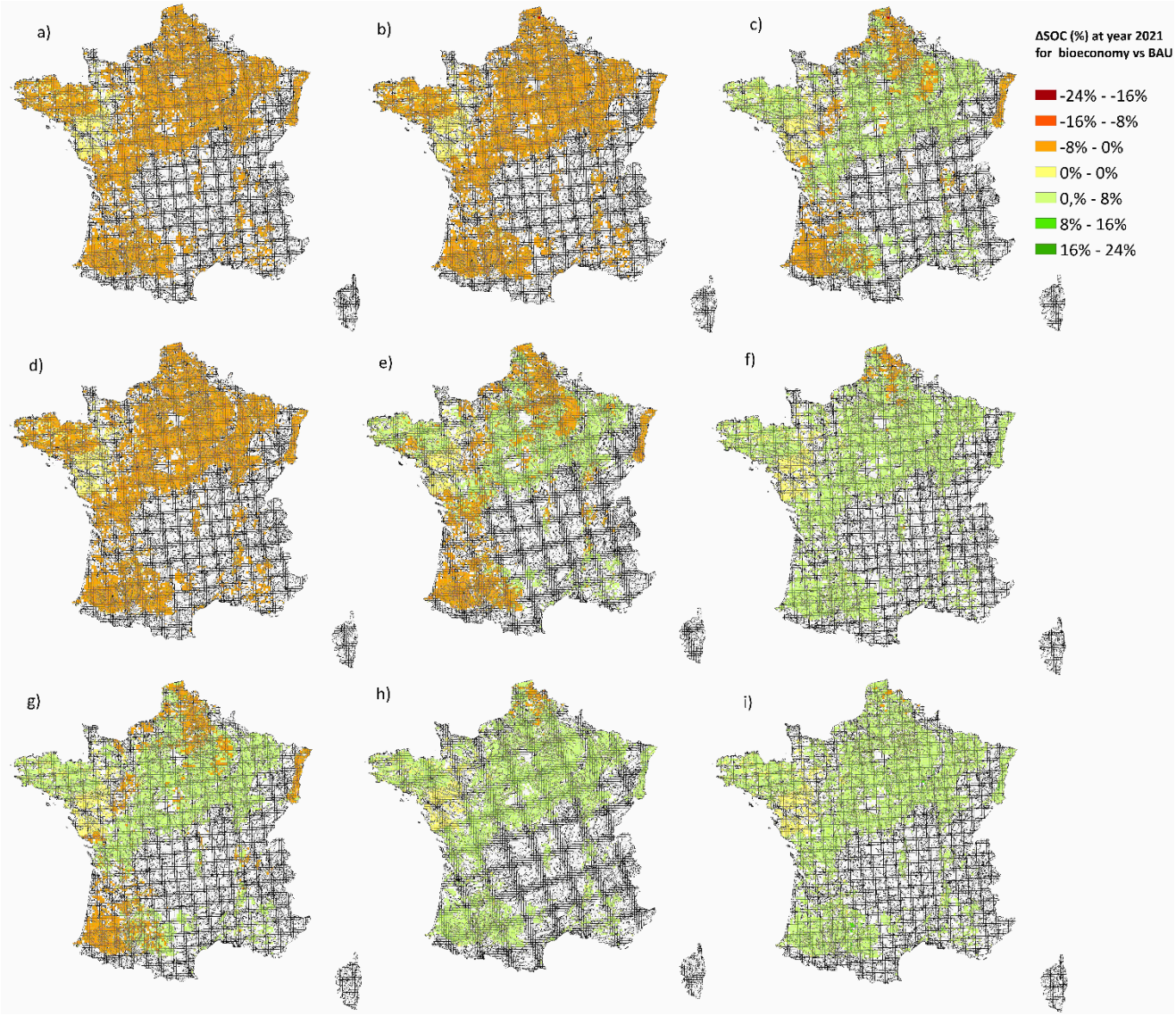

Fig S8. Sensitivity analyses (SA) for the anaerobic digestion scenario: a) LL: Low C_C – Low C_R, b) LM: Low C_C – Mean C_R, c) LH: Low C_C - High C_R, d) ML: Mean C_C – Low C_R, e) MM: Mean C_C – Mean C_R (Main scenario), f) MH: Mean C_C – High C_R, g) HL: High C_C – Low C_R, g) HM: High C_C – Mean C_R, i) HH: High C_C – High C_R

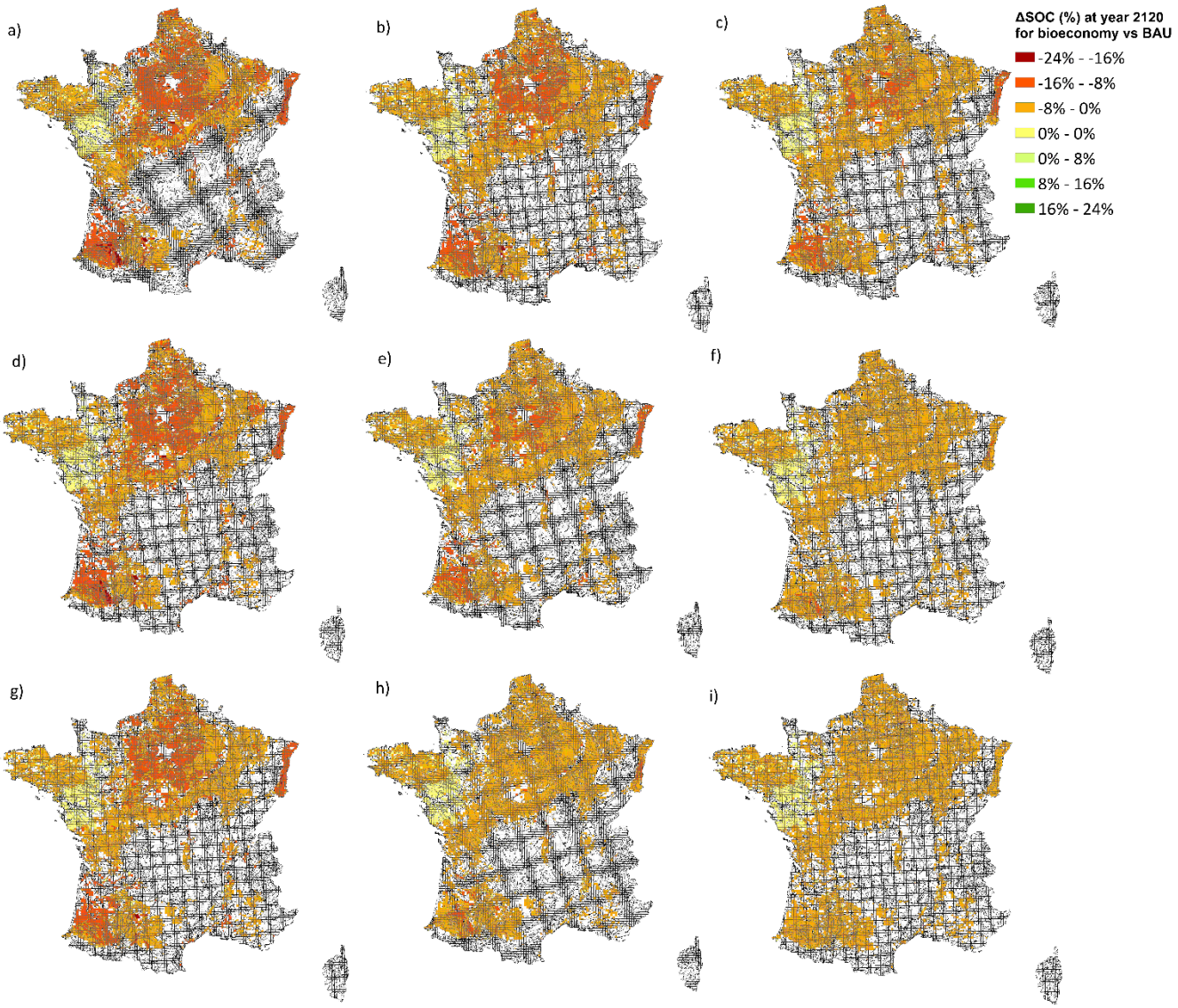

Fig S9. Sensitivity analyses (SA) for the lignocellulosic ethanol scenario: a) LL: Low C_C – Low C_R, b) LM: Low C_C – Mean C_R, c) LH: Low C_C - High C_R, d) ML: Mean C_C – Low C_R, e) MM: Mean C_C – Mean C_R (Main scenario), f) MH: Mean C_C – High C_R, g) HL: High C_C – Low C_R, g) HM: High C_C – Mean C_R, i) HH: High C_C – High C_R

References SI 2.1

[1] Joly D, Brossard T, Cardot H, Cavailhes J, Hilal M, Wavresky P. Les types de climats en France, une construction spatiale. Cybergeo : European Journal of Geography [En ligne], Cartographie, Imagerie, SIG 2010. https://doi.org/10.4000/cybergeo.23155.

[2] GisSol. La texture dominante de l'horizon supérieur des sols agricoles par canton 2011.

[3] Launay C, Constantin J, Chlebowski F, Houot S, Graux A, Klumpp K, et al. Estimating the carbon storage potential and greenhouse gas emissions of French arable cropland using high-resolution modeling. Glob Change Biol 2021;27:1645–61. https://doi.org/10.1111/gcb.15512.

[4] Andrade C, Clivot H, Albers A, Zamora-Ledezma E, Hamelin L. Dataset to assess the soil organic carbon evolution of French croplands in a bioeconomy perspective using the soil model AMG 2022. https://doi.org/10.48531/JBRU.CALMIP/AUEEEJ.

[5] Malyan SK, Kumar SS, Fagodiya RK, Ghosh P, Kumar A, Singh R, et al. Biochar for environmental sustainability in the energy-water-agroecosystem nexus. Renewable and Sustainable Energy Reviews 2021;149:111379. https://doi.org/10.1016/j.rser.2021.111379.

[6] Lehmann J, Joseph S, editors. Biochar for environmental management: science and technology. Reprint. London: Earthscan; 2010.

[7] Andrade C, Albers A, Zamora-Ledezma E, Hamelin L. A review on the interplay between bioeconomy and soil organic carbon stocks maintenance. PREPRINT (Version 2) Available at Research Square 2022. https://doi.org/10.21203/rs.3.rs-1447842/v1.

[8] Molino A, Chianese S, Musmarra D. Biomass gasification technology: The state of the art overview. Journal of Energy Chemistry 2016;25:10–25. https://doi.org/10.1016/j.jechem.2015.11.005.

[9] Jahirul M, Rasul M, Chowdhury A, Ashwath N. Biofuels Production through Biomass Pyrolysis —A Technological Review. Energies 2012;5:4952–5001. https://doi.org/10.3390/en5124952.

[10] Seehar TH, Toor SS, Sharma K, Nielsen AH, Pedersen TH, Rosendahl LA. Influence of process conditions on hydrothermal liquefaction of eucalyptus biomass for biocrude production and investigation of the inorganics distribution. Sustainable Energy Fuels 2021;5:1477–87. https://doi.org/10.1039/D0SE01634A.

[11] Thomsen IK, Olesen JE, Møller HB, Sørensen P, Christensen BT. Carbon dynamics and retention in soil after anaerobic digestion of dairy cattle feed and faeces. Soil Biology and Biochemistry 2013;58:82–7. https://doi.org/10.1016/j.soilbio.2012.11.006.

[12] Swain MR, Singh A, Sharma AK, Tuli DK. Chapter 11 - Bioethanol Production From Rice- and Wheat Straw: An Overview. Bioethanol Production from Food Crops. Sustainable Sources, Interventions, and Challenges, Academic Press; 2019, p. 19.

[13] Bušić A, Marđetko N, University of Zagreb, Faculty of Food Technology and Biotechnology, Pierottijeva 6, 10000 Zagreb, Croatia, Kundas S, Belarussian National Technical University, Power Plant Construction and Engineering Services Faculty, Nezavisimosti Ave. 150, 220013 Minsk, Belarus, Morzak G, et al. Bioethanol Production from Renewable Raw Materials and its Separation and Purification: a Review. Food Technol Biotechnol 2018;56. https://doi.org/10.17113/ftb.56.03.18.5546.

[14] Tonini D, Hamelin L, Astrup TF. Environmental implications of the use of agro-industrial residues for biorefineries: application of a deterministic model for indirect land-use changes. GCB Bioenergy 2016;8:690–706. https://doi.org/10.1111/gcbb.12290.

[15] Bolinder MA, Janzen HH, Gregorich EG, Angers DA, VandenBygaart AJ. An approach for estimating net primary productivity and annual carbon inputs to soil for common agricultural crops in Canada. Agriculture, Ecosystems & Environment 2007;118:29–42. https://doi.org/10.1016/j.agee.2006.05.013.

[16] Clivot H, Mouny J-C, Duparque A, Dinh J-L, Denoroy P, Houot S, et al. Modeling soil organic carbon evolution in long-term arable experiments with AMG model. Environmental Modelling & Software 2019;118:99–113. https://doi.org/10.1016/j.envsoft.2019.04.004.

[17] Hammes K, Torn MS, Lapenas AG, Schmidt MWI. Centennial black carbon turnover observed in a Russian steppe soil. Biogeosciences 2008;5:1339–50. https://doi.org/10.5194/bg-5-1339-2008.

[18] Herath HMSK, Camps-Arbestain M, Hedley MJ, Kirschbaum MUF, Wang T, van Hale R. Experimental evidence for sequestering C with biochar by avoidance of CO_2 emissions from original feedstock and protection of native soil organic matter. GCB Bioenergy 2015;7:512–26. https://doi.org/10.1111/gcbb.12183.

[19] Zimmerman AR. Abiotic and Microbial Oxidation of Laboratory-Produced Black Carbon (Biochar). Environ Sci Technol 2010;44:1295–301. https://doi.org/10.1021/es903140c.

[20] Lehmann J, Abiven S, Kleber M, Pan G, Singh BP, Sohi SP, et al. Persistence of biochar in soil. Biochar for Environmental Management. 2nd Edition, 2015, p. 48.

[21] IPCC. 2019 Refinement to the 2006 IPCC Guidelines for National Greenhouse Gas Inventories - Appendix4: Method for Estimating the Change in Mineral Soil Organic Carbon Stocks from Biochar Amendments: Basis for Future Methodological Development. IPCC; 2019.

[22] Zimmerman A, Gao B. The Stability of Biochar in the Environment. In: Ladygina N, Rineau F, editors. Biochar and Soil Biota, CRC Press; 2013, p. 1–40. https://doi.org/10.1201/b14585-2.

Appendix A2b

Supplementary Information of Chapter 3 – Section 2

The content of this appendix was published as supplementary information of the paper in doi.org/10.1016/j.apenergy.2022.120192 in Applied Energy, and is reproduced with permissions from the journal. This document is a reproduction of the Excel file accompanying the mentioned paper.

The crop residue conundrum: maintaining long-term soil organic carbon stocks while reinforcing the bioeconomy, compatible endeavors?

Supplementary Information 2

Contents

Along this document, the scenarios are represented as: HH; HM; HL; MH; MM; ML; LH; LM; and LL. The first letter represents the C_C coefficient while the second represents the C_R. Letters H, M, and L, represent the level of the parameter as H: high, M: mean, and L: low. Therefore, the combination of two particular letters indicate the level of C_R and C_C tested in the scenario (e.g., HH: high C_C and high C_R).

Table S2.1. SOC change (%) per areas affected (%) at PCU scale. Breaks fixed after considering the max and min values. This sheet allows to compare the tecnologies at the same range of breaks grouped as high recalcitrant or low reclacitrant coproducts

Per PCU by fixed ranges (as shown in maps) 11784 PCU. *To compare the scenarios, Biochar 1 and 2, and Gaschar share the same ranges (0-530, in sets of 106). Hydrochar, Digestate and Molasses share the same ranges (-24 - 24, in sets of 8)*

Bioeconomy scenarios Cc + Cr Combinations	Pyrolysis 1		Pyrolysis 2		Gasification		Hydrothermal liquefaction		Anaerobic digestion		Lignocellulosic ethanol	
	Cranges (%)	Area afected (%)	Cranges (%)	Area afected (%)	Cranges (%)	Area afected (%)	Cranges (%)	Area afected (%)	Cranges (%)	Area afected (%)	Cranges (%)	Area afected (%)
HH	0%-0%	9.76	0%-0%	9.76	0%-0%	9.76	0% - 0%	9.76	-8% - 0%	0.21	-8% - 0%	90.24
	0%-106%	24.41	0%-106%	25.54	0%-106%	84.28	0% - 8%	44.30	0% - 0%	9.76	0% - 0%	9.76
	106%-212%	52.62	106%-212%	54.07	106%-212%	5.70	8% - 16%	41.11	0% - 8%	89.72		
	212%-318%	10.69	212%-318%	9.14	212%-318%	0.25	16% - 24%	4.82	8% - 16%	0.31		
	318%-424%	1.90	318%-424%	1.23								
	424%-530%	0.61	424%-530%	0.26								
HM	0%-0%	9.76	0%-0%	9.76	0%-0%	9.76	0% - 0%	9.76	-8% - 0%	1.77	-16 - %-8%	2.36
	0%-106%	25.59	0%-106%	37.96	0%-106%	85.07	0% - 8%	65.60	0% - 0%	9.76	-8% - 0%	87.87
	106%-212%	54.05	106%-212%	48.08	106%-212%	4.96	8% - 16%	24.64	0% - 8%	88.47	0% - 0%	9.76
	212%-318%	8.66	212%-318%	3.55	212%-318%	0.21						
	318%-424%	1.46	318%-424%	0.65								
	424%-530%	0.48										
HL	0%-0%	9.76	0%-0%	9.76	0%-0%	9.76	0% - 0%	9.76	-8% - 0%	23.27	-24% - -16%	0.22
	0%-106%	27.74	0%-106%	67.22	0%-106%	85.83	0% - 8%	71.72	0% - 0%	9.76	-16 - %-8%	22.57
	106%-212%	55.17	106%-212%	22.04	106%-212%	4.39	8% - 16%	18.52	0% - 8%	66.97	-8% - 0%	67.45
	212%-318%	5.81	212%-318%	0.98	212%-318%	0.02					0% - 0%	9.76
	318%-424%	1.22										
	424%-530%	0.29										
MH	0%-0%	9.76	0%-0%	9.76	0%-0%	9.76	-8% - 0%	0.21	-8% - 0%	3.00	-16 - %-8%	1.22
	0%-106%	34.27	0%-106%	43.18	0%-106%	87.42	0% - 0%	9.76	0% - 0%	9.76	-8% - 0%	89.02
	106%-212%	51.10	106%-212%	43.39	106%-212%	2.82	0% - 8%	90.01	0% - 8%	87.24	0% - 0%	9.76
	212%-318%	4.00	212%-318%	3.14			8% - 16%	0.01				
	318%-424%	0.85	318%-424%	0.52								
	424%-530%	0.02										
MM Standard conditions	0%-0%	9.76	0%-0%	9.76	0%-0%	9.76	-8% - 0%	2.79	-8% - 0%	40.23	-16 - %-8%	11.62
	0%-106%	37.84	0%-106%	60.98	0%-106%	87.93	0% - 0%	9.76	0% - 0%	9.76	-8% - 0%	78.61
	106%-212%	48.08	106%-212%	27.66	106%-212%	2.30	0% - 8%	87.45	0% - 8%	50.01	0% - 0%	9.76
	212%-318%	3.58	212%-318%	1.58								
	318%-424%	0.74	318%-424%	0.02								

Bioeconomy scenarios Cc + Cr Combinations	Pyrolysis 1		Pyrolysis 2		Gasification		Hydrothermal liquefaction		Anaerobic digestion		Lignocellulosic ethanol	
	Cranges (%)	Area afected (%)	Cranges (%)	Area afected (%)	Cranges (%)	Area afected (%)	Cranges (%)	Area afected (%)	Cranges (%)	Area afected (%)	Cranges (%)	Area afected (%)
ML	0%-0%	9.76	0%-0%	9.76	0%-0%	9.76	-8% - 0%	3.60	-8% - 0%	90.24	-24% - -16%	0.83
	0%-106%	43.30	0%-106%	82.82	0%-106%	88.46	0% - 0%	9.76	0% - 0%	9.76	-16 - %-8%	28.81
	106%-212%	43.24	106%-212%	7.17	106%-212%	1.78	0% - 8%	86.64			-8% - 0%	60.60
	212%-318%	3.17	212%-318%	0.24							0% - 0%	9.76
	318%-424%	0.52										
LH	0%-0%	9.76	0%-0%	9.76	0%-0%	9.76	-16 - %-8%	8.95	-8% - -1%	25.50	-16 - %-8%	11.62
	0%-106%	62.05	0%-106%	71.31	0%-106%	89.81	-8% - 0%	81.29	-1% - 0%	9.76	-8% - 0%	78.61
	106%-212%	26.51	106%-212%	17.93	106%-212%	0.42	0% - 0%	9.76	0% - 8%	64.73	0% - 0%	9.76
	212%-318%	1.62	212%-318%	1.00								
	318%-424%	0.06										
LM	0%-0%	9.76	0%-0%	9.76	0%-0%	9.76	-16 - %-8%	15.70	-8% - 0%	90.24	-24% - -16%	0.30
	0%-106%	66.31	0%-106%	82.28	0%-106%	89.95	-8% - 0%	74.53	0% - 0%	9.76	-16 - %-8%	23.81
	106%-212%	22.53	106%-212%	7.60	106%-212%	0.29	0% - 0%	9.76			-8% - 0%	66.12
	212%-318%	1.39	212%-318%	0.36							0% - 0%	9.76
LL	0%-0%	9.76	0%-0%	9.76	0%-0%	9.76	-16 - %-8%	17.47	-8% - 0%	90.24	-24% - -16%	1.47
	0%-106%	71.25	0%-106%	87.66	0%-106%	90.07	-8% - 0%	72.77	0% - 0%	9.76	-16 - %-8%	33.90
	106%-212%	17.96	106%-212%	2.58	106%-212%	0.17	0% - 0%	9.76			-8% - 0%	54.87
	212%-318%	1.03									0% - 0%	9.76

Table S2.1b. SOC change (%) per areas affected (%) at PCU scale. Breaks fixed after considering the max and min values. SA applied: 75% harvest, 50t C limited return

75% Export						
Bioeconomy scenarios Cc + Cr Combinations	HYDROTHERMAL LIQUEFACTION		ANAEROBIC DIGESTION		LIGNOCELLULOSIC ETHANOL	
	Cranges (%)	Area afected (%)	Cranges (%)	Area afected (%)	Cranges (%)	Area afected (%)
MM Standrad Conditions	-8% - 0%	2.79	-8% - 0%	40.23	-16 - %-8%	1.76
	0% - 0%	9.76	0% - 0%	9.76	-8% - 0%	88.47
	0% - 8%	87.45	0% - 8%	50.01	0% - 0%	9.76

50% Export						
Bioeconomy scenarios Cc + Cr Combinations	HYDROTHERMAL LIQUEFACTION		ANAEROBIC DIGESTION		LIGNOCELLULOSIC ETHANOL	
	Cranges (%)	Area afected (%)	Cranges (%)	Area afected (%)	Cranges (%)	Area afected (%)
MM Standrad Conditions	-8% - 0%	2.79	-8% - 0%	40.23	-8% - 0%	90.24
	0% - 0%	9.76	0% - 0%	9.76	0% - 0%	9.76
	0% - 8%	87.45	0% - 8%	50.01		

50 t C limited to return						
	PYROLYSIS 1		PYROLYSIS 2		GASCHAR	
	Cranges (%)	Area afected (%)	Cranges (%)	Area afected (%)	Cranges (%)	Area afected (%)
HH	0%-0%	9.76	0%-0%	9.76	0%-0%	9.76
	0%-106%	87.38	0%-106%	89.24	0%-106%	89.27
	106%-212%	2.86	106%-212%	1.00	106%-212%	0.97
	0%-0%	9.76	0%-0%	9.76	0%-0%	9.76
	0%-106%	88.32	0%-106%	90.21	0%-106%	89.54
	106%-212%	1.92		0.03	106%-212%	0.70
HM	0%-0%	9.76	0%-0%	9.76	0%-0%	9.76
	0%-106%	89.17	0%-106%	90.24	0%-106%	90.04
	106%-212%	1.07			106%-212%	0.20
	0%-0%	9.76	0%-0%	9.76	0%-0%	9.76
	0%-106%	88.01	0%-106%	89.52	0%-106%	89.59
	106%-212%	2.23	106%-212%	0.72	106%-212%	0.65
HL	0%-0%	9.76	0%-0%	9.76	0%-0%	9.76
	0%-106%	88.63	0%-106%	90.21	0%-106%	89.77
	106%-212%	1.61	106%-212%	0.02	106%-212%	0.46
MM Standard conditions	0%-0%	9.76	0%-0%	9.76	0%-0%	9.76
	0%-106%	89.47	0%-106%	90.24	0%-106%	90.16
	106%-212%	0.77			106%-212%	0.08
ML	0%-0%	9.76	0%-0%	9.76	0%-0%	9.76
	0%-106%	88.46	0%-106%	89.67	0%-106%	89.83
	106%-212%	1.78	106%-212%	0.56	106%-212%	0.40
	0%-0%	9.76	0%-0%	9.76	0%-0%	9.76
	0%-106%	88.92	0%-106%	90.22	0%-106%	89.97
	106%-212%	1.32	106%-212%	0.02	106%-212%	0.27
LH	0%-0%	9.76	0%-0%	9.76	0%-0%	9.76
	0%-106%	89.64	0%-106%	90.24	0%-106%	90.21
	106%-212%	0.60			106%-212%	0.02

Table S2.2. SOC change (Bioeconomy vs BAU) at year 2120 for the whole cropland surface modeled. Total SOC change in MtC (total sum of SOC change per PCU). Average SOC change percent for all the cropland surface modeled (SOC change % per PCU). Includes all the Cc and Cr combinations, the exporting rates decrease, and limited application. Export rate: 100 %; coproducts return: 100%

Bioeconomy scenarios $C_C + C_R$ Combinations	Total national SOC change (MtC)	σ	Min	Max	Average national SOC change (%)	σ	Min	Max
PYROLYSIS 1								
MM	774.22	0.08	2.5E-05	0.52	105.45%	69.34%	0.14%	409.15%
HH	1008.76	0.10	3.3E-05	0.68	137.21%	89.83%	0.18%	527.77%
HM	965.31	0.10	3.2E-05	0.65	131.33%	86.04%	0.18%	505.80%
HL	911.00	0.09	3E-05	0.62	123.97%	81.29%	0.16%	478.33%
MH	809.62	0.08	2.6E-05	0.55	110.24%	72.43%	0.14%	427.06%
ML	729.97	0.07	2.3E-05	0.49	99.46%	65.48%	0.13%	386.77%
LH	610.49	0.06	1.9E-05	0.41	83.28%	55.04%	0.11%	326.34%
LM	583.13	0.06	1.8E-05	0.39	79.57%	52.65%	0.10%	312.51%
LL	548.94	0.06	1.7E-05	0.37	74.94%	49.67%	0.09%	295.21%
PYROLYSIS 2								
MM	616.74	0.06	2.05E-05	0.42	83.87%	54.85%	0.11%	321.83%
HH	911.22	0.09	3.02E-05	0.62	123.91%	81.03%	0.17%	475.45%
HM	772.04	0.08	2.63E-05	0.53	104.84%	68.26%	0.15%	398.63%
HL	577.18	0.06	2.08E-05	0.39	78.16%	50.41%	0.12%	291.10%
MH	730.15	0.07	2.37E-05	0.49	99.40%	65.25%	0.13%	384.42%
ML	457.96	0.05	1.60E-05	0.31	62.13%	40.29%	0.09%	234.22%
LH	549.08	0.06	1.72E-05	0.37	74.90%	49.49%	0.10%	293.40%
LM	461.44	0.05	1.47E-05	0.31	62.89%	41.44%	0.08%	245.03%
LL	338.75	0.03	1.13E-05	0.23	46.09%	30.18%	0.06%	177.33%
GASIFICATION								
MM	315.61	0.03	8.62E-06	0.21	43.34%	29.34%	0.05%	177.20%
HH	431.27	0.04	1.27E-05	0.29	59.00%	39.41%	0.07%	235.70%
HM	411.15	0.04	1.20E-05	0.27	56.28%	37.65%	0.07%	225.53%
HL	386.01	0.04	1.11E-05	0.26	52.87%	35.46%	0.06%	212.81%
MH	331.70	0.03	9.19E-06	0.22	45.52%	30.74%	0.05%	185.34%
ML	295.49	0.03	7.91E-06	0.19	40.62%	27.59%	0.04%	167.03%
LH	212.22	0.02	4.95E-06	0.14	29.34%	20.38%	0.03%	124.91%
LM	200.95	0.02	4.55E-06	0.13	27.81%	19.41%	0.03%	119.22%
LL	186.87	0.02	4.05E-06	0.12	25.91%	18.20%	0.02%	112.10%
HYDROTHERMAL LIQUEFACTION								
MM	8.85	1.06E-03	-4.42E-03	0.01	1.12%	0.83%	-1.80%	4.05%
HH	60.06	0.01	4.90E-06	0.05	7.60%	4.89%	0.02%	22.60%
HM	42.92	4.76E-03	3.57E-06	0.04	5.43%	3.51%	0.02%	15.95%
HL	38.96	4.32E-03	3.26E-06	0.03	4.93%	3.19%	0.02%	14.42%
MH	20.67	2.32E-03	-4.65E-04	0.02	2.62%	1.73%	-0.21%	8.11%
ML	6.13	7.95E-04	-0.01	0.01	0.78%	0.65%	-2.27%	3.12%
LH	-32.80	3.64E-03	-0.03	-2.32E-06	-4.15%	2.69%	-13.38%	-0.01%
LM	-37.37	4.15E-03	-0.04	-2.68E-06	-4.72%	3.06%	-15.15%	-0.01%
LL	-38.43	4.26E-03	-0.04	-2.76E-06	-4.86%	3.14%	-15.56%	-0.01%

Bioeconomy scenarios C_C + C_R Combinations	Total national SOC change (MtC)	σ	Min	Max	Average national SOC change (%)	σ	Min	Max
ANAEROBIC DIGESTION								
MM	-0.79	4.25E-04	-0.01	1.45E-03	-0.10%	0.42%	-3.49%	0.74%
HH	23.71	2.65E-03	-1.87E-04	0.02	3.00%	1.97%	-0.08%	9.16%
HM	13.16	1.51E-03	-2.56E-03	0.01	1.67%	1.15%	-1.04%	5.53%
HL	1.44	4.46E-04	-0.01	3.21E-03	0.19%	0.43%	-3.10%	1.51%
MH	7.91	9.68E-04	-4.83E-03	0.01	1.01%	0.77%	-1.96%	3.73%
ML	-10.46	0.07	-0.01	-5.84E-07	-1.32%	0.94%	-5.19%	0.00%
LH	1.14	4.35E-04	-0.01	2.97E-03	0.15%	0.43%	-3.15%	1.41%
LM	-6.77	8.55E-04	-0.01	-2.97E-07	-0.85%	0.69%	-4.54%	0.00%
LL	-15.57	1.77E-03	-0.02	9.81E-07	-1.97%	1.33%	-6.70%	-0.01%
LIGNOCELLULOSIC ETHANOL								
MM	-34.91	3.88E-03	-0.03	-2.49E-06	-4.41%	2.86%	-14.19%	-0.01%
HH	-13.81	1.58E-03	-0.01	-8.44E-07	-1.74%	1.19%	-6.02%	0.00%
HM	-27.00	3.01E-03	-0.03	-1.87E-06	-3.41%	2.23%	-11.13%	-0.01%
HL	-41.95	4.65E-03	-0.04	-3.03E-06	-5.30%	3.43%	-16.92%	-0.01%
MH	-24.36	2.72E-03	-0.02	-1.67E-06	-3.08%	2.02%	-10.11%	-0.01%
ML	-46.87	0.01	-0.04	-3.42E-06	-5.93%	3.82%	-18.83%	-0.02%
LH	-34.91	3.88E-03	-0.03	-2.49E-06	-4.41%	2.86%	-14.19%	-0.01%
LM	-42.83	4.75E-03	-0.04	-3.10E-06	-5.41%	3.50%	-17.26%	-0.02%
LL	-51.80	0.01	-0.05	-3.80E-06	-6.55%	4.22%	-20.74%	-0.02%

Table S2.2. Total SOC change in MtC (total sum of SOC change per PCU). Average SOC change percent for all the cropland surface modeled (SOC change % per PCU). Includes all the Cc and Cr combinations, the exporting rates decrease, and limited application. Export rate: 75 %; coproducts return: 100% Cc: M, Cr: M, Export rate: 50 %; coproducts return: 100% Cc: M, Cr: M

Conversion pathway	Total national SOC change (MtC)	σ	Min	Max	Average national SOC change (%)	σ	Min	Max
Export rate: 75 %; coproducts return: 100% Cc: M, Cr: M								
Hydrothermal liquefaction	6.64	7.97E-04	-3.32E-03	0.01	0.84%	0.62%	-1.35%	3.04%
Anaerobic digestion	-0.59	3.19E-04	-0.01	1.09E-03	-0.07%	0.32%	-2.62%	0.56%
Lignocellulosic ethanol	-26.18	2.91E-03	-0.02	-1.86E-06	-3.31%	2.15%	-10.65%	-0.01%
Export rate: 50 %; coproducts return: 100% Cc: M, Cr: M								
Hydrothermal liquefaction	4.43	5.31E-04	-2.21E-03	4.66E-03	0.56%	0.42%	-0.90%	2.03%
Anaerobic digestion	-0.40	2.13E-04	-4.30E-03	7.27E-04	-0.05%	0.21%	-1.74%	0.37%
Lignocellulosic ethanol	-17.46	1.94E-03	-0.02	-1.24E-06	-2.21%	1.43%	-7.10%	-0.01%

Table S2.2. SOC change (Bioeconomy vs BAU) at year 2120 for the whole cropland surface modeled. Total SOC change in MtC (total sum of SOC change per PCU). Average SOC change percent for all the cropland surface modeled (SOC change % per PCU). Includes all the Cc and Cr combinations, the exporting rates decrease, and limited application. Export rate: 100 %; coproducts return: 50 tC ha^{-1} 100y

Bioeconomy scenarios $C_C + C_R$ Combinations	Total national SOC change (MtC)	σ	Min	Max	Average national SOC change (%)	σ	Min	Max
PYROLYSIS 2								
MM	441.81	0.04	2.49E-05	0.25	58.78%	29.73%	0.14%	139.78%
HH	484.90	0.05	3.32E-05	0.26	64.22%	31.20%	0.18%	146.02%
HM	462.62	0.04	3.17E-05	0.25	61.29%	29.82%	0.18%	139.78%
HL	434.77	0.04	2.98E-05	0.24	57.62%	28.09%	0.16%	131.99%
MH	463.22	0.04	2.62E-05	0.26	61.61%	31.11%	0.14%	146.02%
ML	415.06	0.04	2.33E-05	0.23	55.24%	27.99%	0.13%	131.99%
LH	433.05	0.04	1.91E-05	0.24	57.93%	30.91%	0.11%	144.96%
LM	412.86	0.04	1.81E-05	0.23	55.25%	29.52%	0.10%	138.74%
LL	387.63	0.04	1.69E-05	0.22	51.90%	27.79%	0.09%	130.97%
PYROLYSIS 2								
MM	346.72	0.03	2.05E-05	0.20	46.07%	23.21%	0.11%	110.74%
HH	434.93	0.04	3.02E-05	0.24	57.60%	27.98%	0.17%	131.61%
HM	363.65	0.03	2.63E-05	0.20	48.11%	23.30%	0.15%	110.74%
HL	263.87	0.02	2.08E-05	0.14	34.83%	16.79%	0.12%	81.53%
MH	415.21	0.04	2.37E-05	0.23	55.22%	27.89%	0.13%	131.61%
ML	250.84	0.02	1.60E-05	0.14	33.27%	16.68%	0.09%	81.53%
LH	387.76	0.04	1.72E-05	0.22	51.88%	27.69%	0.10%	130.22%
LM	323.17	0.03	1.47E-05	0.18	43.21%	23.02%	0.08%	108.64%
LL	232.74	0.02	1.13E-05	0.13	31.08%	16.50%	0.06%	78.42%
GASIFICATION								
MM	302.25	0.03	8.62E-06	0.20	40.92%	24.78%	0.05%	120.33%
HH	381.98	0.04	1.27E-05	0.24	51.23%	29.14%	0.07%	139.56%
HM	363.86	0.04	1.20E-05	0.23	48.82%	27.81%	0.07%	133.49%
HL	341.20	0.03	1.11E-05	0.21	45.81%	26.15%	0.06%	125.91%
MH	317.78	0.03	9.19E-06	0.21	43.00%	25.99%	0.05%	125.88%
ML	282.84	0.03	7.91E-06	0.19	38.32%	23.27%	0.04%	113.39%
LH	211.87	0.02	4.95E-06	0.14	29.27%	20.18%	0.03%	121.68%
LM	200.62	0.02	4.55E-06	0.13	27.75%	19.22%	0.03%	116.15%
LL	186.56	0.02	4.05E-06	0.12	25.84%	18.02%	0.02%	109.24%

Table S2.3. Sensitivity Analysis: Combination of 3 levels for 2 factors.***SI is calculated for comparisson of parameters in minimum and maximum vs mean value of each parameter C_C and C_R.*** Cr= Carbon recalcitrance, SI= %Change in output/%change in input, Input is parameter value (C_C or C_R) Output is SOC change

Table S2.3.1 Pyrolysis

Pyrolysis	Input		Outputs				Sensitivity				
$C_C + C_R$ Combinations	Cc	C_R	Total national SOC change (MtC)	σ	Average national SOC change (%)	σ	Change in Output %	Change in C_C %	SI C_C	Change in C_R %	SI C_R
MM	44	95	774.22	0.08	105.45%	69.34%					
HM	54	95	965.31	0.10	131.33%	86.04%	24.54%	22.73%	1.08	0.00%	
LM	34	95	583.13	0.06	79.57%	52.65%	-24.54%	-22.73%	1.08	0.00%	
MH	44	99	809.62	0.08	110.24%	72.43%	4.55%	0.00%		4.21%	1.08
ML	44	90	729.97	0.07	99.46%	65.48%	-5.68%	0.00%		-5.26%	1.08
HH	54	99	1008.76	0.10	137.21%	89.83%	30.12%	22.73%	1.33	4.21%	7.15
HL	54	90	911.00	0.09	123.97%	81.29%	17.57%	22.73%	0.77	-5.26%	-3.34
LH	34	99	610.49	0.06	83.28%	55.04%	-21.03%	-22.73%	0.93	4.21%	-4.99
LL	34	90	548.94	0.06	74.94%	49.67%	-28.93%	-22.73%	1.27	-5.26%	5.50
Range (SA)		90-99	548.94 - 1008.76		74.94 - 137.21		-28.93 - 30.12				

	Min	Max
C_C	34	54
C_R	90	99
Total national SOC change (MtC)	548.94	1008.76
Average national SOC change (%)	74.94%	137.21%
Change in Output %	-28.93%	30.12%

Table S2.3.2 Pyrolysis 2

Pyrolysis 2	Input		Outputs				Sensitivity				
$C_R + C_R$ Combinations	C_R	C_R	Total national SOC change (MtC)	σ	Average national SOC change (%)	σ	Change in Output %	Change in C_C %	SI C_C	Change in C_R %	SI C_R
MM	44	75	616.74	0.06	83.87%	54.85%					
HM	54	75	772.04	0.08	104.84%	68.26%	25.01%	23%	1.10	0.00%	
LM	34	75	461.44	0.05	62.89%	41.44%	-25.01%	-23%	1.10	0.00%	
MH	44	89	730.15	0.07	99.40%	65.25%	18.52%	0%		18.67%	0.99
ML	44	60	457.96	0.05	62.13%	40.29%	-25.93%	0%		-20.00%	1.30
HH	54	89	911.22	0.09	123.91%	81.03%	47.74%	23%	2.10	18.67%	2.56
HL	54	60	577.18	0.06	78.16%	50.41%	-6.81%	23%	-0.30	-20.00%	0.34
LH	34	89	549.08	0.06	74.90%	49.49%	-10.70%	-23%	0.47	18.67%	-0.57
LL	34	60	338.75	0.03	46.09%	30.18%	-45.04%	-23%	1.98	-20.00%	2.25
Range (SA)	34-54	60-89	338.75 - 911.22		46.09 - 123.91		-45.04 - 47.74				

	Min	Max
C_C	34	54
C_R	60	89
Total national SOC change (MtC)	338.75	911.22
Average national SOC change (%)	46.09%	123.91%
Change in Output %	-45.04%	47.74%

Table S2.3.3 Confrontation of results shown in the methodology of Pyrolysis and Pyrolysis 1

Pyrolysis 1	Input		Outputs				Sensitivity		
$C_C + C_R$ Combinations	Cc	C_R	Total national SOC change (MtC)	σ	Average national SOC change (%)	σ	Change in Output %	Change in C_R %	SI C_R
MM 1	44	95	774.22	0.08	105.45%	69.34%			
HM 1	54	95	965.31	0.10	131.33%	86.04%			
LM 1	34	95	583.13	0.06	79.57%	52.65%			
MH 1	44	99	809.62	0.08	110.24%	72.43%			
ML	44	90	729.97	0.07	99.46%	65.48%			
HH	54	99	1008.76	0.10	137.21%	89.83%			
HL	54	90	911.00	0.09	123.97%	81.29%			
LH	34	99	610.49	0.06	83.28%	55.04%			
LL	34	90	548.94	0.06	74.94%	49.67%			
MM 2	44	75	616.74	0.06	83.87%	54.85%	-20.47%	-21.1%	0.97
HM	54	75	772.04	0.08	104.84%	68.26%	-20.17%	-21.1%	0.96
LM	34	75	461.44	0.05	62.89%	41.44%	-20.96%	-21.1%	1.00
MH	44	89	730.15	0.07	99.40%	65.25%	-9.84%	-10.1%	0.97
ML	44	60	457.96	0.05	62.13%	40.29%	-37.54%	-33.3%	1.13
HH	54	89	911.22	0.09	123.91%	81.03%	-9.70%	-10.1%	0.96
HL	54	60	577.18	0.06	78.16%	50.41%	-36.96%	-33.3%	1.11
LH	34	89	549.08	0.06	74.90%	49.49%	-10.06%	-10.1%	1.00
LL	34	60	338.75	0.03	46.09%	30.18%	-38.49%	-33.3%	1.15
Range (SA)	34-54	60-99	338.75-1008.76		46.09 - 137.21		-38.49 - -9.70		

	Min	Max
C_C	34	54
C_R	60	99
Total national SOC change (MtC)	338.75	1008.76
Average national SOC change (%)	46.09%	137.21%
Change in Output %	-38.49%	-9.70%

Table S2.3.4 Gasification

Gasification	Input		Outputs				Sensitivity				
$C_C + C_R$ Combinations	Cc	Cr	Total national SOC change (MtC)	σ	Average national SOC change (%)	σ	Change in Output %	Change in Cc %	SI Cc	Change in Cr %	SI Cr
MM	20	95	315.61	0.03	43.34%	29.34%					
HM	25	95	411.15	0.04	56.28%	37.65%	29.86%	25%	1.19	0%	
LM	14	95	200.95	0.02	27.81%	19.41%	-35.83%	-30%	1.19	0%	
MH	20	99	331.70	0.03	45.52%	30.74%	5.03%	0.00		4%	1.19
ML	20	90	295.49	0.03	40.62%	27.59%	-6.29%	0%		-5%	1.19
HH	25	99	431.27	0.04	59.00%	39.41%	36.14%	25%	1.45	4%	8.58
HL	25	90	386.01	0.04	52.87%	35.46%	22.00%	0.25	0.88	-5%	-4.18
LH	14	99	212.22	0.02	29.34%	20.38%	-32.31%	-30%	1.08	4%	-7.67
LL	14	90	186.87	0.02	25.91%	18.20%	-40.23%	-30%	1.34	-5%	7.64
Range (SA)	14-25	90-99	186.87 - 431.27		25.91-59.07		-40.20 - 36.12				

	Min	Max
C_C	14	25
C_R	90	99
Total national SOC change (MtC)	186.87	431.27
Average national SOC change (%)	25.91%	59.00%
Change in Output %	-40.23%	36.14%

Table S2.3.5 Hydrothermal liquefaction

HTL	Input		Outputs				Sensitivity				
$C_C + C_R$ Combinations	Cc	Cr	Total national SOC change (MtC)	σ	Average national SOC change (%)	σ	Change in Output %	Change in Cc %	SI Cc	Change in Cr %	SI Cr
MM	31	83	8.85	####	1.12%	0.83%					
HM	45	83	42.92	######	5.43%	3.51%	383.46%	45.2%	8.49	0.0%	
LM	12	83	-37.37	######	-4.72%	3.06%	-520.42%	-61.3%	8.49	0.0%	
MH	31	96	20.67	######	2.62%	1.73%	132.99%	0.0%		15.7%	8.49
ML	31	80	6.13	######	0.78%	0.65%	-30.69%	0.0%		-3.6%	8.49
HH	45	96	60.06	0.01	7.60%	4.89%	576.52%	45.2%	12.77	15.7%	36.81
HL	45	80	38.96	######	4.93%	3.19%	338.91%	45.2%	7.50	-3.6%	-93.77
LH	12	96	-32.80	######	-4.15%	2.69%	-468.94%	-61.3%	7.65	15.7%	-29.94
LL	12	80	-38.43	######	-4.86%	3.14%	-532.30%	-61.3%	8.68	-3.6%	147.27
Range (SA)	12-45	80-96	-38.43 - 60.06		-4.86 - 7.60		-532.30 - 576.52				

	Min	Max
C_C	12	45
C_R	80	96
Total national SOC change (MtC)	-38.43	60.06
Average national SOC change (%)	-4.86%	7.60%
Change in Output %	-532.30%	576.52%

Table S2.3.6 Anaerobic digestion

Anaerobic digestion	Input		Outputs				Sensitivity				
$C_C + C_R$ Combinations	Cc	Cr	Total national SOC change (MtC)	σ	Average national SOC change (%)	σ	Change in Output %	Change in Cc %	SI Cc	Change in Cr %	SI Cr
MM	33	68	-0.79	######	-0.10%	0.42%					
HM	40	68	13.16	######	1.67%	1.15%	-1832.65%	21.21%	-86.40	0.00%	
LM	30	68	-6.77	######	-0.85%	0.69%	785.42%	-9.09%	-86.40	0.00%	
MH	33	77	7.91	######	1.01%	0.77%	-1143.48%	0.00%		13.24%	-86.40
ML	33	58	-10.46	0.07	-1.32%	0.94%	1270.54%	0.00%		-14.71%	-86.40
HH	40	77	23.71	######	3.00%	1.97%	-3218.69%	21.21%	-151.74	13.24%	-243.19
HL	40	58	1.44	######	0.19%	0.43%	-292.61%	21.21%	-13.79	-14.71%	19.90
LH	30	77	1.14	######	0.15%	0.43%	-254.11%	-9.09%	27.95	13.24%	-19.20
LL	30	58	-15.57	######	-1.97%	1.33%	1940.46%	-9.09%	-213.45	-14.71%	-131.95
Range (SA)	30-40	58-77	-15.57-23.71		-1.97-3.00		-3218.69 - 1940.46				

	Min	Max
C_C	30	40
C_R	58	77
Total national SOC change (MtC)	-15.57	23.71
Average national SOC change (%)	-1.97%	3.00%
Change in Output %	-3218.69%	#######

Table S2.3.7

Lignocellulosic ethanol	Input		Outputs				Sensitivity				
$C_C + C_R$ Combinations	Cc	Cr	Total national SOC change (MtC)	σ	Average national SOC change (%)	σ	Change in Output %	Change in Cc %	SI Cc	Change in Cr %	SI Cr
MM	24	45	-34.91	######	-4.41%	2.86%					
HM	30	45	-27.00	######	-3.41%	2.23%	-22.69%	25%	-0.91	0%	
LM	18	45	-42.83	######	-5.41%	3.50%	22.69%	-25%	-0.91	0%	
MH	24	60	-24.36	######	-3.08%	2.02%	-30.25%	0%		33%	-0.91
ML	24	28	-46.87	0.01	-5.93%	3.82%	34.29%	0%		-38%	-0.91
HH	30	60	-13.81	######	-1.74%	1.19%	-60.51%	25%	-2.42	33%	-1.82
HL	30	28	-41.95	######	-5.30%	3.43%	20.17%	25%	0.81	-38%	-0.53
LH	18	60	-34.91	######	-4.41%	2.86%	0.00%	-25%	0.00	33%	0.00
LL	18	28	-51.80	0.01	-6.55%	4.22%	48.40%	-25%	-1.94	-38%	-1.28
Range (SA)	18-0	28- 60	-51.80 - -13.81		-6.55 - -1.74		-60.5-8.40				

	Min	Max
C_C	18	30
C_R	28	60
Total national SOC change (MtC)	-51.80	-13.81
Average national SOC change (%)	-6.55%	-1.74%
Change in Output %	-60.51%	48.40%

Table S2.4 SOC change (%) per areas affected (%) at PCU scale (11784). Breaks obtained from Natural Jenks to have the best distribution. This sheet allows to observe the complete range of SOC change for each technology per PCU with the real max and min values. 100% Export

Table S2.4***Per PCU, ranges defined by Jenks natural breaks 11784 PCU . 100% Export rate***

Bioeconomy scenarios	Pyrochar 1		Pyrochar 2		Gaschar	
Cc + Cr Combinations	Cranges (%)	Area afected (%)	Cranges (%)	Area afected (%)	Cranges (%)	Area afected (%)
HH	0 - 49.99	23.76	0 - 44.94	23.71	0- 22.72	24.40
	49.99 - 115.92	13.35	44.94 - 104.63	13.34	22.72 - 51.51	14.86
	115.92 - 172.06	32.90	104.63 - 155.32	32.83	51.51 - 75.56	33.21
	172.06 - 245.25	23.98	155.32 - 221.99	24.13	75.56 - 108.57	21.96
	245.25 - 354.17	4.57	221.99 - 320.49	4.58	108.57 - 157.73	4.12
	354.17 - 527.77	1.45	320.49 - 475.45	1.41	157.73 - 235.7	1.44
HM	0 - 47.98	23.79	0 - 38.09	23.71	0 - 21.67	24.42
	47.98 - 111.15	13.44	38.09 - 88.46	13.24	21.67 - 49.12	14.90
	111.15 - 164.72	32.80	88.46 - 131.25	32.52	49.12 - 72.09	33.17
	164.72 - 235.11	23.97	131.25 - 187.29	24.54	72.09 - 103.55	21.97
	235.11 - 339.23	4.55	187.29 - 269.75	4.60	103.55 - 150.74	4.10
	339.23 - 505.8	1.45	269.75 - 398.63	1.39	150.74 - 225.53	1.44
HL	0 - 45.42	23.85	0 - 25.64	23.06	0 - 20.36	24.43
	45.42 - 105.07	13.41	25.64 - 59.86	10.91	20.36 - 46.15	14.95
	105.07 - 155.6	32.86	59.86 - 87.65	23.19	46.15 - 67.75	33.17
	155.6 - 222.34	23.91	87.65 - 115.18	26.55	67.75 - 97.74	21.93
	222.34- 321.52	4.54	115.18 - 168.82	12.92	97.74 - 142.35	4.10
	321.52 - 478.33	1.43	168.82 - 291.1	3.38	142.35 - 212.81	1.43
MH	0 - 40.5	23.90	0 - 36.45	23.89	0 - 17.88	24.71
	40.5- 93.53	13.44	36.45 - 84.23	13.40	17.88 - 40.18	15.82
	93.53 - 138.45	32.85	84.23 - 124.75	32.80	40.18 - 58.74	32.82
	138.45 - 197.89	23.89	124.75 - 178.33	23.96	58.74 - 84.82	21.29
	197.89 - 286.52	4.50	178.33 - 258.08	4.52	84.82 - 123.94	3.92
	286.52 - 427.06	1.43	258.08 - 384.42	1.43	123.94 - 185.34	1.44
MM	0 - 38.83	23.91	0 - 30.49	23.73	0 - 17.02	24.70
	38.83 - 89.55	13.52	30.49 - 70.79	13.35	17.02 - 38.2	15.86
	89.55 - 132.55	32.96	70.79 - 105.09	32.77	38.2 - 55.94	32.89
	132.55 - 189.65	23.74	105.09 - 149.8	24.14	55.94 - 80.82	21.25
	189.65 - 274.47	4.44	149.8 - 216.08	4.57	80.82 - 117.95	3.83
	274.47 - 409.15	1.43	216.08 - 321.83	1.45	117.95 - 177.2	1.48
ML	0 - 36.83	23.98	0 - 22.68	23.72	0 - 15.6	24.50
	36.83 - 84.75	13.59	22.68 - 52.54	13.27	15.6 - 35.33	15.26
	84.75 - 125.29	33.17	52.54 - 77.78	32.39	35.33 - 52.06	32.96

Bioeconomy scenarios	Pyrochar 1		Pyrochar 2		Gaschar	
Cc + Cr Combinations	Cranges (%)	Area afected (%)	Cranges (%)	Area afected (%)	Cranges (%)	Area afected (%)
	125.29 - 179.3	23.41	77.78 - 110.43	24.47	52.06 - 75.35	21.81
	179.3 - 259.53	4.42	110.43 - 158.93	4.75	75.35%- 109.46	3.92
	259.53 - 386.77	1.43	158.93 - 234.22	1.39	109.46 - 167.03	1.54
LH	0 - 30.98	24.09	0 - 27.86	24.09	0 - 10.91	24.31
	30.98 - 71.14	13.64	27.86 - 63.96	13.61	10.91 - 24.97	14.90
	71.14 - 105.07	33.16	63.96 - 94.46	33.12	24.97 - 37.36	32.97
	105.07 - 150.57	23.29	94.46 - 135.35	23.32	37.36 - 55.36	22.72
	150.57 - 217.78	4.39	135.35 - 195.8	4.41	55.36 - 82.11	3.59
	217.78 - 326.34	1.45	195.8 - 293.4	1.45	82.11 - 124.91	1.51
LM	0 - 29.61	24.10	0 - 23.42	24.08	0 - 10.28	24.36
	29.61 - 67.92	13.61	23.42 - 53.81	13.68	10.28 - 23.57	14.74
	67.92 - 100.34	33.13	53.81 - 79.43	33.19	23.57- 35.38	32.97
	100.34 - 143.95	23.31	79.43 - 113.56	23.20	35.38 - 52.58	22.80
	143.95 - 208.34	4.41	113.56 - 164.48	4.42	52.58 - 78.3	3.62
	208.34 - 312.51	1.45	164.48 - 245.03	1.43	78.3 - 119.22	1.51
LL	0 - 27.94	24.10	0 - 16.88	23.87	0 - 8.91	23.83
	27.94 - 64.05	13.68	16.88 - 39.07	13.42	8.91- 20.59	12.97
	64.05 - 94.63	33.19	39.07 - 57.92	32.92	20.59 - 30.77	28.56
	94.63 - 135.91	23.26	57.92 - 82.57	23.85	30.77 - 43.18	25.88
	135.91 - 196.63	4.33	82.57 - 119.19	4.52	43.18 - 65.99	6.46
	196.63 - 295.21	1.45	119.19 - 177.33	1.43	65.99 - 112.1	2.30

Table S2.4 SOC change (%) per areas affected (%) at PCU scale (11784). Breaks obtained from Natural Jenks to have the best distribution. This sheet allows to observe the complete range of SOC change for each technology per PCU with the real max and min values. 100% ExportTable S2.4***Per PCU, ranges defined by Jenks natural breaks 11784 PCU . 100% Export rate***

Bioeconomy scenarios	Hydrochar		Digestate		Molasses	
Cc + Cr Combinations	Cranges (%)	Area afected %)	Cranges (%)	Area afected (%)	Cranges (%)	Area afected (%)
HH	0- 2.48	22.35	-0.08 - -0.07	0.08	-6.02%- -3.63	7.50
	2.48 - 5.57	12.39	-0.07 - -0.06	0.10	-3.63 - -2.52	16.10
	5.57- 8.18	20.93	-0.06 - 0	9.79	-2.52 - -1.69	26.86
	8.18 - 10.77	17.53	0- 1.88	22.75	-1.69 - -0.84	22.90
	10.77 - 14.17	15.64	1.88 - 4.18	39.26	-0.84 - 0	16.88
	14.17 - 22.6	11.15	4.18 - 9.16	28.02	0 - 0	9.76
HM	0 - 1.75	22.17	-1.04 - -0.59	0.14	-11.13 - -5.98	13.84
	1.75 - 3.96	12.85	-0.59 - -0.27	0.61	-5.98 - -4.21	20.17
	3.96 - 5.87	21.40	-0.27 - 0	10.78	-4.21 - -2.77	28.53
	5.87 - 7.78	17.35	0 - 1.07	23.13	-2.77 - -1.33	13.67
	7.78 - 10.25	15.70	1.07 - 2.39	38.00	-1.33 - -0.01	14.01
	10.25 - 15.95	10.53	2.39 - 5.53	27.34	-0.01 - 0	9.76
HL	0- 1.69	22.72	-3.1 - -1.41	1.63	-16.92 - -9.31	13.33
	1.69 - 3.78	14.77	-1.41 - -0.5	2.19	-9.31 - -6.58	21.02
	3.78 - 5.5	21.28	-0.5 - 0	29.21	-6.58 - -4.35	28.05
	5.5 - 7.18	15.81	0 - 0.26	28.77	-4.35 - -2.11	13.68
	7.18 - 9.37	15.22	0.26 - 0.6	25.30	-2.11 - -0.01	14.15
	9.37 - 14.42	10.21	0.6 - 1.51	12.90	-0.01 - 0	9.76
MH	-0.21 - -0.15	0.18	-1.96 - -1.13	0.49	-10.11 - -5.41	13.72
	-0.15 - -0.06	0.03	-1.13% - -0.52	1.42	-5.41 - -3.8	20.19
	-0.06 - 0	9.76	-0.52 - 0	10.86	-3.8 - -2.51	28.50
	0 - 1.64	22.99	0 - 0.69	24.88	-2.51 - -1.21	13.70
	1.6 - 3.66	39.07	0.69 - 1.55	38.13	-1.21 - -0.01	14.14
	3.66 - 8.11	27.97	1.55 - 3.73	24.23	-0.01 - 0	9.76
MM	-1.78 - -0.98	0.41	-3.49 - -1.26	2.49	-14.19 - -7.75	13.35
	-0.98 - -0.44	1.38	-1.26 - -0.37	15.44	-7.75 - -5.47	20.98
	-0.44 - 0	10.75	-0.37 - 0	32.06	-5.47 - -3.61	28.14
	0 - 0.76	24.43	0 - 0.11	23.06	-3.61 - -1.75	13.66
	0.76 - 1.69	38.16	0.11 - 0.28	18.47	-1.75 - -0.01	14.10
	1.69 - 4.06	24.85	0.28 - 0.74	8.47	-0.01 - 0	9.76
ML	-2.26 - -1.28	0.68	-5.19 - -2.88	7.38	-18.83 - -10.42	13.34
	-1.28 - -0.56	1.49	-2.88 - -1.93	14.23	-10.42 - -7.37	21.08
	-0.56 - 0	11.19	-1.93 - -1.27	27.45	-7.37 - -4.88	27.85
	0 - 0.56	26.53	-1.27 - -0.62	24.35	-4.88 - -2.38	13.60

Bioeconomy scenarios	Hydrochar		Digestate		Molasses	
Cc + Cr Combinations	Cranges (%)	Area afected %)	Cranges (%)	Area afected (%)	Cranges (%)	Area afected (%)
	0.56 - 1.27	38.11	-0.62 - 0	16.83	-2.38 - -0.02	14.37
	1.27 - 3.12	21.99	0 - 0	9.76	-0.02 - 0	9.76
LH	-13.38 - -7.27	13.42	-3.15 - -1.45	1.64	-14.19 - -7.75	13.35
	-7.27 - -5.13	20.93	-1.45 - -0.52	2.24	-7.75 - -5.47	20.98
	-5.13 - -3.39	28.16	-0.52 - 0	31.39	-5.47 - -3.61	28.14
	-3.39 - -1.64	13.64	0 - 0.24	27.91	-3.61 - -1.75	13.66
	-1.64 - -0.01	14.08	0.24 - 0.56	24.50	-1.75 - -0.01	14.10
	-0.01 - 0	9.76	0.56 - 1.41	12.33	-0.01 - 0	9.76
LM	-15.15- -8.31	13.21	-4.54 - -2.27	5.15	-17.26 - -9.51	13.30
	-8.31 - -5.86	21.12	-2.27 - -1.4	11.58	-9.51 - -6.72	21.06
	-5.86 - -3.87	28.12	-1.4 - -0.85	26.11	-6.72- -4.44	28.14
	-3.87- -1.87	13.69	-0.85 - -0.39	29.87	-4.44 - -2.15	13.59
	-1.87 - -0.01	14.10	-0.39 - 0	17.52	-2.15 - -0.02	14.14
	-0.01 - 0	9.76	0- 0	9.76	-0.02 - 0	9.76
LL	-15.56 - -8.53	13.37	-6.7 - -3.99	7.96	-20.74 - -11.5	13.41
	-8.53 - -6.02	21.03	-3.99 - -2.82	16.23	-11.5 - -8.15	21.06
	-6.02 - -3.98	28.04	-2.82- -1.91	26.67	-8.15 - -5.42	27.51
	-3.98 - -1.93	13.68	-1.91 - -0.95	22.44	-5.42 - -2.66	13.69
	-1.93 - -0.01	14.11	-0.95 - 0	16.94	-2.66 - -0.02	14.56
	-0.01 - 0	9.76	0 - 0	9.76	-0.02 - 0	9.76

Table S2.4 ***Per PCU, ranges defined by Jenks natural breaks 11784 PCU . 75% Export rate MM***

HYDROCHAR		DIGESTATE		MOLASSES	
Cranges (%)	Area afected (%)	Cranges (%)	Area afected (%)	Cranges (%)	Area afected (%)
-1.35% - -0.74%	0.41	-2.62% - -0.95%	2.49	-10.65% - -5.81%	13.36
-0.74% - -0.33%	1.38	-0.95% - -0.28%	15.44	-5.81% - -4.1%	20.97
-0.33% - 0%	10.75	-0.28% - 0%	32.06	-4.1% - -2.71%	28.14
0% - 0.57%	24.43	0% - 0.08%	23.06	-2.71% - -1.31%	13.66
0.57% - 1.28%	38.16	0.08% - 0.21%	18.47	-1.31% - -0.01%	14.10
1.28% - 3.04%	24.85	0.21% - 0.56%	8.48	-0.01% - 0%	9.76

Table S2.4*Per PCU, ranges defined by Jenks natural breaks 11784 PCU .50% Export rate MM*

HYDROCHAR		DIGESTATE		MOLASSES	
Cranges (%)	Area afected (%)	Cranges (%)	Area afected (%)	Cranges (%)	Area afected (%)
-0.9% - -0.49%	0.41	-1.74% - -0.63%	2.49	-7.1% - -3.87%	13.35
-0.49% - -0.22%	1.38	-0.63% - -0.19%	15.50	-3.87% - -2.73%	20.98
-0.22% - 0%	10.75	-0.19% - 0%	32.00	-2.73% - -1.8%	28.14
0% - 0.38%	24.43	0% - 0.05%	23.06	-1.8% - -0.87%	13.66
0.38% - 0.85%	38.16	0.05% - 0.14%	18.47	-0.87% - -0.01%	14.10
0.85% - 2.03%	24.85	0.14% - 0.37%	8.47	-0.01% - 0%	9.76

Table S2.4; *Per PCU, ranges defined by Jenks natural breaks 11784 PCU . 50t C applied*

	PYROCHAR 1		PYROCHAR 2		GASCHAR	
	Cranges (%)	Area afected (%)	Cranges (%)	Area afected (%)	Cranges (%)	Area afected (%)
HH	0% - 19.27%	18.23	0% - 17.39%	18.21	0% - 15.79%	22.15
	19.27% - 44.98%	7.08	17.39% - 40.48%	7.17	15.79% - 36.69%	8.09
	44.98% - 65.36%	17.02	40.48% - 58.79%	17.55	36.69% - 53.57%	15.67
	65.36% - 80.89%	26.27	58.79% - 72.65%	25.88	53.57% - 68.06%	25.26
	80.89% - 99.99%	25.94	72.65% - 89.73%	25.72	68.06% - 85.96%	21.92
	99.99% - 146.02%	5.46	89.73% - 131.61%	5.48	85.96% - 139.56%	6.91
HM	0% - 18.42%	18.23	0% - 14.52%	18.03	0% - 14.9%	22.10
	18.42% - 43.04%	7.18	14.52% - 33.79%	7.33	14.9% - 34.56%	7.93
	43.04% - 62.5%	17.42	33.79% - 49.07%	17.45	34.56% - 50.63%	15.31
	62.5% - 77.3%	26.01	49.07% - 60.57%	25.80	50.63% - 64.61%	25.54
	77.3% - 95.6%	25.71	60.57% - 74.57%	25.60	64.61% - 81.77%	22.06
	95.6% - 139.78%	5.45	74.57% - 110.74%	5.80	81.77% - 133.49%	7.05
HL	0% - 17.38%	18.23	0% - 10.59%	17.87	0% - 14.26%	22.18
	17.38% - 40.49%	7.23	10.59% - 24.56%	7.71	14.26% - 33.1%	8.40
	40.49% - 58.8%	17.73	24.56% - 35.6%	17.37	33.1% - 48.29%	16.39
	58.8% - 72.8%	25.83	35.6% - 43.9%	26.20	48.29% - 61.33%	25.17
	72.8% - 90.13%	25.56	43.9% - 53.87%	24.91	61.33% - 77.5%	21.26
	90.13% - 131.99%	5.42	53.87% - 81.53%	5.95	77.5% - 125.91%	6.59
MH	0% - 16.05%	18.25	0% - 14.45%	18.25	0% - 13.22%	22.55
	16.05% - 38.91%	6.25	14.45% - 34.95%	6.31	13.22% - 31.17%	9.07
	38.91% - 59.32%	12.68	34.95% - 53.17%	12.78	31.17% - 46.54%	19.45
	59.32% - 76.17%	27.70	53.17% - 68.18%	27.38	46.54% - 61.31%	28.36
	76.17% - 95.41%	28.39	68.18% - 85.33%	28.40	61.31% - 82.52%	17.03
	95.41% - 146.02%	6.73	85.33% - 131.61%	6.88	82.52% - 125.88%	3.54
MM	0% - 15.31%	18.25	0% - 12.39%	18.27	0% - 12.5%	22.52
	15.31% - 37.1%	6.30	12.39% - 29.81%	6.74	12.5% - 29.5%	8.97
	37.1% - 56.6%	12.78	29.81% - 45%	13.69	29.5% - 44.16%	19.42
	56.6% - 72.66%	27.57	45% - 57.25%	26.79	44.16% - 58.33%	28.46

	PYROCHAR 1		PYROCHAR 2		GASCHAR	
	Cranges (%)	Area afected (%)	Cranges (%)	Area afected (%)	Cranges (%)	Area afected (%)
	72.66% - 91.12%	28.36	57.25% - 71.42%	27.90	58.33% - 78.59%	17.08
	91.12% - 139.78%	6.74	71.42% - 110.74%	6.61	78.59% - 120.33%	3.55
ML	0% - 19.1%	20.12	0% - 9.03%	18.14	0% - 12.33%	22.80
	19.1% - 42.2%	8.32	9.03% - 21.61%	6.84	12.33% - 28.95%	9.82
	42.2% - 59.01%	18.50	21.61% - 32.51%	14.04	28.95% - 42.8%	22.62
	59.01% - 72.69%	27.81	32.51% - 41.3%	26.32	42.8% - 55.86%	26.15
	72.69% - 89.25%	20.47	41.3% - 51.33%	27.58	55.86% - 74.82%	15.35
	89.25% - 131.99%	4.78	51.33% - 81.53%	7.07	74.82% - 113.39%	3.27
LH	0% - 20.54%	21.54	0% - 18.46%	21.54	0% - 9.99%	23.69
	20.54% - 45.8%	9.23	18.46% - 41.18%	9.37	23.12% - 34.42%	28.01
	45.8% - 64.14%	19.85	41.18% - 57.59%	20.32	34.42% - 47.35%	25.79
	64.14% - 79.27%	27.32	57.59% - 71.09%	26.82	47.35% - 71.56%	7.41
	79.27% - 97.83%	18.40	71.09% - 87.57%	18.19	71.56% - 121.68%	2.55
	97.83% - 144.96%	3.65	87.57% - 130.22%	3.75	9.99% - 23.12%	12.55
LM	0% - 19.64%	21.56	0% - 14.96%	21.28	0% - 9.4%	23.68
	19.64% - 43.76%	9.33	14.96% - 33.48%	8.87	9.4% - 21.8%	12.50
	43.76% - 61.3%	20.20	33.48% - 47.21%	19.47	21.8% - 32.54%	27.93
	61.3% - 75.77%	27.10	47.21% - 58.54%	26.82	32.54% - 44.87%	25.87
	75.77% - 93.45%	18.14	58.54% - 72.27%	19.48	44.87% - 68.13%	7.47
	93.45% - 138.74%	3.67	72.27% - 108.64%	4.08	68.13% - 116.15%	2.55
LL	0% - 18.42%	21.56	0% - 10.81%	21.22	0% - 8.7%	23.67
	18.42% - 41.06%	9.26	10.81% - 24.06%	9.12	8.7% - 20.23%	12.52
	41.06% - 57.55%	20.52	24.06% - 33.76%	18.63	20.23% - 30.29%	27.97
	57.55% - 71.24%	26.94	33.76% - 41.83%	26.66	30.29% - 41.95%	25.98
	71.24% - 88.02%	18.03	41.83% - 51.47%	19.85	41.95% - 63.9%	7.31
	88.02% - 130.97%	3.70	51.47% - 78.42%	4.52	63.9% - 109.24%	2.55

Appendix A3a

Data paper

This document is a data paper by itself, serving as companion for Chapter 4. This Data paper describes the creation of the baseline for current cropping systems in Ecuadorian croplands and parallel input data required to run simulation sin RothC for the specific case study deployed in paper 3: *"Modelling the long-term carbon storage potential from recalcitrant matter inputs in tropical arable croplands".*

This Data paper is currently being prepared to be submitted to Data in Brief. The database inhere presented is accessible in https://doi.org/10.48531/JBRU.CALMIP/VLKG8V but remains confidential until the publication of the paper.

Contents

Dataset for defining the spatially explicit baseline of cropping systems in Ecuadorian croplands and estimating the crop residues potential

Christhel Andrade Diaz[a,b*], Ezequiel Zamora-Ledezma[c], Lorie Hamelin[a]

[a] Toulouse Biotechnology Institute (TBI), INSA, INRAE UMR792, and CNRS UMR5504, Federal University of Toulouse, 135 Avenue de Rangueil, F-31077, Toulouse, France

[b] Department of Chemical, Biotechnological and Food Processes, Faculty of Mathematical, Physics and Chemistry Sciences. Universidad Técnica de Manabí (UTM), 130150, Portoviejo, Ecuador.

[c] Ecosystems Functioning and Climate Change Research Group FAGROCLIM, Faculty of Agriculture Engineering. Universidad Técnica de Manabí (UTM), 13132, Lodana, Ecuador.

* andraded@insa-toulouse.fr, christhel.andrade@utm.edu.ec, twitter:@christhell

Keywords

cropping systems, harvestable biomass, high spatial resolution, baseline, SOC, pedoclimatic data

Abstract

This dataset describes the baseline cropping systems of Ecuador and the associated pedoclimatic conditions. A high spatial resolution approach was used to quantify the spatially-explicit theoretical and technical potential yield of ten key crop residues, as well as the inputs to soil and potential supply to the bioeconomy in terms of carbon. Besides, it provides future meteorological data (mean temperature and evapotranspiration) under the representative pathway concentration RCP4.5, in a monthly timestep, spatially explicitly assigned to the cropping systems defined within this baseline. The original data was extracted from the Agricultural and Livestock Public Information System (SIPA; MAG, 2023) of Ecuador. The potential yields were calculated as the average data reported by the Ecuadorian National Continuous Agricultural Production and Surface Survey (ESPAC) for the period 2002-2019. Residue to product ratios (RPR), root to shoot (R:S), root distribution factors in soil profile, crop residues composition are parameters influencing the final C calculation and were determined based on literature review and accompany this database in order to keep the transparency of the data. This database provides all the baseline data required to perform long-term simulations of soil organic carbon for Ecuador.

Specifications table

Subject	Agricultural sciences
Specific subject area	Soil organic carbon modeling in croplands. Assessment of potential C sequestration in agricultural soils.

Type of data	Tables, figures, online database containing excel, csv, and shape files, as well as the scripts used to produce the data.
How the data were acquired	The original data was retrieved from the online database of the Agricultural and Livestock Public Information System (ALPIS; MAG, 2023) of Ecuador and received as courtesy from the Ministry of Agriculture of Ecuador and the Subsecretary of Climate Change of Ecuador. The procedures of data collection are detailed in section 3. Soil bulk density was retrieved from FAO, while parameters required to perform calculations over the data were compiled from exhaustive literature review.
Data format	Analyzed, Filtered
Description of data collection	The primary data was directly retrieved from the SIPA repository as detailed in section 2 and received as courtesy by the original authors. Georeferenced data was manipulated and intersected using ArcGIS. Agricultural production data was managed and processed using R. Climatic data was extracted from the original netcfd files using python, processed with R and then processed with ArcGIS.
Data source location	Ecuador
Data accessibility	List of primary data sources: http://sipa.agricultura.gob.ec/, courtesy from authors (Ministry of Agriculture of Ecuador and Sub-secretary of Climate Change of Ecuador). **Secondary dataset repository** The data has ben deposited in the "TBI - Toulouse Biotechnology Institute - T21018" dataverse at "Data repository for TBI team involved in the following research: "Interactions carbone du sol et utilisation des résidus de culture pour la bioéconomie", (CALMIP 2021 N°T21028) ». Repository name: Dataset for defining the spatially explicit baseline of cropping systems in Ecuadorian croplands and estimating the crop residues potential Data identification number: Direct URL to data: https://doi.org/10.48531/JBRU.CALMIP/VLKG8V.
Related research article	C. Andrade Diaz, E. Balugani, E. Zamora-Ledezma, L. Hamelin, Modelling the long-term carbon storage potential from recalcitrant matter inputs in tropical arable croplands, "Accepted Journal", In Press.

Value of the data

- Average crop yields for 10 key crops to supply bioeconomy in Ecuador are presented
- Theoretical potential of crop residues in Ecuador is presented.
- Potential C contribution to Ecuadorian SOC stocks from 10 key crops have been calculated.
- To our knowledge, this is the first study to systematize and model this type of data for Ecuador on a national scale in a context of bioeconomy and pedoclimatic conditions.
- Baseline current cropping systems in Ecuador are defined.
- This dataset can be used by researchers to model potential bioenergy or biomaterials production using crop residues as feedstock, and to analyze SOC dynamics of the BAU and bioeconomy future perspectives in Ecuador.

Objective

The aim of this dataset is to provide the baseline scenario of current cropping systems in Ecuador and to supply the input data required to model soil organic carbon dynamics in Ecuador, in a high-resolution and spatially explicit manner. The dataset intends to cluster Ecuadorian croplands according to pedology and climatic homogeneity, and determine the potential crop residues available in the clustered area. Moreover, this dataset aims to provide the spatially explicit C inputs from aerial biomass and roots for each crop in the cropping systems, contributing to soil organic carbon dynamics. The specific monthly cumulated precipitations and evapotranspiration, as well as average monthly temperature for the 2020 – 2070 period of the clustered cropping systems is also provided.

1. Data Description

This dataset describes the baseline current cropping systems of Ecuador and the average expected carbon inputs to the soil in croplands dedicated to annual, semi-perennial, and perennial crops. It also quantifies the technically harvestable amount of crop residues that can be potentially mobilized to supply the bioeconomy for bioenergy o biomaterials production. Moreover, this dataset is of high spatial resolution, reported for specific combinations of soil and climate characteristics, known as pedoclimatic units. The daily temperature and precipitation projections from 2020 to 2070 under the Representative Concentration Pathway (RCP) 4.5 were used to calculate potential evapotranspiration for the same future period according to the Thornthwrite equation. The meteorological variables were then processed to be displayed at the scale of the pedoclimatic units in a monthly timestep. This dataset was used to model the long-term (from year 2020 to year 2070) soil organic carbon dynamics in Ecuadorian croplands. The dataset [2] comprises 5 Shapefiles, 13 scripts, 3 excels, 6 csv plus one folder containing 23021 csv files. Also, within this document, we include 3 figures and 3 tables.

Figure 1 deploys the workflow followed to cluster the Ecuadorian croplands by soil and climate characteristics to represent the current cropping systems as pedoclimatic units. **Table 1** presents the total production and harvested surface of the 31 main crops reported in the National Continuous Agricultural Production and Surface Survey (ESPAC) (INEC, 2021) for the period 2016-2019. **Figure 2** shows the share of contribution of each crop to the total national croplands surface and production for the period (2016-2019). **Figure 3** describes the sowing and harvesting calendar of the crops selected to supply the bioeconomy in Ecuador and is used to define the monthly availability of crop residues. **Figure 4** presents the spatially explicit potential of crop residues in PJ (average yield from 2002 to 2019) as well as the crop contribution to that yield, for the APCUs included in the database. **Table 2** presents the crop residues main characteristics and **Table 3** presents the factors allocating the biomass across the plant crop (aerial residues and root biomass). Both tables are used in combination with Table 1 to determine the national crop residues potential.

1. Figure 1: Workflow to cluster Ecuadorian cropping systems in agricultural pedoclimatic units.
2. Table 1: Average crop yield reported for Ecuador for the period 2016 – 2019.
3. Figure 2: Crop share for total national production and surface, period 2016 – 2019.
4. Figure 3: Potential of crop residues at APCU scale. Share of contribution per corp to national potential energy
5. Table 2: Crop residues composition
6. Table 3: Factor required to allocate the crop residues biomass across the whole plant, i.e., aerial biomass (RPR) and root biomass (RtS).

The files included in the data repository [2] are briefly explained in here and detailed in the medata txt file accompanying the database:

7. Shapefile1: Agricultural pedoclimatic units (APCUs) defined
8. Shapefile2: Map presented in Figure 3, showing the spatially-explicit crop residues potential in Ecuador, at APCU scale.
9. Shapefile3: Map of accumulated monthly precipitation at APCU scale (RCP4.5). Scaled from
10. Shapefile4: Map of mean monthly Temperature at APCU scale in timestep (RCP4.5)
11. Shapefile5: Map of accumulated monthly evapotranspiration at APCU (RCP4.5)
12. R Script 1: Determines the yield per crop and per province based on the historical national continuous survey of Ecuador, retrieved from [1].
13. R script 2: script used to input the pedoclimatic data and crop yields in the APCUs created in shapefile 1.

14. R Script 3 and 4: 2 scripts working on tandem to calculate the aboveground and belowground carbon in each APCU.
15. R Scripts 5, 6, and 7: 1 script used to calculate the monthly mean temperature in each APCU, under the RCP 4.5 projections, from 2020 until 2070. 2 scripts used to calculate monthly evapotranspiration according to the Thornthwaite method and then scaled at APCU level.
16. Python script 1 and 2: 2 python scripts used to process the original minimum and maximum temperature, as well as the precipitation netcdf files containing the daily projected data until 2070, under RCP 4.5, cordially supplied by the Sub-secrertary of Climate Change of Ecuador [3]
17. R script 8: Script used to pepare the initial input data used by the soil model in the companion research paper.
18. Python script 3, 4, and 5: Pyhton scripts used to create the R scripts subseting the input data at APCU scale.
19. R script 9: Script used to convert Climate csvs created in this database into shapefiles.
20. Excel 1: Yield per crop per province per year (t ha^{-1} y^{-1})
21. Excel 2: Crop residues potential per APCU in tonne (dry matter), and PJ
22. CSV1: Average yield per crop per APCU in monthly timestep
23. Folder TS: 17118 CSV files: Monthly Potential crop residues in tonne C ha-1 (dry matter) per per crop type, split into aboveground and belowground inputs. Each file corresponds to a separate APCU.
24. CSV2: Initial SOC conditions per PCU. It includes total initial SOC in t C ha -1, as well as the SOC allocated in each soil pool (Decomposable plant matter: DPM, Resistant plant matter: RPM, BIO: Biological pool, HUM: Humified matter, IOM: Inert organic matter)
25. CSV3 and 4: Monthly mean temperature at national scale (longitude and latitude provided) and scaled at APCU level, period 2020 – 2070, RPC4.5
26. CSV5 and 5: Monthly accumulated evapotranspiration at national scale (longitude and latitude provided) and scaled at APCU level, period 2020 – 2070, RPC4.5
27. CSV 6: Monthly accumulated precipitations at APCU level, period 2020 – 2070, RPC4.5
28. Excel 3: Harmonized database to determine coefficients required to calculate the crop residues potential and C inputs. It includes also the parameters describing the characteristics of the coproducts obtained when the crop residues are converted in the bioeconomy
29. Excel 4: Calculation of carbon conversion coefficient for digestate produced from tropical crop residues

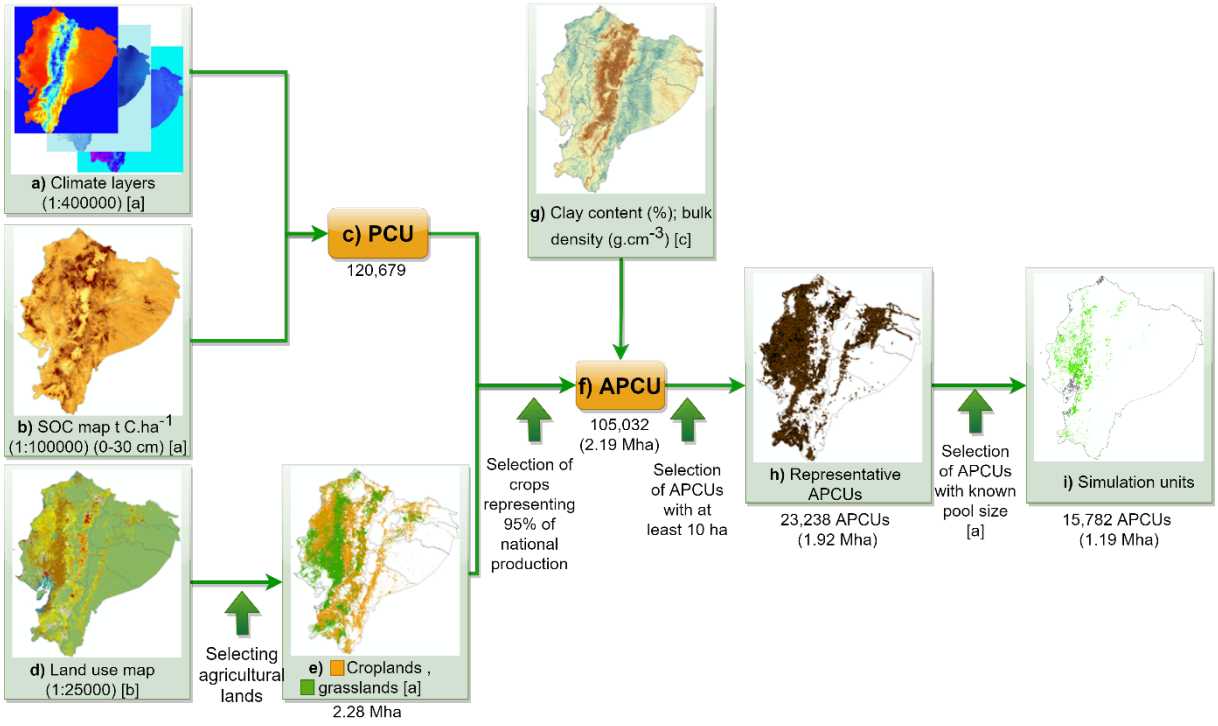

Fig 1. Workflow to create the agricultural pedoclimatic units (APCU) representing the cropping systems in Ecuador. b) climate layers are intersected with a) SOC map at 0-30 cm (1:100 000) to produce c) Pedoclimatic Units (PCU); then the d) Land use map is filtered to agricultural lands, the e) croplands in PCU are selected to produce the national f) APCUs, for which soil clay content and bulk density is assigned. Constraints are applied to the APCUs to define the h) representative APCUs and final selection of i) simulation units based on knowledge of soil pool sizes according to the RothC (Coleman and Jenkinson, 1997) model soil pool distribution.

Table 1. Average national agricultural cropland distribution by crop type for the period 2016-2019 as a representative of current data, retrieved from data reported by INEC (2021). Used to select the crops included in the final database.

Crop	Type	Harvested surface (ha)	Production (tonnes)	Yield (tonne/ha)
Oil palm	Perennial	227494.23	2781615.49	12.23
Avocado	Perennial	4362.97	20421.13	4.68
Banana	Semi-perennial	168790.73	6384856.34	37.92
Barley	Annual	11672.25	16031.39	1.37
Broccoli	Annual	8831.16	145891.25	16.21
Cocoa	Perennial	495263.35	246054.33	0.49
Coffee	Perennial	32402.28	5990.94	0.18
Beans	Annual	33547.15	32245.34	1.27
Faba	Annual	8740.70	20771.37	2.81
Peas	Annual	6420.99	12882.98	2.30
Lemon	Perennial	5022.93	26262.78	5.23
Maize	Annual	412484.08	1462483.58	4.02
Mango	Perennial	16768.00	85826.23	5.16
Onions	Annual	8365.66	37221.27	4.44
Orange	Perennial	15527.79	120169.40	7.74
Orito	Semi-perennial	6007.22	32879.37	5.51
Palmetto	Semi-perennial	6155.29	44452.07	7.15
Passion fruit	Semi-perennial	7450.65	45265.13	6.10
Peanuts	Annual	5649.48	4273.44	0.76
Pineapple	Semi-perennial	4008.35	116261.28	29.15
Plantain	Semi-perennial	111736.73	699589.81	6.35
Potato	Annual	25164.72	350538.43	13.92
Quinoa	Annual	2593.91	3348.73	1.39
Rice	Annual	318548.11	1277486.48	4.05
Soy	Annual	24827.32	33809.98	1.36
Sugarcane	Semi-perennial	127521.45	9465268.38	74.42
Tobacco	Annual	4408.45	5326.39	1.26
Tomato	Annual	1849.69	44029.18	24.31
Tomato (fruit)	Semi-perennial	1756.23	21197.58	11.94
Wheat	Annual	4369.12	7533.39	1.67
Yucca	Annual	15287.90	80856.13	5.30
TOTAL		2123028.90	23630839.57	300.71

[a] Only the harvested surface considered. [b] Sum of the dry and tender crop. [c] Sum of hard and soft maize.

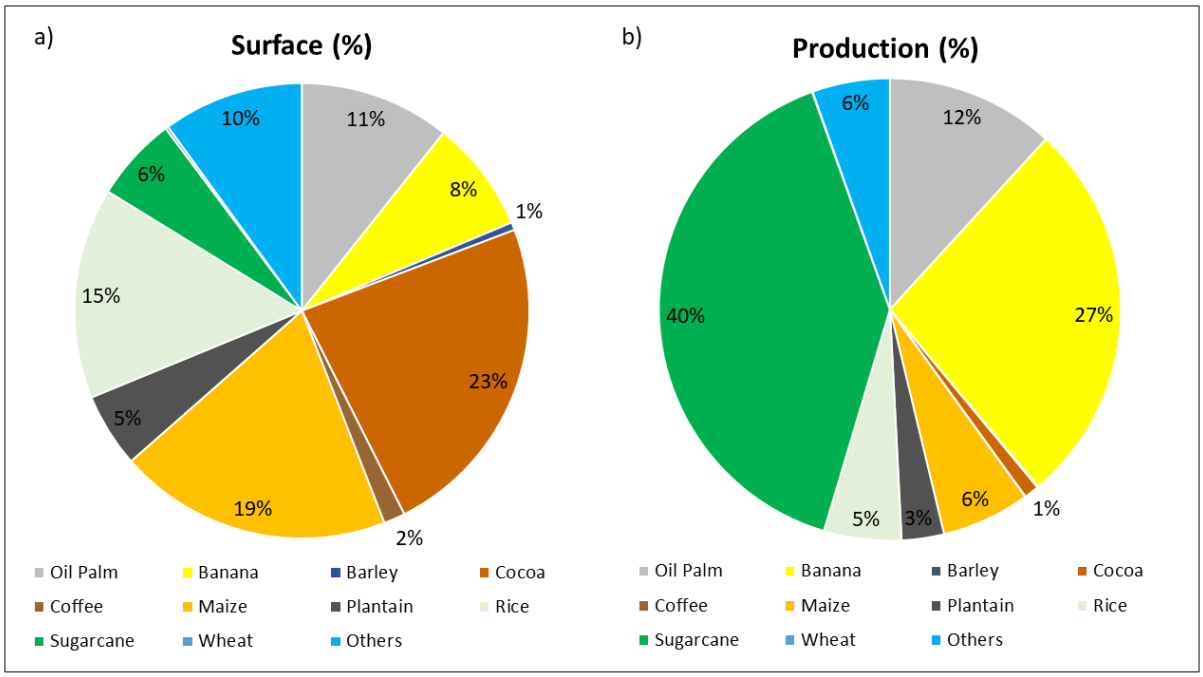

Fig 2. Share of a) harvested surface and b) production reported for the crops selected in this study. Average for the years 2016-2020.

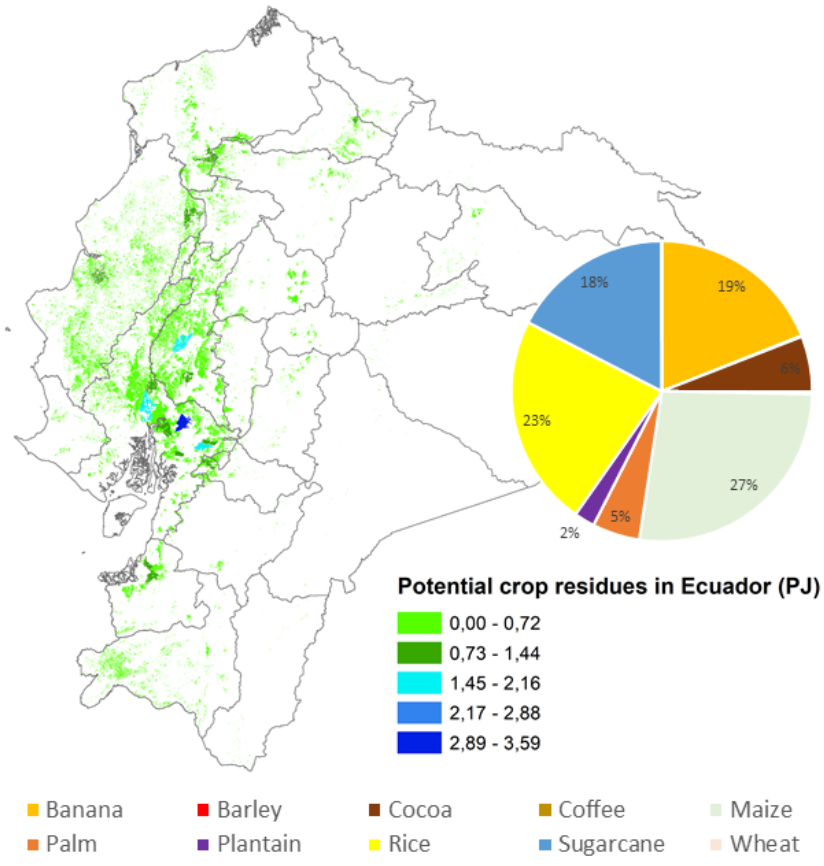

Fig 3. Spatially-explicit theoretical PJ potential of crop residues to supply the bioeconomy and crop contribution to this potential.

Table 2. Main characteristics of the residual biomass included in the database[a]

Crop	Main Product	Aerial biomass			Root[d]	
	Dry matter [b] (%)	Type	C (%)	LHV (MJ kg^{-1})	Distribution at 30 cm depth [c]	Ref.
Oil Palm	15	Fronds, empty fruit bunch, fiber	51.86	16.99	0.97	[5]
Banana - Plantain	15	Leaves, pseudostem, rachis	41.50	11.89 12.79	0.965	[6]
Barley	89	Straw	47.60	15.78	0.94	[7]
Cocoa	85	Husk, branches	46.13	14.86	0.97	[5]
Coffee	85	Husk, branches	50.29	14.93	0.97	[5]
Maize	87	Stover, husk	48.69	16.13	0.952	[7]
Rice	89	Straw, husk	41.00	15.53	0.94	[7]
Sugarcane	83	Straw, leaves	45.65	16.68	0.969	[8]
Wheat	89	Straw	49.09	14.25	0.96	[7]

a Stem from a compilation of data available in the Database Repository, at Andrade et al [2]. Number of digits not to be seen as an indication of precision, but are kept for as input for subsequent calculation.

b As reported by Morais et al. Morais et al. (2019).

c Beta (β) value to calculate the soil C inputs due to root distribution at a given depth, herein at 0 – 30 cm soil profile. Crop specific β values are used here.

d Due to lack of specific data per crop type, the average Carbon content in the roots has been defined as 40% for all the crops based on Bolinder et al., [10]

Table 3. Summary of RPR and RtS parameters considered

Feedstock	Type of residue	Fixed RPR	RPR equation	Yield-dependent RPR [a]	RtS	References
Oil Palm	Fronds	7.75, 5.07, 10.8	-	-	0.25, 0.43, 0.31, 0.39, 0.32, 0.3, 0.3, 0.39, 0.35, 0.08, 0.31	[11], [12], [13], [14], [15], [16], [17], [18],
	Shells	0.72, 1.00, 0.22, 0.04, 0.06				
	Empty fruit bunch	1.45, 0.21, 0.30				
	Fiber	0.15, 1.6, 1.06, 0.14, 0.72, 0.44				
	Average	1.31				
Banana - Plantain	Leaves	0.64, 0.35, 30, 1.5	-	-	0.56, 0.59, 0.065, 0.10, 0.05, 0.049, 0.24	[19], [20], [21], [22], [23],
	Pseudostem	2.97, 5.6, 2.5, 5.00				
	Rachis	0.40, 0.16, 0.15				
	Flowers	0.04				
	Average	3.79[b]				
Barley	Straw	0.80, 1.50, 1.30, 1.50, 1.00, 1.75, 1.00, 1.24, 1.50, 1.30, 1.20, 0.90, 1.00, 1.06, 1.30	1.822*exp(-0.149*Y)	1.60	0.3, 0.33, 0.3, 0.39, 0.35, 0.31, 0.5, 0.5, 0.61, 0.37, 0.32, 0.38, 0.15, 0.31, 0.22	[24], [25], [13], [26], [27], [19], [28]
	Average	1.22				
Cocoa	Husk	0.57, 0.50, 2.23, 1.00, 0.97, 11.5, 12.38	-	-	0.28, 0.23, 0.255, 0.338, 0.31, 0.37, 0.5, 0.52, 0.41, 0.42	[11], [12], [19], [16], [29], [30], [31]
	Average	4.16				
Coffee	Husk	2.10, 0.21, 0.24, 1.16, 5.42, 1.00				[32], [11], [12], [33], [29], [34], [35], [36], [37],
	Average	1.74				

Feedstock	Type of residue	Fixed RPR	RPR equation	Yield-dependent RPR [a]	RtS	References
Maize	Husk	0.20	-	2.18		[32], [38], [11],
	Stover	0.42, 0.78, 2.00, 2.14, 2.30, 1.56, 2.00, 2.32, 0.93, 1.60, 2.00, 1.59, 0.63, 2.50, 1.63, 1.43, 1.30, 2.30	2.656*exp(-0.103*Y)		0.22	[39], [24], [40], [12], [25], [13], [41], [42], [26], [27], [43], [44], [19], [45], [20],
	Average	1.49				[46], [21], [47],
Rice	Husk	0.27, 0.20, 0.57, 0.22, 0.29, 0.63, 1.50, 0.27, 0.23, 3.28, 0.23	- - 2.450*exp(-0.084*Y)	1.89	0.21, 0.16, 0.25, 0.14, 0.16,	[32], [38], [11], [48], [39], [49], [24], [40], [50],
	Straw	1.48, 0.45, 1.36, 1.7, 2.19, 1.045, 1.757, 1.7, 1.23, 1.757			0.16	[51], [52], [12], [25], [53], [13], [33], [26], [27],
	Average	1.10				[43], [44],
Sugarcane	Leaves	0.18, 3.75, 0.13, 0.10, 0.05, 0.34, 0.22, 0.32, 0.3, 0.18, 0.05, 0.19, 0.35, 0.23, 3.26, 0.38, 0.34	-	-	0.17, 0.47, 0.30 0.31	[54], [11], [39], [40], [13], [33], [27], [44], [19], [20], [46], [47],
	Trash	3.26, 0.38, 0.34				[37], [55], [8],
	Average	0.61				[56],
Wheat	Straw	1, 1.08, 1.80, 1.30, 1.20, 1.34, 1.84, 1.75, 0.60, 1.00, 1.26, 1.60, 1.80	2.186*exp(-0.127*Y)	1.95	0.20, 0.14, 0.29, 0.25, 0.56, 0.032,	[38], [39], [24], [40], [25], [13], [26], [27], [45],
	Average	1.35			0.021, 0.23	[10], , [57], [58],

a National average. Calculated for an average yield for 20 years (2002-2019) and as the average of all the provinces. b Average for all residuals parts of banana plant determined by Ulloa-Ortiz et al., 2222 for banana plants in Ecuador. **Database**: [2]

2. Experimental design, materials, and methods

The spatially explicit potential production of crop residues in Ecuador was determined by processing geographical and statistical information retrieved from the National reporting sources [1,59]. High resolution spatial data was manipulated and intersected using ArcGIS [60] and Python [61], while the statistical information corresponding to each explicit location was processed using R [62].

2.1 Pedoclimatic units

The Andes mountain range divides mainland Ecuador in three natural regions (Coastal Plane, Highlands, and Amazonia) with complex and diverse meteorological and soil characteristics, landscapes, and biodiversity [63]. This diversity is reflected in a wide variety of cropping systems that can be represented by clustering the country in the so-called pedoclimatic units (PCU), which are unique combinations of soil properties (i.e., clay content, SOC content) and climatic variables (i.e., temperature and precipitation) [64].

The PCU creation was based on the target zones reported in the National Report of Ecuador for the Global Soil Organic Carbon sequestration map [63,65]. PCUs were produced by intersecting the national SOC stock map at 0 – 30 cm (1:25000) [66] with the climate layers (1:400000) extracted from Terraclimate [67] for the periods 1980 – 2000 and 2001 – 2020. The national land use map (1:25000) harmonized at 1km, with data collected from 2009 to 2015 [68] was then used to locate the PCUs dedicated to croplands, hereon referred as agricultural pedoclimatic units (APCUs). Only the APCUs dedicated to harvest the crops detailed in Fig 2 were included in the final dataset. This selection yielded 105,032 APCU, covering 2.19 Mha, which represent approximately 96% of the national cropland area (annual, semi-perennial and perennial croplands). The bulk density and clay content of the selected APCUs, at 0 – 30 cm, were retrieved from the ISRIC Soilgrids database [69]. Bulk density data were not available for 13512 APCUs, and thus the bulk density of the neighboring APCUs was used as proxy for the missing values. We refined the selection of APCUs, by restricting it to only APCUs with at least 10 ha of area, which yielded 23,021 APCUs representing 87% (1.92 Mha) of the initial selection (84% of total croplands).

2.2 Crops selection

Agricultural land is inhere defined as the share of arable land dedicated to annual, semi-perennial, and perennial crops, as well as cultured pastures (ref:FAO?worldbank?). In 2020, the agricultural land of Ecuador covered 4 333 284 (INEC, 2021; retrieved from MAG, 2023b), of which 2 126 820 ha correspond to annual, semiperennial, and perennial croplands (harvested land only). Despite 147 crops (annual, semi- perennial, and perennial) have been identified in the land use map of

Ecuador [68], only the harvested surface and total production of the main 38 crops are reported in the ESPAC (Table 1) collected every year [59], at a province spatial scale. According to the average last 4 years of the ESPAC (2016 -2019) as a representative of the current cropping systems (INEC, 2021), approximately 95% of the national production is currently characterized by ten crops (i.e., oil palm, banana, cocoa, coffee, maize, plantain, rice, sugarcane, wheat, and barley), which represent a 90% share of the total harvested croplands (Fig 2), and have been deemed as key for bioenergy in Ecuador [29].

Note that while the ESPAC [4] is performed in a yearly basis, the land use map [68] was delivered in 2015, thus a slight difference in the total surface covered in each dataset can be observed (i.e., APCUs represent 96% of the croplands surface reported in the land use map, while it represents 92% of the surface in the 2020 CAPSS). However, since the production level is further converted to yield in tonne ha^{-1} (see section 2.3) and due to the high spatial explicitness of the land use map, the final surface reported corresponds to that of the land use map.

Despite the production and surface use data of Ecuador is collected with high spatial resolution and time frequency, information regarding farming management is currently sparse in the country. The National Agricultural Livestock Registry (RENAGRO) project is currently ongoing to bridge this gap of knowledge with expected results to be available after 2023. Therefore, due to lack of systematically reported data regarding crop rotations and based on **expert's knowledge and grey literature** for the Ecuadorian cropping systems that indicate intensive monoculture systems, crop rotations were not included in the dataset. Therefore, only one crop is reported for a given APCU.

2.3 Spatially explicit biomass potential assessment

The potential biomass available in Ecuadorian croplands was determined for the crops selected in section 2.2, based on the main product yield calculated for each crop. Total production and harvested surface data were retrieved for the period 2002- 2019 from the NCAPPS [4] to calculate the average annual yield in tonne ha^{-1}, per crop and province (Eq 1).

$$Y_{ij} = \frac{Production_{ij}}{Surface_{ij}} \qquad \text{Eq 1}$$

Where, for crop i in province j, Y_{ij} is the primary economic yield in tonne ha^{-1}, $Production_{ij}$ is the total production (tonne), and $Surface_{ij}$ is the harvested surface.

While each crop has a different sowing and harvest calendar (Fig S1 in companion Research paper), the ESPAC data is reported in an annual cumulated basis. Therefore, the monthly yield was

calculated as the annual yield divided by the number of harvesting months reported in the cropping calendar and assigned to the corresponding month.

The potential residual biomass produced in Ecuador was estimated as a function of the primary crop yield (Yij), using reported residue to product (RPR) ratios for each crop (Eq 2). RPR is defined as the ratio of aboveground residual biomass yield (R) to the primary crop yield (Y) dry matter (Table 2 and 3) [70].

$$RPR = \frac{R}{Y} \qquad \text{Eq 2}$$

RPR values could be reported as a fixed value or as a value dependent on Y derived from specific equations [71] . Yield dependent RPRs were used when available and were calculated using the specific RPR equations (Table 3) and the average yield of each crop (2002 – 2020) per province. We then averaged the province-wise yield-dependent RPR values to obtain a national single value per crop. For crops where RPR equations where not available, the residual biomass was calculated using fixed RPR values retrieved from the literature. Fixed RPR values for each residue part of a given crop were collected (Table 3) and the average "residue RPR" per crop was used.

The potential spatially explicit residual biomass produced was calculated for each APCU and for each crop, considering the crop yield, the RPR, and the total surface using Eq 3.

$$Rij = RPRi \; x \; Yij \; x \; Sj \qquad \text{Eq 3}$$

Where, for crop i in APCU j, R_{ij} is the amount of residual biomass produced, RPR_i is the residue to product ratio, Y_{ij} is the primary product dry yield, and S_j is the APCU surface. The theoretical spatially explicit residue production is expressed in terms of energy based on the reported LHV values of each crop residue (Table 2) at an APCU scale (Figure 4). Moreover, the share of contribution of each crop to the total potential at a province scale is also presented in Figure 4.

2.3 Carbon inputs

The potential input of carbon from crop residues to the croplands soil can be calculated as the sum of the above- (i.e., aerial residual biomass) and belowground (i.e., root and root exudates) carbon inputs (Eq 4).

Aboveground carbon inputs were determined by converting the residual aerial biomass (R) into carbon content with the carbon fraction in Table 2. Belowground carbon inputs refers to the C contribution from the root biomass and the extra-root rhizodeposit in soil [10] for the soil profile considered in the study. The root biomass is determined as a fraction of the total shoot biomass (i.e.,

primary yield and residual biomass) using the root to shoot ratio (R:S, Eq5) [72]. The belowground C at 0 – 30 cm depth was determined using Eq 9 and 10, for a root C content of 40% (Bolinder et al., 2007).

$$C\_in_{ij} = C_R + C_{root\_depth} + C_{E\_depth} \quad \text{Eq4}$$

$$C_R = \left(R_{ij} \times C\_res_i\right) \quad \text{Eq5}$$

$$C_{root} = \left(Root_{ij} \times C\_root_i\right) \quad \text{Eq6}$$

$$Root_{ij} = R{:}S \times \left(Y_{ij} + RP_{ij}\right) \quad \text{Eq 7}$$

$$C_E = C_{root} \times 0.65 \quad \text{Eq 8}$$

$$C_{root\_30cm} = C_{root} \times (1 - \beta^{30}) \quad \text{Eq 9}$$

$$C_{E\_30cm} = C_{root\_30cm} \times 0.65 \quad \text{Eq 10}$$

Where, for crop i and APCU j, C_in_{ij} (t C ha^{-1}) is the total carbon input to soil, R_{ij} is the dry residual biomass (tonne ha^{-1}), $Root_{ij}$ is the dry weight of the roots, C_res_i and C_root_i are the C fraction of the residual biomass and root, respectively, as defined in Table 2. The extra-root C was calculated as 65% of the root C (C_{root}) for all the crops in the dataset (i.e., annual, semi-perennial, and perennial), according to [10]. C_{root_30cm} corresponds to the effective root C in the 0 – 30 cm soil profile, C_{E_30cm} corresponds to the C from root exudates in the 0 – 30 cm soil profile, and β is a factor determining the root distribution at a given soil profile (here 30 cm depth).

24 Meteorological variables

We used the RCP4.5 temperature (i.e., maximum and minimum) and precipitation projections, downscaled for Ecuador according to on an ensemble model based on the IPSL-CM5A-MR, MIROC-ESM, GISS-E2-R, CSIRO-Mk3-6-0 global models, performed by the Sub-secretary of Climate Change of the Ministry of Environment, Water and Ecological Transition of Ecuador – MAATE (*data received as courtesy and only available under request to the original authors*). The four models used to produce the ensemble model were selected as the most representatives among a previous test including 15 models. Data was received in a daily timestep and were processed to calculate the monthly cumulated precipitation (mm) and the average monthly temperature (°C), for the period 2020 - 2070. Due to lack of data reporting the mean temperature projected, it was calculated as the average value between the maximum and minimum temperatures in the original database (Eq 11). The temperature data consisted of four variables, namely i) date, ii) longitude, iii) latitude, and iv) temperature. The monthly values were then joined with the PCU shapefile to assign the corresponding temperature to each APCU.

$$T_{mean_i} = \frac{\left(T_{max_i} + T_{min_i}\right)}{2} \quad \text{Eq 11}$$

where, for PCU i, T_{meani} is the mean temperature calculated, T_{maxi} is the maximum reported temperature, and T_{mini} is the minimum reported temperature.

The potential evapotranspirtation (PET) was computed, following Morais et al. (2020), by using the Thornthwaite method [73]. The calculated T_{meani} projected under the RCP4.5 trajectory was used within the Standardized Precipitation Evapotranspiration Index (SPEI package SPEI v1.7, updated 20xx) package [74,75] to calculate the projected future evapotranspiration under the RCP4.5 in each APCU. The original data was extracted, converted from daily to monthly basis, and assigned to the PCUs using Python, while the Tmean and PET data was created using R [62].

The processed meteorological data (Tmean, PET, and precipitation) was produced as CSV files and converted to shapefiles using the sp package of R and assigned to the coordinate system CRS 32717 (WGS84/UTM zone 17S) to be harmonized with APCU shapefile produced in section 2.1. The meteorological data was assigned to the corresponding APCU based on the longitude and latitude using the nearest neighbor (st_nn) function of the nngeo package [76] in R. The st_nn function allows to assign the attributes of one shapefile to another one based on matching the nearest longitude and latitude values in the two shapefiles.

Ethics statement

No ethics approvals were required or sought for this work.

Code Availability

Data analyses were completed in ESRI ArcGIS and no code is supplied. Analyses can be reproduced following spatial analysis steps described in the methods. ----- Scripts for other data is indeed supplied!!

Data Availability

Data is openly available in REPOSITORY.

CFRediT author statement

Christhel Andrade Diaz: Conceptualization, methodology, software, data curation, validation, formal analysis, visualization, writing-original draft preparation; **Lorie Hamelin:** conceptualization, methodology, writing-review and editing, supervision, project administration, funding acquisition; **Ezequiel Zamora-Ledezma: :** Conceptualization, methodology , Writing - review & editing, Funding acquisition, and Supervision.

Acknowledgements

This work was carried out within the framework of the research project Cambioscop (https://cambioscop.cnrs.fr), partly financed by the French National Research Agency, Programme Investissement d'Avenir (ANR-17-MGPA-0006), and Region Occitanie (18015981). C. Andrade was additionally funded by the French Embassy in Ecuador under the Project "Fonds de Solidarité pour Projets Innovants" (FSPI) and the French Ministry for Europe and Foreign Affairs and by a partial Scholarship from the Universidad Técnica de Manabí, Ecuador (UTM)..

The authors would like to thank Wilmer Jimenez and the Ministry of Agriculture of Ecuador for providing the backup data used to produce the Ecuadorian National Report for the Global Soil Organic Carbon Sequestration Potential Map, the Subsecretary of Climate Change of Ecuador for providing the climate projections for Ecuador, and Carlos Robles for helping with the climate data extraction.

Declaration of interests

☐ The authors declare that they have no known competing financial interests or personal relationships that could have appeared to influence the work reported in this paper.

☐ The authors declare the following financial interests/personal relationships which may be considered as potential competing interests:

References

1. MAG. Geoportal del Agro Ecuatoriano: Visor geografico [Internet]. SIPA. 2023. Available from: http://geoportal.agricultura.gob.ec/
2. Andrade Díaz C, Zamora-Ledezma E, Hamelin L. Database: Dataset for defining the spatially explicit baseline of cropping systems in Ecuadorian croplands and estimating the crop residues potential. Dataverse - TBI - Toulouse Biotechnology Institute - T21018. 2023 May;
3. Armenta Porras GE, Villa Cedeño JL, Jácome P. Proyecciones Climáticas de Precipitación y Temperatura para Ecuadorm bajo distintos escenarios de cambio climático. Ecuador: Subsecretaría de Cambio Climático del Ecuador; 2016.
4. INEC. Encuesta de Superficie y Producción Agropecuaria Continua [Internet]. Ecuador: INEC, SENPLADES; 2021. Available from: https://anda.inec.gob.ec/anda/index.php/catalog/912#page=accesspolicy&tab=study-desc
5. Jackson RB, Canadell J, Ehleringer JR, Mooney HA, Sala OE, Schulze ED. A global analysis of root distributions for terrestrial biomes. Oecologia. 1996 Nov 1;108(3):389–411.
6. Araya M. Stratification and spatial distribution of the banana (Musa AAA, Cavendish subgroup, cvs 'Valery' and 'Grande Naine') root system. Proceedings of the International Symposyum - Banana Root System: towards a better understanding for its productive management. 2003;
7. Fan J, McConkey B, Wang H, Janzen H. Root distribution by depth for temperate agricultural crops. Field Crops Research. 2016 Mar 15;189:68–74.
8. Smith DM, Inman-Bamber NG, Thorburn PJ. Growth and function of the sugarcane root system. Field Crops Research. 2005 Jun;92(2–3):169–83.
9. Morais TG, Teixeira RFM, Domingos T. Detailed global modelling of soil organic carbon in cropland, grassland and forest soils. PLOS ONE. 2019;27.
10. Bolinder MA, Janzen HH, Gregorich EG, Angers DA, VandenBygaart AJ. An approach for estimating net primary productivity and annual carbon inputs to soil for common agricultural crops in Canada. Agriculture, Ecosystems & Environment. 2007 Jan 1;118(1):29–42.
11. Rhofita EI, Rachmat R, Meyer M, Montastruc L. Mapping analysis of biomass residue valorization as the future green energy generation in Indonesia. Journal of Cleaner Production. 2022 Jun 20;354:131667.
12. Nelson N, Darkwa J, Calautit J, Worall M, Mokaya R, Adjei E, et al. Potential of Bioenergy in Rural Ghana. Sustainability. 2021 Jan;13(1):381.
13. Mai-Moulin T, Visser L, Fingerman KR, Elbersen W, Elbersen B, Nabuurs GJ, et al. Sourcing overseas biomass for EU ambitions: assessing net sustainable export potential from various sourcing countries. Biofuels, Bioproducts and Biorefining. 2019;13(2):293–324.
14. Suharno I, Dehen YA, Barbara B, Ottay JB. Opportunities for increasing productivity and profitability of oil palm smallholder farmers in Central Kalimantan. Palangkaraya: Palangkaraya Institute for Land use and Agricultural Research (PILAR). 2015;
15. Contreras NER, S AA, Núñez JAG. Inventario de la biomasa disponible en plantas de beneficio para su aprovechamiento y caracterización fisicoquímica de la tusa en Colombia. Palmas. 2015 Dec 1;36(4):41–54.
16. Griffin DW, Schultz MA. Fuel and chemical products from biomass syngas: A comparison of gas fermentation to thermochemical conversion routes. Environmental Progress and Sustainable Energy. 2012;31(2):219–24.
17. Ashraf AN, Zulkefly S, Adekunle SM, Samad MYA. Growth and Biomass yield of Oil Palm (Elaeis guineensis) Seedlings as Influenced by Different Rates of Vermicompost. European Journal of Engineering and Technology Research. 2017 Aug 17;2(8):17–21.

18. Haniff MH, Zuraidah Y, Roslan MMN. Oil palm root study at a northern region in Peninsula Malaysia. International Journal of Agriculture Innovations and Research. 2014;3(3):797–801.
19. Bundhoo ZMA, Surroop D. Evaluation of the potential of bio-methane production from field-based crop residues in Africa. Renewable and Sustainable Energy Reviews. 2019 Nov 1;115:109357.
20. Katherine Rodriguez Caceres, Francy Blanco Patino, Julian Araque Duarte, Viatcheslav Kafarov. Assessment of the energy potential of agricultural residues in non-interconnected zones of colombia: case study of choco and putumayo. Chemical Engineering Transactions. 2016 Jun;50:349–54.
21. Kemausuor F, Kamp A, Thomsen ST, Bensah EC, Østergård H. Assessment of biomass residue availability and bioenergy yields in Ghana. Resources, Conservation and Recycling. 2014 May 1;86:28–37.
22. Ortiz-Ulloa JA, Abril-González MF, Pelaez-Samaniego MR, Zalamea-Piedra TS. Biomass yield and carbon abatement potential of banana crops (Musa spp.) in Ecuador. Environ Sci Pollut Res. 2021 Apr 1;28(15):18741–53.
23. Blomme G, Jacobsen K, Ocimati W, Beed F, Ntamwira J, Sivirihauma C, et al. Fine-tuning banana Xanthomonas wilt control options over the past decade in East and Central Africa. Eur J Plant Pathol. 2014 Jun 1;139(2):271–87.
24. Scarlat N, Martinov M, Dallemand JF. Assessment of the availability of agricultural crop residues in the European Union: Potential and limitations for bioenergy use. Waste Management. 2010 Oct 1;30(10):1889–97.
25. Bentsen NS, Felby C, Thorsen BJ. Agricultural residue production and potentials for energy and materials services. Progress in Energy and Combustion Science. 2014 Feb 1;40:59–73.
26. Esteban L, Pilar C, Carrasco J. An assessment of relevant methodological elements and criteria for surveying sustainable agricultural and forestry biomass byproducts for energy purposes. BioResources. 2008 Aug 1;3.
27. Vaish S, Kaur G, Sharma NK, Gakkhar N. Estimation for Potential of Agricultural Biomass Sources as Projections of Bio-Briquettes in Indian Context. Sustainability. 2022 Jan;14(9):5077.
28. Füllner K, Temperton VM, Rascher U, Jahnke S, Rist R, Schurr U, et al. Vertical gradient in soil temperature stimulates development and increases biomass accumulation in barley. Plant, Cell & Environment. 2012;35(5):884–92.
29. MEER, MCPEC, INP. Atlas Bioenergético del Ecuador. Ecuador: Ministry of Electricity and Renewable Energy; 2014.
30. Borden KA, Anglaaere LCN, Adu-Bredu S, Isaac ME. Root biomass variation of cocoa and implications for carbon stocks in agroforestry systems. Agroforest Syst. 2019 Apr 1;93(2):369–81.
31. Gouvello C, Dayo F, Thioye M. Low-carbon Energy Projects for Development in Sub-Saharan Africa. 2008 Jan 1;
32. Okello C, Pindozzi S, Faugno S, Boccia L. Bioenergy potential of agricultural and forest residues in Uganda. Biomass and Bioenergy. 2013 Sep 1;56:515–25.
33. Waldheim L, Monis M, Verde Leal MR. Biomass Power Generation: Sugar Cane Bagasse and Trash. In: Progress in Thermochemical Biomass Conversion [Internet]. John Wiley & Sons, Ltd; 2001 [cited 2023 May 5]. p. 509–23. Available from: https://onlinelibrary.wiley.com/doi/abs/10.1002/9780470694954.ch41
34. Bingh LP. Opportunities for utilizing waste biomass for energy in Uganda. In 2004 [cited 2023 May 5]. Available from: https://www.semanticscholar.org/paper/Opportunities-for-utilizing-waste-biomass-for-in-Bingh/0491bced642af223d5842123a5b91b0dce9d5be6
35. Ramos LCDS, Carvalho A. SHOOT AND ROOT EVALUATIONS ON SEEDLINGS FROM Coffea GENOTYPES. Bragantia. 1997;56:59–68.
36. Salamanca-Jimenez A, Doane TA, Horwath WR. Nitrogen Use Efficiency of Coffee at the Vegetative Stage as Influenced by Fertilizer Application Method. Frontiers in Plant Science [Internet]. 2017 [cited 2023 May 5];8. Available from: https://www.frontiersin.org/articles/10.3389/fpls.2017.00223
37. Gabisa EW, Gheewala SH. Potential of bio-energy production in Ethiopia based on available biomass residues. Biomass and Bioenergy. 2018 Apr 1;111:77–87.

38. Zhang J, Li J, Dong C, Zhang X, Rentizelas A, Shen D. Comprehensive assessment of sustainable potential of agricultural residues for bioenergy based on geographical information system: A case study of China. Renewable Energy. 2021 Aug 1;173:466–78.
39. Barahira DS, Okudoh VI, Eloka-Eboka AC. Suitability of Crop Residues as Feedstock for Biofuel Production in South Africa: A Sustainable Win-Win Scenario. Journal of Oleo Science. 2021;70(2):213–26.
40. Ying B, Xiong K, Wang Q, Wu Q. Can agricultural biomass energy provide an alternative energy source for karst rocky desertification areas in Southwestern China? investigating Guizhou Province as example. Environ Sci Pollut Res. 2021 Aug 1;28(32):44315–31.
41. Graham RL, Nelson R, Sheehan J, Perlack RD, Wright LL. Current and Potential U.S. Corn Stover Supplies. Agronomy Journal. 2007;99(1):1–11.
42. Coelho ST, Monteiro MB, Karniol M da R, Ghilardi A. Atlas de bioenergia do Brasil. São Paulo. 2012;
43. Alhassan EA, Olaoye JO, Olayanju TMA, Okonkwo CE. An investigation into some crop residues generation from farming activities and inherent energy potentials in Kwara State, Nigeria. IOP Conf Ser: Mater Sci Eng. 2019 Nov;640(1):012093.
44. Ben-Iwo J, Manovic V, Longhurst P. Biomass resources and biofuels potential for the production of transportation fuels in Nigeria. Renewable and Sustainable Energy Reviews. 2016 Sep 1;63:172–92.
45. Khatiwada D, Purohit P, Ackom EK. Mapping Bioenergy Supply and Demand in Selected Least Developed Countries (LDCs): Exploratory Assessment of Modern Bioenergy's Contribution to SDG7. Sustainability. 2019 Jan;11(24):7091.
46. Cardoen D, Joshi P, Diels L, Sarma PM, Pant D. Agriculture biomass in India: Part 1. Estimation and characterization. Resources, Conservation and Recycling. 2015 Sep 1;102:39–48.
47. Hiloidhari M, Das D, Baruah DC. Bioenergy potential from crop residue biomass in India. Renewable and Sustainable Energy Reviews. 2014 Apr 1;32:504–12.
48. Nada RM, Abogadallah GM. Restricting the above ground sink corrects the root/shoot ratio and substantially boosts the yield potential per panicle in field-grown rice (Oryza sativa L.). Physiologia Plantarum. 2016;156(4):371–86.
49. Gondwe KJ, Chiotha SS, Mkandawire T, Zhu X, Painuly J, Taulo JL. An assessment of crop residues as potential renewable energy source for cement industry in Malawi. Journal of Energy in Southern Africa [Internet]. 2017 Dec 23 [cited 2023 May 5];28(4). Available from: https://energyjournal.africa/article/view/4178
50. Chitawo ML, Chimphango AFA. A synergetic integration of bioenergy and rice production in rice farms. Renewable and Sustainable Energy Reviews. 2017 Aug 1;75:58–67.
51. Abstract [Internet]. [cited 2023 May 5]. Available from: http://www.jsrr.jp/3sympo/shin.htm
52. Panwar NL, Rathore NS. Potential of surplus biomass gasifier based power generation: A case study of an Indian state Rajasthan. Mitig Adapt Strateg Glob Change. 2009 Dec 1;14(8):711–20.
53. Li Z, Yagi K. Rice root-derived carbon input and its effect on decomposition of old soil carbon pool under elevated CO2. Soil Biology and Biochemistry. 2004 Dec 1;36(12):1967–73.
54. Singh J, Panesar BS, Sharma SK. Energy potential through agricultural biomass using geographical information system—A case study of Punjab. Biomass and Bioenergy. 2008 Apr 1;32(4):301–7.
55. El-Naggar A, El-Naggar AH, Shaheen SM, Sarkar B, Chang SX, Tsang DCW, et al. Biochar composition-dependent impacts on soil nutrient release, carbon mineralization, and potential environmental risk: A review. Journal of Environmental Management. 2019 Jul 1;241:458–67.
56. Madhav TV, Bindu GSM, Kumar MV, Naik CS. Study on Root Characteristics of Sugarcane (Saccharum officinarum) Genotypes for Moisture Stress. International Journal of Plant & Soil Science. 2017 Sep 12;1–4.

57. Amanullah, Stewart BA, Ullah H. Cool Season C3-Grasses (Wheat, Rye, Barley, and Oats) Differ in Shoot: Root Ratio When Applied With Different NPK Sources. Journal of Plant Nutrition. 2015 Jan 28;38(2):189–201.
58. Carvalho JLN, Hudiburg TW, Franco HCJ, DeLucia EH. Contribution of above- and belowground bioenergy crop residues to soil carbon. GCB Bioenergy. 2017 Aug;9(8):1333–43.
59. MAG. Sistema de Información Pública Agropecuaria [Internet]. Sistemaa de Información Pública Agropecuaria: Estadísticas. 2023. Available from: http://sipa.agricultura.gob.ec/index.php/sipa-estadisticas/estadisticas-productivas
60. ESRI. ArcGIS Desktop. 2020.
61. The Python Language Reference [Internet]. Python documentation. [cited 2023 May 9]. Available from: https://docs.python.org/3/reference/index.html
62. R Core Team. R: A language and environment for statistical computing [Internet]. Viena, Austria: R Foundation for Statistical Computing; 2021. Available from: https://www.R-project.org/
63. Jiménez W, Sánchez D, Ruiz V, Manzano D, Armas D, Jiménez L, et al. Ecuador: SOil Organic Carbon Sequestration Potential National Map. National Report. Version 1.0. Global Soil Partnership. Ministry of Agriculture and Livestock of Ecuador.; 2021. Report No.: 1.0.
64. Andrade Díaz C, Clivot H, Albers A, Zamora-Ledezma E, Hamelin L. The crop residue conundrum: Maintaining long-term soil organic carbon stocks while reinforcing the bioeconomy, compatible endeavors? Applied Energy. 2023 Jan 1;329:120192.
65. FAO. Global Soil Organic Carbon Sequestration Potential Map – GSOCseq v.1.1 : Technical report [Internet]. Rome, Italy: FAO; 2022 [cited 2023 Jan 13]. 179 p. Available from: https://www.fao.org/documents/card/en/c/cb9002en
66. MAG, MAATE, FAO, GSP. Mapeo digital de Carbono orgánico en los suelos del Ecuador. [Internet]. Quito, Ecuador; 2021. Report No.: Segunda Edición. Available from: sipa.agricultura.gob.ec
67. Abatzoglou JT, Dobrowski SZ, Parks SA, Hegewisch KC. TerraClimate, a high-resolution global dataset of monthly climate and climatic water balance from 1958–2015. Sci Data. 2018 Jan 9;5(1):170191.
68. MAG, IEE, SENPLADES. Mapa de cobertura y uso de la tierra del Ecuador continental, 2009- 2015, escala 1: 25.000. Versión editada por el Ministerio de Agricultura y Ganadería 2020. Ecuador; 2015.
69. Hengl T, Jesus JM de, Heuvelink GBM, Gonzalez MR, Kilibarda M, Blagotić A, et al. SoilGrids250m: Global gridded soil information based on machine learning. PLOS ONE. 2017 Feb 16;12(2):e0169748.
70. Karan SK, Hamelin L. Crop residues may be a key feedstock to bioeconomy but how reliable are current estimation methods? Resources, Conservation and Recycling. 2021 Jan;164:105211.
71. Kyryzyuk S, Krupin V, Borodina O, Wąs A. Crop Residue Removal: Assessment of Future Bioenergy Generation Potential and Agro-Environmental Limitations Based on a Case Study of Ukraine. Energies. 2020 Jan;13(20):5343.
72. Rogers HH, Prior SA, Runion GB, Mitchell RJ. Root to shoot ratio of crops as influenced by CO2. Plant Soil. 1995 Jul 1;187(2):229–48.
73. Aschonitis V, Touloumidis D, ten Veldhuis MC, Coenders-Gerrits M. Correcting Thornthwaite potential evapotranspiration using a global grid of local coefficients to support temperature-based estimations of reference evapotranspiration and aridity indices. Earth Syst Sci Data. 2022 Jan 20;14(1):163–77.
74. Vicente-Serrano SM, Beguería S, López-Moreno JI. A Multi-scalar drought index sensitive to global warming: The Standardized Precipitation Evapotranspiration Index – SPEI. Journal of Climate. 2010;23:1696–718.
75. Beguería S, Vicente-Serrano SM, Reig F, Latorre B. Standardized precipitation evapotranspiration index (SPEI) revisited: parameter fitting, evapotranspiration models, tools, datasets and drought monitoring. International Journal of Climatology. 2014;34(10):3001–23.

76. Dorman M, Rush J, Hough I, Russel D, Ranghetti L, Benini A, et al. nngeo: k-Nearest Neighbor Join for Spatial Data [Internet]. 2023 [cited 2023 May 9]. Available from: https://cran.r-project.org/web/packages/nngeo/index.html

Appendix A3b

Supplementary Information of Chapter 4 – Section 1

The content of this appendix is part of the supplementary information accompanying the paper 3 of this thesis and is currently under preparation to be submitted to *peer review*. The numbering of the sections, figures and tables are as presented in the original paper.

The background data of this appendix is available in the following repository: https://doi.org/10.48531/JBRU.CALMIP/VLKG8V

Modelling the long-term carbon storage potential from recalcitrant matter inputs in tropical arable croplands

Christhel Andrade Diaz[a,b*], Enrico Balugani[c], Ezequiel Zamora-Ledezma[d], Lorie Hamelin[a]

[a] Toulouse Biotechnology Institute (TBI), INSA, INRAE UMR792, and CNRS UMR5504, Federal University of Toulouse, 135 Avenue de Rangueil, F-31077, Toulouse, France

[b] Department of Chemical, Biotechnological and Food Processes, Faculty of Mathematical, Physics and Chemistry Sciences. Universidad Técnica de Manabí (UTM), 130150, Portoviejo, Ecuador.

[c] Department of Physics and Astronomy, Università di Bologna, Bologna, Italy

[d] Ecosystems Functioning and Climate Change Research Group - FAGROCLIM, Faculty of Agriculture Engineering. Universidad Técnica de Manabí (UTM), 13132, Lodana, Ecuador.

Supplementary Information I

Table of contents

List of Figures

List of Tables

1. Spatially explicit biomass potential

The detailed methodology and data used to define the APCUs and the spatially explicit carbon inputs in the business-as-usual (BAU) scenario are transparently documented in the companion data paper [1] and the key elements are explored in here.

1.1 Pedoclimatic data

The complex pedoclimatic characteristics of mainland Ecuador, entailing three regions (Coastal Plane, Highlands, and Amazonia)[4] with marked climate and soil characteristics play a role in the regional cropping systems. This rich diversity is well represented in the agricultural pedoclimatic Units (APCUs) developed in this study, built upon the unpublished background data used in the National Report of Ecuador for the Global Soil Organic Carbon sequestration (SOCS) map [2,3] received as a courtesy. The APCUs created by the intersection of georeferenced data reporting the national SOC stocks at 0-30 cm [4], climate layers containing the mean temperature, precipitation, and evapotranspiration (ETP) [5]), and detailed land use information [6] for the period 2009 – 2015 represented approximately 2,28 Mha of croplands. The selection of APCUs including only the crops of interest (Table S1), resulted in 105,032 APCUs representing 96% of the national cropland surface. By limiting the APCUs by the surface extension to at least 10 ha, the number of APCUs was decreased to 23,021, representing 84% of the national croplands. Due to lack of information on crop rotations in Ecuador (further explored in section 1.2) the APCUs were considered as the simulation units in this study. Due to unconformities on the study performed by MAG [3] for the global SOCS map [2,3] (i.e., no SOC stocks simulated and negative size of soil pools) the cropland surface simulated was reduced to 1.19 Mha, which was represented by 15,782 APCUs (see section SI. 3.1).

1.2 Biomass potential

The Ecuadorian National Continuous Agricultural Production and Surface Survey (NCAPSS; [7,8] presents the total annual production and harvested surface of 38 crops at a provincial level. Approximately 95% (average last five years) of the total national production is represented by 10 crops covering 90% of the cropland surface [1] and were thus selected for the APCU creation. Despite Ecuador is recognized as an agricultural country, there is sparse information on crop rotations and the grey literature reports extensive monoculture systems across the country. Therefore, the crops

[4] The region of Galapagos was not considered in this study due to their poor contribution to the national agricultural mix.

included in this study are assumed to be managed in monocultured systems, according to the representative sow-harvest schedule of the country (Fig S1).

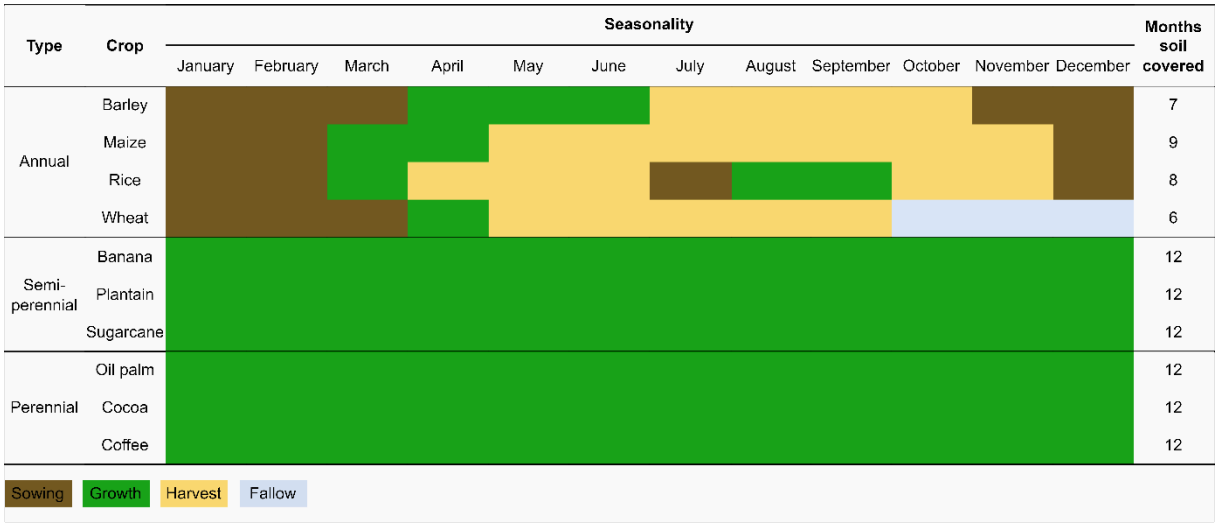

Fig S 10. Sowing and harvest calendar for crop seasonality in Ecuador [9–13].

The spatially explicit potential production of crop residues in Ecuador was determined based on the last 18 years (from 2002 to 2019) of data reported in the NCAPSS, for each APCU, using Eq S1 with the residue to product ratios (RPR) values reported in Table 1, in the companion data paper [1].

$$Rij = RPRi \; x \; Yij \; x \; Sj \qquad \text{(Eq S1)}$$

Where i represents a given crop in a specific j APCU, R is the quantity of residues produced (t DM), RPR is the residue to product ratio, Y is the main product yield (t DM) as determined in “data paper”, and S is the APCU surface.

RPR assumes that the relationship between the primary yield of a crop and the residues generated can be mathematically expressed as a fixed factor or as a function of the crop yield [14]. Nonetheless, the actual quantity of crop residues produced is influenced by a plethora of factors (e.g., soil characteristics, meteorological conditions, farming practices, among others) which challenges the endeavor of quantifying the residue potential of a country. We privileged the use of yield dependent RPRs and when not available an average fixed RPR, derived from the compilation of several studies in Andrade et al. [15], was used for each crop. Table 1 presents the national total crop residues potential per crop, while the spatially explicit amount per APCU is transparently reported in Andrade et al. [15] and in the data paper [1].

The soil model RothC used in this study operates at a monthly timestep, and therefore the annual crop yield, steaming from the annual NCAPPS, was downscaled to monthly inputs using the sow-harvest calendar in the companion Data paper. The vast majority of crops included in this study

are semi-perennial or perennial, thus the harvest cycle is considered to cover a full year and the annual yield is divided by 12 months and equally allocated to each month. The annual crops present their own specific harvest season and the yield is considered to be allocated across the growth and harvest months in an equal proportion. The sowing and fallow months are used to indicate to RothC which are the months exhibiting bare soil, per crop type.

Table S3. Biomass potential for the croplands considered in the study

Crop Type	RPR [a]	LHV ($MJ.kg^{-1}$) [a]	Technical harvestable fraction	Biomass theoretical potential (PJ) [b]	References [c]
Banana	3.79	11.89	0.1	21.37	[16], [17], [18], [19]
Barley	1.60	15.78	0.5	0.13	[20], [21], [14], [22], [23], [24], [25], [16]
Cocoa	4.16	14.86	0.1	6.77	[26], [27], [28], [16], [29], [30], [31], [32]
Coffee	1.75	14.93	0.1	0.27	[33], [26], [28], [23], [34], [31], [35], [36]
Maize	2.18	16.13	0.3	30.54	[33], [37], [26], [38], [39] [21], [14], [40], [27], [28], [22], [23], [41], [25], [42]
Oil Palm	1.31	16.99	0.1	5.75	[26], [28], [23], [43], [44], [17], [30]
Plantain	3.79	12.79	0.1	2.51	[16], [17], [18], [19], [28], [45]
Rice	1.89	15.53	0.4	25.75	[33], [20], [37], [26], [38], [39], [21], [40], [46], [27], [28], [22], [23], [34], [47], [24], [25], [48], [42], [49]
Sugarcane [d]	0.23	16.68	0.1	19.60	[20], [26], [38], [40], [23], [34], [50], [25], [42], [17], [18], [51], [36], [52]
Wheat	1.95	14.25	0.4	0.04	[38], [21], [14], [40], [22], [23], [24], [25], 34] [26], [28], [23], [43], [44], [17], [30]
TOTAL				112.72	

[a] Average value from various sources compiled in Andrade et al. [15]. Here we consider the average of residues produced by each crop, as presented in Data paper.[b] Based on the average yield for 2002-2019. Yield multiplied by the surface of APCU to account only for the surface included in the APCUs. This potential represents 52% of

national croplands in Ecuador; [c] References for RPR and LHV values; [d] Sugarcane is reported as "industrial use" for sugar production and "other uses" in the NCAPSS. Here total production represents the sum of the two types of sugarcane in the NCAPPS.

1.3 Carbon inputs and exports

The carbon inputs to the soil are determined as the sum of the carbon contained in the aerial biomass (i.e., left on the field) and the roots, including root exudates [53,54]. The former source of C is here referred to as aboveground (C_ab) while the latter is considered as belowground (C_be). For the business-as-usual scenario (BAU, described in section 2.1 of main manuscript) the total C inputs correspond to the total C in the crop residues and the root C in soil depth considered in the study (here 0 – 30 cm). For the mitigation scenarios, a fraction of the aboveground C is considered to be harvested based on the technical harvestable fraction (Table S1), render a service to the bioeconomy, and partly returned as recalcitrant carbon through the input of the exogenous organic matter (EOM) remaining after the conversion process (Fig S2).

The characteristics of the crop residues and the type of harvest-machinery available in the country influence the amount of crop residues that can be harvested (technical harvestable fraction). Previous studies [21,55] have reported that approximately 60 – 80 % of the total residue can be collected for cereal crops, based on the cutting height of the harvesting machinery and the average height of the plant. For annual crops (i.e. cereals), the technical harvestable fraction used was the same as in Andrade et al., 2023. While the main crop residue of annual crops is straw, which must be cut to be collected, the semi-perennial and perennial crops produce residues such as husks, leaves and branches, that could be completely collected by the farmers while harvesting the primary product. However, to remain conservative, the technical harvestable percentage was fixed to be 90% for these crop residues. The non-harvestable fraction of residues is considered to be incorporated to the soil and are accounted for the soil C balance.

The spatially explicit carbon inputs for the BAU and mitigation scenarios are openly available in Andrade et al. [15] and the detailed calculation procedure, including the equations used, is transparently reported in data paper [1]. Note that aerial biomass is calculated using RPR whereas root biomass is calculated using root-to-shoot (RtS) ratios, retrieved from the literature, both varying according to the reference source and location. Both RPR and RtS can highly influence the total C inputs and SOC evolution, and are thus considered a source of uncertainty.

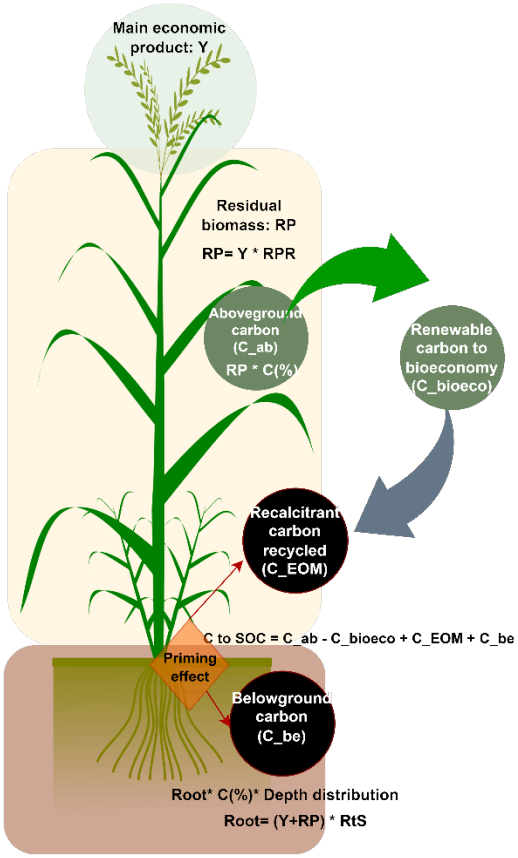

Fig S11. Scheme to determine the C inputs in the soil as calculated in this study. RP: Residues production, Y: primary economic product yield, RPR: Residue to product ratio (specific for each crop), RtS: root to shoot ratio, C_ab: Aboveground carbon, C_be: belowground carbon, C_bioeco: C exported to the bioeconomy through harvesting the crop residues, C_EOM: Carbon in the exogenous organic matter input, SOC: soil organic carbon.

2. Simulation scenarios

This study entails five simulation scenarios, one BAU and four mitigation developments. The BAU represents the current cropping systems where crop residues are not valorised in the bioeconomy. In Ecuador, crop residues are mainly considered a waste and their maintenance in the fields is avoided to prevent the attraction of plagues and to facilitate subsequent sow harvest cycles. The main way of disposal of crop residues in Ecuador is open field incineration instead of ploughing in soils, which is the common practice in developed countries. However, due to lack of data regarding the spatial explicitness, frequency, and amount of crop residues being burned, in this study the BAU considered that crop residues are just left on the field and not burned. The mitigation scenarios comprehend the return of stabilized EOMs to the soils, these being biochar from fast pyrolysis (pyrochar) and gasification (gaschar) processes, hydrochar from hydrothermal liquefaction (HTL), and anaerobic digestion (AD) digestate.

Thermochemical technologies such as gasification, pyrolysis, and HTL, subject the biomass to high degrees of temperature and/or pressure that convert the carbon in the biomass into bio-oil (i.e., pyrolysis and HTL) and syngas [56]. These extreme conditions exert a change in the unconverted carbon molecules. It has been well documented by previous authors [57,58] that the higher the temperature and reaction times, higher the rate of aromatic groups in the remaining unconverted biomass but lesser the amount of residual biomass (i.e., better biofuel yields).

Aromaticity has been found to be directly related to resistance to degradation, aka recalcitrance, while higher degrees of aliphatic components are related to more labile matter [59,60]. This understanding is highlighted when comparing thermochemical processes with the biochemical process of anaerobic digestion. The mild conditions of AD are not enough to cause a change in the type of carbon in the unconverted biomass remaining after the AD process. Therefore, the digestate matter contains the same type of molecule of carbon as the raw biomass (i.e., mainly lignin), with the difference that the labile fraction has been already converted to biogas. In attention to this, the degree of recalcitrance of digestate is markedly lower than that of biochar and the mean residence time is expected to be of only 1 year. A brief description of each conversion pathway, including process conditions, coproducts obtained (under study in this work), and yield of coproduct are detailed in Table S2.

Table S4. Conversion pathways conditions, products, and coproducts [56].

Conversion Pathway	Description	Main product	Coproducts[a]
Pyrolysis	Thermochemical process carried out in absence of oxygen, at 300 – 700°C, lasting from a few seconds to a couple hours, using dry feedstock (DM > 90%). Pyrolysis processes comprising temperatures from 300 – 500°, lasting a couple seconds, are considered to favour the production of bio-oil and are referred to as fast-pyrolysis. In this study, we consider a fast-pyrolysis process.	Bio-oil	Biochar (**pyrochar**), non-condensable gases
Gasification	Thermochemical process carried out in the presence of a limited amount of oxygen (i.e., below combustion requirements), at temperatures ranging from 700°C to 1200°C, using dry feedstock (DM > 90%). Here we include a gasification process carried out at a temperature range of 800 – 1200°C.	Syngas	Char (**gaschar**), tar, ashes
Hydrothermal liquefaction (HTL)	Thermochemical process, similar to pyrolysis, but carried out at lower temperatures (280 – 370°C), lasting approximately 20 to 30 minutes, and using wet biomass (DM < 20%). The HTL process considered in this study includes the use of catalysts to improve the efficiency of the process (i.e., higher bio-oil yields).	Bio-oil	**Hydrochar**, non-condensable gases
Anaerobic digestion (AD)	Biochemical process, carried out in the absence of oxygen and presence of microorganisms that convert the organic fraction of the feedstock into a gas stream mainly composed of CH4 and CO2. AD can be performed in an array of temperature and retention times combination, mainly influenced by the type of microorganism involved in the process. The process requires the use of wet feedstock (DM < 35%) and can be performed using a single feedstock (mono-digestion) or a mixture of feedstock(co-digestion) to attain the desired conditions of initial composition (e.g., DM, C content, C:N ratio, among others). Here we consider a mono-digestion process where the crop residues are mixed with water to attain the desired DM content, with mesophilic temperatures (30 – 50°C) and retention times of 1 to 3 months.	Biogas	**Digestate**

[a] Considered as the EOM returned to soils in this study

3. Soil Model

3.1 Size of the soil pools

The RothC [61] soil model used in this study requires knowledge on the size of each soil pool (see section 2.4.1 of main manuscript) in order to properly allocate the initial soil organic carbon (SOC) stocks. The Ecuadorian contribution to the global SOC sequestration map [2,3] performed a back-run calculation for 500 years, which allowed determining the size of each soil pool in RothC, with high spatial-resolution. The fraction calculated by MAG was then used to set the size of the pools in each APCU. To this end, the SOC reported for each pool was divided by the total SOC (sum of all fractions), at 2040 [3], and this fraction was then multiplied by the initial SOC at 2020 [4] to define the initial amount of SOC (t C ha^{-1}) per pool.

Due to running errors in the original study [3], 6247 APCUs did not present SOC results for 2040, thus they were removed from our database. Moreover, the APCUs with incongruences regarding the size of the soil pools (e.g., negative values) were also removed from the study. The final number of APCUs abided to the requirements of including at least 1 of the crops selected in table S1, at least 10 ha of surface, and reporting the size of each pool was 15,782.

3.2 Size of C input for the mitigation scenarios

The size of C inputs in each mitigation scenario was determined as the C in the original biomass that could be harvested, exported to the bioeconomy, and remain in the coproducts after the bioeconomy conversion process. This value was defined using the C conversion (C_C) coefficient (Eq S1), which defines the percentage of initial C that remains in the coproduct [62].

$$\%C_C = \frac{CpY * CpC}{BmC} * 100 \quad \text{(Eq S2)}$$

where C_C is the carbon conversion (%), CpY is the coproduct yield (kg Cp kg^{-1} biomass), which corresponds to the amount of coproduct resulting from the treatment of 1 kg of feedstock during the bioeconomy process, CpC is the carbon content in the co-product (kg C kg^{-1} Bp), and BmC is the initial carbon content in the biomass (kg C kg^{-1} biomass).

C_C varies in function of the technology and initial feedstock. Here, we used the same C_C values as in Andrade et al. [62] for cereal-like feedstocks and defined a new set of C_C values per technology (Table S1), for the more lignin rich feedstocks in tropical lands (i.e., banana, plantain, cocoa, coffee). The lignin-rich feedstock C_C stems from a literature review including 110 records (i.e., 40 data records for digestate, 40 for pyrochar, and 30 for gaschar), which was not intended to be exhaustive, but a

representative of the difference in C_C between the crop residues found in temperate (higher cellulose content) and tropical (higher lignin content) lands. The data compilation is openly accessible at [15].

Table S5. Carbon conversion (C_C) from initial feedstock to recalcitrant EOM, per crop type and EOM. Initial C content in unconverted crop residue is also presented.

Feedstock [a]	EOM	Initial C content [b] (%)	C_C EOM	References [c]
Banana	Pyrochar	37.88	48.10	[63], [64], [65], [66], [67], [68], [69], [70], [71], [72], [73], [74]
Banana	Gaschar		38.33	[75], [76]
Banana	Hydrochar [d]		84.07	[77], [78], [71]
Banana	Digestate		77.35	[16]
Plantain	Digestate		78.29	[16], [79]
Cocoa	Pyrochar	40.46	59.74	[80], [81], [82], [83], [84], [85], [86], [87], [88], [89]
Cocoa	Gaschar		23.32	[90], [91]
Cocoa	Digestate		71.04	[16], [82]
Coffee	Pyrochar	42.84	47.52	[82], [83], [85], [92], [93], [94], [95], [96], [97], [98], [99], [100], [86], [101]
Coffee	Digestate		55.59	[95], [96], [97]
Oil palm	Pyrochar	44.03	35.59	[102], [103], [104], [105], [106],
Oil palm	Digestate		75.54	[107], [108], [109], [110], [111], [112], [113], [49], [114], [111]
Sugarcane	Digestate	40.68	67.74	[115], [72], [116], [117], [118], [119]

EOM: exogenous organic matter; C_C: carbon conversion coefficient. [a] Type of crop from which the crop residue is obtained. [b] Average initial carbon content (%) in the crop residue. [c] References include the sources retrieved to determine the initial carbon content in the raw feedstock and the CC coefficient. [d] Data available considered conditions for a hydrothermal carbonization process and may overestimate the amount of carbon remaining in the EOM.

For the HTL pathway, the carbon balances reported in literature for the crops selected in the case study were only presented for hydrothermal carbonization (HTC) processes. HTC is performed for

longer times and higher temperatures than HTL [120], with the main product obtained as hydrochar. As the mitigation scenario chosen in this study envisions the provision of feedstock for an HTL pathway where hydrochar is a secondary product (Table S2), the use of carbon balances for HTC would overestimate the C returns in this scenario. Therefore, the C_C for cereal based hydrochar produced under HTL conditions reported in [56] was used as a proxy for the lignocellulosic rich biomass used in this study.

C_C (EOM-wised) was used in Eq (S2) to determine the amount of C from a given co-product that would be applied in a given simulation unit per year.

$$TCpC = Wt(dm)_i * WtCc_i * Cc \qquad \text{(Eq S2)}$$

Where, for crop i, TCpC is the total coproduct C applied [t C ha^{-1} $monh^{-1}$] in an APCU, $Wt(dm)_i$ is the technical harvestable dry mass of crop residues [t crop residues ha^{-1} $month^{-1}$], $WtCc_i$ is the Crop residue carbon content [t C t^{-1} crop]. $Wt(dm)_I$ is determined for each crop in each APCU as explained in section 1.2 while WtCCi is reported in Andrade et al. [15]

3.3 RothC adaptation to include the recalcitrance of various EOMs

The EOM-adapted RothC-Bioeconomy reflects the recalcitrant nature of the EOMs investigated in each mitigation scenario. Recalcitrance is translated to the model across the carbon recalcitrance coefficient (C_R) and the priming effect (PE). The former determines the fraction of carbon resistant to degradation contained in the EOM while the latter expresses the effect on the mineralization rate of SOC exerted by the application of the EOMs in the soil [121].

3.3.1 Carbon recalcitrance

C_R was used as in [62]. To the extent possible, values where taken by groups (i.e., cereal straw, leaves and fibers, and husks/shells). In the case of digestate the same value was used across all the groups due to scarcity of data. The C_R and C_L fractions were taken as reported for the crops/biowaste digestate group in [56], while the k_L and k_R were taken as reported for the ensemble data due to lack of data on the crops/biowaste group. For Pyrochar also the ensemble data was used as this included data for sugarcane and peanut husks that were considered proxies for the groups defined.

3.2.2 Priming effect

The PE can be defined as the change on SOC decomposition rates in response to freshly-added C [121]. It has been observed that in average all the EOMs inhere studied exert a negative effect when applied to soils. A negative PE effect implies slower mineralization rates and thus increased SOC carbon stocks, and it is associated to inputs with high degrees of recalcitrance. On the other hand, positive PE

values, represent faster mineralization rates, attributed to stimulus to the soil microorganisms' dynamics, and is thus associated to less recalcitrant matter and SOC losses [122].

The PE of pyrochar has been fairly well studied. The study by Moura represents the latest global metadata analysis regarding pyrochar PE. The authors compiled 169 studies and reported the change observed on SOC stocks after pyrochar application. The results were categorized in 10 groups, regarding process temperature, raw material, climatic zone, soil properties, among others. Here we selected the results reported for a pyrochar produced in a temperature range of 350-600°C, which is close to the process defined in Table S2. For this group, a 71.4% decrease on SOC mineralization was reported, which was accounted in our study as a negative PE of 0.714. No similar meta-study has been found for gaschar or hydrochar. For the case of gaschar, due to its similarity to pyrochar, we used the value reported by Moura for high temperatures >600°C as a proxy. For gaschar a negative PE of 0.551 was used. For digestate, the PE value was calculated as the average change between control soil and digestate amended soils, based on a data compilation of 79 data records, harmonized in an unpublished database *(unpublished study under construction*). The application of digestate to soils decreased SOC mineralization by 19.70% in average, thus a negative PE of 0.1970 was used.

Hydrochar is a product with a medium degree of recalcitrance, not comparable to pyrochar or gaschar, which have reported mean lives on the hundreds of years [123], while hydrochar mean residence time is on the decadal scale [56]. The PE of hydrochar still remains unclear, with results reporting positive PE of approximately 20% in 1 year of application, and 51-72% native SOC loss after 1 year of application. In this study, due to lack of data, we used the PE of digestate as a proxy for hydrochar. The PE is accounted as a new parameter in RothC-Bioeconomy. For conditions were no PE is foreseen, the default value is 1. It means that the mineralization rate of the soil pools remains unaffected by PE. If the PE of an EOM is negative, then it is included by subtracting 1 – PE. Likewise, for positive PE, it is included in the model by adding 1 + PE.

4. Sensitivity analysis (SA) configuration

The SA was conducted to test the combinations of three levels for the C inputs as EOMs and two levels of recalcitrance, the former defined by C_C and the latter defined by the combination of C_R, C_I, k_R, k_L, and PE. The C_C levels are inhere defined as low, high, and medium while the recalcitrance is referred to a minimum and maximum. The minimum recalcitrance includes the values set as high kL, low kR, high C_L, low C_R, and positive PE. The maximum recalcitrance comprises a low k_L, high k_R, low C_L, high C_R, and negative PE. An extra SA to assess the effect of including PE without changing other recalcitrance parameters was performed for pyrochar. A total of 25 SA scenarios were assessed by these combinations. The values used for the SA combinations are detailed in Table S3

Table S 6. Different combinations of carbon size and recalcitrance of the EOMs considered for sensitivity

Bioeconomy pathways	Recalcitrance (C_R)															Size of carbon (C_C)					
	C_L [a]			k_L (y^{-1}) [a]			C_R [a]			k_R (y^{-1}) [a]			PE			Cereal straw [a]			Fibres and leaves[b]		
	L	M	H	L	M	H	L	M	H	L	M	H	L	M	H	L	M	H	L	M	H
Pyrochar	0.01	0.05	0.09	2.61E+1	1.18E+2	1.90E+2	0.91	0.95	0.99	1.08E-3	3.30E-3	5.00E-3	1.91	1	0.286	0.34	0.44	0.54	0.43	0.51	0.59
Pyrochar[c]	-	0.05	-	-	3.40	-	-	0.95	-	-	3.30E-3	-	-	0.286	-	0.34	0.44	0.54	0.43	0.51	0.59
Gaschar	0.01	0.05	0.09	7.03	6.97E+1	8.08E+1	0.91	0.95	0.99	4.75E-3	7.05E-3	7.96E-2	1.91	1	0.449	0.14	0.20	0.25	0.29	0.31	0.34
Hydrochar[d]	0.03	0.11	0.2	1.68E+1	2.76E+1	4.21E+1	0.8	0.89	0.97	7.55E-2	9.88E-2	1.83E-1	1.91	1	0.803	0.12	0.31	0.45	0.12	0.31	0.45
Digestate	0.23	0.32	0.435	6.31E+1	2.00E+2	3.32E+2	0.555	0.68	0.77	7.30E-1	8.15E-1	2.85E+1	1.91	1	0.803	0.29	0.39	0.49	0.64	0.69	0.80

C_C:,Carbon conversion C_R:Carbon recalcitrant fraction, C_L: carbon labile fraction (1-C_R), PE: Priming effect, k_L: mineralization rate of the labile fraaction, k_R: mineralization rate of the recalcitrant fraction

[a] Value used as in Andrade Díaz et al. (2023). Values are shown with 2 decimals to ensure tractability. [b] Average value from data reported in Andrade et al. [15]. It stems from a database where 110 data records (40 for digestate, 30 for pyrochar, and 30 for gaschar) are compiled and harmonized within this study and is openly accessible at "doi database". PE values of pyrochar and gaschar were defined according to the global meta-analysis by Chagas et al. (2022). PE for pyrochar was used as the percent change of the organic carbon content in the soil observed by the application of biochar produced at medium temperature (350 – 600°C) and the value observed for high temperatures (> 600 °C) was used as proxy for gaschar. PE for digestate was calculated from a meta-analysis (unpublished) including 79 data records contrasting the SOC changes observed after the application of digestate with a control situation where no digestate is applied. [c] One at a time sensitivity for pyrochar scenario, to assess the single effect of PE. Also, k_L was used as reported in Wang et al. (2016) in this scenario. Wang et al. (2016) found a mean residence time of 108 days for the labile fraction, which corresponds to 0.29 years and a k_L of 3.4 y^{-1} [d] No data regarding the hydrochar represented in this study was found, therefore C_C and C_R defined in Andrade Díaz et al. (2023) for cereal residues were used as a proxy. Since HTL processes tolerate wet feedstocks as in AD processes, and the recalcitrance lifetime of hydrochar was found to be on the decadal scale as opposed to the hundreds found for other biochar (pyrochar and gaschar) [57,125], the PE defined for digestate was used as a proxy for hydrochar.

5. BAU scenario results

The BAU scenario predicted an average increase of SOC stocks by 4% at the year 2040. However, in terms of net storage, a total loss of 0.77 Mt C is shown at the national scale at the same period. The SOC sequestration potential map of Ecuador, produced by MAG (unpublished; [3] to contribute to the global SOC sequestration map [2] exhibits similar trends but the net values differ from our results. In fact, the potential SOC loss observed in here is 1.2-fold that observed by Jimenez (0.6 Mt C). However, the study of Jimenez reports potential SOC depletion in the coastal croplands by 2040, while although we observe high losses, no APCU reports SOC depletion in our study (Fig S3). A thorough analysis of the BAU scenario allows depicting that the main difference between our study and that of MAG relies on the C inputs for sugarcane, banana, and maize. This offset in results between the two studies can be explained because the BAU scenario modeled inhere considers that all the potential crop residues will remain on the fields, while in reality the common practice in Ecuador, especially for the case of sugarcane residues, is open-field burning. The study of MAG considers this reality by stablishing the C inputs based on the back-run calculations performed for 500 years, which allows to determine the C inputs that have resulted in the current SOC stocks measured in the country [126].

Although the approach followed by FAO considers the C inputs under the real current practices, our approach based on the use of RPR, RtS, and C composition coefficients to account for the C inputs allows accomplishing our main goal of quantifying the amount of crop residues that can be harvested and returned to soils as recalcitrant EOMs. Moreover, our approach complies with our statement of leaving all the crop residues on fields with no further processing. Therefore, we consider our approach to be correct for the scope and goals of our study. As the results presented in our study are relative, observing the SOC change between the mitigation and BAU scenarios, this effect is accounted in both scenarios and thus does not change the final conclusions retained.

The SOC stocks at year 2040 and 2070 are presented in Fig 3 a and b, respectively. Results show a SOC loss of up to 65% in 79% of the simulated areas by the year 2040. The SOC losses observed in the long term (2070) attain 90%, which represents a net loss of 0.77 MtC. The Northwest region (province of Esmeraldas) as well as some central west areas (province of Manabí) show a change of conclusions between the near- and long-term results. For the year 2040, the North- and Central-west regions depict potential SOC storage, however, if the simulation timeframe is extended until 2070, SOC losses are predicted.

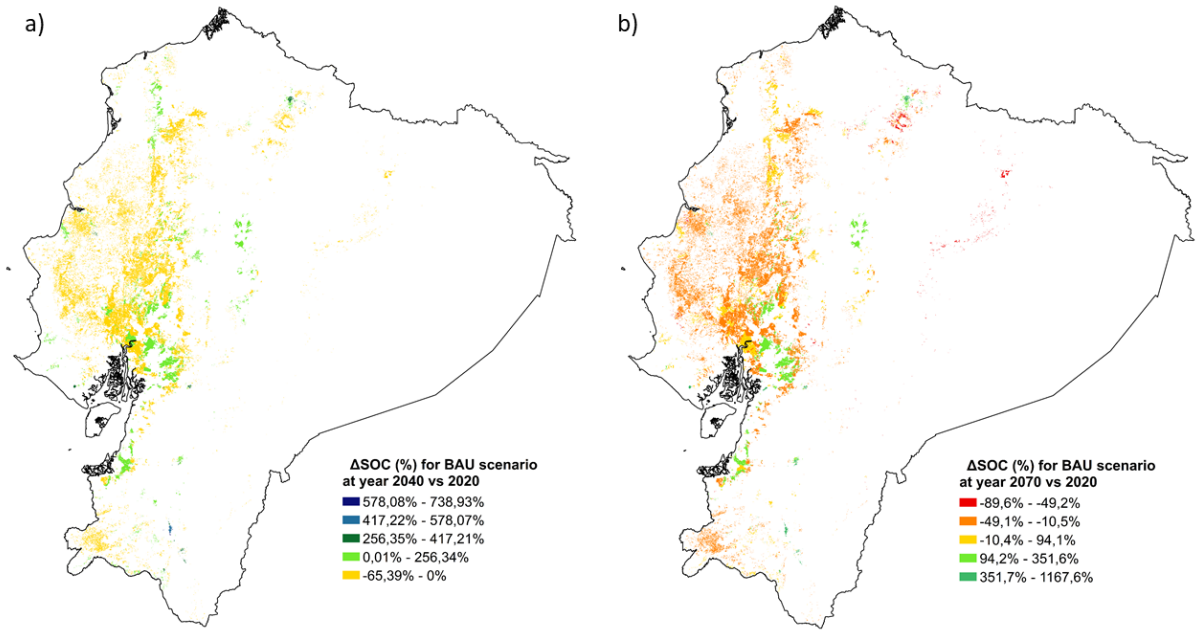

Fig S12. Business as usual scenario SOC evolution a) at year 2040 vs 2020, and b) year 2070 vs 2020

References

1. Andrade Díaz C, Zamora-Ledezma E, Hamelin L. Dataset for defining the spatially explicit baseline of cropping systems in Ecuadorian croplands and estimating the crop residues potential. 2023.
2. FAO. Global Soil Organic Carbon Sequestration Potential Map – GSOCseq v.1.1 : Technical report [Internet]. Rome, Italy: FAO; 2022 [cited 2023 Jan 13]. 179 p. Available from: https://www.fao.org/documents/card/en/c/cb9002en
3. Jiménez W, Sánchez D, Ruiz V, Manzano D, Armas D, Jiménez L, et al. Ecuador: SOil Organic Carbon Sequestration Potential National Map. National Report. Version 1.0. Global Soil Partnership. Ministry of Agriculture and Livestock of Ecuador.; 2021. Report No.: 1.0.
4. MAG, MAATE, FAO, GSP. Mapeo digital de Carbono orgánico en los suelos del Ecuador. [Internet]. Quito, Ecuador; 2021. Report No.: Segunda Edición. Available from: sipa.agricultura.gob.ec
5. Abatzoglou JT, Dobrowski SZ, Parks SA, Hegewisch KC. TerraClimate, a high-resolution global dataset of monthly climate and climatic water balance from 1958–2015. Sci Data. 2018 Jan 9;5(1):170191.
6. MAG, IEE, SENPLADES. Mapa de cobertura y uso de la tierra del Ecuador continental, 2009- 2015, escala 1: 25.000. Versión editada por el Ministerio de Agricultura y Ganadería 2020. Ecuador; 2015.
7. INEC. Encuesta de Superficie y Producción Agropecuaria Continua [Internet]. Ecuador: INEC, SENPLADES; 2021. Available from: https://anda.inec.gob.ec/anda/index.php/catalog/912#page=accesspolicy&tab=study-desc
8. MAG. Geoportal del Agro Ecuatoriano: Visor geografico [Internet]. SIPA. 2023. Available from: http://geoportal.agricultura.gob.ec/
9. Northern South America - Crop Calendars [Internet]. [cited 2023 May 6]. Available from: https://ipad.fas.usda.gov/rssiws/al/crop_calendar/nsa.aspx
10. FAO GIEWS Country Brief on Ecuador - [Internet]. [cited 2023 May 6]. Available from: https://www.fao.org/giews/countrybrief/country.jsp?code=ECU
11. Palm Oil Explorer [Internet]. [cited 2023 May 6]. Available from: https://ipad.fas.usda.gov/cropexplorer/cropview/commodityView.aspx?cropid=4243000&sel_year=2020&rankby=Production
12. FaoCropCalendar [Internet]. [cited 2023 May 6]. Available from: https://cropcalendar.apps.fao.org/#/home
13. Blackmore I, Rivera C, Waters WF, Iannotti L, Lesorogol C. The impact of seasonality and climate variability on livelihood security in the Ecuadorian Andes. Climate Risk Management. 2021 Jan 1;32:100279.
14. Karan SK, Hamelin L. Crop residues may be a key feedstock to bioeconomy but how reliable are current estimation methods? Resources, Conservation and Recycling. 2021 Jan;164:105211.
15. Andrade Díaz C, Zamora-Ledezma E, Hamelin L. Database: Dataset for defining the spatially explicit baseline of cropping systems in Ecuadorian croplands and estimating the crop residues potential. Dataverse - TBI - Toulouse Biotechnology Institute - T21018. 2023 May;
16. Bundhoo ZMA, Surroop D. Evaluation of the potential of bio-methane production from field-based crop residues in Africa. Renewable and Sustainable Energy Reviews. 2019 Nov 1;115:109357.
17. Katherine Rodriguez Caceres, Francy Blanco Patino, Julian Araque Duarte, Viatcheslav Kafarov. Assessment of the energy potential of agricultural residues in non-interconnected zones of colombia: case study of choco and putumayo. Chemical Engineering Transactions. 2016 Jun;50:349–54.
18. Cardoen D, Joshi P, Diels L, Sarma PM, Pant D. Agriculture biomass in India: Part 1. Estimation and characterization. Resources, Conservation and Recycling. 2015 Sep 1;102:39–48.

19. Ortiz-Ulloa JA, Abril-González MF, Pelaez-Samaniego MR, Zalamea-Piedra TS. Biomass yield and carbon abatement potential of banana crops (Musa spp.) in Ecuador. Environ Sci Pollut Res. 2021 Apr 1;28(15):18741–53.
20. Singh J, Panesar BS, Sharma SK. Energy potential through agricultural biomass using geographical information system—A case study of Punjab. Biomass and Bioenergy. 2008 Apr 1;32(4):301–7.
21. Scarlat N, Martinov M, Dallemand JF. Assessment of the availability of agricultural crop residues in the European Union: Potential and limitations for bioenergy use. Waste Management. 2010 Oct 1;30(10):1889–97.
22. Bentsen NS, Felby C, Thorsen BJ. Agricultural residue production and potentials for energy and materials services. Progress in Energy and Combustion Science. 2014 Feb 1;40:59–73.
23. Mai-Moulin T, Visser L, Fingerman KR, Elbersen W, Elbersen B, Nabuurs GJ, et al. Sourcing overseas biomass for EU ambitions: assessing net sustainable export potential from various sourcing countries. Biofuels, Bioproducts and Biorefining. 2019;13(2):293–324.
24. Esteban L, Pilar C, Carrasco J. An assessment of relevant methodological elements and criteria for surveying sustainable agricultural and forestry biomass byproducts for energy purposes. BioResources. 2008 Aug 1;3.
25. Vaish S, Kaur G, Sharma NK, Gakkhar N. Estimation for Potential of Agricultural Biomass Sources as Projections of Bio-Briquettes in Indian Context. Sustainability. 2022 Jan;14(9):5077.
26. Rhofita EI, Rachmat R, Meyer M, Montastruc L. Mapping analysis of biomass residue valorization as the future green energy generation in Indonesia. Journal of Cleaner Production. 2022 Jun 20;354:131667.
27. Arranz-Piera P, Kemausuor F, Addo A, Velo E. Electricity generation prospects from clustered smallholder and irrigated rice farms in Ghana. Energy. 2017 Feb 15;121:246–55.
28. Nelson N, Darkwa J, Calautit J, Worall M, Mokaya R, Adjei E, et al. Potential of Bioenergy in Rural Ghana. Sustainability. 2021 Jan;13(1):381.
29. Barbanera M, Muguerza IF. Effect of the temperature on the spent coffee grounds torrefaction process in a continuous pilot-scale reactor. Fuel. 2020 Feb 15;262:116493.
30. Griffin DW, Schultz MA. Fuel and chemical products from biomass syngas: A comparison of gas fermentation to thermochemical conversion routes. Environmental Progress and Sustainable Energy. 2012;31(2):219–24.
31. MEER, MCPEC, INP. Atlas Bioenergético del Ecuador. Ecuador: Ministry of Electricity and Renewable Energy; 2014.
32. Gouvello C, Dayo F, Thioye M. Low-carbon Energy Projects for Development in Sub-Saharan Africa. 2008 Jan 1;
33. Okello C, Pindozzi S, Faugno S, Boccia L. Bioenergy potential of agricultural and forest residues in Uganda. Biomass and Bioenergy. 2013 Sep 1;56:515–25.
34. Waldheim L, Monis M, Verde Leal MR. Biomass Power Generation: Sugar Cane Bagasse and Trash. In: Progress in Thermochemical Biomass Conversion [Internet]. John Wiley & Sons, Ltd; 2001 [cited 2023 May 5]. p. 509–23. Available from: https://onlinelibrary.wiley.com/doi/abs/10.1002/9780470694954.ch41
35. Bingh LP. Opportunities for utilizing waste biomass for energy in Uganda. In 2004 [cited 2023 May 5]. Available from: https://www.semanticscholar.org/paper/Opportunities-for-utilizing-waste-biomass-for-in-Bingh/0491bced642af223d5842123a5b91b0dce9d5be6
36. Gabisa EW, Gheewala SH. Potential of bio-energy production in Ethiopia based on available biomass residues. Biomass and Bioenergy. 2018 Apr 1;111:77–87.
37. Zhang J, Li J, Dong C, Zhang X, Rentizelas A, Shen D. Comprehensive assessment of sustainable potential of agricultural residues for bioenergy based on geographical information system: A case study of China. Renewable Energy. 2021 Aug 1;173:466–78.
38. Barahira DS, Okudoh VI, Eloka-Eboka AC. Suitability of Crop Residues as Feedstock for Biofuel Production in South Africa: A Sustainable Win-Win Scenario. Journal of Oleo Science. 2021;70(2):213–26.

39. Gondwe KJ, Chiotha SS, Mkandawire T, Zhu X, Painuly J, Taulo JL. An assessment of crop residues as potential renewable energy source for cement industry in Malawi. Journal of Energy in Southern Africa [Internet]. 2017 Dec 23 [cited 2023 May 5];28(4). Available from: https://energyjournal.africa/article/view/4178
40. Ying B, Xiong K, Wang Q, Wu Q. Can agricultural biomass energy provide an alternative energy source for karst rocky desertification areas in Southwestern China? investigating Guizhou Province as example. Environ Sci Pollut Res. 2021 Aug 1;28(32):44315–31.
41. Papendick RI, Moldenhauer WC, United States. Agricultural Research Service. Crop residue management to reduce erosion and improve soil quality : northwest [Internet]. [Washington, D.C.?] : U.S. Dept. of Agriculture, Agricultural Research Service; 1995 [cited 2023 May 5]. 78 p. Available from: http://archive.org/details/cropresiduemanag40pape
42. Ben-Iwo J, Manovic V, Longhurst P. Biomass resources and biofuels potential for the production of transportation fuels in Nigeria. Renewable and Sustainable Energy Reviews. 2016 Sep 1;63:172–92.
43. Suharno I, Dehen YA, Barbara B, Ottay JB. Opportunities for increasing productivity and profitability of oil palm smallholder farmers in Central Kalimantan. Palangkaraya: Palangkaraya Institute for Land use and Agricultural Research (PILAR). 2015;
44. Contreras NER, S AA, Núñez JAG. Inventario de la biomasa disponible en plantas de beneficio para su aprovechamiento y caracterización fisicoquímica de la tusa en Colombia. Palmas. 2015 Dec 1;36(4):41–54.
45. Kemausuor F, Kamp A, Thomsen ST, Bensah EC, Østergård H. Assessment of biomass residue availability and bioenergy yields in Ghana. Resources, Conservation and Recycling. 2014 May 1;86:28–37.
46. Chitawo ML, Chimphango AFA. A synergetic integration of bioenergy and rice production in rice farms. Renewable and Sustainable Energy Reviews. 2017 Aug 1;75:58–67.
47. Forster-Carneiro T, Berni MD, Dorileo IL, Rostagno MA. Biorefinery study of availability of agriculture residues and wastes for integrated biorefineries in Brazil. Resources, Conservation and Recycling. 2013 Aug 1;77:78–88.
48. Alhassan EA, Olaoye JO, Olayanju TMA, Okonkwo CE. An investigation into some crop residues generation from farming activities and inherent energy potentials in Kwara State, Nigeria. IOP Conf Ser: Mater Sci Eng. 2019 Nov;640(1):012093.
49. Kaniapan S, Hassan S, Ya H, Patma Nesan K, Azeem M. The Utilisation of Palm Oil and Oil Palm Residues and the Related Challenges as a Sustainable Alternative in Biofuel, Bioenergy, and Transportation Sector: A Review. Sustainability. 2021 Jan;13(6):3110.
50. Hernández Hernández H 50556, Orduz Prada J 37906, Zapata Lesmes HJ 37907, Cecilia 37908 CRM, Duarte Ortega M 37909. Atlas del potencial energético de la biomasa residual en Colombia /. 2010 [cited 2023 May 5]; Available from: https://repositorio.fedepalma.org/handle/123456789/109170
51. Hiloidhari M, Das D, Baruah DC. Bioenergy potential from crop residue biomass in India. Renewable and Sustainable Energy Reviews. 2014 Apr 1;32:504–12.
52. El-Naggar A, El-Naggar AH, Shaheen SM, Sarkar B, Chang SX, Tsang DCW, et al. Biochar composition-dependent impacts on soil nutrient release, carbon mineralization, and potential environmental risk: A review. Journal of Environmental Management. 2019 Jul 1;241:458–67.
53. Bolinder MA, Janzen HH, Gregorich EG, Angers DA, VandenBygaart AJ. An approach for estimating net primary productivity and annual carbon inputs to soil for common agricultural crops in Canada. Agriculture, Ecosystems & Environment. 2007 Jan 1;118(1):29–42.
54. Clivot H, Mouny JC, Duparque A, Dinh JL, Denoroy P, Houot S, et al. Modeling soil organic carbon evolution in long-term arable experiments with AMG model. Environmental Modelling & Software. 2019 Aug 1;118:99–113.

55. Scarlat N, Fahl F, Lugato E, Monforti-Ferrario F, Dallemand JF. Integrated and spatially explicit assessment of sustainable crop residues potential in Europe. Biomass and Bioenergy. 2019 Mar 1;122:257–69.
56. Andrade C, Albers A, Zamora-Ledezma E, Hamelin L. A review on the interplay between bioeconomy and soil organic carbon stocks maintenance. PREPRINT (version 2) available at Research Square [Internet]. 2022 Mar 16 [cited 2022 Mar 16]; Available from: https://www.researchsquare.com
57. Han L, Sun K, Yang Y, Xia X, Li F, Yang Z, et al. Biochar's stability and effect on the content, composition and turnover of soil organic carbon. Geoderma. 2020 Apr;364:114184.
58. Wang J, Xiong Z, Kuzyakov Y. Biochar stability in soil: meta-analysis of decomposition and priming effects. GCB Bioenergy. 2016 May;8(3):512–23.
59. Ippolito JA, Cui L, Kammann C, Wrage-Mönnig N, Estavillo JM, Fuertes-Mendizabal T, et al. Feedstock choice, pyrolysis temperature and type influence biochar characteristics: a comprehensive meta-data analysis review. Biochar. 2020 Dec;2(4):421–38.
60. Joseph S, Cowie AL, Van Zwieten L, Bolan N, Budai A, Buss W, et al. How biochar works, and when it doesn't: A review of mechanisms controlling soil and plant responses to biochar. GCB Bioenergy. 2021 Aug 26;gcbb.12885.
61. Coleman K, Jenkinson DS. RothC-26.3 - A Model for the turnover of carbon in soil. In: Powlson DS, Smith P, Smith JU, editors. Evaluation of Soil Organic Matter Models [Internet]. Berlin, Heidelberg: Springer Berlin Heidelberg; 1996 [cited 2021 Apr 15]. p. 237–46. Available from: http://link.springer.com/10.1007/978-3-642-61094-3_17
62. Andrade Díaz C, Clivot H, Albers A, Zamora-Ledezma E, Hamelin L. The crop residue conundrum: Maintaining long-term soil organic carbon stocks while reinforcing the bioeconomy, compatible endeavors? Applied Energy. 2023 Jan 1;329:120192.
63. Liao F, Yang L, Li Q, Li YR, Yang LT, Anas M, et al. Characteristics and inorganic N holding ability of biochar derived from the pyrolysis of agricultural and forestal residues in the southern China. Journal of Analytical and Applied Pyrolysis. 2018 Sep 1;134:544–51.
64. Fernandes ERK, Marangoni C, Medeiros SHW, Souza O, Sellin N. SLOW PYROLYSIS OF BANANA CULTURE WASTE: LEAVES AND PSEUDOSTEM. 2012;
65. Sellin N, Krohl DR, Marangoni C, Souza O. Oxidative fast pyrolysis of banana leaves in fluidized bed reactor. Renewable Energy. 2016 Oct 1;96:56–64.
66. Ighalo JO, Adeniyi AG. Thermodynamic modelling and temperature sensitivity analysis of banana (Musa spp.) waste pyrolysis. SN Appl Sci. 2019 Sep;1(9):1086.
67. Adeniyi AG, Ighalo JO, Amosa MK. Modelling and simulation of banana (Musa spp.) waste pyrolysis for bio-oil production. Biofuels. 2021 Aug 9;12(7):879–83.
68. Abdullah N, Sulaiman F, Taib RM, Miskam MA. Pyrolytic oil of banana (Musa spp.) pseudo-stem via fast process. In Kuala Lumpur, Malaysia; 2015 [cited 2022 Dec 7]. p. 100005. Available from: http://aip.scitation.org/doi/abs/10.1063/1.4915212
69. Abdullah N, Mohd Taib R, Mohamad Aziz NS, Omar MR, Md Disa N. Banana pseudo-stem biochar derived from slow and fast pyrolysis process. Heliyon. 2023 Jan 1;9(1):e12940.
70. Taib RM, Abdullah N, Aziz NSM. Bio-oil derived from banana pseudo-stem via fast pyrolysis process. Biomass and Bioenergy. 2021 May 1;148:106034.
71. Mosqueda A, Medrano K, Gonzales H, Takahashi F, Yoshikawa K. Hydrothermal treatment of banana leaves for solid fuel combustion. Biofuels. 2021 Oct 21;12(9):1123–9.
72. Fernandes ERK, Marangoni C, Souza O, Sellin N. Thermochemical characterization of banana leaves as a potential energy source. Energy Conversion and Management. 2013 Nov 1;75:603–8.

73. Alves JLF, da Silva JCG, Sellin N, Prá F de B, Sapelini C, Souza O, et al. Upgrading of banana leaf waste to produce solid biofuel by torrefaction: physicochemical properties, combustion behaviors, and potential emissions. Environ Sci Pollut Res. 2022 Apr 1;29(17):25733–47.
74. Cheng Q, Jiang M, Chen Z, Wang X, Xiao B. Pyrolysis and kinetic behavior of banana stem using thermogravimetric analysis. Energy Sources, Part A: Recovery, Utilization, and Environmental Effects. 2016 Nov 16;38(22):3383–90.
75. Cardona S, Orozco LM, Gómez CL, Solís WA, Velásquez JA, Rios LA. Valorization of banana residues via gasification coupled with electricity generation. Sustainable Energy Technologies and Assessments. 2021 Apr 1;44:101072.
76. Anniwaer A, Chaihad N, Zhang M, Wang C, Yu T, Kasai Y, et al. Hydrogen-rich gas production from steam co-gasification of banana peel with agricultural residues and woody biomass. Waste Management. 2021 Apr 15;125:204–14.
77. Islam MdA, Akber MdA, Limon SH, Akbor MdA, Islam MdA. Characterization of solid biofuel produced from banana stalk via hydrothermal carbonization. Biomass Conv Bioref. 2019 Dec 1;9(4):651–8.
78. Divyabharathi R, Subramanian P. Assessment of Product Yield and Characteristics of Biocrude from Hydrothermal Liquefaction. Research Biotica. 2022 May 3;4(2):42–6.
79. Khan MT, Brulé M, Maurer C, Argyropoulos D, Müller J, Oechsner H. Batch anaerobic digestion of banana waste - energy potential and modelling of methane production kinetics. 18(1).
80. Bahrun A, Fahimuddin MY, Rakian TC, Safuan LO, Kilowasid LOMH. Cocoa Pod Husk Biochar Reduce Watering Frequency and Increase Cocoa Seedlings Growth. International Journal of Environment, Agriculture and Biotechnology [Internet]. 2018 Sep 8 [cited 2023 May 6];3(5). Available from: https://ijeab.com/detail/cocoa-pod-husk-biochar-reduce-watering-frequency-and-increase-cocoa-seedlings-growth/
81. Ogunjobi JK, Lajide L. The Potential of Cocoa Pods and Plantain Peels as Renewable Sources in Nigeria. International Journal of Green Energy. 2015 Apr 3;12(4):440–5.
82. Ghysels S, Acosta N, Estrada A, Pala M, De Vrieze J, Ronsse F, et al. Integrating anaerobic digestion and slow pyrolysis improves the product portfolio of a cocoa waste biorefinery. Sustainable Energy Fuels. 2020;4(7):3712–25.
83. Ramos LF, Soto AR, Huaynate AIO, Gallegos MAC. Extracción e identificación de lípidos polares de las microalgas Nannochloropsis oceanica y Desmodesmus asymmetricus. Revista Colombiana de Química. 2020 May 1;49(2):3–11.
84. Adjin-Tetteh M, Asiedu N, Dodoo-Arhin D, Karam A, Amaniampong PN. Thermochemical conversion and characterization of cocoa pod husks a potential agricultural waste from Ghana. Industrial Crops and Products. 2018 Sep 1;119:304–12.
85. Ngalani GP, Kagho FD, Peguy NNC, Prudent P, Ondo JA, Ngameni E. Effects of coffee husk and cocoa pods biochar on the chemical properties of an acid soil from West Cameroon. Archives of Agronomy and Soil Science. 2022 Feb 10;1.
86. Zinla D, Gbaha P, Koffi PME, Koua BK. Characterization of rice, coffee and cocoa crops residues as fuel of thermal power plant in Côte d'Ivoire. Fuel. 2021 Jan 1;283:119250.
87. Sobamiwa O, Longe OG. Utilization of cocoa-pod pericarp fractions in broiler chick diets. Animal Feed Science and Technology. 1994 Jun 1;47(3):237–44.
88. Daud Z, Kassim ASM, Aripin AM, Awang H, Hatta ZM. Chemical Composition and Morphological of Cocoa Pod Husks and Cassava Peels for Pulp and Paper Production. 2013;
89. Dahunsi SO, Osueke CO, Olayanju TMA, Lawal AI. Co-digestion of Theobroma cacao (Cocoa) pod husk and poultry manure for energy generation: Effects of pretreatment methods. Bioresource Technology. 2019 Jul 1;283:229–41.
90. George J, Arun P, Muraleedharan C. Experimental investigation on co-gasification of coffee husk and sawdust in a bubbling fluidised bed gasifier. Journal of the Energy Institute. 2019 Dec 1;92(6):1977–86.

91. Gunasekaran AP, Chockalingam MP, Padmavathy SR, Santhappan JS. Numerical and experimental investigation on the thermochemical gasification potential of Cocoa pod husk (Theobroma Cacoa) in an open-core gasifier. Clean Techn Environ Policy. 2021 Jul 1;23(5):1603–15.
92. Kiggundu N, Sittamukyoto J. Pryloysis of Coffee Husks for Biochar Production. JEP. 2019;10(12):1553–64.
93. Matoso SCG, Wadt PGS, de Souza Júnior VS, Pérez XLO, Plotegher F. Variation in the properties of biochars produced by mixing agricultural residues and mineral soils for agricultural application. Waste Manag Res. 2020 Sep 1;38(9):978–86.
94. de Carvalho Oliveira F, Srinivas K, Helms GL, Isern NG, Cort JR, Gonçalves AR, et al. Characterization of coffee (Coffea arabica) husk lignin and degradation products obtained after oxygen and alkali addition. Bioresource Technology. 2018 Jun 1;257:172–80.
95. Qiuxia W, Rui X, Jianchang L, Huanyun D, Yage Y, Jiahong H. One study on biogas production potential character of coffee husks. In: 2013 International Conference on Materials for Renewable Energy and Environment. 2013. p. 188–92.
96. Ulsido MD, Zeleke G, Li M. BIOGAS POTENTIAL ASSESSMENT FROM A COFFEE HUSK: AN OPTION FOR SOLID WASTE MANAGEMENT IN GIDABO WATERSHED OF ETHIOPIA. ENGINEERING FOR RURAL DEVELOPMENT.
97. Du N, Li M, Zhang Q, Ulsido MD, Xu R, Huang W. Study on the biogas potential of anaerobic digestion of coffee husks wastes in Ethiopia. Waste Manag Res. 2021 Feb 1;39(2):291–301.
98. Bekalo SA, Reinhardt HW. Fibers of coffee husk and hulls for the production of particleboard. Mater Struct. 2010 Oct 1;43(8):1049–60.
99. de Oliveira JL, da Silva JN, Martins MA, Pereira EG, da Conceição Trindade Bezerra e Oliveira M. Gasification of waste from coffee and eucalyptus production as an alternative source of bioenergy in Brazil. Sustainable Energy Technologies and Assessments. 2018 Jun 1;27:159–66.
100. Mendoza Martinez CL, Saari J, Melo Y, Cardoso M, de Almeida GM, Vakkilainen E. Evaluation of thermochemical routes for the valorization of solid coffee residues to produce biofuels: A Brazilian case. Renewable and Sustainable Energy Reviews. 2021 Mar 1;137:110585.
101. Veiga TRLA, Lima JT, Dessimoni AL de A, Pego MFF, Soares JR, Trugilho PF. Different Plant Biomass Characterizations for Biochar Production. CERNE. 23(4):529–36.
102. Sukiran MA. CONVERSION OF PRE-TREATED OIL PALM EMPTY FRUIT BUNCHES INTO BIO-OIL AND BIO-CHAR VIA FAST PYROLYSIS. JOPR [Internet]. 2018 Mar 9 [cited 2023 May 6]; Available from: http://jopr.mpob.gov.my/conversion-of-pre-treated-oil-palm-empty-fruit-bunches-into-bio-oil-and-bio-char-via-fast-pyrolysis/
103. Abnisa F, Arami-Niya A, Wan Daud WMA, Sahu JN, Noor IM. Utilization of oil palm tree residues to produce bio-oil and bio-char via pyrolysis. Energy Conversion and Management. 2013 Dec 1;76:1073–82.
104. Rahman A, Abdullah N, Sulaiman F. Temperature Effect on the Characterization of Pyrolysis Products from Oil Palm Fronds. In 2014 [cited 2023 May 6]. Available from: https://www.semanticscholar.org/paper/Temperature-Effect-on-the-Characterization-of-from-Rahman-Abdullah/9df0b85ab475f2664c579e40651b4e0493e29e49
105. Sukiran MA, Loh SK, Bakar NA. Production of Bio-oil from Fast Pyrolysis of Oil Palm Biomass using Fluidised Bed Reactor. 2016;
106. Shrivastava P, Kumar A, Tekasakul P, Lam SS, Palamanit A. Comparative Investigation of Yield and Quality of Bio-Oil and Biochar from Pyrolysis of Woody and Non-Woody Biomasses. Energies. 2021 Jan;14(4):1092.
107. Suksong W, Jehlee A, Singkhala A, Kongjan P, Prasertsan P, Imai T, et al. Thermophilic solid-state anaerobic digestion of solid waste residues from palm oil mill industry for biogas production. Industrial Crops and Products. 2017 Jan 1;95:502–11.

108. Srimachai T, Thonglimp V, O-Thong S. Ethanol and Methane Production from Oil Palm Frond by Two Stage SSF. Energy Procedia. 2014 Jan 1;52:352–61.

109. Tepsour M, Usmanbaha N, Rattanaya T, Jariyaboon R, O-Thong S, Prasertsan P, et al. Biogas Production from Oil Palm Empty Fruit Bunches and Palm Oil Decanter Cake using Solid-State Anaerobic co-Digestion. Energies. 2019 Jan;12(22):4368.

110. Piolo JAM, Legowo EH, Widiputri DI. Study of Biogas Production From Palm Oil Solid Wastes: A Review. In Atlantis Press; 2022 [cited 2023 May 5]. p. 155–73. Available from: https://www.atlantis-press.com/proceedings/ic-fanres-21/125968110

111. Chaikitkaew S, Kongjan P, O-Thong S. Biogas Production from Biomass Residues of Palm Oil Mill by Solid State Anaerobic Digestion. Energy Procedia. 2015 Nov 1;79:838–44.

112. Mustafa N., Li C.S., Doevendans T., Chin S.A., Karim Ghani A.W.A. Fluidised bed gasification of oil palm frond (opf) and napier grass (ng): a preliminary study. Chemical Engineering Transactions. 2015 Oct;45:1441–6.

113. Mahmood WMFW, Ariffin MA, Harun Z, Md Ishak NAI, Ghani J, Ab Rahman M. Characterisation and potential use of biochar from gasified oil palm wastes. 2015 Jan 1;10:45–54.

114. Ogi T, Nakanishi M, Fukuda Y, Matsumoto K. Gasification of oil palm residues (empty fruit bunch) in an entrained-flow gasifier. Fuel. 2013 Feb 1;104:28–35.

115. Janke L, Leite A, Nikolausz M, Schmidt T, Liebetrau J, Nelles M, et al. Biogas Production from Sugarcane Waste: Assessment on Kinetic Challenges for Process Designing. International Journal of Molecular Sciences. 2015 Sep;16(9):20685–703.

116. Jorapur R, Rajvanshi AK. Sugarcane leaf-bagasse gasifiers for industrial heating applications. Biomass and Bioenergy. 1997 Jan 1;13(3):141–6.

117. Landell MG de A, Scarpari MS, Xavier MA, Anjos IA dos, Baptista AS, Aguiar CL de, et al. Residual biomass potential of commercial and pre-commercial sugarcane cultivars. Sci agric (Piracicaba, Braz). 2013 Oct;70:299–304.

118. Oliveira FMV, Pinheiro IO, Souto-Maior AM, Martin C, Gonçalves AR, Rocha GJM. Industrial-scale steam explosion pretreatment of sugarcane straw for enzymatic hydrolysis of cellulose for production of second generation ethanol and value-added products. Bioresource Technology. 2013 Feb 1;130:168–73.

119. Oliveira LRM, Nascimento VM, Gonçalves AR, Rocha GJM. Combined process system for the production of bioethanol from sugarcane straw. Industrial Crops and Products. 2014 Jul 1;58:1–7.

120. Castello D, Pedersen T, Rosendahl L. Continuous Hydrothermal Liquefaction of Biomass: A Critical Review. Energies. 2018 Nov 15;11(11):3165.

121. Bastida F, García C, Fierer N, Eldridge DJ, Bowker MA, Abades S, et al. Global ecological predictors of the soil priming effect. Nat Commun. 2019 Aug 2;10(1):3481.

122. Liu W, Qiao C, Yang S, Bai W, Liu L. Microbial carbon use efficiency and priming effect regulate soil carbon storage under nitrogen deposition by slowing soil organic matter decomposition. Geoderma. 2018 Dec 15;332:37–44.

123. Lehmann J, Abiven S, Kleber M, Pan G, Singh BP, Sohi SP, et al. Persistence of biochar in soil. In: Biochar for Environmental Management. 2nd Edition. 2015. p. 48.

124. Chagas JKM, Figueiredo CC de, Ramos MLG. Biochar increases soil carbon pools: Evidence from a global meta-analysis. Journal of Environmental Management. 2022 Mar 1;305:114403.

125. Lehmann J, Cowie A, Masiello CA, Kammann C, Woolf D, Amonette JE, et al. Biochar in climate change mitigation. Nat Geosci. 2021 Dec;14(12):883–92.

126. FAO. Technical Manual Global Soil Organic Carbon Sequestration Potential Map GSOCseq [Internet]. 2022 [cited 2023 May 4]. Available from: https://fao-gsp.github.io/GSOCseq/index.html

Appendix A4a

Supplementary Information of Chapter 5 – Section 1

The content of this appendix is part of the supplementary information accompanying the paper 4 of this thesis. The numbering of the sections, figures and tables are as presented in the original document. The background data of this appendix is available in the following repository: https://doi.org/10.48531/JBRU.CALMIP/1JXQK3

To harvest or not? Tradeoffs between SOC maintenance and overall environmental performance of harvesting crop residues for the bioeconomy

Christhel Andrade Diaz[a,b*], Ezequiel Zamora-Ledezma[c], Lorie Hamelin[a]

[a] Toulouse Biotechnology Institute (TBI), INSA, INRAE UMR792, and CNRS UMR5504, Federal University of Toulouse, 135 Avenue de Rangueil, F-31077, Toulouse, France

[b] Department of Chemical, Biotechnological and Food Processes, Faculty of Mathematical, Physics and Chemistry Sciences. Universidad Técnica de Manabí (UTM), 130150, Portoviejo, Ecuador.

[c] Ecosystems Functioning and Climate Change Research Group FAGROCLIM, Faculty of Agriculture Engineering. Universidad Técnica de Manabí (UTM), 13132, Lodana, Ecuador.

* andraded@insa-toulouse.fr, christhel.andrade@utm.edu.ec, twitter:@christhell

Supplementary Material 1

Table of contents

List of tables

1. Maritime fuels

Maritime shipping is forecasted to increase 3-fold until 2050 in the cargo freight sector [1]. Facing the climate urgency, transition to biofuels is being encouraged within the maritime sector and is specially required in the cargo-freight sector.

As opposed to aviation systems, maritime engines are able to use rather unrefined biofuels, with HFO as the main fuel for cargo shipping historically (ref.). Current transition to low-sulfur content fuels has led to a rapid increase on the number of liquefied natural gas (LNG) operated vessels, reaching a global fleet of over 150 ships [2].

The consumption rate and emissions vary on a ship-by-ship basis and are specific for each fuel and engine type. In this section we present the main parameters required to account for the fuel consumption on-board and related emissions. The equations and parameters have been mainly retrieved from the 4th IMO GHG Study (ref.) which is considered as the main source to model the maritime fuels sector.

As the hydrotreated pyrolysis oil (HPO) considered inhere is composed of lighter carbon chains than HFO, we consider it as a proxy of marine distillate oils (MDO). In the case of cryogenic liquefied biogas, to produce biomethane, the bio-LNG is comparable to fossil-LNG, and thus the parameters for the traditional LNG are considered as well for bio-LNG. For the oil fuels (HFO and HPO) a slow-speed two-stroke (SSD) engine has been considered as the source of propulsion, while the fossil- and bio-LNG assume an Otto-cycle LNG engine [3].

1.1 Specific fuel oil consumption

The specific fuel oil consumption (SFOC) varies with the engine type and the vessel load. The IMO (refers) considers a 80% load as the most efficient baseline; while the minimum required at all times is of 65% (Comer). The proposed SFOC for the fuel and engine combinations selected are presented in Table S1.

Table S 7 Density, energy content, and fuel consumption of maritime fuels [3]

Fuel type	Density ($t.m^{-3}$)	Energy density ($MJ.kg^{-1}$) [a]	Engine type [b]	SFOC ($g.kWh^{-1}$)
Residual (HFO)	0.985	40.2	SSD	175
Distillate (MDO)	0.96	42.7	SSD	165
LNG	0.566	48.0	LNG (Otto-cycle)	166

[a] Resolution MEPC.308(73);(imo 4th); [b] Engine type per fuel type considered in our study

1.2 Emissions [3]

1.2.1 SOx emissions

SOx emissions depend on the Sulphur content and can be calculated using Eq S1

$$SOx = fuel * 2 * 0.97753 * S \quad \text{Eq S1}$$

where SOx are the grams of SOx emitted by gram of fuel, considering S as the Sulphur fraction in the fuel. Eq S1 assumes that 97.753% of the Sulphur content is emitted as SOx and the rest 2.247% is converted to sulphates – sulfites and accounted as particulate matter. SOx emissions in ships are mainly accounted as SO_2, thus the 2 in Eq S1 reflects the ratio of molecular weight of SO_2.

1.2.2 Particulate matter (PM)

The sulfur not emitted as SOx is released as PM. Also, PM2.5 is considered to be 97% of PM10, which varies among fuel types (Eq S2 and S3).

$$PM_{HFO}\left(\frac{g}{kWh}\right) = 1.35 + SFOC * 7 * 0.02247 * (S - 0.0246) \quad \text{Eq S2}$$

$$PM_{MDO}\left(\frac{g}{kWh}\right) = 0.23 + SFOC * 7 * 0.02247 * (S - 0.024) \quad \text{Eq S2}$$

where S represents the sulfur fraction in the fuel.

1.2.3 Emissions factors for all pollutants

Table S 8. Emissions factors for maritime fuels (kg pollutant.tonne-^{1}fuel) [a]

	Fuel type		
Pollutants	HFO	MDO	LNG
CO2	3,114	3,206	2,755
CH4	0.05	0.05	11.96
N2O	0.18	0.18	0.1
NOX	75.9	56.71	13.44
CO2	2.88	2.59	3.97
NMVOC	3.2	2.4	1.59
SOX	50.83	1.37	0.03
PM	7.55	0.9	0.11
PM2.5	6.94	0.83	0.1
BC	0.26	0.38	0.019

[a] Data source: 4th IMO GHG Study [3]

2. Marginal Suppliers

The marginal suppliers along the whole valorization chain must be clearly identified in consequential assessments. Here we considered the energy provision as marginal heat and electricity. Marginal electricity is intrinsically related to the geographical scope, and thus the electricity mix for France already implemented in Ecoinvent 3.9.1 [4] for medium or high voltage (depending on the situation) was employed. The marginal heat supply was designed for an optimal-performant future in terms of energy, and was thus described by an electrified system for its already distribution to the grid.

The marginal heat was implemented according to the high (HT) and low (LT) temperature marginal heat described by Su-ungkavatin [5]. Here, LT heat was used to supply process requiring temperatures below 100°C while HT heat was used for processes with requirements of over 100°C. Table S3 and S4 presents the assumptions followed for the LT and HT marginal heat, respectively.

Table S 9 Marginal LT Heat to supply processes requiring heating temperatures below 100°C: Heat production by heat pump. [a]

Parameters	Amount	Unit	Comments
Heat production, heat pump	1.00	MJ	Process from Ecoinvent adapted to use electricity from France (consequential)
Heat production, heat pump	1.00	MJ	Heat pump is determined to be a major source of the low-temperature heat production, according to the capacity established in the industry (Madeddu et al., 2020). Ecoinvent: Heat, borehole heat pump {FR}| heat production, borehole heat exchanger, brine-water heat pump 10kW | Conseq., U.

a Adapted with authorization of Su-ungkavatin [5]. Further details are described in the original database.

Table S 10 Marginal HT Heat to supply processes requiring heating temperatures above 100°C: Heat production using electric furnace.

Parameters	Amount	Unit	Comments
Heat production, electric arc furnace	**1.00**	**MJ**	Considered for heat applied to the service processes requiring the delivery temperatures of more than 100 °C
Electric arc furnace	9.50E-14	p	Electric arc furnace is applied as the proxy equipment regarding to the use of electrical currents for the heat production in this analysis as it is available in the Ecoinvent. The unit of required electric furnace is calculated from the average lifespan of industrial furnace used in EU as 35 years, with the estimated annual enery consumption of about 130 TWh/year. Ecoinvent: Electric arc furance converter {RER}| production| Conseq., U.
High voltage electricity	0.370	kWh	The electricity consumption of electric furnace is calculated based upon the reported energy efficiency between 0.6 and 0.9, the average value of 0.75 is applied. Data can be retrieved from the study of Madeddu et al. (2020). Ecoinvent: Electricity, high voltage {FR}| market for | Conseq., U.
Assumptions	**Amount**	**Unit**	**Comments**
Avergae energy requirements	0.370	kWh.MJ^{-1} heat	
Assumed lifespan of furnance used in EU	30	years	
Estimated annual energy consumption	130	TWh.year^{-1}	
	3.51E+11	MJ.year^{-1}	
∴ Heat production in a lifespan of furance	1.053E+13	MJ.unit^{-1}	

a Adapted with authorization of Su-ungkavatin [5]. Further details are described in the original database.

3. Scenarios description and Life cycle inventories (LCI)

Here we consider two case scenarios for the production of SMF: i) pyrolyisis bio-oil to replace HFO, and ii) cryogenic liquefied biomethane, referred to as bio-LNG to replace fossil-LNG.

The life cycle inventories (LCI) are built on from previous studies developed for the "base" technologies (i.e., fast pyrolysis and anaerobic digestion) and adapted to include the upgrading stages required to produce drop-in fuels suitable for maritime transport in carrier ships.

The fast-pyrolysis LCI was adapted from the study of Brassard et al. [6] for primary forest residues and adapted to crop residues based on original data for wheat straw kindly supplied by Brassard et al. (*unpublished*). The LCI was expanded, by incorporating the upgrading of the biocrude by a catalytic hydrotreatment process [7]. The LCI for anaerobic digestion was entirely performed using the anaerobic digestion module developed by Javourez [8] and adapted for the specific conditions of cryogenic liquefaction upgrading [9].

The key details considered in each scenario, as well as the main assumptions used in the LCIs are described in the subsequent sections and transparently documented in the SI2 and SI3, both openly available at [10].

3.1 Crop residues composition

This study follows a feedstock-based approach, and thus the initial feedstock is the same in all the compared scenarios. Since the geographical scope of this study has been set in France, a "generic" crop residue based on French crop production distribution has been used in this study based on the distribution and characterization described by Karan and Hamelin [11]. French crops distribution and generic composition are described in Table S3. The total amount of crop residues available in France was determined to be 18.7 Mt dry matter by Andrade Diaz [12].

Table S 11 Generic French crop residue composition [a]

Crop	% Share [b]	Component	Unit	Average value [c]
Wheat	38.66	Water	% ww	13.24
Barley	13.12	Total Solids (TS or DM)	% ww	86.67
Maize	20.32	Volatile Solids (VS)	% TS	93.07
Oats	0.81	Ash	% TS	6.84
Rice	0.20	LHV dry	MJ/kg TS	18.39
Rye	0.19	Cellulose	% TS	38.52
Sorghum	0.52	Hemicellulose	% TS	24.95
Triticale	2.69	Lignin	% TS	13.03
Rape	12.20	Lipids (% crude fat in DM, crude lipids)	% TS	1.25
Soy	0.48	Proteins (total proteins)	% TS	4.08
Sunflower	3.28	C	% TS	47.71
Pea	0.41	H	% TS	5.92
Beans	0.13	O	% TS	43.37
Potato	1.42	N	% TS	1.04
Beet	5.49	S	% TS	0.19
		P	% TS	0.09
		K	% TS	1.19

[a] Ref: Adapted from Karan and Hamelin [11]; [b] Percent distribution at the national scale of France, [c] weighted average value based on the % share.

3.2 Reference scenario or business-as-usual (BAU)

The BAU scenario considers that crop residues (1 tonne wet matter) are ploughed in croplands and decay in the same place where they are generated. No transportation or management is considered in this scenario. The LCI for the BAU was modeled using the Decay on land module for crop residues in Javourez [8]. All the emissions factors considered in this scenario are in Table S4. The decay of crop residues on soils, considers that they will be mineralized in less than two years, therefore 100% of the crop residues will be emitted in a 10-year basis.

Table S 12 Emissions factors related to decay on land [a]

Pathway	Emission factor	Value	Unit	Min	Max	Comment
Decay on land (non-arable)	N_2O_{-N} direct (EF_1)	0.60%	kg N_2O_{-N} .kgN^{-1}	0.001	0.011	[13] *"Other N inputs in wet climates"*
	N_2O_{-N} Fraction volatilized	21.00%	kg(NH_{3-N}+NOx_{-N}) .kgN^{-1}	1E-17	0.31	[13] *volatilization, organic fertilizer*
	N_2O_{-N} indirect vol (EF_4)	1.00%	kg N_2O_{-N}. kg(NH_{3-N}+NOx_{-N}) $^{-1}$	0.002	0.018	[13] *Table 11.3 (EF4)*
	N_2O_{-N} indirect leach (EF_5)	1.10%	kg N_2O_{-N}. $kgNO_{3-N}^{-1}$	1E-17	0.02	[13] *Table 11.3 (EF5)*
	CH_4	3.00%	$kgCH_{4-C}.kgC^{-1}$	0.01	0.1	[11]
	Trapped C	5.00%	$kgC.kgC_{tot}^{-1}$	1E-17	0.1	[11]
Decay on land (arable) [b]	NOx	1.33%	kgNOx-N. kgN^{-1}	0.007	0.026	*Recommended* [14]
	NH_{3-N} (EF)	50.00%	%TAN	0.35	0.65	[15] *Biosolids*
	NO_{3-N}	11%	%Ntot	0.01	0.2	[16] *mineralized N already present in top 20cm of soil assumed neglectable*
	CH_4	0.20%	$kgCH_{4-C}.kgC^{-1}$	1E-17	0.005	[16] *proxy of compost land spreading*
	Trapped CO_2 [c]	1.00%	$kgC.kgC_{tot}^{-1}$	1E-17	0.02	[17]
	MFE-P	60%	%P_applied	50%	70%	[18] *Average residues*
	MFE-K	60%	%K_applied	50%	70%	*Used same as P, as in* [19]
	Ploughing diesel	5.292	$Kg.ha^{-1}$	5	7.5	*Adapted in the "mulching" process of ecoinvent, higher range in* [20]

[a] Retrieved from Decay on Land module by Javourez [8]; [b] considers residues ploughed in soils; c considering carbon sequestration on a 100-year basis. For the crop residues considered, a total 1516.832 CO_2 emissions are associated to ploughing crop residues in soils.

3.3 Hydrodeoxygenated Pyrolysis oil (HPO) system

This scenario considers the production of bio-crude by fast pyrolysis and the consecutive purification by hydrodeoxygenation (HDO) [7,21], which removes O_2 to attain adequate H:C ratios for the stabilized bio-oil to be used as a drop-in fuel. The scenario considers as well the replacement of HFO for marine transportation and accounts for the emissions observed by combusting the HPO. This scenario entails a i) biomass supply and conditioning stage, ii) the fast pyrolysis process, iii) the HDO upgrading, and the iv) HPO combustion.

The biomass supply and pretreatment include the harvesting, transportation storage, size reduction and drying. The preconditioning of the input material results in minor mass losses, of which a 4.8% matter [22] (i.e., 'volatile matter and water) is lost as emissions during storage, 1% of total matter is lost in size reduction and the water content is lost to attain a 10% or less wet content.

The fast pyrolysis process was carried out in an auger reactor, according to the study of Brassard et al. [6], setting the operation conditions at 510°C, during 81 s, with a nitrogen flow rate of 5 $L.min^{-1}$ and condensation temperatures of 120 and 4 °C. The fast pyrolysis produces, along with the biocrude, a liquid fraction hereon referred to as vinegar, a solid biochar, and a syngas stream. The yield obtained in the fast-pyrolysis stage were defined based on the experimental results of Brassard et al., (unpublished) for wheat straw (Table S7).

The biocrude is then upgraded following the HDO process detailed by Jones [7]. The HDO consist on a first stabilization stage followed by two columns were the biocrude reacts with oxygen to displace the oxygen content. The filtered bio-oil from the pyrolysis stage is stabilized at 140-180°C and 1200 psia. The stabilized oil is hydrotreated in two stages. The 1st stage hydrotreating reactor operates at 180-250°C and 2000 psia in a single bed catalytic reactor. The 2nd stage reactor operates at 350-425°C. Ruthenium based catalysts are assumed to be used in the stabilizer and 1st hydrotreating reactor and molybdenum-based catalyst is assumed for the 2nd hydrotreater. The overall HDP process has an oxygen consumption of 5.8% H2/kg treated bio-oil. The process conditions of each stage are reported in Table S8, while the hydrogen requirements and yields observed in each stage for all the products and coproducts are presented in Tables S9.

Table S 13 Fast pyrolysis yields [a]

Parameters	Units	Bio-crude oil	Bio-oil (aqueous phase)	Biochar	Syngas
Yields	% w.b.	**18.77**	**18.30**	**28.10**	
Water content	% w.b.	25.3	71.90		
LHV	MJ/kg	15.22			**6.98**
Phenolics compounds	% mass.		5.80		
Acetic acid	% mass.		5.0		
Ash content	% d.b.			15.44	
Carbon	% d.b.			66.09	
Hydrogen	% d.b.			3.31	
Oxygen	% d.b.			14.38	
Nitrogen	% d.b.			0.710	
Sulfur	% d.b.			0.070	
O/C	molar ratio			0.17	
H/C	molar ratio			0.61	
CO	%vol.				43.26
CO2	%vol.				42.88
H2	%vol.				5.20
CH4	%vol.				7.34
C2H6	%vol.				0.739
C2H4	%vol.				0.583
N2	%vol				

d.d: dry basis, w.b.: wet basis. a Experimental data for the fast pyrolysis of wheat straw, received as courtesy from Brassard et al., [23].

Table S 14 Upgrading conditions. Here, a catalytic hydrodeoxygenation process performed in two columns is considered [7,24]

Process conditions	Units	Stabilization	1st Hydrotreatment	2nd Hydrotreament
Temperature	°C	140	180	410
Pressure	psia	1200	2000	2000
LHSV[a]	volume.h^{-1}.volume_catalyst^{-1}	0.5	0.5	0.22
Catalyst	type		Ru/C	Pt/C/Pd/C
Amount of catalyst	g.kg hydrotreated_bio-oil^{-1}		0.2	0.3

[a] Liquid hourly space velocity

Table S 15. Specific material and energy consumptions in the stabilization process before HDO, with expected yields [7,24]

	Parameter	Value	Unit
Stabilization	H_2 consumption in Stabilization	0.055	H_2 feed.dry oil feed^{-1}
	H_2 consumption	0.08	%w per pyrolysis oil
	H_2 feed/dry oil feed (wt/wt)	0.055	wt.wt^{-1}
	Oil yield in stabilization	96	%
	Gas yield in stabilization	4	%
	CH_4 conversion in Stabilization	3.1	%
	CO_2 conversion in Stabilization	0.6	%
	Acids intermediates	29.5	%
	Carbonyl intermediates	42.9	%
	Extractive intermediates	3.4	%
	Low MW lignin intermediates	20.5	%

Table S 16Specific material and energy consumptions and yields in the first hydrotreatment stage. [7,24]

	Parameter	Value	Unit
Hydrotreating 1st [b]	H_2 input in single stage hydrotreating	74	g.kg^{-1} hydrotraite biofuel
	H_2 consumption	0.18	% pyrolysis oil
	H_2 consumption in Hydrotreating 1	0.07	% per dry oil feed
	Oil yield in 1st Hydrotreating	83	%
	Gas yield in 1st Hydrotreating	7	%
	Water yield in 1st Hydrotreating	10	%
	CH_4 conversion	1.3	%
	CO_2 conversion	3.3	%
	C_2H_6 conversion	2.4	%
	Acids intermediates	11.8	%
	Carbonyl intermediates	4.5	%
	Extractive intermediates	1.9	%
	Low MW lignin intermediates	23.9	%
	High MW lignin intermediates	11.7	%
	Sugar intermediate A	8	%
	Sugar intermediate B	9.2	%
	Phenanthrenes	12.1	%

Table S 17 Specific material and energy consumptions and yields in the second hydrotreatment stage. [7,24]

	Parameter	Value	Unit
Hydrotreating 2nd [c]	H_2 input in two stage hydrotreating	69	$g.kg^{-1}$ hydrotreated bio-oil
	H_2 consumption in Hydrotreating 2	5.54	%wt per pyrolysis oil
	H_2 consumption in Hydrotreating 2	0.21	% per dry oil feed
	Oil yield in 2nd Hydrotreating	48	%
	Gas yield in 2nd Hydrotreating	24	%
	Water yield in 2nd Hydrotreating	28	%
	CO conversion	0.5	%
	CO_2 conversion	9.9	%
	CH_4 conversion	4.7	%
	C_2H_6 conversion	3.7	%
	C_3H_8 conversion	2.6	%
	C_4H_{10} conversion	2.6	%
	H_2S conversion	0.0025	%
	Parafins	12.9	%
	Cyclo C	11.1	%
	Aromatics	5	%
	Phenanthrenes	2.8	%
	Pyrenes	2.8	%
	Diphenyl compounds	0.5	%
	Indans	0.8	%
	Indenes	0.6	%
	Naphtalenes	3	%
	Polynuclear aromatics	2.3	%
	Phenols	2.2	%
	Pentane	3.5	%

Table S 18 Overall hydrogen requirement and yields for the HDO upgrading process

Parameter	Value	Unit	Ref.
HHV	45	$MJ.kg^{-1}$	
LHV	43.02	$MJ.kg^{-1}$	
Hydrotreated oil density	0.85	$g.ml^{-1}$	
H_2 for all hydrotreating	5.8	% per oil feed	
bio-oil yield for all hydrotreating	44	% per dry biocrude	[5]
gas yield for all hydrotreating	26	% per dry biocrude	
water yield for all hydrotreating	30	% per dry biocrude	
C in aqueous phase	0.5	%	[5,8,9]
O in aqueous phase	1.9	%	[5]
C in upgraded oil	68	C/C in pyrolysis oil	
Moisture in Hydrotreated bio-oil	0.1	%	
C in hydrotreated oil	87.5	%	
H in hydrotreated oil	11.95	%	[10]
O in hydrotreated oil	0.5	%	
N in hydrotreated oil	0.05	%	
S in hydrotreated oil	0.005	%	

3.3.1 Mass balance for HPO production

Here, we present the mass balance corresponding to the stabilized biooil production, split by stages of preconditioning (Table S13), fast pyrolysis (Table S14) and HDO upgrading (Tables S15).

Table S 19Mass balance for crop residues supply and conditioning

Parameter	Biomass harvested	Stored biomass	Dried biomass	Grinded biomass
	kg	kg	kg	kg
Total mass	1000.0	954.8	920.9	911.7
Water	132.4	126.0	92.1	91.2
DM	867.6	828.8	828.8	820.5
VM	808.25616	769.5	769.5	761.8
Carbon (C)	413.97	395.5	395.5	391.5
Oxygen (O)	391.62	374.1	374.1	370.4
Hydrogen (H)	51.37	49.07	49.1	48.6
Nitrogen (N)	9.03	8.6	8.6	8.54
Sulfur (S)	1.62	1.5	1.5	1.53
Ashes	59.34	59.34	59.3	58.8
Energy (MJ)				15089.3
Sum DM	867.6	828.8	828.8	820.5

Table S 20Mass balance for the fast pyrolysis process [a]

Prameter	Bio-oil (total)	Bio-crude	Vinegar	Biochar	Syngas
	kg	kg	kg	kg	kg
Total mass	337.96	**171.1**	**166.8**	**256.2**	**317.5**
Water content	163.3	43.3	120.0		
Organic compounds	174.7	127.8	46.9		
Carbon (C)	109.6	80.2	29.4	169.3	112.57
Oxygen (O)	132.1	96.6	35.4	36.8	201.44
Hydrogen (H)	36.6	26.8	9.8	8.48	3.53
Nitrogen (N)	2.6	2.22	0.34	1.82	4.157
Sulfur (S) [b]	0.695	0.45	0.19	0.18	0.65
Ashes	19.196			39.6	
Heat (LHV)		**2604.5**			**1884**
Sum DM	300.7	206.3	75.2	256.2	322.4

[a] Elemental composition of the original matter was received as accounting for ash matter. Therefore, a slight off-calculation is observed in the detailed elemental balance of the pyrolysis products due to the account off ashes. However, the global mass balance (and composition) is correct. [b] Almost all the sulfur-containing bonds in lignin structure can be broken at 550 °C. Also, main sulfur-containing products in the pyrolytic vapors are present as the following small molecular compounds: H2S, SO2, CH3SH, CH3SCH3, and CH3SSCH3, which are in the form of gas or liquids with low boiling points [23]

Table S 21 Mass balance for the hydrotreating upgrade to convert pyrolysis bio-crude into hydrotreated pyrolysis oil (HPO) [a]

Parameters	Pessurized bio-crude	Stabilized biocrude	Gas	Stable bio-oil	Aqueous phase	Gas	Wastewater
	kg	kg	kg	kg	kg	kg	kg
Total mass	**171.1**	**164.3**	**13.88**	56.24	38.35	33.24	43.3
Water	**43.3**	**41.6**		0.06	38.35		
Organic compounds	**127.8**	**122.7**		56.19			
Carbon (C)	**80.20**	**75.94**	4.26	49.16	0.19	30.85	
Oxygen (O)	**96.65**	**95.90**	**0.75**	0.28	33.97	23.95	38.45
Hydrogen (H)	**26.76**	**24.92**	**8.87**	6.71	4.19	18.04	4.84
Nitrogen (N)	**2.22**	**2.22**		0.03		2.19	
Sulfur (S) [b]	**0.45**	**0.45**		0.003		0.44	
Ashes							
Heat (LHV)	**2604.5**	**2604.5**					
Total mass	206.3	199.4	13.9	56.2	38.3	75.5	43.3

3.4 bio-LNG production by anaerobic digestion and cryogenic liquefaction

The second SMF scenario investigated considers that harvested crop residues are pretreated by means of extrusion and comminution and then thy are mixed with water to enter an anerobic digestion process. The biogas produced is purified by cryogenic separation of the CO2 and the recovered biomethane (CH4) is then liquefied and used as maritime biofuel. The liquefied biomethane (bio-LNG) is therefore a replace alternative for fossil LNG. The whole system accounts for the storage of the digestate produced and its use to avoid the application of mineral fertilizers. The biogas system was built upon the anaerobic digestion module developed by Javourez [8] and improved to include the cryogenic liquefaction upgrading process, according to the Cryopure commercial system, and assumptions reported by the Danish Energy agency.

The bio-LNG considers a futuristic energy performant scenario, where the biogas upgrading to bio-LNG by means of cryogenic liquefaction is promoted and the upgrading facilities are close to the actual area where the gas is going to be used, in this case the harbor.

Table S 22 Mass balance of the biogas production.[8]

Stream	Comp.	Crop residues		ex-pretreat feedstock		Ex-storage feedstock		Ex-storageWM feedstock		Digestate		Ex-storage digestate	
WM	**ton**	**1.00**		**0.97**		**0.951**		**8.256**		**7.89**		**7.954**	
DM	kg	867	***86.7%***	841	***86.7%***	826	***87 %***	826	***10 %***	425	***5 %***	405	***5 %***
Proteins	kg	35	*4.1%*	34	*4.1%*	34	*4 %*	34	*4 %*				
Fats	kg	11	*1.3%*	11	*1.3%*	10	*1 %*	10	*1 %*				
Soluble carbs	kg	0	*0.0%*	0	*0.0%*	0	*0 %*	0	*0 %*				
Hemicellulose	kg	216	*25.0%*	210	*25.0%*	206	*25 %*	206	*25 %*				
Cellulose	kg	334	*38.5%*	324	*38.5%*	318	*39 %*	318	*39 %*				
Lignin	kg	113	*13.0%*	110	*13.0%*	108	*13 %*	108	*13 %*				
Ashes	kg	59	*6.8%*	58	*6.8%*	56	*7 %*	56	*7 %*	56	*13 %*	56	*14 %*
Others	kg	98	*11.3%*	95	*11.3%*	94	*11 %*	94	*11 %*				
C	kg	413.5	*47.7%*	401.1	*47.7%*	397.0	*48 %*	397.0	*48 %*	205.5	*48 %*	197.5	*49 %*
N	kg	9.0	*1.0%*	8.7	*1.0%*	8.7	*1 %*	8.7	*1 %*	8.7	*2 %*	8.3	*2 %*
P	kg	0.7	*0.1%*	0.7	*0.1%*	0.7	*0.1%*	0.7	*0.1%*	0.7	*0.2%*	0.7	*0.2%*
H	kg	51.3	*5.9%*	49.8	*5.9%*	49.8	*6.0%*	49.8	*6.0%*	49.8	*11.7%*	48.4	*12.0%*
K	kg	10.4	*1.2%*	10.1	*1.2%*	10.1	*1 %*	10.1	*1 %*	10.1	*2 %*	10.1	*2 %*
O	kg	375.9	*43.4%*	364.6	*43.4%*	353.7	*42.8%*	353.7	*42.8%*	146.1	*34.3%*	135.3	*33.4%*
S	kg	1.6	*0.2%*	1.6	*0.2%*	1.6	*0.2%*	1.6	*0.2%*	0.5	*0.1%*	0.50	*0.1%*
Rest	kg	4.2	*0.5%*	4.1	*0.5%*	4.1	*0.5%*	4.1	*0.5%*	4.1	*1.0%*	4.1	*1.0%*
Energy	GJ	15.61	*18.01*	15.14	*18.01*	14.87	*18.01*	14.87	*18.01*				
mass C:N		*45.9*		*45.9*		*45.9*		*45.9*		*23.7*		*23.9*	
mass C:S		*256*		*256*		*254*		*254*					

3.5 Life cycle inventories (LCI)

The complete LCIss for the HPO and bio-LNG scenarios are transparently documented in “doi database”. It includes all the input and output material and energy flows of the unit operations involved in the SMF production system, including the upgrading, onboard combustion, and avoided/replaced marginals. Here we compile the main assumptions and factors applied in the LCIs.

3.5.1 LCI for HPO scenario

The biomass supply chain includes the process of harvesting the crop residues on the fields and transporting them to the pyrolysis facility. Here, we assumed that the collected residues are transported to a collection platform at 40 km of the field, where they are baled and then they are transported to the pyrolysis facility at 40 km. The collection of the diffuse residues implies a total transportation of 80 km [8], No matter losses are assumed during the collection and baling stages. The straw bales are assumed to be stored in a hay storage structure, designed according to [14] were a 4.8% loss matter takes place. The size reduction is performed with an electrical grinder, while the drying process uses marginal HT heat.

The dust generated during grinding is assumed to be recovered and combusted in an electric furnace for heat production. The design for the combustion process is based on the assumptions in the Combustion module by Javourez [25]. The heat produced is assumed to avoide marginal LT heat (Table S3).

According to Brassard et al. [6,23] in industrial pyrolysis, generally no loss considered. Here we considered the best available technology. This assumption must be further tested in a sensitivity analysis (SA) to determine at which extend the emissions assumptions are important for the overall supply chain.

Table S 23 ***Crop residues harvesting, handling and transportation***

Assumption	Amount	Unit	Ref	Comments
Transport	80.000	tkm	[22]	80 km (13.2% w.c.). Assumed as in the study of [8], where 40 km are defined for the collection of diffuse feedstocks and 40 km are considered for the transport to the pyrolysis plant. Market for transport, freight, lorry >32 metric ton, EURO6, RER [4].
Bale	160	kg	[4]	This is delivering the service of 'bale loading', for 1 straw bale (mass of 160 kg) with bale gripper onto trailer. The service does not include transportation of the bales to the farm. A user wishing to model this service and is aware that within his/her model there is a production of 320 kg of straw while in this service assumes a bale of 160 kg, there the user can model 2 bales of this service for their model
Bale density	200	$kg.m^{-3}$	[23]	Density of one bale of straw

Table S 24 ***Assumptions for the crop residues storage in the HPO scenario***

Assumption	Amount	Unit	Ref	Comment
Total area of a storage building	297.18	m^2	[26],	Total area of a storage building: 50 x 64 ft. (3200 ft2)
Life time	50.00	years		Theorical lifetime of buiding
Storage time	30.00	days	[8]	
Number of bales	117.55	bales	[26],	Calculate the number of bales that can be stored in the building. 18 bales can be stored in 490 ft2 (14 x 35)
CH4pot	0.35	$Nm^3CH_4.kgVS^{-1}$	[8]	Value reviewed by [8]and chosed as intermediate (range: 0.2 - 0.4 %)
MCF	2.00%	% CH_4pot	[6]	From IPCC tier 2 manure management: composting temperate climate
Conversion m3 to kg	0.6684	kg/Nm^3_STP		16.04 g/mol * 24L/mol
N_2O emissions	1	%		1% of the Nitrogen composition by 1.57 (44 g.mol N_2O^{-1}/ 28 mol.gN^{-2}).
CH_4 emissions	-	kg CH_4		$CH_4 = Yield * CH_{4_{pot}} * 0.67MCF$
CO_2 emissions	-	kg CO_2		$CO_2 = Closs - \left(CH_{4_{pot}} * \frac{12}{16}\right) * 44/12$

Table S 25. ***Assumptions for pretreatment of crop residues for HPO: Grinding &drying***

Assumption	Amount	Unit	Ref	Comments
Target moisture	10	%		
Wet mass loss at grinding	1	%WM		Estimated loss as dust
Electricity for chipping (industrial)	0.02	kWh.kgDM^{-1}	[8]	*For grinding and densification. Range 0.02-0.156 reviewed by* [8]*using wood as a proxy*
Inert gas for lock hopper	0.0764	Nm^3.kg DM^{-1}	[5]	Review by [15]. N_2 selected as in [8]
Nitrogen gas density	1.167	kg.Nm^{-3}		Molar mass N2: 28.01 kg/kmol ; Molar volume gas: 24 Nm3/kmol (STP 20°C)
Heat requirement	4.000	MJ.kg^{-1} evaporated water	[6],	To remove water
Heat requirement	6.320	MJ.kg^{-1}water	[8]	
Electricity for drying	0.096	kWh.kgDM^{-1}	[15]	Average energy demand using air blowing drying. Data are derived from literature review (Bujant 2011) and Ecoinvent database. Drying is operated at temperature 80-90 °C. Temperature outlet is about 60 °C (Hannula 2016).
Feeding electricity	5.86	kWh.tDM^{-1}	[5]	Lock hopper feeding system under up to 25 bar. Data are obtained from literature reviews (Swanson 2003; Carven 2014).

Energy consumption to reduce the particle size of biomass feedstock from 25 mm to 3 mm is 443 MJ/drytonne of biomass compared to the 157.5 MJ/dry tonne required to decrease the particle size from 300 mm to 25 mm.

$$Heat_{reauired} = \left(T_{target} - T_{ambient}\right) * \left(cp_{water(liq)} * wate_{fraction}\right) + \left(cp_{solid} * DM_{fraction}\right) + \left(kg_{watzr\_removed} / \left(kg_{wet_{water}} * vap_{water\,lat_{heat}} * 1000\right)\right)$$

Table S 26 ***Dust recovery and combustion for heat production.***

Assumption	Amount	Unit	Ref	Comments
Dust generated during grinding/chipping is assumed recovered in an industrial furnace, small size, on-site (no transportation)				
Initial moisture	13.20	%		As in stored biomass
Energy in dust	15.9624276	$MJ.kgWM^{-1}$	[8]	*For grinding and densification. Range 0.02-0.156 reviewed by* [8]
Furnace efficiency	80	%	[8]	Assumed as reviewed by [8]
Heat generation	12.76994208	$MJ.kgWM^{-1}$		
Dust combustion process taken as a proxy of heat prodcution, wood pellet, 9 kV [11] Ecoinvent [4]process "heat production, wood pellet, at furnace, 9kW, state-of-the-art 2014, CH" used to create the LT Heat avoided process				
	1	**MJ provided**		
	1.03E-06	$Unit.MJ^{-1}$		
	0.00556	$kWh.MJ^{-1}$		
	3.75E+00	*kg ash.tonne$_{ww}^{-1}$*		
Ash	4.46E+00	$kg\ ash.tonneDM^{-1}$		*REMOVED*
Electricité	5.56E-03	kWh		market group for electricity, low voltage
Furnace efficiency	1.03E-06	unit		market for furnace, pellets, 9kW
	1	**kgDM burned**		
	1.19E+00	$kg.kgDM^{-1}$		market for wood ash mixture, pure
	1.48E-03	$kWh.kgDM^{-1}$		market group for electricity, low voltage
	2.74E-07	$unit.kgDM^{-1}$		market for furnace, pellets, 9kW

Table S 27 **Assumptions for designing the fast pyrolysis plant**

Assumption	Amount	Unit	Ref	Comments
Biomass pyrolysed per day	20000	$kg.day^{-1}$	[6]	Assumed as in [2]: Scaled-up to 20 $tonne.day^{-1}$ (Pyroformer from Aston University, 2.5 $t.h^{-1}$ working 8h.day^{-1}).
Working days per year	240	days		
Biomass pyrolysed per year	4800000	kg		
Life time of chemical factory	50	years		
Biomass pyrolysed per year	4800	ton		
Pyrolysis biomass flowrate	2500	$kg.h^{-1}$		
Pyrolysis VS synthetic gas factory	0.54		[4]	Ratio to scale syngas factory in Ecoinvent 3.9.1 for the pyrolysis procedure.
Bio-oil density	1.2	$g.ml^{-1}$	[27]	The density of the liquid bio-crude is very high at around 1.2 $g.ml^{-1}$ compared to light fuel oil at around 0.85 $g.ml^{-1}$. Range 1.1 - 1.3 $g.ml^{-1}$.
Bio-oil + vineagar production	7414	$kg.day^{-1}$		
Bio-oil + vineagar production	370.7	$kg.ton^{-1}_{biomass}$		
Bio-oil + vineagar production	6178.33	$L.day^{-1}$		
LHV biocrude	15.22	$MJ.kg^{-1}$		
Energy - preheating	0.319	$MJ\ kg^{-1}_{biomass}$	[23]	
Energy - heating	1.051	$MJ\ kg^{-1}_{biomass}$		
Energy - Screws	8.77	$MJ\ kg^{-1}_{biomass}$		
Energy - Agitator	0.563	$MJ\ kg^{-1}_{biomass}$		
Synthetic gas factory construction: Building, hall, steel construction	10500	m^2	[4]	This infrastructure process includes land use, buildings and facilities (including dismantling) of a typical biomass gasifier. Process includes the dryer, the comminution equipment, the gasifier and the gas treatment and conditioning facility. Chemical factory, organics (GLO), 33% RER, 67% RoW
Chemical factory construction	12600000	kg	[4]	Estimated composition of the facilities of a chemical plant, based on a distillation unit.

Table S 28 **Condensation** [6]

Assumption	Amount	Unit	Ref.	Comments
Ratio Glycol/Water	0.5		[2]	50/50 ratio water to glycol.
Quantity of liquid	5	$m^{-3}.year^{-1}$	[2]	Per condenser
Cp water	4.185	$kJ.K\text{-}kg^{-1}$		
Cp Glycol	2.2	$kJ.K\text{-}kg^{-1}$		
Density glycol	1.11	$g.cm^{-3}$		
Water flow rate	180	L.h-kg		for 1 kg biomass/h
Water flow rate	1.56	$L\ .min^{-1}kg^{-1}$		
Delta T (C1)	3.1	°C		
Delta T (C2)	0.17	°C		
Pumps				
Power	1	HP	[2]	
Power	0.75	kW		
Pressure	20	PSI		
Capacity	43.2	$L.min^{-1}$		
Water for 1000 kg	180000	L		
Time for 90 L	4.17	min		
Time for 180000 L	69.447	h		
Energy (Heating system)	47.89	MJ	[3]	Considering heating 1 m3 water once a day from 60 to 120°C. Heat losses are compensated by heating during pyrolysis. Considered to be HT heat.
Energy (electricity for pumps)	186.4	MJ	[2]	Calculation pump 1 HP, 43 LPM. Submersible pump
Energy (Cooling system)	17.786	MJ	[2]	Considering cooling 1 m3 water once a day from 21 to 4°C
Energy (Cooling system - continue)	64.03	MJ	[2]	All electricity considered to be medium voltage, FR

Table S 29 **HDO process to upgrading**

Parameter	Value	Unit	Reference
Electricity for hydrotreatng	0.014849147	kWh/kg biooil	[28]
Electricity for hydrotreatng	0.0054428	kwh/MJ produced	[7]
Electricity (total)	0.088	kWh/kg biofuel	[24]
Catalysts lifetime	365	days	[7]
a LHV = HHV - 0.212*H - 0.0245*M - 0.008*Y.,H = Percent hydrogen,M = Percent moisture,Y = Percent oxygen**(2006 IPCC Guidelines, Vol. II, Section 1.4.1.2)**			
biocrude upgraded by day	3754	kg/day	
Working days per year	240	days	
Life time of chemical factory	50	yrs	
Biooil stabilized for life time	45048000	kg	
Biooil flowrate	469.25	kg/h	
Pyrolysis VS synthetic gas factory	0.537313433		
Catalysts lifetime	240	days	
Hydrotreated bio-oil	1651.76	kg/day	
Hydrotreated bio-oil	1943.247059	L/day	
Gas from hydrotreating	976.04	kg/day	
Water from hydrotreating	1126.2	kg/day	
HHV	74329.2	MJ/day	
H2 input	217.73	kg/day	
Catalyst input Ru	0.91	g/day	
Catalyst input Mo	1.357610959	g/day	
Catakyst used for lifetime	27152.21918	g	
Catalyst used per 1 ton biocrude			
Hydrotreated bio-oil	440	kg/ton biocrude	
Hydrotreated bio-oil	517.65	L/ton biocrude	
Gas from hydrotreating	260	kg/ton biocrude	
Water from hydrotreating	300	kg/ton biocrude	
HHV	19800	MJ/ton biocrude	
LHV	18929.7064	MJ/ton biocrude	
H2 input	58	kg/ton biocrude	
Catalyst input Ru	0.24109589	g/ton biocrude	
Catalyst input Mo	0.361643836	g/ton biocrude	
c Ref: Jones et al., 2013			

Biochar is assumed to be spread on fields as in [8]. Below we present the considerations for biochar spreading process according [8] . Besides biochar, biopesticide is also applied to soils, however that inventory is only presented in the complete LCI database [21] due to its length.

Table S 30 **Biochar application**

Assumption	Amount	Unit		Comments
Pathway depend on origin of feedstock (risk management) : Biochar assumed to be appied on land/ temporary storage of gaschar neglicted - no emissions, assumed as stable We don't consider the land use. Biochar is expected to be mixed with fertilizer for spreading				
Water	1.8	kg/kgbiochar	[29]	Facilitates the spreadign of biochar
Increase in maize yield	28 %		[30]	*Likely optimist for France condition (already high yields): represent max threshold (moreover done with T°<550) / [40] reviewed average yield of 10-42%*
Increase in wheat yield	14 %		[30]	
Decrease in N2O emissions	30 %	%_ref		[25] Detailed N emisions are reported in https://doi.org/10.48531/JBRU.CALMIP/1JXQK3
Char application	10	tww/ha	[30]	*Range reviewed by [38], no notable additional effects after 10*
C_sequestrated after 100y	75 %	%C_in	[17]	
C_emited	25 %	%C_in	[17]	Assumed as CO_2-C
Stable carbon	**95 %**	%C_in	[17]	*Meta-review by [13], here values refer to "Gas char" at temperature between 800-1200°C (15 refs)*
Half life	**632**	year	[17]	
Carbon lost after 100y	25 %	%C_in	[17]	
Solid manure spreader	1	tww/tww	[4]	As Javourez 2023. To spread biochar, replacing FR mix
Transport	100	tkm		
Skeletal density	1.5241	g/cm3	[23]	biochar skeletal density was calculated based on the equation as a function of pyrolysis temperature for wood (Brewer et al., 2014)

Syngas combustion modeled as in gasification module by [8] considering in-situ valorization of syngas, modeled as in [19] and [20]. Producer gas is cleaned and cooled before entering the CHP unit, then flue gases are treated (as in [19]), to meet emissions standards of the Directive 2010/75/EU. The full LCI is presented in [21]. Here we show the CHP system created in Ecoinvent 3.9.1 to account for the syngas heat and power valorization. The heat produced is assumed to avoid marginal LT Heat while the electricity avoids marginal medium voltage electricity for France.

Table S 31 **Syngas combustion**

Assumption	Amount	Unit	Ref	Comments
biogas	0.42806	Nm3		
CHP	4.87E-08	unit		
lubricating oil	0.00029189	kg		
waste lubricating oil	-0.00029189	kg		
platinium	6.81E-11	kg		
CH4	0.00022381	kg		
N2O	2.43E-05	kg		
NMVOC	1.95E-05	kg		
CHP inventory proxy				
CHP unit	1.14E-07	units/Nm3	[4]	Adapted from the ecoinvent process CHP
lubricating oil	0.003235246	kg/Nm3	[4]	production from biogas, considering
waste lubricating oil	-0.00323525	kg/Nm3	[4]	equivalent in a Nm3 basis
Calcium hydroxide	0.002611357	kg/MJ_syngas	[31]	For flue gas cleaning (SI of [19])
CHP efficiency				
Electricity generation	35 %	%	[8]	syngas CHP electricity efficiency
LT Heat generation	45 %	%	[8]	syngas CHP electricity efficiency
use of LT heat	50 %	%	[8]	LT heat recovery efficiency

The combustion of the syngas recoverd from the HDO stage is modelled following the same technical assumptions that for the pyrolysis sungas, but accounting for the specific composition and LHV. The HPO and HFO combustion onboard are detailed in the LCI database and were modeled according to the fuel consumption and emissions detailed in section SI1.

The Hydrogen used for HDO was modeled to be produced by alkaline electrolysis at 80°C, 30 bars, according to the gasification module of Javourez [8]. The energy efficiency was parametrized according to Table S21. The full inventory for installations and materials was used as by Javourez, itself built upon an existing pilot plant. The excess heat was assumed to be partly recovered while the oxygen separated

was not recovered. The storage emissions and water discharge were neglected. The H2 plant parametrized according to table x, has a global warming potential 100 years performance of 2.14 kgCO2-eqkH2-1, which is below the threshold defined by the EU comisison (3.0 kgCo2eq.kgH2-1). Here we show the main assumptions and inventory for the hydrogen plant creation (TableS16), while the detailed calculations are presented in SI2, accessible at [21]

Table S 32 Detailed inventory for alkaline electrolysis production of hydrogen. 25]

Alkaline H2 inventory	Amount	Unit	Ref
Deionized water requirements	7.84	Kg.kgH_2	[32]
HHV_hydrogen	80%	%energy_in	[32]
Electricity required	49.2	kWh/kgH2	Calc
KOH (90%)	1.90E-03	kg/kgH2	[24]
Oxygen produced	*7.94*	kg/kgH2	[24]
Heat required	2.6	MJ/kgH2	Calc
Heat released	35.5	MJ/kgH2	Calc
Heat recovery	50%	%heat	Assum
Building hall	1.69E-03	m2/kgH2	[33]
Nitrogen , liquid	2.90E-04	kg/kgH2	[32]
LT heat recovery COP	5.00	kW/kWe	MP module
COP electricity requirements	2.0	kWh/kgH2	Calc
Stack			
Copper {RoW} | production, primary	1.93E-04	kg/kgH2	[34]
Steel, unalloyed {GLO} | market for	1.93E-02	kg/kgH2	[34]
Nickel, 99.5% {GLO} | market for	1.83E-03	kg/kgH2	[34]
Aluminum, primary, ingot, at plant/RNA	4.34E-05	kg/kgH2	[34]
Polyvinylchloride, bulk polymerized {RER} | polyvinylchloride production, bulk polymerization	7.52E-05	kg/kgH2	[34]
Tetrafluoroethylene {RER} | production	7.52E-06	kg/kgH2	[34]
Acrylonitrile-butadiene-styrene copolymer {RER} | production	1.54E-05	kg/kgH2	[34]
Polyphenylene sulfide {GLO} | production	3.28E-05	kg/kgH2	[34]
Polysulfone {GLO} | polysulfone production, for membrane filtration production	2.51E-05	kg/kgH2	[34]
N-methyl-2-pyrrolidone {RER} | production	1.25E-04	kg/kgH2	[34]
Aniline {RER} | production	4.72E-06	kg/kgH2	[34]
Acetic anhydride {RER} | production, ketene route	5.20E-06	kg/kgH2	[34]
Purified terephthalic acid {RER} | production	8.48E-06	kg/kgH2	[34]

Alkaline H2 inventory	Amount	Unit	Ref
Nitric acid, without water, in 50% solution state {RER} | nitric acid production, product in 50% solution state | C	3.18E-06	kg/kgH2	[34]
Hydrochloric acid, without water, in 30% solution state {GLO} | tetrafluoroethane production	1.25E-05	kg/kgH2	[34]
Graphite {RER} | production	4.14E-05	kg/kgH2	[34]
Lubricating oil {RER} production	4.63E-08	kg/kgH2	[34]
Zirconium oxide {RoW} | production	1.06E-04	kg/kgH2	[34]
Carbon monoxide {RER} | production	1.45E-05	kg/kgH2	[34]
Water, decarbonized, at user {RER} | water production and supply, decarbonized	1.06E-03	kg/kgH2	[34]
De-ionized water, reverse osmosis, production mix, at plant, from surface water RER S	8.29E-03	kg/kgH2	[34]
Industrial machine heavy, unspecified {RER} | production	1.54E-08	kg/kgH2	[34]
Plaster mixing {CH} | processing	7.52E-05	kg/kgH2	[34]
Electricity, high voltage {KR} | electricity production, natural gas, conventional power plant	3.47E+00	kJ/kgH2	[34]
Heat, district or industrial, natural gas {KR} | heat and power co-generation, natural gas, conventional power plant	8.48E+00	kJ/kgH2	[34]
Heat, from steam, in chemical industry {RER} | steam production, as energy carrier, in chemical industry	6.74E-02	kJ/kgH2	[34]
Share of O2 used	95%	%generated	Assumed 0%

3.5.2 LCI for bio-LNG production by biogas production in AD and cryogenic liquefaction upgrading

The crop residues are assumed to be harvested and pretreated before storage. The pretreatment consists on size reduction by means of extrusion and comminution [20]. The feedstock is considered to be stored ensiled where part of mass is lost as emission. The stored crop residues are then directed to a mesophilic agitated tank where the anerobic digestion process takes place. The biogas is assumed to be composed of 60% CH4 and the balance of CO_2 [9]. The produced digestate is stored in concrete tanks with emission capture cover. No losses to water or soil are induced by the storage of digestate. The CH_4 in biogas is assumed to be separated by cryogenesis, with recovery of CO_2. The CH4 obtained is of 99.95% of purity and the losses during the process are <1% [35]. The separate biomethane is then liquefied and commercialized to be used as maritime fuel. The assumptions on the substituted fertilizer are presented only in the data repository due to the length.

Table S 33 **Pretreatment of crop residues for the bio-LNG scenario**

Parameter	Amount	Unit	Comment
Comminution	0.0075	kWh/kgDM	*Optim from* [19]
Extrusion	0.007	kWh/kgDM	*Based on Hjorth et al 2011*
	3 %	%WMloss	*All fractions equals, including DM*
Hygienization	247.4	kJ/kgwater	*Adapted to local average T°*
	176.7	kJ/kgDM	*Adapted to local average T°*
Transport	40	km	*Only accounted if diffuse stream*
Forwarding	40	km	*Usually considered 100 for diffuse, but here separated in two. See pyrolysis module*
	0.315	PMH/tww	*to load, haul and unload, conserv by* [36]*Ardolino et al 2019*
Bale loading	160	kg/unit	*This is delivering the service of 'bale loading', for 1 straw bale (mass of 160 kg) with bale gripper onto trailer. The service does not include transportation of the bales to the farm.*

Table S 34 **Emissions from ensiling**

Pollutant	Amount	Unit	Ref	Comment
CO2	1.50 %	%WMin	[12]	*Maximum CO2 released during ensiling*
NH3	0.007	kgNH3/kgCO2	Calc	*Assumed NH3 losses proportional to CO2 losses as in [4]*
molar C:N in	0.02	molN/molC	Calc	
WMloss	1.95 %	%WMin	[12]	*Change in weight after ensiling*

Table S 35 **Anaerobic digestion conditions** [25]

Parameter	Amount	Unit	Ref
Theoretical Methane Potential			
Proteins	0.496	m3CH4/kg	[37]
Fat	1.0008	m3CH4/kg	[37]
Soluble Carbs	0.415	m3CH4/kg	[37]
Hemicelluloses	0.415	m3CH4/kg	[37]
Cellulose	0.415	m3CH4/kg	[37]
Lignin	0	m3CH4/kg	[37]
Ashes	0	m3CH4/kg	[37]
Others	0.415	m3CH4/kg	Assumed
Theoretical Methane production	34.3	m3CH4/ton ex-stor feedstock (after humidity)	Calc
Yield	75 %	%theo	see KPI
Methane production - before losses	25.7	m3CH4/ton ex-stor feedstock (after humidity)	Calc
Apparent Methane potential - before losses	276	m3CH4/tonVS	Calc
Biogas parameters			
CH4	60 %	%biogas	[9]
CO2	40 %	%biogas	Calc
CH4 density	0.714	kg/Nm3	[37]
CH4 LHV	38	MJ/Nm3	[37]
CO2 density	1.87	kg/Nm3	[37]
Biogas density	1.18	kg/Nm3	Calc
Biogas LHV	22.8	MJ/Nm3	Calc
CH4 produced - before losses	18.4	kgCH4/tonex-stor feedstock (after humidity)	Calc
CO2 produced - before losses	33.6	kgCO2/ton	Calc
Biogas	52.0	kgBiogas/ton	
H2S production	0.20 %	%H2S-S	[29]
Losses			
CH4	1 %	%prodbiogas	[38]
CO2	*2.74*	kgCO2/kgCH4	
Flaring	2.8%	%prodBiogas	
Flaring efficiency	98.0%	%CH4	
Energy requirements			
Pre treatment	0.005	kWh/kgDM	
Diesel	0	L/kgWW	
Elec	8 %	Autoconso	
Heat	97.9	kJ/kgWM	
Additional water	7.3	m3/ton_ex_stor	
DM	10 %		
Average T°	13	°C	
Cp water	4.2	kJ/kgWW/°C	[2]
Cp DM	3	kJ/kgWW/°C	[2]
Machines & Building	2.9E-07	unit/m3biogas	[15]

Table S 36 **Digestate storage parameters**

Digestate	Amount	Unit
Water addition	0.02	m3/tonWM
Electricity for pumping	2.9	kWh/tonWM
Emissions		
CH4 MCF	12 %	%BMP
Digestate potential	0.177	m3CH4/kgVS
CH4 emissions - before reduction	0.015	kgCH4/kgVS
Digestate TAN	75 %	%Ntot
NH3	11 %	%TAN
CO2	2.74	kgCO2/kgCH4emi - before reduction
directN20	0.50 %	kgN2O-N/kgN
indirectN20 - frac gas	0.05	
indirectN20	0.01	kgN20/kgfrac(gas+leach)
Nox	1.00 %	%TAN
N2	3	kgN2-N/kgN2O-N
Loss in TAN	7 %	%
Emissions reduction potential	80 %	%CH4&NH3
VS digestate in	87 %	%DM
DM digestate in	5 %	%WM
%N digestate in	2.0%	%DM

Table S 37 **Cryogenic liquefaction assumptions**

Parameter	Amount	Unit	Reference
Biogas purity	99 %	%methane	Yousef et al., 2019
Upgrading electricity	2 %	%biogas	[10]
Compression electricity	1.00 %	%biogas	[10]
Energy requirement	0.009	kWh/MJ	[10]
N2 as refrigerant			
Plant size	2.67E-10	plants/m3 biogas	[39]
Pipeline injection			
Pressuirng biogas	0.12	kWh/Nm3	[10]
Fugitive losses from injection	0.10 %	%biomethane	[10]
Network losses	1.50 %	%biomethane	Ademe, transition(s) 2050
Transport	100	tkm	
Other			
Liquefaction			
Energy requitement	0.75	kWh/kg LBM	
Energy requitement	0.80	kWh/Nm3 raw biogas	
Flow rate			
LHV	48	MJ/kg	
Density	0.428	kg/m3	

References

1. United Nations. Review of Maritime transport 2022: Navigating stormy waters. Geneva: United Nations; 2022. 174 p. (Review of maritime transport / United Nations Conference on Trade and Development, Geneva).
2. Hwang SS, Gil SJ, Lee GN, Lee JW, Park H, Jung KH, et al. Life Cycle Assessment of Alternative Ship Fuels for Coastal Ferry Operating in Republic of Korea. Journal of Marine Science and Engineering. 2020 Sep;8(9):660.
3. IMO. Fourth IMO GHG Study 2020 [Internet]. IMO; 2020. Available from: https://wwwcdn.imo.org/localresources/en/OurWork/Environment/Documents/Fourth%20IMO%20GHG%20Study%202020%20-%20Full%20report%20and%20annexes.pdf
4. Ecoinvent. Ecoinvent 3.9.1 database. 2022.
5. Su-ungkavatin P. Assessing the environmental performance of future sustainable aviation systems: methodological development and evaluation by life cycle assessment. [France]: INSA Toulouse; 2022.
6. Brassard P, Godbout S, Hamelin L. Framework for consequential life cycle assessment of pyrolysis biorefineries: A case study for the conversion of primary forestry residues. Renewable and Sustainable Energy Reviews. 2021 Mar;138:110549.
7. Jones S, Meyer P, Snowden-Swan L, Padmaperuma A, Laboratory PNN. Process Design and Economics for the Conversion of Lignocellulosic Biomass to Hydrocarbon Fuels: Fast Pyrolysis and Hydrotreating Bio-oil Pathway. 2013;97.
8. Javourez U. Transforming residual biomass into food and feed – Towards an LCA optimization platform. [France]: INSA Toulouse; 2023.
9. Pellegrini LA, De Guido G, Langé S. Biogas to liquefied biomethane via cryogenic upgrading technologies. Renewable Energy. 2018 Aug 1;124:75–83.
10. Andrade Díaz C. Database: LCIs for : To harvest or not? Tradeoffs between SOC maintenance and overall environmental performance of harvesting crop residues for the bioeconomy. Datavers.Callisto; 2023.
11. Karan S. Cambioscop RO1: Dataset on characterization, quantity and current use of French residual biomasses. 2022 Nov 28 [cited 2023 May 10];1. Available from: https://data.mendeley.com/datasets/b9sx3h3584
12. Andrade Díaz C, Clivot H, Albers A, Zamora-Ledezma E, Hamelin L. The crop residue conundrum: Maintaining long-term soil organic carbon stocks while reinforcing the bioeconomy, compatible endeavors? Applied Energy. 2023 Jan 1;329:120192.
13. IPCC. Chapter 11 - N2O Emissions From Managed Soils, and Co2 Emissions From Lime and Urea Application. 2019 Refinement to the 2006 IPCC Guidelines for National Greenhouse Gas Inventories. 2019;1–48.
14. Skiba U, Medinets S, Cardenas LM, Carnell EJ, Hutchings NJ, Amon B. Assessing the contribution of soil NOx emissions to European atmospheric pollution. Environ Res Lett. 2021 Feb;16(2):025009.
15. Brockmann D, Pradel M, Hélias A. Agricultural use of organic residues in life cycle assessment: Current practices and proposal for the computation of field emissions and of the nitrogen mineral fertilizer equivalent. Resources, Conservation and Recycling. 2018 Jun 1;133:50–62.
16. Albizzati PF, Tonini D, Astrup TF. A Quantitative Sustainability Assessment of Food Waste Management in the European Union. Environ Sci Technol. 2021 Dec 7;55(23):16099–109.
17. Andrade C, Albers A, Zamora-Ledezma E, Hamelin L. A review on the interplay between bioeconomy and soil organic carbon stocks maintenance. PREPRINT (version 2) available at Research Square [Internet]. 2022 Mar 16 [cited 2022 Mar 16]; Available from: https://www.researchsquare.com
18. Delin S. Fertilizer value of phosphorus in different residues. Soil Use and Management. 2016;32(1):17–26.

19. Lodato C, Hamelin L, Tonini D, Astrup TF. Towards sustainable methane supply from local bioresources: Anaerobic digestion, gasification, and gas upgrading. Applied Energy. 2022 Oct;323:119568.
20. Hamelin L, Naroznova I, Wenzel H. Environmental consequences of different carbon alternatives for increased manure-based biogas. Applied Energy. 2014 Feb;114:774–82.
21. Elliott DC. Transportation fuels from biomass via fast pyrolysis and hydroprocessing. WIREs Energy and Environment. 2013;2(5):525–33.
22. Emery I, Dunn JB, Han J, Wang M. Biomass Storage Options Influence Net Energy and Emissions of Cellulosic Ethanol. Bioenerg Res. 2015 Jun 1;8(2):590–604.
23. Brassard P. Mass balance and LCA inventory of bio-oil production by fast pyrolysis of wheat straw. Unpublished study, received as a courtesy from the authors. 2022;
24. Vienescu DN, Wang J, Le Gresley A, Nixon JD. A life cycle assessment of options for producing synthetic fuel via pyrolysis. Bioresource Technology. 2018 Feb 1;249:626–34.
25. Javourez U. Transforming residual biomass into food and feed, towards an LCA optimization platform - Supporting data. 2023;
26. Overhults D, Bicudo J. Hay storage structures [Internet]. 2016. Available from: https://cpb-us-e1.wpmucdn.com/blogs.cornell.edu/dist/e/1628/files/2016/03/Hay-Storage-Structures-2iygxft.pdf
27. IEA Bioenergy. Task 34: Direct Thermochemical Liquefaction - Pyrolysis bio-oil [Internet]. Task 34: Direct Thermochemical Liquefaction. 2023. Available from: https://task34.ieabioenergy.com/bio-oil/
28. Iribarren D, Peters JF, Dufour J. Life cycle assessment of transportation fuels from biomass pyrolysis. Fuel. 2012 Jul 1;97:812–21.
29. Peters JF, Iribarren D, Dufour J. Biomass Pyrolysis for Biochar or Energy Applications? A Life Cycle Assessment. Environ Sci Technol. 2015 Apr 21;49(8):5195–202.
30. Farhangi-Abriz S, Torabian S, Qin R, Noulas C, Lu Y, Gao S. Biochar effects on yield of cereal and legume crops using meta-analysis. Science of The Total Environment. 2021 Jun;775:145869.
31. Dong J, Tang Y, Nzihou A, Chi Y, Weiss-Hortala E, Ni M. Life cycle assessment of pyrolysis, gasification and incineration waste-to-energy technologies: Theoretical analysis and case study of commercial plants. Science of The Total Environment. 2018 Jun 1;626:744–53.
32. Cvetković SM, Radoičić TK, Kijevčanin M, Novaković JG. Life Cycle Energy Assessment of biohydrogen production via biogas steam reforming: Case study of biogas plant on a farm in Serbia. International Journal of Hydrogen Energy. 2021 Apr 19;46(27):14130–7.
33. Palmer G, Roberts A, Hoadley A, Dargaville R, Honnery D. Life-cycle greenhouse gas emissions and net energy assessment of large-scale hydrogen production via electrolysis and solar PV. Energy Environ Sci. 2021 Oct 13;14(10):5113–31.
34. Lee B, Cho HS, Kim H, Lim D, Cho W, Kim CH, et al. Integrative techno-economic and environmental assessment for green H2 production by alkaline water electrolysis based on experimental data. Journal of Environmental Chemical Engineering. 2021 Dec 1;9(6):106349.
35. Danish Energy Agency, Energinet. Technology Data. Renewable fuels. [Internet]. 2017. Available from: http://www.ens.dk/teknologikatalog
36. Ardolino F, Cardamone GF, Parrillo F, Arena U. Biogas-to-biomethane upgrading: A comparative review and assessment in a life cycle perspective. Renewable and Sustainable Energy Reviews. 2021 Apr;139:110588.

37. Tonini D, Hamelin L, Alvarado-Morales M, Astrup TF. GHG emission factors for bioelectricity, biomethane, and bioethanol quantified for 24 biomass substrates with consequential life-cycle assessment. Bioresource Technology. 2016 May;208:123–33.
38. Hamelin L, Møller HB, Jørgensen U. Harnessing the full potential of biomethane towards tomorrow's bioeconomy: A national case study coupling sustainable agricultural intensification, emerging biogas technologies and energy system analysis. Renewable and Sustainable Energy Reviews. 2021 Mar;138:110506.
39. Florio C, Fiorentino G, Corcelli F, Ulgiati S, Dumontet S, Güsewell J, et al. A Life Cycle Assessment of Biomethane Production from Waste Feedstock Through Different Upgrading Technologies. Energies. 2019 Jan;12(4):718.